U.PORTO
FACULDADE DE CIÊNCIAS
UNIVERSIDADE DO PORTO

PhD

3rd CYCLE

FCUP
2025

U.PORTO

RNA-based therapies for Mucopolysaccharidoses

Juliana Inês Pinto dos Santos

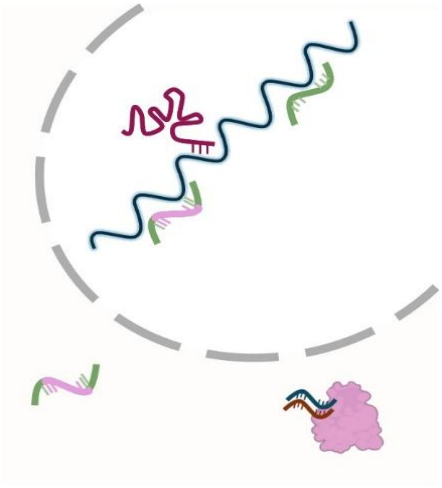
FC

U.PORTO
FACULDADE DE CIÊNCIAS
UNIVERSIDADE DO PORTO

RNA-based therapies for Mucopolysaccharidoses

Juliana Inês Pinto dos Santos
Doctoral Degree in Biology
Department of Biology
Faculty of Sciences of the University of Porto
2025

PhD



RNA-based therapies for Mucopolysaccharidoses

Juliana Inês Pinto dos Santos

Thesis carried out as part of the Doctoral Degree in Biology
Departament of Biology
2025

Supervisor
Doctor Sandra Catarina da Conceição Alves
Principal Researcher
National Health Institute Doutor Ricardo Jorge

Co-supervisors
Doctor Maria Francisca de Lima Magriço Coutinho Reis
Auxiliary Researcher
National Health Institute Doutor Ricardo Jorge

Professor Maria João Prata Martins Ribeiro
Associate Professor with Habilitation
Faculty of Sciences of the University of Porto
Researcher at i3S/IPATIMUP

Agradecimentos

Ao concluir esta etapa desafiadora e enriquecedora, é com profunda gratidão que expresso os meus agradecimentos a todos que, de alguma forma, contribuíram para a realização deste trabalho.

Começo por agradecer ao Conselho Diretivo do Instituto Nacional de Saúde Doutor Ricardo Jorge (INSA) e à Direção do Centro de Saúde Pública Doutor Gonçalves Ferreira (CSPGF), por me terem dado a possibilidade de realizar este trabalho no INSA. À Dra. Glória Isidro, coordenadora do Departamento de Genética Humana, o meu obrigada.

Ao Centro de Estudos de Ciência Animal (CECA) e à Fundação para a Ciência e a Tecnologia (FCT), fontes de financiamento, esta última pela concessão da bolsa individual de doutoramento (SFRH/BD/124372/2016), sem a qual não poderia ter iniciado esta jornada, e pelo financiamento do projeto ASOS2cureMPSIII-2022.04667.PTDC (doi.org/10.54499/2022.04667.PTDC). Agradeço também à associação de doentes americana, *National MPS Society*, pelo financiamento do projeto 2019DGH1642 e ao Laboratório Associado para a Ciência Animal e Veterinária (AL4AnimalS).

À Doutora Sandra Alves, minha orientadora, por há 9 anos me ter dado a oportunidade de “entrar” no seu grupo. Por toda a confiança que depositou em mim, por todas as sugestões e conselhos que me foi dando ao longo deste percurso. Agradeço toda a atenção, orientação e disponibilidade. Nesta reta final, por todas as correções e melhorias que enriqueceram em muito a redação desta tese. Obrigada por estar sempre presente e por me fazer querer continuar a trabalhar neste fantástico grupo de investigação.

À Professora Doutora Maria João Prata, minha co-orientadora, que apesar de fisicamente longe sempre esteve presente quando precisei. Agradeço por todos os conselhos, pela disponibilidade e pelas críticas construtivas que fez na revisão desta tese. Por sempre acreditar que seria capaz e que no fim tudo iria dar certo.

À Francisca, minha co-orientadora, que desde o meu primeiro dia no INSA nunca me deixou “sozinha”. Por todo o apoio, ajuda, compreensão, disponibilidade e partilha de conhecimento que tornaram possível a realização de todo este trabalho. Por sempre ter acreditado nas minhas capacidades e por ver sempre o lado mais positivo e menos sombrio de cada resultado obtido. Agradeço toda a dedicação ao longo destes anos,

pela forma como me acolheu e me quer ver brilhar. Por toda a paciência que sempre teve comigo e pelo sorriso diário mesmo depois de uma noite às claras, sobretudo nesta fase final. Obrigada por teres agarrado esta tese como se fosse tua. Mas, sobretudo, e o mais importante, obrigada pela amizade.

Ao Paulo Gaspar e ao Hugo Rocha, da Unidade de Rastreio Neonatal. Obrigada por toda a ajuda neste trabalho.

Ao Dr. Zé Manel, por diariamente "bater 6 vezes" à porta do *Tzero* após o almoço e nos dar uns minutos de boa disposição, obrigada.

Aos meus colegas e amigos do *Tzero*. Obrigada por me terem acolhido quando cheguei. Por todas as gargalhadas e brincadeiras, pelos almoços diários, pelos momentos de descontração, pelo apoio e amizade. Obrigada pela paciência e preocupação que sempre tiveram comigo e por me aturarem nesta última fase. À Joana, a minha parceira do lado, que começou e que acaba esta etapa comigo. Obrigada pelo companheirismo, pela amizade e pela paciência para os meus desabafos! À Liliana, por toda a orientação que me deu para a realização de parte deste trabalho. Obrigada pelo que me ensinaste e por todos os conselhos. Sem dúvida que sem ti os resultados não tinham tido o sucesso que tiveram. À Marisa, à Luciana e ao Pedro, os meus bioquímicos preferidos. Obrigada pelas conversas e por me fazerem ver sempre a parte positiva de tudo. Obrigada por toda a partilha de conhecimento e por todas as palavras nos momentos que mais precisei. À Olga, pelos sábios conselhos. Ao Diogo e à Lisbeth, que mesmo não estando no *Tzero* fazem parte dele!

Um obrigada especial à Mariana. É com ela que partilho grande parte deste trabalho. Por estar sempre disposta a ajudar, por todos os dias me receber com um grande sorriso e um "bom dia jóia" mesmo sendo 8 da manhã e tendo feito 70 km para ali estar. És a pessoa com mais alegria e boa disposição que conheço e que vê sempre a parte boa de tudo. Sem dúvida que sem ti este trabalho não teria tido tanto sucesso. Obrigada por todo o companheirismo e amizade.

A todos os meus amigos que me acompanharam ao longo desta caminhada. Obrigada pelos momentos de diversão, pelo apoio e pela amizade. Por sempre acreditarem que este dia iria chegar. Um grande obrigada!

Aos meus amigos do PHC, obrigada. Fazem com que o final de dia seja uma animação e com que o exercício físico custe bem menos ☺. Um especial agradecimento à Sandrinha, à Sandra Costa e ao "Tina". Sem vocês o grupo não seria o mesmo.

À Maria e ao João, obrigada pelos jantares de sexta. Obrigada por me fazerem “desligar” do trabalho, pelas conversas e por todas as gargalhadas. Mas sobretudo, obrigada por me deixarem fazer parte da vossa família. Ao Manel e à Maria, as “minhas crianças”, que fazem com que os momentos com eles sejam um dos pontos altos da minha semana, obrigada por aquecerem o coração da Juju! ♡

À minha família. Obrigada por sempre acreditarem que sou capaz. À minha madrinha, Eduardo e João Pedro que “são casa”. À minha avó, por toda a preocupação, por me ter acompanhado desde sempre e ter tanto orgulho em mim e por estar tão ansiosa que esta etapa acabe para irmos festejar ☺

Aos meus pais e irmã, os que mais levam com os meus problemas. São eles que ouvem todas as minhas frustrações e me erguem. Obrigada por todo o carinho, por toda a preocupação e por todo o amor que me dão. É graças a vocês que hoje alcanço esta tão importante etapa.

Resumo

As Doenças Lisossomais de Sobrecarga (DLS) constituem um grupo de doenças hereditárias do metabolismo, na sua maioria associadas a complicações graves e progressivas, incluindo neurodegeneração. Avanços significativos têm sido obtidos quanto à compreensão dos mecanismos moleculares subjacentes a essas doenças, mas os progressos no desenvolvimento de terapias eficazes têm sido muito mais lentos.

Os poucos fármacos atualmente disponíveis para tratar DLS enfrentam vários desafios, especialmente nos subtipos de DLS com envolvimento neurológico, uma vez que tais fármacos são incapazes de atravessar a barreira hematoencefálica (BHE), e assim, não podem mitigar os sintomas neurológicos. Entre as DLS, a Mucopolissacaridose tipo III (MPS III), também conhecida como síndrome de Sanfilippo, destaca-se por ser um dos subgrupos cuja caraterística principal é a neurodegeneração grave. Esta síndrome é causada por deficiências em qualquer uma das enzimas envolvidas na degradação do sulfato de heparano, um tipo de glicosaminoglicano (GAG). Em consequência, sulfato de heparano acumula-se nas células, afetando predominantemente o sistema nervoso central (SNC). Outros órgãos e sistemas também podem ser afetados, embora os sintomas neurológicos representem a caraterística mais distintiva da síndrome de Sanfilippo. Existem quatro subtipos de MPS III (A, B, C e D), classificados com base na enzima deficiente, todos partilhando manifestações clínicas semelhantes.

Atualmente, as opções terapêuticas para a MPS III são muito limitadas. A terapia de substituição enzimática tem sido eficaz em algumas DLS, mas não consegue debelar os sintomas neurológicos devido à incapacidade de atravessar a BHE. Compreende-se, assim, que estejam a ser investigadas diversas abordagens terapêuticas, incluindo terapia génica, terapia de redução de substrato e outras capazes de atravessar a BHE, tendo em vista oferecer melhores alternativas de tratamento, embora nenhuma tenha tradução na prática clínica até hoje. Este cenário reforça a necessidade de procurar novas abordagens terapêuticas capazes de oferecer aos doentes e às suas famílias cuidados mais eficazes, ou seja, de encontrar soluções mais inovadoras para lidar com a doença.

Entre estas, as abordagens terapêuticas baseadas em RNA têm despertado um interesse crescente, o que já se saldou no desenvolvimento de fármacos aprovadas para uso clínico.

Neste trabalho, exploraram-se várias dessas abordagens, incluindo *small nuclear RNAs* (U1 snRNAs) modificados, *small interfering RNAs* (siRNAs), oligonucleótidos *antisense* do tipo *splice-switching* (SSOs) e oligonucleótidos *antisense*

do tipo *gapmers* (gapmer ASOs). Foi possível demonstrar o potencial de estratégias terapêuticas baseadas em RNA para MPS III, abrindo caminho para o desenvolvimento de opções de fármacos mais direcionados e eficazes.

Foram desenvolvidas duas abordagens distintas. Uma focou-se no desenvolvimento duma terapia direcionada para uma mutação específica associada a MPS IIIC, a forma mais desafiante de todas as MPS III. Essa mutação, localizada num local de *splicing* a 5' (c.234+1G>A) resulta na exclusão do exão 2, impedindo a produção da proteína funcional, acetil-CoA: α-glucosaminida N-acetiltransferase (HGSNAT). A outra abordagem, de caráter mais abrangente, visou uma redução de substrato de base genética (gSRT, do inglês *genetic substrate reduction therapy*) tendo como alvo um gene específico, *XYLT1*, envolvido numa etapa inicial da biossíntese dos GAG. Ao reduzir a expressão do *XYLT1*, o objetivo foi diminuir a síntese de sulfato de heparano, atenuando a sua acumulação nas células e tecidos de doentes com MPS III.

Em relação à primeira abordagem, que pretendia restaurar o processo normal de *splicing* desregulado pela mutação c.234+1G>A, este trabalho deu continuidade a um estudo anterior do próprio grupo, avançando na validação pré-clínica da estratégia terapêutica através da realização de estudos *in vivo*. Isto porque já tinham sido obtidos resultados promissores *in vitro* em fibroblastos de doentes tratados com um vetor U1 snRNA modificado totalmente complementar ao local de *splicing* mutado- U1 snRNATC.

Foram construídos dois midigenes, um contendo a sequência normal do *HGSNAT* e o outro a sequência mutada. Os midigines foram transfetados em diferentes linhas celulares modelo para avaliar a sua expressão. Tendo sido confirmada a capacidade para gerar os padrões de *splicing* esperados, testou-se a eficácia do U1 snRNATC nesses sistemas artificiais. Embora o U1 snRNATC tenha sido capaz de modular o *splicing* do midigene mutado, o transcrito resultante não correspondeu ao transcrito normal, apresentando a incorporação de quatro nucleótidos do intrão 2. Apesar destes resultados não terem ido de encontro às expectativas, não foram desencorajantes, uma vez que foram obtidos num sistema artificial destituído, por isso, do adequado contexto genético e epigenético.

Assim, e tendo em conta os resultados anteriores do grupo mostrando que o tratamento com o mesmo U1 snRNATC modificado resultava em cerca de 50% de transcritos normais em fibroblastos de doentes, avançou-se com estudos *in vivo* para avaliar a sua eficácia terapêutica. Começou-se por induzir a expressão transitória dos dois midigenes (normal e mutado) através de injeção hidrodinâmica em ratinhos C57BL/6, o que falhou provavelmente devido a dificuldades técnicas. Tentou-se então uma outra abordagem, em que se promoveu uma expressão mais prolongada utilizando

vetores de vírus adeno-associados (AAV, do inglês *adeno-associated virus*), especificamente o serótipo AAV2/9, conhecido pelo seu tropismo para os tecidos nervoso e hepático.

Os resultados revelaram não só que foi alcançada a expressão prolongada dos vetores em ratinhos FVB/N, mas também que o U1 snRNATC inserido no vetor AAV2/9 foi capaz de restaurar o processo de *splicing* do gene *HGSNAT* mutado num número considerável de animais. Estes resultados constituem um avanço significativo não só para o desenvolvimento de terapias baseadas em RNA para MPS IIIC, mas também, e numa perspetiva mais ampla, para a geração de terapêuticas baseada em U1 snRNAs. Pela primeira vez, conseguiu-se uma correção bem-sucedida de uma mutação localizada na posição +1 de um local de *splicing* a 5', num modelo *in vivo*.

Em relação ao segundo tipo de abordagem, cujo objetivo era desenvolver uma terapia de gSRT, foram avaliadas três classes distintas de moléculas de RNA: siRNAs, SSOs e *gapmer* ASOs. Cada uma foi especificamente desenhada para desencadear um mecanismo de ação diferente, mas convergindo na degradação dos mRNAs alvo, garantindo simultaneamente máxima especificidade e mínimos efeitos *off-target*.

Com siRNAs, forçou-se a modulação artificial do mecanismo de RNA de interferência, utilizando uma *pool* de três siRNAs para silenciar a expressão do *XYLT1*. A avaliação inicial do efeito em fibroblastos de doentes de todos os subtipos de MPS III (A-D) revelou reduções significativas nos níveis de RNA mensageiro (mRNA) do gene-alvo. Porém, a análise cuidada dos problemas que poderiam dificultar a introdução de siRNAs na prática clínica, especialmente relacionados com o atingimento do SNC, levou a enveredar por vias alternativas, mais fáceis de prosseguir quer em termos científicos quer em termos regulamentares respeitantes ao desenvolvimento de medicamentos. Assim, apostou-se num estudo com oligonucleótideos *antisense* (SSOs e *gapmer* ASOs), uma vez que podem chegar ao SNC através de uma injeção intratecal, um método já utilizado na prática clínica para outras doenças.

Inicialmente, considerou-se modular o *splicing* de forma a induzir um *skipping* de exões que levasse ao desfasamento da grelha de leitura, gerando transcritos *out-of-frame* de *XYLT1*, que posteriormente fossem degradados pelo mecanismo de *nonsense-mediated mRNA decay*. Dos cinco SSOs desenhados e testados para esse propósito, selecionaram-se os dois que demonstraram maior eficácia no *skipping* dos exões alvo a nível do mRNA para as análises subsequentes. Não foram observadas reduções nem nos níveis da proteína xilosiltransferase-I (XT-I) nem na acumulação de sulfato de heparano, nos períodos de incubação testados. De momento, não é possível descartar se tal se pode atribuir a longa semi-vida da proteína XT-I aliada à acumulação

substancial de sulfato de heparano, ou se apenas reflete a ausência de ação terapêutica destes específicos SSOs nas concentrações testadas. Estudos futuros serão fundamentais para esclarecer essa questão.

A terceira abordagem para gSRT focou-se no uso de *gapmer* ASOs, moléculas que promovem a degradação do mRNA recrutando a enzima RNase H. Dos cinco gapmers inicialmente testados, foram selecionados para análises adicionais os dois que demonstraram uma maior eficácia na redução dos níveis de mRNA, usando apenas fibroblastos de doentes com MPS IIIC. Os períodos de incubação prolongados revelaram reduções significativas nos níveis da proteína XT-I e de acumulação de sulfato de heparano. O efeito de um dos gapmers manteve-se mesmo 10 dias após a transfeção, reforçando a sua capacidade para originar fármacos de longa duração.

Estes resultados destacam o potencial dos *gapmer* ASOs como uma abordagem de gSRT não apenas para as MPS III, mas também para outras DLS que em o SNC, esteja comprometido, na medida em a administração intratecal de ASOs pode contornar a BHE, permitindo o tratamento de graves distúrbios neurológicos.

Nesta tese, apresentaram-se dados que reforçam o enorme valor das terapias baseadas em RNA para responder às necessidades clínicas das DLS, em particular das MPS III. Tanto estratégias de correção do processo de *splicing* como de redução de substrato evidenciaram a versatilidade e especificidade das terapias de RNA. Ao explorar diferentes modalidades deste tipo de terapias, este trabalho constitui um passo importante no sentido do desenvolvimento de fármacos mais direcionados, eficazes e personalizados para doenças genéticas raras.

No futuro, iremos centrar-nos na otimização das vias de administração de terapias baseadas em RNA, que podem passar pelo uso de nanopartículas lipídicas e/ou administração intratecal para facilitar a passagem pela BHE. Além disso, serão conduzidos estudos pré-clínicos em modelos animais, como o peixe-zebra e roedores, para avaliar a biodistribuição, segurança e eficácia a longo prazo das diversas moléculas.

Os resultados apresentados nesta tese já proporcionam algumas bases importantes para a translação clínica das terapias de RNA, oferecendo novas perspetivas terapêuticas e, assim, esperança para doentes com MPS III ou doenças relacionadas.

Palavras-chave: Doenças Lisossomais de sobrecarga, Mucopolissacaridose tipo III, terapia de redução de substrato de base genética, modulação de splicing, U1snRNAs,

small interfering RNAs, oligonucleótidos do tipo *splice-switcing*, oligonucleótidos do tipo gapmer.

Abstract

Lysosomal storage disorders (LSDs) are a group of inherited metabolic conditions that often lead to severe and progressive complications, including neurodegeneration. While significant progress has been made in understanding the molecular mechanisms underlying these disorders, development of effective therapies is running much more slower.

Treatments face several challenges, particularly for neuronopathic LSDs, concerning which current drugs are unable to cross the blood-brain barrier (BBB) preventing them to mitigate the neurological symptoms. One of the LSD' subgroups more strongly marked by severe neurodegeneration is Mucopolysaccharidoses type III (MPS III), also known as Sanfilippo syndrome. The syndrome is caused by deficiencies in one of the enzymes required for the degradation of heparan sulfate (HS), a type of glycosaminoglycan (GAG). As a result, HS accumulates within cells, predominantly affecting the central nervous system (CNS). Many organ systems may be affected, albeit the neurological degeneration remains the hallmark of the disease. There are four subtypes (A, B, C, and D), classified based on the specific enzyme deficiency, that share similar clinical manifestations.

Currently, treatment options for MPS III are limited. Enzyme replacement therapy, which has shown effectiveness in some other LSDs, fails to address neurological symptoms due to its inability to cross the BBB. Experimental approaches, including gene therapy, substrate reduction therapy and BBB-penetrating treatments, are being explored viewing the development of innovative therapeutic options for MPS III, but the progresses have been too modest. This raises the need to find alternative therapies that can offer patients and their families improved care and more effective solutions. Among them are RNA-based therapeutics, which already have offered some drugs approved for clinical use in a number of diseases.

This work has explored several RNA-based strategies, including engineered U1 snRNAs, small interfering RNAs (siRNAs), splice-switching oligonucleotides (SSOs) and gapmer antisense oligonucleotides (ASOs), in the context of MPS III.

The focus were two main approaches. One involved the development of a mutation-specific strategy, aimed to correct the abnormal splicing process caused by a common splice site mutation in the *HGSNAT* gene (c.234+1G>A), associated with MPS IIIC, the most challenging form of MPS III. The mutation results in exon 2 skipping, preventing the production of a functional acetyl-CoA:α-glucosaminideN-acetyltransferase (HGSNAT) protein.

The other approach, was a broader one that consisted on the development of a genetic substrate reduction therapy (gSRT) to target a particular gene, *XYLT1*, which plays a role in an early step of GAGs biosynthesis. By downregulation *XYLT1* expression, the goal was to decrease the synthesis of HS and its accumulation in the cells and tissues of MPS III patients.

Regarding the first approach, which aimed to rescue the normal splicing process disrupted by the c.234+1G>A mutation, this work builds on our team's previous findings to further advance the preclinical validation of this strategy, now progressing to *in vivo* studies, as *in vitro* evidence had already been obtained using patient-derived fibroblasts. To achieve that, an engineered U1 snRNA vector, fully complementary to the mutated splice site (ss) was used: U1 snRNATC.

We started by developing two distinct midigenes, one containing the wild-type and the other the mutated *HGSNAT* sequence. The midigines were then expressed in different model cell lines. After confirming their ability to generate the expected splicing patterns, we tested the previously designed U1 snRNATC in one of those artificial systems. Although the U1 snRNATC was able to modulate splicing, the resulting transcript differed from the wild-type, incorporating four nucleotides of intron 2. These results did not fit our expectations, but they didn't discourage us because they were obtained in an artificial system that eventually lacked the proper genetic and epigenetic context.

So, recuperating our group's previous findings evidencing that treatment with the same modified U1 snRNATC resulted in about 50% of normal transcripts in patient-derived fibroblasts, we turned to *in vivo* studies to evaluate its therapeutic efficacy.

First, we induced transient expression of both midigenes (wild-type and mutant) through hydrodynamic injection into C57BL/6 mice, which was unsuccessful probably due to technical issues. Next, we proceeded with another approach aimed at achieving a more robust and sustained expression, using adeno-associated virus (AAV) vectors, specifically the AAV2/9 serotype, known for its tropism for neural and hepatic tissues.

Overall, the AAV-mediated delivery enabled sustained expression of our constructs in FVB/N mice. It was also shown that the U1 snRNATC packaged into the AAV2/9 vector restored the correct splicing of AAV-delivered *HGSNAT* mutant in some animals. This represents an important finding in the scope of RNA-based therapies for MPS IIIC, as well in the broader field of U1 snRNA-based therapeutics. It ilustrates the first successful correction of a mutation located at position +1 of a 5’ splice site in an *in vivo* model.

The second type of RNA-based approaches implemented in this thesis, aimed at promoting a genetic substrate reduction therapy (gSRT). Three different RNA molecules were evaluated: siRNAs, SSOs and gapmer ASOs. Each one was designed to trigger a distinct mechanism of action leading to the degradation of target mRNAs, while ensuring high specificity and minimal off-target effects.

With regard to siRNA, which relies on the artificial modulation of the RNA interference mechanism, a pool of three siRNAs was used to silence the expression of our target gene, *XYLT1*. Initial assessments in fibroblasts from patients of all MPS III subtypes (A-D) revealed significant reductions of target mRNA levels. However, the evaluation of the hindrances to overcome viewing the successful introduction in the clinical practice, specially the delivery to the CNS, led us to move to alternative approaches whose development pipeline appeared less problematic. Antisense oligonucleotides (SSOs and gapmer ASOs) were the options, given that they can be delivered to the CNS via intrathecal administration, as was already implemented in the clinical practice for other diseases.

We first thought to modulate splicing by intentionally inducing an out-of-frame exon skipping generating abnormal transcripts of *XYLT1* that could be then targeted for mRNA degradation by nonsense-mediated decay. Among the five SSOs designed and tested, the two that demonstrated a more efficient skipping of the target *XYLT1* exons at mRNA level, were selected for subsequent analysis. No reductions were observed in xylosyltransferase I (XT-I) protein levels or HS accumulation within the tested timeframes. Though, it remains unclear whether that was due to a long XT-I protein half-life combined with substantial pre-existing HS accumulation, or to the absence of therapeutic action of the two SSOs, at least at the tested conditions. Only future studies will shed light on the issue.

The third approach appraised for gSRT, was based on the use of gapmer ASOs, which promote mRNA degradation by recruiting RNase H. Five molecules were designed, two of which demonstrated very high knockdown efficiency at mRNA level. Both were selected for further analysis performed exclusively in MPS IIIC fibroblasts. Extended incubation times revealed significant decreases in XT-I protein levels and HS accumulation. Notably, the effect of one of those gapmers was sustained for 10 days post-transfection, highlighting its potential for long-term therapeutic applications. These findings underscore the transformative potential of gapmer ASOs as a gSRT not only for MPS III but even for other LSDs. This is particularly relevant for disorders with severe CNS manifestations, as intrathecal delivery of ASOs allows them to bypass the BBB.

This thesis adds novel evidence on the immense potential and efficacy of RNA-based therapies to address the unmet clinical needs of LSDs, particularly MPS III. Both splicing correction and substrate reduction strategies underscore the versatility and specificity of RNA therapeutics. By leveraging different RNA modalities, this work represents more one step towards the so long awaited targeted, effective, and personalized treatments for rare genetic diseases.

Our future studies will focus on optimizing the delivery of RNA-based therapies, including the use of lipid nanoparticles or intrathecal administration to bypass the BBB. Developing preclinical studies in animal models, including zebrafish and rodents, is also in our horizon, to assess the biodistribution, safety, and long-term efficacy of these therapies.

The findings already provided in this thesis lay the groundwork for the clinical translation of RNA-based therapies, offering hope for patients with MPS III and related disorders.

Keywords: Lysosomal Storage Disorders, Mucopolysaccharidoses type III, RNA-based therapies, genetic substrate reduction therapy, splicing modulation, U1snRNAs, small interfering RNA, splice-switching oligonucleotides, gapmer antisense oligonucleotides

Table of contents

Resumo ..... ***i***

Abstract ..... ***vi***

List of Tables ..... ***xv***

List of Figures ..... ***xvi***

Abbreviations ..... ***xix***

Introduction ..... ***ii***

1. Where it all begins - the Lysosome: a mini organelle with a major role ***1***

2. What if it fails - the Lysosomal storage disorders ***2***

2.1. What's sweet becomes sour – the Mucopolysaccharidoses 6

2.1.1. Focus on Mucopolysaccharidoses type III (MPS III) 11

3. RNA-based therapeutics ***13***

3.1. RNA drugs acting upon splicing 16

3.1.1. A brief overview of the splicing process 16

3.1.2. Splice-switching oligonucleotides (SSOs) 20

3.1.3. Engineered U1 snRNAs 23

3.2. RNA-therapies acting by gene knockdown 26

3.2.1. Gapmer ASOs and siRNAs 26

3.3. Increasing the efficacy of RNA-based drugs 29

3.3.1. Chemical modifications 29

3.3.2. Disease models 32

3.3.3. Delivery technologies 34

3.4. Current state of RNA therapy development for MPSs 36

3.4.1. Approaches attempting splicing modulation/correction 36

3.4.2. Approaches attempting gene knockdown 38

Aims ***41***

Materials and Methods ***45***

1. Part I ***47***

1.1. Therapeutic approach to correct the c.234+1G>A mutation in the *HGSNAT* gene using an engineered U1snRNA vector fully complementary to the mutant 5'ss of exon 2 – *in vitro* studies 47

1.1.1. Midigene cloning and construction 47

1.1.2. Minicultures 48
1.1.3. Minipreps 49
1.1.4. Sequencing PCR 50
1.1.5. Maxipreps 50
1.1.6. Transfection of the midigenes pHGSNATwt and pHGSNAT+1A in Hep3B and COS-7 cell lines 51
1.1.7. Co-transfection of pHGSNATwt and pHGSNAT+1A midigenes along with a engineered U1 snRNA vector in the HEK293T cell line 52
1.1.8. Analysis of splicing rescue by reverse transcription-polymerase chain reaction (RT-PCR) 53
1.1.8.1. Total RNA extraction 53
1.1.8.2. cDNA synthesis 54
1.1.8.3. RT-PCR and products purification 54
1.2. Therapeutic approach to correct the c.234+1G>A mutation in the *HGSNAT* gene using an engineered U1 snRNA vector fully complementary to the mutant 5'ss of exon 2 – *in vivo* studies 56
1.2.1. Transient expression of the pHGSNATwt or pHGSNAT+1A midigenes in wild-type mice 56
1.2.1.1. Animal procedures 56
1.2.1.2. Hydrodynamic injection and animals sacrifice 56
1.2.1.3. Evaluation of pHGSNATwt and pHGSNAT+1A expression in wild-type mice 58
1.2.1.4. Statistical analysis 58
1.2.2. Sustained expression of the pHGSNATwt or pHGSNAT+1A midigenes in wild-type mice 59
1.2.2.1. Selection of the best performing AAV serotype 59
1.2.2.2. Intraperitoneal injection of different AAV2/9 vectors in wild-type FVB/N mice 60
1.2.2.3. Evaluation of the AAV2/9_HGSNATwt, AAV2/9_HGSNAT+1A, AAV2/9_U1snRNAwt and AAV2/9_U1snRNATC expression in mice and assessment of splicing pattern rescue 63
1.2.2.4. Histological analysis 64
1.2.2.5. Statistical analysis 64

2. Part II 65

2.1. Genetic substrate reduction approaches for Mucopolysaccharidoses type III 65

2.1.1. RNA-based molecules design 65
2.1.1.1. Small interfering RNAs (siRNAs) 65
2.1.1.2. Splice-switching oligonucleotides (SSOs) 65
2.1.1.3. Gapmer antisense oligonucleotides (ASOs) 67
2.1.2. Cell Culture and RNA-based molecules transfection 68
2.1.2.1. Cell culture 68
2.1.2.1.1. siRNAs transfection 68
2.1.2.1.2. SSOs transfection 69
2.1.2.1.3. Gapmer ASOs transfection 69
2.1.3. Evaluation of the effect at mRNA level 69
2.1.3.1. Quantitative real-time PCR (qRT-PCR) - siRNAs and gapmer ASOs experiments 69
2.1.3.2. RT-PCR analysis - SSOs experiments 70
2.1.4. Evaluation of the effect at protein level 71
2.1.4.1. Protein extraction 71
2.1.4.2. Protein quantification 71
2.1.4.3. Sodium Dodecyl Sulphate – Polyacrylamide Gel Electrophoresis (SDS-PAGE) 72
2.1.4.4. Western Blot (wb) 72
2.1.5. Evaluation of the effect at heparan sulfate levels 73
2.1.5.1. Heparan sulfate and dermatan sulphate (DS) quantification by LC-MS/MS 73
2.1.6. Statistical analysis 74

Results and Discussion 75

1. Part I: Therapeutic approach to correct the c.234+1G>A mutation in the HGSNAT gene using an engineered U1 snRNA vector fully complementary to the mutant 5'ss of exon 2 77

1.1. *In vitro* functional studies to evaluate the splicing patterns promoted by *HGSNAT* midigenes and the therapeutic correction potential of the modified U1 snRNA 78
1.1.2. Transfection of pHGSNATwt and pHGSNAT+1A midigenes in Hep3B reproduced the expected splicing pattern 79
1.1.3. Transfection of pHGSNATwt and pHGSNAT+1A midigenes in COS-7 cells also reproduced the expected splicing pattern 80
1.1.4. U1 snRNATC induced a splicing pattern shift 81

1.2. *In vivo* therapeutic approach to correct the c.234+1G>A mutation in the *HGSNAT* gene using an engineered U1 snRNA vector fully complementary to the mutant 5'ss of exon 2 84
1.2.1. Hydrodynamic injection for transient expression of pHGSNATwt and pHGSNAT+1A midigenes in mouse liver to model the human MPS IIIC c.234+1G>A splicing defect 84
1.2.1.1. Splicing pattern analysis of pHGSNATwt and pHGSNAT+1A midigenes in the liver of wild-type C57BL/6 mice: transient expression did not result in widespread expression of the midigenes 87
1.2.2. Sustained expression of the h*HGSNAT*wt and h*HGSNAT*+1A in wild-type FVB/N mice using AAV vectors 89
1.2.2.1. Choosing the adequate AVV vector for delivering the constructs - no major differences were observed on the expression levels induced by different AAV serotypes 91
1.2.2.2. Splicing pattern analysis of h*HGSNAT*wt and h*HGSNAT*+1A in the liver of wild-type FVB/N mice: rescue of the splicing defect by sustained expression of U1 snRNATC 93

2. Part II: Genetic Substrate reduction therapeutic approach for Mucopolysaccharidoses type III - targeting a gene of the GAG biosynthesis.... 100

2.1. Evaluating the siRNA effectiveness in fibroblasts from MPS III patients .. 103
2.2. Exploring antisense oligonucleotides as a novel strategy for genetic substrate reduction therapy in MPS III 105
2.2.1. Evaluating the effect of SSOs on exon skipping of *XYLT1* gene: identifying the most promising molecules 105
2.2.1.1. Evaluating the effect of SSOs on exon skipping of *XYLT1* gene: SSO3 and SSO5 as the most promising molecules 109
2.2.1.2. Evaluating the effect of the exons 9 and 11 skipping on xylosyltransferase I (XT-I) protein expression 110
2.2.1.3. The final effect: can the most promising SSOs decrease heparan sulfate storage? 112
2.2.2. Evaluating the effect of gapmer ASOs on *XYLT1* mRNA relative expression: selecting the most promising molecules 115
2.2.2.1. Evaluating the effect on the *XYLT1* mRNA relative expression using the most promising gapmers: G2 and G3 117
2.2.2.2. The gapmers G2 and G3 have any effect on xylosyltransferase I (XT-I) protein levels? 117

2.2.2.3. Do the gapmers G2 and G3 induce a decrease on heparan sulfate (HS) storage? 119
2.2.3. The “Final assay”: are we working at the correct time points? 121
2.2.3.1. The effect on *XYLT1* expression levels 24 hours after gapmers’ treatment 121
2.2.3.2. Increasing the gapmers’ incubation time to see the effect on xylosyltransferase I protein levels 121
2.2.3.3. Gapmer G2 reduces the storage levels of heparan sulfate at 6 and 10 days post-transfection 122

Conclusions and Future perspectives 127

References 137

Annexes 155

List of Tables

Table 1. Classification and molecular basis of MPS..... 8
Table 2. Cycling conditions for the site-directed mutagenesis.....48
Table 3. Cycling conditions for the sequencing PCR. 50
Table 4. Summary of the experimental scheme followed for transfection of the pHGSNATwt or pHGSNAT+1A midigene and the pEGFP vector and co-transfection of the pHGSNATwt or pHGSNAT+1A midigenes with the U1 snRNAwt or U1 snRNATC vectors and the pEGFP vector. 53
Table 5. Primer sequences used for cDNA amplification of pHGSNATwt and pHGSNAT+1A midigenes as well as pcDNA 3.1® vector. 54
Table 6. Preparation of the Preparation of the quantitative real-time PCR mix..... 60
Table 7. Data on the injections of each AAV2/9 construct in mice and the combinations between them.. 61
Table 8. Primer sequences used for cDNA amplification of constructs expressed in mice. 63
Table 9. Small interfering RNA (siRNA) sequences used in this study. 65
Table 10. Sequences of splice-switching oligonucleotides (SSOs) and their target exons in *XYLT1* gene. 67
Table 11. Sequences of Gapmer ASOs and their target exons in *XYLT1* gene. 68
Table 12. Preparation of the quantitative real-time PCR (qRT-PCR) mix. 70
Table 13. Cycling conditions for the quantitative real-time PCR (qRT-PCR). 70
Table 14. Primer sequences used for cDNA amplification of diferent *HGSNAT* exons. 71
Table 15. List of antibodies used in Western Blot. 73

List of Figures

Figure 1. Schematic representation of lysosomal components and properties**.**. 1
Figure 2. Summary of Lysosomal Storage Disorders (LSDs).. 3
Figure 3. Therapeutic strategies fo Lysosomal Storage Disorders (LSDs)..... 5
Figure 4. Major therapeutic approaches currently under evaluation to target the CNS disease in Mucopolysaccharidoses.. 13
Figure 5. Classification of RNA drugs..... 15
Figure 6. Schematic representation of the splicing process**.**..... 18
Figure 7. Schematic diagram of essential regulatory elements in pre-mRNA splicing.. 19
Figure 8. Simplified overview of the alternative splicing (AS) process.. 20
Figure 9. Mechanism of action of splice-switching oligonucleotides (SSOs). 22
Figure 10. Role of the endogenous U1 snRNP in splicing.. 24
Figure 11. U1 snRNA-mediated therapy for 5' splice site (ss) mutations through restoration of exon recognition and inclusion.. 25
Figure 12. Schematic representation of the mechanism of action of gapmer ASOs**……..**27
Figure 13. Schematic representation of the mechanism of action of short interfering RNAs (siRNAs). 28
Figure 14. Oligonucleotide chemistries..... 31
Figure 15. Schematic representation of the rationale behind the original study by Matos and co-workers 38
Figure 16. Schematic representation of the pcDNA 3.1® vector with the wild-type HGSNAT gene sequence from exon 1 to 18 and partial sequences of intron 1 (437 bp) and intron 2 (435 bp) cloned into the Nhe I and Xba I restriction sites..... 47
Figure 17. Schematic representation of the therapeutic approach with modified U1snRNA to correct the pathogenic effect of the splice site mutation c.234+1G>A in the *HGSNAT* gene. 52
Figure 18. Representative diagram of the experimental assay in wild-typet C57BL/6 mice for analysis the splicing patterns of the pHGSNATwt and pHGSNAT+1A midigenes. . 57
Figure 19. Representative diagram of the experimental assay for AAV serotype selection in wild-type FVB/N mice.. 60
Figure 20. Schematic representation of the pAAV2/9 vector showing (a) wild-type HGSNAT gene sequence from exons 1 to 18, along with partial sequences of introns 1 and 2 and (b) U1 snRNAwt.. 62

Figure 21. Schematic representation of SSOs target sites in corresponding exons of XYLT1 gene. 67
Figure 22. Agarose gel electrophoresis of *HGSNAT* amplification products after Hep3B transfection with pcDNA 3.1-myc, pHGSNATwt and pHGSNAT+1A, for 24 and 48 hours. 80
Figure 23. Electropherogram of a portion of the *HGSNAT* transcript sequence obtained after transfection with two midigenes: a) pHGSNATwt; b) pHGSNAT+1A 80
Figure 24. Agarose gel electrophoresis of *HGSNAT* amplification products after COS-7 transfection with pcDNA 3.1-myc, pHGSNATwt and pHGSNAT+1A, for 24 and 48 hours, respectively 81
Figure 25. Fluorescence microscopy analysis of HEK293T cells co-transfected with the pHGSNATwt midigene and the U1snRNAwt vector (24 hours). 82
Figure 26. Agarose gel electrophoresis of *HGSNAT* amplification products after HEK293T co-transfection with the pEGFP, pHGSNATwt or pHGSNAT+1A midigene vectors, combined with the U1snRNAwt or U1snRNATC during 24 hours. 82
Figure 27. Electropherogram of a segment of the *HGSNAT* transcript sequence obtained after co-transfection of pHGSNAT+1A midigene with U1snRNATC vector. 84
Figure 28. Mean body mass (g) of each animals' group at the beginning and end of the transient expression experiment. 86
Figure 29. Relative mass (g/g-1) of different organs of each animals' group. 87
Figure 30. Agarose gel electrophoresis of *HGSNAT* amplification following the injection of pHGSNATwt and pHGSNAT+1A midigenes into C57BL/6 mice.. 88
Figure 31. Mean body mass (g) of each animal group at the beginning and at the end of the sustained expression experiment. 93
Figure 32. Relative mass (g/g^{-1}) of liver from the animals of different groups for the sustained expression experiment. 94
Figure 33. Agarose gel electrophoresis of h*HGSNAT* amplification following the injection of a) AAV2/9_HGSNATwt and b) AAV2/9_HGSNAT+1A into FVB/N mice; c) result from animal number 11 after a second amplification. 96
Figure 34. Agarose gel electrophoresis of *HGSNAT* amplification following the injection of AAV2/9_HGSNAT+1A into animal 12 (group 3) and corresponding sanger sequencing result, showing the skipping of exon 2. 97
Figura 35. Agarose gel electrophoresis of *HGSNAT* amplification following the injection of AAV2/9_HGSNAT+1A plus AAV2/9_U1snRNATC into FVB/N mice (group 7). 97
Figure 36. Agarose gel electrophoresis of *HGSNAT* following PCR re-amplification of the purified fragments from animals numbers 32 to 35. 98

Figure 37. Electropherogram of segments of the h*HGSNAT* transcript sequence obtained after injection of the AAV2/9_HGSNAT+1A plus AAV2/9_U1snRNATC (group 7) in FVB/N mice..... 98
Figura 38. Schematic representation of the biosynthetic pathway of Glycosaminoglycans (GAGs): heparan sulfate (HS), chondroitin sulfate (CS) and dermatan sulfate (DS).. 101
Figure 39. *XYLT1* mRNA relative expression in patient-derived MPS III fibroblasts.. 104
Figure 40. Agarose gel electrophoresis of *XYLT1* amplification fragments following transfection of MPS IIIA with different SSOs, for 24 and 48 hours..... 107
Figure 41. Agarose gel electrophoresis of *XYLT1* fragment amplification..... 108
Figura 42. Electropherogram of a portion of the *XYLT1* transcript sequence obtained after transfection with SSO3 and SSO5 showing the skipping of exons 9 and 11, respectively..... 109
Figure 43. Agarose gel electrophoresis of *XYLT1* fragments amplification..... 110
Figure 44. Quantification of Xylosiltransferase I (XT-I) protein in MPS III patient-derived fibroblasts after treatment with selected SSOs..... 112
Figure 45. Quantification of Heparan Sulfate (HS) in MPS III patient-derived fibroblasts after treatment with selected SSOs..... 113
Figure 46. *XYLT1* mRNA relative expression in MPS III patient-derived fibroblasts after treatment with the five gapmer ASOs..... 116
Figure 47. Quantification of Xylosyltransferase I (XT-I) in MPS III patient-derived fibroblasts after treatment with selected gapmer ASOs..... 118
Figure 48. Quantification of Heparan Sulfate (HS) in MPS III patient-derived fibroblasts after treatment with selected gapmer ASOs..... 119
Figure 49. *XYLT1* mRNA relative expression in MPS IIIC patient-derived fibroblasts.. 121
Figure 50. Quantification of Xylosyltransferase I (XT-I) in MPS IIIC patient-derived fibroblasts. 122
Figure 51. Quantification of heparan sulfate (HS) in MPS IIIC patient-derived fibroblasts 6 days post-transfection with selected gapmers..... 123
Figure 52. Quantification of heparan sulfate (HS) in MPS IIIC patient-derived fibroblasts 10 days post-transfection with selected gapmers..... 124

Abbreviations

2'-F	2'-fluor
2'-MOE	2'-O-methoxyethyl
2'-OMe	2'-O-methyl
AAV	adeno-associated virus
ALB	albumin
AGO2	argonaute 2
ApoE	apolipoprotein E
ASO	antisense oligonucleotide
BBB	blood-brain barrier
BSA	bovine serum albumin
cDNA	complementary DNA
CNS	central nervous system
CS	chondroitin sulfate
CSF	cerebrospinal fluid
CT	control samples
DBSD	Desbuquois skeletal dysplasia
DGAV	Direção-Geral de Alimentação e Veterinária
DMD	Duchenne muscular dystrophy
DMEM	dulbecco's modified eagle medium
DS	dermatan sulfate
EMA	European Medicines Agency
ERT	enzyme replacement therapy
ESE	exonic splicing enhancers
ESS	exonic splicing silencers
ExSpeU1	exon-specific U1 snRNA
FBS	fetal bovine serum
FELASA	Federation of European Laboratory Animal Science Associations
GAG	glycosaminoglycan
GalNAc	N-acetylgalactosamine-conjugate
gSRT	genetic substrate reduction therapy
HA	hyaluronic acid
HDFa	Human Dermal Fibroblasts, adult
HGMD	human gene mutation database
hnRNP	heterogeneous nuclear ribonucleoprotein

HS	heparan sulfate
HSCT	hematopoietic stem cell transplantation
hTTR	hereditary transthyretin amyloidosis
ICV	intracerebroventricular
IP	intraperitoneal
iPSC	induced pluripotent stem cell
ISE	intronic splicing enhancers
ISS	intronic splicing silencers
IT	intrathecal
IV	intravenous
IVT	intravitreal
KS	keratan sulfate
LC-MS/MS	liquid chromatography-tandem mass spectrometry
LIMP-2	lysosomal integral membrane protein-2
LNA	locked nucleic acid
LNP	lipid nanoparticle
LP2000	Lipofectamine™ 2000
LSD	Lysosomal storage disorder
M6PR	mannose 6-phosphate receptor
MP-6	mannose 6-phosphate
MPS	mucopolysaccharidosis
MPS III	mucopolysaccharidoses type III
mRNA	messenger RNA
MSC	multipotent stem cell
NCL	neuronal ceroid lipofuscinosis
NGS	next generation sequencing
NMD	nonsense-mediated mRNA decay
NT	non-transfected
ORF	open reading frame
OSWG	Oligonucleotide Safety Working Group
PD	pharmacodynamics
Pen-Strep	penicilin/streptomycin
PK	pharmacokinetics
PMO	phosphorodiamidate morpholino oligomer
PNA	peptide-nucleic acid
PO	phosphodiester

pre-mRNA	precursor messenger RNA
PS	phosphorothioate
PTC	premature termination codon
Py	polypyrimidine tract
qRT-PCR	quantitative real-time PCR
RISC	RNA-induced silencing complex
RNAi	RNA interference
RT	room-temperature
RT-PCR	Reverse transcription-polymerase chain reaction
SCA	Spinocerebellar ataxia
SDS-PAGE	sodium dodecyl sulfate – polyacrylamide gel electrophoresis
SF1	splicing factor 1
siRNA	small interfering RNA
Sm	Smith antigen
SMA	Spinal muscular atrophy
SNALP	stable nucleic acid lipid particle
SNAP	soluble NSF attachment protein
SNARE	soluble NSF attachment receptor
snRNP	small nuclear ribonucleoprotein
SR	serine/arginine-rich
SRT	substrate reduction therapy
ss	splice site
SSO	splice-switching oligonucleotide
TTR	transthyretin
U1 snRNA	U1 small nuclear RNA
U2AF	U2 auxiliary factor
US FDA	United States Food and Drug Administration
VUS	variants of unknown significance
WB	western blot
WPRE	Woodchuck hepatitis virus post-transcriptional regulatory element
wt	wild-type
XT-I	xylosyltransferase I
XT-II	xylosyltransferase II

Introduction

The work developed under the scope of this thesis is, in its essence, a proof of principle of the incredible potential of RNA-based drugs in treating or at least slowing down the relentless progression of a currently untreatable group of neuropathic lysosomal storage diseases. Still, the design of an effective therapeutic approach requires not only well-defined assays to assess its efficacy but also a solid scientific rationale. A precise understanding of the target disease, its molecular and biochemical basis, as well as the pathophysiological mechanisms that trigger its associated symptomatology, enables the optimal design, of both the therapeutic approach and the experimental setup to test it.

In that sense, this introduction is organized to first present the conceptual framework of our target diseases, providing a state of the art overview on the broader group of disorders they belong to, and summarizing their peculiarities. Only then will we move on to present the basics on RNA therapeutics, mostly focusing on the particular types of molecules that were used under the scope of this work. Finally, we conclude the chapter with a brief overview on the very few studies that have already attempted using this kind of technology in our particular field of interest.

1. Where it all begins - the Lysosome: a mini organelle with a major role

Lysosomes are membrane-bound organelles with such a prominent role in intracellular degradation that granted them a reputation as 'the garbage disposal system of the cell' [1]. With an acidic lumen filled with over 70 soluble lysosomal enzymes including proteases, lipases, glycosidases, nucleases, phosphatases and sulfatases, lysosomes are responsible for the degradation, processing and recycling of virtually all kinds of macromolecules. Nowadays, it is also known that the lysosome plays a crucial role in controlling anabolic activities. Indeed, it functions as a nutrition sensor and regulates vesicle trafficking, cellular development, and signal transduction (Figure 1) [2,3].

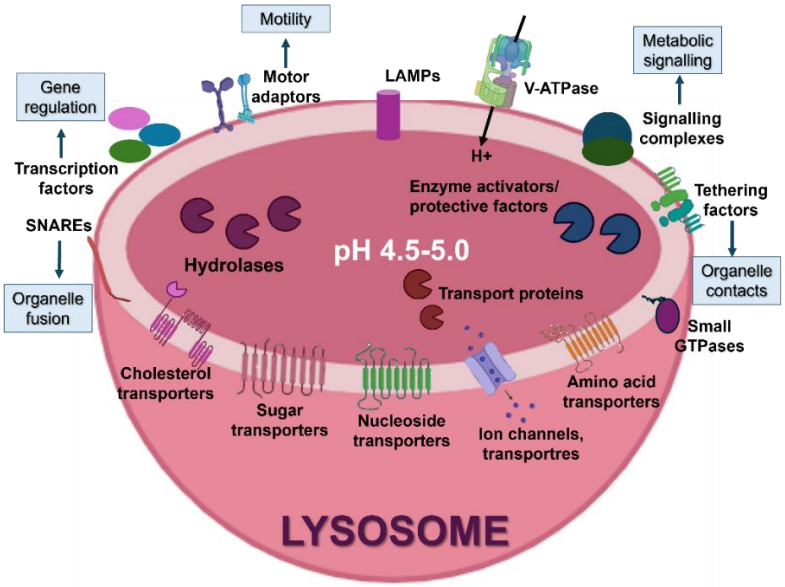


Figure 1. Schematic representation of lysosomal components and properties. Lysosomes contain luminal, membrane-bound, and peripheral proteins. Inside, acid hydrolases break down substrates with the help of activators and protective factors. Transport proteins like NPC intracellular transporter 2 (NPC2) shuttle cholesterol to NPC intracellular transporter 1 (NPC1) for export. The lysosome's acidic environment is sustained by the vacuolar ATP-ase (v-ATPase) located in the membrane. Lysosomal membranes feature glycosylated lysosomal-associated membrane protein (LAMPs) for protection, ion channels, transporters, and solute carriers that export degradation products. SNAP receptors (SNARE) proteins enable lysosomal fusion with organelles. The outer lysosomal surface acts as a hub for protein complexes, including mammalian target of rapamycin complex 1 (mTORC1), transcription factors EB (TFEB/TFE3), and motor adaptors, coordinating nutrient sensing, lysosomal biogenesis, autophagy, and organelle interaction (based on [3]).

All lysosomal enzymes are synthesized in the endoplasmic reticulum, after which they are transported to the Golgi apparatus, where undergo further modifications before

following defined endocytic pathways to the lysosome. In most cases, this process involves the addition of a mannose 6-phosphate (MP-6) tag to the mannose residues of the oligosaccharide chains attached to lysosomal enzymes, allowing them to enter the lysosome via the MP-6 receptors (M6PR). However, certain enzymes reach the destination through alternative trafficking routes, such as β-glucocerebrosidase, which enters the lysosome via the lysosomal integral membrane protein-2 (LIMP-2) [4]. Once inside that organelle enzymes are capable of breaking down various classes of macromolecules, through degradation routes that are essential for diverse cellular processes and ultimately for the cell's homeostasis. Thus, whenever a deficiency of lysosomal enzymes or components of the lysosomal transport machinery occurs, the homeostatic state is disrupted, leading to a series of rare genetic disorders, the so-called Lysosomal storage disorders (LSDs). In addition to deficient enzymatic activity or transport, these diseases can also arise from dysfunctions in lysosomal membrane proteins such as nutrient transporters or ion channels, or even from defects in non-lysosomal proteins.

2. What if it fails - the Lysosomal storage disorders

LSDs are a group of about 70 hereditary monogenic diseases of lysosomal catabolism. While the majority of them are inherited in an autosomal recessive manner, there are three X-linked recessive: Mucopolysaccharidosis (MPS) type II, Fabry disease, and Danon disease.

These disorders have a combined incidence around 1:7700, but according to several authors, this figure may be as high as 1:3000 or even 1:1500 births [5]. LSDs occur due to mutations in genes that code for proteins involved in lysosomal function. Mutations that impair protein functionality result in lysosomal malfunction due to the gradual storage of the undegraded or partially degraded substrates inside the organelle, ultimately leading to cellular dysfunction and death. While in the past, these diseases were classified based on the nature of the accumulated substrate(s), for instance Sphingolipidoses or Mucopolysaccharidoses, recent classifications also focus on their underlying molecular defects [6]. These newer classifications include groups of disorders due to defects in non-enzymatic lysosomal proteins, such as integral membrane protein disorders and post-translational modification defects [7,8] (Figure 2). Also typically classified as LSDs are the Neuronal ceroid lipofuscinoses (NCLs). These atypical lysosomal disorders exhibit distinct characteristics, as the accumulating material in NCLs

is not a disease-specific substrate but the subunit c of mitochondrial ATP synthase or sphingolipid activator proteins A and D (Figure 2). There are many LSDs which are commonly named after the physicians who first described them (e.g. Fabry, Gaucher…)

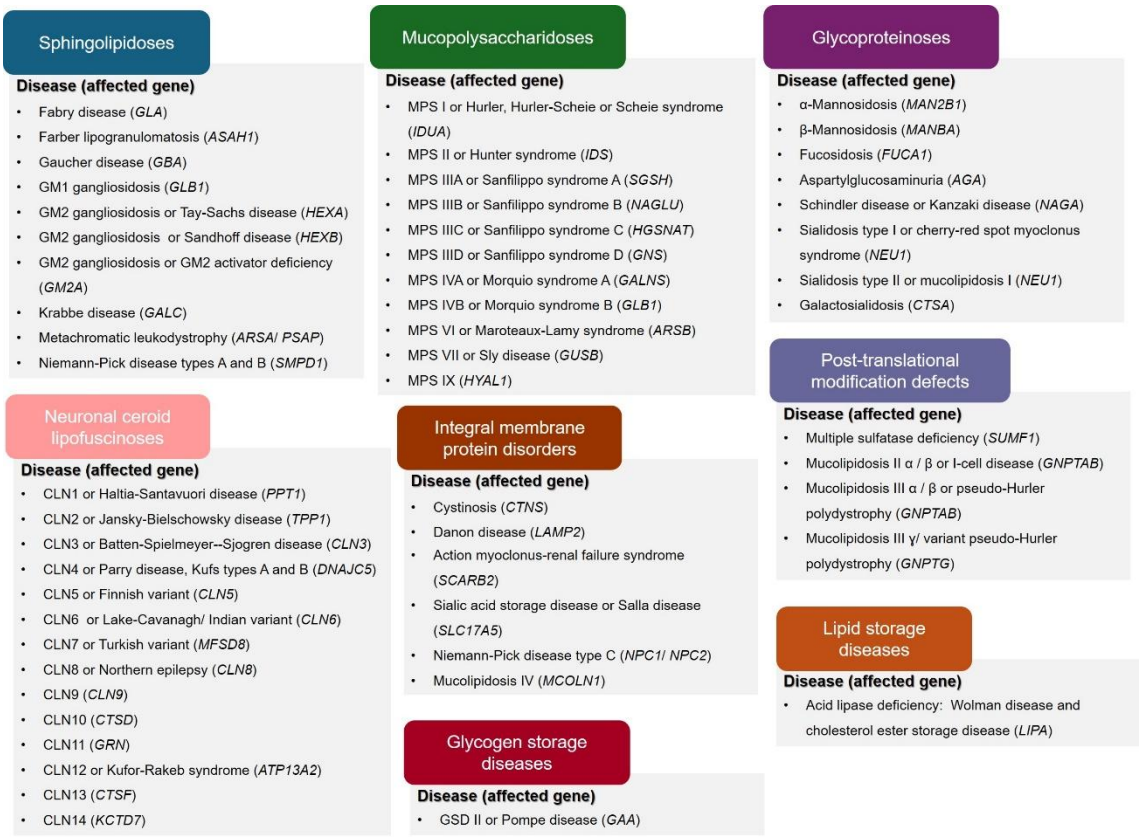


Figure 2. Summary of Lysosomal Storage Disorders (LSDs). These diseases are classified based on the type of accumulated material, such as Sphingolipidoses, Mucopolysaccharidoses, Glycoproteinoses, and Lipid storage diseases. They can also be categorized by defects in integral membrane proteins, post-translational modifications, or lipofuscin metabolism. The gene involved in each disorder is indicated in parentheses (based on [7]).

LSDs are often presented as pediatric neurodegenerative diseases, particularly in the most severe cases. However, as they are heterogeneous disorders, depending on the gene defect and on the biochemical nature of the stored substrates, LSDs can cause a variety of symptoms that can go from skeletal dysmorphia, due to bone pathology to central nervous system (CNS) defects, in addition to symptoms affecting many other organs.

Diagnosis is usually based on the clinical symptoms of the patients, followed by the confirmation of increased storage of particular substrate(s) and the identification of the genetic variants. In most cases, defective or absent enzyme/protein function is also confirmed. This diagnostic workflow usually depends on several tests, such as enzymatic analysis and gene sequencing. Traditionally, molecular genetic testing was performed

by Sanger sequencing to examine the gene associated with the particular substrate accumulation, or encoding the relevant enzyme. More recently, though, the diagnosis using next generation sequencing (NGS) became routine, greatly reducing the time from the onset of patient symptoms and the diagnosis of the disease [9,10].

Based on the type of disorder and the age of diagnosis, LSDs may be classified as congenital or infantile, late-infantile, juvenile and adult types. Usually, the earlier the symptoms appear, the most severe is the disease presentation.

All established therapeutic approaches for LSDs to date are based on the lysosome's physiology, which points to various targets or methods. The first, and perhaps most well-known, is enzyme replacement therapy (ERT), which consist on the regular intravenous (IV) administration of the defective enzyme produced through recombinant DNA technology. These recombinant proteins carry M6P residues on their oligosaccharide chains, facilitating their attachment to M6PR on the cell surface. This interaction allows them to enter the cell, and be directed to the lysosomes, where they break down the accumulated substrates. Another well-known approach, whose rationale was also proposed in the early days of LSD research, is substrate reduction therapy (SRT) that uses small-molecule drugs to inhibit the enzymes that synthesize the storage substances instead of supplying the missing enzyme, thereby reducing the burden on lysosomes. Hematopoietic stem cell transplantation (HSCT) is yet another option, consisting in the transplantation of healthy matched donor cells into the patient, from which the enzyme is then continuously secreted. Pharmacological chaperones are also a treatment alternative that encompass the use of competitive inhibitors at sub-inhibitory concentrations to stabilize the mutant enzyme, thereby extending half-life and improving catalysis. Finally, *ex vivo* gene therapy, involves administering a functional enzyme through the autologous transplant of hematopoietic stem cells, where the genetic defect was corrected *in vitro*, often by genome editing. *In vivo* gene therapy, in other hand, involves the direct injection of non-replicating non-hazardous viral vectors encoding the gene of interest directly into transduced cells, leading to the production of the desired functional enzyme. Both are emerging therapeutic options that are currently under development for some of these diseases (reviewed in [11], Figure 3).

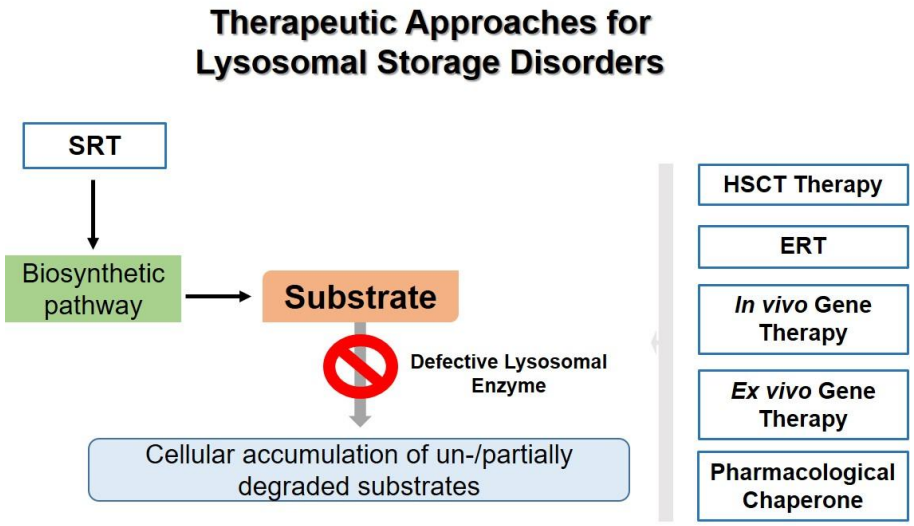


Figure 3. Therapeutic strategies for Lysosomal storage disorders (LSDs). These approaches can act upstream, by inhibiting the synthesis of a gene, or downstream, giving the missing enzyme or inducing its production. SRT- substrate reduction therapy; HSCT – hematopoietic stem cell transplantation; ERT – enzyme replacement therapy.

To date treatments are only available for 14 LSDs. Most of these disorders are only managed symptomatically with supportive care [12]. Amongst the various reasons that underlie the difficulty of developing new and more effective therapies is the inability of currently available options to mitigate the neurological symptoms [8].

This issue is particularly relevant taking into account that more than two-thirds of LSD patients present with neuropathology whose signs often arise at an early age, frequently leading to severe clinical manifestations and premature death [12,13]. Most importantly, even when therapies are available, particularly ERTs, they are only effective in somatic tissues due to their failure to cross the blood–brain barrier (BBB). This leaves untreated the neurological deficits, which are among the most debilitating manifestations of many LSDs. It adds that currently available data suggest that once neurological damage has occurred, it is extremely difficult to revert the phenotype [12].

That is why the development of therapeutic strategies to delay or prevent neurological manifestations in LSD patients represents a major challenge in LSDs' research. Small-molecule drugs are being designed to cross the BBB, even though none can yet reliably reach the brain. A hold promise is gene therapy that directly targets the CNS. It is emerging as an approach potentially more effective to overcome the limitations of the existing treatments, since it is aimed to achieve high concentrations of the therapeutic enzyme in various tissues. It is being accomplished either by transplanting gene-modified hematopoietic stem progenitor cells (*ex vivo*) or by directly administering a viral vector to deliver the therapeutic gene (*in vivo*) [12,14].

2.1. What's sweet becomes sour – the Mucopolysaccharidoses

Amongst the LSDs in which neurological symptoms are very serious are the Mucopolysaccharidoses (MPSs), one of the major LSD groups, accounting for approximately 30% of the cases worldwide [15]. Eight major diseases are currently known: MPSI, II, III, IV, VI, VII, IX and X that result from mutations in genes that code for one of 12 enzymes involved in the degradation of glycosaminoglycans (GAGs). Each enzymatic deficiency underlies one particular MPS (Table 1). For instance, four different enzyme deficiencies trigger an equivalent number of MPS III disorders, all resulting from either deficient or absent degradation of heparan sulfate (HS) [16].

GAGs are linear polysaccharides composed of repeating disaccharide units consisting of hexamine and uronic acid. The five types of GAGs described - HS, dermatan sulfate (DS), chondroitin sulfate (CS), keratan sulfate (KS) and hyaluronic acid (HA) - are present in all human tissues.

When these lysosomal enzymes fail to fulfil their function, those compounds accumulate inside the lysosomes and consequently in cells and tissues, causing progressive damage and a variety of multi-organ clinical manifestations, including cardiovascular disease, respiratory problems, skeletal abnormalities and premature death, with the spectrum and severity of these manifestations varying between and within MPS types [17,18]. Additionally, these compounds can accumulate outside the lysosomes, triggering inflammatory pathways and an innate immune response via the Tool-like receptor 4 and the complement system. Indeed, there is a number of relevant clinical aspects like neuroinflammation, short bones and aortic fragmentation which can arise due to an exacerbated inflammatory response [17].

In general, MPSs are heterogeneous and multisystemic diseases, with manifestations that vary not only between subtypes but also among individuals within the same subtype. These variations significantly impact the patients' quality of life and lifespan. Clinically, MPS patients can be categorized into three groups based on the predominant characteristics of their disease: "visceral phenotype", "neurodegenerative phenotype" and "skeletal phenotype". In general, MPS types I, II, VI and VII present coarse facies, visceromegaly (hepatosplenomegaly), hernias, upper airway obstruction, joint stiffness, heart disease and other skeletal deformities. These main manifestations induce to classify these subtypes within the "visceral phenotype". Short stature is also present in patients with MPS I, II and VII. Additionally, corneal clouding is very frequent in all of these subtypes, except for type II where hearing loss is a prominent symptom, but not associated to ocular symptoms. MPS III patients belong to the "neurodegenerative phenotype" group. In this group, the clinical manifestations typical of

the other MPS subtypes are relatively mild, but there is a marked neurodegeneration, which usually starts between 3 and 5 years of age, often accompanied by behavioral disturbances and hyperactivity. Finally, the “skeletal phenotype” is characteristic of MPS IV patients, who show skeletal dysplasia and many bone abnormalities. These patients are mentally normal but exhibit a short stature. MPS IX, however, is usually not included in these three major groups because its distinctive clinical finding is the presence of joint swellings and synovial masses [17], which is not shared by any other MPS. All MPS diseases are monogenic and transmitted in an autosomal recessive way, except for MPS II that is X-linked. In general, nonsense and frameshift mutations are associated with more severe disease phenotypes, while missense mutations are usually associated to more attenuated forms. Splicing mutations on the other hand, are generally associated with severe forms, but whenever they simultaneously allow for the production of the normal transcript, even in small amounts, a milder phenotype may still present. Despite being a rather high genotype-phenotype correlation that helps to predict the phenotype knowing the mutation at stake, it has to be considered with caution because sometimes it may fail. This knowledge is particularly important for MPS I patients, as the choice of treatment depends on the severity of the disease. If predicting the phenotype on an individual basis is always problematic, it is particularly difficult in the presence of the so-called variants of unknown significance (VUS). That is why it is important to study the impact of each mutation at complementary DNA (cDNA) and protein levels through functional studies, as well as to develop new biomarkers for the assessment and follow-up of both treated and untreated patients [19,20].

Overall, the therapeutic options available for MPS diseases overlap those already described for LSDs in general. Still, they are largely insufficient as of the 12 different subtypes of MPSs only five have approved therapeutic approaches (Table 1).

Currently, ERT and HSCT are the unique approved options for MPS treatment, depending on the subtype and disease severity. As for all treatable LSDs, the earlier the treatment is initiated, the better are its outcomes, and in addition not all available options may be considered depending on the age at diagnosis

Table 1. Classification and molecular basis of MPS [1].

MPS type		Common name(s)	Gene (localization)		Enzyme (type)	Accumulated GAG(s)	Treatment options available
I		Hurler OMIM #607014 / Hurler-Scheie OMIM #607015 / Scheie OMIM #607016	*IDUA* 4p16.3		α-L-iduronidase EC 3.2.1.76 (lysosomal hydrolase)	Dermatan and heparan sulfate	ERT: laronidase (Aldurazyme®) HSCT
II		Hunter Syndrome OMIM #309900	*IDS* Xq28		iduronate-2-sulfatase EC 3.1.6.13 (lysosomal hydrolase)	Dermatan and heparan sulfate	ERT: idursulfase (Elaprase®) HSCT
III	A	Sanfilippo syndrome A OMIM #252900	*SGSH* 17q25.3		*N*-sulphoglucosamine sulphohydrolase EC:3.10.1.1 (lysosomal hydrolase)	Heparan sulfate	-
	B	Sanfilippo syndrome B OMIM #252920	*NAGLU* 17q21		α-N-acetylglucosaminidase EC:3.2.1.50 (lysosomal hydrolase)	Heparan sulfate	
	C	Sanfilippo syndrome C OMIM #252930	*HGSNAT* 8p11.1		HS acetyl-CoA:α-glucosaminide N-acetyltransferase EC:2.3.1.78 (transmembrane hydrolase)	Heparan sulfate	

[1] For an extensive review on each MPS subtype, see Annex 1, review paper 1: Santos JI, Gonçalves M, Matos L, Moreira L, Carvalho S, Prata MJ, Coutinho MF, Alves S. Splicing Modulation as a Promising Therapeutic Strategy for Lysosomal Storage Disorders: The Mucopolysaccharidoses Example. *Life*. 2022 (authored by the PhD candidate).

	D	Sanfilippo syndrome D OMIM #252940	*GNS* 12q14	glucosamine (N-acetyl)-6-sulfatase EC: 3.1.6.14 (lysosomal hydrolase)	Heparan sulfate	
IVA	A	Morquio A OMIM #253000	*GALNS* 16q24.3	N-acetylgalactosamine-6-sulphatase EC 3.1.6.4 (lysosomal hydrolase)	Keratan and chondroitin sulfate	ERT: elosulfase alfa (Vimizim®) HSCT
	B	Morquio B OMIM #253010	*GLB1* 3p21.33	β-galactosidase EC 3.2.1.23 (lysosomal hydrolase)	Keratan and chondroitin sulfate	-
VI		Maroteaux-Lamy syndrome OMIM #253200	*ARSB* 5q11-q13	arylsulfatase B (N-acetylgalactosamine-4-sulfatase) EC 3.1.6.12 (lysosomal hydrolase)	Dermatan sulfate	ERT: galsulfase (Naglazyme®)
VII		Sly syndrome OMIM #253220	*GUSB* 7q21.11	β-D-glucuronidase enzyme EC 3.2.1.31 (lysosomal hydrolase)	Dermatan, keratan and chondroitin sulfate	ERT: vestronidase alfa (Mepsevii™)
IX		Hyaluronidase deficiency OMIM # 601492	*HYAL* 3p21.3	hyaluronidase EC 3.2.1.35 (lysosomal hydrolase)	Hyaluronan	-
X		Arylsulfatase K deficiency OMIM #619698	*ARSK* 5q15	arylsulfatase K EC: 3.1.6.1 (lysosomal hydrolase)	Dermatan sulfate	-

The first trial using a recombinant enzyme to treat MPS was performed in 1997, with MPS I patients, resulting in improvements in mobility, increases in linear growth velocity, reductions in liver volume and in urine GAGs. With the first approval in 2003, since then this type of therapy became available for other MPS subtypes [21]. To be effective, recombinant enzymes must reach the affected tissues, by quickly binding to the M6PR for cellular uptake. The rate of penetrance is higher in organs like liver, spleen and kidney than in bone, cartilage and ocular tissues. A major handicap is that these enzymes are unable to cross the BBB and so to penetrate the CNS, making ERT an ineffective treatment for neurological manifestations, such as those observed in MPS III. In addition, ERT can cause immune reactions in some patients, requiring pre-medications and/or adjustments to the treatment protocol. This therapy also requires lifelong injections, accounting so to its very high costs [14].

HSCT, on the other hand, was first performed in a patient with MPS I in 1981, and since then, more than two hundred patients with MPS have received this treatment with positive impacts on neurocognition (reviewed in [22]). MPS II also began to be elected to HSCT, with at least one hundred patients with severe form having been successfully transplanted, showing clear improvements in biochemical disease markers and somatic symptoms [23]. The application of HSCT for treating other MPS types is considerably less widespread compared to its use in Hurler syndrome.

It is again worth mentioning that the currently approved drugs fail to address CNS lesions, thus not preventing the neuropathological progression of the disorders and resultant neuropsychiatric manifestations. This is a universal hurdle faced not only by MPSs but by virtually every LSD, which justifies the significant efforts that are being done to develop therapies with improved penetration for high-risk tissues, in particular the skeletal and CNS (reviewed in [22]). Among the emerging therapies, gene therapy stands out as a promising approach because it could permanently replace the deficient enzymes. However, one of the major problems is delivery, that in most cases is performed using therapeutic viruses, like adeno-associated virus (AAV), to penetrate the bloodstream or directly the CNS [14,24]. Theoretically, systemic delivery offers lasting improvement in neurological symptoms. Since that is not always achieved, administration of recombinant AAV into the intracerebral space is being extensively studied and trialed for several MPS (reviewed in [25,26]).

Chaperone therapy is another approach under development. Pharmacological chaperones are low-molecular weight compounds mainly used to increase the enzyme activity of a mutated protein. Chaperones have been studied for almost 25 years as a treatment for Gaucher [27,28] and Fabry diseases [29,30] with some molecules being

already in clinical use for both LSDs, particularly for Fabry disease, and according to several studies they may also constitute an option for MPS [31].

SRT, which aims to reduce the bioavailability of the compounds that accumulate in each specific disorder, is also under scrutiny. Small molecules are used to inhibit specific enzymes, balancing synthesis and catabolism rates, and thereby reducing substrate buildup, mitigating cellular damage [32,33]. This approach was first proposed by Norman Radin in 1996 [34]. Theoretically, SRT holds potential to treat neurological forms of LSDs, due to the size and charge of the molecules used that theoretically prone them to cross the BBB. In addition to the potential to treat neurological forms of LSD, STR has the advantage of be a non-invasive treatment option, because SRT drugs have non-immunogenic properties and can be administered orally [35]. To date, however, no effective SRT drugs for MPSs are available [36-38].

2.1.1. Focus on Mucopolysaccharidoses type III (MPS III)

Amongst the broader MPS group, there is one particular subgroup that stands out from all the other types due to its predominant CNS involvement: the so-called MPS III, or Sanfilippo syndrome [13,39]. Indeed, unlike other MPS disorders, which are consensually classified as multisystemic, MPS III is often simply described as a neurodegenerative pediatric disease or, more extremely, as a genetic form of childhood dementia. This does not mean that MPS III patients do not suffer from somatic symptoms, but only that their symptoms are quite mild when compared to the severe and relentless neurological manifestations. The main compound accumulated in MPS III is HS, a GAG whose proper spatiotemporal expression is particularly relevant during early embryogenesis and brain development by mediating cell signaling, migration, and differentiation [40,41]. MPS III can be classified into four subtypes based on the mutated gene and the associated enzyme deficiency: MPS IIIA (OMIM #252900), caused by pathogenic variants in the *SGSH* gene, which encodes *N*-sulphoglucosamine sulphohydrolase (EC:3.10.1.1); MPS IIIB (OMIM #252920), caused by variants in *NAGLU*, which encodes α-N-acetylglucosaminidase (EC:3.2.1.50); MPS IIIC (OMIM #252930) caused by pathogenic variants in the *HGSNAT* gene, encoding heparan-α-glucosaminide N-acetyltransferase (EC:2.3.1.78); and MPS IIID (OMIM #252940), associated with pathogenic variants in the *GNS* gene, leading to a defective or absent glucosamine (N-acetyl)-6-sulfatase (EC: 3.1.6.14). To date, numerous mutations have been identified in each of the 4 genes (197 in *SGSH*, 302 in *NAGLU*, 142 in *HGSNAT* and 34 in *GNS* genes, https://my.qiagendigitalinsights.com/, HGMD Professional 2024.4, accessed on 30 December 2024), and a few robust genotype-phenotype correlations

have been established. Clinically, somatic symptoms are generally mild, although some typical LSD-related features, such as hepatosplenomegaly may occasionally be present. Still, those features are not usually detected during routine clinical assessment.

Recently, a fifth MPS III subtype, referred to as MPS IIIE, has also been proposed [42-46] but still there is an ongoing debate on whether MPS IIIE is a novel human disease or a diagnostic pitfall [47]. Indeed, while there is now plenty of evidence that the genetic knockout of arylsulfatase G in animals (specifically, in dogs and mice) results in biochemical and behavioral abnormalities consistent with MPS III [48], the human phenotype associated with a similar deficiency seems quite different from that of MPS III disease, with no behavioral, cognitive or memory symptoms reported [49,50].

From the strictly therapeutic point of view, MPS III diseases are the most challenging MPS of them all. Thanks to their almost exclusive neurological involvement, standard ERT approaches do not constitute a treatment scenario, since those large molecules are unable to cross the BBB. Although intrathecal (IT) and intracerebroventricular (ICV) administrations could offer a potential route for enzyme delivery, they were long considered very invasive and risky strategies, making them difficult to implement until now. Despite these difficulties, efforts continue to be done in order to develop suitable ERT treatments for MPS III. [51-53].

Still, research efforts to treat MPS III go far beyond ERT. Indeed, a number of therapies are being developed and evaluated in parallel by different consortia worldwide, including HSCT, SRT, anti-inflammatory therapies and gene therapy [39,54]. Some phase I and phase II trials were already successfully completed [55-57], others are still ongoing, but there is still a long way to go in order to evaluate whether any of these approaches can reach the clinic [58].

Of particular interest for this work are previous studies addressing the feasibility of SRT. To the best of our knowledge, two chemical compounds were already tested for MPS III: rhodamine B and genistein. Still, none of them reached the clinic. The first assessment dates back to 1991, when Kaji *et al.* reported that rhodamine B decreases the GAG content of human lip fibroblasts through a functional suppression of polysaccharide chain formation in the process of the GAG production [59]. Since then, various works addressed the potential of rhodamine B in the treatment of MPSs [60-63]. Preclinical studies using rhodamine B in a MPS I mouse model yielded promising results regarding skeletal manifestations [64], However, no clinical trials were later conducted, likely due to reported toxicity and the unknown mechanism through which it inhibited GAG synthesis [65].

Concerning genistein, an open-label study demonstrated the safety of high-dose drug in MPS patients with neurological impairments [66], but a subsequent phase III trial failed to show significant clinical efficacy, including reductions in cerebrospinal fluid (CSF) HS levels or cognitive improvements, with only a modest decrease in urinary GAGs [67].

Thus, MPS III management remains mostly palliative, focusing on addressing behavior issues (aggressiveness, hyperactivity) and sleep disturbances. Overall, the need for additional therapies for MPSs is evident, especially for the neuronopathic subtypes that unfortunately can only benefit from supportive care nowadays. Emerging interventions that hold potential to treat the disease in a personalized way, or at least with high specificity while being easy to test pre-clinically, are attracting much attention. Amongst them, RNA-based therapeutics stands out as one of the most cutting-edge today.

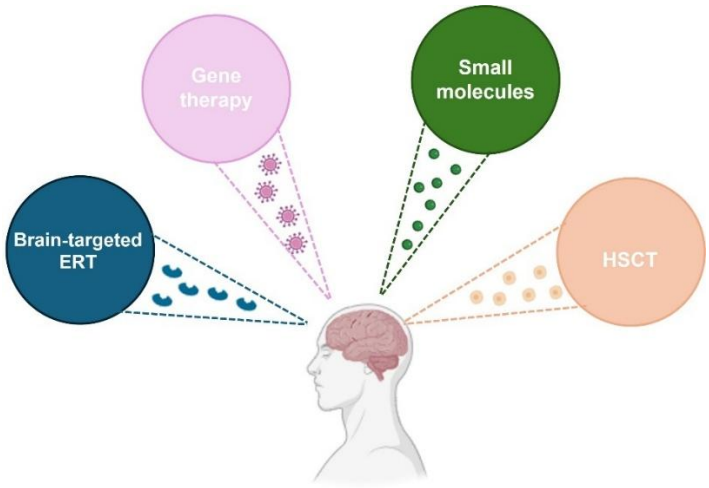


Figure 4. Major therapeutic approaches currently under evaluation to target the CNS disease in Mucopolysaccharidoses. ERT: enzyme replacement therapy; HSCT: hematopoietic stem cell transplantation (based on [68]). Created with BioRender.com.

3. RNA-based therapeutics[2]

RNA was first described as a key player in the flow of genetic information by Crick, in 1958, as a part of the “Central Dogma of Molecular Biology”. Shortly later, the discovery of messenger RNA (mRNA) in 1961, highlighted the role of RNA molecules as key messengers in the translation of genetic information [69-71]. Since then, the study of RNA intensified extraordinarily in order to answering the many questions that were

[2] For an extensive overview on RNA-based therapies, see Annex 3, book chapter 2: Coutinho MF, Matos L, Santos JI, Alves S. RNA Therapeutics: How Far Have We Gone? *Adv Exp Med Biol*. 2019 (co-authored by the PhD candidate).

arising- from its structure, its relationship with DNA and genetic code, its role in protein synthesis to the diversity of RNA molecules and how they were involved in different biological processes (reviewed in [72]).

In 1978, Stephenson and Zamecnik described the first application of RNA base-pairing for therapeutic purposes: they designed an antisense oligonucleotide (ASO) targeting the 35S RNA sequence of the Rous sarcoma virus to inhibit viral replication [73]. Twenty years and many investigations later, the first antisense RNA drug was approved by the United States Food and Drug Administration (US FDA), for the treatment of cytomegalovirus retinitis [74]. Since then, numerous RNA drugs have received approval of the competent entities to treat an increasing range of diseases. This continuous growing on the understanding of RNA biology and chemistry has provided new tools that can be exploited in the development of RNA-based therapeutics (reviewed in [72]). In contrast to DNA-based therapies, which must pass across the cytoplasmic and nuclear membranes, carrying the risk of be integrated into the host genome, some RNA therapies need simply to reach the host cytoplasm, and those that do penetrate the nucleus have no potential for chromosomal integration [72]. Besides these two important advantages, RNA therapies have many other benefits including their capacity to target previously undruggable targets, fast production, long-lasting effects, and no risk of genotoxicity. Additionally, they are particularly useful for rare diseases, such as those addressed in this thesis (reviewed in [75]). Overall, RNA drugs are considered very strong candidates for the development of novel therapeutic strategies, making research on RNA-based therapeutics a rapidly expanding and highly promising field in current days.

RNA drugs may be categorized in different ways, depending on their targets, ultimate purpose, the mechanisms triggered, and there are even some authors who also consider the chemical modifications they harbor. A more comprehensive classification groups them into those that are translated into proteins [for example *in vitro* transcribed mRNA (IVT mRNA)], and those that are not and whose mechanisms of action depend upon interactions with precursor messenger RNAs (pre-mRNAs), mRNAs or proteins, to regulating target gene expression in the cell. This last category includes aptamers, antagomiRs and agomiRs, small-interfering RNAs (siRNAs) and ASOs, collectively known as oligonucleotide therapeutics [75-77], as well as other RNA targeting drugs, such as engineered U1 snRNAs [78]. Over the past decades, the number of studies and the plethora of applications involving these drugs, both in pre-clinical testing and clinical trials, has been growing exponentially, and reviewing all of them would far exceed the scope of this thesis. Thus, since the therapeutic approaches investigated in this work

relied on the use of ASOs, siRNAs (both classified as oligonucleotide-based therapies) and engineered U1 snRNAS, these will be the focus of the next sections.

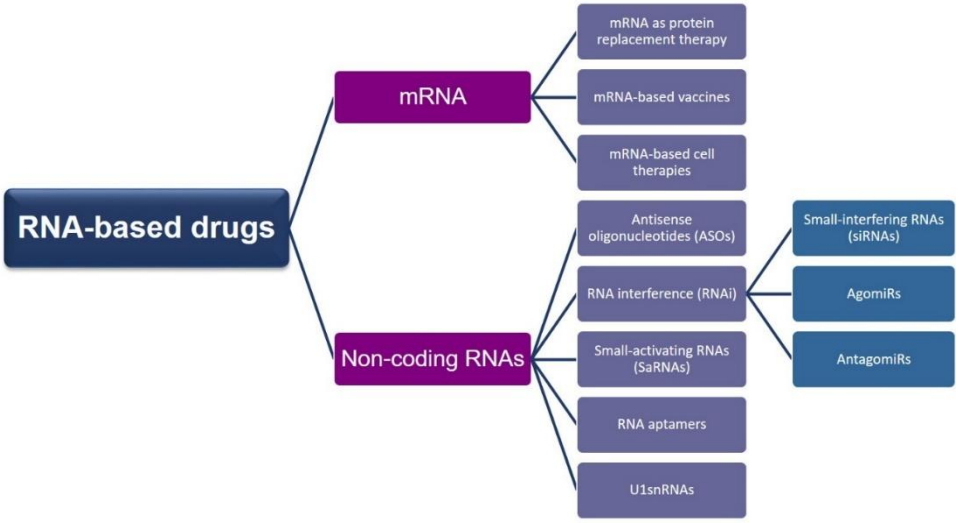


Figure 5. Classification of RNA drugs (based on [79,80]).

Generically, therapeutic oligonucleotides interact with a target RNA following the Watson-Crick base pairing. This interaction can influence different processes including mRNA degradation, pre-mRNA splicing and mRNA translation. Amongst the different mechanisms by which that might occur, the most used are: RNase H-dependent degradation of mRNA a specific type of ASOs, known as gapmers; correction of splicing defects using splice-switching oligonucleotides (SSOs) and engineered U1 snRNAs, and disruption of gene expression by siRNAs.

As mentioned earlier, the development of RNA-based drugs began in the late 1970s with a DNA ASO targeting viral RNA *in vitro*. However, the first regulatory approval was only achieved in 1998. Since then, these therapies have experienced remarkable growth, and by 2023, around 20 had been approved by regulatory bodies such as the FDA and EMA [81]. This progress was made possible through significant advancements in the field.

The first therapeutic oligonucleotides consisted of synthetic, unmodified DNA or RNA molecules. Despite the raised expectations, their clinical utility was limited by several challenges, including susceptibility to nuclease degradation, low affinity for target mRNA, off-target effects, difficulty crossing cell membranes due to their negative charge, and weak plasma protein binding, which led to rapid clearance by the kidneys. To address these problems, a wide range of chemically modified nucleotide analogues has

been developed, greatly enhancing their stability, specificity, and therapeutic potential [82].

Currently, the available therapeutic oligonucleotides and virtually all that are still under analysis have a number of chemical modifications in their phosphate backbone and sugar rings, all of which ultimately contribute to improve their action, by increasing their binding affinity, stability and pharmacodynamic properties. A widely used modification is the incorporation of phosphorothioate (PS) linkages, which enhances bioavailability, cellular uptake, and resistance to nucleases degradation. Likewise, another very frequent modification that enhances stability is the addition of a 2'-O-methyl (2'-OMe) group to the ribose sugar, replacing the 2'-OH group.

These two modifications were among the first to be implemented, and critically boosted advances in oligonucleotides therapies, by enhancing their efficiency particularly through improved affinity for target sequences. Furthermore, the ease of synthesis and somehow affordability have also triggered the researchers' attention. Nowadays, there are several clinical trials with oligonucleotides chemically modified either with PS or 2'-OMe (reviewed in [83,84]).

Other modifications to the ribose sugar that under use include 2'-O-methoxyethyl (2'-MOE), 2'-fluor (2'-F), and locked nucleic acid (LNA). Likewise, modifications to the phosphate backbone include phosphorodiamidate morpholino oligomers (PMOs) and peptide-nucleic acid (PNA).

Still, the primary challenge for expanding the use of RNA-based therapies to a broader range of disorders is the effective delivery to target tissues. The development of delivery technologies, such as conjugates or nanoparticles paired with appropriate administration methods, has progressed significantly, however, many conditions are still waiting for a breakthrough in delivery solutions [85].

In the following sections, we will provide a more detailed description of some RNA therapies. For the sake of simplicity, the RNA therapeutics were divided into two main groups: those that modulate splicing and those that are designed to promote gene knockdown. We will dissert on some already approved RNA-based drugs, while setting the grounds to introduce the two major strategies employed within the scope of this thesis.

3.1. RNA drugs acting upon splicing

3.1.1. A brief overview of the splicing process

To clarify how RNA-based drugs might be splicing modulators, a brief overview on the splicing process will be first presented. It is well known that the expression of

eukaryotic gene(s) requires a series of highly regulated sequential steps, in which non-coding introns are removed from the pre-mRNA while the exonic coding sequences are joined together. This occurs during the process of maturation of the mRNA, which can then be translated into protein. The process of splicing is carried out by a large and dynamic molecular complex called the spliceosome.

RNA splicing was initially discovered in the 1970s, overturning years of thought in the field of gene expression [86,87]. Its central effector, the spliceosome, functions in a cycle encompassing assembly and disassembly, in which five small nuclear ribonucleoprotein (snRNP) complexes (U1, U2, U4/U6 and U5) recognize and assemble each intron to ultimately form a catalytically active spliceosome. An early event in the exon definition is the recognition of the 5' donor splice site (ss) by the U1 snRNP, followed by the binding of splicing factor 1 (SF1) to the branch point and of the U2 auxiliary factor heterodimer (U2AF 65/35) to the polypyrimidine tract (Py) and 3'ss, originating the so-called E complex [88,89].

After that, SF1 is replaced by the U2 snRNP at the branch point, originating the A complex, which allows the interaction between U1 snRNP and U2 snRNP across the exon [88,90]. Then, the U4, U5 and U6 snRNPs are recruited as a preassembled complex, leading to the formation of the so-called B complex. Subsequently, the interaction between U4 and U6 is disrupted and the U6 snRNP base pairs with the 5'ss, displacing U1 snRNP from its initial location and releasing it from the complex, along with the U4 snRNP [91]. At the same time, U6 snRNP interacts extensively with U2 snRNP, bringing the 5'ss and the branch point into close proximity. This signalizes the beginning of the first step of splicing, which originates the C complex containing the free upstream exon and the intron-exon lariat intermediate [90]. This complex completes the second step of the splicing reaction, releasing the intron and joining the exons to form the mature mRNA. At the same time, U2, U5 and U6 snRNPs are also disassembled from the complex and recycled for future reactions ([90,92,93], reviewed in [94]; Figure 6).

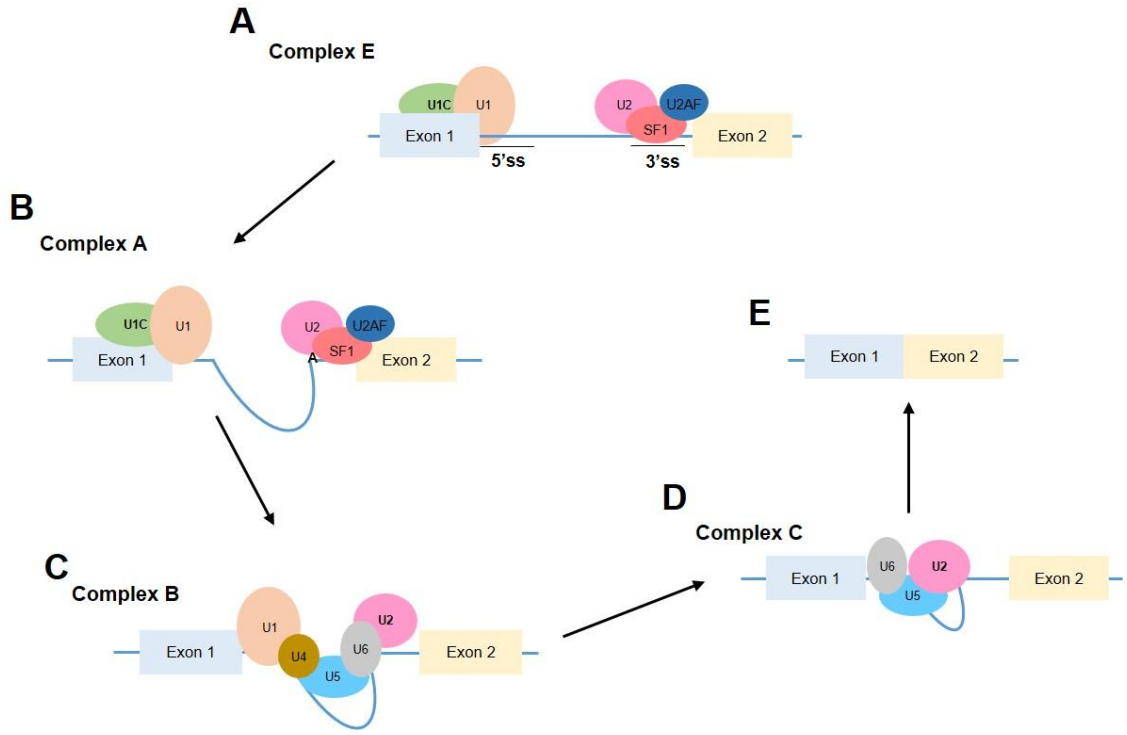


Figure 6. Schematic representation of the splicing process. (A) The formation of the spliceosome begins with U1 small nuclear ribonucleoprotein (snRNP) binding to the donor splice site (ss) and U2 snRNP attaching to the acceptor ss, resulting in the formation of complex E; (B) U2 snRNP then identifies the adenosine at the branch site, leading to the formation of complex A; (C) The U4/U6·U5 tri-snRNP is recruited to the spliceosome, assembling complex B; (D) U4 and U1 dissociate, allowing U6 to replace U1 at the ss, where it interacts with U2, forming complex C and driving the splicing process; (E) The exons are joined together, while the intronic pre-mRNA and spliceosomal snRNPs are released (based on [95]).

Even though the spliceosome drives pre-mRNA processing with great complexity and precision, the mechanism it triggers is quite flexible, relying on a strong regulation by both *cis* and *trans*-acting elements. *Cis*-acting regulatory sequences, including exonic splicing enhancers (ESE) and silencers (ESS) as well as intronic splicing enhancers (ISE) and silencers (ISS), along with RNA-binding protein splicing factors that recognize and bind to these sites play a crucial role in establishing and maintaining alternative splicing patterns. Amongst these proteins are the so-called heterogeneous nuclear ribonucleoproteins (hnRNPs) and serine/arginine-rich (SR) proteins. hnRNPs may either regulate splicing repression by binding to ISS and ESS. On the other hand, SR proteins promote splicing activation, by binding to ISE and ESE ([89,90,96], reviewed in [94]; Figure 7).

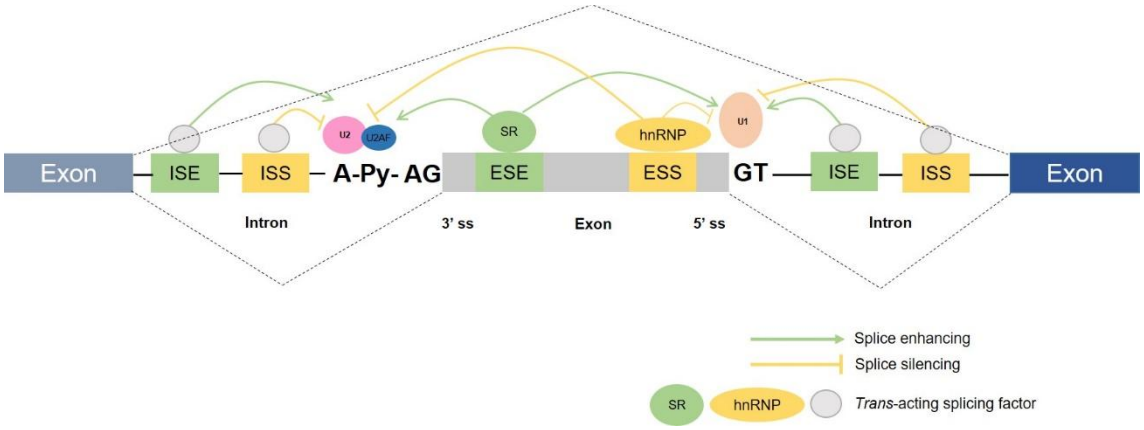


Figure 7. Schematic diagram of essential regulatory elements in pre-mRNA splicing. The selection of splice sites is regulated not only by core *cis*-sequence elements (the 5' and 3' splice sites, ss) and associated 3' sequences (including the polypyrimidine tract, Py, and branch point sequence, A) but also by additional enhancer and silencer elements located within exons and introns. These elements include exonic splicing enhancers and silencers (ESE/ESS) and intronic splicing enhancers and silencers (ISE/ISS). Two primary families of *trans*-acting splicing factors play crucial roles in this process: serine/arginine-rich proteins (SRs) and heterogeneous nuclear ribonucleoproteins (hnRNPs). These regulatory proteins, along with other trans-acting factors, bind to enhancer and silencer elements, interacting with spliceosomal components (depicted in green). These components are associated with the 5' and 3' ss that flank the alternative exon. This interaction can either promote (indicated by a green arrow) or inhibit (indicated by a yellow arrow) the recognition and utilization of the splice site (based on [90]).

Alternative splicing is the process through which a single precursor mRNA can generate a number of alternative mRNAs, allowing considerable proteomic diversity and complexity [97,98]. It is currently estimated that near 95% of human multi-exonic genes are alternatively spliced, which generates different mRNA isoforms. Alternative splicing might involve mechanisms of exon skipping, intron retention, mutually exclusive exons and alternative donor 5’ and acceptor 3’ss [96]. Additionally, alternative polyadenylation and the use of alternative promoters also contribute to alternative splicing. This process can be regulated at the transcription level and at the chromatin structure (reviewed in [94]).

Numerous players need to act in coordination to guarantee the quality of this multitude of tightly regulated processes, concerning which any disruption might affect development, leading to human disease [99] (Figure 8).

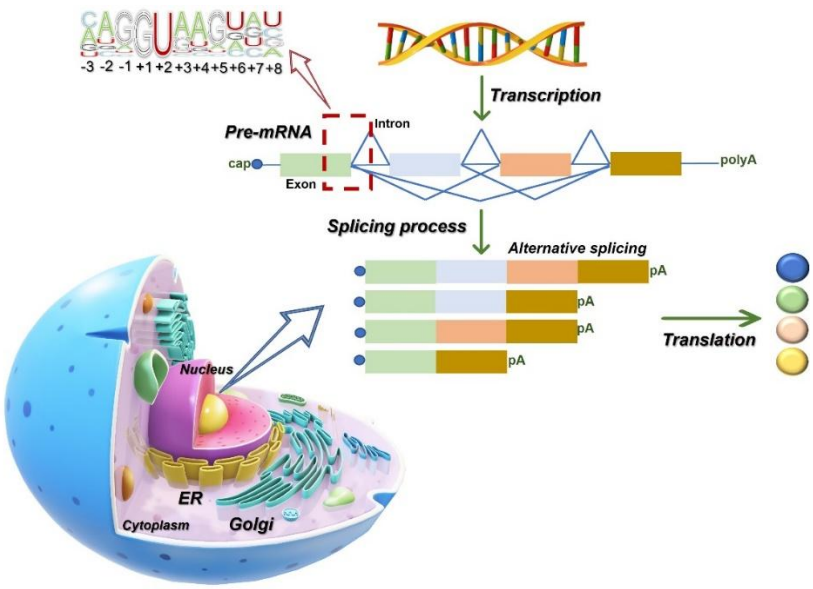


Figure 8. Simplified overview of the alternative splicing (AS) process. The AS process generates mature mRNAs with different exon combinations, resulting in production of different protein isoforms, from the same mRNA. Abbreviations: ER, endoplasmatic reticulum; mRNA, messenger RNA; pre-mRNA, precursor mRNA (adapted from [94]).

In humans, approximately 14% of all disease-associated mutations affect splice sites [100], and as many as 50% of mutations disrupt splicing by altering exonic or intronic silencers or enhancers [101].

This is why splicing modulation has become a central focus of research over the last decades, leading to the development of therapeutic strategies aimed at bypassing the disease-causing effects of mutations (reviewed in [78,94]). Remarkably, splicing modulation is also being used to address mutations that do not directly affect splicing, such for instance is happening is Duchenne muscular dystrophy (DMD), where splicing modulation is employed to induce the skipping of exons containing out-of-frame deletions [102].

Amongst the molecules that are being applied to modulate splicing, a particular class of ASOs, the SSOs, and the engineered U1 snRNAs seem to have particularly high therapeutic potential, and both will be the focus of the two upcoming sections.

3.1.2. Splice-switching oligonucleotides (SSOs)

SSOs are among the most widely used types of ASOs. ASOs are small (~18–30 nucleotides), synthetic, single-stranded nucleic acid polymers (RNA or DNA) with diverse chemistries. They are designed to be complementary to their target sequences through conventional base-pairing and can modulate gene expression via various mechanisms.

ASOs are broadly classified into two major categories: RNase H-competent and steric block ASOs [84,103].

RNase H-competent ASOs, which will be referred to later on (section 3.2.1.) are used for target downregulation by activating RNase H, thus promoting the cleavage of the target mRNA. On the other hand, steric block ASOs lack RNase H activity but can bind to specific sequences within a target transcript, thereby disrupting RNA–RNA or RNA–protein interactions. For instance, they can inhibit translation initiation by targeting the AUG start codon. However, the most widely utilized application of steric block ASOs is the modulation of alternative splicing, with these ASOs frequently referred to as SSOs [84].

SSOs were first described for correction of aberrant splicing in human β-globin pre-mRNAs [104], having progressed furthest in the treatment of other diseases. SSOs are typically 15–25 nucleotides long ASOs that target the pre-mRNA and modulate the splicing process by interfering with the recognition of regulatory splice elements.

Briefly, SSOs enter in the cell nucleus and bind to their target in a sequence-specific manner. By doing so, they block splice-regulatory elements, which are then 'masked' from the splicing apparatus. Ultimately, this leads to an alteration of normal splicing of the targeted transcript. These regulatory elements can be canonical/cryptic ss, branchpoints (*cis*-acting intronic motifs localized approximately 18–40 bases upstream of the 3′ ends of the intron), and/or splicing enhancers and silencers (exonic and intronic). By hiding splice-regulatory elements from the spliceosome, SSOs can selectively induce skipping or inclusion of target exons [105,106] (Figure 9). In this way, SSOs offer an effective and specific way to target and modify splicing in a therapeutic manner.

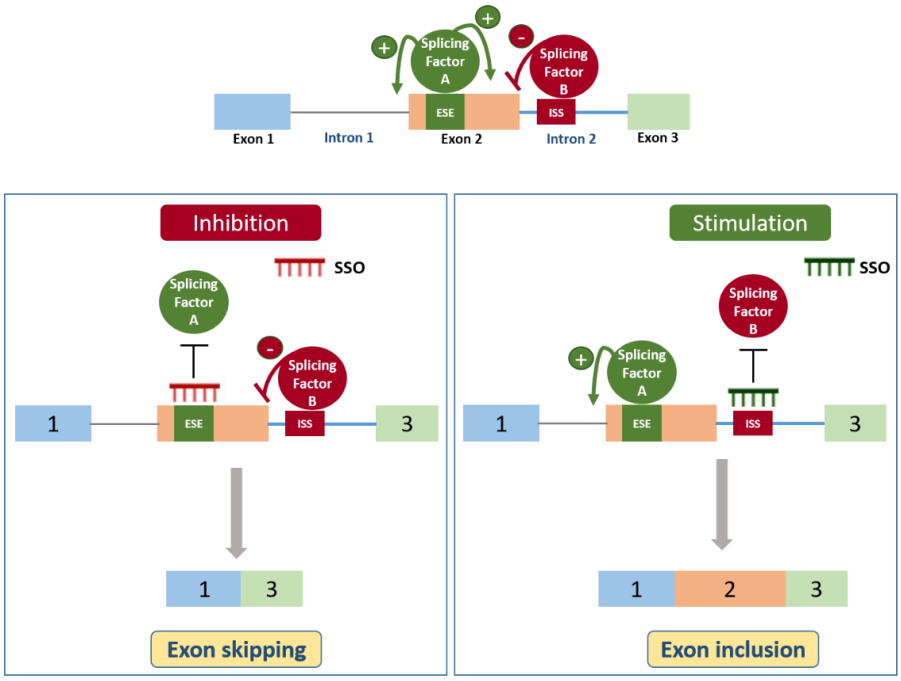


Figure 9. Mechanism of action of splice-switching oligonucleotides (SSOs). Alternative splicing can be manipulated by SSOs. A representation of a pre-mRNA transcript, where introns are represented as lines and exons as boxes (upper). A trans-acting inhibitory splicing factor (SF) protein (red oval) or stimulatory splicing factor (green oval) is seen attached to an intronic splicing silencer (ISS, red) and exonic splicing enhancer (ESE, green), respectively. These splicing factors (SF) proteins influence splice sites that are close to the surrounding exons by either promoting (+) or blocking (−) splicing. The binding of the stimulatory splicing factor to its corresponding enhancer binding site is sterically blocked by an SSO that base pairs to a splicing enhancer sequence. As a result, this block causes exon skipping by interfering with splicing (left panel). On the contrary, when a splicing silencer activity is selectively blocked by an SSO that base pairs to a splicing silencer sequence element, it stops a negatively acting splicing factor from attaching. The subsequent exon inclusion results from splicing at the splice site that is negatively controlled by the silencer element being activated when splicing inhibitory proteins' binding to their cognate binding sequence is disrupted (right panel).

The demonstration that a SSO drug can successfully promote the correction of its targets *in vivo* paved the way to clinical trials of ASOs for treatment of a variety of diseases, namely rare diseases, such as DMD and Spinal muscular atrophy (SMA). Currently, there are five approved drugs for these pathologies, all capable of manipulating pre-mRNA splicing: Eteplirsen (EXONDYS 51™) [107,108], Golodirsen (Vyondys 53™) [109], Viltolarsen (Viltepso®) [110] and Casimersen (Amondys 45™) [111] for the DMD and Nusinersen (Spinraza®) [112,113] for SMA treatment (reviewed in [94]). These ASOs are commonly used to modulate splicing with the primary aim of restoring a fully or partially functional protein. However, they can also be applied for splice corruption, a strategy where an exon is deliberately skipped to disrupt the translation of the target gene. This approach induces aberrant exon skipping, leading to the generation of mRNAs containing premature termination codons (PTCs), which are subsequently degraded through the nonsense-mediated mRNA decay (NMD) pathway.

This highly original approach has already been investigated in a few contexts, such as targeting the *MAPT* gene for tauopathies (e.g., [114]) and the *STAT3* gene, which is hyperactive in several cancers. Notably, the *STAT3*-targeting ASO [115] has advanced to clinical trials, highlighting its therapeutic potential.

Given this context, it is worth saying now that in this work SSOs were tested for therapeutic purposes, precisely having as main goal: to achieve targeted gene knockdown. That will become evident later.

3.1.3. Engineered U1 snRNAs

Another approach to modulate the splicing process, both *in vitro* or *in vivo*, involves the use of synthetic U1 snRNAs engineered to target and restore complementarity at mutant 5'ss. Unlike oligonucleotide-based therapies such as ASOs or siRNAs, these molecules belong to a distinct class of RNA-targeting therapies.

The endogenous U1 snRNA was discovered during the early days of splicing research and identified as a key player in the initial stages of the splicing process [116-118]. Briefly, the U1 snRNA is a 164-nucleotide molecule with a well-defined structure comprising four stem-loops, which primarily functions as a part of the RNP complex called U1 snRNP that also contains three U1-specific proteins (U1A, U1C, and U1-70K) and seven Smith antigen (Sm) proteins ([119,120], reviewed in [121]) (Figure 10a).

For the first step of the splicing process to occur, the 5′ end of the U1snRNA has to interact by complementarity with the moderately conserved sequence of the 5′ss (CAG/GURAGU; R-purine) marking the exon-intron boundary [97]. However, not all base pairs at different 5'ss positions are equally important for this process to occur, and their contribution to splicing roughly correlates with their conservation (Figure 10b). It is understandable that many other additional elements, such as splicing silencer and enhancer motifs, alternative splice sites, secondary structures, and regulatory proteins, can influence the splice site selection once the donor site does not always conform to the consensus sequence and instead can have a degenerate pattern feature ([122], reviewed in [121]).

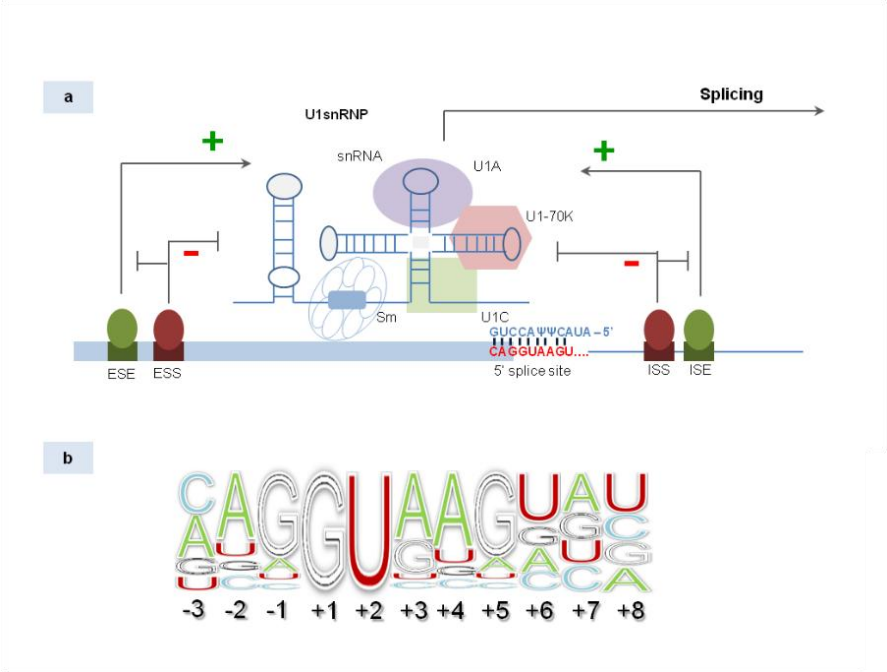


Figure 10. Role of the endogenous U1 snRNP in splicing. (a) The 5' end of U1snRNA base pairs to the 5' splice site (ss) in order to define a functional donor ss. This process is positively and negatively modulated by different splicing factors, which bind to exonic and intronic splicing enhancer and silencer motifs (ESE, ISE, ESS and ISS, respectively). (b) The 5'ss motif. The height of each nucleotide corresponds to its conservation at the corresponding positon (-3 to -1 are exonic positions, while +1 to +8 correspond to intronic positions). The most conserved 5'ss positions are +1 and +2, which determine the 5'ss subtype: the GU subtype accounts for ~99% of 5'ss. Minoritary subtypes have a mismatch to U1 at either +1 or +2 and include the GC and the very rare AU 5' ss. The next most conserved 5' ss positions are -1G and +5G, which form strong G-C base pairs with U1, through three hydrogen bonds. Consensus nucleotides -2A, +3A, +4A, and +6U are also conserved but are generally considered to have a lesser even though important contribution to 5'ss strength because their base pairing to U1 relies in the formation of two hydrogen bonds instead. The 5'ss positions +7 and +8 do not exhibit substantial conservation in humans, yet several lines of evidence indicate that these positions can base-pair to U1 and contribute to splicing. U1snRNP - small nuclear ribonucleoproteins (snRNPs) U1; ESE – exon splicing enhancer; ESS – exon splicing silencer; Sm - spliceosomal Smith-antigen proteins; snRNA - small nuclear RNA; ISS – intronic splicing silencer; ISE – intronic splicing enhancer. (Adapted from [121]).

Splicing mutations at the 5'ss affect U1 snRNA binding hindering spliceosome assembly and subsequent splicing, which can lead to exon skipping, intron retention, or even to the activation of cryptic splice sites. These mutations are common amongst the genetic abnormalities that may cause disease [123,124]. The most deleterious mutations at the 5'ss are those affecting the nearly invariant GU dinucleotide at positions +1 and +2. For the remaining nine positions, the effects on splicing are less obvious. In fact, nucleotide substitutions affecting the less conserved positions can cause splicing defects in some but not all 5'ss, suggesting that the remaining 5'ss positions and/or the overall context dictate the extent to which splicing is disrupted [124,125]. Remarkably, splicing can be restored by using modified U1 snRNA vectors that mimic natural U1 snRNA and are able to bind to the target pre-mRNA. To do this, a sequence that complements the

mutated target sequence must be introduced to the 5' end of U1 snRNA, by site-directed mutagenesis (Figure 11), and the modified U1 snRNA subsequently delivered to its ultimate therapeutic target - the patient.

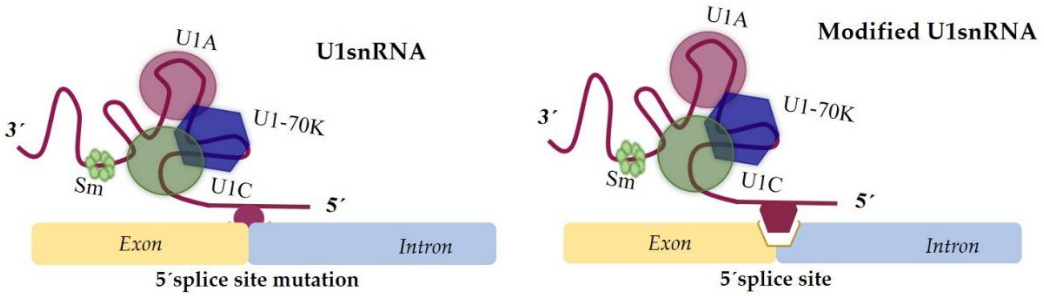


Figure 11. U1 snRNA-mediated therapy for 5' splice site (ss) mutations through restoration of exon recognition and inclusion. The wild-type U1 snRNP cannot bind to the mutated 5'ss, while a mutation-adapted U1 snRNP (first generation particle) may actually bind to that same ss. (Adapted from [94]).

The first evidence suggesting that the 5' end of the U1 snRNA recognizes the 5'ss in mRNA precursors by complementary base pairing dates back to the mid 80s. By then, Zhuang and Weiner tested if a modified U1 snRNAs could correct aberrant splicing patterns caused by mutations affecting the 5'ss [126][3]. Subsequently, a number of studies using cellular and animal models showed that disease-associated mutations in less conserved locations of the 5'ss might be corrected, making them a possible therapy for numerous diseases (reviewed in [78]). In 2003, Baralle and colleagues demonstrated the ability to correct a 5'ss variant (c.288+5G>C) causing exon 3 skipping in Neurofibromatosis type 1 using a U1 snRNA engineered to fully complement the mutated site [127]. Later, Pinotti *et al.*, developed a complementary U1snRNA targeting a mutation in the FVII donor splice site of intron 7 at the +5 position, reducing exon 7 skipping by 50% in COS-7 and Hep3B cells [128] and increasing functional FVII protein levels (135). Similar *in vitro* studies showed the capacity of modified U1 snRNAs to restore splicing in conditions such as retinitis pigmentosa [129,130], Bardet–Biedl syndrome [131], Propionyl-CoA carboxylase deficiency [132], and Tyrosinemia type 1 [133], Fanconi anemia C [134], Shwachman–Diamond syndrome [135], and MPS IIIC [136]. The latter was investigated by our group, with results discussed in detail later in this thesis.

Across various diseases, modified U1 snRNAs have consistently demonstrated their potential to correct splicing defects caused by genetic mutations *in vitro*, paving the way for further *in vivo* investigations. Such studies have already been conducted for

[3] For an extensive overview on U1snRNAs-based therapies, see Annex 2, review paper 2: Gonçalves M, Santos JI, Coutinho MF, Matos L, Alves S. Development of Engineered-U1snRNA Therapies: Current Status. *Int J Mol Sci*. 2023 (co-authored by the PhD candidate).

conditions like FVII clotting deficiency [137], aromatic L-amino acid decarboxylase deficiency [138], and Tyrosinemia type 1 [139].

In addition to the modified U1 snRNA vectors, there is yet another U1snRNA-based strategy being developed the Exon-specific U1 snRNAs (ExSpeU1s). ExSpeU1s are a novel U1 snRNA-based strategy designed to enhance exon inclusion with high specificity while minimizing off-target effects [121]. These molecules target poorly conserved intronic regions downstream of the 5′ss of a specific exon, promoting spliceosome activation and exon definition through the recruitment of splicing factors, thus holding significant therapeutic potential. So far, ExSpeU1s have been mostly tested *in vitro*, but there is a growing amount of data on their potential, with several diseases targeted to date, including ATP8B1 [140] and CDKL5 [141] deficiencies, Hemophilia A [142], Fanconi anemia [143] and Phenylketonuria [144], amongst others.

Overall, even though no engineered U1 snRNA has yet reached the clinic, it is likely to assume that in near future these molecules can be an option for treating diseases caused by splicing mutations. The ongoing researches focusing the optimization of their effectiveness, the understanding of the off-target effects, as well as the search for new delivery strategies, clearly fuel these expectations.

3.2. RNA-therapies acting by gene knockdown

3.2.1. Gapmer ASOs and siRNAs

The RNA transcripts can be knocked down using either gapmer ASOs or siRNAs. Gapmers are used for gene silencing by stimulating RNA cleavage through the recruitment of RNase H. These chimeric ASOs consist of a central block of DNA nucleotides (gap region) for engagement with RNase H, flanked by modified RNA-based structures, 5’ and 3’-wing regions. These wings typically feature 2'-OMe, 2'-MOE, or LNA modifications to improve the binding affinity to target genes as well as to improve stability against exonucleases. For a successful therapeutic applications of gapmers, advancements in their chemistry, particularly in the wings, revealed to be essential to make them more drug-like (more details on this subject can be found in the section 3.3.1.) [84,85,103]. In contrast, the central DNA region of gapmers permits only phosphorothioate (PS) modifications, the inclusion of which depends on the specific design and therapeutic objectives.

RNase H is capable of cleave a phosphodiester bond of a RNA molecule when RNA-DNA duplex exists. So, gapmers can target both mRNA and pre-mRNA, creating a DNA:RNA hybrid of the gapmer core with the target transcript, inducing the recruitment

of RNase H enzyme, either in the nucleus or the cytoplasm. Once recognized these hybrids, RNase H cleaves the duplex structure, causing mRNA degradation and reducing gene expression [145,146] (Figure 12). Decades ago, it was discovered that RNase H-mediated RNA degradation could be a therapeutic strategy for downregulating genes. When it was shown that these chimeric oligos could effectively induce RNase-H-mediated RNA degradation, their appeal as a therapeutic tool increased significantly.

Targeting a mutant mRNA in a therapeutic context may improve disease phenotypes by preventing the toxic effect linked to the expression of a dominant-negative or gain-of-function protein (reviewed in [147]).

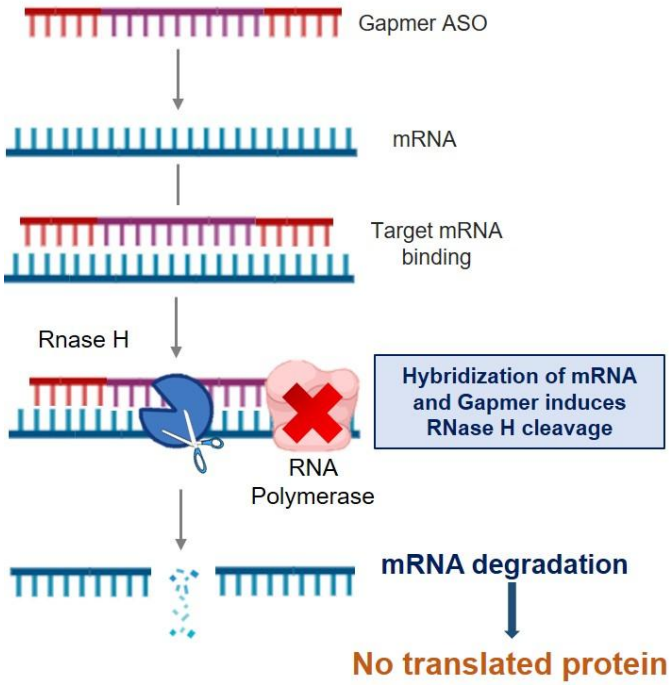


Figure 12. Schematic representation of the mechanism of action of gapmer antisense oligonucleotides (ASOs). The gapmer binds to its target messenger RNA (mRNA), and this complex recruits RNase H. The cleavage position of RNase H in the target mRNA is directed by the position of the DNA building blocks, and the cleaved mRNA is degraded. Consequently, no protein is produced.

Currently, there are four approved gapmers for clinical practice: Inotersen (Tegsedi®) for hereditary transthyretin amyloidosis (hTTR), Volanesorsen (Waylivra™) for the treatment of familial chylomicronaemia syndrome, Tofersen (Qalsody™) for the treatment of amyotrophic lateral sclerosis and, very recently, Eplontersen (Wainua™) for the treatment of polyneuropathy of hTTR in adults, while many others are currently undergoing preclinical evaluation or clinical trials [145,148].

siRNAs are short double-stranded RNAs (20-25 nt) that act by using the RNA interference (RNAi) pathway, a natural cellular defense mechanism useful to recognize and degrade pathogenic RNAs. Once in the cell, the siRNA is incorporated into the RNA-induced silencing complex (RISC), its unwinding occurs and is separated into sense and antisense strands. Only the antisense strand remains within the complex, guiding it to bind to its complementary mRNA. This binding mediates its cleavage and, consequently, its degradation by the cell (Figure 13).

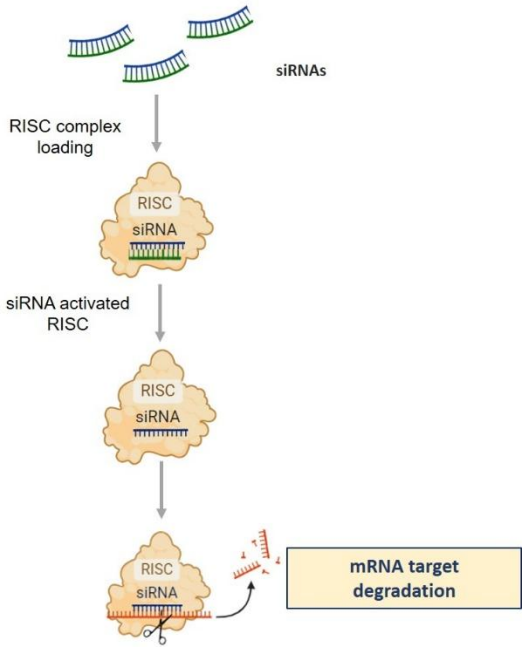


Figure 13. Schematic representation of the mechanism of action of small interfering RNAs (siRNAs). The siRNA contains two short RNAs with terminal overhangs and, when in the cytoplasm, recruits the RISC complex. This complex cleaves the nontargeting passenger strand RNA and then binds to its target mRNA sequence-specifically. The target mRNA is then cleaved by the Argonaute protein and further degraded. Created with BioRender.com

To date, five siRNAs received approval and are used in clinics: Patisiran (Onpattro™) and Vutrisiran (Amvuttra™) for hTTR, Givosiran (Givlaari®), for acute hepatic porphyria, Lumasiran (Oxlumo™) for primary hyperoxaluria type 1, and Inclisiran (Leqvio®) for hypercholesterolemia (reviewed in [76]). Many of the previous mentioned chemical modifications can be used in siRNAs to improve their stability and protection from endonuclease degradation. However, the presence and type of modifications have limitations due to the molecular requirements needed for effective recruitment of RNAi machinery.

Progresses in understanding the molecular mechanisms of activity, cellular uptake, biodistribution and toxicity of ASOs and siRNAs are needed to extend the application of these versatile technologies to many other diseases.

3.3. Increasing the efficacy of RNA-based drugs

Regardless of the disease aimed to treat, several key aspects must be considered to increase efficacy and facilitate clinical translation of RNA-based drugs: having a non-toxic and stable drug, testing it in appropriate models and ensuring efficient delivery. And while going into detail for all these issues, would largely surpass the scope of this thesis as each single topic has a field of research of its own, we will briefly tackle these major subjects over the following sections.

3.3.1. Chemical modifications

As mentioned earlier, both ASOs and siRNAs are synthetic, chemically modified oligonucleotide therapeutics. For an oligo to hold any therapeutic potential, it must closely follow several critical criteria. Specifically, it needs to bind to its target in a sequence-specific manner; have chemical proprieties that facilitates its cellular uptake and activity; resist to nuclease degradation for preventing its degradation and exhibit favorable pharmacokinetics (PK) and pharmacodynamics (PD) to enabler effective delivery to the target tissues. Thus, tailored chemical modifications of DNA and RNA nucleotides were assumed to be a fundamental step in transforming oligonucleotides into viable drugs [149]. Over the years, several chemical modifications were tested and implemented both in the backbone and sugar component, allowing the development of different oligonucleotide chemistries with properties that enhance their potential as therapeutic tools.

The first successful chemical modification of oligonucleotides was the addition of a PS moiety into the backbone, where a non-bridging oxygen in the phosphate group is replaced by sulfur (Figure 14). PS backbone modifications are well-tolerated in ASO designs and do not disrupt RNase H activity. In contrast, siRNAs with PS modifications at every linkage are less active than their phosphodiester (PO) counterparts. Consequently, PS-containing siRNAs are typically modified only at the termini, if at all [84].

Notably, PS was also the first chemical analog to be applied in clinical settings and has been incorporated into many of the molecules currently used in the clinic or under development as potential therapeutics.

While PS modification reduces the oligonucleotide's affinity for its target, it provides critical advantages such as resistance to nucleases, improved overall stability *in vivo*, reduced renal clearance and enhanced tissue retention, thus allowing for greater biodistribution. However, these benefits come with the drawback of an increased risk of

toxicity, primarily due to prolonged tissue retention and extended drug effects [84,85,106,150,151].

To address these limitations, additional chemical modifications have been developed. Beyond backbone modifications, the sugar moiety of nucleotides has become a key target for chemical alterations. Modifications in this region have proven instrumental in further optimizing the properties and enhancing the therapeutic efficacy of oligonucleotides.

The most successful and well-known ones are the 2'-OMe, 2'-MOE and 2′-F alterations (Figure 14) that correspond to the substitution of the hydrogen or hydroxyl group at the 2′-position of the sugar moiety. These modifications improve the drug-like properties of ASOs by increasing their nuclease resistance, prolonging tissue half-life, and enhancing drug effects. For instance, 2′-OMe and 2′-MOE improve the binding affinity of ASOs to their RNA targets by promoting an RNA-like conformation. These modifications also reduce immune reactions, minimize nonspecific protein binding, and lower toxicity compared to the PS backbone modification, with 2′-MOE being notably less toxic than 2′-OMe. Importantly, 2′-MOE is the most advanced modification and is the only 2′-substitute used in FDA-approved ASO drugs [84,85,106]. 2′-ribose modifications are incompatible with RNase H activity and are mainly used in steric block oligonucleotides (such as SSOs) or as flanking regions in gapmer ASOs. For siRNAs, which require compatibility with argonaute 2 (AGO2) loading and slicer activity however, extensive 2′ modifications has been reported using 2'-OMe and 2'-F, highlighting the RNAi machinery's tolerance for chemical modifications [84].

Novel compounds are still being developed, which include among others LNAs, PNAs and PMOs (Figure 14). These modifications can be combined with any one of the previously referred in order to attain greater efficacy.

The LNAs involve modifications to the sugar, specifically a methyl bridge between the 2'-O and 4'-position of the ribose ring, which is why they are considered constrained analogues. This modification has the advantage to increase the affinity for its target but present some toxicity.

The PNA consists of modification in which ribose and the phosphate group of the nucleotide are replaced by a peptide polymer [84,85,106]. PNAs present low cellular uptake, insolubility in water and when administered, are quickly eliminated from the body, which poses a challenge for *in vivo* studies.

The modifications in PMOs are also substantial: the ribose sugar is replaced by a six-membered morpholine ring and the negatively charged phosphodiester backbone is replaced with a neutral phosphorodiamidate backbone [152]. Unlike PS

oligonucleotides, PMOs have neutral charge and, therefore, do not tend to interact with nucleic acid-binding proteins, a feature that significantly improves their tolerability *in vivo*. However, they are also rapidly cleared by the kidney and for this reason exhibit lower accumulation rates in tissues. Ultimately, this means that high doses of PMO oligonucleotides are required to achieve a pharmacological response ([153], reviewed in [154]).

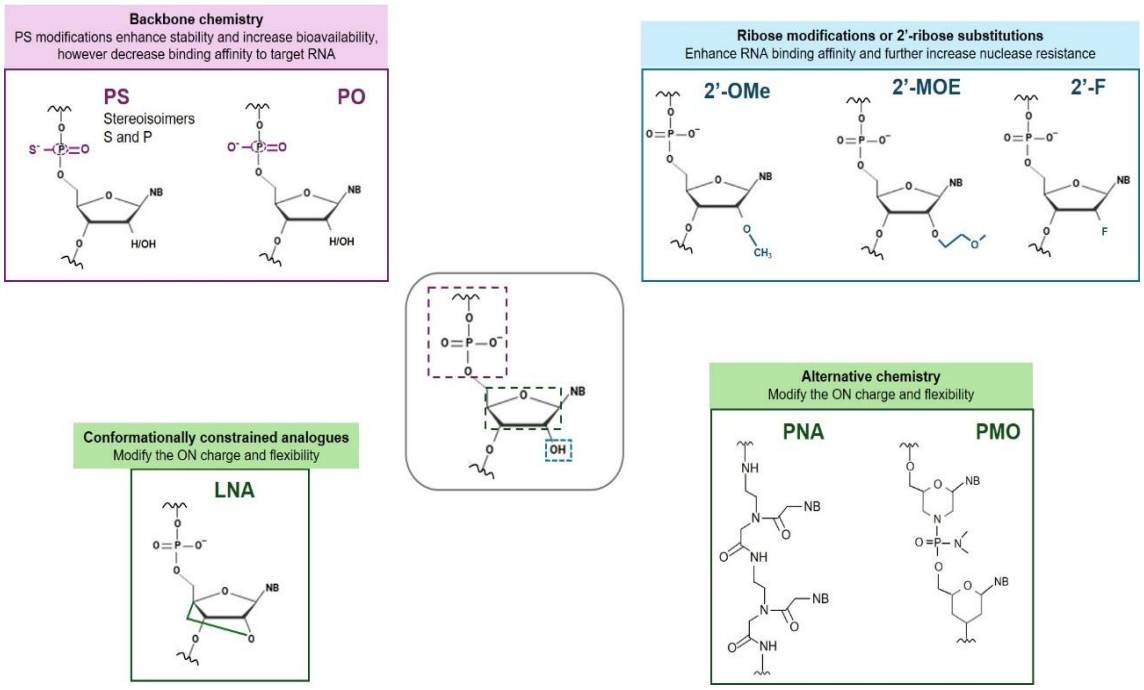


Figure 14. Oligonucleotide chemistries. Commonly used nucleic acid chemistries involve several modifications. The widely adopted phosphorothioate (PS) backbone replaces the natural phosphodiester (PO) structure. Modifications to the ribose at the 2'-O position in RNA and the 2' position in DNA often include 2'-O-methyl (2'-OMe), 2'-O-methoxy-ethyl (2'-MOE), and 2'-fluoro (2'-F), which are among the most frequently used. Conformationally restricted DNA analogues, such as locked nucleic acid (LNA) enhance binding affinity and is constrained by a methyl bridge linking the 2'-O and 4' positions of ribose. Alternative chemistries include nucleobase modifications, such as phosphorodiamidate morpholino oligomers (PMO) and peptide nucleic acids (PNA) (based on [85]).

Overall, the positive impact of chemical modifications over the properties of oligonucleotides has greatly impacted this field, prompting a significant evolution in the last decades and significantly accelerating drug development. Indeed, part of their success as an emerging class of drugs that directly regulates disease-causing genes and their variants, can be attributed to the stability, resistance and efficacy conferred by these modifications (reviewed in [76,149,155]).

3.3.2. Disease models

Disease models are essential not only to decipher the pathogenic mechanisms underlying human diseases, but also to evaluate new therapeutics, concerning which study models able to mimicking the target human pathologies must be recruited. This includes all stages, from the preliminary *in vitro* to the exploratory *in vivo* pre-clinical evaluations.

Both *in vitro* and *in vivo* models are needed for pre-clinical testing of new therapies. *In vitro* models can provide insights into the mechanism of action and efficacy of potential therapies, whereas *in vivo* models are better suited to assess the delivery efficiency and overall potential of therapeutic compounds. Accordingly, most ASO sequence variants are first screened *in vitro*, conducting only to *in vivo* testing the strongest therapeutic candidates [82].

In the LSD field, two major types of models have been employed: patient-derived skin fibroblasts, the classical choice for *in vitro* studies; and genetically engineered mouse models, the gold standard for *in vivo* analyses, not ignoring that both platforms have specific drawbacks. Some of those caveats are even more evident for neurological diseases, such as MPS III[4].

Reconciling optimal proliferation with survival rates *in vitro*, human cell cultures aim to replicate the mechanisms that cells exhibit *in vivo* within a controlled environment [156]. Primary cell cultures offer greater genetic diversity than specific cell lines, but their limited availability and proliferation capability pose challenges. In multisystemic diseases like LSDs, *in vitro* culture of fibroblasts has been often used, since such cells display typical storage phenotypes. Their collection is, however, invasive and causative of distress particularly in children. Moreover, fibroblasts may not replicate the disease mechanisms in specialized cells like neurons, for example, which are non-dividing cells that in neurological LSDs reveal disrupted neurotransmission dynamics. On the other hand, dividing cells like fibroblasts, may temporarily compensate for lysosomal dysfunction, contrarily to neurons, which cannot regenerate any dysfunction that leads to faster and irreversible damage [157,158].

Currently, this conundrum can be addressed through the use of induced pluripotent stem cells (iPSCs) and multipotent stem cells (MSCs), which can differentiate into any somatic cell, including neurons, while also exhibiting unlimited proliferation

[4] For an extensive overview on the existing in vitro models for MPS diseases and on our lab's particular opinion on a specific patient-derived cell type, which holds potential to arise as a novel MPS disease model, see Annex 2, review paper 3: Carvalho S, Santos JI, Moreira L, Gonçalves M, David H, Matos L, Encarnação M, Alves S, Coutinho MF. Neurological Disease Modeling Using Pluripotent and Multipotent Stem Cells: A Key Step towards Understanding and Treating Mucopolysaccharidoses. *Biomedicines*. 2023 (co-authored by the PhD candidate).

capacity ([159], reviewed in [157]). Other *in vitro* models like organoids, bioengineered tissue models and organs-on-chips are increasingly used in both preclinical and clinical research (reviewed in [160-162]).

In MPS research, the generation of patient-derived iPSC has gained momentum, and different tools to generate cells of interest not only for pre-clinical but also for broader pathophysiological evaluations emerged. Still, there are no reports on the use of naturally-occurring MSCs (reviewed in [157]) apart from a work performed by our own team[5] [163]. Similarly, more advanced platforms, such as the above-referred 3D cultures, from organoids to organs-on-a-chip, are still largely unexplored.

Up to now, the most informative preclinical systems for studying medication effects and disease mechanisms in the complex environment of the human biology continue to be animal models such as mice, which is the most used worldwide, including in LSD research. Knockout models for human LSDs are relatively common, as illustrated by the well characterized mouse and zebrafish models available for specific LSD diseases [158], However, animals carrying splicing mutations are absent in the currently available models [164]. This limitation extends to one of the therapies developed in this study involving modified U1 snRNAs.

Most of the mentioned difficulties are being gradually overcome. For example, to evaluate the therapeutic potential of modified U1 snRNAs *in vivo*, various strategies have been developed. Transient expression of constructs carrying the human sequence with a mutation was achieved through hydrodynamic injection of plasmid constructs. For sustained expression, adeno-associated viral (AAV) vectors were employed (reviewed in [78]). A pioneering study by Balestra *et al.* [137] tested both transient and stable expression approaches for generating C57BL/6 mice expressing a splicing mutation in the *FVII* gene, associated with clotting deficiencies. Plasmid constructs were delivered via hydrodynamic injection for transient expression, while AAV vectors of different serotypes were administered intravenously for sustained expression. In both cases, mice carrying the human splicing mutation were obtained, and the mutation-adapted U1 snRNA successfully restored FVII splicing and improved clotting.

In conclusion, the development and application of appropriate disease models are pivotal for advancing our understanding of pathological mechanisms and evaluating novel therapeutic strategies. Significant progress has been made in creating more

[5] This is an original report on the establishment and characterization of a particular type of MSC from patient-derived baby teeth to model MPS II *in vitro*. See Annex 1, original paper 2: Carvalho S, Santos JI, Moreira L, Duarte AJ, Gaspar P, Rocha H, Encarnação M, Ribeiro D, Barbosa Almeida M, Gonçalves M, David H, Matos L, Amaral O, Diogo L, Ferreira S, Santos C, Martins E, Prata MJ, Pereira de Almeida L, Alves S, Coutinho MF. Modeling Lysosomal Storage Disorders in an Innovative Way: Establishment and Characterization of Stem Cell Lines from Human Exfoliated Deciduous Teeth of Mucopolysaccharidosis Type II Patients. *Int J Mol Sci*. 2024 (co-authored by the PhD candidate).

representative *in vitro* and *in vivo* systems, including iPSCs, organoids, and animal models. Still, challenges remain, particularly in modeling specific splicing mutations. Continued innovation in these platforms will be critical to overcome current limitations, accelerating preclinical research, and translating promising therapies into effective clinical treatments.

3.3.3. Delivery technologies

Probably the biggest challenge in designing and testing RNA-based therapeutics is delivery. As potent as they may be, these new classes of therapeutics require effective delivery systems to reach their full potential. To reach the desired targets, oligonucleotides or any other RNA-based drug must overcome numerous hurdles. One of them is that these therapeutic molecules might be subjected to degradation by RNases and entrapment within endosomes. Without protective strategies they will face elimination via renal filtration. Additionally, the relatively large size of some molecules, such as siRNAs for example, prevent passive diffusion across biological membranes into the cytosol.

Much has been done lately viewing the development of specialized drug delivery systems. Advances in nano and materials technologies are being essential to overcome delivery challenges of oligonucleotides, namely thought the use of lipid nanoparticles (LNPs) or the N-acetylgalactosamine-conjugates (GalNAc) (reviewed in [149]). LNPs are nanoparticles with amphipatic lipids that contain a hydrophilic head and a hydrophobic chain and interact with negatively charged therapeutic oligonucleotides. LNPs are important players in siRNAs interaction and delivery, which can be complexed with different ligands to target specific cell receptors, promoting receptor-mediated intake of putative drugs[6]. However, lipoplexes can accumulate in the liver and other filtering organs, limiting thus their effectiveness in penetrating other tissues. Besides they are also prone to induce pro-inflammatory reactions. Many efforts were made to develop a class of nanoparticles that could circumvent these limitations. Zimmerman *et al.*, showed that ionizable cationic LNPs, called stable nucleic acid lipid particles (SNALPs), have high cargo encapsulation efficiency and favor cellular uptake and are able to escape from the endosomes [165,166]. Moreover, they may be engineered to promote targeted delivery to specific receptors. siRNA-LNP complexes bind to apolipoprotein E (ApoE), for example, can enter hepatocytes via ApoE receptors present in cells' membrane. This

[6] For an extensive overview on a potential solution for siRNA delivery to the CNS using a particular type of LNPs, see Annex 2, review paper 4: Coutinho MF, Santos JI, S Mendonça L, Matos L, Prata MJ, S Jurado A, Pedroso de Lima MC, Alves S. Lysosomal Storage Disease-Associated Neuropathy: Targeting Stable Nucleic Acid Lipid Particle (SNALP)-Formulated siRNAs to the Brain as a Therapeutic Approach. *Int J Mol Sci*. 2020 (co-authored by the PhD candidate).

technology was used in a siRNA drug recently approved targeting transthyretin (TTR) mRNA for the treatment of hTTR [167].

Another strategy to improve delivery systems is based on the selection of the appropriate administration route. Clinical success has been achieved with local delivery to the eye, brain, and spinal cord through intravitreal (IVT) and intrathecal (IT) administration, respectively [168,169]. Both methods bypass renal clearance, ensuring prolonged exposure of the oligonucleotides to the cellular microenvironment, which facilitates efficient uptake. The approach represented a game changer for certain RNA-based drugs, particularly ASOs [85] concerning which the major difficulty for therapeutic use is delivery to the target site(s) [82,85]. Surprisingly, despite their large size and highly charged nature, it was demonstrated that ASOs can distribute widely throughout the CNS when delivered into the CSF via IT injection, a method that is safe and well tolerated. This characteristic, which is not shared by other RNA therapies like siRNAs, has significantly facilitated the use of ASOs as a therapeutic approach for a number of CNS disorders [84,170].

The successful role of RNA-based therapies in LSDs is illustrated by Milasen, an ASO approved by the FDA for a single patient with Batten's disease, also administered via IT injection [171]. Ongoing studies are now exploring the use of ASOs for other neurodegenerative disorders, including Spinocerebellar ataxia (SCA) types 1, 2, and 3, Huntington's disease, Alzheimer's disease, Dravet syndrome, Angelman syndrome, and progressive supranuclear palsy [172,173].

Similarly, delivery to the target tissues/organs is a great difficulty in the therapeutic use of engineered U1snRNA vectors. So far, most of the *in vivo* studies were conducted using viral delivery vectors, particularly AAVs, which are expected to be the first to reach clinical trials (reviewed in [78]). However, despite the many modifications introduced in viral vectors, it was not yet possible to neutralize their potential to induce immune reactions, and thus concerns persist. Still, different AAV serotypes with specific tissue tropisms have been described, including serotypes capable of transducing the BBB, making them particularly suitable for delivering therapeutic agents in diseases with neurological symptoms. Furthermore, AAV vectors have shown to mediate long-term *in vivo* expression with little or no acute toxicity. These two are among the main reasons underlying the routine use of AAV vectors in numerous preclinical and clinical trials [174,175], rendering reasonable to assume that AAVs could also provide positive results when used for the targeted delivery of engineered U1 snRNAs.

In conclusion, while significant progress has been made in overcoming the delivery challenges associated with RNA-based therapeutics, continued innovation in

delivery technologies, including nanoparticle systems and viral vectors, will be crucial to unlocking the full potential of these therapies for the treatment of a wide range of diseases, particularly those with neurological involvement.

3.4. Current state of RNA therapy development for MPSs

In the field of LSDs RNA drugs remain largely unexplored, with the existing scarce studies having addressed only a few diseases [176]. For RNA drugs acting upon splicing, two studies relied in rescue strategies involving antisense oligonucleotides for specific mutations associated with Pompe and Niemann-Pick type C diseases [177,178]. Additionally, modified U1snRNAs have been employed to target mutations in Fabry disease and MPSs [136,179], the latter being conducted by our research group. Regarding gene knowckdown technologies, somes studies have been conducted with siRNAs for SRT, namely for Gaucher disease [180] and MPS. For MPSs, while we have reviewed most of them, first in a review on genetic SRT (gSRT) approaches [181], and more recently in an extensive publication on splicing modulation approaches [94], under the scope of this thesis, a brief overview on the existing published pre-clinical studies will also be presented.

3.4.1. Approaches attempting splicing modulation/correction[7]

Among the most successful RNA-based drugs are those that act at the pre-mRNA level to either modulate or correct aberrant splicing patterns. Diseases that are monogenic represent very suited candidates for highly specific mutation-targeted splicing modulation approaches, as is the case of MPSs. In a review paper on the subject published by our team in 2022, 226 MPS-causing mutations were known to affect the pre-mRNA splicing process [94]. Today this number has grown to 257 (https://my.qiagendigitalinsights.com/, HGMD Professional 2024.4, accessed on 30 December 2024) and includes mutations that might occur in *cis*-acting elements, including 5′ss and 3′ss, GU-AG canonical nucleotides, the Py tract, branch point sequences, ESE, ESS, ISE and ISS, which affects their interaction with *trans*-acting factors (SR family proteins and hnRNPs) (reviewed in [94]).

Splice modulation for therapeutic purposes in MPSs using ASOs, was first attempted by our group, in 2015, when the team tried to correct the effect of a silent pathogenic variant in the *IDS* gene, which underlies a severe form of MPS II [179,182].

[7] For an extensive review on splicing modulation as a potential therapeutic strategy Mucopolysaccharidoses, see Annex 2, review paper 1: Santos JI, Gonçalves M, Matos L, Moreira L, Carvalho S, Prata MJ, Coutinho MF, Alves S. Splicing Modulation as a Promising Therapeutic Strategy for Lysosomal Storage Disorders: The Mucopolysaccharidoses Example. *Life*. 2022 (authored by the PhD candidate).

The target mutation occurs in exon 8 of the gene, and corresponds to a single nucleotide change, c.1122 C>T, that was then reclassified as a splicing mutation, contrarily to the initial misclassification as nonsense variant [179]. Actually the team showed that it created a new 5'ss within exon 8, thus affecting exon recognition and dramatically altering the normal *IDS* splicing. In order to block the access of the splicing machinery to that mutant pre-mRNA and circumvent the formation of the aberrantly spliced transcript, four SSOs were designed and tested *in vitro*, in patient-derived fibroblasts: three PMOs and one LNA, all complementary to the region of the newly created 5'ss. Unexpectedly, the SSOs failed to abolish the abnormal transcript, but instead resulted in the appearance of another aberrant splicing product corresponding to the complete skipping of exon 8. Remarkably, this occurred not only on patient's but also in control fibroblasts, indicating that the oligonucleotides were masking an important *cis*-acting element involved in regulation of exon 8 the 5′ss.

The use of modified U1 snRNAs to counteract the effect of MPS IIIC-causing variants, was again first investigated by our group, in 2014 [136]. Modified U1 snRNAs were tested to correct three nucleotide changes affecting distinct donor 5′ ss in the *HGSNAT* gene (c.234+1G>A, c.633+1G>A, and c.1542+4dupA), as well as one mutation affecting acceptor 3′ss (c.372-2A>G). A partial correction of splicing patterns (around 50%) was achieved for the c.234+1G>A mutation, using a modified U1 snRNA that perfectly matched the mutant donor ss in fibroblasts from patients carrying this frequent mutation (Figure 15c). As for the mutations c.633+1G>A and c.1542+4dupA, no rescue was observed following overexpression of the modified U1 snRNAs in patient cells. More attempts like this, further complemented with *in vivo* studies, are needed to fully understand the potential of U1 snRNA-based therapies in MPS III.

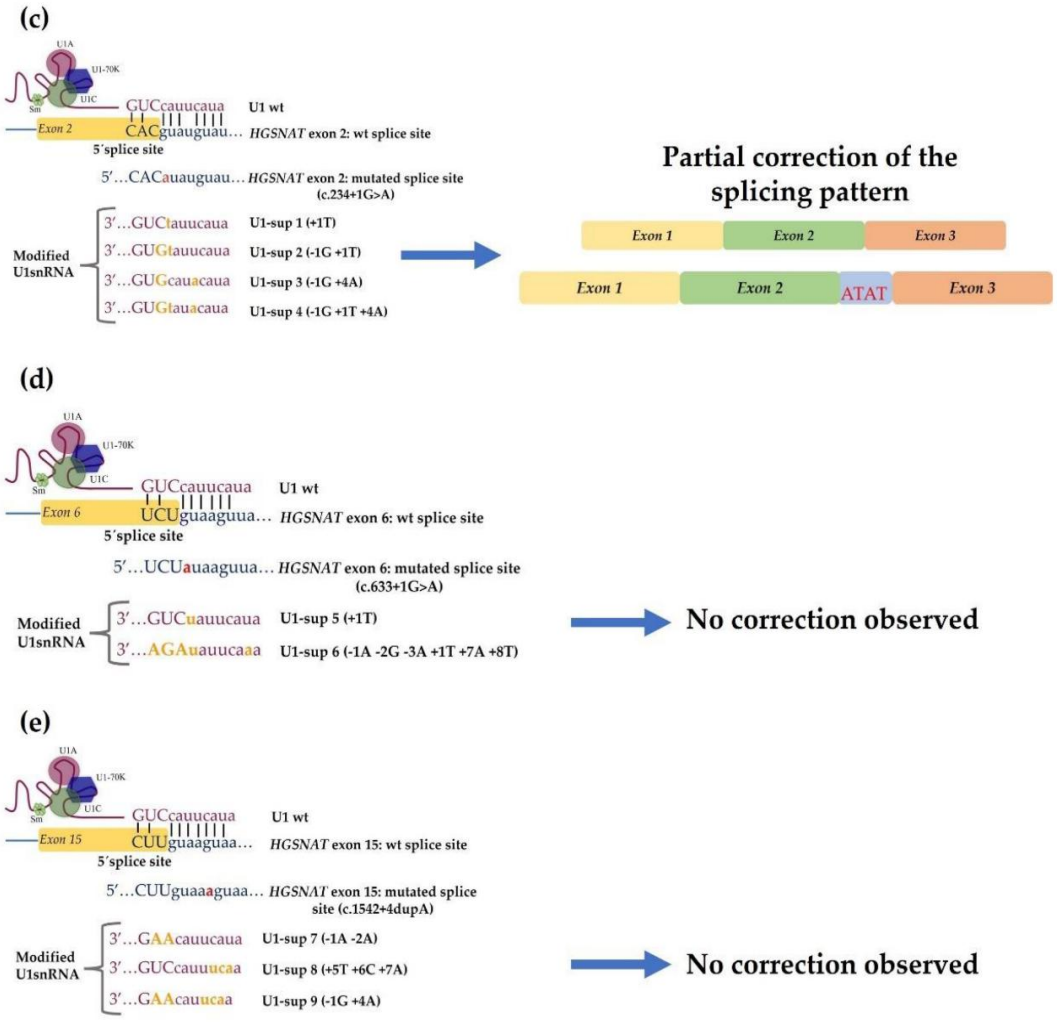


Figure 15. Schematic representation of the rationale behind the original study by Matos and co-workers [136]. This study relies on the therapeutic potential of modified U1 snRNA vectors to correct the pathogenic effects of three independent MPS IIIC-causing variants, along with the results obtained for each case (reproduced from an original review paper authored by the PhD candidate; see Annex 2, review paper 1). (c–e) Various therapeutic strategies involve using different U1 snRNAs to correct the pathogenic splice site mutations in the *HGSNAT* gene (c.234+1G>A, c.633+1G>A, and c.1542+4dupA). For the mutation mentioned in (c), partial recovery of the splicing defect was achieved following treatment with fully adapted U1 snRNA (U1-sup4). Sequence analysis revealed two distinct sequences: one showing a normal splicing pattern and another incorporating the first four base pairs of intron 2 (ATAT). However, for the other two mutations affecting the 5′ss of the *HGSNAT* gene, no correction was detected after applying the modified U1snRNAs. Uppercase letters represent exonic nucleotides, while lowercase letters indicate intronic nucleotides. Base pairing is depicted with vertical lines. The mutant nucleotide is marked in red, and the altered nucleotides in the U1 sequence are shown in orange.

3.4.2. Approaches attempting gene knockdown

Knockdown-replace strategies are being widely tested as gene therapies for gain-of-function mutations causative of diseases. LSDs may also benefit from such strategies, as long as they are designed to target genes playing roles upstream in the

pathophysiological cascade of the diseases. That rationale underlies all SRT approaches for LSDs: any drug that reduces the substrate buildup by balancing its synthesis and catabolism rates may be of therapeutic value. Therefore, targeting specific genes in the biosynthetic cascade that gives rise to the accumulation of undegraded substrate(s), expectedly will lead to decrease of subcellular damage, thus delaying the symptoms. Theoretically, any drug that can target and knockdown a gene within the biosynthetic cascade may be option viewing SRT. However, no research group has yet assessed the feasibility of ASO-driven knockdown approaches.

In 2010, Dziedic and colleagues were pioneers in promoting targeted gene knockdown for SRT purposes in MPS, when they transfected several siRNAs into human MPS IIIA patients' fibroblasts. The goal was to develop a specific inhibitor of GAG synthesis that could work as therapeutic for MPS III. siRNAs were designed to target different genes responsible for coding enzymes involved in the first steps of the biosynthesis of HS, namely: *XYLT1, XYLT2, GALTI* (*B4GALT7*) and *GALTII* (*B3GALT6*). As expected, they observed a decrease in mRNA and protein levels of the targeted genes/proteins when compared to the control samples, as well as considerable impairment in GAG synthesis [183], thus providing an *in vitro* proof of principle of gSRT. Still, no data was presented on its ability to decrease GAG buildup, which is the primary pathophysiological trigger in MPS diseases.

Soon after this seminal work, a similar approach was undertaken by Kaidonis *et al*., who tried lentiviral transfection of MPS I and MPS III skin fibroblasts with shRNAs targeting *EXTL2* and *EXTL3*, two additional genes responsible for coding enzymes involved in the biosynthesis of HS, reaching similar conclusions [184]. Of the six originally designed shRNAs, four reduced target gene expression and GAG synthesis. Furthermore, a significant reduction in GAG storage in MPS IIIA fibroblasts treated with three of the shRNAs was observed. In MPS I fibroblasts, results were less satisfactory [184].

Later on Dziedic and colleagues hypothesized that the simultaneous use of two siRNAs directed to two different genes involved in GAGs synthesis could be more effective than the use of a single one. Disappointingly, they found that combinations of two siRNAs designed to silence the coding genes for isoenzyme pairs (either XT-I and XT-II or CS- GalNAcT-1 and CSGalNAcT-2*)* were slightly more efficient in decreasing GAGs synthesis, but the differences were not statistically significant compared to cells treated with one single siRNA [185]. Thus, no evidence for additive effects was obtained.

However, an important lesson was drawn from this study: it discourages the simultaneous use of two siRNAs instead a single one for therapeutic purposes in MPS;

the timid benefit of using two different molecules did not seem to compensate the associated increased costs and risk of side effects.

Finally, it has to be mentioned another study, conducted by Canals *et al*., in 2015, that relied on the RNAi technology to counteract GAG buildup in MPSs. Two different genes were target, *EXTL2* and *EXTL3* that showed decreased expression after transfection of four different siRNAs in MPS IIIC fibroblasts. Not only GAG synthesis was inhibited but also reduced HS storage, two findings that were confirmed through immunocytochemistry analyses [186].

To the best of our knowledge, these are all the available reports on targeted gene knockdown for therapeutic purposes in MPS diseases, all of them relying on siRNA-based molecules. Among other RNA-based drugs competent to promote gene downregulation, ASOs are clearly gaining momentum, although no gSRT studies have yet been carried out with these molecules. ASOs offer precision and specificity, because they are designed to target specific mRNA sequences, allowing reduction of a specific substrate without broadly affecting other cellular processes. As a consequence, side effects with ASOs are reduced compared to non-specific inhibitors. Both these features are shared by ASOs and siRNAs, which, however, rely in distinct in delivery mechanisms. Unlike siRNAs, which need to be encapsulated or chemically conjugated with different types of ligands, ASOs can be directly targeted to the CNS without such modifications, using IT administration.

Delivery-related issues are often overlooked during the early investigative or *in vitro* stages of research. We believe that to take RNA-based drugs to another level that ensures a smooth clinical translation of the molecules under pre-clinical development, delivery systems cannot be ignored.

Aims

The present work had as main goal to develop RNA-based therapies for Mucopolysaccharidoses type III (MPS III). Today, MPS III disorders, which comprise four subtypes, A-D, all characterized by a severe neurological involvement, still remain without effective therapies available.

Taking advantage of the ability of RNA-based therapeutics to trigger different responses by activating diverse mechanisms of action, we outlined two major research lines. One focused on the design of mutation-specific approaches to correct abnormal splicing events in MPS III-related genes underling known pathologies. The other relied on the selective downregulation of gene(s) involved in the glycosaminoglycans' (GAGs) biosynthetic cascade to promote substrate reduction.

Despite being based on substantially different principles, these two approaches face many common challenges.

This thesis is divided in two major parts, each having its specific aims. Part I addresses the preclinical evaluation of a mutation-specific therapeutic approach for MPS IIIC, the most challenging of all MPS III diseases, using a modified U1 snRNA vector specifically designed to correct the splicing defect caused by a common MPS IIIC-causing variant. Part II is dedicated to the development of a genetic substrate reduction (gSRT) approach applicable to the entire MPS III group, using different candidate molecules, namely small-interfering RNAs (siRNAs), splice-switching oligonucleotides (SSOs), and gapmer antisense oligonucleotides (ASOs), to promote targeted downregulation of a specific gene of GAG biosynthetic pathway.

Part I

General Aim:

Reinforcement of the preclinical evaluation of the therapeutic potential of a previously designed engineered U1 snRNA vector, tested in patient-derived fibroblasts, to counteract the effect of the c.234+1G>A variant in the *HGSNAT* gene, a common mutation underlying a severe form of MPS IIIC.

Specific aims:

- Generation of a midigene for overexpressing the target mutation, enabling functional analysis of the c.234+1G>A variant.

- Evaluation the expression of the midigene, as well as of the potential of the previously designed U1 snRNA vector to correct the c.234+1G>A variant in an artificial *in vitro* system.

- Generation of an *in vivo* model for transient and sustained expressing the human c.234+1G>A variant, to allow for both efficacy and toxicity assessments.

- Evaluation of the ability of the modified U1 snRNA vector to correct the abnormal splicing pattern generated by the c.234+1G>A variant, while assessing its potential risk of toxicity *in vivo*.

Part II

General Aim:

Development and validation of an RNA-based gSRT for MPS III targeting *XYLT1*, a gene involved in the early stage of GAGs' synthesis.

Specific aims:

- Design and *in vitro* validation of three distinct RNA-based therapeutics in MPS III patient-derived fibroblasts: siRNAs, SSOs and ASOs.

- Comparison of the effect of those molecules upon its target gene, *XYLT1*, aimed at choosing the most promising for subsequent analyses.

- Assessment of the capacity of the selected RNA molecules to decrease the *XYLT1*-encoded protein, xylosyltransferase I (XT-I) levels.

- Evaluation of the effectiveness of the best performing drugs to reduce heparan sulfate (HS) storage in MPS III-derived fibroblasts.

Materials and Methods

1. Part I

1.1. Therapeutic approach to correct the c.234+1G>A mutation in the *HGSNAT* gene using an engineered U1snRNA vector fully complementary to the mutant 5'ss of exon 2 – *in vitro* studies

1.1.1. Midigene cloning and construction

For the *in vitro* splicing approach, wild-type (wt) and mutant midigenes were constructed. The wt *HGSNAT* midigene, here designated as pHGSNATwt, includes the human *HGSNAT* gene full coding sequence (exons 1 to 18) as well as partial sequences of intron 1 (437 bp) and intron 2 (435 bp). This midigene was constructed by NZYTech (Lisboa, Portugal) using a synthesized *HGSNAT* gene sequence, which was cloned into the pcDNA 3.1® vector (Invitrogen™, Waltham, Massachusetts, USA) (Figure 16).

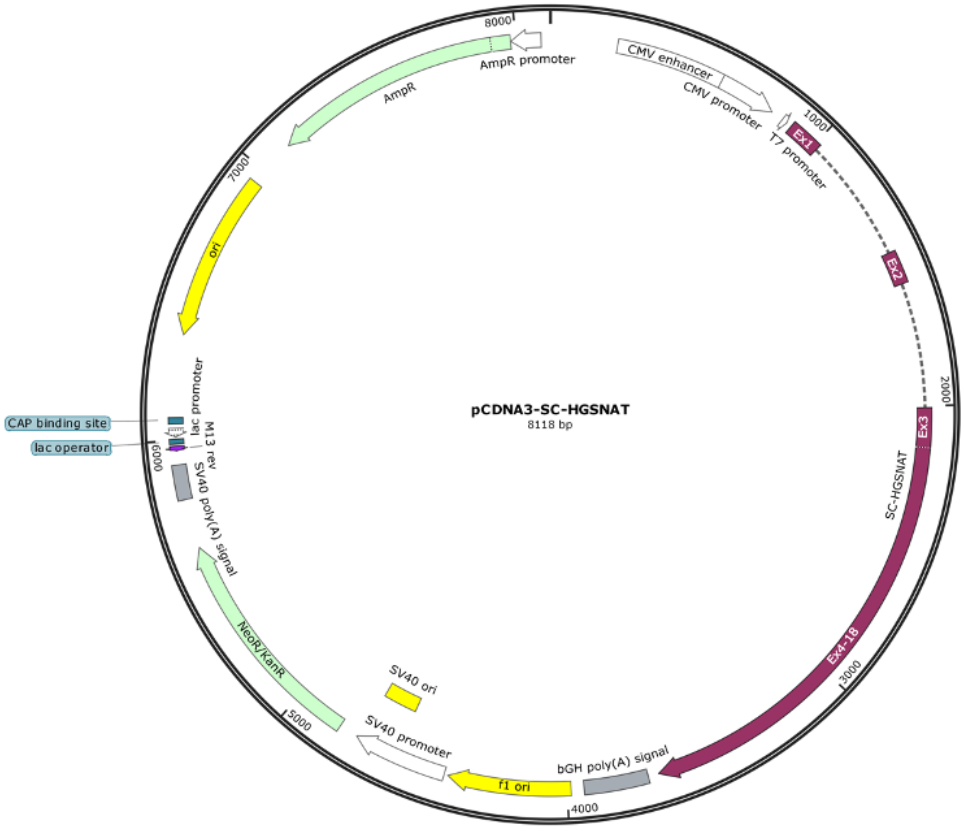


Figure 16. Schematic representation of the pcDNA 3.1® vector with the wild-type *HGSNAT* gene sequence from exon 1 to 18 and partial sequences of intron 1 (437 bp) and intron 2 (435 bp) cloned into the Nhe I and Xba I restriction sites. The full length cloned fragment spans 2780 bp. [Image was created with SnapGene software (San Diego, USA)].

The *HGSNAT* midigene harboring the mutation under study, c.234+1G>A, designated as pHGSNAT+1A, was obtained by site-directed mutagenesis using the QuikChange Lightning Site-Directed Mutagenesis® kit (Agilent, Santa Clara, Califórnia, USA), according to the manufacturer's instructions. In a PCR tube, the reaction was set up as follows: 5 µl of 10X Reaction Buffer, 1 ng/µl of pHGSNATwt plasmid, 2.5 µl of 20 µM mutagenic forward primer, 2.5 µl of 20 µM mutagenic reverse primer, 1 µl of 10 mM dNTP mix, 1.5 µl of QuikSolution Reagent. The reaction volume was then ajusted to 49 µl with Nuclease-free water, and finally 1 µl of QuikChange Lightning Enzyme was added to the reaction tube. The PCR cycling conditions are described in Table 2.

Table 2. Cycling conditions for the site-directed mutagenesis.

Temperature	Time	Cycles
95 °C	2 min	1
95 °C	20 s	18
60 °C	10 s	
68 °C	4 min 30 s	
68 °C	5 min	1

Digestion followed suit, by adding 2 µl of *Dpn* I restriction enzyme, and incubating them for 5 min, at 37 ºC. Next, the transformation took place using XL10-Gold® ultracompetent cells. A tube of cells was thawed on ice, and 45 µl of cells were transferred to a pre-chilled 1.5 mL round bottom tube. Next, 2 µl of ß-mercaptoethanol mix were added, and the tube incubated on ice. Then 2 µl of the mutated plasmid DNA were added and, swirled to mix. After 30 min on ice, the tube was heat-pulsed for 30 s in a 42 °C water-bath, and chilled again for 2 min on ice. Subsequently, 0.5 mL of pre-heated (30 ºC) NZY$^+$ broth were added, and the tube incubated for 1 h, at 37 °C with shaking at 600 rpm. The mixture was then plated in selection plates (LB agar-ampicillin), which were incubated at 37 ºC, for 16-18 h. After this period, the plates were checked for the presence or absence of individual colonies. Sequencing PCR

1.1.2. Minicultures

In order to obtain plasmid DNA minipreps of pHGSNATwt and pHGSNAT+1A, minicultures of selected bacterial colonies from each case were prepared to allow for its growth. Briefly, 5 mL of LB medium (PanReac AppliChem, Barcelona, Spain) containing 5 µl of ampicillin (100 µg/mL) was added to a 15 mL Falcon tube. Using a steril pipette tip, a single bacterial colony was picked and transferred into the medium by pipetting up

and down. The procedure was repeated for 3–5 individual colonies per condition. The tubes were then incubated at 37 °C in an orbital shaking incubator IKA® KS 4000i (Staufen, Germany) at 220 rpm for 16–18 h.

After incubation, part of the bacterial growth was used to make a glycerol stock (also termed glycerolate) in order to preserve the bacteria containing each one of the plasmids of interest. For each glycerolate, 650 µl of bacterial growth and 350 µl of sterile 30% glycerol were combined in an Eppendorf® tube resulting in a final glycerol concentration of ~10%. The stocks were prepared near a flame. The contents of each tube were then mixed by vortexing and each glycerolate stored at -80°C.

1.1.3. Minipreps

To purify plasmid DNA and prepare DNA minipreps, the Monarch® Plasmid Miniprep kit (New England Biolabs®, Ipswich, Massachusetts, USA) was used according to the manufacturer's directions and recommendations. Briefly, 1.5 mL of bacterial culture (from minicultures) was transferred to a 2 mL Eppendorf® tube and centrifuged for 30 s at 16,000 x g. The procedure was repeated two times until all bacterial growth has been pelleted. The supernatant was then discarded, and the pellet resuspended in 200 µl of Plasmid Resuspension Buffer, by pipetting up and down. Next, 200 µl of Plasmid Lysis Buffer was added and the tube was immediately inverted 5-6 times, until the solution turned clear and viscous. One min later, 400 µl of Plasmid Neutralization Buffer was added, and the tube gently inverted until a precipitate formed. Following a 2 min incubation at room-temperature (RT), the tube was centrifuged at 16,000 x g for 5 min, and the supernatant carefully transferred to a spin column. Another centrifugation took place, this time for 1 min, at the same speed. The flow-through was discarded and 200 µl of Wash Buffer 1 was added. The tube was incubated at RT for 5 min being centrifuged again for 1 min, at 16,000 x g. After the flow-through was again discarded, 400 µl of Wash Buffer 2 was added, and the tube centrifuged again for 1 min, at 16,000 x g. The column was then transferred to a new 1.5 mL tube, and 30 µl of Elution Buffer was added. The column was allowed to rest for 3 min, before a final 16,000 x g centrifugation, for 1 min, to elute the plasmid DNA.

The concentration (ng/µl) and purity of plasmid DNA from each miniprep was measured on a NanoDrop® ND-1000 UV-Vis spectrophotometer (Thermo Fisher Scientific, Waltham, Massachusetts, USA). Minipreps were then stored at -20ºC.

1.1.4. Sequencing PCR

In order to confirm the sequence of the *HGSNAT* gene fragment inserted in the pHGSNATwt and the success of the mutagenesis to obtain the pHGSNAT+1A, the different minipreps were subject to sequencing. For this, the PCR was done using the BigDye™ Terminator v3.1 Cycling Sequencing Kit from Applied Biosystems™, followed by Sanger sequencing, which was performed at the Technology and Innovation Unit of the National Institute of Health Dr. Ricardo Jorge, in Lisbon.

Briefly, two tubes were prepared for each sample, containing 1 µl of BigDye™ terminator, 1 µl of sequencing buffer, 5.5 µl of nuclease-free water, 2 µl of DNA template, and 0.5 µl of 5 µM forward or reverse primer. After placing the samples on the thermocycler, the program described in Table 3 was run. The samples were then sent to Lisbon, on ice, for dye-terminator Sanger sequencing in an ABI 3130XL DNA Analyzer.

Table 3. Cycling conditions for the sequencing PCR.

Temperature	Time	Cycles
96 °C	10 min	1
96 °C	10 s	25
50 °C	5 s	
60 °C	4 min	

1.1.5. Maxipreps

For larger scale preparations of the pHGSNATwt and pHGSNAT+1A midigenes, the selected protocol was that of the NucleoBond® Xtra Maxi Plus Endotoxin Free kit (Macherey-Nagel, Düren, Germany), performed to their specifications. Pre-cultures were grown by inoculating 10 µl of bacterial glycerol stock in 5 mL of LB-ampicillin medium, and incubating for 16-18 h, at 37 ºC, with 220 rpm shaking. Then, 3 mL of each pre-culture were transferred into 150 mL LB-ampicillin medium, inside sterile flasks and incubated for another 16-18 h, at 37 ºC, and 220 rpm. The total amount of bacterial cultures was then centrifuged, on a High-Speed PPCO Centrifuge Tubes (Nalgene™ Oak Ridge T, Thermo Fisher Scientific, Waltham, Massachusetts, USA) for 10 min, at 6,000 x g and 4 ºC, and the resulting supernatants discarded. 12 mL of RES-EF buffer were used to resuspend the bacterial pellets followed by the addition of 12 mL of pre-chilled (4 ºC) lysis Buffer LYS-EF, which was added and thoroughly mixed inverting the tubes 5 times. The mixtures were then incubated at RT during 5 min. Afterward, 12 mL of neutralization buffer NEU-EF were added and mixed immediately by inverting the

tubes until the solution lost its blue colour and viscosity. The tubes were then incubated on ice during 5 min. After checking that the suspension was homogeneous, the lysates were loaded onto a column with a filter and the flow-through was discarded. Each column filter was washed with 10 mL of FIL-EF buffer and then removed. Next, in two steps, the columns were washed first with 90 mL of ENDO-EF buffer and then with 45 mL of WASH-EF buffer. After washing, DNAs were eluted using 15 mL of buffer ELU-EF. 10.5 mL of RT isopropanol were then added to the eluates, and the contents of the tubes mixed before being centrifuged for 30 min, at 15,000 x g and 4 ºC. The supernatants were carefully decanted, and the DNA pellets washed using 70 % ethanol, anticipating a new 15,000 x g centrifugation step for 5 min, after which the supernatants were discarded and the final pellets air-dried. Finally, 300 µl of endotoxin free H_2O were added and the tube incubated at RT in an orbital shaking incubator IKA® KS 4000i (Staufen, Germany). Each maxiprep obtained was validated by standard sequencing analysis, as described in step 1.1.4.

1.1.6. Transfection of the midigenes pHGSNATwt and pHGSNAT+1A in Hep3B and COS-7 cell lines

To evaluate the splicing pattern of the pHGSNATwt and pHGSNAT+1A midigenes, transfections were carried out in two standard cell lines, Hep3B and COS-7. Cells were seeded into 6-well plates (10 cm^2) at a density of 4 x 10^5 per well and cultured in Dulbecco's Modified Eagle Medium (DMEM), high glucose, GlutaMAX™, supplemented with 10% fetal bovine serum (FBS), 1% penicilin/streptomycin (Pen-Strep) and 1% Amphotericin B (all reagents from Gibco™, Thermo Fisher Scientific, Waltham, Massachusetts, USA). Cells were maintained at 37 °C with 5% CO_2 and 24 h after seeding, the different cell lines with a confluence between 80 to 90% were transfected with 2 or 3 µg of pHGSNATwt or pHGSNAT+1A midigenes using the transfection reagent Lipofectamine™ 2000 (LP2000), (Invitrogen™, Waltham, Massachusetts, USA).

Briefly, the volume corresponding to 2 µg or 3 µg of each midigene was diluted in Opti-MEM® medium (Gibco™, Thermo Fisher Scientific, Waltham, Massachusetts, USA) until reaching the final volume of 125 µl. For each case, 10 µl of LP2000 were diluted in 115 µl of Opti-MEM™ medium to a final volume of 125 µl. After a period of 10 min incubation at RT, this LP2000 mix was added to the midigene and Opti-MEM™ solution to allow the formation of liposome-nucleic acid complexes, resulting in a total volume of 250 µl. This mixture was then incubated for 20 min at RT.

During complex formation, the culture medium was removed from each well plate, and the cells were washed with 2 ml of 1X PBS. Afterward, 1 mL of DMEM, high glucose,

GlutaMAX™ medium supplemented with 10% FBS, but without antibiotics and Amphotericin B, was added to each plate. Once incubated, the liposome-nucleic acid complexes were added dropwise to each corresponding well, and the cells were incubated at 37 °C with an atmosphere of 5% CO_2 for 5 h. After this period, the culture medium containing the liposome-nucleic acid complexes was removed and 2 mL of supplemented DMEM medium was added to each well. The cells were then kept in the incubator for an additional period of 24 or 48 h after transfection. As a negative control, 2 µg of the empty pcDNA 3.1® vector were also transfected.

To estimate transfection efficacy, the vector pEGFP (Enhanced Green Fluorescent Protein) was transfected along with each of the pHGSNAT midigenes or with the empty pcDNA 3.1® at a 1:1 ratio (Table 4) and cellular fluorescence was subsequently monitored by fluorescent microscopy (Invitrogen™ FLoid™ Cell Imaging Station).

1.1.7. Co-transfection of pHGSNATwt and pHGSNAT+1A midigenes along with a engineered U1 snRNA vector in the HEK293T cell line

In order to evaluate the effect of a modified U1 snRNA vector on the aberrant splicing caused by the c.234+1G>A variant in the *HGSNAT* gene, HEK293T cells were transfected with pHGSNATwt or pHGSNAT+1A midigenes, along with one of the two U 1snRNA vectors already available in our lab [136]: U1 snRNAwt (containing the wild-type sequence of U1 snRNA; kindly provided by Dr. F. Pagani) and U1 snRNA totally complementary (U1 snRNATC) to the mutated 5'ss of *HGSNAT* exon 2 (modified by site-directed mutagenesis[8]) (Figure 17).

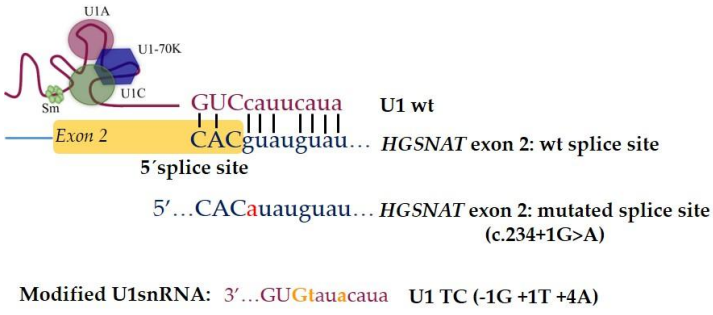


Figure 17. Schematic representation of the therapeutic approach with a modified U1 snRNA to correct the pathogenic effect of the 5' splice site mutation c.234+1G>A in the *HGSNAT* gene. The location of mutation in position

[8] For an extensive review on how to design U1 snRNAs molecules for splicing rescue, see Annex 3, book chapter 1: Matos L, Santos JI, Coutinho MF, Alves S. How to Design U1 snRNA Molecules for Splicing Rescue. *Methods Mol Biol.* 2022 (co-authored by the PhD candidate).

+1 of intron 2 is highlighted in red. The nucleotide changes inserted in the U1snRNA sequence at positions -1, +1 and +4 are illustrated in orange.

To estimate transfection efficacy in the different assays, the vector pEGFP was also co-transfected, and cellular fluorescence was subsequently monitored by fluorescent microscopy (Invitrogen™ FLoid™ Cell Imaging Station). For these assays, HEK293T cells were plated in 6-well plates (10 cm^2) with a density of 8 x 10^5 cells per well. Once the cells reached 80-90% confluence, they were co-transfected in a 1:1:1 ratio with 2 or 3 µg of the p*HGSNAT*wt or mutated midigenes, the U1 snRNAwt or U1 snRNATC vector and the pEGFP vector (Table 4). All transfections were performed using LP2000, following a protocol similar to the one described in point 1.1.6. Cells were collected 24 h post-transfection.

Table 4. Summary of the experimental scheme followed for transfection of the pHGSNATwt or pHGSNAT+1A midigene and the pEGFP vector and co-transfection of the pHGSNATwt or pHGSNAT+1A midigenes with the U1 snRNAwt or U1 snRNATC vectors and the pEGFP vector.

Transfection
2 µg pcDNA3.1® + 2 µg pEGFP
2 µg or 3 µg pHGSNATwt + 2 µg or 3 µg pEGFP
2 µg or 3 µg pHGSNAT+1A + 2 µg or 3 µg pEGFP
Co-transfection
2 µg or 3 µg pHGSNATwt + 2 µg or 3 µg U1snRNATC + 2 µg or 3 µg pEGFP
2 µg or 3 µg pHGSNATwt + 2 µg or 3 µg U1snRNATC + 2 µg or 3 µg pEGFP
2 µg or 3 µg pHGSNAT+1A + 2 µg or 3 µg U1snRNAwt + 2 µg or 3 µg pEGFP
2 µg or 3 µg pHGSNAT+1A + 2 µg or 3 µg U1snRNATC + 2 µg or 3 µg pEGFP

1.1.8. Analysis of splicing rescue by reverse transcription-polymerase chain reaction (RT-PCR)

1.1.8.1. Total RNA extraction

Total RNA was extracted from cell pellets with the GRS Total RNA Kit – Blood & Cultured cells (GRiSP research solutions, Porto, Portugal) following the manufacturer's instructions. The cellular pellets were resuspended in 100 µl of Red Blood Cell Lysis Buffer and lysed by vigorous shaking with 400 µl of Buffer R1 and 4 µl of β-mercaptoethanol, then incubating at RT for 5 min. Afterward, 500 µl of 70% ethanol were added to the lysate and 500 µl of this mixture transferred to an RNA mini spin column, followed by centrifugation at 16,000 x g for 1 min.

After discarding the flow-through, this step was repeated for the remaining sample. Then, 400 µl of Wash Buffer 2 was added to the sample. After that, and to eliminate any DNA residues that could be present in the sample, a mixture of 45 µl of DNase I reaction buffer and 5 µl of DNase I solution was also added and an incubation step of 10-15 minutes at RT performed. Next, three wash steps were carried out, using Wash Buffers 1 and 2, always with centrifugations in between and throwing away the flow-through. After that, a longer centrifugation (3 min) was done to dry the column matrix. Finally, 50 µl of RNase-free water was applied to the center of the column and incubated for 1-2 min at RT. A subsequent 1 min centrifugation was performed to elute RNA. The RNA concentration was then quantified with the UV-Vis spectrophotometer NanoDrop® ND-1000 (Thermo Fisher Scientific, Waltham, Massachusetts, USA), and stored at -80ºC when not used immediately.

1.1.8.2. cDNA synthesis

After RNA extraction and quantification, first-strand cDNA synthesis was performed using the Ready-To-Go™ You-Prime First-Strand Beads kit (Cytiva, Marlborough, Massachusetts, USA), following the manufacturer's instructions. A volume corresponding to 2 µg of RNA was placed in a 1.5 mL Eppendorf® tube, which was then filled with RNase-free water to a total volume of 30 µl and heated for 10 min, at 65 ºC, followed by a thermal shock on ice for 2 min. This RNA solution was then transferred to the supplied tube containing first-strand reaction beads, where 1 µl of oligo $(dT)_{18}$ primer mix (50 µM) (NZYTech, Lisboa, Portugal) and 2 µl of RNase-free water were added, to a final volume of 33 µl. The tubes were incubated for 1 min, before gently vortexing, spinning-down, and incubating them for 1 h, at 37 ºC.

1.1.8.3. RT-PCR and products purification

The RT-PCR analysis was performed using ImmoMix™ Red (Bioline, London, UK) and the primers listed in the Table 5.

Table 5. Primer sequences used for cDNA amplification of pHGSNATwt and pHGSNAT+1A midigenes as well as pcDNA 3.1® vector.

Primer	Oligonucleotide sequence (5' → 3')	Annealing site
pCMV5.1 Fw	GGGACTTTCCAAAATGTCGTA	CMV promoter
Ex3 Rv2	TTCTTTCTCTTCCAAGGTGTC	*HGSNAT* gene
pfGHr1 Rv	TTTATTAGGAAAGGACAGTGGG	pcDNA 3.1®

The amplification program started with an initial denaturation step of 10 min at 95 °C. This was followed by 35 cycles of denaturation at 94 °C (45 s), annealing at 57°C (45 s) and extension at 72 °C (60 s). A final extension step was performed at 72 °C for 10 min. The RT-PCR products were then analysed on a 2% agarose gel and all cDNA fragments of interest were extracted from gel for subsequent purification with the Wizard® SV Gel and PCR Clean-Up System (Promega, Madison, Wisconsin, USA). After the excision of the fragment using a sterile blade, it was transferred to a pre-weighed 1.5 mL Eppendorf® tube. The weight of the gel slice was determined by subtracting the weight of the empty tube from the total weight.

Then, Membrane Binding Solution buffer was added at a ratio of 10 µl of solution per 10 mg of agarose gel slice. The sample was vortexed and incubated at 65 °C for 10 min. Afterward, the dissolved gel mixture was transferred to the SV Minicolumn assembly and incubated for 1 min at RT. A centrifugation step of 1 min at 16,000 x g was performed and the liquid in the Collection Tube discarded. Next, 700 µl of Membrane Wash Solution were added and then the SV Minicolumn centrifuged. As previously, the liquid was discarded and the wash repeated with 500 µl of Membrane Wash Solution.

The sample was again centrifuged at 16,000 x g during 5 min and the flow-through discarded. Following this, an additional centrifugation of 1 min was performed to evaporate any residual ethanol. The SV Minicolumn was then transferred to a clean 1.5 ml microcentrifuge tube and 50 µl of Nuclease-Free Water applied directly to the center of the column without touching the membrane with the pipette tip. The column was incubated for 1 min at RT, followed by a 1 min centrifugation at 16,000 × g to elute the sample. Direct DNA sequencing was then carried out as described in step 1.1.4.

To confirme the identity of the transcripts, the sequences were compared to the *HGSNAT* reference sequence ENSG0000016502 from Ensembl (www.ensembl.org) using the Clustal Omega bioinformatic tool (https://www.ebi.ac.uk/jdispatcher/msa/clustalo). This analysiswas performed to evaluate the effect of the modified U1 snRNA's in rescuing the normal splicing pattern.

1.2. Therapeutic approach to correct the c.234+1G>A mutation in the *HGSNAT* gene using an engineered U1 snRNA vector fully complementary to the mutant 5'ss of exon 2 – *in vivo* studies

1.2.1. Transient expression of the pHGSNATwt or pHGSNAT+1A midigenes in wild-type mice

1.2.1.1. Animal procedures

All the animal procedures were approved by the *Trás-os-Montes e Alto Douro University* (UTAD) and the *Direção-Geral de Alimentação e Veterinária* (DGAV, approval number 021988) according to the national legislation (Decreto-Lei 113, 7 de agosto) and european legislation (Diretive 2010/63/EU).

A total of 25 wt male C57BL/6 mice, with 7 weeks of age were used in this study. The animals were purchased from Charles River Laboratories (France). Upon arrival, the animals were randomly distributed among cages and subjected to a quarantine period that lasted for two weeks, allowing them to adapt to the new animal facility conditions. The animals were kept in controlled environmental conditions, at a temperature of 23 ± 2°C, a photoperiod of 12 h of light and 12 h of darkness and a relative humidity of 50 ± 10%. Animals were housed in hard polycarbonate cages with smooth surfaces and round corners (Dimensions: 375x215x150 mm; Eurostandard Type IV S 1500U, Tecniplast, Italy), coated with core corn (Ultragene, Santa Comba Dão, Portugal). They were fed with a standard pellet diet (Diet Standard 4RF21®, Mucedola, Italy), and tap water bothavailable on an ad libitum basis. In order to calculate the animals' average daily water and food consumption, the masses of water and feed were recorded using a KERN® PLT 6200-2A precision scale (Dias de Sousa S.A., Alcochete, Portugal).

To allow for the body mass record of each animal, mice were individualy identified through markings on the tail with a permanent marker. These brands were refreshed daily. Individual body mass was measured using the previously mentioned precision scale.

1.2.1.2. Hydrodynamic injection and animals sacrifice

After a two-week of acclimatization period, wt C57BL/6 mice were randomly distributed among 5 groups (n=5). The animals were then administered with 1X PBS (negative control) or varying concentrations of the midigene pHGSNATwt or pHGSNAT+1A via hydrodynamic injection in the tail vein to allow for transient liver-directed expression of the respective midigenes.

Based on a published protocol by Balestra *et al.*, [137], the experimental groups received either only 1X PBS solution (negative control) or 1X PBS combined with the volume corresponding to 1 µg/g or 2 µg/g of the pHGSNATwt or pHGSNAT+1A midigene (Figure 18).

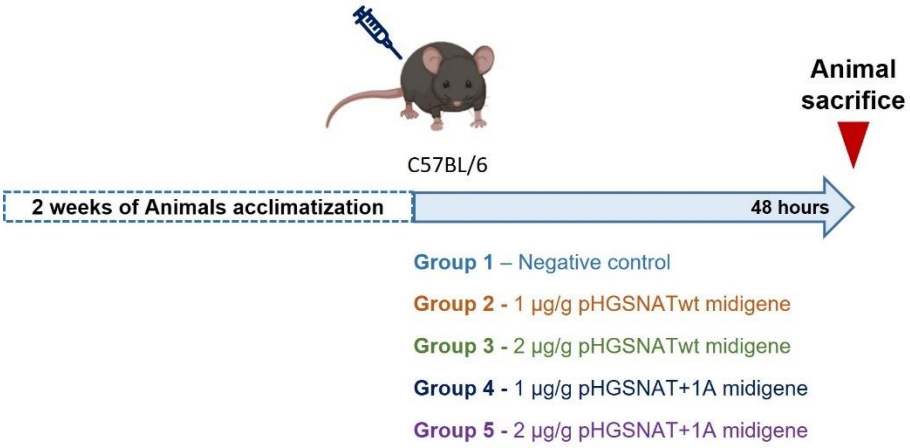


Figure 18. Representative diagram of the experimental assay in wild-type male C57BL/6 mice for analysis the splicing patterns of the pHGSNATwt and pHGSNAT+1A midigenes.

All animals tested received an injection volume equivalent to 7% of their body weight. The calculation of the administered volume for each animal was carried out using two formulae:

$$\text{Volume to inject (mL)} = 7\% \frac{\text{Animal body weight (g)}}{10\ \text{g/mL}} + 0.1\ \text{mL of 1X PBS solution}$$

$$\text{Delivery solution (1X PBS volume in mL)} = \text{Volume to inject(mL)} - \text{volume of midigene (mL) (1 µg/g or 2 µg/g)}$$

After 48 h of incubation, the animals were sacrificed by an overdose of the anesthetic agent Xyslazine (Rompun® 2%, Bayer Healthcare S.A., Kiel, Germany) and Ketamin (Clorketam 1000, injectable solution, Vetoquinol, Barcarena, Portugal) administered intraperitoneally (IP). After verifying that the animals did not respond to stimuli, they were exsanguinated by cardiac puncture, in accordance with FELASA (Federation of European Laboratory Animal Science Associations) guidelines. The organs were then removed, and the spleen, heart, liver, lungs, and kidneys were collected. Each organ was examined macroscopically and any changes found were

registered. All organs were weighed and cuted into small fragments and preserved at -80ºC for subsequent RNA extraction.

1.2.1.3. Evaluation of pHGSNATwt and pHGSNAT+1A expression in wild-type mice

Total RNA was extracted from liver samples using the GRS Total RNA Kit – Tissue (GRiSP research solutions, Porto, Portugal) following the manufacturer's instructions. Approximately 25 mg of frozen liver tissue were cut and transferred to a 1.5 mL RNase-free microcentrifuge tube. To the sample, 400 µl of Buffer R1 and 4 µl of β-mercaptoethanol were added and, using the micropestle provided, tissue sample was grinded. The tissue lysate was then passed throught a 20-G needle syringe 10 times, followed by a 5 min incubation at RT.

Then, a filter column was placed in 2-ml collection tube, and the sample transferred and centrifuged at 1,000 x g for 1 min. The filter column was discarded and 400 µl of 70% ethanol was added to the filtrate, mixing well by shaking vigorously. 500 µl of the sample mixture was then transferred to a RNA mini spin column and centrifuged at 16,000 x g for 2 min. The flow-through was discarded and the remaining sample transferred to the same spin column. The centrifugation step was repeated. Total RNA obtained was then converted into cDNA as described in 1.1.8.2. RT-PCR and sequencing analyses were also performed as previously described for *in vitro* studies (see 1.1.8.3. and 1.1.4., respectively).

1.2.1.4. Statistical analysis

The median daily water and food consumption per animal and the relative organ mass, were calculated using the following formulae:

$$\text{Median water consumption per day (g)} = \frac{\text{Initial water mass} - \text{Final water mass}}{\text{number of days between final and initial weighing x number of animals per cage}}$$

$$\text{Median food consumption per day (g)} = \frac{\text{Initial food mass} - \text{Final food mass}}{\text{number of days between final and initial weighing x number of animals per cage}}$$

$$\text{Relative mass of organs} = \frac{\text{Organ mass}}{\text{Final body mass of animal}}$$

The mean and standard error of the body mass for each animal and the relative mass of each organ were calculated using Microsoft excel® (Microsoft Office®; version 16.49). Subsequently, statistical analysis was performed using the GraphPad Prism® software for Windows (version 8.0.1). Statistical significance between groups was determined by analysis of variance (ANOVA), followed by the Tukey's multiple comparisons test. The significance level of $p<0.05$ was used.

1.2.2. Sustained expression of the pHGSNATwt or pHGSNAT+1A midigenes in wild-type mice

In the first *in vivo* assay, both midigenes (pHGSNATwt and pHGSNAT+1A) were administered to wt C57BL/6 mice using the hydrodynamic injection technique to test their transient expression in the liver of these mice. Moreover, we also tested the sustained expression of both wt and mutant human *HGSNAT* gene cassettes packaged into adeno-associated viral (AAV) vectors, to evaluate the therapeutic effect of our modified U1 snRNATC. For this, we established a collaboration with Prof. Rik Gijsbers from the Leuven Viral Vector Core facility (University of Leuven – Belgium) and four different AAVs were acquired.

1.2.2.1. Selection of the best performing AAV serotype

To select the most effective AAV serotype to be used in our AAV constructs, a specific quantity (9.07×10^9 vector genomes (vg)/ animal) of the serotypes AAV2/5, AAV2/7, AAV2/8 and AAV2/9 was tested in FVB/N mice (n=3) by intravenous (IV) injection.

Two weeks after, the mice were sacrificed and their organs collected, in the same way as referred in section 1.2.1.2. RNA extraction was performed from liver samples using the method described in 1.2.1.3. and converted into cDNA as described in 1.1.8.2. Quantitative real-time PCR (qRT-PCR) was carried out in CFX96 Touch Real-Time PCR Detection System (Bio-Rad Laboratories, California, USA) (Figure 19).

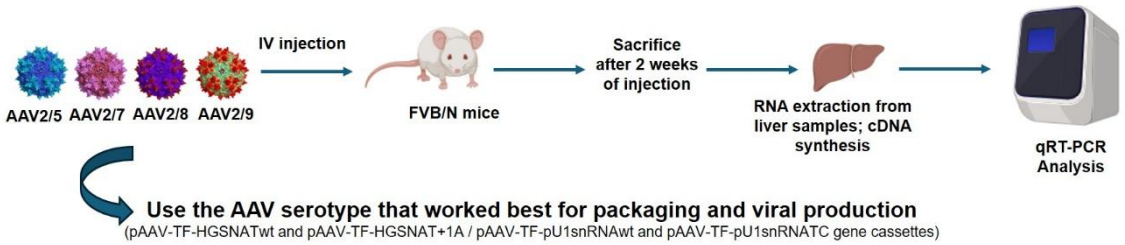


Figure 19. Representative diagram of the experimental assay for AAV serotype selection in wild-type FVB/N mice. IV- intravenous injection.

To analyse the expression levels of each serotype, we had as a target a region of the WPRE (Woodchuck Hepatitis Virus Post-transcriptional Regulatory Element) sequence present in the AAV vector before the bGH poly(A) signal region.

Briefly, a mix containing SsoAdvanced™ Universal SYBR® Green Supermix and primers for the WPRE sequence or for the albumin (*ALB*) gene was prepared as described in table 6. Albumin was used as an internal control for normalization.

Table 6. Preparation of the quantitative real-time PCR mix.

Component	Volume per reaction
SsoAdvanced™ Universal SYBR® Green Supermix (2x)	10 µl
Primer Fw WPRE or *ALB*	2 µl
Primer Rv WPRE or *ALB*	2 µl
Nuclease-free H_2O	5 µl
cDNA	1 µl

In a second assay, and using the remaining volume of each AAV vector solution, an intraperitoneal (IP) injection was also performed to evaluate if there is a difference in the expression efficacy of AAV serotypes due to the administration route. FVB/N mice were used, and all the procedures repeated as listed before.

1.2.2.2. Intraperitoneal injection of different AAV2/9 vectors in wild-type FVB/N mice

A total of 55 wild-type female FVB/N mice, with 4 weeks of age, were purchased to Charles River Laboratories (France). Upon arrival, the animals were maintained in the same conditions described in 1.2.1.1. Then, to validate the engineered U1 snRNA therapeutic approach for the *HGSNAT* 5'ss mutation, the animals were divided into 11 groups of 5 animals each and IP-injected with different combinations and quantities of the AAVs: AAV2/9_HGSNATwt, AAV2/9_HGSNAT+1A, AAV2/9_U1snRNAwt and

AAV2/9_U1snRNATC, as detailed in table 7, with a final injection volume of 400 µl. A dose-dependent effect of the constructs was also tested.

Table 7. Data on the injections of each AAV2/9 construct in mice and the combinations between them. "vg" means vector genome.

Group	AAV	Quantity
1	0.9% saline solution	
2	AAV2/9_HGSNATwt	2.83×10^{10} vg
3	AAV2/9_HGSNAT+1A	2.83×10^{10} vg
4	AAV2/9_HGSNATwt **+** AAV2/9_U1snRNAwt	2.83×10^{10} vg **+** 1.13×10^{11} vg
5	AAV2/9_HGSNATwt **+** AAV2/9_U1snRNATC	2.83×10^{10} vg **+** 1.13×10^{11} vg
6	AAV2/9_HGSNAT+1A **+** AAV2/9_U1snRNAwt	2.83×10^{10} vg **+** 1.13×10^{11} vg
7	AAV2/9_HGSNAT+1A **+** AAV2/9_U1snRNATC	2.83×10^{10} vg **+** 1.13×10^{11} vg
8	AAV2/9_U1snRNATC	1.13×10^{11} vg
9	AAV2/9_HGSNAT+1A	1.13×10^{11} vg
10	AAV2/9_HGSNAT+1A **+** AAV2/9_U1snRNATC	1.13×10^{11} vg **+** 1.13×10^{11} vg
11	AAV2/9_HGSNAT+1A **+** AAV2/9_U1snRNATC	1.13×10^{11} vg **+** 2.26×10^{11} vg

A schematic representation of AAV2/9 vectors containing the human HGSNATwt and U1 snRNAwt sequences can be seen in Figure 20 (the corresponding mutant constructs are not displayed).

After 2 weeks of incubation the animals were sacrificed according to described in 1.2.1.2.

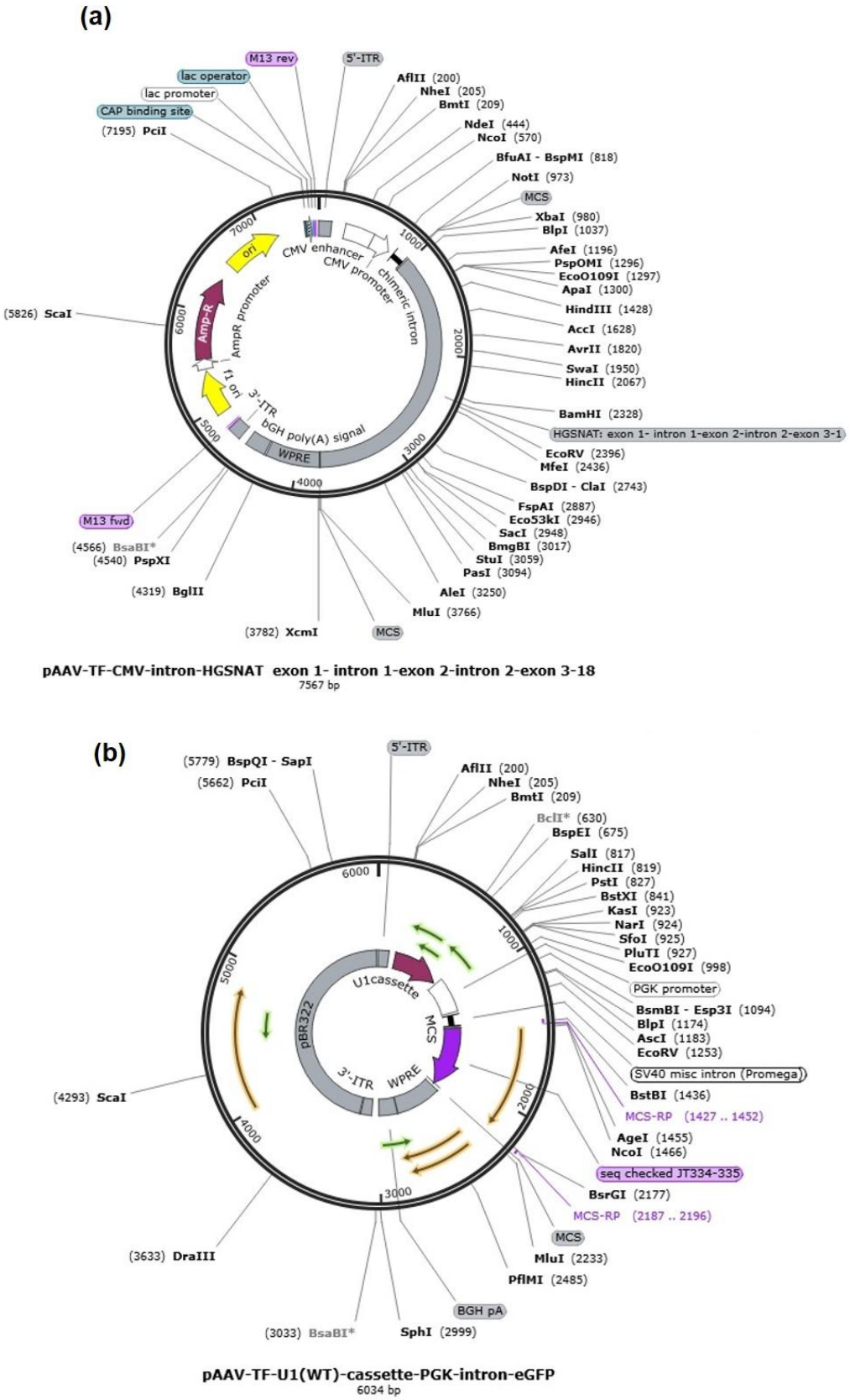


Figure 20. Schematic representation of the AAV2/9 vector containing the (a) human wild-type *HGSNAT* gene sequence from exons 1 to 18, along with partial sequences of introns 1 and 2 and (b) U1 snRNA wild-type sequence. [Image was created with SnapGene software (San Diego, USA)].

1.2.2.3. Evaluation of the AAV2/9_HGSNATwt, AAV2/9_HGSNAT+1A, AAV2/9_U1snRNAwt and AAV2/9_U1snRNATC expression in mice and assessment of splicing pattern rescue

Total RNA was extracted as previously referred (see 1.2.1.3.) The cDNA synthesis and RT-PCR were also performed as described before but using the combination of primers described in table 8.

Table 8. Primers sequence used for cDNA amplification of constructs expressed in mice.

Primer	Oligonucleotide sequence (5' → 3')	Annealing site
pCMV5.1 Fw	GGGACTTTCCAAAATGTCGTA	CMV promoter
Ex1 Fw	TCTTCGGGGCGCGATGCCCA	*HGSNAT* gene (exon 1)
Ex3 Rv1	CCTGCTTTTGGACTCTGAGG	*HGSNAT* gene (exon 3)
Ex3 Rv2	TTCTTTCTCTTCCAAGGTGTC	*HGSNAT* gene (exon 3)

We designed specific primers for the human *HGSNAT* sequence, taking into account the mismatch sites between the mouse and human genomes. Additionally, one of the *forward* primers was designed to anneal with the promoter sequence of the human cytomegalovirus (CMV), which is located located upstream of the *HGSNAT* gene in the construct (see Figure 20a). The CMV promoter is included in plasmids because it is a strong, constitutive promoter that drives high levels of gene expression in mammalian cells.

For RT-PCR analysis, two different combinations of primers were used: a) Ex1 Fw/ Ex3 Rv1 and b) pCMV5.1 Fw/ Ex3 Rv2, depending of the fragment to be amplified. The first combination was used to amplify an *HGSNAT* fragment comprising exons 1 to 3 in animals injected with AAV2/9_HGSNATwt (group 2) and in animals injected with AAV2/9_HGSNAT+1A plus AAV2/9_U1snRNATC (group 7). The second combination of primers allows for the detection of exon 2 skipping and was used in animals injected with AAV2/9_HGSNAT+1A (group 3).

For the first combination of primers (a), the amplification program consisted of an initial step of 10 min at 95 °C, followed by 40 cycles of denaturation, annealing and extension at 94 °C (45 s), 56 °C (45 s) and 72 °C (30 s), respectively, and a final extension at 72 °C for 10 min. For the second (b), the protocol was quite similar, but with an annealing temperature of 60 °C (45 s) and an extension time of 1 minute per cycle. The sequencing analyses were performed as previously described for *in vitro* studies (see 1.1.4.).

1.2.2.4. Histological analysis

The organs collected in the necropsy were immersed in 10% neutral buffered formaldehyde (ITW Reagents, Germany) for at least 24 h (ITW Reagents, Germany). Sections of paraffin-embedded samples were stained with hematoxylin and eosin (H&E) and observed by light microscopy.

Immunohistochemical studies were performed to investigate possible histological alterations in the liver of the mice due to the AAVs expression. These analyses were made in collaboration with Doctor Ana Canadas Sousa from ICBAS (Instituto de Ciências Biomédicas Abel Salazar), University of Porto, Portugal.

1.2.2.5. Statistical analysis

The mean and standard error of the body mass for each animal as well as the relative mass of each organ, were calculated using Microsoft excel® (Microsoft Office®; version 16.49). Subsequently, statistical analysis was performed using the same method described in 1.2.1.4.

2. Part II

2.1. Genetic substrate reduction approaches for Mucopolysaccharidoses type III

2.1.1. RNA-based molecules design

2.1.1.1. Small interfering RNAs (siRNAs)

A pool of three different siRNAs targeting the *XYLT1* gene, along with one negative control, was designed and synthesized by riboxx RNA Technologies (Riboxx GmbH, Radebeul, Germany) (Table 9). These siRNAs are synthetic double stranded RNAs (dsRNA) well-validated for RNAi, with a typical length of 24 bp, and are composed of adenosines, cytosines, guanosines and uridines. iBONi siRNAs harbor no chemical modifications apart from an RNAi-cap, whose patent was pending when this work started. According with studies from the company who developed this technology, in addition to conferring resistance to serum nucleases, the RNAi-cap technology also increaed the overall potency of siRNA and reduced off-target effects [187].

Table 9. Small-interfering RNA (siRNA) sequences used in this study.

Designation	siRNA sequence (5' -> 3')		Size (nt)
	guide	passenger	
Negative control	ACAACAUUCAUAUAGCUGCCCCC	GGGGGCAGCUAUAUGAAUGUUGU	23
siRNA pool anti-*XYLT1*	UAAAUAUCUAAAGUGUCCCCC	GGGGGACACUUUAGAUAUUUA	21
	AUAUUCUACAAACCUCCGGCCCCC	GGGGGCCGGAGGUUUGUAGAAUAU	24
	AUAAAUCAUUCUCAGGCAGCCCCC	GGGGGCUGCCUGAGAAUGAUUUAU	24

2.1.1.2. Splice-switching oligonucleotides (SSOs)

For the design and selection of the most promising SSOs, we followed the guidelines and parameters previously described by Aartsma-Rus [188,189]. Since our ultimate goal was to achieve gene-specific knockdown, we designed ASOs complementary to constitutive exons of the *XYLT1* pre-mRNAs to promote aberrant exon skipping. To do so, we started by extracting the mature mRNA sequence for the target

gene (*XYLT1*) from GenBank (https://www.ensembl.org/Homo_sapiens/Transcript/Exons?db=core;g=ENSG00000103489;r=16:17101769-17470960;t=ENST00000261381) and selecting the exons whose sequence is not a multiplie of 3 nucleotides, as their removal would disturb the open reading frame (ORF) and generate premature termination codon (PTC)-containing mRNAs. Theoretically, those abnormally truncated mRNAs would then be degraded through nonsense-mediated mRNA decay. For *XYLT1*, which is composed of 12 exons, there were seven different exons whose skipping held potential to have the desired effect: 3, 4, 5, 7, 9, 10, or 11. Thus, those were our targets for the upcoming assessments.

Briefly, the secondary structure of each target exon and its respective flanking intronic regions (50 bp each) was assessed using the mfold software (http://www.unafold.org/mfold/applications/rna-folding-form.php) [190]. From the most stable structures mfold identified, partially open and partially closed regions were selected for further analysis as these are the most appropriate locations for SSO binding. Next, the information regarding the secondary structure of the transcript was combined with the data collected from ESEfinder 3.0 software concerning the presence of enhancers along the sequence of the exon in order to select those regions where both analysis overlap, that is, the partially open and partially closed regions that also contain the highest number of predicted enhancer elements.

Having the target regions established, several potential SSO ASOs were designed spanning around 20 nucleotides, and their sequences tested for a number of parameters. First, their GC content and melting temperature (Tm) were assessed, and only the sequences with a GC content between 40-60% and a Tm above 48 °C were selected. Next, free energy of the SSO and SSO-SSO complexes was calculated using the software RNAstructure (http://rna.urmc.rochester.edu/RNAstructureWeb/index.html) [191]: for the first, the option “Predict a Secondary Structure” was selected and for the second, the option “bifold” was chosen. Ideally, the free energy of the SSO should be above -4, while the free energy of the SSO-SSO complexes should be above -15. Using the same software (and the option “bifold”), the binding energy between each putative SSO and the target sequence was calculated. This binding energy is a measure of the strength of the annealing between the SSO and its target sequence and should ideally be between 21 and 28 for optimal results [189]. Finally, after narrowing the number of SSOs to the most promising candidates, those sequences were subjected to a BLAST analysis using the nucleotide BLAST tool hosted by the NCBI database

(https://blast.ncbi.nlm.nih.gov/Blast.cgi) and Ensembl Blast (http://www.ensembl.org/Multi/blastview), in order to ensure their uniqueness and avoid the possibility of off-target effects. Sequences that shared a certain degree of homology with other related or unrelated genes were avoided (stretches of 15 or more homologous nucleotides), allowing a maximum of five mismatches, as oligonucleotides with up to five mismatches have been reported to successfully bind to their targets and induce exon skipping. As final step, we used "The Human Protein Atlas project" webtool (http://www.proteinatlas.org/) [192] to examine the expression of the genes with the highest levels of similarity to our oligonucleotides and select those SSOs which affected the least amount of tissues, reducing the possibility of off-target effects in multiple organs.

Ultimately, only SSOs targeting exons 4, 5, 9, 10 and 11 of *XYLT1* gene were selected, as only for these exons could we design SSO ASOs that met all (the above-referred) criteria. SSOs were synthesized and purified by Eurogentec (Seraing, Belgium) as 2'-MOE RNA molecules containing a full-length phosphorothioate (PS) backbone. The sequences of the SSOs are listed in table 10.

Table 10. Sequences of splice-switching oligonucleotides (SSOs) and their target exons in *XYLT1* gene.

SSO designation	SSO sequence (5' -> 3')	Target exon
SSO 1	GCATGTACTCCACGGAGTCC	Exon 4
SSO 2	TGTACTGCCTGGAGACCTGGA	Exon 5
SSO 3	TACAAGGTGAGTGTCACGTC	Exon 9
SSO 4	TTACCTCGGAAAACTGAAGC	Exon 10
SSO 5	GCAACGAGGAATTTGGTCTC	Exon 11

The localization scheme of each SSO is represented in Figure 21.

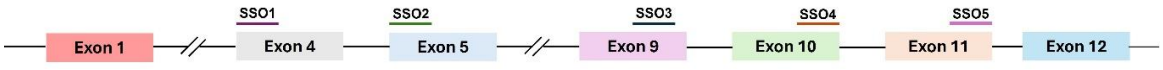


Figure 21. Schematic representation of SSOs target sites in corresponding exons of *XYLT1* gene.

2.1.1.3. Gapmer antisense oligonucleotides (ASOs)

Five different gapmer ASOs targeting the *XYLT1* gene, along with one negative control were synthesized by IDT (Integrated DNA Technologies, Coralville, Johnson County, Iowa, United States) (Table 10). These ASOs are 5-10-5 gapmers using fully

PS-modified linkages with a central segment of 10-mer DNA flanked by 5-mer 2'MOE on both wings.

Table 1. Sequences of Gapmer ASOs and their target exons in *XYLT1* gene. NA- not applicable.

Gapmer designation	Gapmer sequence (5' -> 3')	Target exon
Scramble	CCTATAGGACTATCCAGGAA	*NA*
G1	CGATGCAGGTAATTAGAGCG	5
G2	GTCAGCAAGGAAGTAGAGGT	10
G3	GTCAGGCTCATCGTAGACAT	9
G4	GCAACACATCTGGCTAGGAT	12
G5	ACAATCTTGGGACCAGGAGA	3'UTR

2.1.2. Cell Culture and RNA-based molecules transfection

2.1.2.1. Cell culture

Fibroblasts of the four subtypes of MPS type III disease (MPS IIIA, IIIB, IIIC and IIID) were purchased from the biobank at Istituto Giannina Gaslini (Genoa, Italy). The cells were cultered in DMEM (Gibco™, Thermo Fisher Scientific, Waltham, Massachusetts, USA) high glucose medium, supplemented with GlutaMAX™ and 10% FBS (Gibco™, Thermo Fisher Scientific, Waltham, Massachusetts, USA), 1% Pen-Strep (Gibco, Thermo Fisher Scientific, Waltham, Massachusetts, USA), and 1% Amphotericin B (Gibco™, Thermo Fisher Scientific, Waltham, Massachusetts, USA) at 37 °C and 5% CO_2. Once the cells reached around 80% confluence, they were either passaged into new flasks or frozen in vials for cryopreservation, depending on the experimental requirements. This process was repeated up to 3 times before proceeding with the transfection experiments. For all experiments, fibroblasts were seeded in 6-well plates at 1,8 x 10^5 cells per well and/ or in T-75 flasks at a density of 1,125 x 10^6 per flask, depending of the subsequent analysis. Specifically, for RT-PCR, qRT-PCR and Liquid chromatography-tandem mass spectrometry (LC-MS/MS) cells were plated in 6-well while T75 flasks were used for WB analysis. The cells were seeded 24 h prior to transfection and incubated under the same conditions described above.

2.1.2.1.1. siRNAs transfection

Fibroblasts from all four MPS III subtypes were cultured as described in 2.1.2.1. Cells were plated in 6-well plates and transfected with a siRNA pool using riboxx® FECT as the transfection reagent at a final concentration of 20 nM. Fibroblasts were harvested 24 and 48 h post-transfection for subsequent qRT-PCR analysis.

2.1.2.1.2. SSOs transfection

Fibroblasts at 80% confluency were transfected with 5 ordered SSOs, at different concentrations namely 100, 200 and 300 nM. The SSOs were mixed with Opti-MEM™ (Gibco™, Thermo Fisher Scientific, Waltham, Massachusetts, USA) containing 10 µl of LP2000 (Invitrogen™, Carlsbad, USA) in a 6-well plate, according to the manufacturer's instructions. As already referred on section 1.1.6., where midigenes transfection was described, after 5 h of transfection, the medium was replaced with fresh DMEM containing FBS and Pen-Strep.

The cells were harvested for RT-PCR analysis, as described later, at 24 and 48h post- transfection. After this analysis, the 2 most promising SSOs along with the best concentration, were selected for further experiments. Again, cells were seeded in T-75 flasks, in order to increase the amount of transfected cells, allowing for two distinct analyses: western-blot (WB) and LC-MS/MS. SSOs were transfected under the same conditions refered above, but the volume of the transfection reagent was increased to 75 µl. Cells were harvested 48 and 72 h after transfection.

2.1.2.1.3. Gapmer ASOs transfection

Similar to what has been described for SSOs' transfection, fibroblasts from all four MPS III subtypes at 65-70% confluency were transfected with the five 2'-MOE PS gapmers at 100 nM. For qRT-PCR, cells were harvested 24 and 48 h after transfection, and the best performing gapmer ASOs were selected. After this, fibroblasts were seeded in 6-well plates and in T-75 flasks, depending on the subsequent analysis (as referred in 2.1.2.1.2.). Twenty-four hours later, the two selected gapmers were transfected, under the same conditions described for SSOs. Cells were harvested at various time points for different analyses: 24 h post-transfection for qRT-PCR, 72 and 96 h for WB and at 6 and 10 days for LC-MS/MS.

2.1.3. Evaluation of the effect at mRNA level

2.1.3.1. Quantitative real-time PCR (qRT-PCR) - siRNAs and gapmer ASOs experiments

For the siRNAs and gapmer ASOs, the first tier test to assess treatment efficacy was the confirmation of decreased target gene expression levels by qRT-PCR. Total RNA was extracted from stored pellets using the GRS Total RNA Kit – Blood & Cultured cells (GRiSP research solutions, Porto, Portugal), as described previously (see 1.1.8.1.) and reverse transcribed into cDNA with the Ready-To-Go™ You-Prime First-Strand

Beads kit (Cytiva, Marlborough, Massachusetts, USA) as referred in 1.1.8.2. using 0.5 or 1 µg of total RNA.

qRT-PCR was carried out in a CFX96 Touch Real-Time PCR Detection System (Bio-Rad Laboratories, California, USA). The qRT-PCR mix is summarized in the following in table 11, included primePCR™ SYBR Green Assays for *XYLT1* and *GAPDH* along with SsoAdvanced™ Universal SYBR® Green Supermix, with a final volume of 20 µl.

Table 2. Preparation of the quantitative real-time PCR (qRT-PCR) mix.

Component	Volume per reaction
SsoAdvanced™ Universal SYBR® Green Supermix (2x)	10 µl
PrimePCR™ SYBR Green Assays	1 µl
Nuclease-free H_2O	Variable
cDNA	3 µl or 2 µl

The 96-well plate was then sealed using and adhesive cover for spin-down and placed in the thermocycler for amplification, following the program described in table 12.

Table 3. Cycling conditions for the quantitative real-time PCR (qRT-PCR).

Temperature	Time	Cycles
95 °C	30 s	1
95 °C	15 s	40
60 °C	30 s	

The relative expression of *XYLT1* was calculated using the Livak method ($2^{-\Delta\Delta Ct}$ method) [193], using *GAPDH* as the internal control for normalization.

2.1.3.2. RT-PCR analysis - SSOs experiments

For the SSOs experiments, on the other hand, the first tier test for assessing treatment efficacy was the analysis of splicing patterns. Total RNA was extracted and reverse-transcribed into cDNA using the method described before (section 1.1.8.2.). Next, the PCR analysis was performed using ImmoMix™ Red (Bioline, London, UK) and the primers listed in the table 13. The amplification program was as follows: an initial step of 10 min at 95 °C, and then 35 cycles of 96 °C (45 s), 56/ 58 °C (45 s) and 72 °C (60 s), with a final extension cycle of 10 min at 72 °C. PCR products were then analysed on 2%

agarose gels, and all cDNA fragments obtained were excised from the gel and purified with the Wizard® SV Gel and PCR Clean-Up System (Promega, Madison, Wisconsin, USA). Direct DNA sequencing was carried out in an ABI 3130xl DNA Analyzer (Applied Biosystems, Foster City, California, USA) (as described in section 1.1.4.). To confirm the transcripts identity, sequences were compared to the *XYLT1* reference sequence ENSG00000103489 (www.ensembl.org) using the Clustal Omega bioinformatics tool (https://www.ebi.ac.uk/jdispatcher/msa/clustalo).

Table 4. Primers sequences used for cDNA amplification of diferent *HGSNAT* exons.

RT-PCR fragments	Oligonucleotide sequence (5' → 3')	Tm (ºC)
XYLT1-exon 4/5F	GCTGATGCCTGAGAAGGTGA	58
XYLT1-exon 4/5R	GAGAGAAACGCCACCAACTG	58
XYLT1-exon 9F	GCCAGTACAAGCACATCGT	56
XYLT1-exon 9R	CAGCAAGGAAGTAGAGGTGC	56
XYLT1-exon 10F	CTTGTACCACTCCTTTGCCC	56
XYLT1-exon 10R	CACGGTCACATTAGGTCCCT	56
XYLT1-exon 11F	CTCTGGAGACCTGGGTGATG	56
XYLT1-exon 11R	CGGGGTTTAGGCTCTGGAA	56

2.1.4. Evaluation of the effect at protein level

2.1.4.1. Protein extraction

Frozen cell pellets were thawed on ice and ressuspended in an adequate amount of RIPA buffer (25 mM Tris, pH = 7.6, 150 mM NaCl, 1 % nonidet P40, 1% sodium deoxycholate and 0.1% SDS) with 0.0 % Protease Inhibitor cocktail (Sigma-Aldrich®, St. Louis, Missouri, EUA). The suspensions were kept on ice for 1 h, resuspending every 10 min, before being centrifuged for 5 min, at 3,000 x g, and 4 ºC. The supernatant was then collected into a new 1.5 mL Eppendorf® tube and stored at -20°C until further use.

2.1.4.2. Protein quantification

Total protein quantification was carried out with the Pierce™ BCA Protein Assay Kit (Thermo Scientific™ , Waltham, Massachusetts, USA). Standard dilutions of Bovine Serum Albumin (BSA), provided with the kit, were prepared according to the manufacturer's instructions. Briefly, 10 µl of each sample or BSA standard was pipetted

into the wells of a 96-well microplate (in duplicate), followed by the addition of 80 µl of Working Reagent to each well. The plate was then incubated for 30 min, at 37 ºC.

After cooling the plate to RT, the absorbance was measured at 562 nm, using the spectrophotometer VICTOR® Nivo™ plate reader (PerkinElmer, Inc, Waltham, Massachusetts, USA). The average Abs_{562} blank value was substracted from all standard and sample readings. A standard curve was then generated by plotting the blank-corrected Abs_{562} values of each BSA standard *vs.* its concentration. Linear regression analysis showed a very strong correlation ($R^2 \geq 0.99$). This standard curve was then used to determine the total protein concentration for each sample tested.

2.1.4.3. Sodium Dodecyl Sulphate – Polyacrylamide Gel Electrophoresis (SDS-PAGE)

For SDS-PAGE, 20 µg of protein was mixed with 5 µl of 4X NuPAGE™ LDS Sample Buffer (Invitrogen™, Thermo Fisher Scientific, Waltham, Massachusetts, USA), 2 µl of 10X NuPAGE™ Sample Reducing Agent (Invitrogen™, Thermo Fisher Scientific, Waltham, Massachusetts, USA), and MiliQ water to a final volume of 20 µl. The mix was heated to 70 °C, for 10 min prior to electrophoresis. The PROTEAN® Tetra System was used, with 4–15% Mini-PROTEAN® TGX Stain-Free™ Protein Gels and a buffer dam (Bio-Rad Laboratories, California, USA). The upper and lower buffer chambers were filled with 10X Tris/Glycine/SDS Buffer.

Then, 5 µl of protein ladder was loaded onto the first well of each gel, and 20 µl of each denatured sample mix was loaded onto the remaining wells. A constant voltage of 200 V was set on the power source, and the electrophoresis ran for 35 - 40 min.

2.1.4.4. Western Blot (wb)

Following SDS-PAGE, the stratified proteins were transferred from the gel to a nitrocellulose membrane. A so-called “transfer sandwich” was assembled using blotting paper and held together by a plastic cassette. The cassette was then placed inside the Trans-Blot Turbo Transfer System, and the transfer took 30 min at a constant amperage of 20 mA. The membrane was then incubated with blocking solution (5% Non-Fat Dry Milk (NFDM)/TBST) milk for 2 h, at RT, on a shaker. Then, the blocked membrane was cut into two sections, around the 70 kDa molecular weight marker. Each section was then incubated overnight with its respective primary antibody, at 4 °C, on a shaker (table 14). The lower half of the membrane, corresponding to the proteins of lower molecular weight, was incubated with α-tubulin antibody (the loading control used in this study) (Sigma-Aldrich, St. Louis, Missouri, USA), diluted 1:5000 in blocking buffer. The upper

section, containing the heavier proteins was incubated with α-XYLT1 antibody (US Biological Life technologies, Massachusetts, USA), diluted 1:1000 in blocking buffer.

After washing the membrane 3 times for 10 min with wash buffer, both membrane sections were incubated for 1 h with the respective secondary antibodies. The lower section, containing the antibody-bound tubulin protein, was incubated with goat α-mouse IgG-HRP antibody (invitrogen™, Thermo Fisher Scientific, Waltham, Massachusetts, USA) diluted 1:5000 in blocking buffer. The upper section, containing the XYLT1 antibody-bound protein, was incubated with the mouse α-rabbit IgG-HRP antibody (Santa Cruz Biotechnology, Dallas, Texas, USA) diluted 1:5000 in blocking buffer (table 14).

Table 5. List of antibodies used in Western Blot.

Antibody	Dilution	Host species	Company
α-XYLT1	1:1000	Rabbit	US Biological
α-tubulin	1:5000	Mouse	Sigma-Aldrich
α-rabbit IgG-HRP	1:5000	Mouse	Santa Cruz Biotechnology
α-mouse IgG-HRP	1:5000	Goat	Invitrogen™

The sections were then washed again 3 times for 10 min, after which they were incubated with ECL solution for 5 min, protected from the light. Excess solution was drained, and the image was captured on a ChemiDoc™ XRS+ imaging system (Bio-Rad Laboratories, California, USA).

2.1.5. Evaluation of the effect at heparan sulfate levels

2.1.5.1. Heparan sulfate and dermatan sulphate (DS) quantification by LC-MS/MS

Heparan sulfate (HS) and dermatan sulphate (DS) levels were quantified by LC-MS/MS in MPS III cell homogenates, treated or non-treated with the selected SSOs and gapmer ASOs, after butanolysis reaction, according to the method recently described by Forni and co-workers [194]. Briefly, cell homogenates were prepared by sonication, and their protein concentration determined with the same method described in section 2.1.4.2. Each individual cell homogenate was aliquoted into two different plates, one for HS and one for DS. The samples were then dried under a stream of nitrogen and 75 µl of 3N HCl in N-butanol was added to each plate well. For HS measurements, samples were incubated for 60 min at 90 °C. For DS measurements, on the other hand, samples were heated for 25 min at 65 °C.

After the incubations, samples were cooled to RT for 10 min and dried again under a stream of nitrogen. Then, 30:70 (v/v) water/acetonitrile solution was added to the samples: 100 µl for HS quantification and 250 µl for DS quantification. After a brief vortex, the HS samples were combined with their respective DS counterparts and vortexed again. Finally, dimers derived from the butanolysis reaction were chromatographed on a HPLC using a gradient of acetonitrile and water (LC column: Gemini® 3µm C6-Phenyl 110 Å,100 x 2 mm, from Phenomenex) and detected on a triple quadrupole mass spectrometer (API4000 QTRAP,Sciex, Danaher Corporation, Washington, D.C., USA). Samples were quantified by interpolation from a calibration curve prepared to cover a concentration range of 0.39 to 50 µg/mL.

2.1.6. Statistical analysis

All experiments were performed at least three times, with data presented as mean ± standard deviation. To compare the means between groups, one-way ANOVA was performed, followed by Tukey's multiple comparisons test. Differences were considered statistically significant if the p-value was less than 0.05. All tests were performed using GraphPad Prism® software for Windows (version 8.0.1).

Results and Discussion

1. Part I: Therapeutic approach to correct the c.234+1G>A mutation in the *HGSNAT* gene using an engineered U1 snRNA vector fully complementary to the mutant 5'ss of exon 2

In the absence of an animal model carrying the homologous c.234+1G>A mutation, the need arose to find an effective option to evaluate the therapeutic efficacy of our modified U1 snRNA *in vivo.* Only that would allow to continue the preclinical validation of this the therapeutic strategy, as *in vitro* evidence had already been obtained using patient-derived fibroblasts carrying this variant in homozygosity [136].

The generation of such an animal model, would be quite time-consuming and expensive, particularly having in mind a knock-in mouse or a humanized model expressing that human variant. Thus, we followed an alternative path, having opted to generate a mouse capable of expressing the human *HGSNAT* sequence including both the wild-type (wt) and the c.234+1G>A variants.

To achieve this, a midigene containing the coding sequence of the human *HGSNAT* gene alongside partial sequences of introns 1 and 2 (pHGSNATwt) was constructed. Using site-directed mutagenesis, we generated a mutant version, pHGSNAT+1A, incorporating the G-to-A transition at position +1 of intron 2. The primary objective was to generate mouse models expressing these midigenes in the liver to evaluate the therapeutic efficacy of the mutation-specific modified U1 snRNA vector. However, our initial tests were conducted *in vitro* using various cell lines to assess the ability of both midigenes to replicate the splicing patterns of the wild-type and mutant variants, as well as the capacity of the U1 snRNA to rescue the defective splicing caused by the c.234+1G>A variant.

This strategy was inspired on that applied in a previous study by Balestra *et al.,* [137], who used hydrodynamic injection as well as AAVs to promote the expression in the liver of wild-type mice of a plasmid harboring the sequence of their target gene. In that original work it had been assessed the therapeutic potential of an exon-specific U1snRNA to correct a disease-causing variant of Hemophilia B, using an elegant experimental design that allowed not only for splicing rescue assessments *in vivo*, but also for toxicity studies. Thus, drawing upon their methodology, we adapted a similar approach for the c.234+1G>A *HGNSAT* variant.

Initially, transient expression of our constructs was attempted via hydrodynamic injection. However, due to the low expression levels of both midigenes, likely resulting from technical limitations, we opted for sustained expression using AAV vectors. In this approach, co-injection of our modified U1 snRNA, also delivered via AAV vectors, successfully corrected the mutant splicing defect, demonstrating the feasibility of our therapeutic strategy.

Overall, the results obtained through these *in vitro and in vivo* studies, are summarized and extensively documented over the following sections.

1.1. *In vitro* functional studies to evaluate the splicing patterns promoted by *HGSNAT* midigenes and the therapeutic correction potential of the modified U1 snRNA

Before proceeding to *in vivo* studies, it was preliminary tested if the pHGSNATwt and pHGSNAT+1A midigenes (wild-type and harboring the mutation, respectively) reproduced the expected splicing patterns *in vitro*, transfecting them into two different cell lines: COS-7 and Hep3B. Briefly, the pHGSNATwt midigene, was expected to produce a normal transcript, whereas the pHGSNAT+1A midigene was expected to promote the skipping of exon 2. Once the Hep3B and COS-7 cell lines were established and adequately passaged, they were transfected with either one of the two midigenes. As a negative control, an empty pcDNA 3.1® plasmid (without the insertion of the *HGSNAT* gene sequence) was also transfected. Subsequently, molecular analysis of the cDNA derived from the various transfections was performed.

For the RT-PCR reaction, in order to amplify only the *HGSNAT* fragments produced by the midigenes, but not inadvertently endogenous transcripts, a specific pair of primers was used. The forward primer pairs in a region of the plasmid pcDNA 3.1® (located just before the multiple cloning site of the vector), while the reverse primer targeted the end of *HGSNAT* exon 3, encompassing exon 2. Amplicon sizes were evaluated and compared with those expected for the wild-type and mutant transcripts and then sequenced.

Having checked the ability of our newly generated *HGSNAT* midigenes to promote the expression of the desired transcripts, we proceeded to evaluate the capacity of a previously selected U1 snRNA vector to correct the mutant transcript. As already referred, concerning this U1 snRNA vector, which is fully complementary to the 5'ss of exon 2 harboring the c.234+1G>A variant, its therapeutic potential had already been tackled in MPS IIIC patients' fibroblasts carrying the this mutation [136].

In this work, HEK293T cells were co-transfected with either the pHGSNATwt or the pHGSNAT+1A midigenes together with the U1 snRNAwt or the U1 snRNA vector fully complementary (wherein referred to as U1 snRNATC) vectors, in all possible combinations, and the resulting splicing patterns analysed. Again, amplicons were sequenced to confirm whether they contained the desired correction, meaning that the co-transfection of the pHGSNAT+1A and U1 snRNATC vectors resulted in the inclusion of exon 2, without unpredicted effects consequent to the co-transfection itself, or to the introduction of an exogenous U1 snRNA.

1.1.2. Transfection of pHGSNATwt and pHGSNAT+1A midigenes in Hep3B reproduced the expected splicing pattern

Hep3B cells were transfected with different plasmids, including pcDNA 3.1®, pHGSNATwt, and pHGSNAT+1A, and incubated for 24 and 48 hours. Agarose gel electrophoresis of cDNA fragments obtained from RNA extracted from cells transfected with pcDNA 3.1® (control) showed the presence of a fragment with, approximately, 400 bp as expected (Figure 22).

For cells transfected with the pHGSNATwt midigene, it was possible to observe a band with around 500 bp (534 bp) that corresponds to the normal transcript at both concentrations and incubation times. Notably, for the 48 h incubation period, the intensity of transcripts is greater when compared with that obtained 24 hours post-transfection.

On the other hand, the intensity of bands from cDNA of cells transfected with midigene pHGSNAT+1A was lower, but still at both concentrations and incubation times tested a band of approximately 400 bp (426 bp) was detected, fitting well the expectation for an amplificon with exon 2 skipping.

All bands of interest were excised, purified and sequenced. A normal transcript was observed in the case of pHGSNATwt transfection whereas a transcript with exon 2 skipping was obtained from pHGSNAT+1A midigene transfection (Figure 23).

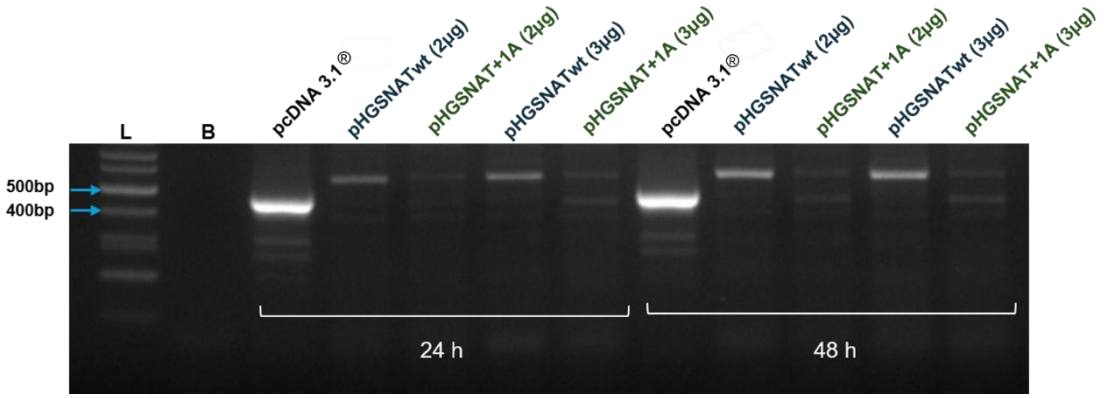


Figure 22. Agarose gel electrophoresis of *HGSNAT* amplification products after Hep3B transfection with pcDNA 3.1®, pHGSNATwt and pHGSNAT+1A, for 24 and 48 hours. L: ladder; B: White; pcDNA 3.1® (2 µg), pHGSNATwt and pHGSNAT+1G (2 µg and 3 µg).

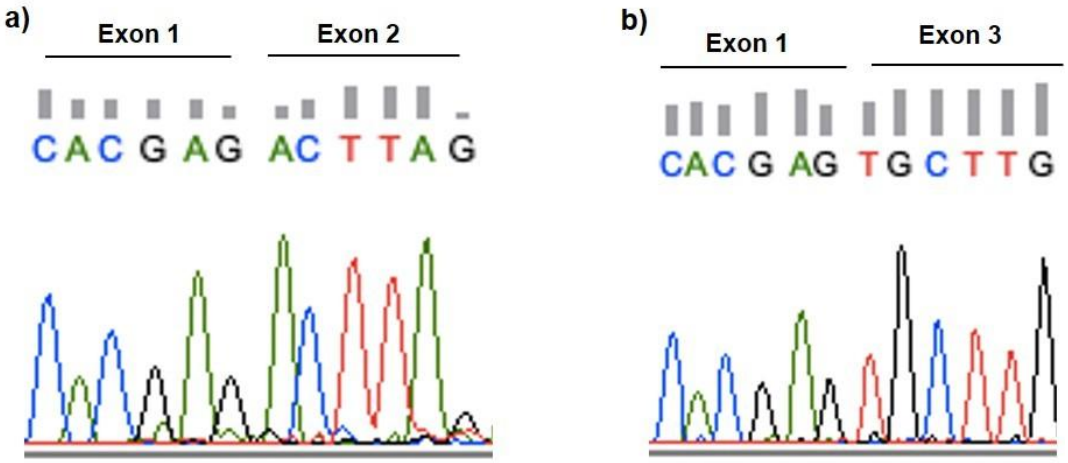


Figure 23. Electropherogram of a portion of the *HGSNAT* transcript sequence obtained after transfection with two midigenes: a) pHGSNATwt; b) pHGSNAT+1A.

1.1.3. Transfection of pHGSNATwt and pHGSNAT+1A midigenes in COS-7 cells also reproduced the expected splicing pattern

As expected, when the same experiments were performed in COS-7 cells, similar results were observed for all conditions. Agarose gel analysis of RT-PCR products from cells transfected with the pHGSNATwt midigene showed the presence of a fragment of around 500 bp (534 bp), which was later confirmed to correspond to the wild-type transcript.

Regarding the cells transfected with the pHGSNAT+1A midigene, it was also possible to detect the presence of a band corresponding to a transcript with *HGSNAT* exon 2 skipping for all tested conditions (Figure 24; pHGSNAT+1A lanes, in green).

Again, the amplicons with the expected size were excised and sequenced, revealing a sequence identical to that observed in cells Hep3B (Figure 23).

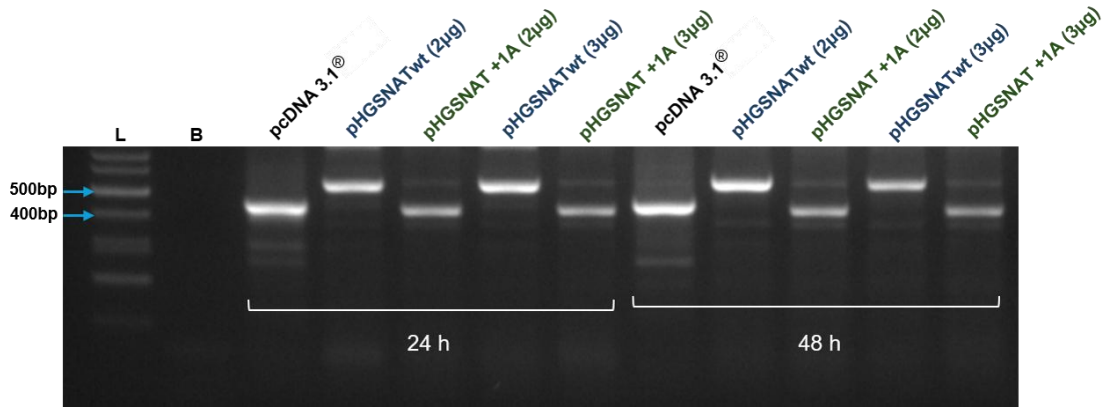


Figure 24. Agarose gel electrophoresis of *HGSNAT* amplification products after COS-7 transfection with pcDNA 3.1®, pHGSNATwt and pHGSNAT+1A, for 24 and 48 hours, respectively. L: ladder; B: White; pcDNA 3.1® (2 µg), pHGSNATwt and pHGSNAT+1G (2 µg and 3 µg).

1.1.4. U1 snRNATC induced a splicing pattern shift

After confirming the ability of the *HGSNAT* midigenes to promote the expression of either wild-type or mutant transcripts, a new set of experiments was performed to assess whether the therapeutic agent U1 snRNATC would allow for the intended correction. This time, all was conducted in a HEK293T cell line, consisting of immortalized human embryonic kidney cells, which were available in our lab with fewer passages and optimized growth conditions.

The plasmids pHGSNATwt or pHGSNAT+1A were co-transfected with one of the two U1snRNA vectors: wild-type or U1 snRNATC (fully complementary to the 5'ss of the c.234+1G>A allele sequence; see Material and Methods, 1.1.7, for further details). To evaluate the transfection efficiency, co-transfections with the pEGFP vector were also performed. Twenty-four hours after initiating the experiment, cells were observed under a fluorescence microscope, and high fluorescence levels were detected for all the tested conditions, as depicted in Figure 25.

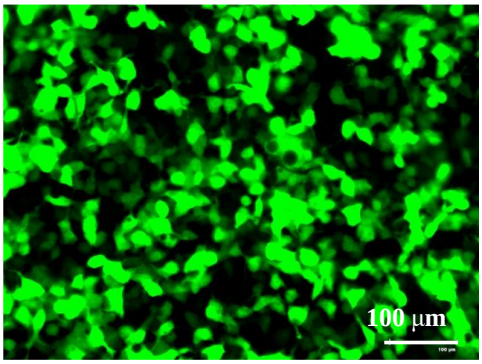


Figure 25. Fluorescence microscopy analysis of HEK293T cells co-transfected with the pHGSNATwt midigene and the U1 snRNAwt vector (24 hours).

As soon as the co-transfection assays were completed, samples were prepared for RNA extraction, followed by cDNA synthesis and RT-PCR analysis. As depicted in Figure 26 for the untreated pHGSNATwt (blue lanes) and pHGSNAT+1A (green lanes) midigenes, RT-PCR confirmed the presence of the expected splicing patterns. The same was also possible for the treated pHGSNATwt samples (with both U1 snRNAwt and U1 snRNATC). For the treated pHGSNAT+1A samples, amplicon sizes were also in line with those expected after treatment with either the wild-type U1 snRNA or the U1 snRNATC.

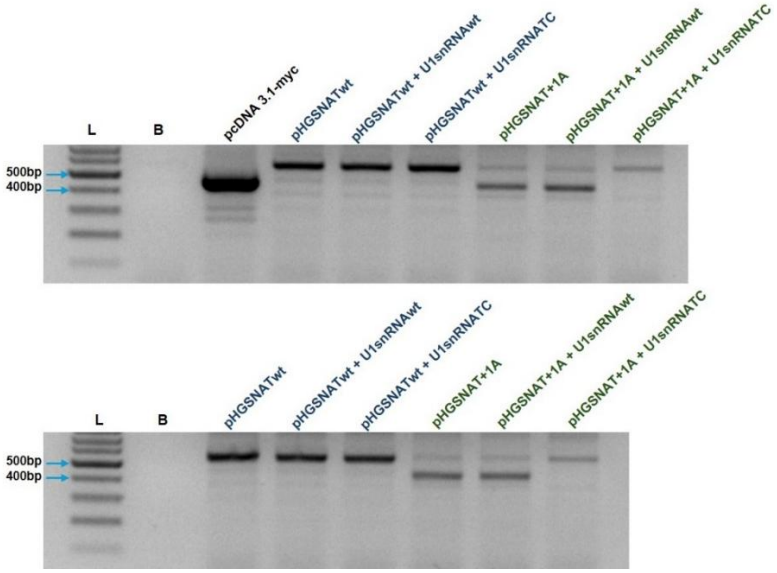


Figure 26. Agarose gel electrophoresis of *HGSNAT* amplification products after HEK293T co-transfection with the pEGFP, pHGSNATwt or pHGSNAT+1A midigene vectors, combined with the U1 snRNAwt or U1 snRNATC during 24 hours. L: ladder; B: blank. Top panel: 2 µg of midigene; Bottom panel: 3 µg of midigene.

Briefly, for the non-treated pHGSNATwt (blue lanes) and pHGSNAT+1A (green lanes) samples, the splicing patterns observed after gel agarose electrophoresis mimicked those already observed in Hep3B and COS-7 cells transfected with the same

midigenes. A fragment of around 500 bp was detected, corresponding to the 534 bp amplicon generated from the normal transcript, while a 426 bp fragment, corresponding to the exon 2 skipping, was observed for the mutant midigene.

Regarding the co-transfections of the wild-type midigene with either U1 snRNAwt or U1 snRNATC, performed as controls, no changes were observed in the electrophoretic profiles. In both cases, a fragment of normal size was detected, identical to that observed for the transfection with the pHGSNATwt midigene alone.

Regarding the tests with the pHGSNAT+1A midigene, differences were observed when it was co-transfected with the U1 snRNAwt or with the U1 snRNATC. Co-transfection with U1 snRNAwt revealed an amplification product of around 400 bp, corresponding the skipping of *HGSNAT* exon 2. However, co-transfection with the fully complementary U1 snRNA, the U1 snRNATC, resulted a shift in the splicing pattern, as was denoted by the presence of a band of around 500 bp detected after gel electrophoresis.

All relevant fragments were excised from the gel, purified and sequenced. However, not all fragments displayed the expected sequences. Summarizing:

a) For the co-transfection of pHGSNATwt with the pEGFP vector or with any of the tested U1 snRNA vectors, the sequences corresponded to the normal transcript (i.e., including exon 2);

b) For the co-transfection of the pHGSNAT+1A midigene with pEGFP or with the U1snRNA wt, the sequences displayed the skipping of exon 2;

c) Undesirably, for the co-transfection of the pHGSNAT+1A with the U1 snRNATC, the sequences not only included the full exon 2 but also the first four nucleotides of intron 2 (ATAT) preceding it. The pattern observed was compatible with homozygosity, supporting the absence of the normal transcript after treatment (Figure 27), though the similar size of that amplicon and that of the normal transcript when inferred by agarose gel electrophoresis (Figure 26, last lane: pHGSNAT+1A + U1 snRNATC).

In a certain sense, these were disappointing results, though they were not entirely unexpected. In fact, the presence of this aberrant transcript had already been observed in patients' fibroblasts, where it represented around 50% of the transcripts, while in the remaining 50%, splicing did occur in a correct way [136].

This original observation was actually the trigger for the studies here undertaken. In HEK293T cells, however, this otherwise encouraging pattern shifted towards the presence of the mutant transcript instead of the desirable normal one.

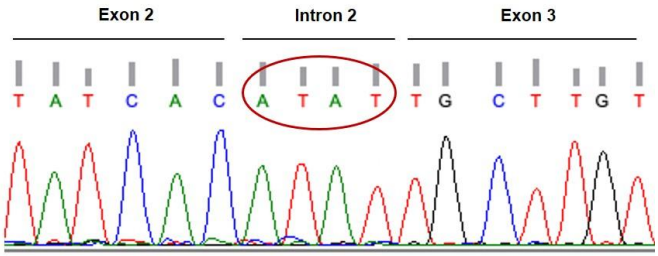


Figure 27. Electropherogram of a segment of the *HGSNAT* transcript sequence obtained after co-transfection of pHGSNAT+1A midigene with U1 snRNATC vector. The insertion of the first four nucleotides from intron 2 is highlighted by the red circle.

1.2. *In vivo* therapeutic approach to correct the c.234+1G>A mutation in the *HGSNAT* gene using an engineered U1 snRNA vector fully complementary to the mutant 5'ss of exon 2

Although the aforementioned results observed in HEK293T cells were not as positive as those obtained by our team in patient-derived fibroblasts, we were convinced that the initial results with endogenous *HGSNAT* levels in patient samples, should not be disregarded.

Thus, an *in vivo* assay appeared to be the most logical next step, aiming to provide definitive proof of whether treatment with the U1 snRNA vector fully complementary to the c.234+1G>A variant may be of therapeutic value or not.

Due to the reasons already presented, in this work we used as a proxy for *in vivo* assessment, the midigenes that had been successfully generated and whose effect mimicked that of the target mutation *in vitro*, following the protocol reported by other researchers [137]. So, plasmid vectors were used to promote the expression of human *HGSNAT* wild-type or c.234+1G>A in mice.

Several assays were carried out, to evaluate the expression of our target mutation in the liver of two different wild-type mouse strains. Our ultimate goal was to check whether the splicing pattern observed after *in vivo* treatment mirrored that seen in the aforementioned cell lines, or resembled the one observed in patients' fibroblasts.

1.2.1. Hydrodynamic injection for transient expression of pHGSNATwt and pHGSNAT+1A midigenes in mouse liver to model the human MPS IIIC c.234+1G>A splicing defect

To explore the expression of the human MPS IIIC c.234+1G>A splicing defect in the liver, midigenes were administered to mice via hydrodynamic injection into the lateral tail vein.

Hydrodynamic delivery was first established in 1999 as a simple and efficient non-viral method for the delivery of plasmids to hepatocytes in mice. Its underlying rationale is actually quite simple. When a remarkably high volume of plasmid-containing solution is injected into the mouse tail vein, it causes a rapid increase in blood pressure and temporarily slows down circulation. As a result, the heart is not able to quickly recirculate plasmid DNA after it passes through the inferior vena cava. Instead, blood flows back into the liver through the portal vein, leading to a rapid increase in liver volume and to a transiently increased permeability of the capillary endothelium. This enlarges pores in cell membranes, allowing the plasmid DNA to enter the cells and remain there once pores close [195,196]. This physical process prevents plasmid DNA from being degraded by DNA enzymes in the bloodstream and enhances transfection efficiency. Regardless of its inherent risks associated with injecting solution volumes as high as 8-10% of the mouse body weight, the method was later adapted to accommodate the delivery of various biologically active materials to cells in various organs in a variety of animal species through systemic or local injection [197]. Still, the traditional tail vein-injection in wild-type mice remains the most widely used approach. The assay conducted as part of this thesis followed the protocol described in the material and methods section 1.2.1.2.

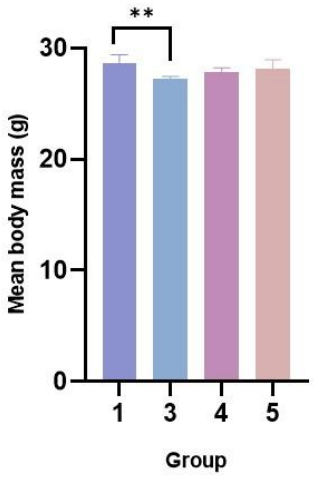
Administration of compounds by hydrodynamic injection is a complex technique that often poses difficulties in execution. In this case, despite the extensive experience of the operator who carried out the test, none of the animals in group 2 (pHGSNATwt 1 µg/g) survived after the injection. Consequently, only the results obtained from the remaining groups, which experienced no mortality, are presented.

The morphometric analysis of C57BL/6 mice revealed significant variations in body mass across experimental groups. The average body mass estimated at the beginning of the study revealed statistically significant differences ($p<0.005$) from the values observed in groups 1 and 3. At the end of the experiment, the animals from group 1 (control group) had a higher average body mass when compared to the groups 3 ($p<0.0001$), 4 ($p<0.001$) and 5 ($p<0.005$). Additionally, animals from group 3 showed a lower average body mass when compared to group 5 ($p<0.05$) (Figure 28). No other statistically significant differences were observed among the groups at the beginning or the end of the study.

a)

Group	Initial body mass	Final body mass
Group 1 (negative control)	28.64 ± 0.74	28.42 ± 0.66
Group 3 [pHGSNATwt (2 µg/g)]	27.22 ± 0.22	25.56 ± 0.22
Group 4 [pHGSNAT+1A (1 µg/g)]	27.84 ± 0.37	26.50 ± 0.51
Group 5 [pHGSNAT+1A (2 µg/g)]	28.14 ± 0.80	26.86 ± 0.64

b)



c)

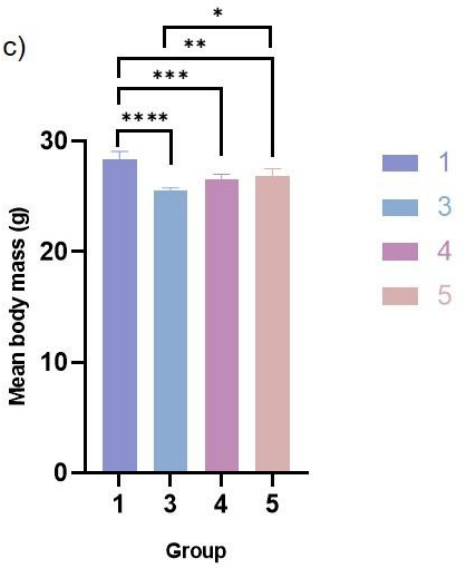


Figure 28. Mean body mass (g) of each animals' group at the beginning and end of the transient expression experiment. a) Table showing the mean ± standard error of body mass for each group (initial and final). b) Graphs obtained after statistical analysis of the data. Comparisons between groups were performed using a one-way ANOVA and a Tukey's multiple comparisons test as a posthoc comparator (*p < 0.05, **p < 0.005, ***p < 0.001, ****p < 0.0001).

Forty-eight hours after the beginning of the assay, the animals were sacrificed and submitted to postmortem examination. Necropsy showed macroscopic damages in the organs of some animals. Changes were noted in the spleen of one animal from group 1 (control), in two animals from group 3 (pHGSNATwt, 2 µg/g) and in three animals from group 4 (pHGSNAT+1A, 1 µg/g). Additionally, two animals from group 5 (pHGSNAT+1A, 2 µg/g) had liver damage. The average relative mass of each organ was calculated, revealing differences in liver mass values when comparing the control group (group 1) to other groups (data with *p* values are presented only for the liver) (Figure 29).

a)

	Group 1 (negative control)	Group 3 pHGSNATwt (2 µg/g)	Group 4 pHGSNAT+1A (1µg/g)	Group 5 pHGSNAT+1A (2 µg/g)
Heart	0.0049 ± 0.0002	0.0052 ± 0.0003	0.0051 ± 0.0003	0.0052 ± 0.0004
Lung	0.0053 ± 0.0003	0.0061 ± 0.0002	0.0058 ± 0.0002	0.0067 ± 0.0002
Spleen	0.0033 ± 0.0002	0.0028 ± 0.0004	0.0025 ± 0.0002	0.0032 ± 0.0004
Liver	0.0600 ± 0.0002	0.0507 ± 0.0003	0.0468 ± 0.0030	0.0483 ± 0.0040
Right kidney	0.0060 ± 0.0002	0.0067 ± 0.0002	0.0064 ± 0.0004	0.0071 ± 0.0005
Left kidney	0.0060 ± 0.0002	0.0065 ± 0.0001	0.0060 ± 0.0004	0.0067 ± 0.0005

b)

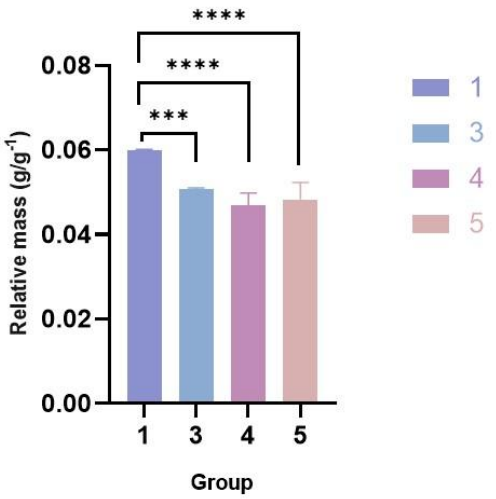


Figure 29. Relative mass (g/g^{-1}) of different organs of each animals' group. a) table presenting the mean ± standard error of organ mass for each group (g/g^{-1}). b) graph obtained after statistical analysis of liver data from animals across different groups. Comparisons between groups were performed using an one-way ANOVA and by Tukey's multiple comparisons test as a posthoc comparator (***p < 0.001, ****p < 0.0001).

1.2.1.1. Splicing pattern analysis of pHGSNATwt and pHGSNAT+1A midigenes in the liver of wild-type C57BL/6 mice: transient expression did not result in widespread expression of the midigenes

Molecular analysis of RNA extracted from liver samples of different animals was performed using the same primers previously utilized in the *in vitro* experiments, along with additional primer combinations for the *HGSNAT* gene. Agarose gel electrophoresis analysis of the resulting *HGSNAT* fragments (Figure 30), showed that the pHGSNATwt midigene was not expressed in any of the 5 animals. In contrast, animals administered with the pHGSNAT+1A midigene, showed a faint band in the region of interest (426 bp)

in some cases (7, 8, 12, 13 and 15). However, only in the case of animal number 12 was it possible to extract the corresponding band from gel, allowing its re-amplification and sequencing. It was confirmed the presence of the human *HGSNAT* transcript without exon 2, demonstrating that pHGSNAT+1A midigene expression occurred in the liver of this animal.

While this is only a preliminary result, it indicates that it might be possible to obtain an animal model to evaluate *in vivo* the effectiveness of the fully complementary U1snRNA vector in restoring the splicing caused by the presence of the c.234+1G>A variant.

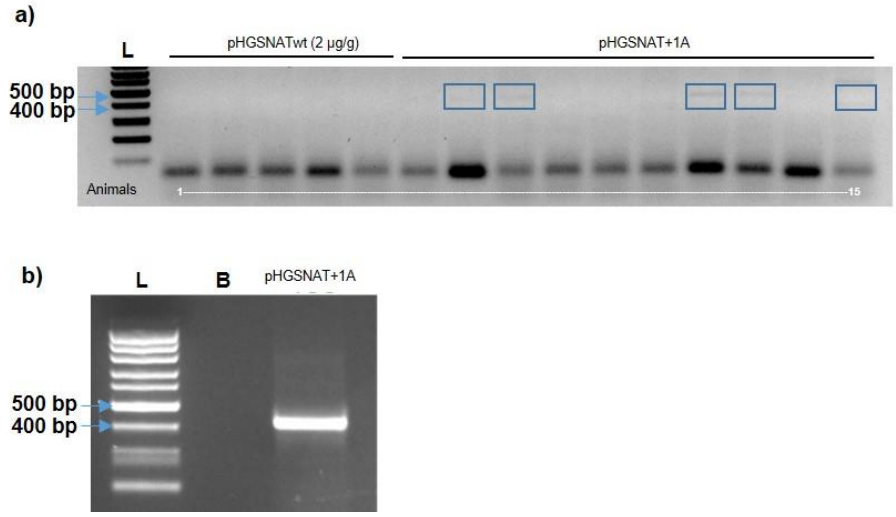


Figure 30. Agarose gel electrophoresis of *HGSNAT* amplification following the injection of pHGSNATwt and pHGSNAT+1A midigenes into wild-type C57BL/6 mice. a) Animals administered with the pHGSNATwt or pHGSNAT+1A midigenes; b) Band corresponding to PCR re-amplification of the purified fragment from animal number 12. L: ladder; B: blank.

It is worth mentioning that the absence of detectable h*HGSNAT* transcripts in most cases was completely unexpected, as our plasmids had been specifically designed to ensure appropriate gene expression after hydrodynamic injection, namely by harboring a strong cytomegalovirus (CMV) promoter.

The capacity of this promoter for driving transgene expression in mouse liver after hydrodynamic gene transfer was well demonstrated by Al-Dosari and co-workers, in 2006 [198]. Through a straightforward luciferase assay, the team evaluated the activities of 14 promoters in driving the expression of that well-known reporter gene. Their systematic analysis spanned four different groups of promoters, including viral promoters, promoters with or without known hepatic activity, and stress-responsive promoters. Amongst the viral promoters was that of CMV, one of the most commonly used and also the select promoter for this work. Remarkably, from the whole panel of 14

promoters, the most active ones were the CMV and AAT promoters. Adding up to this, Balestra and co-workers, in their pivotal work on U1 snRNA-driven correction of transiently expressed splicing variants in mice liver, also used a non-liver specific promoter (SV40) and still the hydrodynamic tail-vein injection approach guaranteed an appreciable delivery of plasmid DNA with significant transgene expression, mainly in liver [137].

All this augmented the initial believe that our design was rational and optimized for successful target gene expression following hydrodynamic injection. Consequently, it does not seem plausible to attribute the lack or inefficient expression of the target gene to the plasmids themselves. More reasonably the failure seems to lie in the injection protocol, concerning which several factors may have accounted for. On the one hand, the mouse strain used in this study (C57BL/6, often referred to as "black 6") is known for its aggressive temperament, and much more hyperactive behavior compared to other mouse strains. In addition, there is another technical challenge common to all transgenic mouse lines derived from black strains, which regards the high difficulty in performing tail vein injections in these mice, as the veins stand poorly contrasted against the dark skin, making them hard to identify.

Since other authors have managed to perform successful hydrodynamic injections in C57BL/6 mice [199,200], regardless the challenges, we must admit that our experience with this injection protocol still needs to be improved. For instance, when we performed hydrodynamic injections administering a volume that corresponded to 10% of the mice's body weight, the animals unfortunately died. This prompted us to lower the injection volume to 7%, which is slightly lower than recommended threshold for this type of injection (8-9% of mouse's total body weight). Probably a few adjustments will help us to optimize this injection technique in a near future.

Another scenario could imply the obvious choice of an albine mouse strain. Reportedly, these mice are easier to handle, in part due to the docile temperament. Furthermore, their tail veins would be much easier to observe.

Given these shortcomings, which realistically could not be solved in the time available to conclude this thesis, an alternative delivery strategy was experimented.

1.2.2. Sustained expression of the h*HGSNAT*wt and h*HGSNAT*+1A in wild-type FVB/N mice using AAV vectors

As an alternative delivery system, our choice fell upon a method known to promote high and sustained levels of gene expression, in contrast to the transient expression provided by the hydrodynamic injection protocol.

Additionally, taking into account the issues regarding the mouse strain used for the hydrodynamic injection studies, the sustained expression assays were done with FVB/N, an inbred mouse strain assumed to be highly suitable for transgenic analyses. FVB/N mice (named after its susceptibility to Friend leukemia virus B), have been often the choice for the generation of transgenic mice by pronuclear microinjection, due to the large and prominent pronuclei in fertilized FVB/N eggs, a feature that facilitates microinjection of DNA. The strain also has a vigorous reproductive performance with consistently large litters, thus increasing the probability of generating viable progeny of the desired phenotype [201].

In this study, we used adeno-associated virus (AAV) vectors to achieve the sustained expression of both the wild-type (h*HGSNAT*wt) and mutant (h*HGSNAT*+1A) midigenes, thereby establishing an *in vivo* model to evaluate the therapeutic effect of the modified U1 snRNA.

Firstly, 4 different AAVs (AAV2/5, AAV2/7, AAV2/8 and AAV2/9) were acquired from the Leuven Viral Vector Core facility (University of Leuven – Belgium) and tested in FVB/N mice to identify which most effectively drove transgene expression.

The assessment involved 3 animals per group that were IV injected with each of the four AAVs, all harboring a reference sequence for the reporter WPRE. The experiment was carried out according to the representative diagram presented in the Material and Methods section 1.2.1.1.

All animals that received the AAV2/8 died shortly after injection and one animal from each of every other group also died. Thus, results were only obtained for the remaining three pairs of animals. Two weeks later, the animals who survived were sacrificed and the expression potency of the AVV-delivered gene assessed through standard procedures. The analysis of AAVs expression was carried out by quantitative real time-PCR (qRT-PCR), measuring the expression levels of the WPRE, whose sequence was inserted into the recombinant AAV vectors.

No finding led to exclude any particular serotype. However, considering that the target organ for the therapeutic approach under investigation would be the brain, and following the recommendations of our international consultants from the Leuven Viral Vector Core facility, the serotype 9 was considered to be the most suitable backbone for constructing the AAV2/9_HGSNATwt, AAV2/9_HGSNAT+1A, AAV2/9_U1snRNAwt and AAV2/9_U1snRNATC vectors [202].

Still aiming at working with a well-designed experimental protocol, a pilot study with the remaining volume of AAV vectors was conducted to compare the effectiveness of intraperitoneal (IP) versus intravenous (IV) injections, evaluating differences in target

gene expression based on the injection route. Based on the analysis, the IP administration was chosen for the final assay, which was carried out as described in material and methods section, 1.2.3.2. The conventional standard operation procedures were followed to monitor each animal throughout the entire assay. The body mass of each animal was recorded at two different time points, the beginning and the end of the experimental assay. Identical precautions were taken during sacrifice and post-mortem analysis. At the end of the protocol the animals were euthanized and their organs were collected, weighed and preserved at - 80ºC.

The molecular analysis of RNA extracted from liver samples of different animals was carried out with four primers designed: for CMV promotor and exon 1 (forward primers) and two for exon 3 (reverse primers), of the *HGSNAT* gene, after an alignment between mouse and human sequences of the gene. The primers designed had one to three mismatches between the two sequences, at the 3' end of the primer to ensure specificity to the human sequence.

The results obtained for this second subset of *in vivo* studies, will be presented in detail in the following sections.

1.2.2.1. Choosing the adequate AVV vector for delivering the constructs - no major differences were observed on the expression levels induced by different AAV serotypes

Animals in group 1 were injected with the AAV2/5 serotype, those in group 2 with AAV2/7, and those in groups 3 and 4 with the AAV2/8 and AAV2/9 serotypes, respectively. The analysis of AAV2/5, AAV2/7 and AAV2/9 expression, in liver samples from the injected animals, showed similar results in the different serotypes. However, since groups 1 and 2 had only two animals each, and group 4 had only one, statistical analysis could not be performed.

Overall, the expression results fell within the expected range for a successful AAV injection for all tested animals, providing no technical reasons to exclude any of the tested AAV serotypes.

For many years AAV2 was the standard serotype used in CNS applications, but more recently, several other AAV serotypes, including AAV5, AAV6, AAV8 and AAV9, have been characterized and tested for neuronal tropism and overall transduction efficiency in neurons, providing in general positive results. Additionally, numerous hybrid AAV vectors have been engineered using capsid protein of AAV serotypes 1-9 with the genome of AAV serotype 2. Increasing evidence suggests that capsid protein is a major determinant of cellular tropism and transduction efficiency of AAV vectors [26].

However, many of these studies also indicated that neuronal subtypes respond differently to viral transduction, making serotype selection an important consideration when designing experiments aimed at the development of CNS-targeted therapies [203]. Notably, AAV9 has already shown interesting results after IV delivery in different animal models of several diseases, including LDSs and motor neuron diseases, opening the way to the first clinical trials in the field [204,205].

Some of those trials were so successful that AAV9-based gene therapy is currently a reality, with one drug already available in the market, Zolgensma (onasemnogene abeparvovec) [206-208]. It uses an AAV9 vector to deliver a functional copy of the *SMN1* gene to motor neurons, which are deficient in individuals with SMA. Several AAV9-based therapies for MPS are progressing through clinical trials, highlighting potential to address both systemic and CNS manifestations of both disorders (reviewed in [14,209]).

In MPS IIIA, for instance, a study based on systemic IV injections of AAV9 to transduce brain cells was successfully conducted in preclinical models [210] and later translated into an ongoing gene therapy clinical trial [58]. Another study using a canine model of MPS IIIA also employed an AAV9 vector carrying the gene for the missing enzyme. After delivery into the cerebrospinal fluid (CSF), the vector enabled long-lasting and widespread expression of the therapeutic gene without causing toxicity, maintaining its effects for seven years post-treatment [211].

Altogether, the AAV9 expression analysis combined with the amount of data supporting the advantages of the AAV9 for therapies aiming at the CNS, led us to select this serotype to construct the different vectors we intended to test.

To increase the chances of success of this novel AAV-based assay, the effectiveness of IP versus IV injections in driving target gene expression was also evaluated.

The remaining volume of AAVs that was not used in the serotype choice assay, was administered to mice by IV and IP routes to compare the differential expression promoted by these two methods.

Apparently, the highest expression levels were observed in the IP-injected animal, but again no statistical analysis could be performed. For the moment interindividual variability cannot be ruled out as a factor influencing the observed difference in expression, an issue that deserves future investigation.

Not ignoring the fragility of the result we refer to as it was based on a single animal per condition it was the finding that based the choice of IP injection as the method to administrate the AAV2/9 constructs in mice.

1.2.2.2. Splicing pattern analysis of h*HGSNAT*wt and h*HGSNAT*+1A in the liver of wild-type FVB/N mice: rescue of the splicing defect by sustained expression of U1 snRNATC

To investigate whether modified U1 snRNA (U1 snRNATC) was able to mediate correction of the HGSNAT+1A splicing mutation, the HGSNAT+1A and the U1 snRNATC expression cassettes were packaged into AAV2/9. As shown in Table 7 in the Materials and Methods section, different combinations of midigene and U1 molecules were performed for mice administration. A dose of 2.83 $x10^{10}$ vg of each midigene, pHGSNATwt and pHGSNAT+1A, was chosen. For the U1 snRNAwt and U1 snRNATC the dose was 1.13 x 10^{11} vg. Additionally, other doses were also administered in different mice in order to verify if there was a dose-related effect of the midigene and/ or U1 snRNATC.

Morphometric parameters of FVB/N mice were carefully monitored throughout the whole experiment. The mean body mass was calculated at the beginning and the end of the study and no statistically significant differences between the groups were observed ($p>0.05$) (Figure 31).

a)

Group	Initial body mass	Final body mass
1	20.68 ± 1.00	22.91 ± 1.07
2	21.13 ± 1.14	22.25 ± 0.89
3	21.12 ± 1.80	22.73 ± 2.38
4	21.79 ± 1.69	23.99 ± 1.44
5	22.01 ± 1.55	23.81 ± 1.22
6	20.43 ± 0.68	23.03 ± 1.01
7	21.23 ± 1.59	23.32 ± 1.90
8	20.44 ± 1.18	23.85 ± 3.26
9	20.52 ± 0.85	23.38 ± 1.79
10	19.75 ± 1.43	21.62 ± 1.94
11	22.56 ± 0.94	24.74 ± 1.42

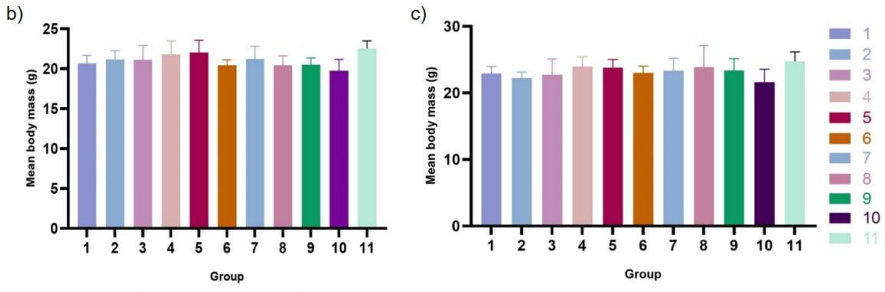


Figure 31. Mean body mass (g) of each animal group at the beginning and at the end of the sustained expression experiment. a) table with mean ± standard error of mean body mass of each animal groups (mean ± standard error). b)

statistically treated data of initial body mass c) statistically treated data of final body mass. Comparisons between groups were analysed using a one-way ANOVA and a Tukey's multiple comparisons test as a posthoc comparator.

Two weeks after the beginning of the assay, the animals were sacrificed and necropsied, without evidencing any macroscopic organs' damages. The average relative mass of each organ was calculated and some statistically significant differences were found in liver mass between group 9 and groups 3, 4, 7, 8 (*p<0.05) and group 6 (**p<0.005) (Figure 32).

a)

	Group 1	Group 2	Group 3	Group 4	Group 5	Group 6
Heart	0.007 ± 0.002	0.005 ± 0.001	0.005 ± 0.001	0.005 ± 0.001	0.005 ± 0,001	0.004 ± 0.001
Lung	0.007 ± 0.001	0.007 ± 0.000	0.007 ± 0.001	0.006 ± 0.001	0.007 ± 0,001	0.007 ± 0.001
Spleen	0.005 ± 0.000	0.006 ± 0.000	0.005 ± 0.000	0.005 ± 0.001	0.005 ± 0,001	0.005 ± 0.001
Liver	0.059 ± 0.002	0.059 ± 0.003	0.058 ± 0.004	0.058 ± 0.003	0.059 ± 0,002	0.057 ± 0.002
Right kidney	0.007 ± 0.001	0.007 ± 0.000	0.007 ± 0.001	0.007 ± 0.000	0.007 ± 0,001	0.006 ± 0.001
Left kidney	0.008 ± 0.001	0.007 ± 0.000	0.007 ± 0.001	0.007 ± 0.000	0.006 ± 0.000	0.006 ± 0.001
Brain	0.015 ± 0.001	0.016 ± 0.002	0.016 ± 0.003	0.015 ± 0.002	0.015 ± 0.002	0.013 ± 0.002

	Group 7	Group 8	Group 9	Group 10	Group 11
Heart	0.005 ± 0.000	0.005 ± 0.001	0.005 ± 0.001	0.005 ± 0.001	0.004 ± 0.001
Lung	0.007 ± 0.001	0.008 ± 0.002	0.007 ± 0.001	0.007 ± 0,000	0.006 ± 0.000
Spleen	0.005 ± 0.001	0.005 ± 0.000	0.005 ± 0.000	0.005 ± 0.001	0.005 ± 0.001
Liver	0.058 ± 0.007	0.058 ± 0.004	0.067 ± 0.005	0.062 ± 0.003	0.062 ± 0.003
Right kidney	0.007 ± 0.001	0.007 ± 0.001	0.007± 0.001	0.006 ± 0.001	0.007 ± 0.000
Left kidney	0.007 ± 0.001	0.007 ± 0.000	0.007 ± 0.000	0.007 ± 0.001	0.007 ± 0.000
Brain	0.014 ± 0.001	0.015 ± 0.003	0.015 ± 0.002	0.015 ± 0.002	0.015 ± 0.002

b)

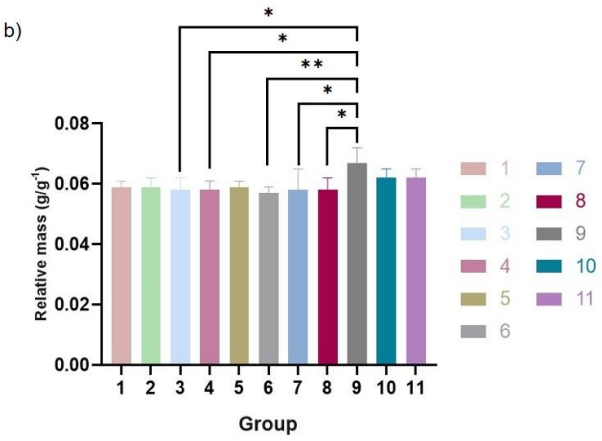


Figure 32. Relative mass (g/g^{-1}) of liver from the animals of different groups for the sustained expression experiment. a) table with mean ± standard error of mass of animal organs (mean ± standard error) (g/g^{-1}). b) graph obtained after statistical treatment of data from animals' liver of different groups. Comparisons between groups were analysed using an one-way ANOVA and a Tukey's multiple comparisons test as a posthoc comparator (*p < 0.05, **p < 0.005).

Immunohistochemical analysis revealed irrelevant signs of toxicity associated with AAVs vectors. The most notable changes, despite minimal, were related to degeneration (rarefaction of the cytoplasm - ballooning cells, cloudy hepatocytes and swollen hepatocytes) alongside with signs of hepatocyte regeneration such as binucleation, mitoses and enlarged single nuclei). Inflammation and fibrosis were the most frequent manifestations, although very discreet, with the inflammation predominantly located in the periportal regions.

Mallory bodies or acidophil bodies appeared in most cases, as it is usually associated with inflammation and fibrosis. Animals 25 and 26 exhibited small foci of necrosis with neutrophils, representing an important but very focal and discrete change.

Currently, there are no specific formal guidelines for the preclinical testing of ASO drugs. Their testing principles generally follows the general ICH M3(r2) guidelines for small molecules, as recommended by the International Council for Harmonisation of Technical Requirements for Pharmaceuticals for Human Use, US FDA, or European Medical Agency (EMA). However, recent initiatives by the Oligonucleotide Safety Working Group (OSWG) and other working groups, along with numerous sponsors and regulators that recognize the uniqueness of these RNA-based drugs, are trying to shift this scenario publishing a series of white papers with numerous consensus recommendations. Regardless of the parameters analysed or the guidelines followed, toxicity evaluation in pre-clinical development is pivotal to ensure the future success of a novel drug. Unfortunately, however, this issue is often neglected as efficacy is generally the primary objective of pre-clinical assessments. That was not the case here, where the performed immunohistochemical analyses strongly support minimal risks of toxicity associated to this U1 snRNATC drug.

Herein, we are presenting only the analysis of the most relevant groups from our *in vivo* experimental assays: groups 2, 3, and 7, which correspond to mice injected with AAV2/9_HGSNATwt, AAV2/9_HGSNAT+1A, and AAV2/9_HGSNAT+1A plus AAV2/9_U1snRNATC, respectively. In the near future, molecular analysis will also be conducted for all other groups included in the experiment.

After molecular analysis, the expected expression of the h*HGSNAT* in mouse liver samples was confirmed by detecting the anticipated splicing patterns. Following IP injection of AAV2/9_HGSNATwt (group 2 animals), a transcript with all exons was observed, whereas the injection of AAV2/9_HGSNAT+1A (group 3 animals) resulted in the detection of a transcript with the skipping of exon 2 (Figure 33). Group 2 consists of animals numbered 6 to 10, which were injected with the wild-type vector, while group 3 includes animals numbered 11 to 15, which received the mutant vector.

Since different primer combinations were used for the two groups (see material and methods section), the expected size of the amplification products also differed: a band of approximately 200 bp was anticipated for AAV2/9_HGSNATwt-injected animals, while a 400 bp band was for the AAV2/9_HGSNAT+1A injected animals. That was the pattern we observed after agarose gel electrophoresis as presented in Figure 33a and 33b, respectively. For the animal number 11, no band was detected in the first RT-PCR. However, when the procedure was repeated, the expected band was observed (Figure 33c). The corresponding bands were extracted from the gel and sequenced, confirming the presence of the expected h*HGSNAT* fragments.

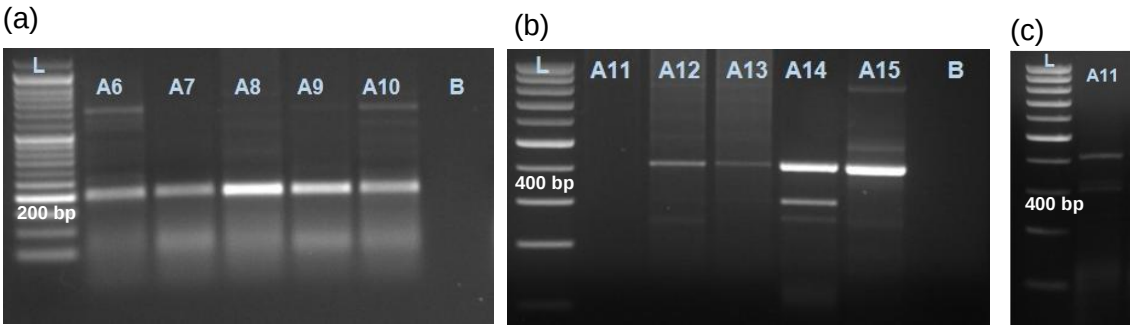


Figure 33. Agarose gel electrophoresis of h*HGSNAT* amplification following the injection of a) AAV2/9_HGSNATwt and b) AAV2/9_HGSNAT+1A into FVB/N mice; c) result from animal number 11 after a second amplification. The animals numbered between 6 and 10 are from group 2 (injected with AAV2/9_HGSNATwt) and the animals numbered between 11 and 15 are from group 3 (injected with AAV2/9_HGSNAT+1A). A: animal; L: ladder; B: blank.

Ideally, all three tested groups should be analysed using both primer pairs. However, amplification using the Ex1 Fw/Ex3 Rv1 primer pair in groups 2 and 7 and the pCMV5.1 Fw/Ex3 Rv2 primer pair in group 3 has proven to be more challenging.

An attempt was made to amplify the h*HGSNAT* fragment in group 3 animals, which were injected with AAV2/9_HGSNAT+1A, using the same primer pair as for groups 2 and 7 (Ex1 Fw/Ex3 Rv1). One animal, number 12, has already been amplified with this primer pair and sequenced, confirming the skipping of exon 2. The amplicon has a 84 bp (Figure 34), supporting the specificity of our analysis.

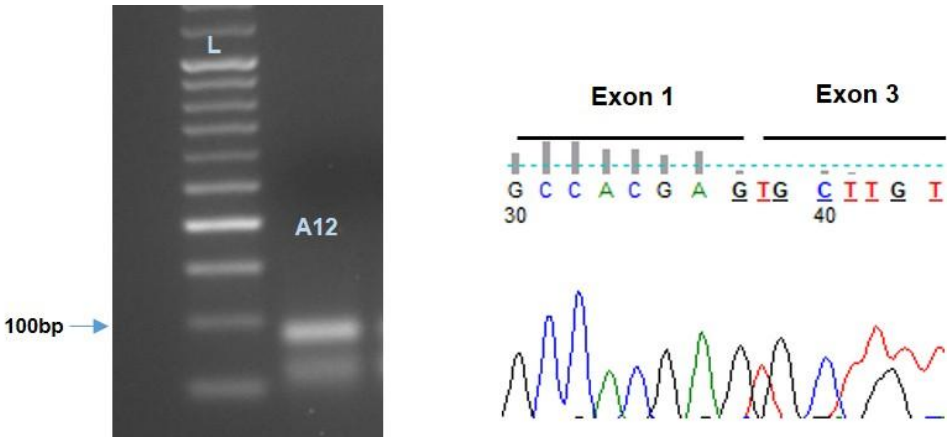


Figure 34. Agarose gel electrophoresis of h*HGSNAT* amplification following the injection of AAV2/9_HGSNAT+1A into animal 12 (group 3) and corresponding Sanger sequencing result, showing the skipping of exon 2. A: animal; L: ladder.

Remarkably, the results observed in the animals injected with the target disease-causing variant along with the modified U1 snRNA vector (AAV2/9_HGSNAT+1A plus AAV2/9_U1snRNATC), even surpassed positively those obtained in patient-derived cells in our previously published study [136].

The h*HGSNAT* splicing pattern in samples obtained from animals belonging to group 7, those selected to evaluate the rescue of the splicing defect, demonstrated a clear U1 snRNATC-mediated correction of the splicing impairment caused by the c.234+1G>A variant.

In four of the five injected animals, the inclusion of the exon 2 was achieved, as a band with 200 bp was present in the electropherogram, which was later confirmed to harbor the desired h*HGNSAT* sequence. For animal number 31, however, it was not seen any amplification product with the expected size (Figure 35).

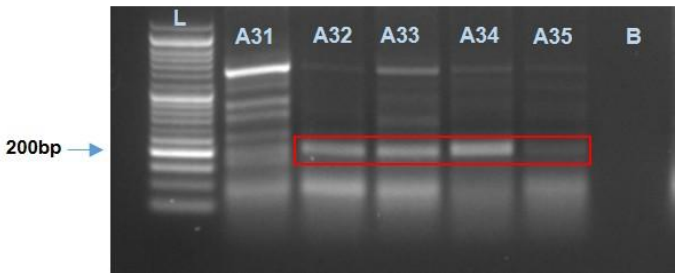


Figura 35. Agarose gel electrophoresis of h*HGSNAT* amplification following the injection of AAV2/9_HGSNAT+1A plus AAV2/9_U1snRNATC into FVB/N mice (group 7). A: animal; L: ladder; B: blank.

To improve the quality of the Sanger sequencing results, the bands corresponding to the expected fragment size were extracted from the gel, and re-amplified (Figure 36) prior to sequencing (Figure 37).

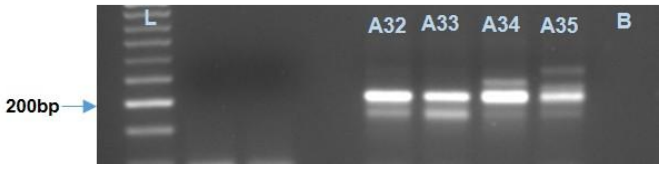


Figure 36. Agarose gel electrophoresis of h*HGSNAT* following PCR re-amplification of the purified fragments from animals numbers 32 to 35. A: animal; L: ladder; B: blank.

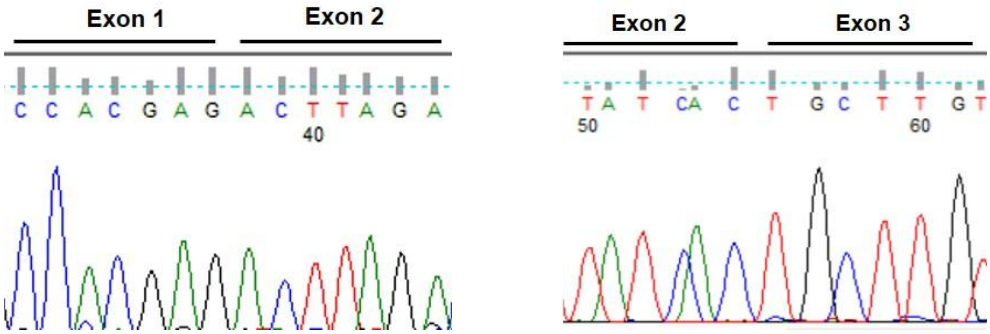


Figure 37. Electropherogram of segments of the h*HGSNAT* transcript sequence obtained after injection of the AAV2/9_HGSNAT+1A plus AAV2/9_U1snRNATC (group 7) in FVB/N mice. Exon boundaries are highlighted above the electropherogram peaks. The Sanger sequencing analysis confirmed the correct inclusion of exon 2.

This final result clearly stimulates further studies and pre-clinical assessments aimed at eventual clinical translation. It also emphasizes the importance of testing new drugs in animal models rather than relying only in *in vitro* systems. Indeed, when this approach was tested in a model cell line, HEK293T, we did not observe the rescue of the splicing defect under investigation. Instead, we obtained the inclusion of exon 2 but with four nucleotides of the intron 2 attached. Still, grounded on the positive results obtained in 2014 by our group in patient-derived fibroblasts [136], and considering they were observed in a setting that more closely mimicked a real-life situation, we decided to proceed with the *in vivo* studies. This was a bold move, considering no correction was obtained when the target mutation was overexpressed in a model cell line co-transfected with the U1 snRNA drug under development. Artificial systems continue to be a gold-standard for pre-clinical assessments of RNA [212], and many potential drugs have been discarded based on their inability to promote the expected splicing patterns in such systems [132,141,143].

All acknowledge that *in vitro* systems cannot fully replicate the complexity of living beings biochemical processes. Testing new drugs for humans in animal models is

essential, providing insights that cell culture testing alone cannot offer [213,214], including on pharmacokinetics, pharmacodynamics, toxicology, safety assessments, immune responses and behavioral and neurological effects. They also play a crucial role in preclinical research, enabling to anticipate outcomes and gain a deeper understanding of intricate biological processes [215,216].

Furthermore, animal testing is advantageous due to the shorter lifespans of animals, which allows for comprehensive life cycle analysis and reduces the duration of experiments [215-217]. In the case of this study, our *in vivo* observations completely support the importance of this type of assessments.

There are issues that cannot be ignored when considering an *in vivo* assay, namely the need for a rational design, aligned with the universal principles outlined by Russell and Burch, in 1959, [218] known as the 3Rs.

3Rs come from Reduction, Refinement and Replacement, which have been the ethical basis upon which virtually every protocol that makes use of animals for research is designed. More recently, it has been proposed a fourth “R”, which stands for Responsibility, to incorporate not only the well-being of experimental animals but also the social and scientific implications of animal experimentation. Accordingly, *in vivo* studies must be well-grounded in ethical principles and supported by sufficient preliminary data, so that no animal is harmed or used if no benefit is expected to arise from its sacrifice.

Altogether, the promising results obtained for the U1 snRNATC approach *in vivo* are currently being compiled and discussed for publication (see Annex 1; original paper *under preparation*).

2. Part II: Genetic Substrate reduction therapeutic approach for Mucopolysaccharidoses type III - targeting a gene of the GAG biosynthesis

Comparatively to mutation-specific therapeutic approaches, genetic substrate reduction therapy (gSRT) is a broader strategy that in the scope of MPSs has the advantage of being applicable not only to patients with MPS III but also to those with other forms of MPS, regardless of their specific mutations.

In this study, the target was a step upstream the enzymatic defect that indirectly influences disease progression.

SRT has been proven to be efficient in several LSD, having driven the development of two drugs that are currently commercially available: miglustat and eliglustat tartrate, which were already introduced into clinical practice. However, both drugs have been associated with some adverse events and their mechanisms of action are far from being fully understood (the subject has been reviewed in a publication related to this thesis [32]). Besides, none of the drugs is RNA-based. The originality of this work lies in having designed and tested several RNA-based molecules to promote an efficient decrease in GAGs biosynthesis.

In the context of MPS diseases, an RNA-based approach as explored in this thesis holds potential to overcome many limitations of the currently available drugs, because each RNA drug has a single, well-defined target, upon which it works with high specificity. With a well-defined target, it is much easier to understand the mechanism of action the drug is triggering.

The rationale followed in this work was quite simple: if GAGs synthesis decreased by acting upon specific genes on the biosynthetic pathway (Figure 38), that decrease would actively reduce substrate accumulation, very likely slowing down the MPS III's pathophysiology.

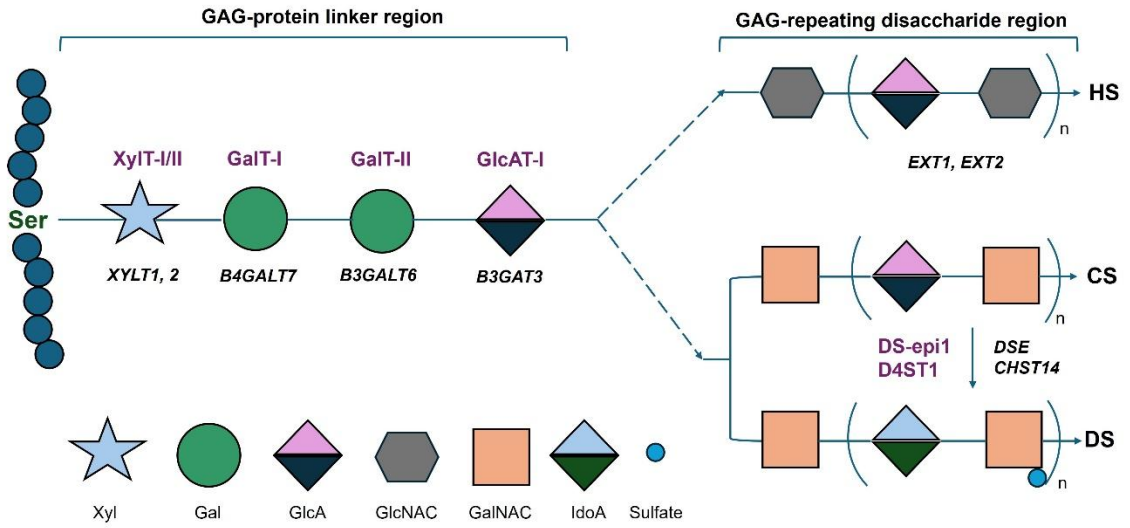


Figura 38. Schematic representation of the biosynthetic pathway of Glycosaminoglycans (GAGs): heparan sulfate (HS), chondroitin sulfate (CS) and dermatan sulfate (DS). The enzymes (highlighted in purple) and their corresponding genes (in black) are labeled near the sugar symbols. The process begins with the synthesis of core proteins, followed by the initiation of GAG-protein linker region synthesis. XylT-I/II enzymes transfer a Xyl unit to a specific serine (Ser) residue in the endoplasmic reticulum. After that, the synthesis of the linker region occurs in the Golgi through the sequential addition of two Gal molecules by GalT-I/II, and then a GlcA molecule, catalyzed by GlcAT-I. Adding GalNAc to the linker determines the growth of the GAG chain to CS/DS synthesis. CS biosynthesis involves alternating additions of GlcA and GalNAc, with additional modifications by sulfotransferases. DS formation begins when GlcA in the chondroitin backbone is converted into IdoA by DS-epi1, creating the dermatan backbone, which is further modified by sulfation of GalNAc by D4ST1. Alternatively, the addition of GlcNAc to the linker signals the start of HS synthesis. HS chain polymerization is carried out by enzymes encoded by the *EXT1* and *EXT2* genes. Abbreviations: Ser, serine; HS, heparan sulfate; CS, chondroitin sulfate; DS, dermatan sulfate; XylT-I/II, xylosyltransferases I/II; GalT-I/II, galactosyltransferases I/II; GlcAT-I:, Glucuronyltransferase I; DS-epi1, dermatan sulfate epimerase 1; D4ST1, dermatan 4-O-sulfotransferase 1; Xyl, xylose; Gal, galactose; GlcA, glucuronic acid; GlcNAc: N-acetylglucosamine; GalNAc, N-acetylgalactosamine; IdoA, iduronic acid (based on [219]).

XYLT1 was here selected as the target gene to downregulate HS synthesis mainly due to the compelling evidence that its inhibition leads to a significant reduction in GAG synthesis, as shown for instance in experiments using siRNAs [183,185].

Furthermore, the side effects of inducing a decrease in a protein' synthesis were also taken into account, since they inadvertently could lead to the onset of other diseases different from the one we wanted to ameliorate. Some *XYLT1* variants have been reported as pathogenic, associated with Desbuquois skeletal dysplasia (DBSD) or Baratela-Scott syndrome. DBSD is an autosomal recessive disease characterized by skeletal dysplasia, joint dislocations, short stature, and facial abnormalities [220-222]. Baratela-Scott syndrome is marked by short stature, skeletal dysplasia, facial dysmorphisms, and developmental delays [223]. As regards DBSD, it was demonstrated that *XYLT1* mutations impair GAG biosynthesis, and low levels of GAGs and proteoglycans in fibroblasts from affected individuals were reported [220]. Recently,

Taieb *et al*., provided a deeper understanding of the role of *XYLT1* in the onset of the disease, demonstrating that xylosyltransferase I (XT-I) plays a crucial role in chondrocyte maturation rather than differentiation, highlighting its importance in cartilage development and disease progression [224]. All this meant that under-expression of *XYLT1* could be problematic.

However, we thought that a transient downregulation of *XYLT1* would be less likely to adversely affect cell function not only for the transient nature of the therapeutic intervention per se, but also because there is another enzyme, xylosyltransferase II (XT-II), that could partially compensate for the inhibited synthesis of XT-I. XT-I is broadly expressed and primarily involved in general GAG synthesis, which makes it a good therapeutic target, whereas XT-II has a more restricted expression profile and is associated with more specialized functions [225]. So, we believe that targeting *XYLT1* holds potential therapeutic effect while minimizing harmful effects for patients, given that our goal is to reduce HS synthesis rather than abolish it entirely [225-227].

Moreover, the kind of drugs we are addressing do not achieve complete gene knockout. They require continuous application, which is expected to result in a controlled reduction of XT-I expression and, consequently, of HS synthesis, with the aim of halting disease progression.

Three different types of RNA-based drugs were designed to downregulate the expression of a gene involved in HS biosynthesis, the *XYLT1*: siRNAs, SSOs and gapmer ASOs.

Depending on the type of molecule under test, different workflows were performed. To analyse the effects of siRNAs and gapmer ASOs, qRT-PCR was performed to assess whether the treatment resulted in a decrease in the *XYLT1* mRNA relative expression. On the other hand, the effects of SSOs were evaluated using RT-PCR. These ASOs were designed to induce the skipping of selected exons in the *XYLT1*, disrupting its reading frame and introducing a premature termination codon (PTC). Expectedly, treatment with these molecules will cause a shift on the splicing pattern.

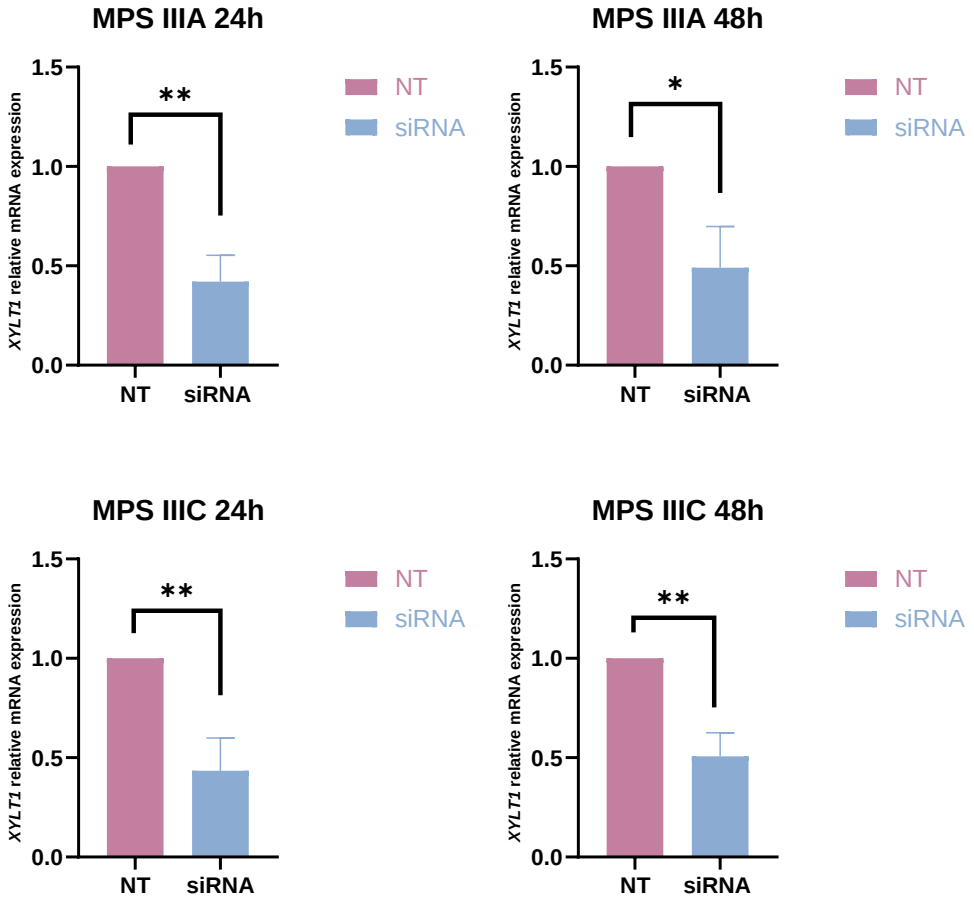
Initially, the transfection of each molecule was performed in all MPS III subtype cell lines to evaluate its effect at RNA level. As we had designed multiple molecules for the same purpose, it was not feasible to implement the entire pre-clinical pipeline for all of them. Therefore, only the best performing molecules were selected to proceed for the macroassays in which larger quantities of cells were needed to perform not only qRT-PCR or RT-PCR, but also WB and LC-MS/MS, to evaluate their effects on protein expression and HS storage, respectively.

2.1. Evaluating the siRNA effectiveness in fibroblasts from MPS III patients

Viewing this therapeutic approach, RNAi was selected as the mechanism of choice, using siRNAs as effectors.

siRNAs are double-stranded RNA molecules that hybridize with a specific mRNA sequence, leading to its degradation. Having this in mind, a pool of three siRNAs targeting the *XYLT1* gene was designed.

cDNA analysis was performed on samples collected 24 and 48 hours after transfecting patients' fibroblasts to assess the relative expression of *XYLT1* mRNA compared to cells transfected only with riboxx® FECT, here defined as non-transfected (NT). qRT-PCR analysis revealed that the siRNA pool induced a significant decrease of the target gene expression compared to NT cells, at both time points analysed (Figure 39).



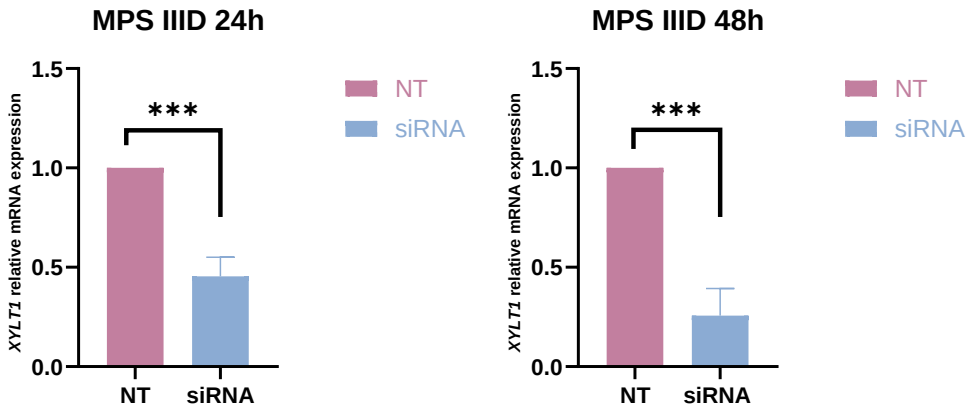


Figure 39. *XYLT1* mRNA relative expression in patient-derived MPS III fibroblasts. The siRNA pool was transfected in IIIA, IIIC and IIID subtypes, for 24 and 48 hours, and the *XYLT1* levels quantified through qRT-PCR, for 3 independent experiments (n=3). *GAPDH* was used as endogenous control. Comparisons between groups were analysed using the t-student test (*p < 0.05, **p < 0.005, ***p < 0.001).

From now on, and in order to foster possible clinical translation of this approach, further steps would be necessary taken: each of the three siRNAs comprising the pool, would have to be tested individually to evaluate its effects. Plus, to be tested in animal models and latter delivered to human patients, siRNAs cannot be administered naked: siRNAs are rapidly degraded by RNases and filtrated in the kidney, thereby requiring a delivery system for effective transport to target cells [228,229].

Stable nucleic acid lipid particles (SNALPs), are a unique class of liposomes with a high cargo encapsulation efficiency and the potential to be designed to facilitate targeted delivery to particular receptors. SNALPs represent one of the most widely adopted RNAi delivery technology. Thus, these lipid nanoparticles would probably be our vehicles of choice to deliver siRNA-based therapies to MPS patients, particularly those suffering from neurological forms of these diseases, as we have extensively discussed in the introduction [230].

Finally, there is yet another challenge that must be addressed when using siRNAs as therapeutic tools: the need for continuous delivery of the siRNA molecules to cells to ensure an efficient and stable effect on the target cells.

As this discussion highlights, the hurdles a siRNA-based gSRT approach would overcome are many, and would probably delay its future clinical translation. That is why alternative approaches were explored and tested in this thesis.

2.2. Exploring antisense oligonucleotides as a novel strategy for genetic substrate reduction therapy in MPS III

In this study, an alternative approach for using siRNA for gSRT was also explored involving a different class of RNA-based therapeutics: antisense oligonucleotides (ASOs). In cell culture experiments, siRNAs are often preferred over ASOs due to the simplicity in identifying potent molecules and the ease of obtaining unmodified RNA with high activity. In contrast, ASOs require chemical modifications to achieve intracellular activity [231]. Additionally, while siRNAs are double-stranded providing them with great stability, which is particularly advantageous for *in vitro* studies, ASOs are single-stranded. However, the stability advantage of siRNAs does not necessarily extend to *in vivo* applications or clinical use. Furthermore, siRNAs may carry a higher risk of off-target effects, as both the sense and antisense strands can potentially be active [232]. The choice between ASOs and siRNAs ultimately depends on the specific context, with delivery considerations playing a crucial role in the development of compounds for animal studies or therapeutic applications. Delivering siRNAs to the CNS is more challenging, but, on the other hand, ASOs offer more versatile delivery options, allowing for safe and localized administration. For example, intrathecal (IT) injection enables broad CNS distribution and has shown therapeutic efficacy in conditions such as SMA, Amyotrophic lateral sclerosis, and Batten disease [145]. These findings prompted us to explore the therapeutic potential of ASOs in this study.

We invested in two distinct approaches - splice-switching oligonucleotides (SSOs) and gapmer ASOs - to assess their therapeutic efficacy for MPS III.

To our knowledge, no previous assessments were ever made on the use of ASOs for genetic modulation of lysosomal related biosynthetic pathways in the context of SRT. This represents the first study of its kind, not only in MPS, but also in the broader LSD field.

2.2.1. Evaluating the effect of SSOs on exon skipping of *XYLT1* gene: identifying the most promising molecules

Our initial approach to an ASO-mediated gSRT for MPS III was a splicing modulation approach. We used SSOs to block splicing and induce exon skipping, effectively removing the target exon from the mRNA. Yet, instead of skipping exons to generate in frame transcripts, typically employed to circumvent the deleterious effects of mutations harbored in those exons, we aimed at skipping exons in a way that would produce out-of-frame transcripts. By doing so, we would effectively disrupt the open

reading frame (ORF), inducing a frameshifting that would subsequently result in the appearance of a PTC and ultimately cause the decay of the *XYLT1* mRNA. This is a very original strategy for applying SSOs, since they are usually used to generate functional ORFs, regardless of whether they were aimed to promote the inclusion or exclusion of specific exons. Overall, all SSOs approved for therapy fall into one of these two types [105,106]. Only a few reports exist on the use of SSOs for ORF disruption and mRNA degradation.

The design of efficient SSOs is not trivial. To guarantee an accurate design, there is a well-documented list of rules that must be followed (see the Materials and Methods section 2.1.1.2.) aimed at increasing the probability of the oligonucleotides trigger the desired effect. In this work, all SSOs were designed strictly adhering to these guidelines.

It was also necessary to incorporate specific chemical modifications into that design, in order to make them potential therapeutic tools. Thus, the SSOs tested here had a PS backbone, to increase resistance to degradation by nucleases, and a modification at the 2' sugar position, which among other advantages also made them resistant to RNase H: 2'-O-methoxyethyl (2'-MOE). This chemistry is one of the two that have already been adopted in clinically approved splice-switching drugs, as for instance is Spinraza®, a fully 2′-MOE-PS splice-switching drug used for the therapy of SMA.

Five different SSOs were designed each one targeting a distinct exon of *XYLT1* gene (see table 10 in Material and Methods). By starting with a reasonable number of SSOs, our goal was to increase the probability of efficient exon skipping.

Initially, 200 nM of each SSO were transfected into patients-derived fibroblasts, and cDNA analysis was performed 24 and 48 hours later.

The RT-PCR showed a transcript corresponding to the skipping of the target exon, in most cases, with the effect being most pronounced with the following two: SSO3, which induced the skipping of exon 9, resulting in a band with 390 bp, and SSO5, which induced the exon 11 skipping resulting in a band with 160 bp. This experiment was done for all MPS III subtypes under the same conditions, and similar results were obtained for all. For the sake of simplicity, only the results for MPS IIIA are depicted here (Figure 40).

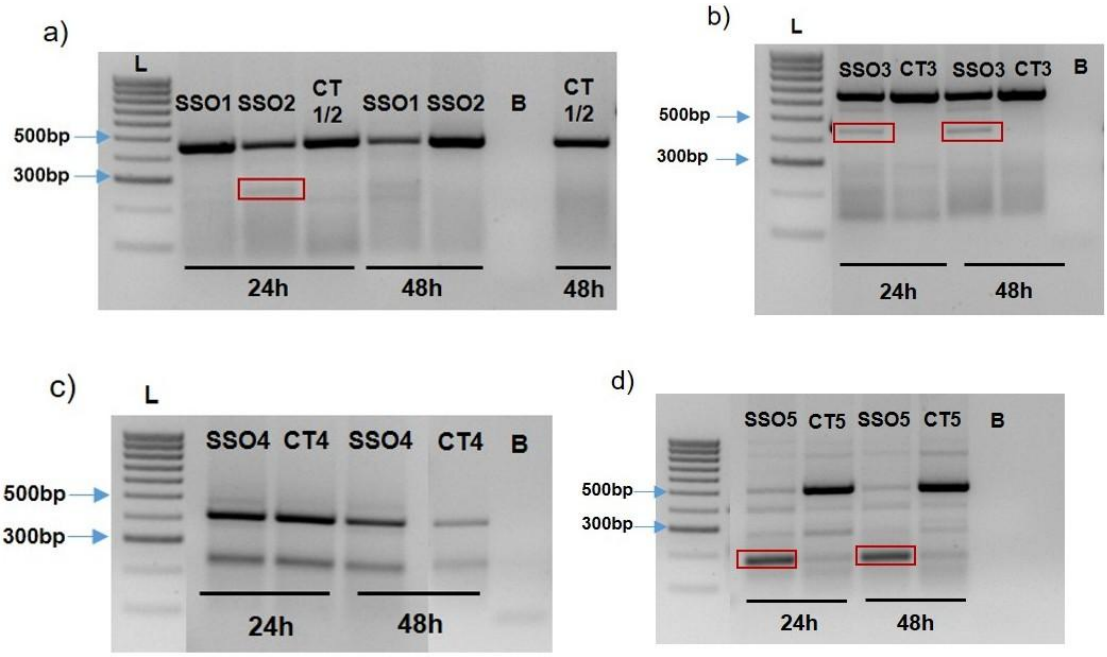


Figure 40. Agarose gel electrophoresis of *XYLT1* amplification fragments following transfection of MPS IIIA with different SSOs, for 24 and 48 hours. The splice-switching oligonucleotides (SSOs) are numbered from 1 to 5. SSO1- splice-switching oligonucleotide 1; SSO2- splice-switching oligonucleotide 2; SSO3- splice-switching oligonucleotide ; SSO4- splice-switching oligonucleotide 4; SSO5- splice-switching oligonucleotide 5. a) SSO1 as a target exon 4 and SSO2 as a target exon 5 (for fragments amplification was used the same pair of primers); b) SSO3 as a target exon 9; c) SSO4 as a target exon 10; d) SSO5 as a target exon 11. The bands corresponding to the fragments with exon skipping are highlighted by a red box. CT- control; L- ladder; B- blank.

Before moving on to the macroassays, where XT-I protein and HS storage levels were measured, a concentration-response study was performed. For clinical application, it is essential to work with the minimum effective concentration, reducing the likelihood of side effects associated with these RNA drugs. So, a balance between the best effect at the lowest concentration must be achieved. Three different concentrations of each SSO (100, 200 and 300 nM) were tested in each MPS III subtype (A-D) at two different time points (24 and 48 hours post-transfection).

For SSO1, no bands corresponding to the skipping of the exon 4 were observed, even though the band corresponding to the wild-type transcript (449 bp) lose intensity after transfection with SSO at 200 and 300 nM for 48 hours. For SSO2, at both time-points analysed, transfection with 200 and 300 nM resulted in an increase in the intensity of the band corresponding to exon 5 skipping (309 bp) and a decrease in the intensity of the band corresponding to the wild-type transcript (449 bp). For SSO3 and SSO4, no differences were observed. For SSO4 at 300 nM the wild-type band resulted in a

decrease in the intensity but the same was observed for the band corresponding to the exon skipping.

For SSO5, which we consider the most promising, the band corresponding to the skipping of exon 11 (160 bp) was more intense when the transfection was performed with 200 nM. Additionally, the wild-type band (494 bp) showed reduced intensity at this SSO concentration both at 24 and 48 hours (Figure 41). Interestingly, it is also worth mentioning that the wild-type band was actually more intense after transfection with 300 nM compared to that observed for 200 nM. Based on these results, the 200 nM was selected as the concentration to proceed to the following assays.

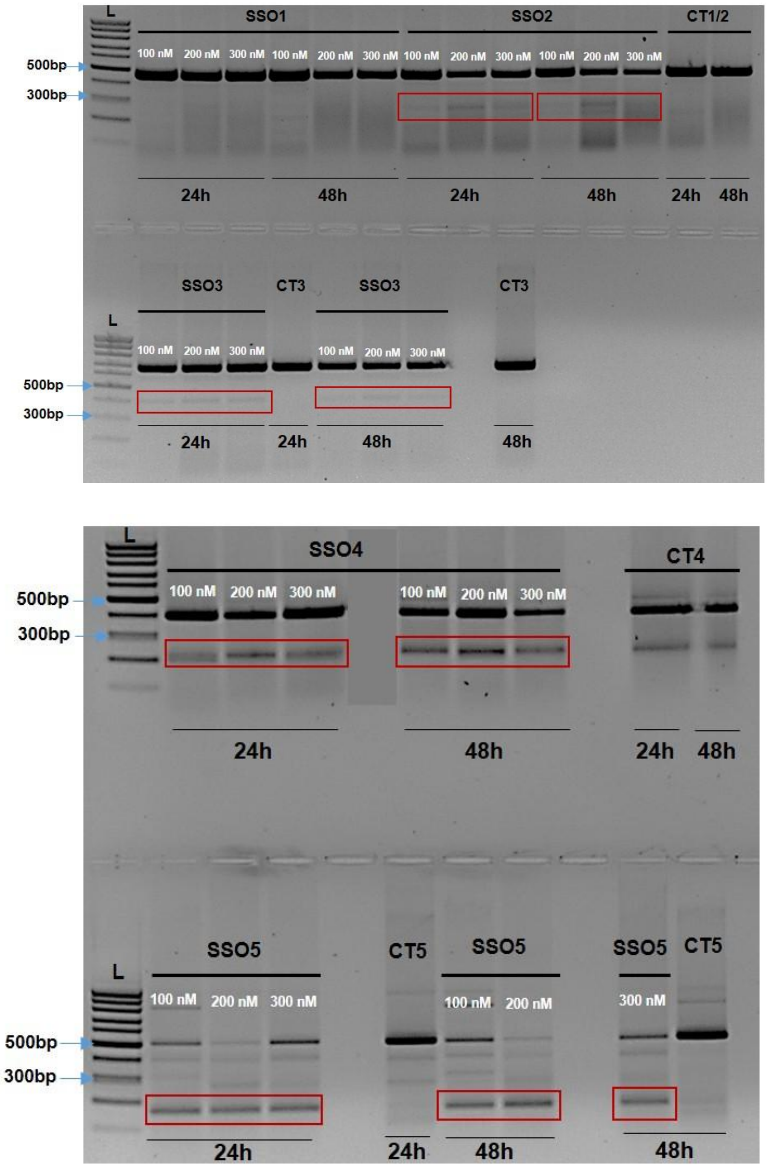


Figure 41. Agarose gel electrophoresis of *XYLT1* fragment amplification. MPS IIIA fibroblasts were transfected with different SSOs' concentrations, for 24 and 48 hours. SSOs are numbered from 1 to 5. The bands corresponding to the fragment with exon skipping are highlighted by the red box. SSO1- splice-switching

oligonucleotide 1; SSO2- splice-switching oligonucleotide 2; SSO3- splice-switching oligonucleotide ; SSO4- splice-switching oligonucleotide 4; SSO5- splice-switching oligonucleotide 5; CT- control; L- ladder.

Whenever a band corresponding to the expected exon skipping size appeared, it was excised, purified and sequenced (Figure 42). For SSOs 2, 3 and 5 it was possible to obtain a sequence that confirmed the expected exon skipping. For SSO4, however, it was never possible to obtain a sequence that clearly confirmed the absence of exon 10 (data not shown).

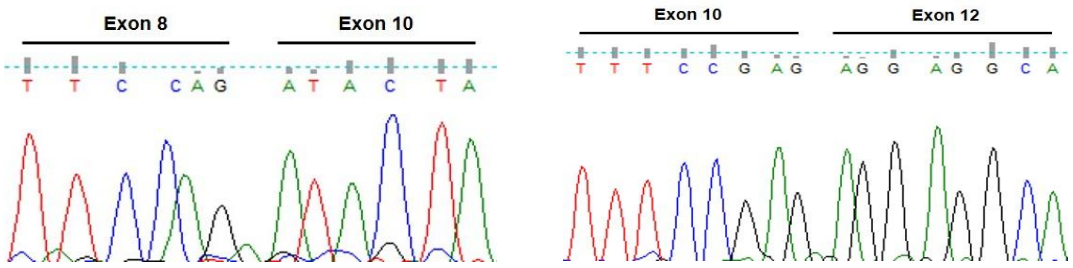


Figura 42. . Electropherogram of a portion of the *XYLT1* transcript sequence obtained after transfection with SSO3 and SSO5 showing the skipping of exons 9 and 11, respectively.

Due to time and financial limitations only the two most promising SSOs, SSO3 and SSO5, were selected for further testing to evaluate their efficacy on protein levels and HS storage.

2.2.1.1. Evaluating the effect of SSOs on exon skipping of *XYLT1* gene: SSO3 and SSO5 as the most promising molecules

The optimal concentration of SSO3 and SSO5 was determined and then we proceeded with the macroassay. To evaluate the efficacy of the molecules on HS storage, our ultimate readout, 200 nM of SSOs 3 and 5 were transfected in all MPS III subtypes, for 24 and 48 hours. Agarose gel analysis of RT-PCR products obtained after transfection of SSO3 showed a fragment with 390 bp, corresponding to the expected skipping of exon 9.

On the other hand, in control samples (CT) a fragment with 654 bp was observed, which corresponded to the normal transcript size (Figure 43). Results of the SSO5 transfection were also in line with the predictions: in the CT lane, a fragment corresponding to the normal transcript expected to have 494 bp was observed, while the lanes that corresponded to SSO5 transfection exhibited a second fragment of around 160 bp (exon 11 skipping), alongside the normal amplicon (Figure 43). Results were similar for both time points tested in all patient fibroblast MPS III subtypes (Figure 43).

Bands of interest were excised, purified and sequenced, which allowed to confirm the skipping of the target exons as well as the presence and integrity of the normal transcript.

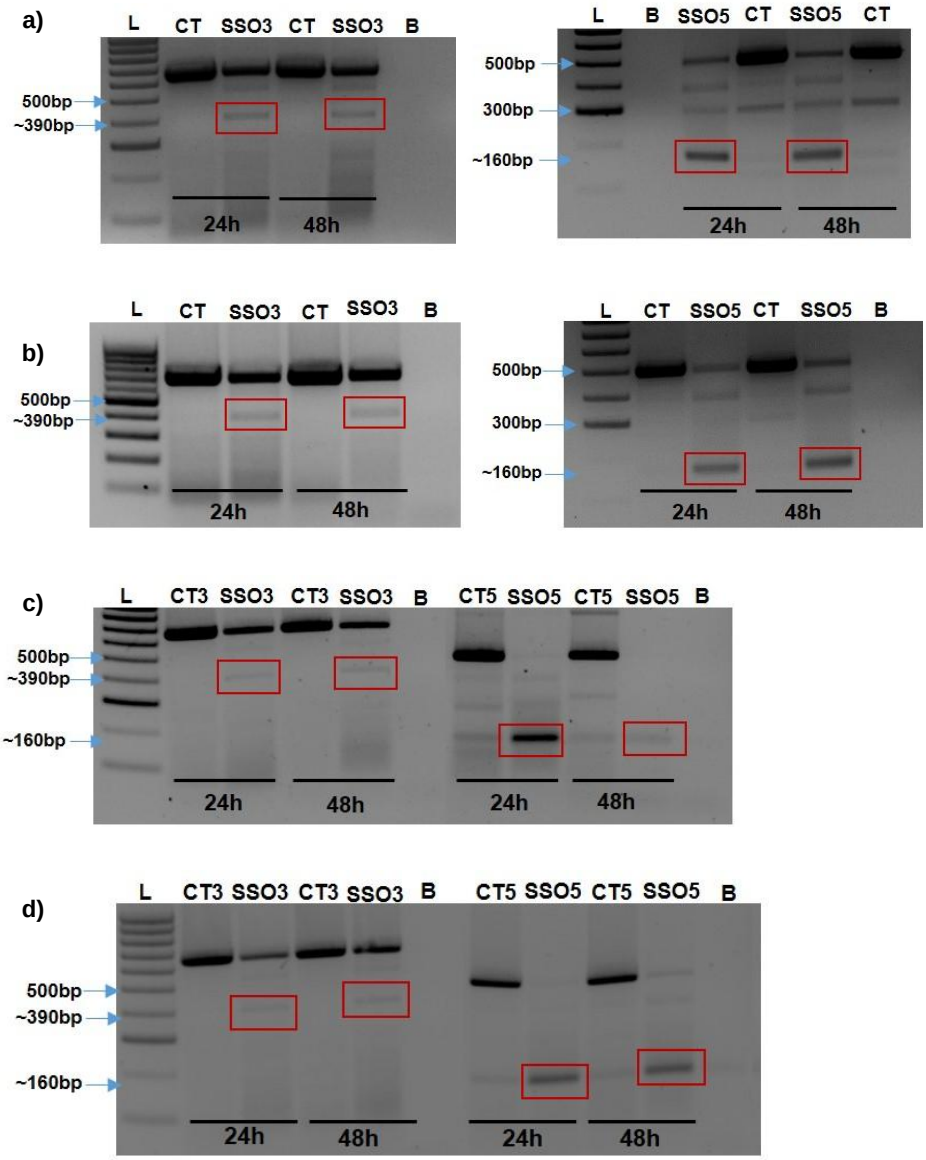


Figure 43. Agarose gel electrophoresis of *XYLT1* fragments amplification. SSO3 and SSO5 were transfected for 24 and 48 hours in MPS III patient-derived fibroblasts. Data show the RT-PCR analysis of all MPS III subtypes: a) MPS IIIA; b) MPS IIIB; c) MPS IIIC and d) MPS IIID. The bands corresponding to the fragments with exon skipping are highlighted with a red box. SSO3- splice-switching oligonucleotide 3; SSO5- splice-switching oligonucleotide 5; CT- control; L- ladder; B- blank.

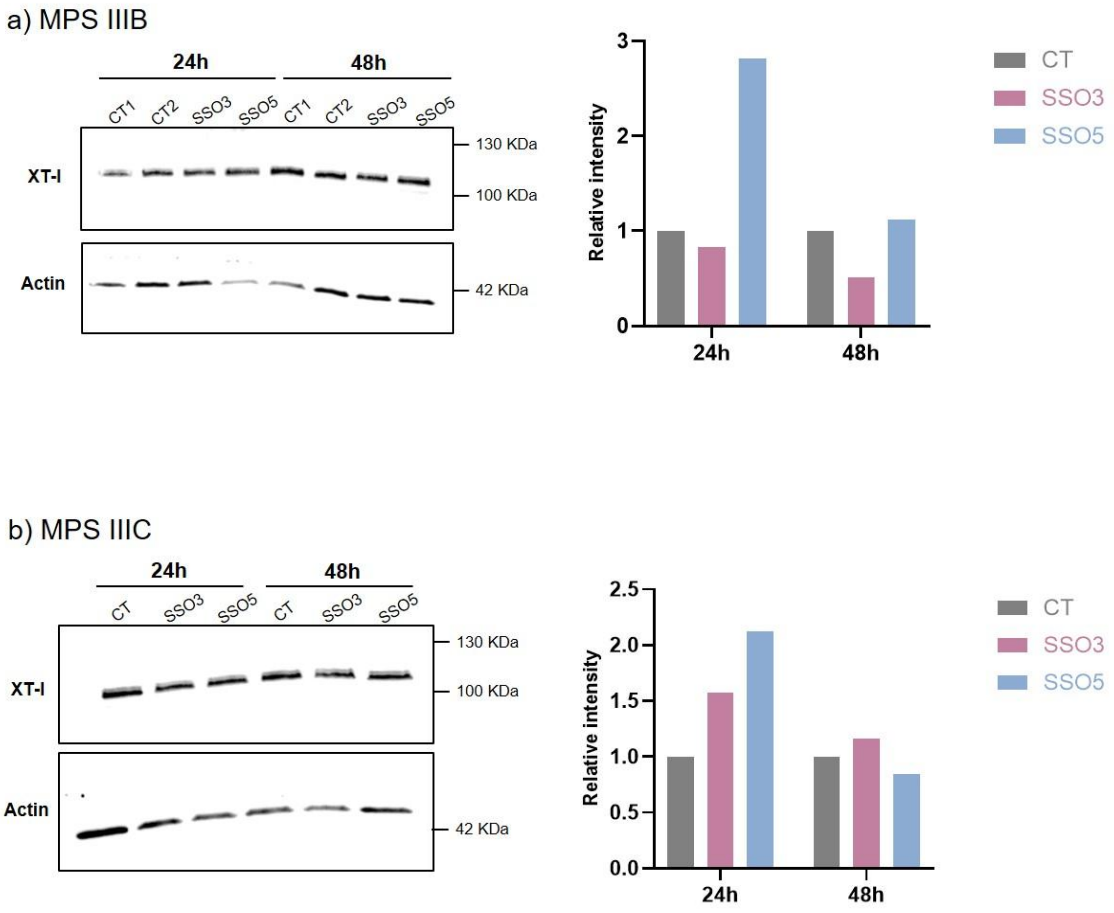
2.2.1.2. Evaluating the effect of the exons 9 and 11 skipping on xylosyltransferase I (XT-I) protein expression

Once the effect of the selected SSOs was double-checked at mRNA level, we proceeded to evaluate whether this resulted in a reduced expression of the

corresponding protein. To achieve this, XT-I the first enzyme in the post-translational biosynthesis of GAG chains in proteoglycans was detected by WB, in both treated and untreated MPS III samples. The treated samples correspond to pellets from MPS III cultures that received the SSOs while the control (untreated samples), refer to MPS III cultures subjected to the full transfection protocol but without SSO treatment.

WB analysis was performed 24 and 48 hours after transfection but no differences in protein expression were observed when compared to the control, despite the detection of the expected exon-skipped band at both time points. For MPS IIIA, WB analysis did not reveal any protein band (data not shown). Although the corresponding cell line was from the same biobank as the other three, shipped at the same time, and established under the same conditions in our laboratory, it already had a higher number of passages prior to arrival.

The WB results for MPS IIIB, IIIC and IIID are presented below (Figure 44).



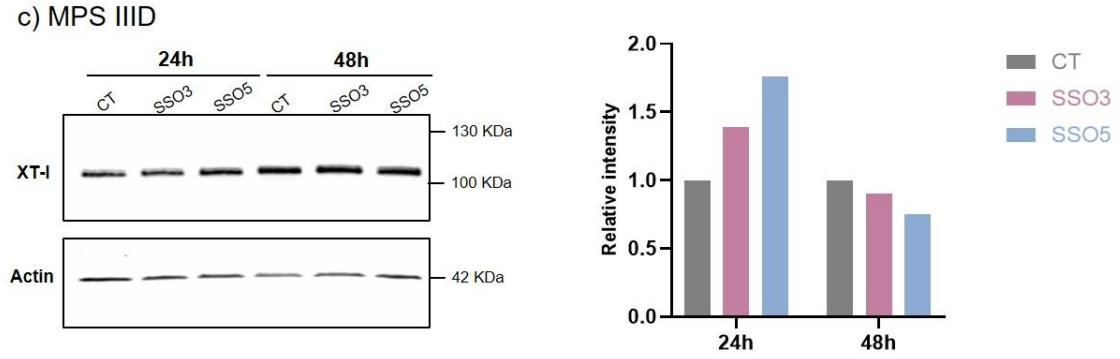


Figure 44. Quantification of Xylosiltransferase-I (XT-I) protein in MPS III patient-derived fibroblasts after treatment with selected SSOs. Quantification was performed 24 and 48 hours post-transfection of SSO3 and SSO5. The left panel displays a representative WB showing XT-I protein levels in fibroblasts from MPS III patients: a) MPS IIIB; b) MPS IIIC; c) MPS IIID, comparing transfected and non-transfected (control – CT) samples, with Actin used as a loading control. The right panel displays the relative quantification of XT-I protein levels, normalized to Actin, from a single experiment (n=1).

The experimental protocol was only carried once for each of the cell lines, but results obtained were consistent across the three subtypes.

Overall, no reduction in XT-I levels was observed at 24 and 48 hours post-treatment. At 24 hours, an increase in band intensity was detected in transfected cells compared to those not transfected with the SSOs, particularly with SSO5. However, potential technical issues cannot be ruled out, as the actin pattern observed in the lanes corresponding to the SSO5 samples at 24 hours and CT1 at 48 hours revealed a suboptimal protein transfer.

The overall conclusion we could draw from both incubation time points is that the span of time does not imply significant changes in XT-I expression levels; particularly at 48 h post-transfection, levels were quite consistent across all three cell lines. This result lead us to hypothesize that the XT-I half-life might be longer than 48 hours, and being so, the treatment's effect on protein levels may only become evident beyond this time point. Since no data on this aspect is currently available in the literature, it would be necessary to extend the incubation period in MPS III fibroblasts to clarify the hypothesis.

2.2.1.3. The final effect: can the most promising SSOs decrease heparan sulfate storage?

The accumulation of HS is the major intracellular hallmark of these disorders, representing the trigger for the pathophysiological cascade. Therefore, the ultimate *in vitro* assessment of the therapeutic potential of any drug for MPS must always involve the accurate measurement of that GAG or, at the very least, the combined assessment

of all GAGs. Here, we took advantage of the availability in house of a triple quadrupole mass spectrometer to implement an exceptionally sensitive method to measure our GAG of interest, HS, after a simple butanolisis reaction.

Using this method, HS levels were evaluated by LC-MS/MS in all MPS III subtypes, from cell pellets collected 24 and 48 hours after transfection. The results were normalized to total protein levels. No decrease in HS storage was observed (Figure 45), a somehow discouraging result, although in line with our observations regarding XT-I levels.

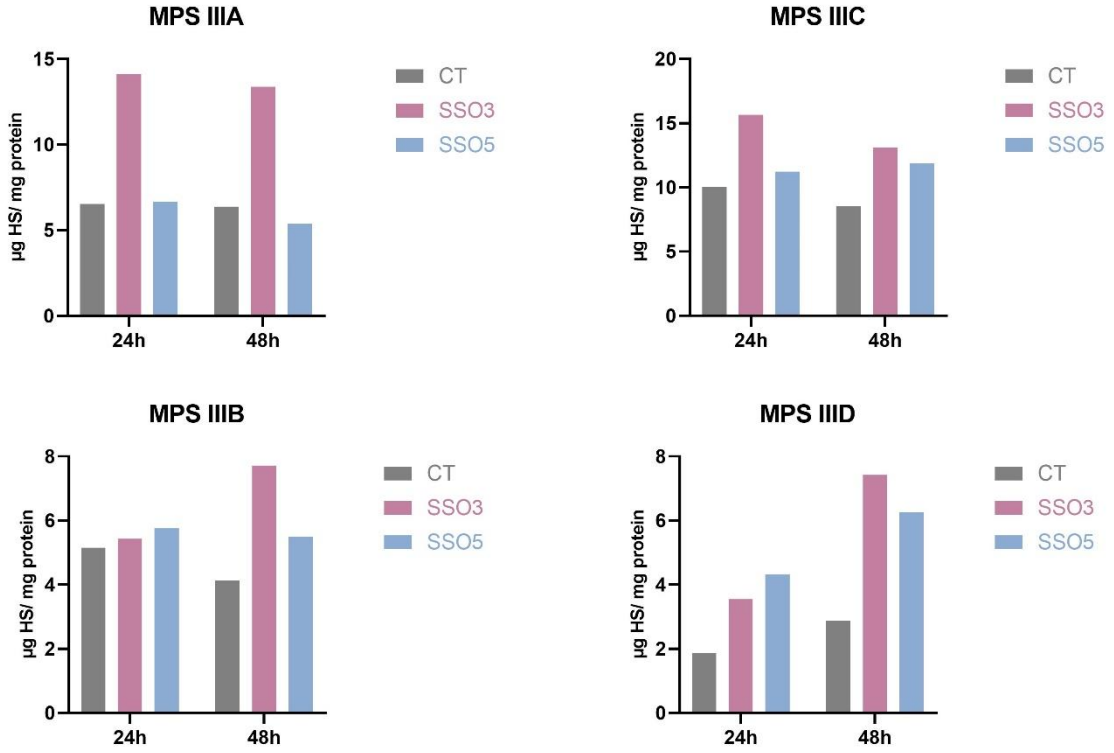


Figure 45. Quantification of Heparan Sulfate (HS) in MPS III patient-derived fibroblasts after treatment with selected SSOs. SSO3 and SSO5 were transfected in fibroblasts from all MPS III patient subtypes, for 24 and 48 hours. Results are expressed as µg HS per mg protein (µg HS/mg protein). Data refer to one experiment for each subtype (n=1).

The protocol has not been replicated, again due to time and financial constraints, but a pattern emerged from the combined analysis of the results.

Concerning the protein and substrate accumulation levels, probably the 24-48 hours timeframe may be too short to capture any effect on overall HS levels, especially considering that the used gSRT drugs are acting upon a very early gene of the biosynthetic pathway of this GAG. This is particularly relevant in a disease setting, where HS is already abnormally accumulated. The result is in line with the non-observation of

decrease on the overall XT-I levels at any of these time points. Taking into account these two independent assessments, the incubation time should be still extended, to guarantee exhaustive translation of all mRNA in the cell offering better conditions to assess the effect of the SSOs. Another factor that should be explored in the future relates with XT-I half-life.

Also mandatory will be to increase the number of tests per cell line, making at least triplicate experiments for every MPS III subtype.

At this point in the work, the pattern that arose was consistent in the four MPS III cell lines. We stress that all experiments were performed independently, at different moments, with cells at different passages and no two cell lines were transfected simultaneously in the same day.

It cannot be discarded that the apparent lack of effect over storage may only reflect an inefficient or insufficient knockdown. If both SSOs were able to efficiently trigger the desired skipping *in vitro*, none was sufficiently potent to abolish the presence of the normal transcripts. This is relevant because it can mean that, while part of the *XYLT1* mRNA is targeted for degradation via mRNA decay, there remains a considerable fraction being correctly processed. According to our observations, in both SSO3- and SSO5-treated cells, the normal amplicon was the prominent one, at least for the tested PCR conditions.

No other amplification conditions were attempted because nothing lead to suspect that PCR products already obtained did not reflect the relative expression levels of the wild-type and ORF-deficient transcripts. PCR bias may occur due to intrinsic differences in the amplification efficiency of templates, or to the inhibition of amplification by the self-annealing of the most abundant templates during the late stages of PCR. However, it is clear unlikely that PCR bias could underlie the same pattern that consistently arise across all the tested SSOs. Besides, the wild-type amplicon was always detected, in most cases corresponding to the band with the highest intensity. Since shorter fragments are easier to amplify than longer ones, PCR artifacts are more prone to produce short amplicons. That also did not fit our observation, since the bands with higher intensities corresponded to the large amplicons where target exons were skipped (shorter fragments), and lower intensities in the non-skipped/ wild-type bands (longer fragments).

The entire approach now addressed still needs much improvement. Until then, we can only speculate on the therapeutic potential these particular SSOs may hold.

2.2.2. Evaluating the effect of gapmer ASOs on *XYLT1* mRNA relative expression: selecting the most promising molecules

The final RNA therapeutic approach explored for gSRT was the gapmer ASOs. These molecules contain a gap region that enables recognition by RNase H, surrounded by nucleotides containing modifications that enhance the stability of the oligonucleotide and its ability to bind to RNA molecules, resulting in more efficient mRNA degradation.

Gapmer ASOs are well validated therapeutic agents, with four drugs currently approved. We believe they may represent a class of therapeutics for gSRT, as they hold the potential to offer a targeted approach for diseases caused by substrate accumulation. Because gapmers induce mRNA degradation, in principle they may have more potent silencing effects.

Here, we selected 2'-MOE-PS gapmers, which are known for their improved stability, resistance to nucleases, and strong RNA-binding affinity. This class of ASOs effectively degrade mRNA through RNase H-mediated cleavage while minimizing off-target effects, ensuring sustained efficacy both *in vitro* and potentially *in vivo*. This chemical modification has become the most successful in its class, offering a more favorable safety profile as evidenced by numerous clinical studies. Notably, the gapmer ASOs currently approved for therapeutic use are 20-mer, 2'-MOE-PS gapmers, similar to those tested in this study, highlighting their potential for clinical application [81,233].The rationale for the gapmers experiments followed the same approach as described for the SSOs assays: five gapmer ASOs (2'-MOE-PS) targeting the *XYLT1* gene were selected and tested in all MPS III subtypes, at an initial concentration of 50 nM. This initial concentration was chosen based on previously studies in which the same type of ASOs were used in *in vitro* tests. Since our goal was not only to assess the effect of the drug, but also to evaluate cellular responses to the treatment, if a high cell mortality rate was observed, the concentration could be reduced. That did not happen, and so in a second phase of the study the tested concentration was double to 100 nM, a concentration within the range described in similar studies [234].

To evaluate the relative expression of *XYLT1* mRNA, the cDNA analysis was performed in samples collected 24 and 48 hours after transfecting patients' fibroblasts with each gapmer. As controls, we used untreated cells, which are cells originated from the same cell lines and subjected to the transfection protocol but without the addition of the gapmer. The qRT-PCR analysis revealed that all tested gapmers were able to induce a significant decrease of the *XYLT1* gene expression compared to untreated cells (Figure 46). However, the effect was more pronounced with gapmers G2 and G3. These two

gapmers were selected proceeded to macroassay to test their efficacy on XT-I protein levels and HS accumulation.

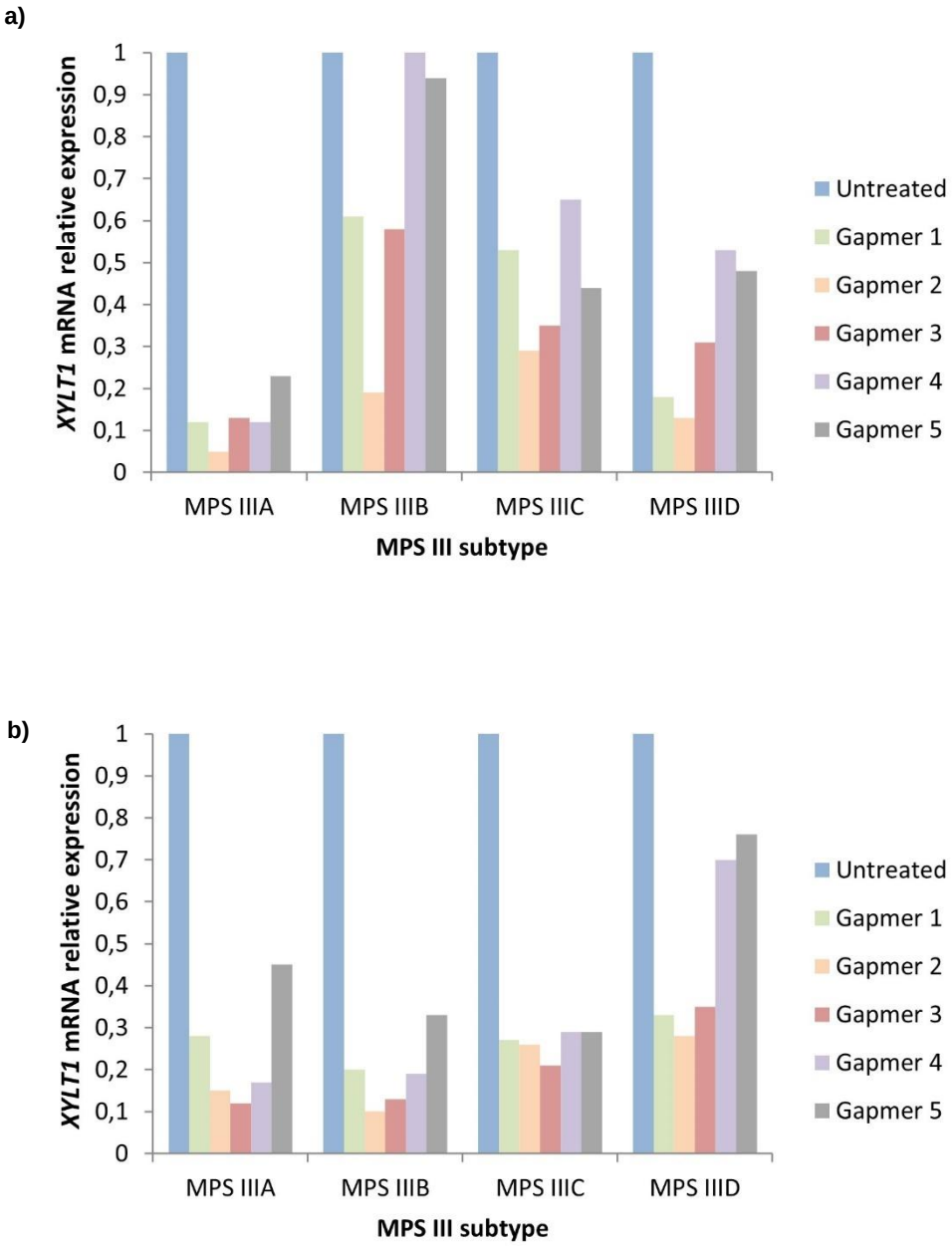


Figure 46. *XYLT1* mRNA relative expression in MPS III patient-derived fibroblasts after treatment with the five gapmer ASOs. Results are from all subtypes, after transfection of five different gapmer ASOs. The effect was evaluated a) 24 hours and b) 48 hours post-transfection. Data refers to a single experiment for each subtype (n=1).

2.2.2.1. Evaluating the effect on the *XYLT1* mRNA relative expression using the most promising gapmers: G2 and G3

G2 and G3 were independently transfected in all MPS III fibroblasts subtypes, at 100 nM, to analyse their effect on XT-I protein and on HS storage. Taking into account the results obtained in the SSOs experiments, where no effects on protein and HS levels were observed at the time points analysed, we decided to extended the incubation periods from the beginning. For practical reasons, the qRT-PCRs were not repeated, and the subsequent experiments that we will refer to as 'macroassays', included only protein and HS assessments.

2.2.2.2. The gapmers G2 and G3 have any effect on xylosyltransferase I (XT-I) protein levels?

After 48 and 72 hours of gapmers' incubation, XT-I levels were analysed. As depicted in Figure 47, no differences were observed in the MPS IIIA and IIID cell lines. In the MPS IIIB cell line, an apparent decrease in the intensity of the bands was observed in the samples incubated with gapmers. However, due to the absence of a control sample, due to technical problems, it was not possible to perform the relative quantification analysis at 72 hours, preventing to determine whether the decrease was maintained or became more pronounced. It was not possible to analyse protein levels in MPS IIIC cell line due to difficulties with the WB technique. Although a signal was obtained after chemiluminescent protein detection, it was too faint and uneven to allow for reliable interpretation. Since the detection of such signal permitted to exclude inadequate image acquisition, we inferred that our observation was the result of a sub-optimal protein transfer.

Only a single experiment was performed per cell line, but unlike what had been seen for the SSO, no consistent pattern emerged across all cell lines. While no decrease in protein expression was observed after the treatment with G2 or G3 in the MPS IIIA and IIID cell lines, for the MPS IIIB cell line, XT-I levels decreased after treatment, regardless of the gapmer used.

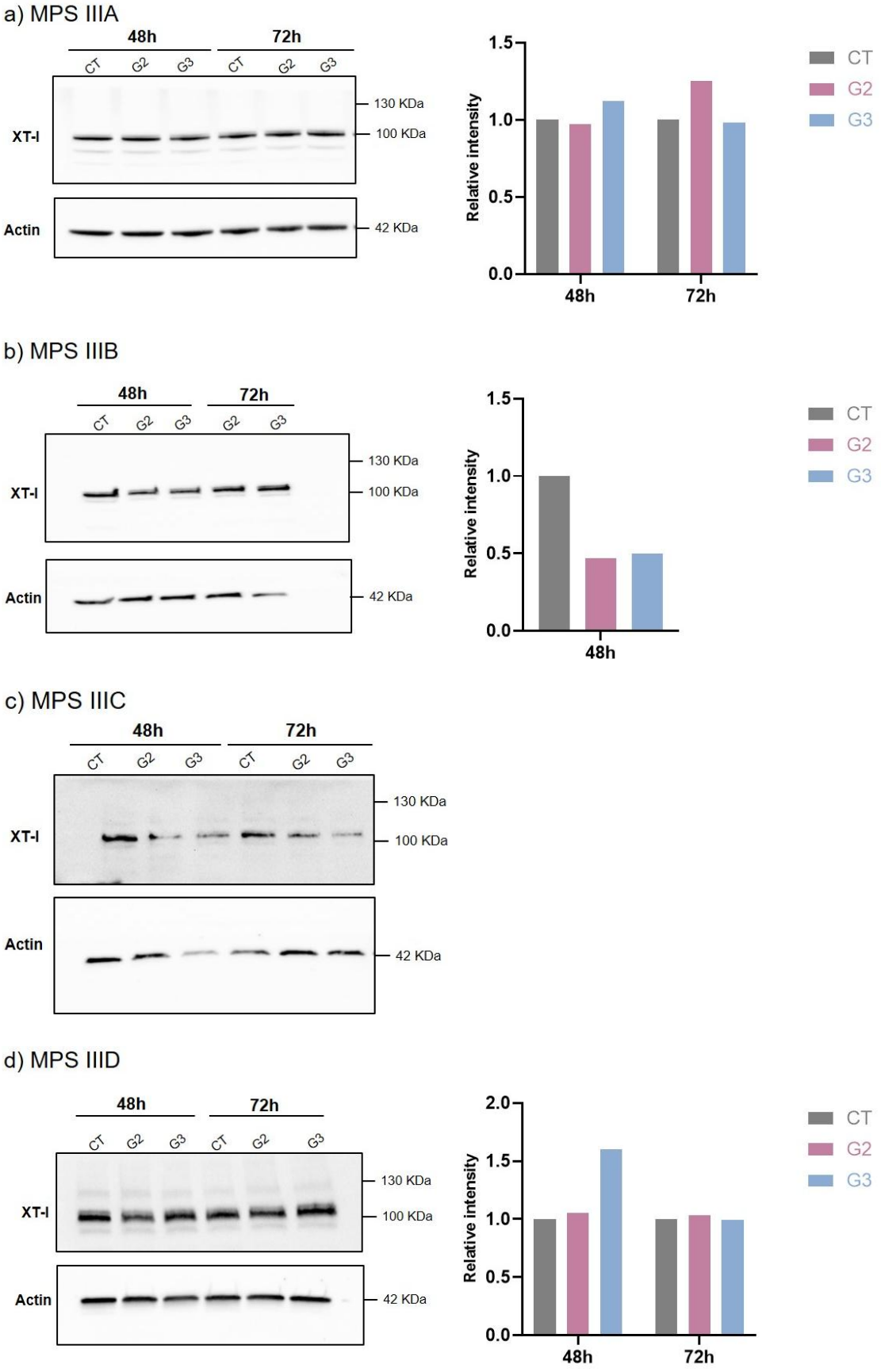


Figure 47. Quantification of Xylosyltransferase I (XT-I) in MPS III patient-derived fibroblasts after treatment with selected gapmer ASOs. The results display the XT-I levels 48 and 72 hours post-transfection of gapmers G2

and G3. The left panel displays a representative WB showing XT-I protein levels in fibroblasts from MPS III patients: a) MPS IIIA; b) MPS IIIB; c) MPS IIIC, and d) MPS IIID, transfected with G2 and G3 gapmers and non-transfected (control – CT), with Actin as a loading control. The right panel displays the quantification of the relative XT-I protein levels, normalized to Actin, for a single experiment (n=1). For MPS IIIB no quantification at 72 hours is shown and for MPS IIIC no quantification at any of the time points is presented.

2.2.2.3. Do the gapmers G2 and G3 induce a decrease on heparan sulfate (HS) storage?

The HS levels were also measured by LC-MS/MS, in cell pellets collected for all MPS III subtypes at 48 and 72 hours after transfection, using the methodology applied for protein analysis. The assessment could not be performed for MPS IIIB due to the lack of available samples and again the results were normalized to the protein quantity (Figure 48).

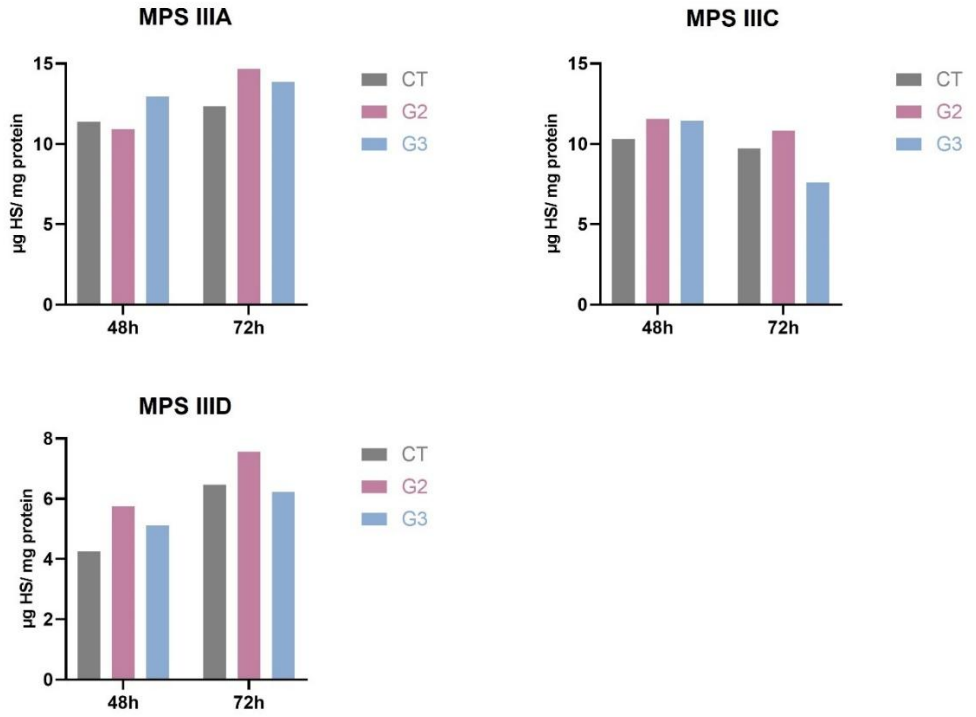


Figure 48. Quantification of Heparan Sulfate (HS) in MPS III patient-derived fibroblasts after treatment with selected gapmer ASOs. The results display the HS levels 48 and 72 hours post-transfection of gapmers G2 and G3 in subtypes A, C and D. Results are expressed in µg HS per mg protein. Data refer to a single experiment for each subtype (n=1).

No decrease on HS storage levels was observed in the samples (Figure 48). This is not surprising for the MPS IIIA and IIID cell lines, as no decrease in XT-I protein levels had been detected. For MPS IIIC, where it was not possible to quantify target protein levels, the results at 48 hours showed similar HS levels in treated and non-treated cells.

As observed for MPS IIIA and IIID, any change would be towards an increase instead of the desired reduction, at last for the first time point assessed. However, for the pellets collected 72 hours post-transfection, the response pattern was a bit different for the cells treated with gapmer number 3 (G3), where a slight decrease on HS levels was observed. This was the unique observation at 48-72 hours that seemed somehow meaningful, but its accuracy not be confirmed by the protein assessment experiments. Also inopportunely, the only cell line revealing a decrease in XT-I protein levels during the first round of macroassays, MPS IIIB, was the one for which HS assessments could not be performed.

Overall, these results convinced us that it would be necessary to increase the incubation times for the protein and substrate accumulation analysis, instead of repeating the whole experimental setup without changes. Then, a second round of macroassays was performed extending the gapmers' incubation time and focusing the study on a specific subtype, MPS IIIC, rather than including all MPS III subtypes. This option was driven by the challenges encountered previously, such as the low growth rate of subtypes A and B, which often hindered our ability to perform all the measurements necessary to draw robust conclusions. Moreover, MPS IIIC is the most complicate subtype in terms of therapeutics as the deficient enzyme- acetyl-CoA:α-glucosaminide N-acetyltransferase, is not a lumen hydrolase but rather a transmembrane protein of the lysosome. Consequently, ERT is not a viable option for patients with MPS IIIC. Furthermore, acetyl-CoA:α-glucosaminide N-acetyltransferase is not targeted to the lysosome via the M6P pathway, which implies that a recombinant version of this enzyme could be efficiently taken up by cells through M6PR, which is the fundamental mechanism of ERT. Currently, MPS IIIC is the MPS III subtype with the fewest therapeutic approaches being explored in clinical trials.

For this final experimental round, where only MPS IIIC patient-derived fibroblasts were involved, the cell pellets were collected at 24 hours to assess the treatment's effect on mRNA; at 72 and 96 hours to evaluate the XT-I protein levels and, finally, 6 and 10 days post-gapmers transfection to quantify the HS levels. These time points were in line with previous studies by Canals *et al.*, who observed a more pronounced decrease in GAGs storage 7 and 14 days post-transfection of patient fibroblasts with siRNAs [186].

Although those authors targeted different genes within the GAGs' biosynthetic cascade, their elegant strategy motivated us to adopt a revised and improved protocol. A control gapmer, targeting a different mRNA and referred to as "scramble", was included in this study to reinforce the specificity of the gapmers under analysis in promoting the expected substrate reduction.

2.2.3. The “Final assay”: are we working at the correct time points?

2.2.3.1. The effect on *XYLT1* expression levels 24 hours after gapmers’ treatment

qRT-PCR analysis was performed 24 hours after transfection of gapmers G2 and G3 at a concentration of 100 nM in MPS IIIC patient-derived fibroblasts. A scramble gapmer was also included as a control to assess the effect our two *XYLT1*-specific gapmers. The results showed a significant decrease in the target gene expression compared to cells transfected with scramble ASO, which is consistent with previous observations. The effect was more pronounced with gapmer G2, which reduced expression to around 10% ($p < 0.0001$). However, gapmer G3 also showed a notable effect with a decrease of about 70% in *XYLT1* mRNA expression ($p<0.001$) (Figure 49).

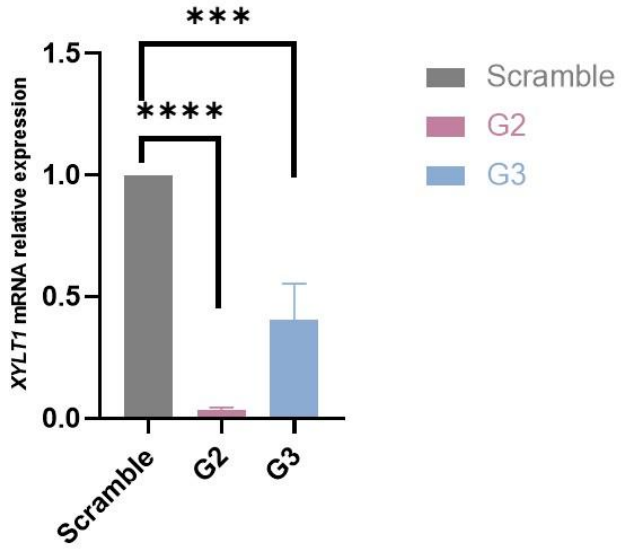


Figure 49. XYLT1 mRNA relative expression in MPS IIIC patient-derived fibroblasts. Quantification was performed 24 hours after transfection of gapmers G2 and G3, by qRT-PCR in three independent experiments (n=3). *GAPDH* was used as endogenous control. Statistical comparisons between groups were performed using one-way ANOVA and a Tukey's multiple comparisons test as a post-hoc comparator (***$p < 0.001$, ****$p < 0.0001$).

2.2.3.2. Increasing the gapmers’ incubation time to see the effect on xylosyltransferase I protein levels

Before addressing whether a decrease on HS storage levels could be achieved after treatment with the G2 and G3 gapmers, we first wanted to verify whether the decreases observed in *XYLT1* expression levels were translated into a reduction on levels of the encoded protein, XT-I. For this, XT-I levels were quantified by comparing band intensities in cells transfected with gapmers G2 and G3 to those transfected with

the scramble gapmer. As expected, at 72 and 96 hours post-transfection, MPS IIIC fibroblasts showed a reduction in XT-I protein levels. This decrease was in alignment with the high inhibition of *XYLT1* mRNA expression, indicating a corresponding decrease at the protein level. In these experiments, α-tubulin, a highly expressed cell protein, was used as a loading control for the WB analysis (Figure 50).

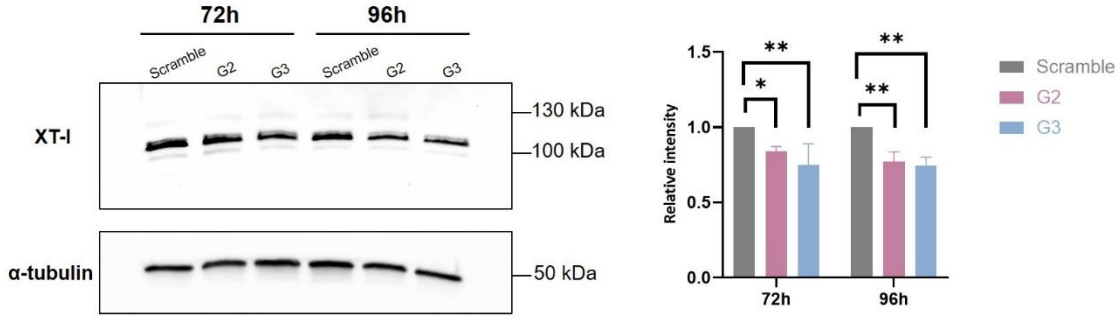


Figure 50. Quantification of Xylosyltransferase I (XT-I) in MPS IIIC patient-derived fibroblasts. The left panel displays a representative western blot showing XT-I protein levels in MPS IIIC patients' fibroblasts 72 and 96 hours post-transfection with gapmers (scramble, G2 and G3), using α-tubulin as the loading control. The right panel displays the relative quantification of the XT-I protein levels, normalized to α-tubulin, from three independent experiments (n=3). Statistical comparisons between G2 or G3 transfected cells and cells transfected with the scramble gapmer were performed using two-way ANOVA followed by Tukey's multiple comparisons test as a post-hoc comparator (*$p < 0.05$, **$p < 0.005$).

2.2.3.3. Gapmer G2 reduces the storage levels of heparan sulfate at 6 and 10 days post-transfection

Finally, we moved on to quantify our ultimate therapeutic target: HS storage. To do so, HS levels were measured by LC-MS/MS in cell pellets collected 6 days after transfection. Apart from the cells treated with the scramble control, MPS IIIC fibroblasts transfected with the transfection reagent alone and not exposed to any gapmer, either targeted or scramble, were also included. This additional samples, referred as non-transfected (NT), allowed us to assess whether the scramble gapmer or the transfection reagent itself had any effect on HS accumulation.

The HS levels were also evaluated in a control cell line, with no disease, Human Dermal Fibroblasts, adult (HDFa), to verify the accumulation pattern. These cells were platted and collected at the same time as the others (6 days). Data were normalized to protein quantity.

In MPS IIIC NT fibroblasts, HS levels were 9.92 µg / mg protein. As expected, a very similar amount of HS was detected in fibroblasts transfected with the scramble gapmer: 9.91 µg / mg protein.

The cells treated with gapmers G2 and G3 demonstrated a reduction in HS levels: 6.82 and 8.26 µg HS/ mg protein, respectively. For reference, HS levels in HDFa cells had a mean of 3.79 µg HS/ mg protein.

When comparing HS levels between HDFa to MPS IIIC fibroblasts (both non-transfected and those treated with the scramble ASO), the levels of HS were significantly lower in HDFa cells ($p < 0.0001$).

The results also showed that the gapmer G2 had a positive effect on reducing HS storage, compared to the scramble gapmer ($p < 0.05$). Although not statistically significant, a decreasing trend is observed when comparing the HS levels of the cells treated with the scramble ASO with the cells transfected with the gapmer G3 (Figure 51).

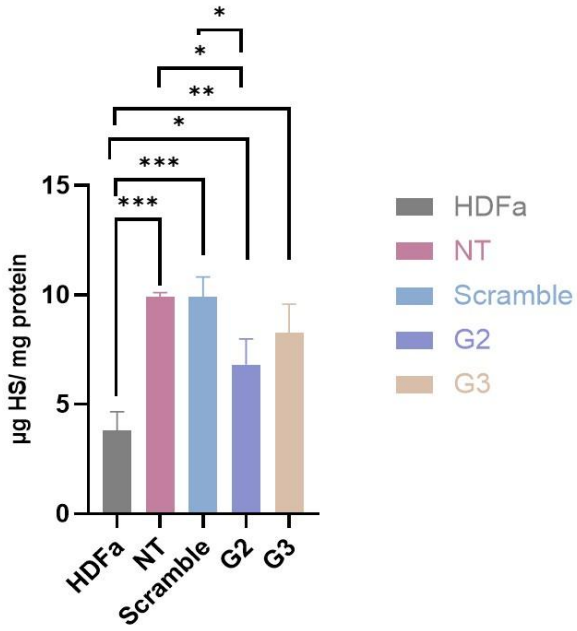


Figure 51. Quantification of heparan sulfate (HS) in MPS IIIC patient-derived fibroblasts 6 days post-transfection with selected gapmers. HS levels were measured in MPS IIIC patients' fibroblasts 6 days post-transfection with gapmers (scramble, G2 and G3) and in the human dermal fibroblast (HDFa) cell line. Results are expressed in µg HS per mg of protein. Statistical comparisons between groups were performed using one-way ANOVA and a Tukey's multiple comparisons test as a post-hoc comparator (*$p < 0.05$, **$p < 0.005$, ***$p < 0.001$). NT: Non-transfected MPS IIIC fibroblasts.

To check whether the effect of the best performing gapmer, G2, persisted over time, we have evaluate its ability to reduce the HS storage in fibroblasts from MPS IIIC patients 10 days post transfection. Gapmer G3 was also included in this analysis, despite the lack of statistical significance observed 6 days after transfection, in order to verify whether its effect was consistently lower than that of gapmer G2, or if it required a longer timeframe to reach statistical significance, unlike gapmer G2.

The results demonstrated that the effect of gapmer G2 is maintained over time, compared to fibroblasts transfected with gapmer scramble ($p < 0.05$). A trend towards a reduction (not statistical significant) was once again detected with gapmer G3 (Figure 52). Not surprisingly, patients' fibroblasts showed a pronounced increase in HS storage over time (with means ranging from 9.91 to 17.12 µg HS/ mg protein), since these cells are not able to degrade HS.

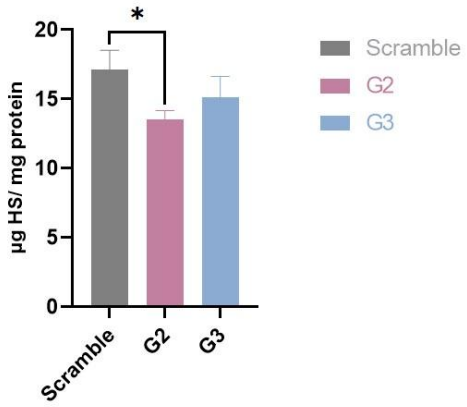


Figure 52. Quantification of heparan sulfate (HS) in MPS IIIC patient-derived fibroblasts 10 days post-transfection with selected gapmers. HS levels were measured in MPS IIIC patients' fibroblasts 10 days post-transfection with gapmers (scramble, G2 and G3). Results are expressed in µg HS per mg of protein. Statistical comparisons between groups were performed using one-way ANOVA and a Tukey's multiple comparisons test as a post-hoc comparator (*$p < 0.05$).

Altogether, the results obtained for the MPS IIIC cell line are remarkable, as they provide proof of concept that 2'-MOE-PS gapmers can effectively downregulate *XYLT1* expression, while demonstrating that reducing XT-I levels leads to a substantial decrease in HS accumulation, thus acting upon the primary cause of MPS IIIC pathology.

Our study reinforces that gSRT could be a valuable therapeutic strategy for LSDs with significant neurological involvement. Also noteworthy, this is the first study to provide a quantitative analysis on the effect one such approach may have upon HS *in vitro*. By doing so, we are assessing the true disease biomarker, which is well-established as the trigger of the pathophysiological cascade. Before, the unique study had specifically assessed HS alone was that of Canals *et al*., in 2015 [186]. However, their analysis was not conducted in a quantitative manner. The results for HS were qualitative, instead, and acquired through immunocytochemistry.

The successful use of ASOs in CNS-related disorders, such as spinal muscular atrophy [235] and Batten disease [171] further supports their applicability to MPS III [84,85,236-238].

Future research should focus on *in vivo* validation in animal models, such as zebrafish or rodents, to evaluate biodistribution, safety, and long-term efficacy, paving the way for clinical translation.

Altogether, the pioneer results obtained for the MPS IIIC cell line, were recently compiled, discussed, and accepted for publication (see Annex 1; original manuscript #1).

Conclusions and Future perspectives

In this work, several questions were answered in the context of RNA-based therapeutics for MSP III and the new findings provided an important advance in the field. Naturally that many other novel and challenging questions have also arisen, opening prospects for future researches.

In this last section, we summarize the main conclusions we were able to draw from these proof-of-principle studies on the potential of several different RNA-based approaches to counteract different forms of the complex childhood-onset dementia MPS III, while outlining the next steps to further validate the most promising ones.

Part I

In the first part of this work, we carried out *in vitro* and *in vivo* studies to explore the potential of an U1 snRNA engineered vector (U1 snRNATC), fully complementary to the mutated 5'ss of the exon 2 of the *HGSNAT* gene as a therapeutic strategy to correct the common disease-causing splicing variant, c.234+1G>A. This mutation leads to the skipping of *HGSNAT* exon 2, underlying a severe form of MPS IIIC. Thus, our goal was to rescue this splicing defect and restore the normal transcript. Initial *in vitro* analysis in two different cell lines, Hep-3B and COS-7, validated that the constructed midigenes, the wild-type (pHGSNATwt) and the midigene carrying the mutation under study (pHGSNAT+1A), were able to replicate the expected splicing patterns when expressed in those cells. Similar splicing patterns were also obtained for another cell line existing in the lab, HEK293T, which has a faster growth rate. This particular feature lead us to consider HEK293T cells as a more suitable option to pursue with the *in vitro* studies.

After co-transfecting the pHGSNATwt or pHGSNAT+1A midigenes with the U1 snRNAwt and/or U1 snRNATC in HEK293T cells, it was possible to demonstrate the reliability of this model for studying the capacity of the engineered U1 snRNATC rescue the splicing defect. However, despite the co-transfection of the midigene harboring the mutation with our therapeutic candidate, U1 snRNATC, resulted in the inclusion of exon 2, it brought along four additional nucleotides from intron 2, thus generating an equally aberrant transcript.

Nonetheless, taking into account that these *in vitro* systems are highly artificial and do not fully replicate the human biological processes by lacking genomic context, and given that we obtained approximately 50% restoration of normal transcripts in patient-derived fibroblasts treated with the same modified U1snRNA engineered vector in our previously published work [136], we decided to proceed with the *in vivo* studies.

In the absence of an animal model carrying the target mutation, it was sought an alternative approach to evaluate the therapeutic efficacy of our modified U1snRNA *in vivo*. Having the collaboration of our international consultors from the University of Ferrara, who previously published a study using the same method [137], we have promoted the transient expression of pHGSNATwt and pHGSNAT+1A in C57BL/6 wild-type mouse. To evaluate potential differences in expression, two different plasmid doses were injected, using hydrodynamic injection, a challenging method of administration, which had already been reported to promote efficient non-viral delivery of plasmids to hepatocytes in mice. Unfortunately, despite the extensive experience of the operator who carried out the test, a high mortality rate was obtained. Overall, no animal from the group that received pHGSNATwt 1 µg/g survived. Furthermore, the molecular analysis of the remaining animals showed that the pHGSNATwt midigene was not expressed in any of the five animals who received 2 µg/g of the plasmid. However, in some animals administered with pHGSNAT+1A, it was possible to observe a very faint band in the region of interest, after agarose gel electrophoresis of the target PCR product. Still, only in one animal it was possible to sequence the band and confirm the presence of the human *HGSNAT* transcript lacking exon 2, confirming the desired liver-targeted expression of the injected pHGSNAT+1A midigene. In general, however, these results imply that the attempted hydrodynamic injection protocol failed to successfully promote a sufficient expression to enable robust preclinical testing of our modified U1snRNA vector.

As many technical hurdles were encountered, we decided to explore an alternative delivery method known to promote high and sustained levels of target gene expression: Adeno-associated virus (AAV) vector-mediated delivery. Additionally, also the mouse strain was changed in our second round of *in vivo* studies, having been substituted by FVB/N instead, an inbred mouse strain commonly preferred for transgenic analyses.

AAV vectors were used to enable prolonged expression of both the wild-type and mutant midigenes, thereby creating an *in vivo* model for assessing the therapeutic potential of the modified U1snRNA. However, before generating the AAV constructs, it was necessary to select the appropriate serotype where the midigenes and the U1 snRNA molecules would be inserted. To this end, four different AAV serotypes were tested by IV injection, followed by quantitative real-time PCR of their expression. The results showed no major differences in the expression levels among the tested serotypes.

This observation, paired with the fact that the brain is the primary target organ for the therapeutic approach under investigation, indicated that AAV2/9 was the optimal vector for achieving robust and sustained transgene expression, leveraging its documented tropism for neural and hepatic tissues. This choice was further validated by our international collaborators from the Leuven Viral Vector Core facility, who synthesized the AAV2/9_HGSNATwt, AAV2/9_HGSNAT+1A, AAV2/9_U1snRNAwt, and AAV2/9_U1snRNATC vectors.

Subsequent *in vivo* studies using this novel experimental setup provided evidence supporting the efficacy of U1snRNATC in rescuing the splicing defect caused by the c.234+1G>A mutation. Briefly, the treatment with the vector fully complementary to the mutated 5'ss, the AAV2/9_U1snRNATC, resulted in the complete inclusion of exon 2 in four out of five animals injected with AAV2/9_HGSNAT+1A. Moreover, the absence of significant toxicity associated with AAV2/9-mediated delivery further supports the translational potential of this approach for clinical applications.

Overall, this finding represents a significant milestone not only in the development of RNA-based therapies for MPS IIIC but also in the design and evaluation of U1snRNA-based therapeutics in general, as it represents the first successful correction of a +1 5'ss mutation, in an *in vivo* model. Finally, it must be emphasized the critical role of the *in vivo* models in the development of any therapeutic. While *in vitro* systems are essential for initial evaluations of any potential drug, as provide good readouts at RNA, protein, or even functional levels, they cannot fully capture the complexity of a whole organism's physiological conditions. The successful *in vivo* correction here demonstrated highlights the importance of ethically conducted animal studies to achieve meaningful scientific results.

Future efforts should focus on optimizing delivery techniques, investigating dose-response dynamics, and evaluating long-term therapeutic effects in clinically relevant animal models. These steps will be pivotal in advancing U1snRNA-based therapies toward clinical implementation and meeting the unmet needs of patients with MPS IIIC.

Part II

In the second part of this work, we explored a genetic substrate reduction therapy (gSRT) for Mucopolysacharidoses type III (MPS III). We focused on the use of RNA-based drugs to decrease the synthesis of a particular glycosaminoglycan (GAG), which accumulates in this particular syndrome: heparan sulfate (HS). However, our approach can be applied to other subtypes of MPS, as we targeted a gene involved in an early step of the GAGs biosynthesis - *XYLT1*. This gene encodes for a protein that catalyzes

the first step in the biosynthesis of several GAGs, including not only HS but also chondroitin sulfate and dermatan sulfate. Ultimately, this means that any approach actively targeting this gene for downregulation could reduce the levels of those other GAGs, thus holding potential to ameliorate the pathology of other MPS types that accumulate them.

We took advantage of three different types of RNA molecules, each with a distinct mechanism of action. The first ones were small interfering RNAs (siRNAs) that act by using the RNA interference (RNAi) pathway, and upon binding to the target mRNA mediate its cleavage and, consequently, its degradation by the cell. The second were splice-switching oligonucleotides (SSOs), a type of antisense oligonucleotides (ASOs) commonly used to modulate the splicing process of their target transcript. The third were gapmer ASOs, used for gene silencing by inducing RNA cleavage through the recruitment of RNase H.

We started by testing a low concentration (20 nM) of a pool of three anti- *XYLT1* siRNAs in fibroblasts from patients with all MPS III subtypes (A-D). Its effect was evaluated 24 and 48 hours post-transfection and significant reductions (50-70%) in the relative expression of our target gene were observed. These results provided proof of concept on the effect of the siRNA pool at the RNA level. However, while siRNAs showed a reasonable performance, their clinical translation faces some hurdles, with the major one likely being efficient and sustained delivery to the CNS, which was our primary therapeutic target. That is why alternative strategies were investigated in in the course of the work.

The second gSRT approach for MPS III was fundamentally centered on splicing modulation. Specifically, we employed SSOs to interfere with constitutive splicing and induce out-of-frame exon skipping, thereby removing the target exon from the mRNA. By doing so, we expected to disrupt the open reading frame (ORF), causing a frameshift that leads to the generation of a premature stop codon (PTC), ultimately triggering the degradation of the *XYLT1* mRNA through the nonsense-mediated mRNA decay (NMD) mechanism. This strategy diverges from the traditional use of SSOs, which are typically employed to restore functional proteins.

Five 2‘-MOE-PS SSOs were designed to achieve substrate reduction, with careful selection of the targeted *XYLT1* exons. The five candidates were transfected into MPS III patient-derived fibroblasts to select the most effective ones. The selection criterion was the ability of each SSO to induce the skipping of the target exon, decreasing the synthesis of the normal transcript and increasing that of the aberrant transcript. Additionally, three different concentrations of each candidate were tested with 200 nM

proving to be the most effective for subsequent analyses. After evaluating the results, SSO3 and SSO5 were considered the most suiatable candidates as they demonstrated a more pronounced effect, skipping correctly their target exons at both time-points analysed.

At the same time-points, the levels of xylosyltransferase I (XT-I), the enzyme encoded by *XYLT1*, and HS storage were evaluated. However, despite success at RNA-level, no significant reductions were observed. We hypothesized that it could require longer incubation periods for XT-I protein levels to reflect the reductions seen at the mRNA level. The same for HS storage, which we considered plausible to be reflected even later. Overall, although additional studies would have to be performed in order to fully clarify this issue, the incomplete knockdown of wild-type transcripts which were still present alongside the desired exon-skipped ones, suggests that the SSO potency was insufficient to achieve the desired effect. Still, considering the significant therapeutic potential of SSOs, this approach will undergo further testing, with extended incubation times. Only after these additional studies it will be possible to draw definitive conclusions about their true therapeutic value. Until then, we can only speculate on the potential these specific SSO candidates may offer.

Not discarding SSOs might have a therapeutic action, we then proceeded to explore the third type of RNA-based drugs used for gSRT: gapmer ASOs. Five potential therapeutic molecules were synthetized, all with the same chemical modifications, the 2'-MOE-PS. After their test in MPS III cell lines at different concentrations, the most promising candidates, gapmers G2 and G3, were selected based on their capacity to decrease the *XYLT1* relative expression. These two drugs were subsequently transfected into patient-derived fibroblasts to evaluate their effect on XT-I levels and HS storage. Grounded on our previous experience trying to measure XT-I decreases after SSO treatment, we increased the gapmers' incubation time to 72 hours, performing the first protein analyses 48 and 72 hours post- transfection. Once again, no differences were observed between non-transfected cells and those treated with the two gapmers. However, a slight decrease in HS levels was noted in G3-treated cells at 72 hours. These results were compelling enough to consider that increasing the incubation times for protein and substrate accumulation analysis would be more effective than simply repeating the experiment without any further modifications. With this in mind, we proceeded with a second round of macroassays, extending the incubation time for the gapmers under analysis. Another change we made to the initial experimental setup, was to narrow the focus to a single MPS III subtype, MPS IIIC, rather than including all subtypes. Among the various subtypes, MPS IIIC is the one that poses the greatest

therapeutic challenge, as it results from a deficiency of a lysosomal transmembrane protein/enzyme. This made it the choice for our study, as it seemed worthwhile to invest in an alternative therapeutic approach.

In this final macroassay, gapmers G2 and G3 demonstrated significant reductions in *XYLT1* mRNA expression, with G2 achieving the highest knockdown rates. Extended gapmers' incubation periods, 72 and 98 hours, confirmed a concomitant decrease in XT-I protein levels. Most importantly, a significant reduction in HS storage was observed 6 days after G2 treatment, whose effect was maintained over 10 days post-transfection, demonstrating long-lasting therapeutic potential. In contrast, for gapmer G3, only a decreasing trend in HS levels was observed when comparing the results to the scramble ASO-treated samples. Overall, the interesting results obtained for the MPS IIIC cell line, open a window for further investigations. Already envisaged are similar studies with the two best performing gapmers (G2 in particular) in other MPS III lines, namely the ones we have available in our lab, as well as new MPS III lines, which will be acquired for this purpose.

Additional preclinical assessments aimed at eventual clinical translation, may also include the analysis of secondary storage patterns and/or evaluation of altered pathophysiological mechanisms, known to be affected in MPS III.

The *in vitro* results must also be validated in animal models to assess the biodistribution, safety, and long-term efficacy of gapmer ASOs. Already under development in our lab are studies in MPS III zebrafish models [239], which will allow to evaluate whether this novel gapmer-based treatment holds potential to ameliorate the MPS III phenotype. If the results are positive, rodent models may be used later on to provide additional insights into the therapeutic potential and dosing regimens required for clinical applications.

While further studies are still needed to fully validate its potential, the ability of our gapmer ASO to reduce HS storage *in vitro* is surely a remarkable observation, which may prompt beneficial advances in the treatment of the MPS III syndromes, where a lack of therapeutic options is a strong concern. The use of ASOs for CNS disorders further underscores their potential, as they can be delivered intrathecally to bypass the blood-brain barrier, thus addressing the severe neurological symptoms associated with MPS III.

Final Remarks

Overall, the work described in this thesis, is a tour-de-force on the potential of various RNA-based therapeutic approaches for the molecular, biochemical and, ultimately, phenotypic correction of the genetic defects and their subsequent consequences (e.g. abnormal accumulation of un- or partially-degraded substrates), which underlie a life-threatening group of diseases, known as MPS III, or Sanfilippo syndrome.

All the studies developed relied in original approaches within the broader field of LSDs, were scarce research has been done on the benefits of RNA-based therapeutics.

Innovative in work was also the first attempt to validate a therapeutic approach *in vivo.* That has greatly benefited from the input and expertise of several national and international researchers, as well as the collaboration of experienced operators in conducting hands-on *in vivo* studies.

Numerous challenges were faced, from which we learnt valuable lessons. We had to optimize many protocols and refine conventional experimental setups, adjusting delivery vectors, injection methods, concentration ranges and time-points for different experimental readouts. Hopefully, the successes and failures here reported will illuminate additional studies that ultimately can be translated into the clinical pratice.

The work underscores the transformative potential of personalized RNA-based strategies, paving the way for future advancements in the treatment of not only MPS III and related diseases, but also other rare diseases.

References

1. De Duve, C. The lysosome. *Sci Am* **1963**, *208*, 64-72, doi:10.1038/scientificamerican0563-64.
2. Parenti, G.; Andria, G.; Ballabio, A. Lysosomal storage diseases: from pathophysiology to therapy. *Annu Rev Med* **2015**, *66*, 471-486, doi:10.1146/annurev-med-122313-085916.
3. Ballabio, A.; Bonifacino, J.S. Lysosomes as dynamic regulators of cell and organismal homeostasis. *Nat Rev Mol Cell Biol* **2020**, *21*, 101-118, doi:10.1038/s41580-019-0185-4.
4. Braulke, T.; Bonifacino, J.S. Sorting of lysosomal proteins. *Biochim Biophys Acta* **2009**, *1793*, 605-614, doi:10.1016/j.bbamcr.2008.10.016.
5. Fuller, M.; Meikle, P.; Hopwood, J. *Epidemiology of lysosomal storage diseases: an overview. In: Fabry Disease: Perspectives from 5 Years of FOS*; Mehta, A., Beck, M., Sunder-Plassmann, G., Eds.; Oxford PharmaGenesis: Oxford, 2006.
6. Filocamo, M.; Morrone, A. Lysosomal storage disorders: molecular basis and laboratory testing. *Hum Genomics* **2011**, *5*, 156-169, doi:10.1186/1479-7364-5-3-156.
7. La Cognata, V.; Guarnaccia, M.; Polizzi, A.; Ruggieri, M.; Cavallaro, S. Highlights on Genomics Applications for Lysosomal Storage Diseases. *Cells* **2020**, *9*, doi:10.3390/cells9081902.
8. Platt, F.M.; d'Azzo, A.; Davidson, B.L.; Neufeld, E.F.; Tifft, C.J. Lysosomal storage diseases. *Nat Rev Dis Primers* **2018**, *4*, 27, doi:10.1038/s41572-018-0025-4.
9. Mokhtariye, A.; Hagh-Nazari, L.; Varasteh, A.R.; Keyfi, F. Diagnostic methods for Lysosomal Storage Disease. *Rep Biochem Mol Biol* **2019**, *7*, 119-128.
10. Zanetti, A.; D'Avanzo, F.; Bertoldi, L.; Zampieri, G.; Feltrin, E.; De Pascale, F.; Rampazzo, A.; Forzan, M.; Valle, G.; Tomanin, R. Setup and Validation of a Targeted Next-Generation Sequencing Approach for the Diagnosis of Lysosomal Storage Disorders. *J Mol Diagn* **2020**, *22*, 488-502, doi:10.1016/j.jmoldx.2020.01.010.
11. Fernández-Pereira, C.; San Millán-Tejado, B.; Gallardo-Gómez, M.; Pérez-Márquez, T.; Alves-Villar, M.; Melcón-Crespo, C.; Fernández-Martín, J.; Ortolano, S. Therapeutic Approaches in Lysosomal Storage Diseases. *Biomolecules* **2021**, *11*, doi:10.3390/biom11121775.
12. Ellison, S.; Parker, H.; Bigger, B. Advances in therapies for neurological lysosomal storage disorders. *J Inherit Metab Dis* **2023**, *46*, 874-905, doi:10.1002/jimd.12615.
13. Heon-Roberts, R.; Nguyen, A.L.A.; Pshezhetsky, A.V. Molecular Bases of Neurodegeneration and Cognitive Decline, the Major Burden of Sanfilippo Disease. *J Clin Med* **2020**, *9*, doi:10.3390/jcm9020344.
14. Rossi, A.; Brunetti-Pierri, N. Gene therapies for mucopolysaccharidoses. *J Inherit Metab Dis* **2024**, *47*, 135-144, doi:10.1002/jimd.12626.
15. Viana, G.M.; Priestman, D.A.; Platt, F.M.; Khan, S.; Tomatsu, S.; Pshezhetsky, A.V. Brain Pathology in Mucopolysaccharidoses (MPS) Patients with Neurological Forms. *J Clin Med* **2020**, *9*, doi:10.3390/jcm9020396.
16. Coutinho, M.F.; Lacerda, L.; Alves, S. Glycosaminoglycan storage disorders: a review. *Biochem Res Int* **2012**, *2012*, 471325, doi:10.1155/2012/471325.
17. Giugliani, R. *The Mucopolysaccharidoses , in Lysosomal Storage Disorders - a practical guide*; Wiley-Blackwell: UK, 2013.
18. Rapoport, D.M.; Mitchell, J.J. Pathophysiology, evaluation, and management of sleep disorders in the mucopolysaccharidoses. *Mol Genet Metab* **2017**, *122S*, 49-54, doi:10.1016/j.ymgme.2017.08.008.
19. Kubaski, F.; Osago, H.; Mason, R.W.; Yamaguchi, S.; Kobayashi, H.; Tsuchiya, M.; Orii, T.; Tomatsu, S. Glycosaminoglycans detection methods: Applications of

mass spectrometry. *Mol Genet Metab* **2017**, *120*, 67-77, doi:10.1016/j.ymgme.2016.09.005.

20. Peters, H.; Ellaway, C.; Nicholls, K.; Reardon, K.; Szer, J. Treatable lysosomal storage diseases in the advent of disease-specific therapy. *Intern Med J* **2020**, *50 Suppl 4*, 5-27, doi:10.1111/imj.15100.
21. Chen, H.H.; Sawamoto, K.; Mason, R.W.; Kobayashi, H.; Yamaguchi, S.; Suzuki, Y.; Orii, K.; Orii, T.; Tomatsu, S. Enzyme replacement therapy for mucopolysaccharidoses; past, present, and future. *J Hum Genet* **2019**, *64*, 1153-1171, doi:10.1038/s10038-019-0662-9.
22. Penon-Portmann, M.; Blair, D.R.; Harmatz, P. Current and new therapies for mucopolysaccharidoses. *Pediatr Neonatol* **2023**, *64 Suppl 1*, S10-S17, doi:10.1016/j.pedneo.2022.10.001.
23. Tanaka, A.; Okuyama, T.; Suzuki, Y.; Sakai, N.; Takakura, H.; Sawada, T.; Tanaka, T.; Otomo, T.; Ohashi, T.; Ishige-Wada, M.; et al. Long-term efficacy of hematopoietic stem cell transplantation on brain involvement in patients with mucopolysaccharidosis type II: a nationwide survey in Japan. *Mol Genet Metab* **2012**, *107*, 513-520, doi:10.1016/j.ymgme.2012.09.004.
24. Wood, S.R.; Bigger, B.W. Delivering gene therapy for mucopolysaccharide diseases. *Front Mol Biosci* **2022**, *9*, 965089, doi:10.3389/fmolb.2022.965089.
25. Wang, D.; Tai, P.W.L.; Gao, G. Adeno-associated virus vector as a platform for gene therapy delivery. *Nat Rev Drug Discov* **2019**, *18*, 358-378, doi:10.1038/s41573-019-0012-9.
26. Issa, S.S.; Shaimardanova, A.A.; Solovyeva, V.V.; Rizvanov, A.A. Various AAV Serotypes and Their Applications in Gene Therapy: An Overview. *Cells* **2023**, *12*, doi:10.3390/cells12050785.
27. Narita, A.; Shirai, K.; Itamura, S.; Matsuda, A.; Ishihara, A.; Matsushita, K.; Fukuda, C.; Kubota, N.; Takayama, R.; Shigematsu, H.; et al. Ambroxol chaperone therapy for neuronopathic Gaucher disease: A pilot study. *Ann Clin Transl Neurol* **2016**, *3*, 200-215, doi:10.1002/acn3.292.
28. de la Mata, M.; Cotán, D.; Oropesa-Ávila, M.; Garrido-Maraver, J.; Cordero, M.D.; Villanueva Paz, M.; Delgado Pavón, A.; Alcocer-Gómez, E.; de Lavera, I.; Ybot-González, P.; et al. Pharmacological Chaperones and Coenzyme Q10 Treatment Improves Mutant β-Glucocerebrosidase Activity and Mitochondrial Function in Neuronopathic Forms of Gaucher Disease. *Sci Rep* **2015**, *5*, 10903, doi:10.1038/srep10903.
29. Germain, D.P.; Hughes, D.A.; Nicholls, K.; Bichet, D.G.; Giugliani, R.; Wilcox, W.R.; Feliciani, C.; Shankar, S.P.; Ezgu, F.; Amartino, H.; et al. Treatment of Fabry's Disease with the Pharmacologic Chaperone Migalastat. *N Engl J Med* **2016**, *375*, 545-555, doi:10.1056/NEJMoa1510198.
30. Müntze, J.; Gensler, D.; Maniuc, O.; Liu, D.; Cairns, T.; Oder, D.; Hu, K.; Lorenz, K.; Frantz, S.; Wanner, C.; et al. Oral Chaperone Therapy Migalastat for Treating Fabry Disease: Enzymatic Response and Serum Biomarker Changes After 1 Year. *Clin Pharmacol Ther* **2019**, *105*, 1224-1233, doi:10.1002/cpt.1321.
31. Losada Díaz, J.C.; Cepeda Del Castillo, J.; Rodriguez-López, E.A.; Alméciga-Díaz, C.J. Advances in the Development of Pharmacological Chaperones for the Mucopolysaccharidoses. *Int J Mol Sci* **2019**, *21*, doi:10.3390/ijms21010232.
32. Coutinho, M.F.; Santos, J.I.; Alves, S. Less Is More: Substrate Reduction Therapy for Lysosomal Storage Disorders. *Int J Mol Sci* **2016**, *17*, doi:10.3390/ijms17071065.
33. Cox, T.M. Substrate reduction therapy for lysosomal storage diseases. *Acta Paediatr Suppl* **2005**, *94*, 69-75; discussion 57, doi:10.1111/j.1651-2227.2005.tb02116.x.
34. Radin, N.S. Treatment of Gaucher disease with an enzyme inhibitor. *Glycoconj J* **1996**, *13*, 153-157, doi:10.1007/BF00731489.

35. Platt, F.M.; Jeyakumar, M.; Andersson, U.; Heare, T.; Dwek, R.A.; Butters, T.D. Substrate reduction therapy in mouse models of the glycosphingolipidoses. *Philos Trans R Soc Lond B Biol Sci* **2003**, *358*, 947-954, doi:10.1098/rstb.2003.1279.
36. Yue, W.W.; Mackinnon, S.; Bezerra, G.A. Substrate reduction therapy for inborn errors of metabolism. *Emerg Top Life Sci* **2019**, *3*, 63-73, doi:10.1042/ETLS20180058.
37. Piotrowska, E.; Jakóbkiewicz-Banecka, J.; Tylki-Szymanska, A.; Liberek, A.; Maryniak, A.; Malinowska, M.; Czartoryska, B.; Puk, E.; Kloska, A.; Liberek, T.; et al. Genistin-rich soy isoflavone extract in substrate reduction therapy for Sanfilippo syndrome: An open-label, pilot study in 10 pediatric patients. *Curr Ther Res Clin Exp* **2008**, *69*, 166-179, doi:10.1016/j.curtheres.2008.04.002.
38. Sawamoto, K.; Stapleton, M.; Alméciga-Díaz, C.J.; Espejo-Mojica, A.J.; Losada, J.C.; Suarez, D.A.; Tomatsu, S. Therapeutic Options for Mucopolysaccharidoses: Current and Emerging Treatments. *Drugs* **2019**, *79*, 1103-1134, doi:10.1007/s40265-019-01147-4.
39. Pearse, Y.; Iacovino, M. A Cure for Sanfilippo Syndrome? A Summary of Current Therapeutic Approaches and their Promise. *Med Res Arch* **2020**, *8*, doi:10.18103/mra.v8i2.2045.
40. Inatani, M.; Irie, F.; Plump, A.S.; Tessier-Lavigne, M.; Yamaguchi, Y. Mammalian brain morphogenesis and midline axon guidance require heparan sulfate. *Science* **2003**, *302*, 1044-1046, doi:10.1126/science.1090497.
41. Yu, C.; Griffiths, L.R.; Haupt, L.M. Exploiting Heparan Sulfate Proteoglycans in Human Neurogenesis-Controlling Lineage Specification and Fate. *Front Integr Neurosci* **2017**, *11*, 28, doi:10.3389/fnint.2017.00028.
42. Spahiu, L.; Behluli, E.; Peterlin, B.; Nefic, H.; Hadziselimovic, R.; Liehr, T.; Temaj, G. Mucopolysaccharidosis III: Molecular basis and treatment. *Pediatr Endocrinol Diabetes Metab* **2021**, *27*, 201-208, doi:10.5114/pedm.2021.109270.
43. Rintz, E.; Banacki, M.; Ziemian, M.; Kobus, B.; Wegrzyn, G. Causes of death in mucopolysaccharidoses. *Mol Genet Metab* **2024**, *142*, 108507, doi:10.1016/j.ymgme.2024.108507.
44. Sahin, O.; Thompson, H.P.; Goodman, G.W.; Li, J.; Urayama, A. Mucopolysaccharidoses and the blood-brain barrier. *Fluids Barriers CNS* **2022**, *19*, 76, doi:10.1186/s12987-022-00373-5.
45. Trabszo, C.; Ramms, B.; Chopra, P.; Lüllmann-Rauch, R.; Stroobants, S.; Sproß, J.; Jeschke, A.; Schinke, T.; Boons, G.J.; Esko, J.D.; et al. Arylsulfatase K inactivation causes mucopolysaccharidosis due to deficient glucuronate desulfation of heparan and chondroitin sulfate. *Biochem J* **2020**, *477*, 3433-3451, doi:10.1042/BCJ20200546.
46. Winner, L.K.; Rogers, M.L.; Snel, M.F.; Hemsley, K.M. Biomarkers for predicting disease course in Sanfilippo syndrome: An urgent unmet need in childhood-onset dementia. *J Neurochem* **2023**, *166*, 481-496, doi:10.1111/jnc.15891.
47. Wiśniewska, K.; Wolski, J.; Żabińska, M.; Szulc, A.; Gaffke, L.; Pierzynowska, K.; Węgrzyn, G. Mucopolysaccharidosis Type IIIE: A Real Human Disease or a Diagnostic Pitfall? *Diagnostics (Basel)* **2024**, *14*, doi:10.3390/diagnostics14161734.
48. Kowalewski, B.; Lamanna, W.C.; Lawrence, R.; Damme, M.; Stroobants, S.; Padva, M.; Kalus, I.; Frese, M.A.; Lübke, T.; Lüllmann-Rauch, R.; et al. Arylsulfatase G inactivation causes loss of heparan sulfate 3-O-sulfatase activity and mucopolysaccharidosis in mice. *Proc Natl Acad Sci U S A* **2012**, *109*, 10310-10315, doi:10.1073/pnas.1202071109.
49. Khateb, S.; Kowalewski, B.; Bedoni, N.; Damme, M.; Pollack, N.; Saada, A.; Obolensky, A.; Ben-Yosef, T.; Gross, M.; Dierks, T.; et al. A homozygous founder missense variant in arylsulfatase G abolishes its enzymatic activity causing

atypical Usher syndrome in humans. *Genet Med* **2018**, *20*, 1004-1012, doi:10.1038/gim.2017.227.
50. De Falco, A.; Karali, M.; Criscuolo, C.; Testa, F.; Barillari, M.R.; Scarpato, M.; Gaudieri, V.; Cuocolo, A.; Russo, A.; Nigro, V.; et al. Late-onset mucopolysaccharidosis type IIIA mimicking Usher syndrome. *Am J Med Genet A* **2024**, *194*, e63517, doi:10.1002/ajmg.a.63517.
51. Jones, S.A.; Breen, C.; Heap, F.; Rust, S.; de Ruijter, J.; Tump, E.; Marchal, J.P.; Pan, L.; Qiu, Y.; Chung, J.K.; et al. A phase 1/2 study of intrathecal heparan-N-sulfatase in patients with mucopolysaccharidosis IIIA. *Mol Genet Metab* **2016**, *118*, 198-205, doi:10.1016/j.ymgme.2016.05.006.
52. Wijburg, F.A.; Whitley, C.B.; Muenzer, J.; Gasperini, S.; Del Toro, M.; Muschol, N.; Cleary, M.; Sevin, C.; Shapiro, E.; Bhargava, P.; et al. Intrathecal heparan-N-sulfatase in patients with Sanfilippo syndrome type A: A phase IIb randomized trial. *Mol Genet Metab* **2019**, *126*, 121-130, doi:10.1016/j.ymgme.2018.10.006.
53. Whitley, C.B.; Vijay, S.; Yao, B.; Pineda, M.; Parker, G.J.M.; Rojas-Caro, S.; Zhang, X.; Dai, Y.; Cinar, A.; Bubb, G.; et al. Final results of the phase 1/2, open-label clinical study of intravenous recombinant human N-acetyl-α-d-glucosaminidase (SBC-103) in children with mucopolysaccharidosis IIIB. *Mol Genet Metab* **2019**, *126*, 131-138, doi:10.1016/j.ymgme.2018.12.003.
54. Seker Yilmaz, B.; Davison, J.; Jones, S.A.; Baruteau, J. Novel therapies for mucopolysaccharidosis type III. *J Inherit Metab Dis* **2021**, *44*, 129-147, doi:10.1002/jimd.12316.
55. Lysogene. Long-term Follow-up of Sanfilippo Type A Patients Treated by Intracerebral SAF-301 Gene Therapy. Available online: https://clinicaltrials.gov/study/NCT02053064?term=NCT02053064&rank=1 (accessed on 30 December 2024).
56. Abeona Therapeutics, I. Gene Transfer Clinical Trial for Mucopolysaccharidosis (MPS) IIIB (MPSIIIB). Available online: https://clinicaltrials.gov/study/NCT03315182?term=NCT03315182&rank=1 (accessed on 30 December 2024).
57. Tardieu, M.; Zérah, M.; Husson, B.; de Bournonville, S.; Deiva, K.; Adamsbaum, C.; Vincent, F.; Hocquemiller, M.; Broissand, C.; Furlan, V.; et al. Intracerebral administration of adeno-associated viral vector serotype rh.10 carrying human SGSH and SUMF1 cDNAs in children with mucopolysaccharidosis type IIIA disease: results of a phase I/II trial. *Hum Gene Ther* **2014**, *25*, 506-516, doi:10.1089/hum.2013.238.
58. Inc, U.P. Phase I/II/III Gene Transfer Clinical Trial of scAAV9.U1a.hSGSH. **2024 [cited 03.01.2025]**.
59. Kaji, T.; Kawashima, T.; Sakamoto, M. Rhodamine B inhibition of glycosaminoglycan production by cultured human lip fibroblasts. *Toxicol Appl Pharmacol* **1991**, *111*, 82-89, doi:10.1016/0041-008x(91)90136-3.
60. Roberts, A.L.; Thomas, B.J.; Wilkinson, A.S.; Fletcher, J.M.; Byers, S. Inhibition of glycosaminoglycan synthesis using rhodamine B in a mouse model of mucopolysaccharidosis type IIIA. *Pediatr Res* **2006**, *60*, 309-314, doi:10.1203/01.pdr.0000233037.00707.da.
61. Roberts, A.L.; Rees, M.H.; Klebe, S.; Fletcher, J.M.; Byers, S. Improvement in behaviour after substrate deprivation therapy with rhodamine B in a mouse model of MPS IIIA. *Mol Genet Metab* **2007**, *92*, 115-121, doi:10.1016/j.ymgme.2007.06.016.
62. Roberts, A.L.; Fletcher, J.M.; Moore, L.; Byers, S. Trans-generational exposure to low levels of rhodamine B does not adversely affect litter size or liver function in murine mucopolysaccharidosis type IIIA. *Mol Genet Metab* **2010**, *101*, 208-213, doi:10.1016/j.ymgme.2010.06.008.

63. Piotrowska, E.; Jakóbkiewicz-Banecka, J.; Barańska, S.; Tylki-Szymańska, A.; Czartoryska, B.; Wegrzyn, A.; Wegrzyn, G. Genistein-mediated inhibition of glycosaminoglycan synthesis as a basis for gene expression-targeted isoflavone therapy for mucopolysaccharidoses. *Eur J Hum Genet* **2006**, *14*, 846-852, doi:10.1038/sj.ejhg.5201623.
64. Derrick-Roberts, A.L.K.; Jackson, M.R.; Pyragius, C.E.; Byers, S. Substrate Deprivation Therapy to Reduce Glycosaminoglycan Synthesis Improves Aspects of Neurological and Skeletal Pathology in MPS I Mice. *Diseases* **2017**, *5*, doi:10.3390/diseases5010005.
65. Dire, D.J.; Wilkinson, J.A. Acute exposure to rhodamine B. *J Toxicol Clin Toxicol* **1987**, *25*, 603-607, doi:10.3109/15563658708992660.
66. Kim, K.H.; Dodsworth, C.; Paras, A.; Burton, B.K. High dose genistein aglycone therapy is safe in patients with mucopolysaccharidoses involving the central nervous system. *Mol Genet Metab* **2013**, *109*, 382-385, doi:10.1016/j.ymgme.2013.06.012.
67. Ghosh, A.; Rust, S.; Langford-Smith, K.; Weisberg, D.; Canal, M.; Breen, C.; Hepburn, M.; Tylee, K.; Vaz, F.M.; Vail, A.; et al. High dose genistein in Sanfilippo syndrome: A randomised controlled trial. *J Inherit Metab Dis* **2021**, *44*, 1248-1262, doi:10.1002/jimd.12407.
68. Zanetti, A.; Tomanin, R. Targeting Neurological Aspects of Mucopolysaccharidosis Type II: Enzyme Replacement Therapy and Beyond. *BioDrugs* **2024**, *38*, 639-655, doi:10.1007/s40259-024-00675-0.
69. Crick, F.H. On protein synthesis. *Symp Soc Exp Biol* **1958**, *12*, 138-163.
70. Brenner, S.; Jacob, F.; Meselson, M. An unstable intermediate carrying information from genes to ribosomes for protein synthesis. *Nature* **1961**, *190*, 576-581, doi:10.1038/190576a0.
71. Gros, F.; Hiatt, H.; Gilbert, W.; Kurland, C.G.; Risebrough, R.W.; Watson, J.D. Unstable ribonucleic acid revealed by pulse labelling of Escherichia coli. *Nature* **1961**, *190*, 581-585, doi:10.1038/190581a0.
72. Mollocana-Lara, E.C.; Ni, M.; Agathos, S.N.; Gonzales-Zubiate, F.A. The infinite possibilities of RNA therapeutics. *J Ind Microbiol Biotechnol* **2021**, *48*, doi:10.1093/jimb/kuab063.
73. Zamecnik, P.C.; Stephenson, M.L. Inhibition of Rous sarcoma virus replication and cell transformation by a specific oligodeoxynucleotide. *Proc Natl Acad Sci U S A* **1978**, *75*, 280-284, doi:10.1073/pnas.75.1.280.
74. Roehr, B. Fomivirsen approved for CMV retinitis. *J Int Assoc Physicians AIDS Care* **1998**, *4*, 14-16.
75. Kim, Y.K. RNA therapy: rich history, various applications and unlimited future prospects. *Exp Mol Med* **2022**, *54*, 455-465, doi:10.1038/s12276-022-00757-5.
76. Sparmann, A.; Vogel, J. RNA-based medicine: from molecular mechanisms to therapy. *EMBO J* **2023**, *42*, e114760, doi:10.15252/embj.2023114760.
77. Zhu, Y.; Zhu, L.; Wang, X.; Jin, H. RNA-based therapeutics: an overview and prospectus. *Cell Death Dis* **2022**, *13*, 644, doi:10.1038/s41419-022-05075-2.
78. Gonçalves, M.; Santos, J.I.; Coutinho, M.F.; Matos, L.; Alves, S. Development of Engineered-U1 snRNA Therapies: Current Status. *Int J Mol Sci* **2023**, *24*, doi:10.3390/ijms241914617.
79. Guerriaud, M.; Kohli, E. RNA-based drugs and regulation: Toward a necessary evolution of the definitions issued from the European union legislation. *Front Med (Lausanne)* **2022**, *9*, 1012497, doi:10.3389/fmed.2022.1012497.
80. Zhang, C.; Zhang, B. RNA therapeutics: updates and future potential. *Sci China Life Sci* **2023**, *66*, 12-30, doi:10.1007/s11427-022-2171-2.
81. Egli, M.; Manoharan, M. Chemistry, structure and function of approved oligonucleotide therapeutics. *Nucleic Acids Res* **2023**, *51*, 2529-2573, doi:10.1093/nar/gkad067.

82. Godfrey, C.; Desviat, L.R.; Smedsrød, B.; Piétri-Rouxel, F.; Denti, M.A.; Disterer, P.; Lorain, S.; Nogales-Gadea, G.; Sardone, V.; Anwar, R.; et al. Delivery is key: lessons learnt from developing splice-switching antisense therapies. *EMBO Mol Med* **2017**, *9*, 545-557, doi:10.15252/emmm.201607199.
83. Moumné, L.; Marie, A.C.; Crouvezier, N. Oligonucleotide Therapeutics: From Discovery and Development to Patentability. *Pharmaceutics* **2022**, *14*, doi:10.3390/pharmaceutics14020260.
84. Roberts, T.C.; Langer, R.; Wood, M.J.A. Advances in oligonucleotide drug delivery. *Nat Rev Drug Discov* **2020**, *19*, 673-694, doi:10.1038/s41573-020-0075-7.
85. Hammond, S.M.; Aartsma-Rus, A.; Alves, S.; Borgos, S.E.; Buijsen, R.A.M.; Collin, R.W.J.; Covello, G.; Denti, M.A.; Desviat, L.R.; Echevarría, L.; et al. Delivery of oligonucleotide-based therapeutics: challenges and opportunities. *EMBO Mol Med* **2021**, *13*, e13243, doi:10.15252/emmm.202013243.
86. Berget, S.M.; Moore, C.; Sharp, P.A. Spliced segments at the 5' terminus of adenovirus 2 late mRNA. *Proc Natl Acad Sci U S A* **1977**, *74*, 3171-3175, doi:10.1073/pnas.74.8.3171.
87. Chow, L.T.; Gelinas, R.E.; Broker, T.R.; Roberts, R.J. An amazing sequence arrangement at the 5' ends of adenovirus 2 messenger RNA. *Cell* **1977**, *12*, 1-8, doi:10.1016/0092-8674(77)90180-5.
88. Chen, M.; Manley, J.L. Mechanisms of alternative splicing regulation: insights from molecular and genomics approaches. *Nat Rev Mol Cell Biol* **2009**, *10*, 741-754, doi:10.1038/nrm2777.
89. De Conti, L.; Baralle, M.; Buratti, E. Exon and intron definition in pre-mRNA splicing. *Wiley Interdiscip Rev RNA* **2013**, *4*, 49-60, doi:10.1002/wrna.1140.
90. Matera, A.G.; Wang, Z. A day in the life of the spliceosome. *Nat Rev Mol Cell Biol* **2014**, *15*, 108-121, doi:10.1038/nrm3742.
91. Will, C.L.; Lührmann, R. Spliceosome structure and function. *Cold Spring Harb Perspect Biol* **2011**, *3*, doi:10.1101/cshperspect.a003707.
92. Shi, Y. Mechanistic insights into precursor messenger RNA splicing by the spliceosome. *Nat Rev Mol Cell Biol* **2017**, *18*, 655-670, doi:10.1038/nrm.2017.86.
93. Yan, C.; Wan, R.; Shi, Y. Molecular Mechanisms of pre-mRNA Splicing through Structural Biology of the Spliceosome. *Cold Spring Harb Perspect Biol* **2019**, *11*, doi:10.1101/cshperspect.a032409.
94. Santos, J.I.; Gonçalves, M.; Matos, L.; Moreira, L.; Carvalho, S.; Prata, M.J.; Coutinho, M.F.; Alves, S. Splicing Modulation as a Promising Therapeutic Strategy for Lysosomal Storage Disorders: The Mucopolysaccharidoses Example. *Life (Basel)* **2022**, *12*, doi:10.3390/life12050608.
95. Aísa-Marín, I.; García-Arroyo, R.; Mirra, S.; Marfany, G. The Alter Retina: Alternative Splicing of Retinal Genes in Health and Disease. *Int J Mol Sci* **2021**, *22*, doi:10.3390/ijms22041855.
96. Tazi, J.; Bakkour, N.; Stamm, S. Alternative splicing and disease. *Biochim Biophys Acta* **2009**, *1792*, 14-26, doi:10.1016/j.bbadis.2008.09.017.
97. Suñé-Pou, M.; Limeres, M.J.; Moreno-Castro, C.; Hernández-Munain, C.; Suñé-Negre, J.M.; Cuestas, M.L.; Suñé, C. Innovative Therapeutic and Delivery Approaches Using Nanotechnology to Correct Splicing Defects Underlying Disease. *Front Genet* **2020**, *11*, 731, doi:10.3389/fgene.2020.00731.
98. Kim, H.K.; Pham, M.H.C.; Ko, K.S.; Rhee, B.D.; Han, J. Alternative splicing isoforms in health and disease. *Pflugers Arch* **2018**, *470*, 995-1016, doi:10.1007/s00424-018-2136-x.
99. Cieply, B.; Carstens, R.P. Functional roles of alternative splicing factors in human disease. *Wiley Interdiscip Rev RNA* **2015**, *6*, 311-326, doi:10.1002/wrna.1276.
100. Soemedi, R.; Cygan, K.J.; Rhine, C.L.; Wang, J.; Bulacan, C.; Yang, J.; Bayrak-Toydemir, P.; McDonald, J.; Fairbrother, W.G. Pathogenic variants that alter

protein code often disrupt splicing. *Nat Genet* **2017**, *49*, 848-855, doi:10.1038/ng.3837.
101. Cartegni, L.; Chew, S.L.; Krainer, A.R. Listening to silence and understanding nonsense: exonic mutations that affect splicing. *Nat Rev Genet* **2002**, *3*, 285-298, doi:10.1038/nrg775.
102. Lim, K.R.; Maruyama, R.; Yokota, T. Eteplirsen in the treatment of Duchenne muscular dystrophy. *Drug Des Devel Ther* **2017**, *11*, 533-545, doi:10.2147/DDDT.S97635.
103. Dhuri, K.; Bechtold, C.; Quijano, E.; Pham, H.; Gupta, A.; Vikram, A.; Bahal, R. Antisense Oligonucleotides: An Emerging Area in Drug Discovery and Development. *J Clin Med* **2020**, *9*, doi:10.3390/jcm9062004.
104. Dominski, Z.; Kole, R. Restoration of correct splicing in thalassemic pre-mRNA by antisense oligonucleotides. *Proc Natl Acad Sci U S A* **1993**, *90*, 8673-8677, doi:10.1073/pnas.90.18.8673.
105. Havens, M.A.; Hastings, M.L. Splice-switching antisense oligonucleotides as therapeutic drugs. *Nucleic Acids Res* **2016**, *44*, 6549-6563, doi:10.1093/nar/gkw533.
106. Chen, S.; Heendeniya, S.N.; Le, B.T.; Rahimizadeh, K.; Rabiee, N.; Zahra, Q.U.A.; Veedu, R.N. Splice-Modulating Antisense Oligonucleotides as Therapeutics for Inherited Metabolic Diseases. *BioDrugs* **2024**, *38*, 177-203, doi:10.1007/s40259-024-00644-7.
107. Syed, Y.Y. Eteplirsen: First Global Approval. *Drugs* **2016**, *76*, 1699-1704, doi:10.1007/s40265-016-0657-1.
108. Young, C.S.; Pyle, A.D. Exon Skipping Therapy. *Cell* **2016**, *167*, 1144, doi:10.1016/j.cell.2016.10.050.
109. Heo, Y.A. Golodirsen: First Approval. *Drugs* **2020**, *80*, 329-333, doi:10.1007/s40265-020-01267-2.
110. Dhillon, S. Viltolarsen: First Approval. *Drugs* **2020**, *80*, 1027-1031, doi:10.1007/s40265-020-01339-3.
111. Shirley, M. Casimersen: First Approval. *Drugs* **2021**, *81*, 875-879, doi:10.1007/s40265-021-01512-2.
112. Finkel, R.S.; Mercuri, E.; Darras, B.T.; Connolly, A.M.; Kuntz, N.L.; Kirschner, J.; Chiriboga, C.A.; Saito, K.; Servais, L.; Tizzano, E.; et al. Nusinersen versus Sham Control in Infantile-Onset Spinal Muscular Atrophy. *N Engl J Med* **2017**, *377*, 1723-1732, doi:10.1056/NEJMoa1702752.
113. Finkel, R.S.; Chiriboga, C.A.; Vajsar, J.; Day, J.W.; Montes, J.; De Vivo, D.C.; Bishop, K.M.; Foster, R.; Liu, Y.; Ramirez-Schrempp, D.; et al. Treatment of infantile-onset spinal muscular atrophy with nusinersen: final report of a phase 2, open-label, multicentre, dose-escalation study. *Lancet Child Adolesc Health* **2021**, *5*, 491-500, doi:10.1016/S2352-4642(21)00100-0.
114. Anthony, K. RNA-based therapeutics for neurological diseases. *RNA Biol* **2022**, *19*, 176-190, doi:10.1080/15476286.2021.2021650.
115. Reilley, M.J.; McCoon, P.; Cook, C.; Lyne, P.; Kurzrock, R.; Kim, Y.; Woessner, R.; Younes, A.; Nemunaitis, J.; Fowler, N.; et al. STAT3 antisense oligonucleotide AZD9150 in a subset of patients with heavily pretreated lymphoma: results of a phase 1b trial. *J Immunother Cancer* **2018**, *6*, 119, doi:10.1186/s40425-018-0436-5.
116. Lerner, M.R.; Boyle, J.A.; Mount, S.M.; Wolin, S.L.; Steitz, J.A. Are snRNPs involved in splicing? *Nature* **1980**, *283*, 220-224, doi:10.1038/283220a0.
117. Mount, S.M.; Pettersson, I.; Hinterberger, M.; Karmas, A.; Steitz, J.A. The U1 small nuclear RNA-protein complex selectively binds a 5' splice site in vitro. *Cell* **1983**, *33*, 509-518, doi:10.1016/0092-8674(83)90432-4.
118. Rogers, J.; Wall, R. A mechanism for RNA splicing. *Proc Natl Acad Sci U S A* **1980**, *77*, 1877-1879, doi:10.1073/pnas.77.4.1877.

119. West, S. The increasing functional repertoire of U1 snRNA. *Biochem Soc Trans* **2012**, *40*, 846-849, doi:10.1042/BST20120058.
120. Kondo, Y.; Oubridge, C.; van Roon, A.M.; Nagai, K. Crystal structure of human U1 snRNP, a small nuclear ribonucleoprotein particle, reveals the mechanism of 5' splice site recognition. *Elife* **2015**, *4*, doi:10.7554/eLife.04986.
121. Coutinho, M.F.; Matos, L.; Santos, J.I.; Alves, S. RNA Therapeutics: How Far Have We Gone? *Adv Exp Med Biol* **2019**, *1157*, 133-177, doi:10.1007/978-3-030-19966-1_7.
122. Raponi, M.; Baralle, D. Can donor splice site recognition occur without the involvement of U1 snRNP? *Biochem Soc Trans* **2008**, *36*, 548-550, doi:10.1042/BST0360548.
123. Buratti, E.; Chivers, M.; Královicová, J.; Romano, M.; Baralle, M.; Krainer, A.R.; Vorechovsky, I. Aberrant 5' splice sites in human disease genes: mutation pattern, nucleotide structure and comparison of computational tools that predict their utilization. *Nucleic Acids Res* **2007**, *35*, 4250-4263, doi:10.1093/nar/gkm402.
124. Roca, X.; Krainer, A.R.; Eperon, I.C. Pick one, but be quick: 5' splice sites and the problems of too many choices. *Genes Dev* **2013**, *27*, 129-144, doi:10.1101/gad.209759.112.
125. Roca, X.; Olson, A.J.; Rao, A.R.; Enerly, E.; Kristensen, V.N.; Børresen-Dale, A.L.; Andresen, B.S.; Krainer, A.R.; Sachidanandam, R. Features of 5'-splice-site efficiency derived from disease-causing mutations and comparative genomics. *Genome Res* **2008**, *18*, 77-87, doi:10.1101/gr.6859308.
126. Zhuang, Y.; Weiner, A.M. A compensatory base change in U1 snRNA suppresses a 5' splice site mutation. *Cell* **1986**, *46*, 827-835, doi:10.1016/0092-8674(86)90064-4.
127. Baralle, M.; Baralle, D.; De Conti, L.; Mattocks, C.; Whittaker, J.; Knezevich, A.; Ffrench-Constant, C.; Baralle, F.E. Identification of a mutation that perturbs NF1 agene splicing using genomic DNA samples and a minigene assay. *J Med Genet* **2003**, *40*, 220-222, doi:10.1136/jmg.40.3.220.
128. Pinotti, M.; Rizzotto, L.; Balestra, D.; Lewandowska, M.A.; Cavallari, N.; Marchetti, G.; Bernardi, F.; Pagani, F. U1-snRNA-mediated rescue of mRNA processing in severe factor VII deficiency. *Blood* **2008**, *111*, 2681-2684, doi:10.1182/blood-2007-10-117440.
129. Tanner, G.; Glaus, E.; Barthelmes, D.; Ader, M.; Fleischhauer, J.; Pagani, F.; Berger, W.; Neidhardt, J. Therapeutic strategy to rescue mutation-induced exon skipping in rhodopsin by adaptation of U1 snRNA. *Hum Mutat* **2009**, *30*, 255-263, doi:10.1002/humu.20861.
130. Glaus, E.; Schmid, F.; Da Costa, R.; Berger, W.; Neidhardt, J. Gene therapeutic approach using mutation-adapted U1 snRNA to correct a RPGR splice defect in patient-derived cells. *Mol Ther* **2011**, *19*, 936-941, doi:10.1038/mt.2011.7.
131. Schmid, F.; Glaus, E.; Barthelmes, D.; Fliegauf, M.; Gaspar, H.; Nürnberg, G.; Nürnberg, P.; Omran, H.; Berger, W.; Neidhardt, J. U1 snRNA-mediated gene therapeutic correction of splice defects caused by an exceptionally mild BBS mutation. *Hum Mutat* **2011**, *32*, 815-824, doi:10.1002/humu.21509.
132. Sánchez-Alcudia, R.; Pérez, B.; Pérez-Cerdá, C.; Ugarte, M.; Desviat, L.R. Overexpression of adapted U1snRNA in patients' cells to correct a 5' splice site mutation in propionic acidemia. *Mol Genet Metab* **2011**, *102*, 134-138, doi:10.1016/j.ymgme.2010.10.013.
133. Scalet, D.; Sacchetto, C.; Bernardi, F.; Pinotti, M.; van de Graaf, S.F.J.; Balestra, D. The somatic FAH C.1061C>A change counteracts the frequent FAH c.1062+5G>A mutation and permits U1snRNA-based splicing correction. *J Hum Genet* **2018**, *63*, 683-686, doi:10.1038/s10038-018-0427-x.

134. Hartmann, L.; Neveling, K.; Borkens, S.; Schneider, H.; Freund, M.; Grassman, E.; Theiss, S.; Wawer, A.; Burdach, S.; Auerbach, A.D.; et al. Correct mRNA processing at a mutant TT splice donor in FANCC ameliorates the clinical phenotype in patients and is enhanced by delivery of suppressor U1 snRNAs. *Am J Hum Genet* **2010**, *87*, 480-493, doi:10.1016/j.ajhg.2010.08.016.
135. Peretto, L.; Tonetto, E.; Maestri, I.; Bezzerri, V.; Valli, R.; Cipolli, M.; Pinotti, M.; Balestra, D. Counteracting the Common Shwachman-Diamond Syndrome-Causing. *Int J Mol Sci* **2023**, *24*, doi:10.3390/ijms24044024.
136. Matos, L.; Canals, I.; Dridi, L.; Choi, Y.; Prata, M.J.; Jordan, P.; Desviat, L.R.; Pérez, B.; Pshezhetsky, A.V.; Grinberg, D.; et al. Therapeutic strategies based on modified U1 snRNAs and chaperones for Sanfilippo C splicing mutations. *Orphanet J Rare Dis* **2014**, *9*, 180, doi:10.1186/s13023-014-0180-y.
137. Balestra, D.; Faella, A.; Margaritis, P.; Cavallari, N.; Pagani, F.; Bernardi, F.; Arruda, V.R.; Pinotti, M. An engineered U1 small nuclear RNA rescues splicing defective coagulation F7 gene expression in mice. *J Thromb Haemost* **2014**, *12*, 177-185, doi:10.1111/jth.12471.
138. Lee, N.C.; Lee, Y.M.; Chen, P.W.; Byrne, B.J.; Hwu, W.L. Mutation-adapted U1 snRNA corrects a splicing error of the dopa decarboxylase gene. *Hum Mol Genet* **2016**, *25*, 5142-5147, doi:10.1093/hmg/ddw323.
139. Balestra, D.; Scalet, D.; Ferrarese, M.; Lombardi, S.; Ziliotto, N.; C Croes, C.; Petersen, N.; Bosma, P.; Riccardi, F.; Pagani, F.; et al. A Compensatory U1snRNA Partially Rescues FAH Splicing and Protein Expression in a Splicing-Defective Mouse Model of Tyrosinemia Type I. *Int J Mol Sci* **2020**, *21*, doi:10.3390/ijms21062136.
140. van der Woerd, W.L.; Mulder, J.; Pagani, F.; Beuers, U.; Houwen, R.H.; van de Graaf, S.F. Analysis of aberrant pre-messenger RNA splicing resulting from mutations in ATP8B1 and efficient in vitro rescue by adapted U1 small nuclear RNA. *Hepatology* **2015**, *61*, 1382-1391, doi:10.1002/hep.27620.
141. Balestra, D.; Giorgio, D.; Bizzotto, M.; Fazzari, M.; Ben Zeev, B.; Pinotti, M.; Landsberger, N.; Frasca, A. Splicing Mutations Impairing CDKL5 Expression and Activity Can be Efficiently Rescued by U1snRNA-Based Therapy. *Int J Mol Sci* **2019**, *20*, doi:10.3390/ijms20174130.
142. Lombardi, S.; Leo, G.; Merlin, S.; Follenzi, A.; McVey, J.H.; Maestri, I.; Bernardi, F.; Pinotti, M.; Balestra, D. Dissection of pleiotropic effects of variants in and adjacent to F8 exon 19 and rescue of mRNA splicing and protein function. *Am J Hum Genet* **2021**, *108*, 1512-1525, doi:10.1016/j.ajhg.2021.06.012.
143. Mattioli, C.; Pianigiani, G.; De Rocco, D.; Bianco, A.M.; Cappelli, E.; Savoia, A.; Pagani, F. Unusual splice site mutations disrupt FANCA exon 8 definition. *Biochim Biophys Acta* **2014**, *1842*, 1052-1058, doi:10.1016/j.bbadis.2014.03.014.
144. Martínez-Pizarro, A.; Dembic, M.; Pérez, B.; Andresen, B.S.; Desviat, L.R. Intronic PAH gene mutations cause a splicing defect by a novel mechanism involving U1snRNP binding downstream of the 5' splice site. *PLoS Genet* **2018**, *14*, e1007360, doi:10.1371/journal.pgen.1007360.
145. Lauffer, M.C.; van Roon-Mom, W.; Aartsma-Rus, A.; Collaborative, N. Possibilities and limitations of antisense oligonucleotide therapies for the treatment of monogenic disorders. *Commun Med (Lond)* **2024**, *4*, 6, doi:10.1038/s43856-023-00419-1.
146. Kanatsu, K.; Takahashi, Y.; Sakaguchi, T.; Kim, D.-S.; Murota, M.; Shan, M.; Fukami, K.; Itano, W.; Kikuta, K.; Yoshimura, H.; et al. *Discovery and characterization of stereodefined PMO-gapmers targeting tau*; 2024.
147. Lim, K.R.Q.; Yokota, T. Invention and Early History of Gapmers. *Methods Mol Biol* **2020**, *2176*, 3-19, doi:10.1007/978-1-0716-0771-8_1.

148. Nie, T. Eplontersen: First Approval. *Drugs* **2024**, *84*, 473-478, doi:10.1007/s40265-024-02008-5.
149. Adachi, H.; Hengesbach, M.; Yu, Y.T.; Morais, P. From Antisense RNA to RNA Modification: Therapeutic Potential of RNA-Based Technologies. *Biomedicines* **2021**, *9*, doi:10.3390/biomedicines9050550.
150. Eckstein, F. Phosphorothioates, essential components of therapeutic oligonucleotides. *Nucleic Acid Ther* **2014**, *24*, 374-387, doi:10.1089/nat.2014.0506.
151. Geary, R.S. Antisense oligonucleotide pharmacokinetics and metabolism. *Expert Opin Drug Metab Toxicol* **2009**, *5*, 381-391, doi:10.1517/17425250902877680.
152. Summerton, J. Morpholino antisense oligomers: the case for an RNase H-independent structural type. *Biochim Biophys Acta* **1999**, *1489*, 141-158, doi:10.1016/s0167-4781(99)00150-5.
153. Yokota, T.; Lu, Q.L.; Partridge, T.; Kobayashi, M.; Nakamura, A.; Takeda, S.; Hoffman, E. Efficacy of systemic morpholino exon-skipping in Duchenne dystrophy dogs. *Ann Neurol* **2009**, *65*, 667-676, doi:10.1002/ana.21627.
154. Gupta, S.; Sharma, S.; Kundu, J.; Pattanayak, S.; Sinha, S. Morpholino oligonucleotide-mediated exon skipping for DMD treatment: Past insights, present challenges and future perspectives. *Journal of Biosciences* **2023**, *48*, doi:10.1007/s12038-023-00365-z.
155. Rinaldi, C.; Wood, M.J.A. Antisense oligonucleotides: the next frontier for treatment of neurological disorders. *Nat Rev Neurol* **2018**, *14*, 9-21, doi:10.1038/nrneurol.2017.148.
156. Philippeos, C.; Hughes, R.D.; Dhawan, A.; Mitry, R.R. Introduction to cell culture. *Methods Mol Biol* **2012**, *806*, 1-13, doi:10.1007/978-1-61779-367-7_1.
157. Carvalho, S.; Santos, J.I.; Moreira, L.; Gonçalves, M.; David, H.; Matos, L.; Encarnação, M.; Alves, S.; Coutinho, M.F. Neurological Disease Modeling Using Pluripotent and Multipotent Stem Cells: A Key Step towards Understanding and Treating Mucopolysaccharidoses. *Biomedicines* **2023**, *11*, doi:10.3390/biomedicines11041234.
158. Gaudioso, Á.; Silva, T.P.; Ledesma, M.D. Models to study basic and applied aspects of lysosomal storage disorders. *Adv Drug Deliv Rev* **2022**, *190*, 114532, doi:10.1016/j.addr.2022.114532.
159. Brooks, I.R.; Garrone, C.M.; Kerins, C.; Kiar, C.S.; Syntaka, S.; Xu, J.Z.; Spagnoli, F.M.; Watt, F.M. Functional genomics and the future of iPSCs in disease modeling. *Stem Cell Reports* **2022**, *17*, 1033-1047, doi:10.1016/j.stemcr.2022.03.019.
160. Zhao, Z.; Chen, X.; Dowbaj, A.M.; Sljukic, A.; Bratlie, K.; Lin, L.; Fong, E.L.S.; Balachander, G.M.; Chen, Z.; Soragni, A.; et al. Organoids. *Nat Rev Methods Primers* **2022**, *2*, doi:10.1038/s43586-022-00174-y.
161. Mullis, A.S.; Kaplan, D.L. Functional bioengineered tissue models of neurodegenerative diseases. *Biomaterials* **2023**, *298*, 122143, doi:10.1016/j.biomaterials.2023.122143.
162. Wang, H.; Ning, X.; Zhao, F.; Zhao, H.; Li, D. Human organoids-on-chips for biomedical research and applications. *Theranostics* **2024**, *14*, 788-818, doi:10.7150/thno.90492.
163. Carvalho, S.; Santos, J.I.; Moreira, L.; Duarte, A.J.; Gaspar, P.; Rocha, H.; Encarnação, M.; Ribeiro, D.; Barbosa Almeida, M.; Gonçalves, M.; et al. Modeling Lysosomal Storage Disorders in an Innovative Way: Establishment and Characterization of Stem Cell Lines from Human Exfoliated Deciduous Teeth of Mucopolysaccharidosis Type II Patients. *Int J Mol Sci* **2024**, *25*, doi:10.3390/ijms25063546.

164. Montes, M.; Sanford, B.L.; Comiskey, D.F.; Chandler, D.S. RNA Splicing and Disease: Animal Models to Therapies. *Trends Genet* **2019**, *35*, 68-87, doi:10.1016/j.tig.2018.10.002.
165. Zimmermann, T.S.; Lee, A.C.; Akinc, A.; Bramlage, B.; Bumcrot, D.; Fedoruk, M.N.; Harborth, J.; Heyes, J.A.; Jeffs, L.B.; John, M.; et al. RNAi-mediated gene silencing in non-human primates. *Nature* **2006**, *441*, 111-114, doi:10.1038/nature04688.
166. Pham, T.T.; Chen, H.; Nguyen, P.H.D.; Jayasinghe, M.K.; Le, A.H.; Le, M.T. Endosomal escape of nucleic acids from extracellular vesicles mediates functional therapeutic delivery. *Pharmacol Res* **2023**, *188*, 106665, doi:10.1016/j.phrs.2023.106665.
167. Akinc, A.; Maier, M.A.; Manoharan, M.; Fitzgerald, K.; Jayaraman, M.; Barros, S.; Ansell, S.; Du, X.; Hope, M.J.; Madden, T.D.; et al. The Onpattro story and the clinical translation of nanomedicines containing nucleic acid-based drugs. *Nat Nanotechnol* **2019**, *14*, 1084-1087, doi:10.1038/s41565-019-0591-y.
168. Haché, M.; Swoboda, K.J.; Sethna, N.; Farrow-Gillespie, A.; Khandji, A.; Xia, S.; Bishop, K.M. Intrathecal Injections in Children With Spinal Muscular Atrophy: Nusinersen Clinical Trial Experience. *J Child Neurol* **2016**, *31*, 899-906, doi:10.1177/0883073815627882.
169. Cideciyan, A.V.; Jacobson, S.G.; Drack, A.V.; Ho, A.C.; Charng, J.; Garafalo, A.V.; Roman, A.J.; Sumaroka, A.; Han, I.C.; Hochstedler, M.D.; et al. Effect of an intravitreal antisense oligonucleotide on vision in Leber congenital amaurosis due to a photoreceptor cilium defect. *Nat Med* **2019**, *25*, 225-228, doi:10.1038/s41591-018-0295-0.
170. Schoch, K.M.; Miller, T.M. Antisense Oligonucleotides: Translation from Mouse Models to Human Neurodegenerative Diseases. *Neuron* **2017**, *94*, 1056-1070, doi:10.1016/j.neuron.2017.04.010.
171. Kim, J.; Hu, C.; Moufawad El Achkar, C.; Black, L.E.; Douville, J.; Larson, A.; Pendergast, M.K.; Goldkind, S.F.; Lee, E.A.; Kuniholm, A.; et al. Patient-Customized Oligonucleotide Therapy for a Rare Genetic Disease. *N Engl J Med* **2019**, *381*, 1644-1652, doi:10.1056/NEJMoa1813279.
172. Di Francesco, V.; Chua, A.J.; Huang, D.; D'Souza, A.; Yang, A.; Bleier, B.S.; Amiji, M.M. RNA therapies for CNS diseases. *Adv Drug Deliv Rev* **2024**, *208*, 115283, doi:10.1016/j.addr.2024.115283.
173. Amanat, M.; Nemeth, C.L.; Fine, A.S.; Leung, D.G.; Fatemi, A. Antisense Oligonucleotide Therapy for the Nervous System: From Bench to Bedside with Emphasis on Pediatric Neurology. *Pharmaceutics* **2022**, *14*, doi:10.3390/pharmaceutics14112389.
174. Kido, J.; Sugawara, K.; Nakamura, K. Gene therapy for lysosomal storage diseases: Current clinical trial prospects. *Front Genet* **2023**, *14*, 1064924, doi:10.3389/fgene.2023.1064924.
175. Parenti, G.; Pignata, C.; Vajro, P.; Salerno, M. New strategies for the treatment of lysosomal storage diseases (review). *Int J Mol Med* **2013**, *31*, 11-20, doi:10.3892/ijmm.2012.1187.
176. Dardis, A.; Buratti, E. Impact, Characterization, and Rescue of Pre-mRNA Splicing Mutations in Lysosomal Storage Disorders. *Genes (Basel)* **2018**, *9*, doi:10.3390/genes9020073.
177. Rodríguez-Pascau, L.; Coll, M.J.; Vilageliu, L.; Grinberg, D. Antisense oligonucleotide treatment for a pseudoexon-generating mutation in the NPC1 gene causing Niemann-Pick type C disease. *Hum Mutat* **2009**, *30*, E993-E1001, doi:10.1002/humu.21119.
178. Ham, K.A.; Johnsen, R.D.; Tchan, M.; Wilton, S.D.; Aung-Htut, M.T. Developing Therapeutic Splice-Correcting Antisense Oligomers for Adult-Onset Pompe

Disease with c.-32-13T>G Mutation. *Methods Mol Biol* **2023**, *2587*, 239-251, doi:10.1007/978-1-0716-2772-3_14.

179. Matos, L.; Gonçalves, V.; Pinto, E.; Laranjeira, F.; Prata, M.J.; Jordan, P.; Desviat, L.R.; Pérez, B.; Alves, S. Functional analysis of splicing mutations in the IDS gene and the use of antisense oligonucleotides to exploit an alternative therapy for MPS II. *Biochim Biophys Acta* **2015**, *1852*, 2712-2721, doi:10.1016/j.bbadis.2015.09.011.
180. Diaz-Font, A.; Chabás, A.; Grinberg, D.; Vilageliu, L. RNAi-mediated inhibition of the glucosylceramide synthase (GCS) gene: A preliminary study towards a therapeutic strategy for Gaucher disease and other glycosphingolipid storage diseases. *Blood Cells Mol Dis* **2006**, *37*, 197-203, doi:10.1016/j.bcmd.2006.07.002.
181. Coutinho, M.F.; Santos, J.I.; Matos, L.; Alves, S. Genetic Substrate Reduction Therapy: A Promising Approach for Lysosomal Storage Disorders. *Diseases* **2016**, *4*, doi:10.3390/diseases4040033.
182. Matos, L.; Gonçalves, V.; Pinto, E.; Laranjeira, F.; Prata, M.J.; Jordan, P.; Desviat, L.R.; Pérez, B.; Alves, S. Data in support of a functional analysis of splicing mutations in the IDS gene and the use of antisense oligonucleotides to exploit an alternative therapy for MPS II. *Data Brief* **2015**, *5*, 810-817, doi:10.1016/j.dib.2015.10.011.
183. Dziedzic, D.; Wegrzyn, G.; Jakóbkiewicz-Banecka, J. Impairment of glycosaminoglycan synthesis in mucopolysaccharidosis type IIIA cells by using siRNA: a potential therapeutic approach for Sanfilippo disease. *Eur J Hum Genet* **2010**, *18*, 200-205, doi:10.1038/ejhg.2009.144.
184. Kaidonis, X.; Liaw, W.C.; Roberts, A.D.; Ly, M.; Anson, D.; Byers, S. Gene silencing of EXTL2 and EXTL3 as a substrate deprivation therapy for heparan sulphate storing mucopolysaccharidoses. *Eur J Hum Genet* **2010**, *18*, 194-199, doi:10.1038/ejhg.2009.143.
185. Dziedzic, D.; Narajczyk, M.; Gabig-Cimińska, M.; Jakóbkiewicz-Banecka, J. Simultaneous siRNA-mediated silencing of pairs of genes coding for enzymes involved in glycosaminoglycan synthesis. *Acta Biochim Pol* **2012**, *59*, 293-298.
186. Canals, I.; Benetó, N.; Cozar, M.; Vilageliu, L.; Grinberg, D. EXTL2 and EXTL3 inhibition with siRNAs as a promising substrate reduction therapy for Sanfilippo C syndrome. *Sci Rep* **2015**, *5*, 13654, doi:10.1038/srep13654.
187. Nolte, A.; Ott, K.; Rohayem, J.; Walker, T.; Schlensak, C.; Wendel, H.P. Modification of small interfering RNAs to prevent off-target effects by the sense strand. *N Biotechnol* **2013**, *30*, 159-165, doi:10.1016/j.nbt.2012.10.001.
188. Aartsma-Rus, A.; van Vliet, L.; Hirschi, M.; Janson, A.A.; Heemskerk, H.; de Winter, C.L.; de Kimpe, S.; van Deutekom, J.C.; 't Hoen, P.A.; van Ommen, G.J. Guidelines for antisense oligonucleotide design and insight into splice-modulating mechanisms. *Mol Ther* **2009**, *17*, 548-553, doi:10.1038/mt.2008.205.
189. Aartsma-Rus, A. Overview on AON design. *Methods Mol Biol* **2012**, *867*, 117-129, doi:10.1007/978-1-61779-767-5_8.
190. Zuker, M. Mfold web server for nucleic acid folding and hybridization prediction. *Nucleic Acids Res* **2003**, *31*, 3406-3415, doi:10.1093/nar/gkg595.
191. Reuter, J.S.; Mathews, D.H. RNAstructure: software for RNA secondary structure prediction and analysis. *BMC Bioinformatics* **2010**, *11*, 129, doi:10.1186/1471-2105-11-129.
192. Pontén, F.; Jirström, K.; Uhlen, M. The Human Protein Atlas--a tool for pathology. *J Pathol* **2008**, *216*, 387-393, doi:10.1002/path.2440.
193. Livak, K.J.; Schmittgen, T.D. Analysis of relative gene expression data using real-time quantitative PCR and the 2(-Delta Delta C(T)) Method. *Methods* **2001**, *25*, 402-408, doi:10.1006/meth.2001.1262.

194. Forni, G.; Malvagia, S.; Funghini, S.; Scolamiero, E.; Mura, M.; Della Bona, M.; Villanelli, F.; Damiano, R.; la Marca, G. LC-MS/MS method for simultaneous quantification of heparan sulfate and dermatan sulfate in urine by butanolysis derivatization. *Clin Chim Acta* **2019**, *488*, 98-103, doi:10.1016/j.cca.2018.11.001.
195. Liu, F.; Song, Y.; Liu, D. Hydrodynamics-based transfection in animals by systemic administration of plasmid DNA. *Gene Ther* **1999**, *6*, 1258-1266, doi:10.1038/sj.gt.3300947.
196. Zhang, G.; Budker, V.; Wolff, J.A. High levels of foreign gene expression in hepatocytes after tail vein injections of naked plasmid DNA. *Hum Gene Ther* **1999**, *10*, 1735-1737, doi:10.1089/10430349950017734.
197. Suda, T.; Yokoo, T.; Kanefuji, T.; Kamimura, K.; Zhang, G.; Liu, D. Hydrodynamic Delivery: Characteristics, Applications, and Technological Advances. *Pharmaceutics* **2023**, *15*, doi:10.3390/pharmaceutics15041111.
198. Al-Dosari, M.; Zhang, G.; Knapp, J.E.; Liu, D. Evaluation of viral and mammalian promoters for driving transgene expression in mouse liver. *Biochem Biophys Res Commun* **2006**, *339*, 673-678, doi:10.1016/j.bbrc.2005.11.063.
199. Li, J.; Yao, Q.; Liu, D. Hydrodynamic cell delivery for simultaneous establishment of tumor growth in mouse lung, liver and kidney. *Cancer Biol Ther* **2011**, *12*, 737-741, doi:10.4161/cbt.12.8.16442.
200. Gao, M.; Ma, Y.; Cui, R.; Liu, D. Hydrodynamic delivery of FGF21 gene alleviates obesity and fatty liver in mice fed a high-fat diet. *J Control Release* **2014**, *185*, 1-11, doi:10.1016/j.jconrel.2014.03.047.
201. Taketo, M.; Schroeder, A.C.; Mobraaten, L.E.; Gunning, K.B.; Hanten, G.; Fox, R.R.; Roderick, T.H.; Stewart, C.L.; Lilly, F.; Hansen, C.T. FVB/N: an inbred mouse strain preferable for transgenic analyses. *Proc Natl Acad Sci U S A* **1991**, *88*, 2065-2069, doi:10.1073/pnas.88.6.2065.
202. Manfredsson, F.P.; Rising, A.C.; Mandel, R.J. AAV9: a potential blood-brain barrier buster. *Mol Ther* **2009**, *17*, 403-405, doi:10.1038/mt.2009.15.
203. Andrews, M.R. Gene therapy in the CNS-one size does not fit all. *Gene Ther* **2021**, *28*, 393-395, doi:10.1038/s41434-020-00196-9.
204. Saraiva, J.; Nobre, R.J.; Pereira de Almeida, L. Gene therapy for the CNS using AAVs: The impact of systemic delivery by AAV9. *J Control Release* **2016**, *241*, 94-109, doi:10.1016/j.jconrel.2016.09.011.
205. Gessler, D.J.; Tai, P.W.L.; Li, J.; Gao, G. Intravenous Infusion of AAV for Widespread Gene Delivery to the Nervous System. *Methods Mol Biol* **2019**, *1950*, 143-163, doi:10.1007/978-1-4939-9139-6_8.
206. Lowes, L.P.; Alfano, L.N.; Arnold, W.D.; Shell, R.; Prior, T.W.; McColly, M.; Lehman, K.J.; Church, K.; Sproule, D.M.; Nagendran, S.; et al. Impact of Age and Motor Function in a Phase 1/2A Study of Infants With SMA Type 1 Receiving Single-Dose Gene Replacement Therapy. *Pediatr Neurol* **2019**, *98*, 39-45, doi:10.1016/j.pediatrneurol.2019.05.005.
207. Thomsen, G.; Burghes, A.H.M.; Hsieh, C.; Do, J.; Chu, B.T.T.; Perry, S.; Barkho, B.; Kaufmann, P.; Sproule, D.M.; Feltner, D.E.; et al. Biodistribution of onasemnogene abeparvovec DNA, mRNA and SMN protein in human tissue. *Nat Med* **2021**, *27*, 1701-1711, doi:10.1038/s41591-021-01483-7.
208. Mercuri, E.; Muntoni, F.; Baranello, G.; Masson, R.; Boespflug-Tanguy, O.; Bruno, C.; Corti, S.; Daron, A.; Deconinck, N.; Servais, L.; et al. Onasemnogene abeparvovec gene therapy for symptomatic infantile-onset spinal muscular atrophy type 1 (STR1VE-EU): an open-label, single-arm, multicentre, phase 3 trial. *Lancet Neurol* **2021**, *20*, 832-841, doi:10.1016/S1474-4422(21)00251-9.
209. de Castro, M.J.; Del Toro, M.; Giugliani, R.; Couce, M.L. Gene Therapy for Neuronopathic Mucopolysaccharidoses: State of the Art. *Int J Mol Sci* **2021**, *22*, doi:10.3390/ijms22179200.

210. Fu, H.; Cataldi, M.P.; Ware, T.A.; Zaraspe, K.; Meadows, A.S.; Murrey, D.A.; McCarty, D.M. Functional correction of neurological and somatic disorders at later stages of disease in MPS IIIA mice by systemic scAAV9-hSGSH gene delivery. *Mol Ther Methods Clin Dev* **2016**, *3*, 16036, doi:10.1038/mtm.2016.36.
211. Marcó, S.; Haurigot, V.; Jaén, M.L.; Ribera, A.; Sánchez, V.; Molas, M.; Garcia, M.; León, X.; Roca, C.; Sánchez, X.; et al. Seven-year follow-up of durability and safety of AAV CNS gene therapy for a lysosomal storage disorder in a large animal. *Mol Ther Methods Clin Dev* **2021**, *23*, 370-389, doi:10.1016/j.omtm.2021.09.017.
212. Cooper, T.A. Use of minigene systems to dissect alternative splicing elements. *Methods* **2005**, *37*, 331-340, doi:10.1016/j.ymeth.2005.07.015.
213. Vázquez-Domínguez, I.; Garanto, A. Considerations for Generating Humanized Mouse Models to Test Efficacy of Antisense Oligonucleotides. *Methods Mol Biol* **2022**, *2434*, 267-279, doi:10.1007/978-1-0716-2010-6_18.
214. Aartsma-Rus, A.; van Putten, M. The use of genetically humanized animal models for personalized medicine approaches. *Dis Model Mech* **2019**, *13*, doi:10.1242/dmm.041673.
215. Soufizadeh, P.; Mansouri, V.; Ahmadbeigi, N. A review of animal models utilized in preclinical studies of approved gene therapy products: trends and insights. *Lab Anim Res* **2024**, *40*, 17, doi:10.1186/s42826-024-00195-6.
216. Mukherjee, P.; Roy, S.; Ghosh, D.; Nandi, S.K. Role of animal models in biomedical research: a review. *Lab Anim Res* **2022**, *38*, 18, doi:10.1186/s42826-022-00128-1.
217. Singh, V.K.; Seed, T.M. How necessary are animal models for modern drug discovery? *Expert Opin Drug Discov* **2021**, *16*, 1391-1397, doi:10.1080/17460441.2021.1972255.
218. Russell, W.M.S.; Burch, R.L. *The principles of humane experimental technique*; Welfare, W.U.U.F.f.A., Ed.; 1959 (as reprinted 1992).
219. Ritelli, M.; Cinquina, V.; Giacopuzzi, E.; Venturini, M.; Chiarelli, N.; Colombi, M. Further Defining the Phenotypic Spectrum of B3GAT3 Mutations and Literature Review on Linkeropathy Syndromes. *Genes (Basel)* **2019**, *10*, doi:10.3390/genes10090631.
220. Bui, C.; Huber, C.; Tuysuz, B.; Alanay, Y.; Bole-Feysot, C.; Leroy, J.G.; Mortier, G.; Nitschke, P.; Munnich, A.; Cormier-Daire, V. XYLT1 mutations in Desbuquois dysplasia type 2. *Am J Hum Genet* **2014**, *94*, 405-414, doi:10.1016/j.ajhg.2014.01.020.
221. Jamsheer, A.; Olech, E.M.; Kozłowski, K.; Niedziela, M.; Sowińska-Seidler, A.; Obara-Moszyńska, M.; Latos-Bieleńska, A.; Karczewski, M.; Zemojtel, T. Exome sequencing reveals two novel compound heterozygous XYLT1 mutations in a Polish patient with Desbuquois dysplasia type 2 and growth hormone deficiency. *J Hum Genet* **2016**, *61*, 577-583, doi:10.1038/jhg.2016.30.
222. Guo, L.; Elcioglu, N.H.; Iida, A.; Demirkol, Y.K.; Aras, S.; Matsumoto, N.; Nishimura, G.; Miyake, N.; Ikegawa, S. Novel and recurrent XYLT1 mutations in two Turkish families with Desbuquois dysplasia, type 2. *J Hum Genet* **2017**, *62*, 447-451, doi:10.1038/jhg.2016.143.
223. LaCroix, A.J.; Stabley, D.; Sahraoui, R.; Adam, M.P.; Mehaffey, M.; Kernan, K.; Myers, C.T.; Fagerstrom, C.; Anadiotis, G.; Akkari, Y.M.; et al. GGC Repeat Expansion and Exon 1 Methylation of XYLT1 Is a Common Pathogenic Variant in Baratela-Scott Syndrome. *Am J Hum Genet* **2019**, *104*, 35-44, doi:10.1016/j.ajhg.2018.11.005.
224. Taieb, M.; Ghannoum, D.; Barré, L.; Ouzzine, M. Xylosyltransferase I mediates the synthesis of proteoglycans with long glycosaminoglycan chains and controls chondrocyte hypertrophy and collagen fibers organization of in the growth plate. *Cell Death Dis* **2023**, *14*, 355, doi:10.1038/s41419-023-05875-0.

225. Huang, Y.F.; Mizumoto, S.; Fujita, M. Novel Insight Into Glycosaminoglycan Biosynthesis Based on Gene Expression Profiles. *Front Cell Dev Biol* **2021**, *9*, 709018, doi:10.3389/fcell.2021.709018.
226. Mizumoto, S.; Ikegawa, S.; Sugahara, K. Human genetic disorders caused by mutations in genes encoding biosynthetic enzymes for sulfated glycosaminoglycans. *J Biol Chem* **2013**, *288*, 10953-10961, doi:10.1074/jbc.R112.437038.
227. Götting, C.; Kuhn, J.; Kleesiek, K. Human xylosyltransferases in health and disease. *Cell Mol Life Sci* **2007**, *64*, 1498-1517, doi:10.1007/s00018-007-7069-z.
228. Yan, J.; Zhang, H.; Li, G.; Su, J.; Wei, Y.; Xu, C. Lipid nanovehicles overcome barriers to systemic RNA delivery: Lipid components, fabrication methods, and rational design. *Acta Pharm Sin B* **2024**, *14*, 579-601, doi:10.1016/j.apsb.2023.10.012.
229. Sajid, M.I.; Moazzam, M.; Kato, S.; Yeseom Cho, K.; Tiwari, R.K. Overcoming Barriers for siRNA Therapeutics: From Bench to Bedside. *Pharmaceuticals (Basel)* **2020**, *13*, doi:10.3390/ph13100294.
230. Coutinho, M.F.; Santos, J.I.; S Mendonça, L.; Matos, L.; Prata, M.J.; S Jurado, A.; Pedroso de Lima, M.C.; Alves, S. Lysosomal Storage Disease-Associated Neuropathy: Targeting Stable Nucleic Acid Lipid Particle (SNALP)-Formulated siRNAs to the Brain as a Therapeutic Approach. *Int J Mol Sci* **2020**, *21*, doi:10.3390/ijms21165732.
231. Gagnon, K.T.; Corey, D.R. Guidelines for Experiments Using Antisense Oligonucleotides and Double-Stranded RNAs. *Nucleic Acid Ther* **2019**, *29*, 116-122, doi:10.1089/nat.2018.0772.
232. Gareri, C.; Polimeni, A.; Giordano, S.; Tammè, L.; Curcio, A.; Indolfi, C. Antisense Oligonucleotides and Small Interfering RNA for the Treatment of Dyslipidemias. *J Clin Med* **2022**, *11*, doi:10.3390/jcm11133884.
233. Sang, A.; Zhuo, S.; Bochanis, A.; Manautou, J.E.; Bahal, R.; Zhong, X.B.; Rasmussen, T.P. Mechanisms of Action of the US Food and Drug Administration-Approved Antisense Oligonucleotide Drugs. *BioDrugs* **2024**, *38*, 511-526, doi:10.1007/s40259-024-00665-2.
234. Aguti, S.; Cheng, S.; Ala, P.; Briggs, S.; Muntoni, F.; Zhou, H. Strategies to improve the design of gapmer antisense oligonucleotide on allele-specific silencing. *Mol Ther Nucleic Acids* **2024**, *35*, 102237, doi:10.1016/j.omtn.2024.102237.
235. Chiriboga, C.A.; Swoboda, K.J.; Darras, B.T.; Iannaccone, S.T.; Montes, J.; De Vivo, D.C.; Norris, D.A.; Bennett, C.F.; Bishop, K.M. Results from a phase 1 study of nusinersen (ISIS-SMN(Rx)) in children with spinal muscular atrophy. *Neurology* **2016**, *86*, 890-897, doi:10.1212/WNL.0000000000002445.
236. Brunet de Courssou, J.B.; Durr, A.; Adams, D.; Corvol, J.C.; Mariani, L.L. Antisense therapies in neurological diseases. *Brain* **2022**, *145*, 816-831, doi:10.1093/brain/awab423.
237. McDowall, S.; Aung-Htut, M.; Wilton, S.; Li, D. Antisense oligonucleotides and their applications in rare neurological diseases. *Front Neurosci* **2024**, *18*, 1414658, doi:10.3389/fnins.2024.1414658.
238. Sumner, C.J.; Miller, T.M. The expanding application of antisense oligonucleotides to neurodegenerative diseases. *J Clin Invest* **2024**, *134*, doi:10.1172/JCI186116.
239. Carvalho, S.; Moreira, L.; Santos, J.I.; Gaspar, P.; Gonçalves, M.; Matos, L.; David, H.; Encarnação, M.; Ribeiro, D.; Duarte, A.J.; et al. Help Comes from Unexpected Places: How a Tiny Fairy and a Tropical Fish may help us Model Mucopolysaccharidoses. *Endocr Metab Immune Disord Drug Targets* **2023**, doi:10.2174/0118715303277318231024055425.

Annexes

ANNEX 1 – ORIGINAL PAPERS

Authored by the PhD candidate

Original Paper#1 - Santos JI, Gonçalves M, Almeida MB, Rocha H, Duarte AJ, Matos L, Moreira LV, Encarnação M, Gaspar P, Prata MJ, Coutinho MF, Alves S. mRNA Degradation as a Therapeutic Solution for Mucopolysaccharidosis Type IIIC: Use of Antisense Oligonucleotides to Promote Downregulation of Heparan Sulfate Synthesis.

Original Paper (*Under preparation*) - Santos JI*, Gonçalves M*, Coutinho MF, Moreira LV, Prata MJ, Pires MJ, Oliveira P, Balestra D, Pinotti M, Van den Haute C, Gijsbers R, Alves S*, Matos L*. In vivo proof of principle on the therapeutic potential of an engineered U1 small nuclear RNA to rescue the most common Mucopolysaccharidosis type IIIC splice variant, c.234+1G>A.

Co-Authored by the PhD candidate

Original Paper#2 - Carvalho S, Santos JI, Moreira L, Duarte AJ, Gaspar P, Rocha H, Encarnação M, Ribeiro D, Barbosa Almeida M, Gonçalves M, David H, Matos L, Amaral O, Diogo L, Ferreira S, Santos C, Martins E, Prata MJ, Pereira de Almeida L, Alves S, Coutinho MF. Modeling Lysosomal Storage Disorders in an Innovative Way: Establishment and Characterization of Stem Cell Lines from Human Exfoliated Deciduous Teeth of Mucopolysaccharidosis Type II Patients.

Original Paper#3 - Coutinho MF, Encarnação M, Matos L, Silva L, Ribeiro D, Santos JI, Prata MJ, Vilarinho L, Alves S. Molecular Characterization of a Novel Splicing Mutation underlying Mucopolysaccharidosis (MPS) type VI-Indirect Proof of Principle on Its Pathogenicity.

International Journal of
Molecular Sciences

MDPI

Article

mRNA Degradation as a Therapeutic Solution for Mucopolysaccharidosis Type IIIC: Use of Antisense Oligonucleotides to Promote Downregulation of Heparan Sulfate Synthesis

Juliana Inês Santos [1,2,3,4], Mariana Gonçalves [1,2,3,5], Matilde Barbosa Almeida [1,2,3,6], Hugo Rocha [7], Ana Joana Duarte [1,2,3,8], Liliana Matos [1,2,3], Luciana Vaz Moreira [1,2,3], Marisa Encarnação [1,2,3], Paulo Gaspar [7], Maria João Prata [4,9], Maria Francisca Coutinho [1,2,3] and Sandra Alves [1,2,3,*]

1 Research and Development Unit, Department of Human Genetics, National Institute of Health Doutor Ricardo Jorge, INSA I.P., Rua Alexandre Herculano, 321, 4000-055 Porto, Portugal; juliana.santos@insa.min-saude.pt (J.I.S.); mariana.goncalves@insa.min-saude.pt (M.G.); matilde.almeida@insa.min-saude.pt (M.B.A.); ana.duarte@insa.min-saude.pt (A.J.D.); liliana.matos@insa.min-saude.pt (L.M.); luciana.moreira@insa.min-saude.pt (L.V.M.); marisa.encarnacao@insa.min-saude.pt (M.E.); francisca.coutinho@insa.min-saude.pt (M.F.C.)
2 Center for the Study of Animal Science, CECA-ICETA, University of Porto, Praça Gomes Teixeira, Apartado 55142, 4051-401 Porto, Portugal
3 Associate Laboratory for Animal and Veterinary Sciences, AL4AnimalS, Faculty of Veterinary Medicine, University of Lisbon, Avenida da Universidade Técnica, 1300-477 Lisboa, Portugal
4 Biology Department, Faculty of Sciences, University of Porto, Rua do Campo Alegre, 4169-007 Porto, Portugal; mprata@ipatimup.pt
5 Centre for the Research and Technology of Agro-Environmental and Biological Sciences, CITAB, Inov4Agro, University of Trás-os-Montes and Alto Douro, 5000-801 Vila Real, Portugal
6 Department of Medical Sciences, Campus Universitário de Santiago, Edifício da Saúde, Agra do Crasto, 3810-193 Aveiro, Portugal
7 Newborn Screening, Metabolism and Genetics Unit, Department of Human Genetics, National Institute of Health Doutor Ricardo Jorge, INSA I.P., Rua Alexandre Herculano, 321, 4000-055 Porto, Portugal; hugo.rocha@insa.min-saude.pt (H.R.); paulo.gaspar@insa.min-saude.pt (P.G.)
8 School of Medicine and Biomedical Sciences (ICBAS), University of Porto, Rua de Jorge Viterbo Ferreira 228, 4050-313 Porto, Portugal
9 Health Research and Innovation Institute, University of Porto, R. Alfredo Allen 208, 4200-135 Porto, Portugal
* Correspondence: sandra.alves@insa.min-saude.pt

check for updates

Academic Editor: Anne Vejux

Received: 3 January 2025
Revised: 29 January 2025
Accepted: 30 January 2025
Published: 1 February 2025

Citation: Santos, J.I.; Gonçalves, M.; Almeida, M.B.; Rocha, H.; Duarte, A.J.; Matos, L.; Moreira, L.V.; Encarnação, M.; Gaspar, P.; Prata, M.J.; et al. mRNA Degradation as a Therapeutic Solution for Mucopolysaccharidosis Type IIIC: Use of Antisense Oligonucleotides to Promote Downregulation of Heparan Sulfate Synthesis. *Int. J. Mol. Sci.* **2025**, *26*, 1273. https://doi.org/10.3390/ijms26031273

Copyright: © 2025 by the authors. Licensee MDPI, Basel, Switzerland. This article is an open access article distributed under the terms and conditions of the Creative Commons Attribution (CC BY) license (https://creativecommons.org/licenses/by/4.0/).

Abstract: Mucopolysaccharidosis type IIIC is a neurodegenerative lysosomal storage disorder (LSD) characterized by the accumulation of undegraded heparan sulfate (HS) due to the lack of an enzyme responsible for its degradation: acetyl-CoA:α-glucosaminide N-acetyltransferase (HGSNAT). Classical treatments are ineffective. Here, we attempt a new approach in genetic medicine, genetic substrate reduction therapy (gSRT), to counteract this neurological disorder. Briefly, we used synthetic oligonucleotides, particularly gapmer antisense oligonucleotides (ASOs), to target the synthesis of the accumulated compounds at the molecular level, downregulating a specific gene involved in the first step of HS biosynthesis, *XYLT1*. Our goal was to reduce HS production and, consequently, its accumulation. Initially, five gapmer ASOs were designed and their potential to decrease *XYLT1* mRNA levels were tested in patient-derived fibroblasts. Subsequent analyses focused on the two best performing molecules alone. The results showed a high inhibition of the *XYLT1* gene mRNA (around 90%), a decrease in xylosyltransferase I (XT-I) protein levels and a reduction in HS storage 6 and 10 days after transfection (up to 21% and 32%, respectively). Overall, our results are highly promising and may represent the initial step towards the development of a potential therapeutic option not only for MPS IIIC, but virtually for every other MPS III form. Ultimately, the same principle may also apply to other neuropathic MPS.

Keywords: Lysosomal Storage Disorders (LSDs); Mucopolysaccharidosis type III (MPS III); genetic substrate reduction therapy (gSRT); RNA therapeutics; antisense oligonucleotides (ASOs); gapmer ASOs

1. Introduction

The therapeutic potential of RNA-based therapies has gained significant attention, especially with the rapid development of messenger RNA (mRNA) vaccines during the COVID-19 pandemic. However, RNA therapeutics have been under development for over 40 years. One of the most promising strategies in this field involves the use of antisense oligonucleotides (ASOs), a novel class of drugs tailored for personalized medicine. ASOs target RNA based on sequence complementarity, and some of the most widely used types are gapmer ASOs, which mediate mRNA cleavage by recruiting RNase H [1–3]. Therapeutic ASOs are chemically modified to enhance their properties, increasing their resistance to nucleases and improving target binding affinity. Phosphorothioate (PS) linkages, along with modifications at the 2′ position of ribose, such as 2′-O-methoxy-ethyl (2′-MOE), are frequently employed to improve efficacy of therapeutic oligonucleotides. However, modifications other than PS do not activate RNase H. Gapmer ASOs overcome this by using a central PS core that activates RNase H, with "wings" composed of PS and additional modifications that enhance ASOs efficacy [4,5].

Other than their specificity and ability to target otherwise "undruggable" targets, ASOs have proven particularly effective in treating central nervous system (CNS) disorders. Intrathecal (IT) delivery of ASOs in particular has shown broad CNS distribution and therapeutic efficacy, as evidenced by approved treatments for conditions such as spinal muscular atrophy [6,7], amyotrophic lateral sclerosis [8], and Batten disease [9]. Thus, numerous ongoing studies are exploring the use of ASOs for other neurodegenerative disorders through IT administration, including spinocerebellar ataxia types 1, 2 and 3, Huntington's disease, Alzheimer's disease, Dravet syndrome, Angelman syndrome, and progressive supranuclear palsy [3,10].

Mucopolysaccharidoses (MPSs) are a subgroup of lysosomal storage disorders (LSDs), comprising 11 disorders across seven subtypes. These disorders are caused by defects in the degradation of glycosaminoglycans (GAGs), namely dermatan, heparan, keratan, and chondroitin sulfates [11–13]. Specifically, MPS type III results from a deficiency in the catabolism of heparan sulfate (HS), with MPS III subtypes A, B, C, and D being caused by deficiencies in heparan-N-sulfatase, N-acetyl-α-D-glucosaminidase, acetyl-CoA:α-glucosaminide N-acetyltransferase, and N-acetylglucosamine-6-sulfatase, respectively. Clinically, these subtypes present with severe CNS degeneration and cognitive decline accompanied by mild somatic disease, unlike other MPS types that may or may not present CNS involvement, while also displaying numerous somatic symptoms, some of which extremely severe and debilitating. While enzyme replacement therapies (ERTs) are available for some MPS types, they do not cross the blood–brain barrier (BBB) and are ineffective for MPS III, which remains an unresolved clinical challenge [13,14].

Given the success of ASOs in treating CNS disorders, this study aimed at investigating their potential as a novel genetic substrate reduction therapy (gSRT) for MPS III. The therapeutic rationale is clear: the HS biosynthetic pathway is well characterized, so we propose using ASOs to downregulate a key gene in this pathway to reduce HS production and accumulation.

Interestingly, substrate reduction therapies (SRTs) have already been approved for certain LSDs, such as miglustat and eliglustat tartrate for Gaucher disease, and miglustat for

Niemann–Pick disease type C [15]. Chemical and genetic SRTs have also been explored for MPS diseases, some only at pre-clinical levels, while others have actually reached clinical trials [16]. The chemical approach involves the use of small molecules such as genistein, a soy-derived isoflavone, and rhodamine B, both of which act as non-specific inhibitors of GAGs synthesis, and have been investigated in various studies [17–19]. For genistein, an open-label study with 22 MPS patients with neurological impairments demonstrated the safety of high-dose genistein [20]. However, a subsequent phase III double-blind, randomized, placebo-controlled trial using high-dose genistein aglycone failed to show significant reductions in cerebrospinal fluid (CSF) HS levels or cognitive improvements, and showed no significant clinical efficacy in MPS III, with only a modest reduction in urinary GAGs [21].

These results emphasize the need for further investigation, and highlight the risks of choosing a drug that does not directly target the intended pathway as a potential therapeutic agent, in this case the GAG biosynthetic cascade, but that instead acts upon a third party, hoping to trigger feedback mechanisms that will ultimately affect the target. Regarding rhodamine B, a study in 2017 using an MPS I mouse model suggested its potential as a promising standalone or adjunct therapy, particularly for skeletal manifestations. Weekly injections of 1 mg/kg rhodamine B for six months in MPS I knockout mice yielded promising results [22]. However, no clinical trials have been conducted to date, likely due to the reported toxic effects of rhodamine B [23]. Also noteworthy is the fact that the mechanism of action through which rhodamine B inhibits GAG synthesis is completely unknown.

The gSRT developed so far have relied on siRNAs. While showing promising in vitro [19,24,25], their clinical translation remains challenging, primarily due to the complexities of siRNA delivery. Effective nanocarriers capable of crossing the BBB are essential for overcoming these challenges [4,5].

In this study, we used gapmer ASOs (2′-MOE-PS) to downregulate the *XYLT1* gene, which encodes xylosyltransferase I (XT-I), a key enzyme in the early stages of GAGs biosynthesis (HS, chondroitin sulfate and dermatan sulfate). By targeting *XYLT1*, we aim to reduce HS, the specific GAG that is accumulated in affected cells and tissues of MPS III patients, potentially slowing disease progression. This approach offers several advantages not only over other potential LSD treatment options, but also over other forms of SRT, including the potential to treat multiple diseases that share the same accumulating substrates, while ensuring remarkable target specificity. Instead of a "one-compound-for-one-disease" model, our gSRT strategy could support a "one-compound-for-several-diseases" approach, reducing treatment costs and expanding the number of patients who would ultimately benefit from it.

Here, we present a proof of concept for our approach in MPS IIIC (MIM#252930), using patient-derived fibroblasts as a preliminary model. We chose MPS IIIC because, unlike other MPS types, it is caused by defects in an enzyme that is quite challenging: acetyl-CoA:α-glucosaminide N-acetyltransferase (HGSNAT; EC:2.3.1.78). Unlike most MPS-related proteins, this enzyme is not a lysosomal hydrolase but a transmembrane protein of the lysosome. Consequently, therapeutic options for this disease are much more limited, as ERT is not a viable option for these patients. Overall, our results demonstrated significant reductions in *XYLT1* mRNA and protein levels in these fibroblasts, along with a notable decrease in HS levels following ASO treatment.

2. Results

2.1. Evaluation of XYLT1 mRNA Expression: Effect of Designed Gapmers

Five distinct 2′-MOE-PS gapmer oligonucleotides were designed to downregulate the expression of *XYLT1*, a gene involved in the initial step of the HS biosynthesis (Table 1).

The design considered that gapmers have a central stretch of 10 DNA nucleotides flanked on each side by a wings of 5 nucleotides containing 2′-MOE modifications in the sugar ring too. These modifications increase nuclease resistance, protecting the ends of the ASO, avoid or reduce an immune response, and increase target binding affinity.

Additionally, PS bonds were included throughout the gapmer to increase stability and plasma protein binding, thereby improving its pharmacokinetic properties. Gapmers bind to their target RNA and form a stretch of double-stranded RNA–DNA hybrid that is recognized and disrupted via RNase H-mediated cleavage of the RNA strand.

To test the gapmers' efficacy in downregulating *XYLT1* mRNA, each gapmer (100 nM) was transfected not only in MPS IIIC patients' fibroblasts but also into patient-derived cell lines from all the other MPS III substypes: MPS IIIA (MIM#252900), MPS IIIB (MIM#252920) and MPS IIID (MIM#252940). The effect was assessed 24 and 48 h post-transfection, by the relative quantification of *XYLT1* expression, revealing high levels of inhibition. All treated cells showed that *XYLT1* mRNA expression levels reduced at 24 h post-transfection, with most of them displaying a further reduction at 48 h. However, the magnitude of the effect varied between cell lines and among the tested gapmers (Figure 1). Overall, at 24 h, the highest decreases were observed in the MPS IIIA cell line, ranging from nearly 95% to 80%, while the MPS IIIB cell line displayed the smallest reductions, ranging from 80% to only 5%. At 48 h, however, the reductions were more consistent across the four cell lines, varying from a maximum decrease of approximately 90% observed in MPS IIIA and MPS IIIB cells treated with gapmers number 2 and 3 (G2 and G3), respectively. For the MPS IIIC cell line in particular, *XYLT1* levels remained consistently lower at both 24 and 48 h. *GAPDH* was used as an endogenous control for normalization. A similar trend was observed in all cases: the inhibition effect was different between the five gapmers, with G2 and G3 seeming the two most promising ones as they showed a more consistent effect on target expression inhibition at both time points analyzed for the four different cell lines tested. Still, aiming at ensuring the reliability of the results, two novel rounds of experiments were performed in the MPS IIIC cell line (n = 3). Overall, the observed results closely mimicked those obtained for the independent cell lines, with G2 and G3 showing a higher knockout power while presenting the lowest standard deviation (see the Supplementary Materials; Figure S1), and thus being selected for a further analysis of their effect on XT-I levels and HS storage.

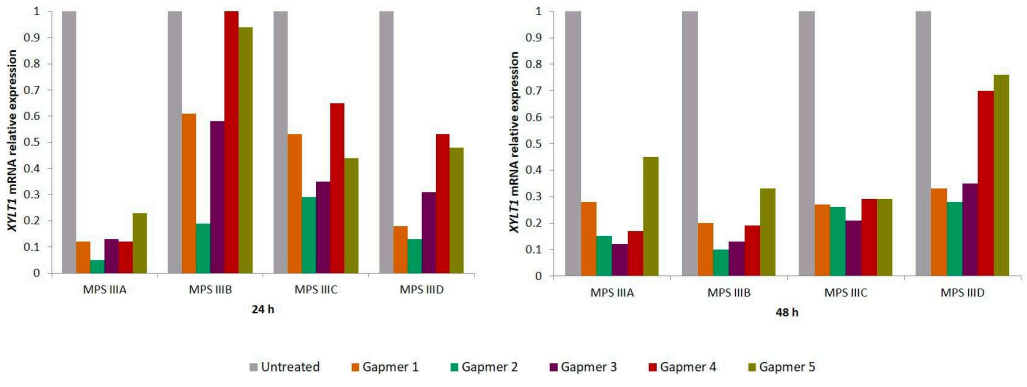


Figure 1. *XYLT1* mRNA relative expression in MPS III (A–D) patients' fibroblasts, after transfection with five different gapmer antisense oligonucleotides (100 nM). Expression levels were assessed at 24 and 48 h post-transfection. Data represent a single experiment per cell line (n = 1).

Table 1. Sequences of gapmer ASOs and their target exon in the *XYLT1* gene. NA—not applicable.

Gapmer Designation	Gapmer Sequence (5′ -> 3′)	Target Exon
Scramble	CCTATAGGACTATCCAGGAA	NA
G1	CGATGCAGGTAATTAGAGCG	5
G2	GTCAGCAAGGAAGTAGAGGT	10
G3	GTCAGGCTCATCGTAGACAT	9
G4	GCAACACATCTGGCTAGGAT	12
G5	ACAATCTTGGGACCAGGAGA	3′UTR

2.2. Inhibition of XYLT1 mRNA with Best-Performing Gapmers: G2 and G3

Following the selection of the most promising gapmer ASOs, transfection was repeated on fibroblasts from a MPS IIIC patient, and the effect on RNA levels was analyzed by qRT-PCR 24 h later. For this assay, a scramble gapmer was used as a negative control. Consistent with previous observations, cells transfected with G2 and G3 showed a significant inhibition of *XYLT1* mRNA expression compared to cells treated with the scramble ASO. The inhibitory effect was more pronounced with G2 as expression levels around 10% (corresponding to 90% reduction) were observed. For fibroblasts treated with G3, a decrease of about 70% in *XYLT1* mRNA expression was observed (Figure 2).

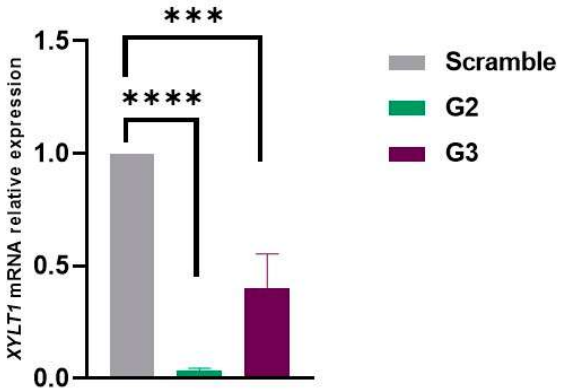


Figure 2. *XYLT1* mRNA relative expression in MPS IIIC patient's fibroblasts, 24 h after transfection with gapmers G2 and G3, quantified by qRT-PCR in three independent experiments ($n = 3$). *GAPDH* was used as endogenous control. Statistical comparisons between groups were performed using one-way ANOVA and Tukey's multiple comparisons test as a post hoc comparator (*** $p < 0.001$, **** $p < 0.0001$).

2.3. Decrease in Xylosyltrasferase I Levels After Treatment with G2 and G3

Before we addressed our ultimate goal, which was to check whether a decrease on HS was visible after treatment, we sought to clarify whether the decreases we had seen in *XYLT1* expression levels did actually translate into a decrease in the levels of the protein it encodes, XT-I. XT-I quantification was conducted by comparing band intensities in cells transfected with gapmers G2 and G3 to those transfected with the scramble gapmer. At 72 and 96 h post-transfection, MPS IIIC fibroblasts showed a decrease in XT-I protein levels, as expected. This reduction is in alignment with the observed high inhibition of *XYLT1* mRNA expression, indicating a corresponding decrease at the protein level. α-tubulin was used as control (Figure 3).

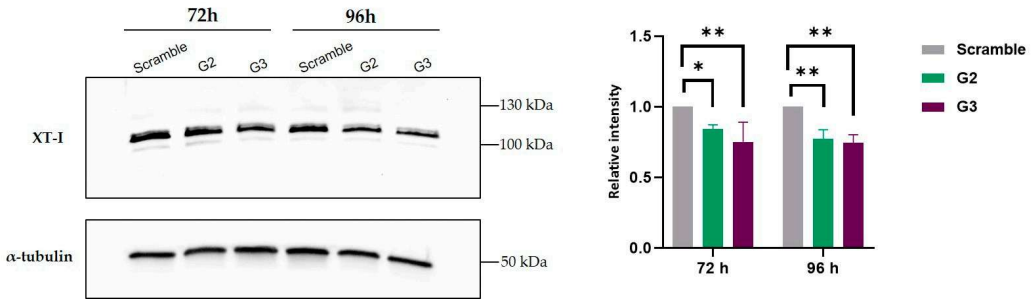


Figure 3. XT-I quantification. The left panel displays a representative Western blot showing XT-I protein levels in MPS IIIC patient's fibroblasts transfected with gapmers (scramble, G2 and G3), using α-tubulin as the loading control. The right panel displays the quantification of the relative XT-I protein levels, normalized to α-tubulin, from three independent experiments (n = 3). Statistical comparisons between G2- or G3-transfected cells and cells transfected with the scramble gapmer were performed using two-way ANOVA followed by Tukey's multiple comparisons test as a post hoc comparator (* $p < 0.05$, ** $p < 0.005$).

2.4. Decrease on Heparan Sulfate Levels

Finally, we moved on to quantify our ultimate therapeutic target: HS storage. To achieve this, HS levels were measured by LC-MS/MS in cell pellets collected 6 and 10 days after transfection. Apart from the scramble control, which was also included in all the previous experiments, MPS IIIC fibroblasts transfected with the transfection reagent alone and not exposed to any gapmer, either targeted or scramble, were included in these experiments. This additional condition allowed us to check whether both the scramble gapmer and the transfection itself had any effect on HS accumulation, and is referred to as non-transfected (NT) here.

The HS levels were also measured in a control cell line with no disease, Human Dermal Fibroblasts adult (HDFa), to verify the accumulation pattern. These cells were platted and collected at the same time as the others (6 days). The results were normalized to protein quantity. In MPS IIIC NT fibroblasts, HS levels were 9.92 µg/mg protein. As expected, a very similar amount of HS was detected in fibroblasts transfected with the scramble gapmer: 9.91 µg/mg protein.

The cells treated with gapmers G2 and G3 demonstrated a reduction in HS levels: 6.82 and 8.26 µg HS/mg protein, respectively. For reference, HS levels in HDFa cells had a mean of 3.79 µg HS/mg protein.

When comparing HS levels between HDFa to those of MPS IIIC fibroblasts (NT and/or treated with the scramble ASO), the levels of HS were significantly lower in the first ($p < 0.0001$), as expected.

The results also showed that the gapmer G2 had a positive impact on HS storage, compared to the scramble gapmer ($p < 0.05$). Although not statistically significant, a decreasing trend is observed when comparing the HS levels of the samples treated with the scramble ASO with the cells transfected with the gapmer G3 (Figure 4).

To check whether the effect of the best performing gapmer, G2, persisted over time, we also tested its ability to reduce HS accumulation in fibroblasts from MPS IIIC patients 10 days after transfection. Gapmer G3 was also included in this analysis, even though the effect seen 6 days after transfection had no statistical significance, in order to verify whether its effect was consistently lower than that of gapmer G2, or needed a longer timeframe to reach statistical significance, unlike gapmer G2.

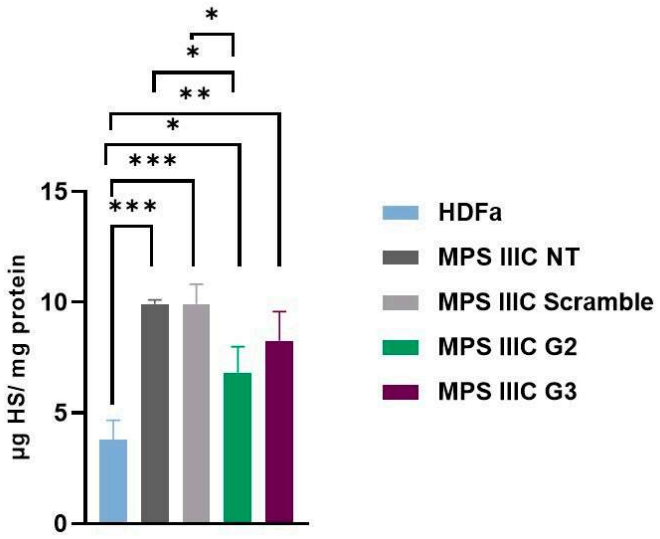


Figure 4. Quantification of heparan sulfate (HS). HS levels were measured in MPS IIIC patient's fibroblasts 6 days post-transfection with gapmers (scramble, G2 and G3) and in the human dermal fibroblast (HDFa) cell line. Results are expressed in µg HS per mg protein. Statistical comparisons between groups were performed using one-way ANOVA and Tukey's multiple comparisons test as a post hoc comparator (*** $p < 0.001$, ** $p < 0.005$, * $p < 0.05$). NT: non-transfected MPS IIIC fibroblasts.

The results showed that the effect of gapmer G2 is maintained over time, compared to that of fibroblasts transfected with the gapmer scramble ($p < 0.05$). A trend toward a reduction was detected, once again, with gapmer G3 (Figure 5). Not surprisingly, patient's fibroblasts showed a pronounced increase in HS storage with time (with means of 9.91 to 17.12 µg HS/mg protein), since these cells are not able to degrade HS.

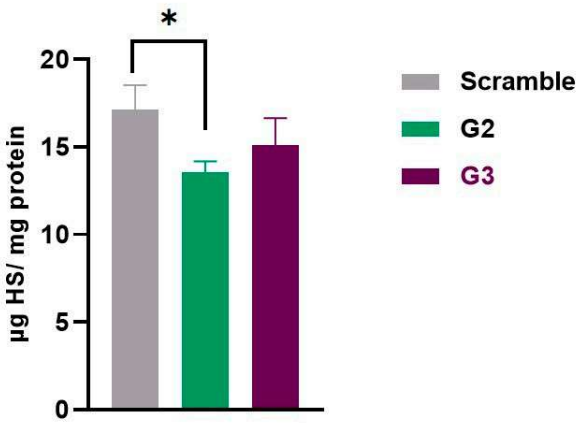


Figure 5. Quantification of heparan sulfate (HS). HS levels were measured in MPS IIIC patient's fibroblasts 10 days post-transfection with gapmers (scramble, G2 and G3). Results are expressed in µg HS per mg protein. Statistical comparisons between groups were performed using one-way ANOVA and Tukey's multiple comparisons test as a post hoc comparator (* $p < 0.05$).

Overall, from an initial panel of five putative candidates, there was one particular gapmer which fulfilled all criteria to qualify as a potential therapeutic molecule: not only did it reduce its target mRNA and protein levels, but also showed a positive effect in reducing HS storage in patient cells: G2. After a single transfection, it achieved the highest reduction 6 days post-transfection (higher than 20%), but its effect was still statistically significant 4 days later (i.e., 10 days post-transfection).

3. Discussion

In this study, we investigated the use of gapmer ASOs as a potential gSRT for MPS IIIC, focusing on downregulating *XYLT1* to reduce the synthesis of XT-I. By targeting XT-I, a key enzyme in GAG synthesis, we aimed to address the pathological accumulation of our target GAG, HS in MPS IIIC. XT-I catalyzes the transfer of UDP-xylose to serine residues on acceptor proteins, a critical step in GAG chain formation. Inhibiting XT-I could broadly reduce GAG synthesis, making it a promising target for multiple MPS subtypes [26]. One of the main reasons for selecting *XYLT1* as the target gene in our initial attempt to downregulate HS synthesis is the compelling evidence from previous studies demonstrating that its inhibition leads to a significant reduction in GAG synthesis, as shown in experiments using siRNAs [27,28].

Mutations in *XYLT1* are implicated in specific genetic disorders, including Desbuquois skeletal dysplasia (DBSD) and Baratela–Scott syndrome. DBSD is an autosomal recessive disease characterized by skeletal dysplasia, joint dislocations, short stature, and facial abnormalities [29–31]. Baratela–Scott syndrome presents with short stature, skeletal dysplasia, facial dysmorphisms, and developmental delays [32]. Studies on DBSD have demonstrated that *XYLT1* mutations impair GAG biosynthesis, with Bui et al. reporting low levels of GAGs and proteoglycans in fibroblasts from affected individuals [29]. A recent study by Taieb et al. provided a deeper understanding of the role of *XYLT1* in the onset of the disease, demonstrating that XT-I plays a crucial role in chondrocyte maturation rather than differentiation, highlighting its importance in cartilage development and disease progression [33].

Another important factor supporting the selection of our target gene was the assumption that the transient downregulation of *XYLT1* will not adversely affect cell function, as another enzyme, XT-II, encoded by the *XYLT2* gene, can partially compensate for it. Mutations in *XYLT2* are also associated with a disease phenotype known as spondylo-ocular syndrome, which is characterized by short stature, retinal detachment, amblyopia, nystagmus, heart valve defects, bone fragility, and mild learning difficulties. Again, the levels of GAGs and XT-I activity in the dermal fibroblasts of a patient were lower than in those of healthy subjects [34].

XYLT1 and *XYLT2* exhibit differential expression across various cell types and tissues. However, both isoforms show broad expression levels in fibroblasts [35] and in the cerebral cortex [36], which is particularly important in the context of our study. Additionally, XT-I and XT-II are expressed in a highly overlapping pattern in adult mice [37]. However, importantly, studies in mouse models and expression analyses across various cell lines have demonstrated that these two xylosyltransferases exhibit both temporally and tissue-specific expression patterns during development [33,35,38–41]. Additionally, some studies in mouse models have revealed reduced GAG concentrations, along with corresponding alterations in proteoglycan expression, as a result of mutations in both genes [38,40].

Another important argument in favor of our approach comes from a study by Dziedzic et al. in 2012 [28], which, in a similar context of using RNA therapies to downregulate GAG biosynthesis, demonstrated that silencing *XYLT1* alone resulted in a substantial decrease in GAG synthesis, whereas the simultaneous silencing of *XYLT1* and *XYLT2* provided only a marginal additional effect.

Based on these findings, we decided to begin our approach by targeting *XYLT1*, as this strategy could help minimize potential harmful effects for patients, given the possibility that *XYLT2* may partially compensate for the loss of *XYLT1*, a factor that should not be overlooked. However, our objective was to reduce, rather than completely eliminate, *XYLT1* gene expression. It is important to note that ASOs do not achieve complete gene knockout.

Instead, their continuous application is expected to result in a controlled reduction in XT-I expression, and, consequently, in HS synthesis, with the aim of halting disease progression.

With that objective, in this study, we used 2′-MOE-PS gapmers, leveraging their enhanced stability, nuclease resistance, and high RNA binding affinity. These second-generation ASOs are known to achieve effective mRNA degradation via RNase H-mediated cleavage without affecting unrelated transcripts, critical for sustained efficacy in vitro and potentially in vivo. This second-generation modification has emerged as the most successful chemistry, having a more favorable safety profile, as suggested by a number of clinical studies. Indeed, the ASOs already available for therapy are 20-mer, 2′-MOE-PS gapmers, such as our tested gapmers, thus showing their potential for clinical translation [42,43]. Initially, we designed and tested five gapmers targeting *XYLT1* and evaluated their effect in four different cell lines. Our rationale for this preliminary assessment was straightforward: although this study focuses on MPS IIIC, any drug or therapeutic molecule acting upon an early step of the GAG biosynthetic cascade has the potential to benefit not only MPS IIIC, but also any other MPS subtypes. Thus, it would be worth assessing its performance in other MPS, particularly those in more urgent need for a therapeutic solution. While only a single experiment was performed for each cell line, the emerging pattern observed across the four MPS III cell lines suggests that G2 and G3 are the most effective, with G2 showing superior results across almost all tested conditions, even in these first assessments. Subsequent experiments in triplicate in fibroblasts from our target disorder alone, MPS IIIC, confirmed these preliminary findings, demonstrating that both gapmers reduced *XYLT1* mRNA and XT-I protein levels, with G2 achieving significant reductions in HS storage in MPS IIIC fibroblasts. It is also worth mentioning that the tested concentration of 100 nM falls within the range typically used for hard-to-transfect cells, such as fibroblasts. It is also within the normal range used for preclinical assessments and later shown to hold sufficient potency to display a therapeutic effect without compromising off-targets.

For instance, Aguti et al. studied the silencing efficiency of gapmer ASOs with 2′-OMe, 2′-MOE, and LNA chemistries. While optimizing allele-specific designs, they used a starting concentration of 100 nM, matching ours. Lower concentrations (10–80 nM for 2′-OMe and 1.25–20 nM for 2′-MOE/LNA) failed to achieve efficient silencing [44].

Therefore, the observed results confirm the efficacy namely of gapmer 2 and highlight its potential for translation to in vivo studies, where it will be possible to better assess the side effects of our therapy. These side effects could be related to the RNA drugs being administered [5] as well as to the pathway we are targeting. Recently, a study by Kleine et al. observed a strong stress response, oxidative stress, senescence and apoptosis following the knockout of *XYLT1* [41], an observation that should not be neglected. Other relevant insights into potential off-targets or cross-effects may also come from the direct measurement of our target's isoform, XT-II.

Our results validate the proof of concept that 2′-MOE-PS gapmers can effectively downregulate *XYLT1* expression. Furthermore, our data demonstrate that reducing XT-I levels leads to a substantial decrease in HS accumulation, thus acting upon the primary cause of MPS IIIC pathology. This specificity is advantageous for treating MPS IIIC, as HS reduction may alleviate neurological symptoms. The ability of ASOs to cross the BBB via IT delivery enhances their therapeutic potential, overcoming the limitations of traditional SRTs like miglustat and eliglustat tartrate, which fail to target the CNS and often have systemic side effects [15].

For MPS, two chemical compounds, rhodamine B and genistein, have demonstrated the ability to reduce GAG production. However, their mechanisms of action on GAG synthesis remain nonspecific and not fully understood, and their translation to clinical practice has not been successful [19]. In contrast, genetic substrate reduction approaches offer a

more targeted strategy, addressing the root cause of the disease with greater specificity, and clinical translation, particularly that using ASOs, appears more feasible. Previous gSRT efforts for MPS relied on siRNAs. Unlike ASOs, siRNAs face significant challenges in delivery, particularly to the CNS, as they require conjugation with other molecules or encapsulation in nanocarriers [3]. For example, Dziedzic et al. carried out the siRNA targeting of *XYLT1*, *XYLT2*, B4GALT7, and B3GALT6 in MPS IIIA fibroblasts, achieving reductions in mRNA and protein levels and impaired GAG synthesis [27]. Similarly, Kaidonis et al. employed shRNAs via lentiviral transfection to inhibit *EXTL2* and *EXTL3* in MPS I and MPS III fibroblasts, yielding comparable results [24]. More recently, Canals et al. tested siRNAs targeting *EXTL2* and *EXTL3* in MPS IIIC fibroblasts, achieving significant HS reductions as early on as in the first 3 days, peaking at 14 days post-treatment. However, translation to the clinic was hampered by the difficulties in the *in vivo* delivery of siRNAs [25].

Our study reinforces that gSRT could be a valuable therapeutic strategy for LSDs with significant neurological involvement. Also noteworthy is that this is the first study to provide a quantitative analysis on the effect one such approach may have upon HS in vitro. In this way, we have assess the true disease biomarker, which is well established as the trigger of the pathophysiological cascade. The only other study that has specifically assessed HS alone is that of Canals et al., carried out in 2015 [25]. However, their analysis was not conducted in a quantitative manner. The results for HS were qualitative, instead, and acquired through immunocytochemistry [25].

The successful use of ASOs in CNS-related disorders, such as spinal muscular atrophy [45] and Batten disease [9], further supports their applicability to MPS III [4,5,46–48]. With our work, we aim to raise awareness among LSD researchers about the potential of using ASOs as a substrate reduction therapy, and to replicate the promising results obtained with siRNAs, but now utilizing a molecule with more accessible delivery. Future research targeting other genes, such as those already targeted by siRNAs and mentioned earlier, that measure other GAGs and explore additional downstream pathways related to HS accumulation will be important in informing the choice of the best possible target for gSRT, as well as in further validating the specificity of the approach. Equally crucial is the focus on in vivo validation in animal models, such as zebrafish or rodents, to evaluate biodistribution, safety, and long-term efficacy, paving the way for clinical translation.

4. Materials and Methods

4.1. Gapmer Antisense Oligonucleotides Design

Five different gapmers targeting the *XYLT1* gene, along with one negative control, (scramble ASO) were synthesized by IDT (Integrated DNA Technologies, Coralville, Johnson County, IA, USA). These ASOs are 5-10-5 gapmers that have fully PS-modified linkages with a central segment of 10-mer DNA flanked by 5-mer 2′MOE on both wings.

4.2. Cell Culture and Transfection

MPS III (A to D) patient-derived fibroblasts were obtained from the Istituto Giannina Gaslini biobank (Genoa, Italy). A commercial adult Human Dermal Fibroblast, adult (HDFa) cell line available in the lab was used as a control in all experiments. Cells were cultured in Dulbecco's Modified Eagle Medium (DMEM; Gibco™, Thermo Fisher Scientific, Waltham, MA, USA), high glucose levels, GlutaMAX™ Supplement supplemented with 10% fetal bovine serum (FBS; Gibco™, Thermo Fisher Scientific, Waltham, MA, USA), 1% penicillin/streptomycin (P/S; Gibco™, Thermo Fisher Scientific, Waltham, MA, USA) and 1% Amphotericin B (Gibco™, Thermo Fisher Scientific, Waltham, MA, USA) at 37 °C and 5% CO_2. The day before ASOs transfection, 1.8×10^5 cells were seeded in a 6-well plate and in 1.125×10^6 in 75 cm^2 flasks, depending on the subsequent analyses.

Fibroblasts at confluence 65–70% were transfected with the 5 ordered gapmers at 100 nM. For this, each gapmer ASO was mixed with Opti-MEM (Gibco™, Thermo Fisher Scientific, Waltham, MA, USA) containing 10 µL Lipofectamine™ 2000 (Invitrogen™, Thermo Fisher Scientific, Waltham, MA, USA) for each 10 cm^2 of growth surface area, at room temperature (RT), for 20 min. During this incubation time, the medium of the seeded cells was changed and replaced with the same fresh DMEM referred to above, but without P/S and Amphotericin B. After the referred incubation, gapmer ASOs were added to cells.

Cells were harvested at different time points for different analyses: at 24 h post-transfection for *XYLT1* relative expression analyses; at 72 and 96 h for protein measurement; and at 6 and 10 days for HS quantification. We decided to select different incubation periods to analyze the effects on the mRNA, protein, and HS levels based on the methodology described in previous studies [25,27,28], as well as on the results obtained from our own experience.

4.3. Quantitative Real-Time PCR Assay

Total RNA was extracted using GRS Total RNA Kit—Blood & Cultured cells (GRiSP research solutions, Porto, Portugal) following the manufacturer's protocol. After reverse-transcription with the Ready-To-Go™ You-Prime First-Strand Beads kit (Cytiva, Marlborough, MA, USA), quantitative real-time PCR was conducted on a CFX96 Touch Real-Time PCR Detection System (Bio-Rad Laboratories, Hercules, CA, USA). PCR reactions were prepared in a final volume of 20 µL using 2× SsoAdvanced™ Universal SYBR® Green Supermix (2×) and PrimePCR™ SYBR Green Assays as follows: PrimePCR™ Template for SYBR® Green Assay: *XYLT1*, Human (qHsaCIP0030871); PrimePCR™ Template for SYBR® Green Assay: *GAPDH*, Human (qHsaCEP0041396). Thermal cycling conditions were 95 °C for 30 s, 40 cycles of denaturation at 95 °C for 30 s, and annealing and extension at 60 °C for 30 s. Each measurement was performed in triplicate and the threshold cycle (Ct) the fractional cycle number at which the amount of amplified target reached a fixed threshold was determined. The relative expression of *XYLT1* was calculated using the Livak method ($2^{-\Delta\Delta Ct}$ method), with *GAPDH* serving as the internal control for normalization.

4.4. Western Blot Analyses

For Western blot analysis, patient-derived fibroblasts grown in 75 cm^2 flasks and transfected with 100 nM of the best-performing gapmers were harvested 72 and 96 h after transfection. Total protein extracts were homogenized in a RIPA buffer (25 mM Tris, pH = 7.6, 150 mM NaCl, 1% nonidet P40, 1% sodium deoxycholate and 0.1% SDS) supplemented with a 0.01% Protease Inhibitor Cocktail (Sigma-Aldrich®, St. Louis, MO, USA). Cell lysis was achieved by keeping the solution on ice for 1 h with resuspension every 10 min, followed by brief centrifugation. Total protein quantification was carried out with the Pierce™ BCA Protein Assay Kit (Thermo Scientific™, Waltham, MA, USA). A total of 20 µg of protein was loaded on a 4–15% Mini-PROTEAN® TGX Stain-Free™ Protein Gels (Bio-Rad Laboratories, Hercules, CA, USA). After electrophoresis, proteins were transferred to a nitrocellulose membrane using a Trans-Blot Turbo Transfer System (Bio-Rad Laboratories, Hercules, CA, USA), for 30 min at 20 mA. The membrane was then incubated with blocking solution (5% NFDM/TBS-T) for 2 h at RT, with gentle agitation on a shaker. The membrane was cut into two sections, around the 70 kDa molecular weight marker, and incubated overnight at 4 °C on a shaker with the primary antibodies rabbit anti-*XYLT1* (1:1000, Catalogue# 043941, US Biological, Salem, MA, USA) and mouse anti-α-tubulin (1:5000, Catalogue# T6199, Sigma-Aldrich, St. Louis, MO, USA), with the latter as a control. The next day, after washing in 0.5% TBS-T, bound antibodies were detected using HRP-conjugated goat anti-mouse IgG (1:5000, Catalogue# 31431, Invitrogen™ Thermo

Fisher Scientific, Waltham, MA, USA) and mouse anti-rabbit IgG (1:5000, Catalogue# sc-2357, Santa Cruz Biotechnology Dallas, TX, USA) for 1 h at RT. Membranes were incubated with ECL solution, and an image was captured using the ChemiDoc™ XRS+ imaging system (Bio-Rad Laboratories, Hercules, CA, USA).

4.5. Heparan Sulfate Quantification

HS and DS levels were quantified by liquid chromatography–tandem mass spectrometry (LC-MS/MS) in MPS IIIC cell homogenates, transfected with the best-performing gapmer ASOs, after the butanolysis reaction, according to the method originally described by Forni and co-workers for urine samples [49] and slightly modified in house to accommodate for cell lysates [50]. Briefly, cell homogenates were prepared by sonication, and their protein concentration was determined using the same method described for the Western blot analyses. Each cell homogenate was divided into two different plates, one for HS and another for DS. Samples were then dried under a stream of nitrogen, and 75 µL of 3 N HCl in N-butanol was added to each plate well.

For HS measurements, samples were incubated for 60 min at 90 °C, while for DS measurements, samples were heated for 25 min at 65 °C. After those incubations, samples were cooled back to RT for 10 min and dried again using the same method. Then, 30:70 water/acetonitrile (*v*/*v*) solution was added to samples: 100 µL for HS and 250 µL for DS quantification. After a brief vortex, the HS samples were combined with their respective DS counterparts and vortexed again. Finally, dimers derived from butanolysis reactions were separated by HPLC using a gradient of acetonitrile and water (LC column: Gemini® 3 µm C6-Phenyl 110 Å, 100 × 2 mm, from Phenomenex, Torrance, CA, USA) and detected using a triple quadrupole mass spectrometer, API4000 QTRAP (Sciex, Danaher Corporation, Washington, DC, USA). Sample quantification was performed by interpolation from a calibration curve (covering a concentration range from 0.39 to 50 µg/mL).

4.6. Statistical Analyses

All experiments were performed at least three times, with data presented as mean ± standard deviation. To compare the means between groups, one-way ANOVA was performed, followed by Tukey's multiple comparisons test. Differences were considered statistically significant if the *p*-value was less than 0.05. All tests were performed using GraphPad Prism® software for Windows (version 8.0.1).

5. Conclusions

This study provides a proof of concept for the use of gapmer ASOs in reducing HS accumulation in MPS IIIC fibroblasts, supporting the further preclinical development of gSRT for MPS IIIC and potentially other MPS III subtypes. By targeting the biosynthetic pathway of all GAGs, this approach not only addresses the primary cause of cellular damage in MPS IIIC that is caused by HS accumulation but also opens up avenues for a broader therapeutic strategy within the field of lysosomal storage disorders. The results presented here underline the potential of ASOs to fulfill unmet clinical needs for CNS-targeted therapies, providing a foundation for future investigations into ASO-based interventions in MPS III.

Taken together, our results indicate that this approach is able to promote a reduction in mRNA levels of our target gene and, consequently, of our target protein, which translate into a notable reduction in the HS synthetic pathway after 6 and 10 days. Although further research is needed, this is a promising approach with the potential to be used as a complementary therapy to obtain synergic effects with other treatments developed to accelerate the rate of HS degradation and/or excretion out of the cell. Furthermore, in the

future, our strategy could be a viable option not only for older patients (in helping to slow disease progression), but also for younger patients awaiting more permanent solutions, such as gene therapy or gene editing.

Supplementary Materials: The following supporting information can be downloaded at: https://www.mdpi.com/article/10.3390/ijms26031273/s1.

Author Contributions: Conceptualization, J.I.S., M.F.C. and S.A.; gapmer antisense oligonucleotides design, J.I.S., M.G. and S.A.; cell culture, J.I.S., M.G. and M.B.A.; qRT-PCR, J.I.S., M.G., M.B.A. and L.V.M.; Western blot, J.I.S., A.J.D. and M.E.; LC-MS/MS, M.F.C., J.I.S., H.R. and P.G.; statistical analysis, J.I.S., M.F.C. and L.M.; writing—original draft preparation, J.I.S. and S.A.; writing—review and editing, M.F.C. and S.A.; critical review: M.J.P. and S.A.; figures and tables: J.I.S. and M.G.; supervision: M.F.C. and S.A.; project administration: S.A.; funding acquisition: S.A. All authors have read and agreed to the published version of the manuscript.

Funding: This work was financed by national funds through FCT—Fundação para a Ciência e a Tecnologia, I.P., within the scope of the project ASOS2cureMPSIII-2022.04667.PTDC (https://doi.org/10.54499/2022.04667.PTDC). The authors would like to thank Sanfilippo Children's Foundation (2019DGH1656), SPDM (2019DGH1629), CECA (UIDB/00211/2020) and AL4AnimalS (LA/P/0059/2020).

Institutional Review Board Statement: The study was conducted in accordance with the Declaration of Helsinki, and approved by the Ethics Committee of National Institute of Health Doutor Ricardo Jorge (date of approval 9 October 2023).

Informed Consent Statement: Informed consent was obtained from all subjects involved in the study.

Data Availability Statement: Data are contained within the article and Supplementary Materials.

Conflicts of Interest: The authors declare no conflicts of interest.

Abbreviations

The following abbreviations are used in this manuscript:

LSDs	Lysosomal storage disorders
MPS III	Mucopolysaccharidosis type III
gSRT	Genetic substrate reduction therapy
ASOs	Antisense oligonucleotides
HS	Heparan sulfate
XT-I	Xylosyltransferase I
XT-II	Xylosyltransferase II
PS	Phosphorothioate
IT	Intrathecal
MPSs	Mucopolysaccharidoses
GAGs	Glycosaminoglycans
ERTs	Enzyme replacement therapies
BBB	Blood–brain barrier
SRTs	Substrate reduction therapies
CSF	Cerebrospinal fluid
DMEM	Dulbecco's Modified Eagle Medium
FBS	Fetal bovine serum
LC-MS/MS	Liquid chromatography-tandem mass spectrometry
NT	Non-transfected
HDFa	Adult Human Dermal Fibroblasts
DBSD	Desbuquois skeletal dysplasia
RT	Room temperature

References

1. Dhuri, K.; Bechtold, C.; Quijano, E.; Pham, H.; Gupta, A.; Vikram, A.; Bahal, R. Antisense Oligonucleotides: An Emerging Area in Drug Discovery and Development. *J. Clin. Med.* **2020**, *9*, 2004. [CrossRef]
2. Lauffer, M.C.; van Roon-Mom, W.; Aartsma-Rus, A.; Collaborative, N. Possibilities and limitations of antisense oligonucleotide therapies for the treatment of monogenic disorders. *Commun. Med.* **2024**, *4*, 6. [CrossRef] [PubMed]
3. Di Francesco, V.; Chua, A.J.; Huang, D.; D'Souza, A.; Yang, A.; Bleier, B.S.; Amiji, M.M. RNA therapies for CNS diseases. *Adv. Drug Deliv. Rev.* **2024**, *208*, 115283. [CrossRef] [PubMed]
4. Roberts, T.C.; Langer, R.; Wood, M.J.A. Advances in oligonucleotide drug delivery. *Nat. Rev. Drug Discov.* **2020**, *19*, 673–694. [CrossRef] [PubMed]
5. Hammond, S.M.; Aartsma-Rus, A.; Alves, S.; Borgos, S.E.; Buijsen, R.A.M.; Collin, R.W.J.; Covello, G.; Denti, M.A.; Desviat, L.R.; Echevarría, L.; et al. Delivery of oligonucleotide-based therapeutics: Challenges and opportunities. *EMBO Mol. Med.* **2021**, *13*, e13243. [CrossRef] [PubMed]
6. Tizzano, E.F.; Finkel, R.S. Spinal muscular atrophy: A changing phenotype beyond the clinical trials. *Neuromuscul. Disord.* **2017**, *27*, 883–889. [CrossRef] [PubMed]
7. De Vivo, D.C.; Bertini, E.; Swoboda, K.J.; Hwu, W.L.; Crawford, T.O.; Finkel, R.S.; Kirschner, J.; Kuntz, N.L.; Parsons, J.A.; Ryan, M.M.; et al. Nusinersen initiated in infants during the presymptomatic stage of spinal muscular atrophy: Interim efficacy and safety results from the Phase 2 NURTURE study. *Neuromuscul. Disord.* **2019**, *29*, 842–856. [CrossRef]
8. Blair, H.A. Tofersen: First Approval. *Drugs* **2023**, *83*, 1039–1043. [CrossRef] [PubMed]
9. Kim, J.; Hu, C.; Moufawad El Achkar, C.; Black, L.E.; Douville, J.; Larson, A.; Pendergast, M.K.; Goldkind, S.F.; Lee, E.A.; Kuniholm, A.; et al. Patient-Customized Oligonucleotide Therapy for a Rare Genetic Disease. *N. Engl. J. Med.* **2019**, *381*, 1644–1652. [CrossRef]
10. Amanat, M.; Nemeth, C.L.; Fine, A.S.; Leung, D.G.; Fatemi, A. Antisense Oligonucleotide Therapy for the Nervous System: From Bench to Bedside with Emphasis on Pediatric Neurology. *Pharmaceutics* **2022**, *14*, 2389. [CrossRef]
11. Neufeld, E.F.; Muenzer, J. The Mucopolysaccharidoses. In *The Metabolic Basis of Inherited Disease*, 8th ed.; Scriver CR: Austin, TX, USA; McGraw-Hill: New York, NY, USA, 2001; pp. 3421–3453.
12. Muenzer, J. Overview of the mucopolysaccharidoses. *Rheumatology* **2011**, *50* (Suppl. S5), v4–v12. [CrossRef]
13. Coutinho, M.F.; Lacerda, L.; Alves, S. Glycosaminoglycan storage disorders: A review. *Biochem. Res. Int.* **2012**, *2012*, 471325. [CrossRef] [PubMed]
14. Penon-Portmann, M.; Blair, D.R.; Harmatz, P. Current and new therapies for mucopolysaccharidoses. *Pediatr. Neonatol.* **2023**, *64* (Suppl. S1), S10–S17. [CrossRef] [PubMed]
15. Platt, F.M.; d'Azzo, A.; Davidson, B.L.; Neufeld, E.F.; Tifft, C.J. Lysosomal storage diseases. *Nat. Rev. Dis. Primers.* **2018**, *4*, 27. [CrossRef]
16. Coutinho, M.F.; Santos, J.I.; Matos, L.; Alves, S. Genetic Substrate Reduction Therapy: A Promising Approach for Lysosomal Storage Disorders. *Diseases* **2016**, *4*, 33. [CrossRef] [PubMed]
17. Piotrowska, E.; Jakóbkiewicz-Banecka, J.; Tylki-Szymanska, A.; Liberek, A.; Maryniak, A.; Malinowska, M.; Czartoryska, B.; Puk, E.; Kloska, A.; Liberek, T.; et al. Genistin-rich soy isoflavone extract in substrate reduction therapy for Sanfilippo syndrome: An open-label, pilot study in 10 pediatric patients. *Curr. Ther. Res. Clin. Exp.* **2008**, *69*, 166–179. [CrossRef] [PubMed]
18. Roberts, A.L.; Thomas, B.J.; Wilkinson, A.S.; Fletcher, J.M.; Byers, S. Inhibition of glycosaminoglycan synthesis using rhodamine B in a mouse model of mucopolysaccharidosis type IIIA. *Pediatr. Res.* **2006**, *60*, 309–314. [CrossRef] [PubMed]
19. Seker Yilmaz, B.; Davison, J.; Jones, S.A.; Baruteau, J. Novel therapies for mucopolysaccharidosis type III. *J. Inherit. Metab. Dis.* **2021**, *44*, 129–147. [CrossRef]
20. Kim, K.H.; Dodsworth, C.; Paras, A.; Burton, B.K. High dose genistein aglycone therapy is safe in patients with mucopolysaccharidoses involving the central nervous system. *Mol. Genet. Metab.* **2013**, *109*, 382–385. [CrossRef] [PubMed]
21. Ghosh, A.; Rust, S.; Langford-Smith, K.; Weisberg, D.; Canal, M.; Breen, C.; Hepburn, M.; Tylee, K.; Vaz, F.M.; Vail, A.; et al. High dose genistein in Sanfilippo syndrome: A randomised controlled trial. *J. Inherit. Metab. Dis.* **2021**, *44*, 1248–1262. [CrossRef]
22. Derrick-Roberts, A.L.K.; Jackson, M.R.; Pyragius, C.E.; Byers, S. Substrate Deprivation Therapy to Reduce Glycosaminoglycan Synthesis Improves Aspects of Neurological and Skeletal Pathology in MPS I Mice. *Diseases* **2017**, *5*, 5. [CrossRef]
23. Dire, D.J.; Wilkinson, J.A. Acute exposure to rhodamine B. *J. Toxicol. Clin. Toxicol.* **1987**, *25*, 603–607. [CrossRef] [PubMed]
24. Kaidonis, X.; Liaw, W.C.; Roberts, A.D.; Ly, M.; Anson, D.; Byers, S. Gene silencing of *EXTL2* and *EXTL3* as a substrate deprivation therapy for heparan sulfate storing mucopolysaccharidoses. *Eur. J. Hum. Genet.* **2010**, *18*, 194–199. [CrossRef] [PubMed]
25. Canals, I.; Benetó, N.; Cozar, M.; Vilageliu, L.; Grinberg, D. *EXTL2* and *EXTL3* inhibition with siRNAs as a promising substrate reduction therapy for Sanfilippo C syndrome. *Sci. Rep.* **2015**, *5*, 13654. [CrossRef]
26. Mizumoto, S.; Ikegawa, S.; Sugahara, K. Human genetic disorders caused by mutations in genes encoding biosynthetic enzymes for sulfated glycosaminoglycans. *J. Biol. Chem.* **2013**, *288*, 10953–10961. [CrossRef] [PubMed]

27. Dziedzic, D.; Wegrzyn, G.; Jakóbkiewicz-Banecka, J. Impairment of glycosaminoglycan synthesis in mucopolysaccharidosis type IIIA cells by using siRNA: A potential therapeutic approach for Sanfilippo disease. *Eur. J. Hum. Genet.* **2010**, *18*, 200–205. [CrossRef] [PubMed]
28. Dziedzic, D.; Narajczyk, M.; Gabig-Cimińska, M.; Jakóbkiewicz-Banecka, J. Simultaneous siRNA-mediated silencing of pairs of genes coding for enzymes involved in glycosaminoglycan synthesis. *Acta. Biochim. Pol.* **2012**, *59*, 293–298. [CrossRef]
29. Bui, C.; Huber, C.; Tuysuz, B.; Alanay, Y.; Bole-Feysot, C.; Leroy, J.G.; Mortier, G.; Nitschke, P.; Munnich, A.; Cormier-Daire, V. *XYLT1* mutations in Desbuquois dysplasia type 2. *Am. J. Hum. Genet.* **2014**, *94*, 405–414. [CrossRef] [PubMed]
30. Jamsheer, A.; Olech, E.M.; Kozłowski, K.; Niedziela, M.; Sowińska-Seidler, A.; Obara-Moszyńska, M.; Latos-Bieleńska, A.; Karczewski, M.; Zemojtel, T. Exome sequencing reveals two novel compound heterozygous *XYLT1* mutations in a Polish patient with Desbuquois dysplasia type 2 and growth hormone deficiency. *J. Hum. Genet.* **2016**, *61*, 577–583. [CrossRef] [PubMed]
31. Guo, L.; Elcioglu, N.H.; Iida, A.; Demirkol, Y.K.; Aras, S.; Matsumoto, N.; Nishimura, G.; Miyake, N.; Ikegawa, S. Novel and recurrent *XYLT1* mutations in two Turkish families with Desbuquois dysplasia, type 2. *J. Hum. Genet.* **2017**, *62*, 447–451. [CrossRef] [PubMed]
32. LaCroix, A.J.; Stabley, D.; Sahraoui, R.; Adam, M.P.; Mehaffey, M.; Kernan, K.; Myers, C.T.; Fagerstrom, C.; Anadiotis, G.; Akkari, Y.M.; et al. GGC Repeat Expansion and Exon 1 Methylation of *XYLT1* Is a Common Pathogenic Variant in Baratela-Scott Syndrome. *Am. J. Hum. Genet.* **2019**, *104*, 35–44. [CrossRef]
33. Taieb, M.; Ghannoum, D.; Barré, L.; Ouzzine, M. Xylosyltransferase I mediates the synthesis of proteoglycans with long glycosaminoglycan chains and controls chondrocyte hypertrophy and collagen fibers organization of in the growth plate. *Cell Death. Dis.* **2023**, *14*, 355. [CrossRef]
34. Munns, C.F.; Fahiminiya, S.; Poudel, N.; Munteanu, M.C.; Majewski, J.; Sillence, D.O.; Metcalf, J.P.; Biggin, A.; Glorieux, F.; Fassier, F.; et al. Homozygosity for frameshift mutations in *XYLT2* result in a spondylo-ocular syndrome with bone fragility, cataracts, and hearing defects. *Am. J. Hum. Genet.* **2015**, *96*, 971–978. [CrossRef]
35. Roch, C.; Kuhn, J.; Kleesiek, K.; Götting, C. Differences in gene expression of human xylosyltransferases and determination of acceptor specificities for various proteoglycans. *Biochem. Biophys. Res. Commun.* **2010**, *391*, 685–691. [CrossRef] [PubMed]
36. Huang, Y.F.; Mizumoto, S.; Fujita, M. Novel Insight Into Glycosaminoglycan Biosynthesis Based on Gene Expression Profiles. *Front. Cell. Dev. Biol.* **2021**, *9*, 709018. [CrossRef]
37. Condac, E.; Silasi-Mansat, R.; Kosanke, S.; Schoeb, T.; Towner, R.; Lupu, F.; Cummings, R.D.; Hinsdale, M.E. Polycystic disease caused by deficiency in xylosyltransferase 2, an initiating enzyme of glycosaminoglycan biosynthesis. *Proc. Natl. Acad. Sci. USA* **2007**, *104*, 9416–9421. [CrossRef]
38. Mis, E.K.; Liem, K.F.; Kong, Y.; Schwartz, N.B.; Domowicz, M.; Weatherbee, S.D. Forward genetics defines *XYLT1* as a key, conserved regulator of early chondrocyte maturation and skeletal length. *Dev. Biol.* **2014**, *385*, 67–82. [CrossRef] [PubMed]
39. Taylan, F.; Mäkitie, O. Abnormal Proteoglycan Synthesis Due to Gene Defects Causes Skeletal Diseases with Overlapping Phenotypes. *Horm. Metab. Res.* **2016**, *48*, 745–754. [CrossRef]
40. Sivasami, P.; Poudel, N.; Munteanu, M.C.; Hudson, J.; Lovern, P.; Liu, L.; Griffin, T.; Hinsdale, M.E. Adipose tissue loss and lipodystrophy in xylosyltransferase II deficient mice. *Int. J. Obes.* **2019**, *43*, 1783–1794. [CrossRef] [PubMed]
41. Kleine, A.; Kühle, M.; Ly, T.D.; Schmidt, V.; Faust-Hinse, I.; Knabbe, C.; Fischer, B. Xylosyltransferase-Deficiency in Human Dermal Fibroblasts Induces Compensatory Myofibroblast Differentiation and Long-Term ECM Reduction. *Biomedicines* **2024**, *12*, 572. [CrossRef] [PubMed]
42. Egli, M.; Manoharan, M. Chemistry, structure and function of approved oligonucleotide therapeutics. *Nucleic. Acids. Res.* **2023**, *51*, 2529–2573. [CrossRef]
43. Sang, A.; Zhuo, S.; Bochanis, A.; Manautou, J.E.; Bahal, R.; Zhong, X.B.; Rasmussen, T.P. Mechanisms of Action of the US Food and Drug Administration-Approved Antisense Oligonucleotide Drugs. *BioDrugs* **2024**, *38*, 511–526. [CrossRef] [PubMed]
44. Aguti, S.; Cheng, S.; Ala, P.; Briggs, S.; Muntoni, F.; Zhou, H. Strategies to improve the design of gapmer antisense oligonucleotide on allele-specific silencing. *Mol. Ther. Nucleic. Acids.* **2024**, *35*, 102237. [CrossRef]
45. Chiriboga, C.A.; Swoboda, K.J.; Darras, B.T.; Iannaccone, S.T.; Montes, J.; De Vivo, D.C.; Norris, D.A.; Bennett, C.F.; Bishop, K.M. Results from a phase 1 study of nusinersen (ISIS-SMN(Rx)) in children with spinal muscular atrophy. *Neurology* **2016**, *86*, 890–897. [CrossRef]
46. Brunet de Courssou, J.B.; Durr, A.; Adams, D.; Corvol, J.C.; Mariani, L.L. Antisense therapies in neurological diseases. *Brain* **2022**, *145*, 816–831. [CrossRef]
47. McDowall, S.; Aung-Htut, M.; Wilton, S.; Li, D. Antisense oligonucleotides and their applications in rare neurological diseases. *Front. Neurosci.* **2024**, *18*, 1414658. [CrossRef] [PubMed]
48. Sumner, C.J.; Miller, T.M. The expanding application of antisense oligonucleotides to neurodegenerative diseases. *J. Clin. Investig.* **2024**, *134*, e186116. [CrossRef] [PubMed]

49. Forni, G.; Malvagia, S.; Funghini, S.; Scolamiero, E.; Mura, M.; Della Bona, M.; Villanelli, F.; Damiano, R.; la Marca, G. LC-MS/MS method for simultaneous quantification of heparan sulfate and dermatan sulfate in urine by butanolysis derivatization. *Clin. Chim. Acta* **2019**, *488*, 98–103. [CrossRef] [PubMed]
50. Carvalho, S.; Santos, J.I.; Moreira, L.; Gonçalves, M.; David, H.; Matos, L.; Encarnação, M.; Alves, S.; Coutinho, M.F. Neurological Disease Modeling Using Pluripotent and Multipotent Stem Cells: A Key Step towards Understanding and Treating Mucopolysaccharidoses. *Biomedicines* **2023**, *11*, 1234. [CrossRef] [PubMed]

Disclaimer/Publisher's Note: The statements, opinions and data contained in all publications are solely those of the individual author(s) and contributor(s) and not of MDPI and/or the editor(s). MDPI and/or the editor(s) disclaim responsibility for any injury to people or property resulting from any ideas, methods, instructions or products referred to in the content.

In vivo proof of principle on the therapeutic potential of an engineered U1 small nuclear RNA to rescue the most common Mucopolysaccharidosis type IIIC splice variant, c.234+1G>A

Juliana I. Santos[1,2,3,4]*, Mariana Gonçalves[1,2,3,5]*, Maria Francisca Coutinho[1,2,3], Luciana Vaz Moreira[1,2,3,], Maria João Prata[4,6], Maria João Pires[5], Paula Oliveira[5], Dario Balestra[7], Mirko Pinotti[7], Chris Van den Haute[8,9], Rik Gijsbers[10], Sandra Alves[1,2,3]*, Liliana Matos[1,2,3]*

[1] Research and Development Unit, Department of Human Genetics, National Institute of Health Doutor Ricardo Jorge, INSA I.P., Rua Alexandre Herculano, 321, 4000-055 Porto, Portugal;

[2] Center for the Study of Animal Science - Instituto de Ciências, Tecnologias e Agroambiente da Universidade do Porto, CECA-ICETA, University of Porto, Praça Gomes Teixeira, Apartado 55142, 4051-401 Porto, Portugal;

[3] Associate Laboratory for Animal and Veterinary Sciences, AL4AnimalS, Faculdade de Medicina Veterinária, Avenida da Universidade Técnica, 1300-477 Lisboa, Portugal;

[4] Biology Department, Faculty of Sciences, University of Porto, Rua do Campo Alegre, 4169-007 Porto, Portugal;

[5] Centre for the Research and Technology of Agro-Environmental and Biological Sciences, CITAB, Inov4Agro, University of Trás-os-Montes and Alto Douro, 5000-801 Vila Real, Portugal;

[6] Health Research and Innovation Institute, University of Porto, R. Alfredo Allen 208, 4200-135 Porto, Portugal

[7] Department of Life Sciences and Biotechnology and Laboratorio per le Tecnologie delle Terapie Avanzate (LTTA), University of Ferrara, Ferrara, Italy

[8] Leuven Viral Vector Core, KU Leuven, 3000 Leuven, Belgium.

[9] Laboratory for Neurobiology and Gene Therapy, Department of Neurosciences, Leuven Brain Institute, KU Leuven, 3000 Leuven, Belgium.

[10] Department of Pharmaceutical and Pharmacological Sciences, KU Leuven, 3000 Leuven, Belgium; Leuven Viral Vector Core, KU Leuven, 3000 Leuven, Belgium

**These authors contributed equally to this work*

Abstract

Inherited defects in the acetylation of heparan sulfates (HS), which is catalyzed by the lysosomal multipass transmembrane protein heparan-alpha-glucosaminide N-acetyltransferase (HGSNAT), cause Mucopolysaccharidosis III type C (MPS IIIC), an untreatable neuropathic lysosomal storage disease (LSD). Here we address the ability of an engineered small nuclear RNA U1 (U1 snRNA) totally complementary to the 5' splice site of the *HGSNAT* gene exon 2 harboring the common MPS IIIC-causing

pathogenic variant to rescue abnormal pre-mRNA splicing, correcting its molecular consequences. While we had already provided proof of principle on its potential *in vitro*, by demonstrating that this molecule was capable of a partial correction of the splicing pattern defect in fibroblasts derived from a patient harboring the target mutation, c.234+1G>A, no *in vivo* studies had been performed yet. Here we assessed the rescue of that mutation, which causes a severe form of MPS IIIC, by that modified U1 snRNA (U1 snRNATC) in a murine model. Briefly, we generated mice expressing the human *HGSNAT* c.234+1G>A variant using adeno-associated viral (AAV) vector-mediated delivery and evaluated the ability of the modified U1 snRNATC to rescue the associated splicing defect. Mice were injected with AAV2/9 vectors carrying either the wild-type or mutant *HGSNAT* sequence, alone or in combination with the therapeutic U1 snRNATC, which was also delivered via AAV2/9.

Analysis of liver samples revealed that U1 snRNATC successfully restored normal splicing in four out of five treated animals, leading to correct exon 2 inclusion in the mature *HGSNAT* mRNA. Moreover, histological and morphometric assessments showed no significant toxicity associated with AAV-mediated delivery. Overall, our findings provide the first *in vivo* evidence supporting the use of modified U1 snRNAs as a potential therapeutic approach for MPS IIIC and highlight their broader applicability in correcting splicing defects.

Key Words

Mucopolysaccharidosis III type C (MPS IIIC); Lysosomal Storage Diseases (LSD); Mouse model; Splicing mutation; modified U1 snRNA; AAV-mediated delivery

Introduction

Mucopolysaccharidosis III type C (MPS IIIC; OMIM# 252930) is a lysosomal storage disorder (LSD) caused by deficiency of acetyl-CoA:α-glucosaminide N-acetyltransferase, an enzyme located in the lysosomal membrane (HGSNAT; EC:2.3.1.78) [1]. It is one of the four subtypes of Sanfilippo syndrome, or MPS III, an autosomal recessive form of childhood dementia caused by pathogenic variants in the genes encoding proteins involved in the intra-lysosomal degradation of heparan sulphate (HS) [2].

As a group, MPS III tends to present early in life, with symptoms beginning to appear around age 3-5 years. It is characterized by a progressive and relentless neurocognitive deterioration, which is first noticeable as a regression in development, with patients

losing milestones and previously acquired skills as the disease progresses. Ultimately, this process culminates in the loss of functional abilities, and premature death usually occurring in the second or third decade of life (reviewed in [3,4]). Amongst the most noticeable and challenging MPS III symptoms are neurobehavioral manifestations, such as hyperactivity, agitation, destructiveness, distress/screaming and social disengagement (reviewed in [3]). MPS IIIC, in particular, presents a significant challenge to researchers worldwide, as it eludes the major therapeutic possibilities since its associated enzyme is incapable of free diffusion or cross-correction due to its transmembrane nature. That feature poses additional challenges to the development of therapies based on enzyme replacement and gene correction, two of the major therapeutic approaches under development for other MPS III diseases. That is why alternative strategies must be explored to address this disorder. RNA-based therapeutics represent a rational and effective alternative to the conventional approaches, for their specificity, fast development and production, and good prospects for clinical translation. Amongst the various RNA-based therapeutic molecules, modified U1 small nuclear RNAs (U1 snRNAs) are emerging as a promising strategy to rescue 5' splicing defects (reviewed in [5]).

Although MPS IIIC is not exclusively caused by mutations that affect splicing, there is a significant number of disease-causing variants that directly affect this process. According to recent data from the Human Gene Mutation Database (HGMD) (https://my.qiagendigitalinsights.com/, HGMD Professional 2024.4, accessed on 28 January 2025), approximately 20% of the pathogenic variants reported for *HGSNAT*, the gene encoding the enzyme whose deficiency underlies MPS IIIC, are classified as splicing substitutions. However, more important than the relative percentage of or even the total number of splicing variants, is their prevalence among MPS IIIC families.

One particular mutation affecting the constitutive exon 2 splice donor site of the *HGSNAT* gene, c.234+1G>A, has been documented in various populations, particularly around the Mediterranean basin. This mutation has been identified in patients and families from Spain, Morocco [6,7], Italy [8], Turkey, France [9,10], Portugal [11] and Tunisia [12]. Even though no extensive study has been performed in these patients, the ones that were subjected to polymorphism and haplotype analyses were found to share a common haplotype. This finding supports the hypothesis of a single origin for this mutation, at least among Spanish and Moroccan patients [7]. Adding up to this preliminary assessment is the geographical distribution of the mutation, which also seems compatible with a common origin. Indeed, to the best of our knowledge there is only one patient out of the Mediterranean basin, known to harbor this pathogenic variant: the first Korean case of MPS IIIC [13]. Regardless of its origin and distribution, truth is this variant

is relatively common amongst affected families and individuals. Any therapeutic approach targeting this variant would hold potential benefits for a significant number of MPS IIIC patients. That is why it emerged as an attractive target for our research. Synthetic U1 snRNAs were first demonstrated to have therapeutic potential, particularly when modified to enhance recognition of specific mutations, especially those affecting the 5′ splice-site (5′ss) [14]. Since then, numerous studies using cellular and animal models have expanded the evidence supporting the ability of modified U1 snRNAs to mediate gene therapy-based correction of splicing defects underlying various genetic diseases (reviewed in [5]).

As every other RNA-based drug, modified U1 snRNAs work by sequence complementarity, exploiting their base-pairing ability to target specific splicing regulatory sequences in the RNAs of interest. For this, the 5′ end of U1 snRNA must be modified to complement the mutated target sequence. Usually, these modifications are made by site-directed mutagenesis on a plasmid that contains the U1 snRNA sequence, a promoter, and a termination sequence (reviewed in [5]).

Ultimately, the principle underlying the use of modified U1 snRNAs for therapeutic purposes is quite straightforward: it leverages the crucial role that U1 snRNA plays in promoting donor splice site recognition and mediating the first step in the spliceosome assembly, along with the technical ability to artificially modify its sequence. This allows to target specific splicing regulatory sequences in the RNAs of interest, promoting their recognition.

By anchoring a modified U1 snRNA to a mutant sequence that would otherwise evade recognition by the endogenous U1 snRNA, one may hope to rescue several splicing mutations. Among the most successful attempts to promote splice donor site recognition by modified U1 snRNAs, thereby recovering normal splicing patterns, are studies in Neurofibromatosis type 1 [15], severe coagulation factor VII (FVII) deficiency [16], Retinitis pigmentosa [17,18] and Bardet–Biedl syndrome [19]. For LSDs, however, particularly for MPS diseases, there are not many studies addressing the therapeutic potential of these molecules [11,20]. Inspired by some of the previously referred positive results in non-LSD diseases, our team sought to develop modified U1 snRNAs to correct the effects of three independent *HGSNAT* mutations in the donor splice site, including the c.234+1G>A. Although not all the tested modified U1 snRNAs molecules were able to rescue the normal splicing process in fibroblast samples from patients harboring the target mutations, one particular engineered U1 snRNA vector was able to partially restore the normal splicing pattern in patient-derived fibroblasts homozygous for the c.234+1G>A mutation. This vector promoted correct recognition of exon 2 and its subsequent inclusion in the mature *HGSNAT* mRNA [11].

In this study, we challenged that modified U1 snRNA-mediated strategy in wild-type (wt) mice expressing the human *HGSNAT* c.234+1G>A pathogenic variant through recombinant adeno-associated viral (AAV) vector administration. We observed that co-injecting the *HGSNAT* mutant together with the previously referred modified U1 snRNA (designated U1 snRNATC) resulted in the appearance of the normally spliced transcript.

Materials and Methods

Construction and in vivo evaluation of HGSNAT Midigenes

To achieve sustained expression and evaluate the in vivo therapeutic potential of our engineered/modified U1 snRNA approach, different AAV vectors were constructed by the Leuven Viral Vector Core facility (collaboration with Prof. Rik Gijsbers, University of Leuven, Belgium). Firstly, to evaluate which is the best serotype to be used in our AAV constructs, a specific quantity (9.07 x 10^9 vg/animal) of four AAV serotypes (AAV2/5, AAV2/7, AAV2/8, and AAV2/9) was tested in wild-type FVB/N mice (n=3) via intravenous (IV) injection. Then, the AAV expression levels in mice liver samples was assessed by qRT-PCR (CFX96 Touch Deep Well Real-Time PCR Detection System, Bio-Rad Laboratories, California, USA), targeting the WPRE sequence within the AAV vectors. Based on this preliminary assessment, no AAV serotype was excluded, and AAV2/9 was selected given that it is the most suitable option for future applications in neurodegenerative disorders such as MPS IIIC. Consequently, the gene cassettes of the HGSNATwt, HGSNAT+1A and the engineered U1 snRNATC were packaged into AAV2/9 vectors. The cassette of AAV2/9_HGSNATwt contains the full HGSNAT coding sequence (exons 1–18) along with partial intronic regions (437 bp of intron 1 and 435 bp of intron 2), the AAV2/9_HGSNAT+1 has the same full HGSNAT sequence but with the c.234+1G>A variant and the engineered U1 snRNATC contains the U1 snRNA sequence modified to be totally complementary to the mutant 5'ss of exon 2.

Finally, to optimize the experimental design, a pilot study was developed to compare intraperitoneal (IP) and IV delivery efficacies. IP administration was selected for the final assay based on target gene expression analysis.

Animal procedures

All procedures were approved by the *Trás-os-Montes e Alto Douro University* (UTAD) and *Direção-Geral de Alimentação e Veterinária* (DGAV) (approval number 021988) according to the national legislation (Decreto-Lei 113, 7 de agosto) and European legislation (Diretiva 2010/63/EU). Six-week old female FVB/N mice were randomly divided in 3 groups of 5 mice each and IP-injected with different combinations and

quantities of the AAVs: AAV2/9_HGSNATwt, AAV2/9_HGSNAT+1A and AAV2/9_U1snRNATC, as listed in Table 1, with a final volume of 400 µl.

Table 1. Data of injections of each construct in mice and combinations between them. vg means *vector genome*.

Group	AAV	Quantity
A	AAV2/9_HGSNATwt	2.83×10^{10} vg
B	AAV2/9_HGSNAT+1A	2.83×10^{10} vg
C	AAV2/9_HGSNAT+1A **+** AAV2/9_ U1snRNATC	2.83×10^{10} vg **+** 1.13×10^{11} vg

After two weeks of IP injection, all animals were sacrificed by an IP overdose administration of ketamine (Eutasil 200 mg/mL, Ceva, Algés, Portugal) and xylazine (Rompun® 20 mg/mL, Bayer Healthcare S.A., Kiel, Germany), followed by exsanguination by cardiac puncture, as recommended by FELASA (Federation for Laboratory Animal Science Associations). Then, a complete necropsy of each animal was performed and all organs were collected (heart, lung, spleen, liver, kidneys and brain).

Evaluation of the AAV2/9_HGSNATwt, AAV2/9_HGSNAT+1A and AAV2/9_U1snRNATC expression in mice and of the splicing pattern rescue

For *HGSNAT* transcript analysis, total RNA was isolated from random sections of mouse liver tissue with the GRS Total RNA Kit – Tissue (GRiSP research solutions, Porto, Portugal), and reverse-transcribed with the Ready-To-Go™ You-Prime First-Strand Beads kit (Cytiva, Marlborough, Massachusetts, USA). Both protocols were performed in accordance with the manufacturers' instructions. As a rule, 5 µg of total RNA were used per sample for cDNA synthesis. Then, the RT-PCR analysis was conducted using the *HGSNAT* gene primers listed in Table 2, specifically designed to account for sequence mismatches between the mouse and human genomes. Each primer contained one to three mismatches at the 3' end to ensure specificity to the human sequence. Additionally, one forward primer was designed to anneal to the human cytomegalovirus (CMV) promoter region, located upstream of the *HGSNAT* gene cassette in the construct (Table 2). Two distinct primer sets were used for amplifications: (a) Ex1 Fw/Ex3 Rv1, designed to amplify an *HGSNAT* fragment spanning exons 1–3 was applied to samples from animals injected with AAV2/9_HGSNATwt (group A) and those receiving

AAV2/9_HGSNAT+1A alongside AAV2/9_U1snRNATC (group C); and (b) pCMV5.1 Fw/Ex3 Rv2, an additional pair of primers that also allows for the detection of exon 2 skipping was used in animals injected with AAV2/9_HGSNAT+1A (group B).

Table 2. Primers sequences used for human cDNA amplification of AAV2/9_HGSNAT constructs expressed in mice.

Primer	Oligonucleotide sequence (5' → 3')	Annealing site
pCMV5.1 Fw	GGGACTTTCCAAAATGTCGTA	CMV promoter
Ex1 Fw	TCTTCGGGGCGCGATGCCCA	*HGSNAT* gene (exon 1)
Ex3 Rv1	CCTGCTTTTGGACTCTGAGG	*HGSNAT* gene (exon 3)
Ex3 Rv2	TTCTTTCTCTTCCAAGGTGTC	*HGSNAT* gene (exon 3)

Histological analysis

The organs collected in the necropsy were immersed in 10% neutral buffered formaldehyde (ITW Reagents, Germany) for at least 24 hours. Sections of paraffin-embedded samples were stained with hematoxylin and eosin (H&E) and observed by light microscopy.

Immunohistochemical studies were performed to search for possible histological alterations in mice liver due to the AAVs expression.

Statistical analysis

The mean and standard error of body mass for each animal, as well as the relative mass of each organ, were calculated. Additionally, the median daily water and food consumption per animal were assessed. Subsequently, statistical analysis was performed using the GraphPad Prism® program to Windows (version 6.0). Statistical significance between groups was determined by analysis of variance (ANOVA), followed by the Tukey's multiple comparisons test. The significance level used was $p<0.05$.

Results

Splicing Patterns of AAV2/9_HGSNATwt and AAV2/9_HGSNAT+1A vectors in the liver of FVB/N Mice

A dose of 2.83 × 10^{10} vg of AAV2/9_HGSNATwt and AAV2/9_HGSNAT+1A vectors was administered to mice in group A and group B, respectively. Two weeks post-injection, the RNA was extracted from mice liver samples, and the RT-PCR analysis confirmed the expected expression of human *HGSNAT* (h*HGSNAT*) by detecting the anticipated splicing patterns. In AAV2/9_HGSNATwt-injected mice (group A), a transcript containing all exons was observed, while in AAV2/9_HGSNAT+1A-injected animals (group B), exon 2 skipping was detected. Due to the use of different primer sets for each group, the expected PCR product sizes vary and are approximately 200 bp for AAV2/9_HGSNATwt-injected mice and around 400 bp for AAV2/9_HGSNAT+1A-injected mice. The transcripts pattern was confirmed by agarose gel electrophoresis, as shown in Figure 1. All fragments were then subjected to Sanger sequencing, which confirmed the expected sequences in each case.

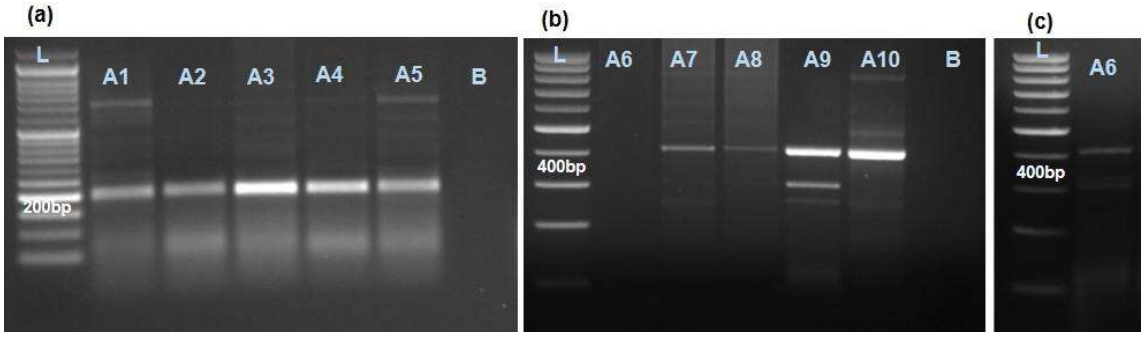


Figure 1. Agarose gel electrophoresis of h*HGSNAT* amplification following the injection of a) AAV2/9_HGSNATwt and b) AAV2/9_HGSNAT+1A into FVB/N mice; c) result from animal number 6 after a second amplification. The animals numbered between 1 and 5 are from group A (injected with AAV2/9_HGSNATwt) and the animals numbered between 6 and 10 are from group B (injected with AAV2/9_HGSNAT+1A). A: animal; L: ladder; B: blank (negative control).

Evaluation of the engineered U1 snRNA-mediated rescue of h*HGSNAT* mRNA splicing in mice

The analysis of the h*HGSNAT* splicing pattern in samples from group C, comprising animals injected with the disease-causing variant alongside the modified U1 snRNA vector (AAV2/9_HGSNAT+1A plus AAV2/9_U1snRNATC) to assess splicing defect correction, revealed a clear U1 snRNATC-mediated rescue of the splicing impairment caused by the c.234+1G>A variant. In four out of five injected animals, exon 2 inclusion

was successfully restored, as evidenced by the presence of a 200 bp band, later confirmed to contain the expected human *HGSNAT* sequence. Only in one animal (number 11), no amplification product of the expected size was detected (Figure 2).

To improve the quality of Sanger sequencing results, bands corresponding to the expected fragment size were extracted from the gel (Figure 2a) and re-amplified by PCR before sequencing (Figure 2b). The sequencing results clearly demonstrate exon 2 rescue, without retention of the first four nucleotides of intron 2 - an even more favorable outcome than previously observed in patient-derived fibroblasts in our earlier study (Figure 2c).

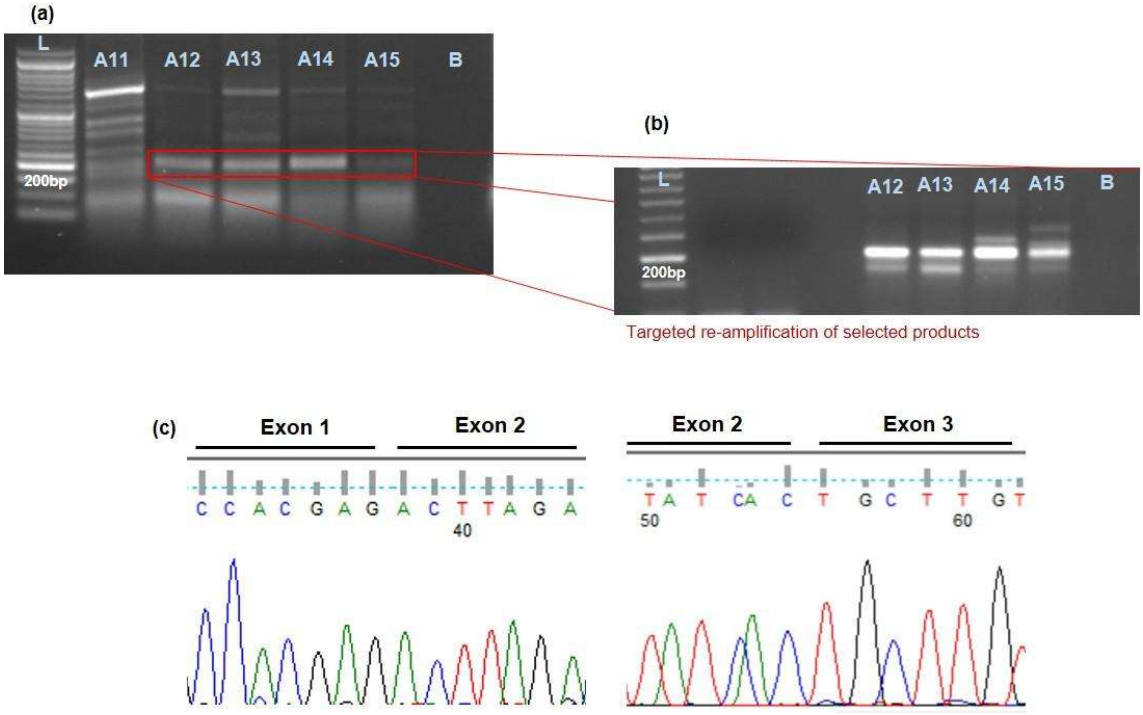


Figure 2. (a) Agarose gel electrophoresis of h*HGSNAT* amplification following the injection of AAV2/9_HGSNAT+1A plus AAV2/9_U1snRNATC into FVB/N mice (group C). (b) Agarose gel electrophoresis of h*HGSNAT* following PCR re-amplification of the purified fragments from animals numbers 12 to 15. (c) Electropherogram of segments of the h*HGSNAT* transcript sequence obtained after injection of the AAV2/9_HGSNAT+1A plus AAV2/9_U1snRNATC (group C) in FVB/N mice. Exon boundaries are highlighted above the electropherogram peaks. The Sanger sequencing analysis confirmed the correct inclusion of exon 2. A: animal; L: ladder; B: blank (negative control).

Morphometric and Histological Assessment of FVB/N Mice

Morphometric parameters of FVB/N mice were carefully monitored throughout the experiment. Two weeks post-injection, animals were sacrificed, and necropsy revealed no macroscopic organ damage. No significant differences were observed regarding

mean body mass (g) of each animal group at the beginning and at the end of the experiment between any of the groups. The same was observed for the relative organ mass analysis for heart, lung, spleen, liver, kidneys and brain ($p > 0.05$) (See Supplementary Material, Figure S1 and S2). Immunohistochemical analysis indicated minimal or largely irrelevant toxicity associated with AAV vectors injection. The most notable alterations, yet mild, included hepatocyte degeneration (cytoplasmic rarefaction, ballooning cells, and swollen hepatocytes) alongside signs of regeneration (binucleation, mitoses, and enlarged nuclei). Inflammation and fibrosis, though discreet, were predominantly observed in periportal regions. Mallory and acidophil bodies, typically linked to inflammation and fibrosis, were present in most cases.

Discussion

In this study, we further validated the potential of an engineered U1 snRNA to rescue the splicing defect caused by the MPS IIIC-causing variant c.234+1G>A, whose prevalence has already been extensively discussed, correcting its molecular consequences at the *HGSNAT* pre-mRNA splicing level.

In a previous study validating this strategy *in vitro* [11], we designed and constructed four distinct modified U1 snRNAs with increasing complementarity to the mutated c.234+1G>A splice donor site. The first had a single nucleotide change at the U1 snRNA position matching the +1 position of the mutant 5'ss. The second and the third had two changes, at positions -1 +1, and -1 +4, respectively. The fourth included three independent nucleotide changes at positions -1, +1 and +4, making it totally complementary to the mutant 5' ss sequence (Figure 3). The therapeutic potential of each of these molecules was first assessed in an artificial system, using COS-7 cells expressing recombinant human *HGSNAT* sequences, either wt or with the c.234+1G>A variant. Firstly, cells were transfected with wt and mutant minigene constructs and the subsequent cDNA analysis showed that the minigene-derived splicing patterns closely resembled those observed in control and patients' cDNAs obtained from fibroblasts. Then, in other experiments, the mutant minigene was co-transfected with each of the four modified U1snRNAs, but no correction of the splicing pattern was observed. Three of them did produce a band of apparently normal size, but sequencing analysis revealed that while exon 2 was included as intended, the first four bases of intron 2 (ATAT) were also retained due to the activation of an alternative donor splice site, resulting in an aberrant transcript [11].

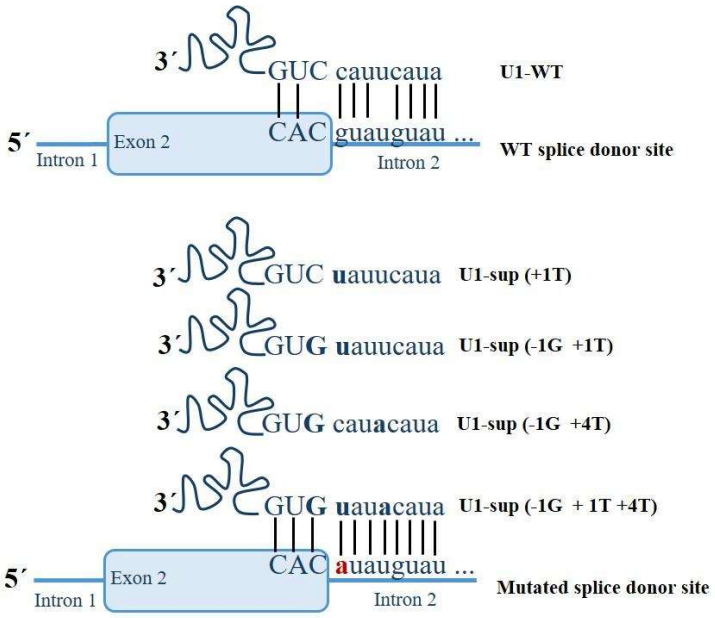


Figure 3. Summary of the different U1 snRNA adaptations attempted by Matos and co-workers to correct the pathogenic effect of the c.234+1G>A donor splice site (ss) mutation on the *HGSNAT* gene. A schematic illustration of base pairing between the U1 wild-type (U1WT) and the wild-type 5'ss of the *HGSNAT* gene exon 2 is presented. The position of the c.234+1G>A variant in the mutant 5'ss is marked in red. The different engineered U1 snRNAs designed to target it (designated as U1-sup, for suppressor) are also shown. The U1 sequence changes are illustrated in bold (adapted from [11]).

While the transient transfection of minigene constructs into model cell lines (e.g. HeLa, Hep3B, COS-1, COS-7, or HEK293) is a well-established and widely used assay for analyzing loss- and gain-of-function effects on *cis*-elements and *trans*-acting factors involved in splicing regulation, it remains an artificial system with inherent limitations. Furthermore, despite being one of the first approaches used to evaluate a molecule's potential to modulate abnormal splicing, its results may not fully reflect the complexity of splicing regulation in physiological conditions. For example, it is now well-known that different cell lines can exhibit different ratios of alternative splicing patterns for reasons that are unrelated to the natural regulation that occurs in the tissue of interest. In an extensive review on use of minigene systems to dissect alternative splicing elements, published nearly 20 years ago, Cooper comments on his lab's own experience, clearly stating that expression of the same minigene in several different and commonly used cell lines, resulted in a variety of splicing efficiencies [23], an observation that is actually mimicked by our own. Indeed, when the same modified U1 snRNAs were tested in fibroblasts from two different MPS IIIC patients homozygous for the c.234+1G>A variant, treatment with varying amounts of the fully adapted U1 snRNA [originally referred to as U1-sup4 (−1G + 1T + 4A)] resulted in a partial recovery of the splicing defect, yielding

two distinct sequences: one with normal splicing and the other incorporating the first four bases of intron 2 [11].

Encouraged by these positive results, in this work we challenged that modified U1 snRNA *in vivo*, to check whether it was able to produce similar outcomes. Briefly, we adapted our strategy from an engineered U1 snRNA approach for Hemophilia B developed by Balestra *et al.*, [24] who used AAVs to express in wild-type mouse liver a modified U1 snRNA enabling both splicing rescue and toxicity assessments *in vivo*. Following their methodology, we applied a similar approach to the c.234+1G>A *HGSNAT* variant using an AAV2/9 vector as the backbone for constructing three different vectors: AAV2/9_HGSNATwt, AAV2/9_HGSNAT+1A and AAV2/9_U1snRNATC. These vectors were delivered via IP injection to drive the expression of the human *HGSNAT* sequences of interest and of the modified U1 snRNA in wild-type mice. This approach seemed more feasible compared to the ideal scenario, which would probably be the generation of a genetically modified humanized mouse model. However, such a model would be too expensive and laborious to validate a strategy that had so many confounding elements *in vitro*, with different platforms delivering different results on its potential, and whose ultimate target patient population, while representative within the MPS IIIC cohort, is relatively small. Actually, even when funds are available and pre-clinical assessments *in vitro* are compiling, there are several considerations to weigh before generating a genetically modified mouse model to assess the therapeutic effect of RNA-based molecules. Those issues have been reviewed elsewhere [25], but we can still point out a few key points. First, it is essential to compare the gene sequence and structure between human and mouse to ensure it is similar and no relevant exons for the study or protein function are missing. Next, it is necessary to verify that the gene of interest is expressed in the proper murine issue (or, at the very least, in the tissue under study). Additionally, assessing the feasibility of humanization by either homologous recombination in embryonic stem cells or genome editing techniques is a step that ought to be discussed with experts on those techniques at specialized institutes or companies. Finally yet importantly, it is necessary to validate the approach *in vitro* in mouse cells, i.e., to check whether the splicing machinery in mouse will allow proper splicing of the humanized transcript or gene, and recapitulate the human splicing defect that the study aims to correct within the mouse molecular background [25]. Adding up to these issues there are also ethical constraints [26], with researchers being actively encouraged to carefully select the variants they chose to generate humanized models, e.g. prioritizing them according with their prevalence [27]. Overall, the approach we used here is an elegant alternative to such a demanding protocol.

Our *in vivo* studies using this experimental setup provided evidence for the efficacy of the U1sn RNATC in rescuing the splicing defect caused by the c.234+1G>A splicing substitution. Briefly, the treatment with the vector fully complementary to the mutated 5'ss, the AAV2/9_U1snRNATC, resulted in the full inclusion of exon 2 in four of the five animals injected also with the AAV2/9_HGSNAT+1A. Overall, this observation marks a significant milestone not only in the development of RNA-based therapies for MPS IIIC but also in the design and evaluation of U1 snRNA-based therapeutics in general, as it represents the first successful correction of a +1 mutation, in an *in vivo* model. Also noteworthy is the absence of significant toxicity associated with AAV2/9-mediated delivery, which further supports the translational potential of this approach to the clinics. Apart from the obvious trigger for subsequent studies and additional pre-clinical assessments aimed at their ultimate clinical translation, this study also provides a significant insight on the irreplaceable role *in vivo* studies play in the U1 snRNA drug development pipeline, highlighting their importance in truly understanding the therapeutic potential of a given molecule.

At this stage, however, further studies are needed to fully assess the therapeutic potential of this molecule, specifically by determining whether U1 snRNATC-mediated correction of *HGSNAT* pre-mRNA processing translates into increased HGSNAT activity and reduced HS levels in treated samples or animals. Additionally, further evaluation of toxicity and potential side effects of this modified U1 snRNA *in vivo* is essential.

Conclusion

There is an urgent unmet medical need for patients with MPS IIIC, whose current treatment is merely symptomatic and supportive, aimed at managing and alleviating individual symptoms instead of addressing the disease at its root cause. In this study, we successfully developed a murine model expressing the human *HGSNAT* c.234+1G>A variant through AAV vector-mediated delivery and evaluated the ability of a modified U1snRNA (U1snRNATC) to rescue the splicing defect associated with this severe mutation. Our results demonstrated that the U1snRNATC effectively restored normal splicing in four out of five treated animals, leading to the correct inclusion of exon 2 in the mature *HGSNAT* mRNA.

While the identification of an optimal model to assess the sequence-dependent efficacy and safety of modified U1 snRNAs, as of other RNA-based drugs remains a challenge, our approach provides a valuable proof of concept for their potential *in vivo* application.

By leveraging a modified U1 snRNA strategy, we directly target the pre-mRNA process, triggering the production of a correctly spliced transcript, which could restore *HGSNAT* expression. This type of intervention at the pre-mRNA level enables gene expression restoration at physiological levels while bypassing the hurdles of delivering a larger gene as required for a gene therapy approach, even though relying on the same type of vectors. Furthermore, it is well-established that, for most LSDs, even a modest increase in functional protein levels can lead to a significant improvement in the disease phenotype. Therefore, even if low amounts of HGSNAT protein are produced, they could still have a therapeutic effect.

Although this modified U1snRNA molecule is specifically designed to correct a single pathogenic variant and does not offer a universal solution for treating MPS IIIC, given its highly heterogeneous mutational landscape, it holds significant promise as a personalized therapeutic approach from a cost-effectiveness perspective. By targeting a disease-causing variant that is relatively common within the MPS IIIC population, it ensures a broader patient pool, which may also facilitate subsequent investments in drug development and recruitment for clinical studies.

Supplementary Material

a)

Group	Initial body mass	Final body mass
A	21.13 ± 1.14	22.25 ± 0.89
B	21.12 ± 1.80	22.73 ± 2.38
C	21.23 ± 1.59	23.32 ± 1.90

b)

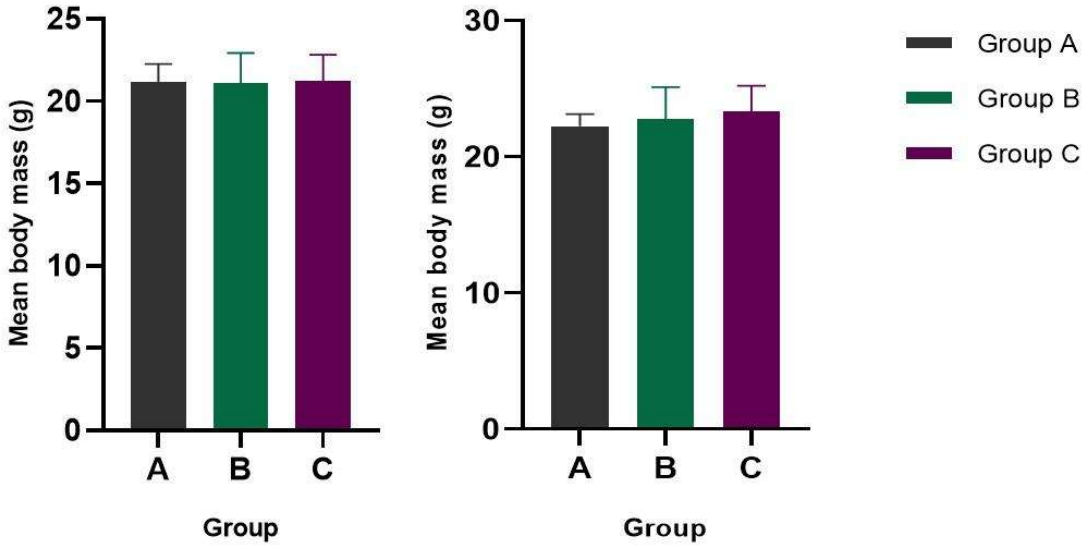


Figure S1. Mean body mass (g) of each animal group at the beginning and at the end of the experiment. a) Table with mean ± standard error of mean body mass of animals from groups A, B and C; b) Statistically treated data of initial body mass (left) and of final body mass (right) of animals' groups. Comparisons between groups were analyzed using a one-way ANOVA and a Tukey's multiple comparisons test as a posthoc comparator.

a)

	Group A	Group B	Group C
Heart	0.005 ± 0.001	0.005 ± 0.001	0.005 ± 0.000
Lung	0.007 ± 0.000	0.007 ± 0.001	0.007 ± 0.001
Spleen	0.059 ± 0.003	0.058 ± 0.004	0.058 ± 0.007
Liver	0.007 ± 0.000	0.007 ± 0.001	0.007 ± 0.001
Right kidney	0.007 ± 0.000	0.007 ± 0.001	0.007 ± 0.001
Left kidney	0.006 ± 0.000	0.005 ± 0.000	0.005 ± 0.001
Brain	0.016 ± 0.002	0.016 ± 0.003	0.014 ± 0.001

b)

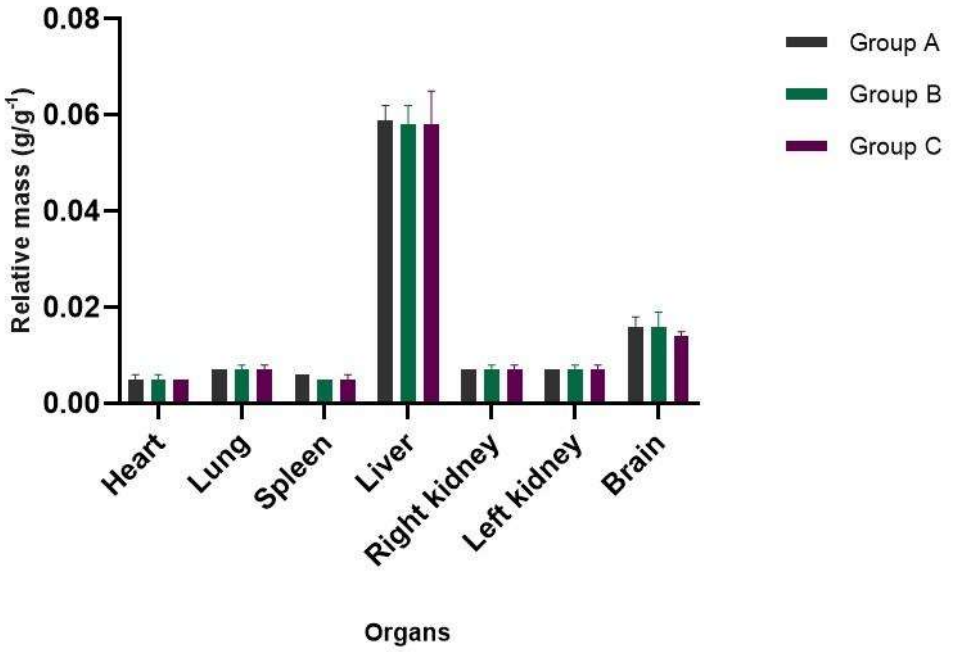


Figure S2. Relative mass (g/g^{-1}) of organs from the animals of different groups. a) Table with mean ± standard error of mass of animal organs from groups A, B and C; b) Statistically treated data of relative organs mass of animals' groups. Comparisons between groups were analyzed using a Two-way ANOVA and a Tukey's multiple comparisons test as a posthoc comparator.

References

1. Klein, U.; Kresse, H.; von Figura, K. Sanfilippo syndrome type C: deficiency of acetyl-CoA:alpha-glucosaminide N-acetyltransferase in skin fibroblasts. *Proc Natl Acad Sci U S A* **1978**, *75*, 5185-5189, doi:10.1073/pnas.75.10.5185.
2. Matalon, D.; Matalon Rd, K.M.; Matalon, R. *Chapter 35 - The mucopolysaccharidoses*, Rosenberg's Molecular and Genetic Basis of Neurological and Psychiatric Disease (Sixth Edition) ed.; Roger N. Rosenberg, Pascual, J.M., Eds.; 2020; Volume 1.
3. Heon-Roberts, R.; Nguyen, A.L.A.; Pshezhetsky, A.V. Molecular Bases of Neurodegeneration and Cognitive Decline, the Major Burden of Sanfilippo Disease. *J Clin Med* **2020**, *9*, doi:10.3390/jcm9020344.
4. Muschol, N.; Giugliani, R.; Jones, S.A.; Muenzer, J.; Smith, N.J.C.; Whitley, C.B.; Donnell, M.; Drake, E.; Elvidge, K.; Melton, L.; et al. Sanfilippo syndrome: consensus guidelines for clinical care. *Orphanet J Rare Dis* **2022**, *17*, 391, doi:10.1186/s13023-022-02484-6.
5. Gonçalves, M.; Santos, J.I.; Coutinho, M.F.; Matos, L.; Alves, S. Development of Engineered-U1snRNA Therapies: Current Status. *Int J Mol Sci* **2023**, *24*, doi:10.3390/ijms241914617.
6. Hrebícek, M.; Mrázová, L.; Seyrantepe, V.; Durand, S.; Roslin, N.M.; Nosková, L.; Hartmannová, H.; Ivánek, R.; Cízkova, A.; Poupetová, H.; et al. Mutations in TMEM76* cause mucopolysaccharidosis IIIC (Sanfilippo C syndrome). *Am J Hum Genet* **2006**, *79*, 807-819, doi:10.1086/508294.
7. Canals, I.; Elalaoui, S.C.; Pineda, M.; Delgadillo, V.; Szlago, M.; Jaouad, I.C.; Sefiani, A.; Chabás, A.; Coll, M.J.; Grinberg, D.; et al. Molecular analysis of Sanfilippo syndrome type C in Spain: seven novel HGSNAT mutations and characterization of the mutant alleles. *Clin Genet* **2011**, *80*, 367-374, doi:10.1111/j.1399-0004.2010.01525.x.
8. Fedele, A.O.; Filocamo, M.; Di Rocco, M.; Sersale, G.; Lübke, T.; di Natale, P.; Cosma, M.P.; Ballabio, A. Mutational analysis of the HGSNAT gene in Italian patients with mucopolysaccharidosis IIIC (Sanfilippo C syndrome). Mutation in brief #959. Online. *Hum Mutat* **2007**, *28*, 523, doi:10.1002/humu.9488.
9. Ruijter, G.J.; Valstar, M.J.; van de Kamp, J.M.; van der Helm, R.M.; Durand, S.; van Diggelen, O.P.; Wevers, R.A.; Poorthuis, B.J.; Pshezhetsky, A.V.; Wijburg, F.A. Clinical and genetic spectrum of Sanfilippo type C (MPS IIIC) disease in The Netherlands. *Mol Genet Metab* **2008**, *93*, 104-111, doi:10.1016/j.ymgme.2007.09.011.
10. Feldhammer, M.; Durand, S.; Mrázová, L.; Boucher, R.M.; Laframboise, R.; Steinfeld, R.; Wraith, J.E.; Michelakakis, H.; van Diggelen, O.P.; Hrebícek, M.; et al. Sanfilippo syndrome type C: mutation spectrum in the heparan sulfate acetyl-CoA: alpha-glucosaminide N-acetyltransferase (HGSNAT) gene. *Hum Mutat* **2009**, *30*, 918-925, doi:10.1002/humu.20986.
11. Matos, L.; Canals, I.; Dridi, L.; Choi, Y.; Prata, M.J.; Jordan, P.; Desviat, L.R.; Pérez, B.; Pshezhetsky, A.V.; Grinberg, D.; et al. Therapeutic strategies based on modified U1snRNAs and chaperones for Sanfilippo C splicing mutations. *Orphanet J Rare Dis* **2014**, *9*, 180, doi:10.1186/s13023-014-0180-y.
12. Ouesleti, S.; Coutinho, M.F.; Ribeiro, I.; Miled, A.; Mosbahi, D.S.; Alves, S. Update of the spectrum of mucopolysaccharidoses type III in Tunisia: identification of three novel mutations and in silico structural analysis of the missense mutations. *World J Pediatr* **2017**, *13*, 374-380, doi:10.1007/s12519-017-0005-x.
13. Huh, H.J.; Seo, J.Y.; Cho, S.Y.; Ki, C.S.; Lee, S.Y.; Kim, J.W.; Park, H.D.; Jin, D.K. The first Korean case of mucopolysaccharidosis IIIC (Sanfilippo syndrome type C) confirmed by biochemical and molecular investigation. *Ann Lab Med* **2013**, *33*, 75-79, doi:10.3343/alm.2013.33.1.75.
14. Zhuang, Y.; Weiner, A.M. A compensatory base change in U1snRNA suppresses a 5' splice site mutation. *Cell* **1986**, *46*, 827-835, doi:10.1016/0092-8674(86)90064-4.

15. Baralle, M.; Baralle, D.; De Conti, L.; Mattocks, C.; Whittaker, J.; Knezevich, A.; Ffrench-Constant, C.; Baralle, F.E. Identification of a mutation that perturbs NF1 agene splicing using genomic DNA samples and a minigene assay. *J Med Genet* **2003**, *40*, 220-222, doi:10.1136/jmg.40.3.220.
16. Pinotti, M.; Rizzotto, L.; Balestra, D.; Lewandowska, M.A.; Cavallari, N.; Marchetti, G.; Bernardi, F.; Pagani, F. U1-snRNA-mediated rescue of mRNA processing in severe factor VII deficiency. *Blood* **2008**, *111*, 2681-2684, doi:10.1182/blood-2007-10-117440.
17. Tanner, G.; Glaus, E.; Barthelmes, D.; Ader, M.; Fleischhauer, J.; Pagani, F.; Berger, W.; Neidhardt, J. Therapeutic strategy to rescue mutation-induced exon skipping in rhodopsin by adaptation of U1snRNA. *Hum Mutat* **2009**, *30*, 255-263, doi:10.1002/humu.20861.
18. Glaus, E.; Schmid, F.; Da Costa, R.; Berger, W.; Neidhardt, J. Gene therapeutic approach using mutation-adapted U1snRNA to correct a RPGR splice defect in patient-derived cells. *Mol Ther* **2011**, *19*, 936-941, doi:10.1038/mt.2011.7.
19. Schmid, F.; Glaus, E.; Barthelmes, D.; Fliegauf, M.; Gaspar, H.; Nürnberg, G.; Nürnberg, P.; Omran, H.; Berger, W.; Neidhardt, J. U1snRNA-mediated gene therapeutic correction of splice defects caused by an exceptionally mild BBS mutation. *Hum Mutat* **2011**, *32*, 815-824, doi:10.1002/humu.21509.
20. Ferri, L.; Covello, G.; Caciotti, A.; Guerrini, R.; Denti, M.A.; Morrone, A. Double-target Antisense U1snRNAs Correct Mis-splicing Due to c.639+861C>T and c.639+919G>A GLA Deep Intronic Mutations. *Mol Ther Nucleic Acids* **2016**, *5*, e380, doi:10.1038/mtna.2016.88.
21. Pagani, F.; Buratti, E.; Stuani, C.; Bendix, R.; Dörk, T.; Baralle, F.E. A new type of mutation causes a splicing defect in ATM. *Nat Genet* **2002**, *30*, 426-429, doi:10.1038/ng858.
22. Matos, L.; Santos, J.I.; Coutinho, M.F.; Alves, S. How to Design U1snRNA Molecules for Splicing Rescue. *Methods Mol Biol* **2022**, *2434*, 89-102, doi:10.1007/978-1-0716-2010-6_5.
23. Cooper, T.A. Use of minigene systems to dissect alternative splicing elements. *Methods* **2005**, *37*, 331-340, doi:10.1016/j.ymeth.2005.07.015.
24. Balestra, D.; Faella, A.; Margaritis, P.; Cavallari, N.; Pagani, F.; Bernardi, F.; Arruda, V.R.; Pinotti, M. An engineered U1 small nuclear RNA rescues splicing defective coagulation F7 gene expression in mice. *J Thromb Haemost* **2014**, *12*, 177-185, doi:10.1111/jth.12471.
25. Vázquez-Domínguez, I.; Garanto, A. Considerations for Generating Humanized Mouse Models to Test Efficacy of Antisense Oligonucleotides. *Methods Mol Biol* **2022**, *2434*, 267-279, doi:10.1007/978-1-0716-2010-6_18.
26. Arechavala-Gomeza, V.; Garanto, A. Antisense RNA Therapeutics: A Brief Overview. *Methods Mol Biol* **2022**, *2434*, 33-49, doi:10.1007/978-1-0716-2010-6_2.
27. Aartsma-Rus, A.; van Putten, M. The use of genetically humanized animal models for personalized medicine approaches. *Dis Model Mech* **2019**, *13*, doi:10.1242/dmm.041673.

International Journal of
Molecular Sciences

MDPI

Article

Modeling Lysosomal Storage Disorders in an Innovative Way: Establishment and Characterization of Stem Cell Lines from Human Exfoliated Deciduous Teeth of Mucopolysaccharidosis Type II Patients

Sofia Carvalho [1,2,3,4], Juliana Inês Santos [1,2,3,5], Luciana Moreira [1,2,3], Ana Joana Duarte [1,2,3,6], Paulo Gaspar [7], Hugo Rocha [7], Marisa Encarnação [1,2,3], Diogo Ribeiro [1,2,3], Matilde Barbosa Almeida [1,2,3,8], Mariana Gonçalves [1,2,3,9], Hugo David [1,2,3,5], Liliana Matos [1,2,3], Olga Amaral [1,2,3], Luísa Diogo [10], Sara Ferreira [10], Constança Santos [10], Esmeralda Martins [11], Maria João Prata [5,12], Luís Pereira de Almeida [4], Sandra Alves [1,2,3,*,†] and Maria Francisca Coutinho [1,2,3,*,†]

1 Research and Development Unit, Department of Human Genetics, National Institute of Health Doutor Ricardo Jorge, INSA I.P., Rua Alexandre Herculano, 321, 4000-055 Porto, Portugal; sofia.carvalho@insa.min-saude.pt (S.C.); juliana.santos@insa.min-saude.pt (J.I.S.); luciana.moreira@insa.min-saude.pt (L.M.); ana.duarte@insa.min-saude.pt (A.J.D.); marisa.encarnacao@insa.min-saude.pt (M.E.); diogo.ribeiro@insa.min-saude.pt (D.R.); matilde.almeida@insa.min-saude.pt (M.B.A.); mariana.goncalves@insa.min-saude.pt (M.G.); hugoddavid@hotmail.com (H.D.); liliana.matos@insa.min-saude.pt (L.M.); olga.amaral@insa.min-saude.pt (O.A.)
2 Center for the Study of Animal Science—Institute of Sciences, Technologies and Agro-Environment, CECA-ICETA, University of Porto, Praça Gomes Teixeira, Apartado 55142, 4051-401 Porto, Portugal
3 Associate Laboratory for Animal and Veterinary Sciences, AL4AnimalS, Faculty of Veterinary Medicine, University of Lisboa, Avenida da Universidade Técnica, 1300-477 Lisboa, Portugal
4 Faculty of Pharmacy, University of Coimbra, Polo das Ciências da Saúde, Azinhaga de Santa Comba, 3000-548 Coimbra, Portugal; luispa@ff.uc.pt
5 Biology Department, Faculty of Sciences, University of Porto, Rua do Campo Alegre, 4169-007 Porto, Portugal; mprata@ipatimup.pt
6 School of Medicine and Biomedical Sciences (ICBAS), Faculty of Porto, Rua de Jorge Viterbo Ferreira 228, 4050-313 Porto, Portugal
7 Newborn Screening, Metabolism and Genetics Unit, Department of Human Genetics, National Institute of Health Doutor Ricardo Jorge, INSA I.P., Rua Alexandre Herculano, 321, 4000-055 Porto, Portugal; paulo.gaspar@insa.min-saude.pt (P.G.); hugo.rocha@insa.min-saude.pt (H.R.)
8 Department of Medical Sciences, Campus Universitário de Santiago, Edifício da Saúde, Agra do Crasto, 3810-193 Aveiro, Portugal
9 Centre for the Research and Technology of Agro-Environmental and Biological Sciences, CITAB, Inov4Agro, University of Trás-os-Montes and Alto Douro, 5000-801 Vila Real, Portugal
10 Centro de Referência de Doenças Hereditárias do Metabolismo do Centro Hospitalar Universitário de Coimbra, CR-DHM (CHUC), Praceta Professor Mota Pinto, 3004-561 Coimbra, Portugal; ld@chuc.min-saude.pt (L.D.); saralopesferreira@chuc.min-saude.pt (S.F.); 12944@chuc.min-saude.pt (C.S.)
11 Centro Hospitalar Universitário do Porto, Hospital de Santo António, CHPorto, Largo do Prof. Abel Salazar, 4099-001 Porto, Portugal; esmeralda.martins@chporto.min-saude.pt
12 Health Research and Innovation Institute, University of Porto, i3S, Rua Alfredo Allen 208, 4200-135 Porto, Portugal
* Correspondence: sandra.alves@insa.min-saude.pt (S.A.); francisca.coutinho@insa.min-saude.pt (M.F.C.)
† These authors contributed equally to this work.

check for updates

Citation: Carvalho, S.; Santos, J.I.; Moreira, L.; Duarte, A.J.; Gaspar, P.; Rocha, H.; Encarnação, M.; Ribeiro, D.; Barbosa Almeida, M.; Gonçalves, M.; et al. Modeling Lysosomal Storage Disorders in an Innovative Way: Establishment and Characterization of Stem Cell Lines from Human Exfoliated Deciduous Teeth of Mucopolysaccharidosis Type II Patients. *Int. J. Mol. Sci.* **2024**, *25*, 3546. https://doi.org/10.3390/ijms25063546

Academic Editors: Tzong-Shyuan Lee and Tianhua Niu

Received: 29 December 2023
Revised: 18 March 2024
Accepted: 20 March 2024
Published: 21 March 2024

Copyright: © 2024 by the authors. Licensee MDPI, Basel, Switzerland. This article is an open access article distributed under the terms and conditions of the Creative Commons Attribution (CC BY) license (https://creativecommons.org/licenses/by/4.0/).

Abstract: Among the many lysosomal storage disorders (LSDs) that would benefit from the establishment of novel cell models, either patient-derived or genetically engineered, is mucopolysaccharidosis type II (MPS II). Here, we present our results on the establishment and characterization of two MPS II patient-derived stem cell line(s) from deciduous baby teeth. To the best of our knowledge, this is the first time a stem cell population has been isolated from LSD patient samples obtained from the dental pulp. Taking into account our results on the molecular and biochemical characterization of those cells and the fact that they exhibit visible and measurable disease phenotypes, we consider these cells may qualify as a valuable disease model, which may be useful for both pathophysiological

assessments and in vitro screenings. Ultimately, we believe that patient-derived dental pulp stem cells (DPSCs), particularly those isolated from human exfoliated deciduous teeth (SHEDs), may represent a feasible alternative to induced pluripotent stem cells (iPSCs) in many labs with standard cell culture conditions and limited (human and economic) resources.

Keywords: mucopolysaccharidosis type II; disease modeling; in vitro models; induced pluripotent stem cells (iPSCs); dental pulp stem cells (DPSCs); stem cells from human exfoliated deciduous teeth (SHEDs)

1. Introduction

Mucopolysaccharidosis type II (MPS II; #MIM 309900; #ORPHA 580), also known as Hunter syndrome, is a rare genetic disorder that is inherited as an X-linked trait, with an incidence ranging from 0.38 to 1.09 per 100,000 live male births (reviewed in [1]). This disorder belongs to the group of lysosomal storage disorders (LSDs) and is caused by a deficiency in the lysosomal enzyme iduronate 2-sulfatase (IDS; EC 3.1.6.13), which catalyzes the hydrolysis of 2-sulfate groups of dermatan sulfate (DS) and heparan sulfate (HS). Therefore, its deficit causes the pathological accumulation of these two glycosaminoglycans (GAGs), which translates into a multisystemic disease also affecting the brain in at least two thirds of cases (reviewed in [2]).

As many other LSDs, this disorder was first described more than 100 years ago, in 1917, by the Canadian physician Charles Hunter, from whom it got its most colloquial designation [3]. Since then, numerous advances have been made regarding our understanding of this rare disease. It was shown to be a progressive and multi-systemic pathology, and its major causes were disclosed, both at biochemical [4] and molecular levels [5,6], with the disease mapping to the *IDS* gene (HGNC ID: 5389) on chromosome X, which encodes for the lysosomal enzyme previously mentioned. At a genetic level, for example, we now know that Hunter syndrome is characterized by a significant heterogeneity, as no highly recurring mutations have been reported so far, even though some variants seem to be slightly more frequent (reviewed in [7]). Also at the clinical level, much has been discovered since the disorder was first reported. Indeed, what was once thought to be a single disease with two quite divergent clinical presentations, either severe or attenuated (depending on the length of survival and presence/absence of neurological disease), is now known to be a continuum between the two forms, with disease severity linked to relative levels of IDS enzyme (reviewed in [8]). In general, MPS II clinical signs and symptoms include coarse facial features, skeletal deformities and joint stiffness, growth retardation, organomegaly, and significant respiratory and cardiac impairments [9]. Neurological involvement has also been reported in at least two thirds of cases [10–12]. Patients also present ENT (ear, nose, and throat) manifestations, sleep disturbances and obstructive apnea [13]. Visual symptoms may also be prominent [14]. According to the natural history of the disease, death occurs typically before adulthood for the most severe forms, while patients suffering from milder forms may usually survive until later in adult life [12] (reviewed in [2]). Also at a subcellular level, much has been learnt on the disease pathophysiology. Increased accumulation of DS and HS was shown to impair numerous cellular functions, including cell adhesion, endocytosis, intracellular trafficking, and intracellular ionic balance. It was also demonstrated to promote nitric oxide synthesis and trigger an inflammatory cascade, with numerous deleterious effects [15]. However, a full characterization of this cascade of secondary cellular events is still lacking (reviewed in [15]).

Currently, the standard of care for MPS II patients is enzyme replacement therapy (ERT), i.e., the intravenous administration of a functional recombinant version of the deficient enzyme. ERT has been shown to reduce urinary GAG levels and liver and spleen volumes in MPS II patients [16] (reviewed in [8]), with real-world data further suggesting that therapy may also improve other somatic cardiorespiratory parameters [17] (reviewed

in [8]). Still, it does hold a number of limitations, namely, its inability to cross the blood–brain barrier and act over the neurological symptoms, an issue which is common to virtually all ERT formulations developed so far, regardless of the LSD they apply to. To overcome the limitations of the ERT approach, some modifications to the traditional ERT protocol have actually been tested, including changes in the administration route, the introduction of modified fusion proteins, and the use of alternative hosts for enzyme production (reviewed in [2]). However, some challenges do persist, such as the treatment's inability to act over the neurological symptoms, its high cost, and life-long dependence [18].

Altogether, the need for deeper understanding of the pathophysiological mechanisms that underlie the disorder and for more effective treatments to counteract it justify the need for a cellular in vitro model that accurately recapitulates the disease phenotype in hard-to-reach/hard-to-treat cells, e.g., those derived from the nervous and/or skeletal systems. Regarding neurons in particular, the use of induced pluripotent stem cells (iPSCs) to model neurogenetic disorders is well established, for example, the function of cortical neurons from patient-derived fibroblasts or blood cells is now well documented and numerous studies in MPS II-derived iPSCs have already been published, with remarkable results and insights on the neuropathology of this disorder [19–21] (reviewed in [22]). However, there are notable drawbacks to using these de-differentiated, reprogrammed cells as in vitro models for molecular studies, mostly their high cost and time-consuming technology validation. That is why we are working with a completely different patient-derived cellular model: an alternative, less invasive and less laborious, source of stem cells, the so-called dental mesenchymal stem cells (DMSCs), which can be isolated from different sources in the oral cavity (reviewed in [22]).

Here, we report the establishment of two independent MPS II-derived cultures of stem cells from human exfoliated deciduous teeth (SHEDs) and their subsequent characterization at molecular, biochemical and pathophysiological levels. The existence of this small population of dental pulp stem cells (DPSC) was first reported by Miura and co-workers in 2003 [23], when SHEDs were first isolated from primary teeth that were lost due to the eruption of permanent teeth. That initial paper already provided remarkable insights into this particular population of DMSCs, demonstrating their high proliferative capacity and their ability to differentiate into a variety of cell types, including neural cells, adipocytes, and odontoblasts. Those authors also attempted their in vivo transplantation, showing that SHEDs were able to induce bone formation, generate dentin, and survive in mouse brain [23]. Thanks to the efforts of many independent teams working in different fields, these highly proliferative cells are now fully characterized and their mesenchymal stem cell (MSC) expression profile disclosed ([24–26], reviewed in [27]). Soon enough, this DMSC population was considered to hold great promise for regenerative medicine approaches and other cell-based therapies. Indeed, numerous studies have shown that autologous transplantation of SHEDs, for example, may be a safe and promising approach for both dentin and pulp regeneration (reviewed in [28]), but their applications far exceed the orthodontic field, as SHEDs have also been tested for their regenerative potential against spinal cord injury [29–31], hypoxic–ischemic brain injury [32], ovariectomy-induced osteoporosis [33], liver fibrosis [34], and systemic lupus erythematosus [35]. And that potential lies not only in the cells themselves but also in the conditioned media one may collect from their culture, as elegantly shown by Katahira and co-workers in a recent study, where they immortalized a SHED cell line and analyzed the effects of its conditioned medium on cutaneous pressure ulcers [36].

In the LSD field, however, DMSCs (and SHEDs in particular) are mostly unknown and their potential unexplored. As such, here we addressed the question of whether these cells could be used, not for therapeutic purposes, but for disease modeling, as they are well known to retain the ability to differentiate into several cell lineages that represent disease-relevant cell types, not only for MPS II, but for LSDs in general (e.g., chondrocytes, osteoblasts, and neuronal cell types; reviewed in [37]). To the best of our knowledge, this was the first time that SHEDs were isolated from LSD patients.

Briefly, we have not only successfully confirmed the DMSC identity of the established MPS II SHEDs but also assessed their LSD phenotype. Regarding their stemness potential, the MPS II-derived SHED cell lines described here presented an expression pattern characteristic of an MSC line, with high expression levels of *CD105*, *CD73* and *CD90* and a weak but still detectable expression of the pluripotency genes *Nanog*, *Oct3-4* and *Sox2*. They were also able to differentiate into endoderm, ectoderm and mesoderm. Also noteworthy, our results so far clearly demonstrate that the typical MPS subcellular phenotype is already present in the established MPS II-derived SHED cell lines. We have also briefly tackled whether secondary accumulation of lysolipids can be detected in those lines using a biomarker panel approach. Overall, this is an original contribution to the LSD field, as it demonstrates the existence of an easily accessible, non-invasive source of MSCs that exhibit visible and measurable LSD subcellular phenotypes. Importantly, those can be collected from severely affected individuals (those who suffer from infantile forms of these disorders). It seems most valuable to use these methods in order to better establish patient-specific models to understand the cellular dynamics of the disease in the donor patients of such cells.

2. Results

2.1. Establishment of Primary SHED Cell Cultures from Patients and Controls

In this study, two unconventional MPS II samples were used to establish novel patient-derived MSC lines in house: SHEDs. The teeth included in the study were non-carious, had no previous restorations, and had no reports of prior trauma, even though one was surgically extracted (that from patient MPS II, 2.01). All other samples were spontaneously exfoliated teeth (namely, those obtained from patients MPS II, 2.02 and controls 01 and 02, here termed Ctrl.01 and Ctrl.02).

Upon reception of the biological sample, dental pulp was extracted, enzymatically digested, and left to grow in poly-D-lysine or vitronectin-coated 12-well plates. Cells derived from the dental pulp were visible within 1–2 weeks. Then, in a process that took anywhere from two weeks to one month, we could observe a population of SHEDs, morphologically characterized by spindle-shape cells, similar to fibroblasts (Figure 1a), which initially formed small colonies (Figure 1b) that were left to grow until they reached sub-confluence (Figure 1c). Throughout the whole process, which involved the establishment of the primary cultures, their passage, freezing and thawing, SHED cell viability and morphology were checked using a light microscope and any relevant alteration noted. All established cell lines shared the same morphological features, regardless of whether they were derived from patients or controls.



(**a**) (**b**) (**c**)

Figure 1. Optical microscope images (4×) of an MPS II-derived SHED primary culture. Undifferentiated SHEDs have a spindle shape similar to fibroblasts. (**a**) Fusiform format; (**b**) small colony formation (CFU-F); (**c**) sub-confluence. Cells were observed using a Leica DMIL inverted contrasting microscope (Leica Microsystems, Wetzlar, Germany) with 4× magnification.

2.2. The Established SHED Cell Lines Share an MSC Phenotype Identity

The MSC phenotype of the established SHED cultures was assessed through different protocols, namely, quantitative real-time reverse-transcription polymerase chain reaction (qRT-PCR) analysis of different stem cell markers and multi-lineage differentiation assays.

Regarding the qRT-PCR analysis, total RNA was successfully extracted not only from cultured SHEDs but also from an iPSC line already available in the lab (INSAi002-A; derived from Fabry fibroblasts [38]). The extracted RNA samples were reverse-transcribed into cDNA, and specific gene expression was assessed (Table 1). In summary, *CD34* was not detected as expected for SHEDs. *CD105*, *CD73* and *CD90* were highly expressed and *CD166*, *MHC I* and *CD117* showed strong to moderate expression. The pluripotency genes *Nanog*, *Oct3-4* and *Sox2* were also expressed, although weakly (Ct value > 35). Moreover, weak expression of *MHC II* was also detected in SHEDs. The expression levels observed for the iPSC line are also summarized in Table 1. Briefly, INSAi002-A iPSCs displayed high expression levels of *CD105*, *CD73*, *CD90*, and *Oct-3/4* and moderate expression levels of *MHC II*, *Nanog*, and *Sox-2*. Absolute ΔCt valuescalculated using glyceraldehyde 3-phosphate dehydrogenase (*GAPDH)* and β-actin *(ACTB)* as housekeeping genes are listed in Table S1.

Table 1. Relative expression levels of several markers, including *CD105*, *CD73*, *CD90* and *CD166* (MSC markers), *Sox-2*, *Oct-3/4*, and *Nanog* (pluripotency markers), *CD117*, *CD34*, *MHC I* and *MHC II*, in SHEDs from patients and controls, and also iPSCs derived from Fabry fibroblasts. Differences were based on qRT-PCR results and calculated using the standard ΔCt method, with *GAPDH* and *ACTB* as housekeeping genes.

Marker	SHEDs (2.01)	SHEDs (2.02)	iPSCs (INSAi002-A)
CD105	***	***	***
CD73	***	***	***
CD90	***	***	***
CD166	***	***	
MHC I	***	***	
Sox-2	*	*	**
Oct-3/4	*	*	***
Nanog	*	*	**
CD117	**	**	
CD34	*	*	*
MHC II	*	**	**

*** Strong expression; ** moderate expression; * weak expression.

Further insights on the stem nature of the established SHED cell lines came from multi-lineage differentiation assays using a human pluripotent stem cell functional identification kit (R&D Systems, Minneapolis, MN, USA). This kit contains especially formulated media supplements and growth factors that can be used to differentiate human pluripotent stem cells into endoderm, ectoderm and mesoderm. It is a fast protocol, which relies on 2- to 4-day incubations with those media, and also includes antibodies to characterize each of the three primordial germ layers: Sox17 for endoderm; Otx2 for ectoderm; and Brachyury for mesoderm. Not surprisingly, all established cell lines stained positive for each respective marker, thus confirming their capacity to differentiate into each of the three germ layers (Figure 2a).

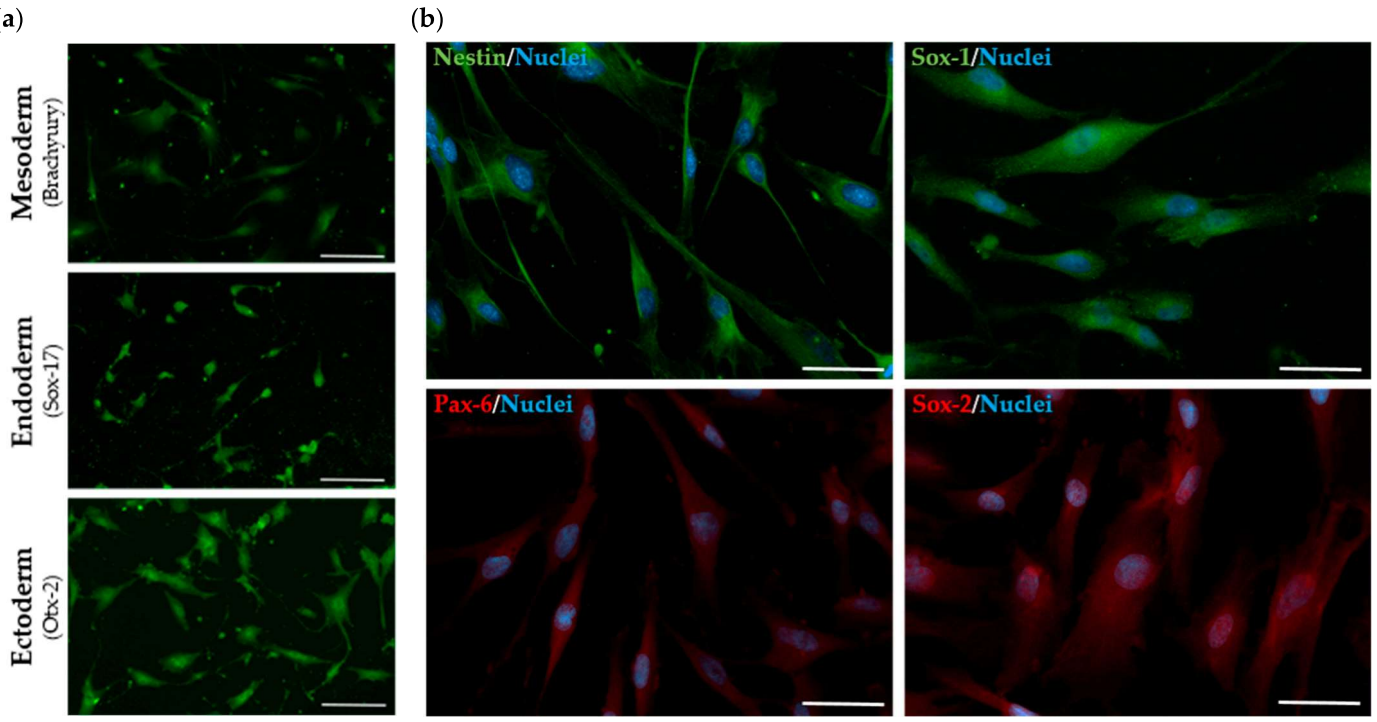


Figure 2. Immunostaining of MPS II-derived SHEDs. (**a**) Confirmation of 3-germ-layer differentiation capacity: mesoderm (top), endoderm (middle), ectoderm (down). (**b**) Confirmation of neural progenitor cell (NPC) stage of SHEDs: Nestin and Sox-1 (top line); Pax-6 and Sox-2 (bottom line). Scale bar: 50 μm. Images were acquired using a DM400 M fluorescence microscope (Leica, Wetzlar, Germany).

2.3. The Established SHED Cell Lines Express Major NPC Markers

As a final characterization step of the established SHED cell lines, the early DMSC commitment to their so-called "neuronal fate" was also confirmed. This study was performed in primary SHED cells before any neuronal differentiation protocol was attempted, and relied on the use of a commercially available kit. Briefly, their neural progenitor cell (NPC) stage was analyzed based on the expression of major NPC markers (Nestin, Sox-1, Sox-2 and Pax-6), with a positive fluorescence pattern observed for all four markers evaluated (Figure 2b). No significant differences were detected between healthy and MPS II cell lines in early passages (from passage 5 to passage 7).

2.4. The Established MPS II-Derived SHED Cell Lines Display Disease-Related Biochemical and Molecular IDS Defects

Whenever an MPS tooth was received in the laboratory, the only information available was the type of MPS from which the patient it belonged suffered. Therefore, as soon as its derived SHED cell line was established and the first vials stored, cell pellets were collected and used for mutational analyses and enzyme activity assays.

2.4.1. The Presence of Pathogenic *IDS* Variants Was Confirmed in the Established MPS II Patient-Derived SHED Cell Lines

For molecular analyses, DNA was successfully extracted from both MPS II patient-derived SHED cultures, and standard amplification and Sanger sequencing protocols were employed to analyze the nine *IDS* exons plus their surrounding intronic regions, as previously reported [39]. Whenever standard procedures were not enough to identify the disease-causing variant, additional studies were performed, namely, restriction fragment length polymorphism (RFLP) [39] (see Materials and Methods, Section 4.4.1).

Briefly, Case 2.01 was confirmed to carry a rearrangement involving recombination between intron 7 of the *IDS* gene and sequences located distally of exon 3 in the *IDS* pseudogene (*IDS-2*) [GAATC > AGAGG (*IDSP1* > *IDS*)]. This recombination event had already

been reported, and is known to cause a partial inversion of the *IDS* gene [40]. Conversely, Case 2.02 was shown to be hemizygous for a variant much more straightforward to detect: the previously reported c.22C > T (p.R8*) nonsense mutation [40]. Both identified genotypes were in accordance with an MPS II phenotype.

2.4.2. IDS Enzyme Activity Is Significantly Decreased in MPS II Patient-Derived SHED Cells

When the IDS activity was measured with the fluorescent substrate 4-methylumbelliferyl (4MU)-α-L-iduronate-2-sulfate in SHED cell lysates from both controls and the two independent MPS II patients, no activity could be detected in case 2.01 or 2.02, whilst control Ctrl.01 and Ctrl.02 cells showed normal IDS activity (Figure 3a). The other lysosomal enzymatic assays performed were within the normal range in all the SHED lysates (Supplementary Figure S1).

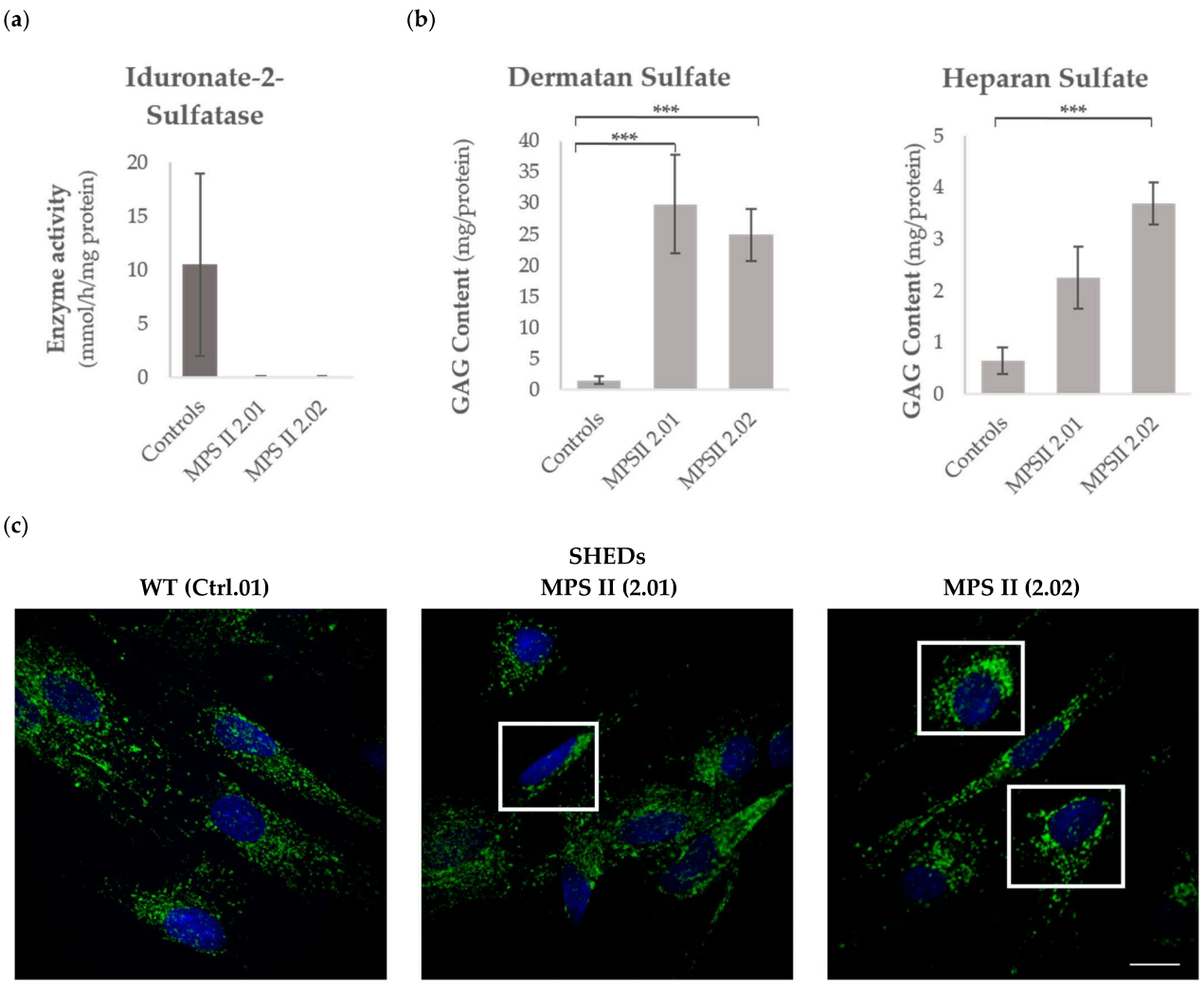


Figure 3. Biochemical profile of SHEDs. (**a**) IDS enzyme activity. Data are presented as means ± SEM (n = 3) *** $p < 0.0005$. (**b**) HS and DS levels of control- and MPS II-derived SHEDs. (**c**) Representative confocal images of control (left) and MPS II-derived SHEDs (middle and right) immunostained for lysosomal-associated membrane protein 1 (LAMP1). Scale bar: 25 µm. The outlined regions (white squares) highlight the different lysosomal positioning in controls vs. patient-derived SHEDs, with more pronounced LAMP1 staining in the perinuclear region of MPS II SHEDs. Images were acquired using a TCS-SPE confocal microscope (Leica, Wetzlar, Germany).

2.5. MPS II Patient-Derived SHED Cells Exhibit a Subcellular LSD Phenotype

Subsequently, the LSD phenotype of the established MPS II patient-derived phenotype was assessed. Briefly, we checked not only the primary GAG storage, which is known to trigger the whole MPS II pathophysiological cascade, but also the lysosomal localization pattern, to check whether it was altered.

2.5.1. GAG Accumulation Is Evident in MPS II Patient-Derived SHED Cells, despite Their High Proliferation Rate

Decreased (or absent) IDS activity in MPS II patients is known to cause an intracellular and extracellular accumulation of two major GAGs, namely, HS and DS. Thus, the levels of those two GAGs were measured by liquid chromatography–mass spectrometry/mass spectrometry (LC-MS/MS), and both MPS II SHED cultures showed evident GAG accumulation when compared with control SHEDs (Figure 3b).

2.5.2. LAMP1 Staining Is Altered in Patient-Derived SHED Cells

Accumulation of DS and HS causes lysosomal hypertrophy and an increase in the number of lysosomes in cells. Therefore, any method that allows for an evaluation of the number, size and sub-cellular localization of these disease-relevant organelles may provide relevant data on the health/disease status of a given cell line. Here, we chose to perform a lysosomal-associated membrane protein 1 (LAMP1) immunostaining protocol in control vs. MPS II cells. LAMP1 is one of the most abundant lysosomal membrane proteins, nicely correlating with lysosomal dysfunction, as its overexpression reflects abnormal accumulation of lysosomes. Overall, the pathological phenotype was quite evident, with MPS II cells presenting a prominent LAMP1-positive perinuclear fluorescence when compared to controls (Figure 3c).

2.6. MPS II Patient-Derived SHED Cells Present Normal Lysosphingolipid Levels

Apart from the primary accumulation of GAGs (assessed in Section 2.5.1), secondary storage of lipids is also known to play a role in the pathophysiological cascade that gives rise to MPS symptoms. Here, we used a multiplexed LC-MS/MS method to simultaneously quantify four different glycosphingolipid biomarkers [Lyso-Gb3, Glc-Sph, Lyso-SM, and PPCS (initially referred to as Lyso-SM-509)] in our MPS II SHEDs vs. controls, and observed normal levels of all four lysosphingolipids in the samples analyzed (Table S2).

3. Discussion

Here, we describe the establishment and characterization of two MPS II patient-derived SHED cell lines (named 2020TF-MPS2.01 and 2020TF-MPS2.02) while addressing their modeling potential for this severe condition by evaluating whether they display visible and measurable MPS subcellular features.

Briefly, we successfully implemented a protocol developed by Goorha and Reiter [41] for efficacious remote tooth collection and subsequent dental pulp extraction for growth and expansion of that particular subset of DMSCs, and applied it in two independent MPS II cases and a significant number of controls (>30). As originally reported by Goorha and Reiter, the process of growing these particular DMSCs can take anywhere from 1 to 2 weeks, and—at least in our hands—there seems to be no particular correlation between the size of the pulp or the time it takes to arrive at the lab (as long as the 48/72 h interval is ensured) and the time it takes for the first cells/colonies to become visible in the plate. Overall, the whole method is well described in the publication we refer to, and it is not hard to implement in a lab with standard cell culture conditions, regardless of whether the operators have had experience with other sorts of stem cells, namely, iPSCs.

Technically, MSCs are classified as multipotent stem cells and not as pluripotent stem cells. Still, as we have already seen, they do present a positive expression pattern of *Oct-3/4*, *Nanog*, and *Sox-2*, which are standard pluripotency markers [42–44]. DMSCs in general and SHEDs in particular have been known to express those markers for quite a while. In fact,

that characteristic was already reported in healthy SHEDs back in 2006 in an original paper by Kerkis et al. [24], where their stemness character was confirmed [25]. Nevertheless, the expression level of any of these markers when compared with other commonly assessed MSCs markers is known to be weak. These data correlate nicely with our results, where all SHED cell lines presented with positive expression levels of these three pluripotency markers, but at a level that was significantly lower than that seen for specific MSC markers (*CD105*, *CD90*, and *CD73*). They also seem to be in accordance with what we saw on the iPSC cell line we used as a control (INSAi002-A; derived from Fabry fibroblasts [38]): while positive, the levels of expression of *Oct-3/4*, *Nanog*, and *Sox-2* were much lower in the established multipotent SHED cell lines than in the truly pluripotent iPSC line, which was triggered to overexpress those markers through a reprogramming protocol with Yamanaka factors. Remarkably, no studies comparing the expression levels of stemness markers between DMSCs and iPSCs are available, at least that we are aware of. Therefore, these results become even more interesting.

Specific MSC markers were also measured in both healthy and disease-derived SHEDs, as well as in the iPSC line INSAi002-A, and overall, the results were in line with what would be expected according to the literature: MSC markers (*CD105*, *CD90*, and *CD73*) were the ones that displayed higher expression levels, thus supporting the MSC phenotype of the established SHEDs. The two remaining markers assessed, *CD34* and *MHC II*, are commonly described as absent in MSCs [45,46]. They did, however, show positive expression, even though with significantly lower levels than those observed for *CD105*, *CD90*, and *CD73*. They were actually comparable with the ΔCt value observed for the pluripotency markers. While this result seems unaligned with MSC requirements, as they are reported in the bibliography, when we look at individual papers where SHED and DPSC expression patterns for these markers were assessed, this observation is actually common. For example, recently, positive expression levels of *MHC II* were reported in a commercially available DPSC line and considered a normal aspect [47]. Additionally, there is already literature commenting on the possibility that the absence of expression of those markers may not be mandatory for a cell to be classified as MSC, once several MSCs have been shown to express, at least to some extent, both of them [45,46].

Adding to our qRT-PCR results regarding the MSC phenotype are our results on the differentiation capacity of the established SHED cell lines into distinct cell types. Traditionally, one of the listed requirements to identify MSCs is their ability to differentiate into three different cell types: adipocytes, osteocytes and chondrocytes [48]. More recently, though, many authors have argued those requirements should be updated to include cells from the three germ layers ectoderm, mesoderm, and endoderm [49]. That is why we chose to perform a novel (and faster) 4-day-long tri-lineage differentiation protocol, through which our MPS II patient-derived SHED cell lines were forced to differentiate into ectoderm, endoderm and mesoderm. Overall, the protocol worked precisely as anticipated, with the cells staining positive for all tested markers, regardless of the differentiation attempted.

Still, there was yet another assessment we considered to be relevant regarding the overall nature of the established cell lines, regardless of their health/disease status. SHEDs have a behavior similar to neuronal precursor cells. Indeed, there are now numerous publications providing evidence that SHEDs express neuronal and glial cell markers, owing to the neural crest-cell origin of the dental pulp [50] (reviewed in [51]). And in fact, staining of neuronal markers in SHEDs not subjected to any type of neurodifferentiation protocol, revealed a positive fluorescence pattern for all four markers evaluated—Nestin, Sox-1, Pax-6 and Sox-2—further validating the assumption that SHEDs may actually be classified as NPCs, as stated by several different authors.

Having extensively demonstrated the stemness capacity of all established SHED cell lines and further characterized them as NPCs, we moved on to analyze whether they were able to mimic the primary defect underlying the MPS II phenotype in the patients from whom they were derived. Thus, a careful molecular characterization of their associated genotypes was performed, together with a quantification of each one's defective enzyme.

Unsurprisingly, when the two established MPS II cell lines were molecularly characterized, both cases were shown to harbor pathogenic *IDS* variants. Case 2.01 was shown to be hemizygous for a complex rearrangement that results from a recombination event between intron 7 of the *IDS* gene and sequences located distally of exon 3 in the *IDS* pseudogene (*IDS*-2) [GAATC > AGAGG (*IDSP1* > *IDS*)] and causes a partial inversion of the *IDS* gene [40]. Case 2.02 was shown to be hemizygous for the previously reported c.22C > T (p.R8*) nonsense mutation [52]. This mutation had already been reported in different populations, correlating either with severe or intermediate forms of the disease [52–54]. Altogether, both mutations may easily correlate with severe, early-onset phenotypes, as those presented by both patients included in this study (see Table 2).

Table 2. Summary of the most relevant clinical data from each MPS II patient, including age of diagnosis, symptoms and age of starting treatment.

Case	Age of Diagnosis (Years)	Symptoms	Age of Starting Treatment (Years)
2.01	3	Coarse facies, stiff joints, etc. Post-natal macroglossia Mild psychomotor development retardation; Interventricular communication (IVC) and patent ductus arteriosus (PDA); Moderate aortic insufficiency and left ventricular hypertrophy; Hydrocele; Chronic nasal obstruction without recurrent otitis or hearing deficit.	-
2.02	2	Inguinal hernias; Claw hands; Low stature; Hypertrichosis; Hepatomegaly; Cardiac involvement.	4

Accordingly, when IDS enzyme activity was measured in the lysate of MPS II patients' SHEDs, it was shown to drop to zero (Figure 3a).

While the results so far already testify to the overall potential of patient-derived SHED cell lines to accurately express a measurable LSD phenotype, the ones we will now focus on further highlight the uniqueness of this cell model.

Our results regarding MPS II-related primary storage in patient-derived SHEDs, for example, are worthy of additional discussion. Briefly, when we quantified DS and HS in healthy and diseased SHED cell lysates by butanolysis derivatization [55], significant differences were observed between patients and controls, with both MPS II samples showing GAG accumulation (Figure 3b). This is particularly relevant when compared with the results other authors have achieved with MPS II iPSC-derived cell lines. Currently, there are numerous reports on the generation of MPS II human iPSC lines. Still, not all papers evaluated the LSD phenotype they present. Instead, most publications focus only on the iPSCs' generation and characterization protocol, already well established to validate an iPSC line: they report the method of reprogramming, present proof on the established cell line(s') pluripotency and differentiation potential; assess identity compared to the cells they were reprogrammed from, as well as their karyotype to confirm it remains normal; double-check the presence of the original disease-causing variant, and rule out mycoplasma contamination. There is, however, an original publication by Kobolák and co-workers [20] where numerous analyses were performed, not only in MPS II-derived iPSCs but also, and perhaps most importantly, in NPCs and terminally differentiated (TD) neurons generated from them. Briefly, they used iPSC lines generated from three independent MPS II patients,

a healthy control, and a carrier, to generate NPCs and TD neuronal cells, and compared results amongst all those lines. Curiously, all the three MPS II NPC cultures analyzed in that work showed lower total GAG levels ($p < 0.05$) compared to either control or carrier cell lines. For the hallmark accumulation to (finally) be observed, the authors had to promote the terminal differentiation of those MPS II iPSC-derived NPCs into cortical neural cells. Only then could a marked GAG accumulation be detected, though for two of the three MPS II cell lines alone. The third patient-derived MPS II neuronal cell line did not differ significantly from the control cell line [20] (reviewed in [22]). This is significantly different from our own observation in MPS II SHED cell lines, where GAG storage was quite evident. And while we cannot find the reasoning for this discrepant observation, it is (quite) obvious that the results further highlight the disease modeling potential of this simple and easily accessible type of stem cell.

Similar results were obtained regarding LAMP1 staining. Again, the established MPS II SHEDs showed obvious differences compared to the controls, a pattern that is in accordance with previous reports from other teams that observed increased LAMP1 levels in LSD animal models, as well as in human patients. For MPS II in particular, Morimoto and co-workers recently reported increased Lamp1 staining in the brains of MPS II mice. Importantly, when those mice were treated with the recombinant enzyme idursulfase, irrespective of the dosing regimen, intensity decreased in most regions of the brain. Those observations further support the assumption that abnormal Lamp1 staining in MPS II correlates with lysosomal dysfunction [56]. Altered staining patterns for both LAMP1 and LAMP2 were also observed in MPS II iPSC-derived neural stem cells [21]. Remarkably, however, this pattern was not seen in all MPS II-derived neural stem cells reported so far. Indeed, in the original publication by Kobolák et al. [20], to which we have already referred, significant differences between patient- and control-derived cells were only observed in TD neuronal cells, where indeed MPS II samples showed cell-type specific differences in their LAMP2 staining patterns, with many more $LAMP2^+$ vacuoles in $GFAP^+$ astrocytes than in $MAP2^+$ neurons [20]. Again, these significant differences between the novel, naturally occurring stem cell model here reported (patient-derived SHEDs) and its iPSC-derived equivalent (NPCs) further highlight the advantage of establishing this type of cell line.

Finally, we moved on to check whether it was possible to document any downstream effects of the observed primary GAG storage with routine methods. As such, we checked whether a biomarker panel approach for lysosphingolipid quantification could help us obtain an insight into the common downstream pathophysiological mechanism(s) leading to intracellular dysfunction in these disorders. Lysosphingolipids are free sphingoid bases that can be accurately quantified by LC-MS/MS and have great diagnostic value for a number of LSDs characterized by the disturbed catabolism of sphingolipids, the so-called glycosphingolipidoses. Indeed, increased levels of glycolysosphingolipids are present in tissue and plasm of several sphingolipidoses, and some of them have actually been validated as disease biomarkers, namely, globotriaosylsphingosine (Lyso-Gb3) glucosyl-sphingosine (Glc-Sph) and phosphorylcholine-sphingosine (Lyso-SM) for Fabry, Gaucher and Niemann–Pick type A/B diseases, respectively [57]. However, disruptions of the glycosphingolipid degradation pathways are implicated not only in glycophingolipidoses but also in other LSDs, including MPSs [15]. And it is true that not only there is a well-documented secondary accumulation of lipids in MPS diseases (MPS II included) [21,58] but also there is an increasing body of evidence documenting significant elevations of several glycophingolipidose biomarkers in other LSDs, including neuronopathic forms of MPSs [59]. That is why we tried to address the question of whether any of those biomarkers could be altered in the cell lines under analysis.

While for the two patients here analyzed, no large increases in any of the assessed lysosphingolipids were seen, we do consider it relevant to perform this kind of analysis in other cell models of non-glycosphingolipid diseases, as they may give us an insight into other relevant pathways that can be secondarily impaired. Here, we used exactly the same method that we have implemented in-house for diagnostic purposes in plasma/leukocyte

samples. For other labs like ours, with a strong component of diagnostic services, this may be an interesting second-tier test in newly established cell models without requiring additional investment. We are currently recruiting more patients for deciduous tooth collection. In the future, additional analyses will be performed in the established cell lines.

It is also worth reinforcing that there are many other DMSCs, which may be collected from the oral cavity (Figure 4). We have focused our attention on SHEDs, because they may be collected in a non-invasive way in pediatric patients. However, other sources may be considered, particularly for adult patients with milder forms of the disorders, who tend to be diagnosed later in life. A good example is the use of adult human third molar teeth, from where DMSCs may also be isolated. While there are slight variations in the protocols described in the literature for the isolation of DPSCs from this source, the overall method is not significantly different from the one reported here for SHED cell culture.

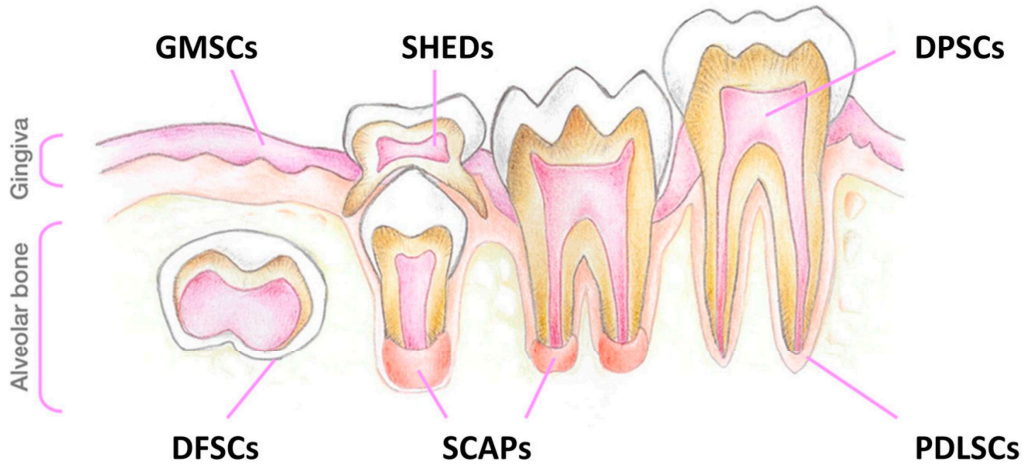


Figure 4. Schematic drawing illustrating the different sources of dental mesenchymal stem cells (DMSCs) in the oral cavity. Abbreviations: GMSCs, gingiva-derived mesenchymal stem cells; DFSCs, dental follicle stem cells; SHEDs, stem cells from exfoliated deciduous teeth; SCAPs, stem cells from the apical papilla; DPSCs, dental pulp stem cells; PDLSCs, periodontal ligament stem cells (reproduced from [22]).

Overall, this type of sample would allow for a significant increase on the number of eligible patients, because their recruitment platform would be much larger than the current one: it would move from children who are currently losing their baby teeth to virtually any patient, regardless of his/her age. The fact that the surgical removal of human third molars (also known as wisdom teeth) is the most common surgical procedure in the orthodontic field, which also adds to the interest in implementing this protocol and asking for this type of sample. This picture is probably even more prominent in individuals who suffer from MPS, particularly from the skeletal forms of these disorders. In fact, some of the most common and obvious orofacial abnormalities in MPS patients are maxillomandibular abnormalities. GAG accumulation in soft tissues, cartilage, and bones and secondary cellular responses to accumulated GAGs are probably the culprit for abnormalities in orofacial soft tissues, orofacial bones, and teeth [60]. That is why MPS patients are frequently subjected to tooth-removal surgeries, among other orofacial interventions.

Finally, it is also worth mentioning that while we recognize the therapeutic potential any stem cell line may eventually hold, particularly in a field where hematopoietic stem cell transplantation (HSCT) is a feasible and recommended approach for a few disorders, depending on the severity of the phenotype and the age of the patient, our goal with this work was never to either establish or characterize SHED cell lines for therapeutic purposes. The cells we isolated present the same genetic defect harbored by their donor; therefore, only after gene editing (e.g., CRISPR-Cas system) would they be suitable for transplantation. Plus, as these cells are isolated from naturally exfoliated baby teeth, one would only have

access to that sample when these patients started losing their teeth, i.e., at about age 6 or later. And that is certainly late for HSCT approaches, as it is well documented for other MPS [namely, MPS I with central nervous system (CNS) affection] that HSCT only works in children who are less than 2.5 years of age. Additionally, it is also worth mentioning that the protocol we used here is not suitable to establish clinical-grade stem cells.

Altogether, our results show that this patient-derived sample is a much faster and more economical way to establish a stem cell model, and it also holds the potential to display disease-relevant sub-cellular features. Thus, patient-derived SHEDs may be assessed not only to allow a better understanding of the pathophysiological mechanisms underlying the disorder but also to evaluate the potential impact of novel therapeutic approaches in vitro.

4. Materials and Methods

4.1. Materials

Methanol, acetonitrile, chloroform, and ethanol were from Fisher Chemicals. Formic acid and DMSO were from Sigma-Aldrich (Gillingham, UK). All solvents were HPLC-grade. Water used was Milli-Q grade (Milipore, UK). Antibodies used in this study are listed in Table 3. All other specific reagents and materials are listed in the following subsections.

Table 3. Antibodies used in this study.

		Antibody	Dilution	Company Cat# and RRID
Primary Antibodies	Germ Layer Markers	Goat Anti-Human Brachyury Polyclonal Antibody, unconjugated (Mesoderm)	1:10	R&D Systems (Minneapolis, MN, USA) Cat# AF2085, RRID:AB_2200235
		Goat Anti-Human Sox17 Polyclonal Antibody, unconjugated (Endoderm)	1:10	R&D Systems Cat# AF1924, RRID:AB_355060
		Goat Anti-Human Otx2 Polyclonal Antibody, unconjugated (Ectoderm)	1:10	R&D Systems Cat# AF1979, RRID:AB_2157172
	Neural Stem Cell Markers	Mouse Anti-Human Nestin Monoclonal Antibody	1:49	Thermo Fisher Scientific (Waltham, MA, USA) Cat# MA1-110 (A24345)
		Rabbit Anti-Human PAX6	1:49	Thermo Fisher Scientific Cat# (A24340)
		Goat Anti-Human SOX1	1:49	Thermo Fisher Scientific Cat# (A24347)
		Rabbit Anti-Human SOX2	1:49	Thermo Fisher Scientific Cat# (A24339)
	LAMP1 Staining	Mouse Anti-Human LAMP-1 Monoclonal Antibody	1:200	Santa Cruz Biotechnology, Inc. (Dallas, TX, USA) Cat# sc-20011
Secondary Antibodies		Alexa Fluor 488 Donkey anti-Goat IgG (H + L) Cross-Adsorbed Secondary Antibody	1:200	Thermo Fisher Scientific Cat# A-11055, RRID:AB_2534102
		Alexa Fluor™ 488 Donkey Anti-Mouse; for use with anti-Nestin	1:249	Thermo Fisher Scientific Cat# (A24350)
		Alexa Fluor™ 488 Donkey Anti-Goat; for use with anti-SOX1	1:249	Thermo Fisher Scientific Cat# (A24349)
		Alexa Fluor™ 555 Donkey Anti-Rabbit; for use with anti-PAX6 or anti-SOX2	1:249	Thermo Fisher Scientific Cat# (A24342)
		Alexa Fluor™ 594 Donkey Anti-Rabbit; for use with anti-PAX6 or anti-SOX2	1:249	Thermo Fisher Scientific Cat# (A24343)

4.2. Patients and Samples

4.2.1. Patient 1 (Case MPS 2.01)

Patient 1 was the first child of a non-consanguineous couple. While there was no access to a complete family tree, family history records included a reference to the mother's learning difficulties and another to a disabled maternal cousin (son of a maternal great aunt), who died in childhood without diagnosis.

At 22 months, initial signs of developmental delay, mostly regarding language, were reported, accompanied by other clinical features, which included wide-based gait with knee flexion and motor agitation. It was also at this age that a first reference was made to a "rough face" in the records of an objective examination of pediatric consultations.

By then, the patient's skeletal and somatic features included coarse facies, stiff joints and postnatal macroglossia. Some cardiac manifestations were also detected, namely, interventricular communication (IVC) and patent ductus arteriosus (PDA), both solved by now. At 35 months, thickening of the aortic valve was detected. Additionally, moderate aortic insufficiency and left ventricular hypertrophy were also referenced. ENT manifestations were also present, including chronic nasal obstruction, even though no recurrent otitis or hearing deficit have been detected so far. Finally, mild psychomotor development retardation was also reported.

Upon objective examination at the metabolic and genetic consultation (also at 35 months of age), the child displayed relatively understandable language and showed important emotional lability. His dysmorphic features (namely, coarse face, abundant and thickened eyebrows, macroglossia apparent, abnormal posture with knee flexion and wide-based gait and limitation in elbow extension, slight pectus carinatum with far apart nipples and preputial ring punctiform) were considered suggestive of MPS and the child was referred for molecular and biochemical diagnosis. There was no evidence of hepatosplenomegaly or hernias. Regarding evolution of weight gain and head circumference, there was a positive crossing of percentiles of the various parameters: height at percentile (P) 85–97, weight at P > 97 [with body mass index (BMI) at P > 99, which corresponds to a Z-score > 3SD (where SD stands for standard deviation of the reference population)] and head circumference at P > 97.

4.2.2. Patient 2 (Case MPS 2.02)

Patient 2 is a 6-year old male child, diagnosed at 2 years old with MPS type II. The child presented with multisystemic involvement, which included not only several classical musculoskeletal features of the disease (inguinal hernias, claw hands and low stature) but also a series of other symptoms, which included hypertrichosis, hepatomegaly and cardiac involvement (minimal mitral regurgitation). Later, he underwent otorhinolaryngological surgery to perform bilateral myringotomy and tubes with adenoidectomy. Currently, his inguinal hernias have already corrected. Recently (June 2022), his global psychomotor development was assessed and considered normal. Nevertheless, he developed an orthopedic condition with joint restrictions, which requires physiotherapy.

4.2.3. Biological Samples

Deciduous teeth (i.e., "baby" teeth) from two independent MPS II patients and from an equal number of controls were acquired.

Briefly, the process of sample collection was performed as follows: all subjects included in this study, either wild-type (WT) controls or MPS II patients, received a tooth collection kit, which included a parafilm-sealed Falcon tube filled with adequate transport media accompanied by return instructions, a biohazard bag, plus a prefilled delivery form. Also included in the kit was an informed consent form to be completed by the participant's legal representative, a summary of the project and its objectives, and a flyer with major recommendations and frequently asked questions (See Figure S2). The families were instructed to store the Falcon tube in the refrigerator (4 °C) and to place the tooth in it, virtually as soon as it fell (within 20 min), and send it to the lab within 24 h.

While we received more than 50 deciduous teeth and established over 30 independent control cell lines from them, most of the results here reported were obtained through the analyses of only two of those controls (here termed Ctrl.01 and Ctrl.02). An exception was made for enzyme activity and LC-MS/MS assays, where a significantly higher number of controls was included, to account for interindividual differences.

In general, the deciduous teeth used in this work were spontaneously exfoliated teeth. However, for patient 1 (MPS II, 2.01), a surgically extracted deciduous tooth was received.

4.3. Cell Cultures

4.3.1. Establishment of Primary SHED Cell Cultures

The whole protocol for the establishment of primary SHED cell cultures was derived from that published by Goorha and Reiter in 2017 [41] for remote tooth collection of exfoliated teeth and subsequent production of DPSC cultures for differentiation or storage, with minor alterations. In detail, upon every tooth reception, and after a careful inspection of the transport medium to discard possible microbial contamination, teeth were broken open under sterile conditions, using a sterilized hammer. The dental pulp was then pulled out and placed into preheated washing media [saline solution, with PenStrep (50 U/mL) fungizone (1.25 µg/mL)] in a small petri dish, where it was minced into smaller fragments. After a brief centrifugation, the minced pulp was resuspended in fresh DPSC culture medium [DMEM/F12 (1:1) with 20% FBS, PenStrep (50 U/mL) and fungizone (50 U/mL)] containing 3 mg/mL collagenase (Gibco, Thermo Fisher Scientific, Waltham, MA, USA) and 1–4 mg/mL dispase (Neutral Protease Grade II, Roche, Basel, Switzerland) and incubated for 1 h at 37 °C. Following enzymatic digestion, samples were centrifuged at 448× *g* during 5 min, resuspended in 1 mL of DPSC culture medium and seeded in a single well of a poly-D-lysine- (Gibco, Thermo Fisher Scientific, Waltham, MA, USA) or vitronectin (Thermo Fisher Scientific, Waltham, MA, USA)-coated 12-well tissue culture plate. The plate was then left to incubate overnight in a standard 37 °C incubator, with 5% CO_2. The following day, supernatant was removed from the well and briefly centrifuged to spin down the floating, unattached cells. The resulting pellet was resuspended in fresh DPSC culture media and seeded in another coated well from the same plate. Cultures were washed with the previously described washing solution and media changed twice a week, up until cells reached sub-confluence (80–90%).

4.3.2. Passage, Freezing and Thawing of SHED Cell Cultures

Again, in accordance with the original protocol developed by Goorha and Reiter [41], SHED cultures were passaged at a ratio of 1:3, according to the following rationale: one part was sub-cultured for passage, and the remaining two were frozen for future applications. In higher passages, when there was no need to assure the maximum possible number of stored vials to ensure the preservation of the cell line, parts 2 and 3 were frequently used to generate pellets for subsequent analyses. For cell detachment, Accutase (GRiSP, Lda., Porto, Portugal) was used. Early-passage cells were frozen for long-term storage in liquid nitrogen, in culture media supplemented with 15% DMSO (Sigma-Aldrich, St. Louis, MO, USA), according to standard freezing protocols.

4.4. Molecular Analyses

4.4.1. Genotype Assessment by PCR and Sanger Sequencing

Genomic DNA was automatically extracted and purified from cell pellets on a BioRobot EZ1 instrument (QIAGEN, Germantown, MD, USA) using the EZ1 DNA Tissue Kit (QIAGEN, Germantown, MD, USA). Previously reported primers [39] covering all *IDS* exons and their surrounding intronic regions, as well as its promoter region, were used to sequence the gene of interest. Each PCR reaction was carried out using approximately 40 ng of genomic DNA, 1X the PCR reaction mix ImmoMix™ Red (Bioline, London, UK) and 0.25 µM of each primer. For some particular fragments, betaine and/or DMSO were also used to enhance the PCR amplification of the target region (conditions available upon

request). Then, samples were heated to 95 °C for 7 min, followed by 35 cycles of denaturation, annealing and extension. The final extension was completed by 5 min at 72 °C. The amplified fragments were purified with illustra ExoStar™ 1-Step (GE Healthcare Life Sciences, Buckinghamshire, UK) and sequenced using a BigDye Terminator v1.1 Cycle Sequencing Kit (Applied Biosystems, Foster City, CA, USA) on an ABI PRISM 3130xl Genetic Analyser (Applied Biosystems, Foster City, CA, USA). Results were analyzed with FINCHTV sequence analysis software, version 1.3.1. Sequencing profiles were compared with the *IDS* reference sequence ENST00000340855.11 [https://www.ensembl.org (accessed on 1 December 2023)] using the Clustal Omega multiple sequence alignment bioinformatic tool [https://www.ebi.ac.uk/Tools/msa/clustalo/ (accessed on 1 December 2023)]. The presence of the variants found in both patients was also confirmed at cDNA level. Briefly, total RNA was extracted from independent cell pellets using GRS Total RNA-Blood & Cultured Cells Kit (GRiSP, Lda., Porto, Portugal). 1 µg of RNA was reverse-transcribed using the Ready-To-Go You-Prime First-Strand Beads kit (GE Healthcare Life Sciences, Chicago, IL, USA), according to the manufacturer's instructions.

Importantly, only after fully genotyping the patients were the results confirmed by the clinicians, who had access to the patients' clinical file and molecular results from previous analyses.

4.4.2. qRT-PCR Analyses

qRT-PCR was performed for MSCs' related gene sequences from Bio-Rad® (Bio-Rad Laboratories, Hercules, CA, USA) to confirm the DPSC/MSC phenotype identity of the established cell lines: *CD34* (qHsaCID0007456), *CD90/THY1* (qHsaCED0036661), *CD73/NT5E* (qHsaCID0036556), *CD105/ENG* (qHsaCID0010800), *CD166/ALCAM* (qHsaCID0037887), *CD117/c-kit* (qHsaCID0008692), *Sox2* (qHsaCED0036871), *Oct-3/4/POU5F1* (qHsaCED0038334), *MHC I/HLA-A* (qHsaCED0037388), *MHC II/HLA-DRA* (qHsaCED0037296) and housekeeping genes: *ACTB* (qHsaCED0036269), *GAPDH* (qHsaCED0038674).

Total RNA was extracted as described in the previous section, and reverse-transcribed using the same kits. Nevertheless, for qRT-PCR analyses, lower amounts of total RNA were used for cDNA synthesis (0.5–1 µg). qPCR was performed in a Bio-Rad CFX 96 Touch Real-Time PCR Detection System (Bio-Rad Laboratories, Hercules, CA, USA) apparatus using the iTAQTM SYBR® Green Supermix (Bio-Rad Laboratories, Hercules, CA, USA). All plates were designed to contain duplicates of targeted human genes as well as a negative control. Recommended Bio-Rad PrimePCR cycling protocol was employed in all cases: 95 °C for 2 min (activation), 40 cycles comprising 95 °C for 5 s (denaturation), 60 °C for 30 s (annealing), and 65–95 °C (0.5 °C increment), 5 s/step (melt curve). The number of cycles for each well was recorded. Data were processed using Bio-Rad CFX® Manager Software 3.1 (Bio-Rad Laboratories, Hercules, CA, USA). Fold differences were calculated using the standard ΔCq method with *GAPDH* and *ACTB* as housekeeping genes.

4.5. Biochemical Analyses

4.5.1. Fluorometric IDS Enzyme Assay

Control (WT) and MPS II-derived SHEDs were used in the determination of IDS enzyme activity. Briefly, cell homogenates were prepared by sonication, and their protein concentration determined using the Pierce™ BCA Protein Assay Kit (TermoFisher Scientific, Waltham, MA, USA) and measured by spectrophotometer (VICTOR® Nivo™ Plate Reader, PerkinElmer Inc., Waltham, MA, USA). Then, the IDS enzyme activity was assayed using fluorogenic substrate 4MU-α-L-iduronate-2-sulfate, according to the method described by Voznyi et al. [61], and the fluorescence was measured in the fluorimeter (VICTOR® Nivo™ Plate Reader, PerkinElmer Inc, Waltham, MA, USA). The enzyme activity was determined according to a calibration curve constructed using 4MU, and normalized to 1 mg/mL of protein.

4.5.2. Other Enzymatic Assays for Additional Lysosomal Enzymes

Other lysosomal enzyme activities were also measured in control (WT) and MPS II-derived SHEDs, namely, beta-galactosidase (GLB1, E.C. 3.2.1.23, the enzyme deficient in either GM1-gangliosidosis or MPS IVB), beta-glucuronidase (GUSB, E.C. 3.2.1.31, the enzyme deficient in MPS VII), hexosaminidase A (HEXA, E.C. 3.2.1.52, the enzyme deficient in GM2-gangliosidosis), alpha-N-acetyl-glucosaminidase (NAGLU, E.C. 3.2.1.50, the enzyme deficient in MPS IIIB) and alpha-galactosidase (GLA, E.C. 3.2.1.22, the enzyme deficient in Fabry disease). All measurements relied on the breakdown of specific 4MU substrates, except for that of arylsulfatase B (ARSB, E.C. 3.1.6.12), which relied on the use of an artificial chromogenic, substrate 4-nitrocatechol sulfate [62,63]. The enzyme activity was determined according to a calibration curve done with 4MU, and normalized to 1 mg/mL of protein.

4.5.3. Glycosaminoglycans Quantification by LC-MS/MS

GAGs were quantified by simultaneous analysis of DS and HS in WT and MPS II-derived SHED homogenates, by LC-MS/MS, after butanolysis reaction, according to the method recently described by Forni and co-workers [55,64]. While initially described to perform HS and DS analysis in urine samples, this method was adapted to quantify the same compounds in cell homogenates. Briefly, cell homogenates were prepared by sonication, and their protein concentration determined with the same method described in Section 4.5.1. Each individual cell homogenate was divided into two different sample tubes, one for HS and another for DS. Samples were then dried under a stream of nitrogen and 75 µL of 3N HCl in N-butanol added to each vial. For HS measurements, samples were incubated for 60 min at 90 °C. For DS measurements, on the other hand, samples were heated for 25 min at 65 °C. After those incubations, samples were cooled back to room temperature for 10 min and dried under a stream of nitrogen. 100 µL of a 30:70 water/acetonitrile (v/v) solution were then added to each HS tube, and 250 µL to each DS tube and briefly vortexed. Then, the DS samples were combined with their respective HS counterparts and vortexed again. Finally, dimers derived from butanolysis reactions were chromatographed on HPLC using a gradient of acetonitrile and water (LC column: Gemini® 3 µm C6-Phenyl 110 Å, 100 × 2 mm, from Phenomenex, Torrance, CA, USA) and detected on a triple quadrupole mass spectrometer (API4000 QTRAP from Sciex, Redwood City, CA, USA). Samples were quantified by interpolation from the calibration curve (prepared to cover a concentration range from 0.39 to 50 µg/mL for HS and from 1.56 to 100 µg/mL for DS using seven different levels) and reported in mg/mL. Then, HS and DS were normalized to protein concentration and finally reported as mg/mg protein.

4.5.4. LAMP1 Immunostaining

LAMP1 immunostaining was performed as previously reported in Encarnação et al. [65]. Briefly, WT and MPS II-derived SHEDs were seeded (approximately 25,000 cells/well) in 8-well chamber slides (Nunc, Roskilde, Denmark), fixed with 4% PFA/PBS for 30 min, quenched with 0.05 M NH_4Cl, permeabilized in ice-cold methanol for 10 min, and blocked with 5% BSA (Sigma-Aldrich, St. Louis, MO, USA), according to standard procedures. Coverslips were washed three times in PBS and once in water, mounted (Fluoroshield™ with DAPI, Sigma-Aldrich, St. Louis, MO, USA) and examined by fluorescence microscopy (Leica TCS-SPE confocal microscope; Leica, Wetzlar, Germany). Spectral detection adjusted for the emission of DAPI and Alexa Fluor™ fluorochromes using the 405-, 488-, and 546-laser lines, respectively. Digital images were analyzed using ImageJ version 2.0.0. Details on the antibodies used and their respective dilutions are listed in Table 3.

4.5.5. Lysosphingolipid Quantification by LC-MS/MS

Simultaneous quantification of sphingoid bases (lysosphingolipids) were quantified by LC-MS/MS as previously reported [57]. Cell pellets were lysed by sonication on ice, and a lysolactosylceramide internal standard was added to each sample. Protein concentration

for each sample was determined with the same method described in Section 4.5.1. Then, sphingoid bases were extracted from cell lysates by a modified Bligh and Dyer extraction with acidic buffer [66]. Briefly, a mixture of chloroform:methanol was added to the samples, stirred an subsequently centrifuged for protein precipitation. Then, chloroform:methanol:water was used to extract the sphingoid bases, which were eluted in the upper phase after subsequent rounds of stirring and centrifugation. Eluted sphingoid bases were dried under a stream of nitrogen and reconstituted in methanol for LC-MS/MS detection on a triple-quadrupole mass spectrometer (API4000 QTRAP from Sciex, Redwood City, CA, USA). Samples were quantified by interpolation from the calibration curve and reported in pmolg/mL, and subsequently normalized to protein concentration (pmolg/mg protein).

4.6. Multi-Lineage Differentiation Protocol

The multi-lineage differentiation capacity of the established SHED cell lines was assessed with a straightforward protocol to promote SHEDs differentiation into the three germ layers.

Briefly, control and patient-derived SHEDs (px5–px7) were plated onto 24-well plates (8000 viable cells/cm^2) and cultured in standard media until reaching a confluency of 70–80% of culture surface. The Human Pluripotent Stem Cell Functional Identification Kit (R&D Systems, Minneapolis, MN, USA) was then used to differentiate into endoderm and ectoderm, according to the manufacturer's instructions. For mesoderm differentiation, however, a slight alternation to the original protocol was performed, by adding the CHIR99021 supplement (Stemcell Technologies, Vancouver, BC, Canada), a WNT pathway activator, to the Differentiation Base Media Supplement (50X), which is part of the kit Stem Cell Functional Identification, as previously reported [38]. For the immunocytochemistry, antibodies against Otx2, Brachyury, and Sox17 were used as markers for ectoderm, mesoderm and endoderm, respectively. Briefly, seeded SHEDs were fixed in 4% paraformaldehyde (Sigma-Aldrich, St. Louis, MO, USA) for 10 min, incubated with PBST with 1% BSA (Sigma-Aldrich, St. Louis, MO, USA) for 30 min and stained by standard immunofluorescence procedures. Cells were analyzed on DM400 M fluorescence microscope (Leica, Wetzlar, Germany). Antibodies are listed in Table 3.

4.7. Statistical Analysis

Statistical analysis was performed using GraphPad PrismVR (version 9, GraphPad Software, La Jolla, CA, USA). Results are presented as means ± standard error of the mean (SEM). Comparisons between groups were performed by one-way analysis of variance followed by Tukey's multiple comparisons test. Differences were considered statistically significant when $p \leq 0.05$. Significant results between groups are presented using the symbol (*). Significance results are also indicated according to p values with one, two, three or four of the symbols (*) corresponding to $0.01 < p \leq 0.05$, $0.001 < p \leq 0.01$, $0.0001 < p \leq 0.001$ and $p \leq 0.0001$, respectively.

5. Conclusions

Here, we present our results on the establishment and characterization of two MPS II patient-derived stem cell lines from deciduous teeth. Quite remarkably, hallmark LSD features, namely, the presence of storage (GAGs, in this particular case) and of an abnormal LAMP1 staining pattern, are already evident in these cells. This is particularly relevant, since those features were not reported by other groups in MPS II-derived iPSCs [19]. Instead, iPSCs seem to need further differentiation in order to show the storage phenotype, which usually becomes evident only in NPCs or neural stem cells [19,20]. Altogether, this is a completely new observation in the field, and we believe it holds potential to set a new trend for investigating not only the subcellular pathology of virtually any LSD but also any gene expression changes that may occur in these pathologies. It may also allow for reliable genotype–phenotype correlations, as soon as significant samples from the same disorder are collected and their derived cell lines established.

Overall, this method relies on a non-invasive, cost-effective approach that can be set as a routine in any lab with standard cell culture conditions. By incredibly diminishing the costs associated with the establishment of a pluripotent cell line (which would otherwise rely on expensive, laboriouso and time-consuming iPSC generation and characterization protocols), this protocol may allow a significant number of laboratories to establish their first LSD-derived stem cell lines. The fact that some of the major LSD pathological hallmarks are already evident in the SHED state, even before any differentiation protocol is attempted, further validates the modeling potential of these dental-derived MSC cultures for this challenging group of disorders.

Having documented the major primary LSD pathological hallmarks in the established cell lines, our goal is now to increase the catalogue of MPS diseases with immortalized/established SHED cell lines, as well as that of available phenotypes for the same disease. Then, we will perform comparative analyses on a number of additional parameters, including secondary storage of lipids [not only by lysosphingolipid biomarker quantification as performed here, but also by analyzing GM2 and GM3 gangliosides, bis(monoacylglycero)phosphate and total cholesterol levels], and pathophysiological assessments [e.g., evaluations of the apoptosis rate or endoplasmic reticulum (ER) stress levels].

Supplementary Materials: The supporting information can be downloaded at https://www.mdpi.com/article/10.3390/ijms25063546/s1.

Author Contributions: Conceptualization, M.F.C. and S.A.; cell culture, S.C., J.I.S., D.R. and M.F.C.; molecular analysis, S.C., M.G. and M.F.C.; qRT-PCR, S.C., J.I.S., M.G., L.M. (Luciana Moreira) and A.J.D.; immunofluorescence/immunostaining, S.C., A.J.D., H.D. and M.E.; LC-MS/MS, M.F.C., J.I.S., M.B.A. and H.R.; enzyme activities, S.C., M.F.C. and P.G.; statistical analysis, S.C., M.F.C., J.I.S., L.M. (Luciana Moreira), P.G. and H.R.; clinical characterization, L.D., S.F., C.S. and E.M.; resources, M.F.C., S.A., M.E. and O.A.; data curation, S.C., J.I.S., M.E. and L.M. (Luciana Moreira); writing—original draft preparation, S.C. and M.F.C.; writing—review and editing, S.A. and L.M. (Luciana Moreira); critical review, O.A., L.M. (Liliana Matos) and M.J.P.; figures and tables, S.C. and M.F.C.; supervision, L.P.d.A. and S.A.; project administration, M.F.C. and P.G.; funding acquisition, M.F.C., M.E., O.A. and S.A. All authors have read and agreed to the published version of the manuscript.

Funding: This work was financed by national funds through FCT—*Fundação para a Ciência e a Tecnologia*, I.P., within the scope of the project EXPL/BTM-SAL/0659/2021 (http://doi.org/10.54499/EXPL/BTM-SAL/0659/2021). This work was also partially supported by Sanfilippo Children's Foundation (2019DGH1656/SCF2019I&D) and the Portuguese Society for Metabolic Disorders, SPDM (*Bolsa SPDM de apoio à investigação Dr. Aguinaldo Cabral 2018*; 2019DGH1629/SPDM2018I&D). Some specific tasks also benefited from additional funds: LAMP1 staining was performed according to the method implemented under the scope of the ongoing FCT project EXPL/BTM-TEC/1477/2021 and using its associated reagents; similarly, the differentiation into the three-germ-layer protocol was performed using a kit acquired and implemented under the scope of another FCT project, previously conducted in the lab (PTDC/BIM-MEC/4762/2014).

Institutional Review Board Statement: The study was conducted in accordance with the Declaration of Helsinki and approved by the Ethics Committee of the National Institute of Health Dr. Ricardo Jorge, INSA, I.P. (date of approval 28 June 2020).

Informed Consent Statement: Written informed consent had been obtained from the subjects who provided their samples for SHED cell lines' establishment and, whenever necessary/adequate, subsequent differentiation into disease-relevant cell lines.

Data Availability Statement: Data are contained within the article and Supplementary Materials.

Acknowledgments: The authors wish to thank the many different people who greatly contributed to the overall success of this project: (1) the patients and their families, for agreeing to participate in this study and gently providing us their baby teeth right after they fell; (2) the numerous families, who have donated control (WT) teeth for the extraction of stem cells, aiming to help us further understand a rare genetic disorder, of which most of them had never heard; (3) everyone who contributed to disseminating this project and spreading our "Call for volunteers" appeal, from patient associations (namely, *Associação Sanfilippo Portugal; Associação Portuguesa de Doenças do Lisossoma*, APL;

and RD-Portugal) to science communicators, journalists, and opinion-makers (namely, Cristina Nobre Soares, Luís Aguiar-Conraria, Ana Stilwell, Isabel Stilwell, Vera Gouveia Barros and Marco Neves); and finally (4) the Portuguese company Little Drops of Water, who gently offered each one of our volunteers a tiny hand-painted resin figure of the tooth fairy. Special thanks to Raquel Neiva for technical assistance in the simultaneous quantification of lysosphingolipid quantified by LC-MS/MS.

Conflicts of Interest: The authors declare no conflicts of interest.

References

1. Khan, S.A.; Peracha, H.; Ballhausen, D.; Wiesbauer, A.; Rohrbach, M.; Gautschi, M.; Mason, R.W.; Giugliani, R.; Suzuki, Y.; Orii, K.E.; et al. Epidemiology of Mucopolysaccharidoses. *Mol. Genet. Metab.* **2017**, *121*, 227–240. [CrossRef] [PubMed]
2. D'Avanzo, F.; Rigon, L.; Zanetti, A.; Tomanin, R. Mucopolysaccharidosis Type II: One Hundred Years of Research, Diagnosis, and Treatment. *Int. J. Mol. Sci.* **2020**, *21*, 1258. [CrossRef]
3. Hunter, C. A Rare Disease in Two Brothers. *Proc. R. Soc. Med.* **1917**, *10*, 104–116. [CrossRef]
4. Bach, G.; Eisenberg, F.; Cantz, M.; Neufeld, E.F. The Defect in the Hunter Syndrome: Deficiency of Sulfoiduronate Sulfatase. *Proc. Natl. Acad. Sci. USA* **1973**, *70*, 2134–2138. [CrossRef] [PubMed]
5. Wilson, P.J.; Meaney, C.A.; Hopwood, J.J.; Morris, C.P. Sequence of the Human Iduronate 2-Sulfatase (IDS) Gene. *Genomics* **1993**, *17*, 773–775. [CrossRef]
6. Wilson, P.J.; Morris, C.P.; Anson, D.S.; Occhiodoro, T.; Bielicki, J.; Clements, P.R.; Hopwood, J.J. Hunter Syndrome: Isolation of an Iduronate-2-Sulfatase CDNA Clone and Analysis of Patient DNA. *Proc. Natl. Acad. Sci. USA* **1990**, *87*, 8531–8535. [CrossRef] [PubMed]
7. Froissart, R.; Da Silva, I.M.; Maire, I. Mucopolysaccharidosis Type II: An Update on Mutation Spectrum. *Acta Paediatr. Int. J. Paediatr.* **2007**, *96*, 71–77. [CrossRef]
8. Horgan, C.; Jones, S.A.; Bigger, B.W.; Wynn, R. Current and Future Treatment of Mucopolysaccharidosis (MPS) Type II: Is Brain-Targeted Stem Cell Gene Therapy the Solution for This Devastating Disorder? *Int. J. Mol. Sci.* **2022**, *23*, 4854. [CrossRef]
9. Fesslová, V.; Corti, P.; Sersale, G.; Rovelli, A.; Russo, P.; Mannarino, S.; Butera, G.; Parini, R. The Natural Course and the Impact of Therapies of Cardiac Involvement in the Mucopolysaccharidoses. *Cardiol. Young* **2009**, *19*, 170–178. [CrossRef]
10. Jones, S.A.; Parini, R.; Harmatz, P.; Giugliani, R.; Fang, J.; Mendelsohn, N.J. The Effect of Idursulfase on Growth in Patients with Hunter Syndrome: Data from the Hunter Outcome Survey (HOS). *Mol. Genet. Metab.* **2013**, *109*, 41–48. [CrossRef]
11. Wraith, J.E.; Scarpa, M.; Beck, M.; Bodamer, O.A.; De Meirleir, L.; Guffon, N.; Meldgaard Lund, A.; Malm, G.; Van Der Ploeg, A.T.; Zeman, J. Mucopolysaccharidosis Type II (Hunter Syndrome): A Clinical Review and Recommendations for Treatment in the Era of Enzyme Replacement Therapy. *Eur. J. Pediatr.* **2008**, *167*, 267–277. [CrossRef]
12. Tomanin, R.; Zanetti, A.; D'Avanzo, F.; Rampazzo, A.; Gasparotto, N.; Parini, R.; Pascarella, A.; Concolino, D.; Procopio, E.; Fiumara, A.; et al. Clinical Efficacy of Enzyme Replacement Therapy in Paediatric Hunter Patients, an Independent Study of 3.5 Years. *Orphanet J. Rare Dis.* **2014**, *9*, 129. [CrossRef]
13. Moreira, G.A.; Kyosen, S.O.; Patti, C.L.; Martins, A.M.; Tufik, S. Prevalence of Obstructive Sleep Apnea in Patients with Mucopolysaccharidosis Types I, II, and VI in a Reference Center. *Sleep. Breath.* **2014**, *18*, 791–797. [CrossRef]
14. Martin, R.; Beck, M.; Eng, C.; Giugliani, R.; Harmatz, P.; Muñoz, V.; Muenzer, J. Recognition and Diagnosis of Mucopolysaccharidosis II (Hunter Syndrome). *Pediatrics* **2008**, *121*, e377–e386. [CrossRef]
15. Fecarotta, S.; Tarallo, A.; Damiano, C.; Minopoli, N.; Parenti, G. Pathogenesis of Mucopolysaccharidoses, an Update. *Int. J. Mol. Sci.* **2020**, *21*, 2515. [CrossRef]
16. Lampe, C.; Bosserhoff, A.K.; Burton, B.K.; Giugliani, R.; de Souza, C.F.; Bittar, C.; Muschol, N.; Olson, R.; Mendelsohn, N.J. Long-Term Experience with Enzyme Replacement Therapy (ERT) in MPS II Patients with a Severe Phenotype: An International Case Series. *J. Inherit. Metab. Dis.* **2014**, *37*, 823–829. [CrossRef]
17. Muenzer, J.; Botha, J.; Harmatz, P.; Giugliani, R.; Kampmann, C.; Burton, B.K. Evaluation of the Long-Term Treatment Effects of Intravenous Idursulfase in Patients with Mucopolysaccharidosis II (MPS II) Using Statistical Modeling: Data from the Hunter Outcome Survey (HOS). *Orphanet J. Rare Dis.* **2021**, *16*, 1–14. [CrossRef] [PubMed]
18. Parini, R.; Deodato, F. Intravenous Enzyme Replacement Therapy in Mucopolysaccharidoses: Clinical Effectiveness and Limitations. *Int. J. Mol. Sci.* **2020**, *21*, 2975. [CrossRef] [PubMed]
19. Rybová, J.; Ledvinová, J.; Sikora, J.; Kuchař, L.; Dobrovolný, R. Neural Cells Generated from Human Induced Pluripotent Stem Cells as a Model of CNS Involvement in Mucopolysaccharidosis Type II. *J. Inherit. Metab. Dis.* **2018**, *41*, 221–229. [CrossRef]
20. Kobolák, J.; Molnár, K.; Varga, E.; Bock, I.; Jezsó, B.; Téglási, A.; Zhou, S.; Lo Giudice, M.; Hoogeveen-Westerveld, M.; Pijnappel, W.P.; et al. Modelling the Neuropathology of Lysosomal Storage Disorders through Disease-Specific Human Induced Pluripotent Stem Cells. *Exp. Cell Res.* **2019**, *380*, 216–233. [CrossRef]
21. Hong, J.; Cheng, Y.S.; Yang, S.; Swaroop, M.; Xu, M.; Beers, J.; Zou, J.; Huang, W.; Marugan, J.J.; Cai, X.; et al. IPS-Derived Neural Stem Cells for Disease Modeling and Evaluation of Therapeutics for Mucopolysaccharidosis Type II. *Exp. Cell Res.* **2022**, *412*, 113007. [CrossRef]

22. Carvalho, S.; Santos, J.I.; Moreira, L.; Gonçalves, M.; David, H.; Matos, L.; Encarnação, M.; Alves, S.; Coutinho, M.F. Neurological Disease Modeling Using Pluripotent and Multipotent Stem Cells: A Key Step towards Understanding and Treating Mucopolysaccharidoses. *Biomedicines* **2023**, *11*, 1234. [CrossRef]
23. Miura, M.; Gronthos, S.; Zhao, M.; Lu, B.; Fisher, L.W.; Robey, P.G.; Shi, S. SHED: Stem Cells from Human Exfoliated Deciduous Teeth. *Proc. Natl. Acad. Sci. USA* **2003**, *100*, 5807–5812. [CrossRef]
24. Kerkis, I.; Kerkis, A.; Dozortsev, D.; Stukart-Parsons, G.C.; Gomes Massironi, S.M.; Pereira, L.V.; Caplan, A.I.; Cerruti, H.F. Isolation and Characterization of a Population of Immature Dental Pulp Stem Cells Expressing OCT-4 and Other Embryonic Stem Cell Markers. *Cells Tissues Organs* **2006**, *184*, 105–116. [CrossRef]
25. Huang, G.T.J.; Gronthos, S.; Shi, S. Critical Reviews in Oral Biology & Medicine: Mesenchymal Stem Cells Derived from Dental Tissues vs. Those from Other Sources: Their Biology and Role in Regenerative Medicine. *J. Dent. Res.* **2009**, *88*, 792–806. [CrossRef]
26. Pivoriuunas, A.; Surovas, A.; Borutinskaite, V.; Matuzevičius, D.; Treigyte, G.; Savickiene, J.; Tunaitis, V.; Aldonyte, R.; Jarmalavičiuute, A.; Suriakaite, K.; et al. Proteomic Analysis of Stromal Cells Derived from the Dental Pulp of Human Exfoliated Deciduous Teeth. *Stem Cells Dev.* **2010**, *19*, 1081–1093. [CrossRef]
27. Rodríguez-Lozano, F.J.; Bueno, C.; Insausti, C.L.; Meseguer, L.; Ramírez, M.C.; Blanquer, M.; Marín, N.; Martínez, S.; Moraleda, J.M. Mesenchymal Stem Cells Derived from Dental Tissues. *Int. Endod. J.* **2011**, *44*, 800–806. [CrossRef]
28. Yoshida, S.; Tomokiyo, A.; Hasegawa, D.; Hamano, S.; Sugii, H.; Maeda, H. Insight into the Role of Dental Pulp Stem Cells in Regenerative Therapy. *Biology* **2020**, *9*, 160. [CrossRef]
29. Taghipour, Z.; Karbalaie, K.; Kiani, A.; Niapour, A.; Bahramian, H.; Nasr-Esfahani, M.H.; Baharvand, H. Transplantation of Undifferentiated and Induced Human Exfoliated Deciduous Teeth-Derived Stem Cells Promote Functional Recovery of Rat Spinal Cord Contusion Injury Model. *Stem Cells Dev.* **2012**, *21*, 1794–1802. [CrossRef]
30. Nicola, F.d.C.; Marques, M.R.; Odorcyk, F.; Arcego, D.M.; Petenuzzo, L.; Aristimunha, D.; Vizuete, A.; Sanches, E.F.; Pereira, D.P.; Maurmann, N.; et al. Neuroprotector Effect of Stem Cells from Human Exfoliated Deciduous Teeth Transplanted after Traumatic Spinal Cord Injury Involves Inhibition of Early Neuronal Apoptosis. *Brain Res.* **2017**, *1663*, 95–105. [CrossRef]
31. Nishii, T.; Osuka, K.; Nishimura, Y.; Ohmichi, Y.; Ohmichi, M.; Suzuki, C.; Nagashima, Y.; Oyama, T.; Abe, T.; Kato, H.; et al. Protective Mechanism of Stem Cells from Human Exfoliated Deciduous Teeth in Treating Spinal Cord Injury. *J. Neurotrauma* **2024**, *41*. [CrossRef]
32. Yamagata, M.; Yamamoto, A.; Kako, E.; Kaneko, N.; Matsubara, K.; Sakai, K.; Sawamoto, K.; Ueda, M. Human Dental Pulp-Derived Stem Cells Protect against Hypoxic-Ischemic Brain Injury in Neonatal Mice. *Stroke* **2013**, *44*, 551–554. [CrossRef]
33. Liu, Y.; Wang, L.; Liu, S.; Liu, D.; Chen, C.; Xu, X.; Chen, X.; Shi, S. Transplantation of SHED Prevents Bone Loss in the Early Phase of Ovariectomy-Induced Osteoporosis. *J. Dent. Res.* **2014**, *93*, 1124–1132. [CrossRef]
34. Yamaza, T.; Alatas, F.S.; Yuniartha, R.; Yamaza, H.; Fujiyoshi, J.K.; Yanagi, Y.; Yoshimaru, K.; Hayashida, M.; Matsuura, T.; Aijima, R.; et al. In Vivo Hepatogenic Capacity and Therapeutic Potential of Stem Cells from Human Exfoliated Deciduous Teeth in Liver Fibrosis in Mice. *Stem Cell Res. Ther.* **2015**, *6*, 1–16. [CrossRef]
35. Sonoda, S.; Yamaza, T. A New Target of Dental Pulp-Derived Stem Cell-Based Therapy on Recipient Bone Marrow Niche in Systemic Lupus Erythematosus. *Int. J. Mol. Sci.* **2022**, *23*, 3479. [CrossRef]
36. Katahira, Y.; Murakami, F.; Inoue, S.; Miyakawa, S.; Sakamoto, E.; Furusaka, Y.; Watanabe, A.; Sekine, A.; Kuroda, M.; Hasegawa, H.; et al. Protective Effects of Conditioned Media of Immortalized Stem Cells from Human Exfoliated Deciduous Teeth on Pressure Ulcer Formation. *Front. Immunol.* **2023**, *13*, 1010700. [CrossRef]
37. Victor, A.K.; Reiter, L.T. Dental Pulp Stem Cells for the Study of Neurogenetic Disorders. *Hum. Mol. Genet.* **2017**, *26*, R166–R171. [CrossRef]
38. Duarte, A.J.; Ribeiro, D.; Santos, R.; Moreira, L.; Bragança, J.; Amaral, O. Induced Pluripotent Stem Cell Line (INSAi002-A) from a Fabry Disease Patient Hemizygote for the Rare p.W287X Mutation. *Stem Cell Res.* **2020**, *45*, 101794. [CrossRef]
39. Alves, S.; Mangas, M.; Prata, M.; Ribeiro, G.; Lopes, L.; Ribeiro, H.; Pinto-Basto, J.; Lima Reis, M.; Lacerda, L. Molecular Characterization of Portuguese Patients with Mucopolysaccharidosis Type II Shows Evidence That the IDS Gene Is Prone to Splicing Mutations. *J. Inherit. Metab. Dis.* **2006**, *29*, 743–754. [CrossRef]
40. Lagerstedt, K.; Karsten, S.L.; Carlberg, B.M.; Kleijer, W.J.; Tönnesen, T.; Pettersson, U.; Bondeson, M.L. Double-Strand Breaks May Initiate the Inversion Mutation Causing the Hunter Syndrome. *Hum. Mol. Genet.* **1997**, *6*, 627–633. [CrossRef]
41. Goorha, S.; Reiter, L.T. Culturing and Neuronal Differentiation of Human Dental Pulp Stem Cells. *Curr. Protoc. Hum. Genet.* **2017**, *2017*, 21.6.1–21.6.10. [CrossRef] [PubMed]
42. Pesce, M.; Schöler, H.R. *Oct-4*: Gatekeeper in the Beginnings of Mammalian Development. *Stem Cells* **2001**, *19*, 271–278. [CrossRef] [PubMed]
43. Mitsui, K.; Tokuzawa, Y.; Itoh, H.; Segawa, K.; Murakami, M.; Takahashi, K.; Maruyama, M.; Maeda, M.; Yamanaka, S. The Homeoprotein Nanog Is Required for Maintenance of Pluripotency in Mouse Epiblast and ES Cells. *Cell* **2003**, *113*, 631–642. [CrossRef] [PubMed]
44. Avilion, A.A.; Nicolis, S.K.; Pevny, L.H.; Perez, L.; Vivian, N.; Lovell-Badge, R. Multipotent Cell Lineages in Early Mouse Development Depend on SOX2 Function. *Genes Dev.* **2003**, *17*, 126–140. [CrossRef] [PubMed]
45. Grau-vorster, M.; Laitinen, A.; Nystedt, J.; Vives, J. HLA-DR Expression in Clinical-Grade Bone Marrow-Derived Multipotent Mesenchymal Stromal Cells: A Two-Site Study. *Stem Cell Res. Ther.* **2019**, *9*, 164. [CrossRef]

46. Sidney, L.E.; Branch, M.J.; Dunphy, S.E.; Dua, H.S.; Hopkinson, A. Concise Review: Evidence for CD34 as a Common Marker for Diverse Progenitors. *Stem Cells* **2014**, *32*, 1380–1389. [CrossRef]
47. Campos, J.M.; Sousa, A.C.; Caseiro, A.R.; Pedrosa, S.S.; Pinto, P.O.; Branquinho, M.V.; Amorim, I.; Santos, J.D.; Pereira, T.; Mendonça, C.M.; et al. Dental Pulp Stem Cells and Bonelike®for Bone Regeneration in Ovine Model. *Regen. Biomater.* **2019**, *6*, 49–59. [CrossRef] [PubMed]
48. Dominici, M.; Le Blanc, K.; Mueller, I.; Slaper-Cortenbach, I.; Marini, F.C.; Krause, D.S.; Deans, R.J.; Keating, A.; Prockop, D.J.; Horwitz, E.M. Minimal Criteria for Defining Multipotent Mesenchymal Stromal Cells. The International Society for Cellular Therapy Position Statement. *Cytotherapy* **2006**, *8*, 315–317. [CrossRef]
49. McNiece, I. Subsets of Mesenchymal Stromal Cells. *Cytotherapy* **2007**, *9*, 301–302. [CrossRef]
50. Chai, Y.; Jiang, X.; Ito, Y.; Bringas, P.; Han, J.; Rowitch, D.H.; Soriano, P.; Mcmahon, A.P.; Sucov, H.M. Fate of the Mammalian Cranial Neural Crest during Tooth and Mandibular Morphogenesis. *Development* **2000**, *1679*, 1671–1679. [CrossRef]
51. Kashyap, R. SHED—Basic Structure for Stem Cell Research. *J. Clin. Diagn. Res.* **2015**, *9*, ZE07–ZE09. [CrossRef]
52. Vafiadaki, E.; Cooper, A.; Heptinstall, L.E.; Hatton, C.E.; Thornley, M.; Wraith, J.E. Mutation Analysis in 57 Unrelated Patients with MPS II (Hunter's Disease). *Arch. Dis. Child.* **1998**, *79*, 237–241. [CrossRef]
53. Lualdi, S.; Tappino, B.; Di Duca, M.; Dardis, A.; Anderson, C.J.; Biassoni, R.; Thompson, P.W.; Corsolini, F.; Di Rocco, M.; Bembi, B.; et al. Enigmatic in Vivo Iduronate-2-Sulfatase (IDS) Mutant Transcript Correction to Wild-Type in Hunter Syndrome. *Hum. Mutat.* **2010**, *31*, 1261–1285. [CrossRef]
54. Filocamo, M.; Bonuccelli, G.; Corsolini, F.; Mazzotti, R.; Cusano, R.; Gatti, R. Molecular Analysis of 40 Italian Patients with Mucopolysaccharidosis Type II: New Mutations in the Iduronate-2-Sulfatase (IDS) Gene. *Hum. Mutat.* **2001**, *18*, 164–165. [CrossRef] [PubMed]
55. Forni, G.; Malvagia, S.; Funghini, S.; Scolamiero, E.; Mura, M.; Della Bona, M.; Villanelli, F.; Damiano, R.; la Marca, G. LC-MS/MS Method for Simultaneous Quantification of Heparan Sulfate and Dermatan Sulfate in Urine by Butanolysis Derivatization. *Clin. Chim. Acta* **2019**, *488*, 98–103. [CrossRef] [PubMed]
56. Morimoto, H.; Kida, S.; Yoden, E.; Kinoshita, M.; Tanaka, N.; Yamamoto, R.; Koshimura, Y.; Takagi, H.; Takahashi, K.; Hirato, T.; et al. Clearance of Heparan Sulfate in the Brain Prevents Neurodegeneration and Neurocognitive Impairment in MPS II Mice. *Mol. Ther.* **2021**, *29*, 1853–1861. [CrossRef] [PubMed]
57. Mirzaian, M.; Wisse, P.; Ferraz, M.J.; Marques, A.R.A.; Gaspar, P.; Oussoren, S.V.; Kytidou, K.; Codée, J.D.C.; van der Marel, G.; Overkleeft, H.S.; et al. Simultaneous Quantitation of Sphingoid Bases by UPLC-ESI-MS/MS with Identical 13C-Encoded Internal Standards. *Clin. Chim. Acta* **2017**, *466*, 178–184. [CrossRef] [PubMed]
58. Dekaban, A.S.; Constantopoulos, G. Mucopolysaccharidosis Types I, II, III A and V Pathological and Biochemical Abnormalities in the Neural and Mesenchymal Elements of the Brain. *Acta Neuropath.* **1977**, *39*, 1–7. [CrossRef] [PubMed]
59. Spiewak, J.; Doykov, I.; Papandreou, A.; Hällqvist, J.; Mills, P.; Clayton, P.T.; Gissen, P.; Mills, K.; Heywood, W.E. New Perspectives in Dried Blood Spot Biomarkers for Lysosomal Storage Diseases. *Int. J. Mol. Sci.* **2023**, *24*, 10177. [CrossRef] [PubMed]
60. de Bode, C.J.; Dogterom, E.J.; Rozeboom, A.V.J.; Langendonk, J.J.; Wolvius, E.B.; van der Ploeg, A.T.; Oussoren, E.; Wagenmakers, M.A.E.M. Orofacial Abnormalities in Mucopolysaccharidosis and Mucolipidosis Type II and III: A Systematic Review. *JIMD Rep.* **2022**, *63*, 621–629. [CrossRef]
61. Voznyi, Y.N.; Keulemans, J.L.M.; Van Diggelen, O.P. A Fluorimetric Enzyme Assay for the Diagnosis of MPS II (Hunter Disease). *J. Inherit. Metab. Dis.* **2001**, *24*, 675–680. [CrossRef] [PubMed]
62. Chamoles, N.A.; Blanco, M.B.; Gaggioli, D.; Casentini, C. Hurler-like Phenotype: Enzymatic Diagnosis in Dried Blood Spots on Filter Paper. *Clin. Chem.* **2001**, *47*, 2098–2102. [CrossRef] [PubMed]
63. Civallero, G.; Michelin, K.; de Mari, J.; Viapiana, M.; Burin, M.; Coelho, J.C.; Giugliani, R. Twelve Different Enzyme Assays on Dried-Blood Filter Paper Samples for Detection of Patients with Selected Inherited Lysosomal Storage Diseases. *Clin. Chim. Acta* **2006**, *372*, 98–102. [CrossRef] [PubMed]
64. Forni, G.; Malvagia, S.; Funghini, S.; Scolamiero, E.; Mura, M.; Della Bona, M.; Villanelli, F.; Damiano, R.; la Marca, G. Data in Support for the Measurement of Heparan Sulfate and Dermatan Sulfate by LC–MS/MS Analysis. *Data Brief* **2018**, *21*, 2398–2404. [CrossRef]
65. Encarnação, M.; Coutinho, M.F.; Cho, S.M.; Cardoso, M.T.; Ribeiro, I.; Chaves, P.; Santos, J.I.; Quelhas, D.; Lacerda, L.; Leão Teles, E.; et al. NPC1 Silent Variant Induces Skipping of Exon 11 (p.V562V) and Unfolded Protein Response Was Found in a Specific Niemann-Pick Type C Patient. *Mol. Genet. Genom. Med.* **2020**, *8*, e1451. [CrossRef]
66. Bligh, E.G.; Dyer, W.J. A Rapid Method of Total Lipid Extraction and Purification. *Can. J. Biochem. Physiol.* **1959**, *39*, 911–917. [CrossRef]

Disclaimer/Publisher's Note: The statements, opinions and data contained in all publications are solely those of the individual author(s) and contributor(s) and not of MDPI and/or the editor(s). MDPI and/or the editor(s) disclaim responsibility for any injury to people or property resulting from any ideas, methods, instructions or products referred to in the content.

diagnostics

MDPI

Case Report

Molecular Characterization of a Novel Splicing Mutation Underlying Mucopolysaccharidosis (MPS) Type VI—Indirect Proof of Principle on Its Pathogenicity

Maria Francisca Coutinho [1,2,†], Marisa Encarnação [1,2,3,†], Liliana Matos [1,2], Lisbeth Silva [1,3], Diogo Ribeiro [1,2], Juliana Inês Santos [1,4], Maria João Prata [4,5], Laura Vilarinho [1,2,3] and Sandra Alves [1,2,*]

1 Research and Development Unit, Department of Human Genetics, INSA, 4000-055 Porto, Portugal; francisca.coutinho@insa.min-saude.pt (M.F.C.); marisa.encarnacao@insa.min-saude.pt (M.E.); liliana.matos@insa.min-saude.pt (L.M.); lisbeth.silva@insa.min-saude.pt (L.S.); diogo.ribeiro@insa.min-saude.pt (D.R.); juliana.santos@insa.min-saude.pt (J.I.S.); laura.vilarinho@insa.min-saude.pt (L.V.)

2 Center for the Study of Animal Science, CECA-ICETA, University of Porto, Praça Gomes Teixeira, 55142, 4051-401 Porto, Portugal

3 Newborn Screening, Metabolism and Genetics Unit, Department of Human Genetics, INSA, 4000-055 Porto, Portugal

4 Biology Department, Faculty of Sciences, University of Porto, 4150-179 Porto, Portugal; mprata@ipatimup.pt

5 i3S—Health Research and Innovation Institute, University of Porto, 4200-135 Porto, Portugal

* Correspondence: sandra.alves@insa.min-saude.pt; Tel.: +351-223-401-100

† These authors contributed equally to the work.

Received: 13 December 2019; Accepted: 16 January 2020; Published: 21 January 2020



Abstract: Here, we present the molecular diagnosis of a patient with a general clinical suspicion of Mucopolysaccharidosis, highlighting the different tools used to perform its molecular characterization. In order to decrease the turnaround time for the final report and contribute to reduce the "diagnostic odyssey", which frequently afflicts affected families, the proband's sample was simultaneously screened for mutations in a number of lysosomal function-related genes with targeted next-generation sequencing (NGS) protocol. After variant calling, the most probable cause for disease was a novel *ARSB* intronic variant, c.1213+5G>T [IVS6+5G>T], detected in homozygosity. In general, homozygous or compound heterozygous mutations in the *ARSB* gene, underlie MPS type VI or Maroteaux-Lamy syndrome. Still, even though the novel c.1213+5G>T variant was easy to detect by both NGS and Sanger sequencing, only through indirect studies and functional analyses could we present proof of principle on its pathogenicity. Globally, this case reminds us that whenever a novel variant is detected, its pathogenicity must be carefully assessed before a definitive diagnosis is established, while highlighting alternative approaches that may be used to assess its effect in the absence RNA/cDNA sample(s) from the proband. This is particularly relevant for intronic variants such as the one here reported. Special attention will be given to the use of reporter minigene systems, which may be constructed/designed to dissect the effect of this sort of alterations, providing an insight into their consequences over the normal pre-mRNA splicing process of the affected gene.

Keywords: mucopolysaccharidosis type VI (MPS VI); lysosomal storage disorders (LSDs); next-generation sequencing (NGS); splicing mutation; functional studies

1. Introduction

Lysosomal Storage Disorders (LSDs) are sometimes challenging to diagnose due to the wide spectrum of phenotypes that the patients may present [1]. Indeed, the recognition of LSDs clinical features requires clinical expertise, as most of them are not specific and can be caused by defects in other metabolic pathways (mitochondrial and peroxisomal) [1–4]. Therefore, it is common to have a long period between the onset of the first symptoms and the definitive diagnosis. Moreover, even in the presence of typical clinical signs and symptoms, samples and diagnostic tests are different for each group of lysosomal disorders, being often specific of a given disease [1,4]. This is one of the major reasons why definitive diagnosis of LSDs requires a close collaboration between laboratory specialists and clinicians, in order to reach a correct diagnosis in the shortest time. Biochemical genetic testing (BGT) in particular, which includes the determination of the enzymatic activity of lysosomal hydrolases, is feasible for most LSDs and essential for the diagnosis of primary lysosomal enzyme deficiency. In fact, the majority of patients is initially screened by enzyme assays and only after that the molecular studies are performed to determine the disease-causing mutation(s). In families with an already identified causative molecular defect, mutation analysis may be performed directly. Mutation analysis is done through molecular genetic testing (MGT), which can be performed either on DNA or RNA and comprises a range of different approaches for investigating the entire gene-coding regions and exon-intron boundaries, as well as the 5′ and 3′ untranslated regions (UTRs). It is not only useful but frequently necessary to confirm the enzymatic diagnosis of LSDs. For LSDs resulting from non-enzymatic lysosomal proteins, MGT is absolutely essential for a proper diagnosis [2]. Additionally, it is the identification of mutations in the proband and its family that allows for accurate, rapid and reliable MGT for other family members, including prenatal diagnosis. Naturally, the pathological significance of a novel variant has to be investigated before its application to diagnosis and counseling [3].

Whatever the case, MGT has not been used extensively as the primary diagnostic test for LSDs but this paradigm may be about to change thanks to the advent of the so-called next-generation sequencing (NGS), with its unprecedented throughput, scalability and speed [5]. This technology allows the sequencing of either the whole genome/exome or that of selected panels of genes, through a process known as targeted sequencing. Targeted sequencing in particular is now implemented in many labs and this technology is actively speeding up the solution of several diagnostic problems in the LSDs field, as demonstrated by several teams [6–18]. While being well known that with this unparalleled capacity, NGS is speeding up molecular diagnostics, it is also true that whenever a novel variant is detected, its pathogenicity must be carefully assessed. Furthermore, most specialist laboratories are still working with more traditional methods. Recently published statistics state that currently about 85–90% of LSDs cases are still diagnosed by demonstrating a deficiency of the activity of a lysosomal enzyme [3]. Finally, even for the laboratories where NGS technology is already available, it should always be considered whether a targeted panel will be the most obvious choice, as there are several preliminary screens that can point out, if not the individual disease, at least the subgroup to which it belongs.

For example, for the Mucopolysaccharidoses (MPS) subgroup, the preliminary screen in urine is a routine test that should always be considered. There are 11 different MPSs, resulting from deficiencies in any of the enzymes involved in the stepwise degradation of glycosaminoglycans (GAGs). Deficiencies in each of those enzymes result in different disorders, all sharing a series of clinical features, though in variable degrees: MPS I (OMIMs #607014; # 607015; # 607016); MPS II (#309900); MPS IIIA (#252900), IIIB (#252920), IIIC (#252930) and IIID (#252940); MPS IV A (#253000) and IV B (#253010); MPS VI (#253220); MPS VII (#253200) and MPS IX (#601492). Typical symptoms include organomegally, dysostosys multiplex and coarse facies. Central nervous system (CNS), hearing, vision and cardiovascular function may also be compromised [19].

Traditionally, MPSs are recognized through analysis of urinary GAGs. Over the years, several methods have been devised to allow both qualitative identification and quantitative measurements of the accumulated subtrate(s) [20–24]. Still, initial screenings of urinary GAGs allow discrimination

between broad classes of MPSs but cannot distinguish subgroups. In fact, as happens with many other LSDs, complete and definitive diagnosis may only be accessed through a combination of enzymatic assays and molecular analyses. Currently, there are countless specialist laboratories in Europe where those biochemical and genetic tests are carried out. Nevertheless, developing countries often lack the necessary resources/expertise for proper laboratory diagnosis of this type of rare genetic diseases. Being one of the laboratories where MGT for virtually all LSDs (MPSs included) is available for research purposes, we receive several samples from developing countries, whose clinicians and/or centers struggle to get a molecular characterization of affected individuals. Some of our results concerning those studies have already been published [25]. Still, every now and again, a case pops up to highlight how tricky and delicate this process can be, especially in non-optimal circumstances, i.e., without knowing the patient's clinical picture or assessing their biochemical study and in the absence of proper or sufficient sample(s).

Here, we present our results on the molecular characterization of one of those cases: a patient with a general clinical suspicion of MPS that we have received from Tunisia. Initial studies were performed in gDNA, by NGS with in a custom gene panel for LSDs that includes 86 genes implicated in lysosomal function. After variant calling, a novel homozygous mutation was detected in the *ARSB* gene, encoding arylsulfatase B, the enzyme deficient in MPS VI (Maroteaux-Lamy syndrome): c.1213+5G>T (IVS6+5G>T). Additional analyses included segregation studies through classical sequencing, cDNA sequencing of the *ARSB* gene of the proband's father, and functional analysis based on reporter minigenes. Altogether, these methods allowed for the full molecular characterization of the novel mutation here described and the indirect assessment of its effect on the normal *ARSB* pre-mRNA splicing.

2. Materials and Methods

2.1. Samples

Here, we studied a female patient from Tunisia with clinical suspicion of MPS. No further information was provided. Informed consent for genetic research was obtained from the individual guardians. Biological samples from healthy donors were also analyzed. The studies were conducted in agreement with the Declaration of Helsinki and approved by the Ethics Committee of Instituto Nacional de Saúde Dr. Ricardo Jorge (2015DGH1062 and 2016DGH1312), where biological samples were obtained.

2.2. Next-Generation Sequence Analysis

Genomic DNA was automated extracted and purified from total blood on a BioRobot EZ1 instrument (QIAGEN, Germantown, MD, USA), using the EZ1 DNA Blood 350 µL Kit (QIAGEN). An NGS-targeted panel covering exonic regions and intronic flanking regions of 86 genes was used. For library preparation, 500 ng of the previously extracted gDNA were used, according to the manufacture protocol (Agilent, Santa Clara, CA, USA). The step-by-step capture protocol is available online (Sureselect QXT Targeted Enrichment for Illumina Multiplexed Sequencing Protocol). The pool was prepared, denaturated, diluted and the sequencing was performed on an Illumina MiSeq platform according to the manufacture protocol for paired-end 150 base pair reads.

Custom-panel design for NGS was prepared with Sure Design software (Agilent Technologies) for the Targeted Enrichment System and Illumina platform based on the last genome build available (*H. sapiens*, hg19, GRCh37, 02.2009) and by selecting for a 150 base-pair read length. The target parameters were the coding exons and the UTRs, including a region extension of 25 bases from the 3′ end and 25 bases from the 5′ end (based on RefSeq database). The stringency parameter was selected to maximize the coverage. The MiSeq Reporter software (Illumina, San Diego, CA, USA) was used for sample demultiplexing and FASTQ file generation. Alignment and variant calling were performed using Surecall (Agilent); variant annotation, on the other hand, was performed using wANNOVAR (http://wannovar.wglab.org/).

2.3. Molecular Diagnosis

PCR amplification of *ARSB* exons and adjacent intronic regions, as well as from the promoter region of the gene, was done with specific primers. Each PCR reaction was carried out with specific primers using approximately 40 ng of genomic DNA, 1X the PCR reaction mix ImmoMix™ Red (Bioline, London, UK) and 0.25 μM of each primer (primer sequences and PCR annealing temperatures available on Supplementary Table S1). Thereafter, the samples were heated to 95 °C for 7 min, followed by 35 cycles of denaturation, annealing and extension. The final extension was completed by 5 min at 72 °C.

The amplified fragments were purified with illustra ExoStar™ 1-Step (GE Healthcare Life Sciences, Buckinghamshire, UK) and sequenced using a BigDye Terminator Cycle Sequencing Kit (Applied Biosystems, Foster City, CA, USA) on an ABI PRISM 3130xl Genetic Analyser (Applied Biosystems). Results were analyzed with the sequence analysis software FINCHTV, version 1.3.1. Sequencing profiles were compared with the *ARSB* reference sequence ENST00000264914.8 (https://www.ensembl.org/index.html) using the Clustal Omega multiple sequence alignment bioinformatic tool (https://www.ebi.ac.uk/Tools/msa/clustalo/).

The presence of the novel mutation was confirmed in two independent experimental assays by Sanger sequencing. Additionally, 50 healthy donors were screened for the newly identified *ARSB* mutation trough gDNA sequencing.

2.4. RT-PCR Analysis

Total cellular RNA was isolated from blood using the PAXgene Blood RNA System (QIAGEN), and reverse transcribed using the Ready-To-Go You-Prime First-Strand Beads (GE Healthcare Life Sciences). The *ARSB* cDNA was then amplified with specific primers (Supplementary Table S1). Amplification reactions were performed in a total volume of 25 μL containing 12.5 μL of 1X ImmoMix™ Red (Bioline), 2.5 to 5 μL of cDNA and 0.5 μM of each primer. After an initial period of 7 min at 95 °C to activate the Taq polymerase and denaturation of 3 min at 94 °C, the reaction continued for 35 cycles at 94 °C for 30 s, 45 s at annealing temperature, extension at 72 °C for 60 s and a final extension for 10 min at 72 °C.

2.5. Bioinformatic Analysis

In order to better understand the potential effect of the novel mutation over to the pre-mRNA splicing, the Human Slicing Finder (HSF)—version 3.1 bioinformatic software (http://www.umd.be/HSF/index.html) was used. The HSF system combines 12 different algorithms to identify and predict mutations' effect on splicing motifs including the acceptor and donor splice sites, the branch point and auxiliary sequences known to either enhance or repress splicing: Exonic Splicing Enhancers (ESEs) and Exonic Splicing Silencers (ESSs). These algorithms are based on either PWM matrices, Maximum Entropy principle or Motif Comparison method. Overall, this website incorporates data from other well-known bioinformatics tools which may be individually used to evaluate the potential effect of novel mutations such as MaxEntScan [26], ESEfinder [27] and Rescue-ESE [28], while integrating new matrices to identify hnRNP A1, Tra2-β and 9G8 [29].

2.6. Minigene Construction

For the splicing analysis of the novel *ARSB* variant [c.1213+5G>T (IVS6+5G>T)], wild-type (WT) and mutant minigene reporter vectors were constructed. Patient and control genomic DNA including 250 bp of the intron 5, the whole exon 6 and 245 bp of intron 6, upstream the variant were amplified. A *XhoI* (Forward primer: 5' ATA TAT CTC GAG CCA GAA TCA TTT TTT AAA 3') and *BamHI* (Reverse primer: 5' ATA TAT GGA TCC GAG AGT TCA ATG GCT TAA 3') restriction enzyme cleavage site was added to each oligonucleotide. The fresh products were then subcloned into the TOPO vector (Invitrogen, Carlsbad, CA, USA), according to the manufactor's guidelines. The inserts were restricted with *XhoI* and *BamHI* and after band excision, subsequently purified with Wizard SV Gel and PCR

Clean-Up system (Promega, Madison, WI, USA). Then, using the Rapid Ligation Kit (Roche Applied Science, Indianapolis, IN, USA), the inserts were cloned into the pSPL3 vector (Exon Trapping System, Life Technologies, Gibco, NY, USA). All clones were verified by DNA sequencing.

2.7. In Vitro Splicing Assays

For the functional splicing assays, Hep3B cells were seeded in 6-well plates (3×10^5) and 24 h later transfected with either WT or mutant minigenes (2 μg) using Lipofectamine 2000 (Invitrogen) according to the manufacturer's instructions. In this study, 24 h post-transfection cells were collected, total RNA was extracted and cDNA synthesized for subsequent amplification with vector-specific primers (SD6 and SA2—sequences available upon request). The amplified products were separated by agarose gel electrophoresis and purified either after band excision (as described in the previous section) or directly by using illustra ExoStar™ 1-Step (GE Healthcare). Purified amplicons were directly sequenced in an ABI Prism 3130xl genetic analyzer (Applied Biosystems).

2.8. Mutation Nomenclature

The Ensembl sequence ENST00000264914.8 of *ARSB* gene was used as reference for residue numbering. Mutation nomenclature followed the guidelines and recommendations of the Human Genome Variation Society (http://varnomen.hgvs.org/) [30].

3. Results

3.1. Next-Generation Sequencing

The complete list of variants identified in the studied patient using the NGS-targeted panel is presented on Supplementary Table S2. In summary, after variant annotation and filtering steps on the LSDs customized panel, two non-polymorphic variants were detected in MPS-related genes: a known *IDUA* missense mutation in heterozygosity (c.G1225C; p.G409R) [31] and a novel homozygous variant affecting the +5 position of *ARSB* intron 6 (c.1213+5G>T; IVS6+5G>T). Taking into account that both MPS I (caused by mutations in the IDUA gene) and MPS VI (caused by mutations in the *ARSB* gene) are autosomal recessive diseases, and no other pathogenic mutations were detected in heterozygosity in the *IDUA* gene, the most probable cause for disease seemed to be the novel *ARSB* intronic variant. Still, a number of studies had yet to be done in order to assess its pathogenicity.

Concerning the implementation of the NGS technology and the reliability of the obtained sequences, the mean per-base coverage depth for the designed panels was 260-fold, and 97% of the bases were covered by more than 20-fold.

3.2. gDNA Screening of the Proband, Segregation Studies and In Silico Analysis of the Newly Identified VUS (c.1213+5G>T [IVS6+5G>T])

After classical sequencing of the *ARSB* gene, the presence of the novel c.1213+5G>T (IVS6+5G>T) variant was confirmed in homozygosity (Figure 1a). Apart from this novel variant of uncertain significance (VUS), only non-pathogenic single nucleotide polymorphism (SNPs) were detected.

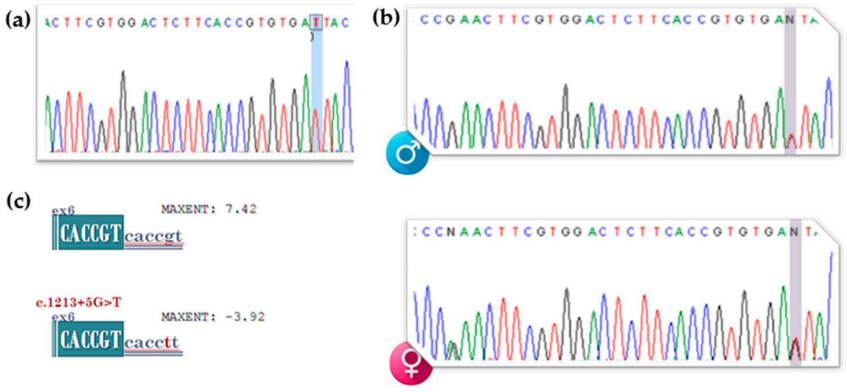


Figure 1. Molecular diagnosis of the patient by classical gDNA screening of the *ARSB* gene: detection of the novel c.1213+5G>T (IVS6+5G>T) mutation. Electropherogram highlighting the affected residue (**a**) in the patient and (**b**) parents. (**c**) *In silico* predictions on the effect of the novel mutation over the splice-site junctions. Score predictions by the MaxEntScan bioinformatic tool.

Targeted segregation studies, which consisted on the amplification of exon 6 and its flanking intronic regions on gDNA samples from the proband's parents, confirmed the presence of the IVS6(+5) VUS in heterozygosity (Figure 1b). Finally, *in silico* tools also predicted this VUS to be pathogenic, by disrupting the normal 5′ constitutive splice site of exon 6. Particularly, the MaxEntScan splicing score for the 5′ constitutive wt splice site (7.42) was much higher than that predicted when the mutant T was inserted in the +5 position (−3.92; −152.7% variation), clearly pointing to a direct effect over the normal *ARSB* pre-mRNA splicing (Figure 1c). Ideal MaxEntScan splice-site scores are: 11.81 (5′ss) and 13.59 (3′ss). Concerning the predictions on the effect of this VUS over the sequence's constitutive enhancer motifs, the ESE finder matrices predicted that the mutant T inserted in the +5 position would severely affect a constitutive ESE site for SRSF6 (SRp55), while generating two novel potential ESE sites, for SRSF2 (SC35) and SRSF5 (SRp40).

Finally, the mutation was not found in gnomAD, a genome aggregation database that spans 125,748 exome sequences and 15,708 whole-genome sequences from unrelated individuals sequenced as part of various disease-specific and population genetic studies. The mutation was also not listed in the 1000 genome nor in the 5000 exome.

3.3. cDNA Screening and Splicing Pattern Analysis

In order to assess the effect of the VUS under analysis, a sample of the proband was requested for RNA extraction and subsequent reverse transcription into cDNA. It was not possible to establish a skin biopsy for fibroblast culture. Therefore, RNA was extracted from total blood of the proband's father. The *ARSB* cDNA was then amplified with specific primers and, surprisingly, its transcript pattern was similar to that observed for a control (Figure 2).

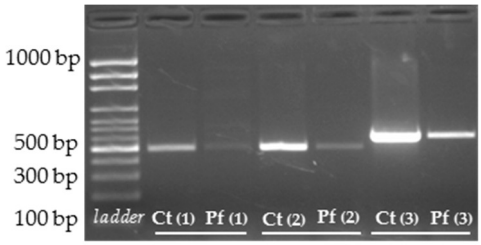


Figure 2. RT-PCR amplification of RNA extracted from the proband's father (Pf), carrier of the novel c.1213+5G>T [IVS6+5G>T] mutation. Total *ARSB* cDNA was amplified in three different fragments (1–3). The amplification of a control sample (Ct) is also presented.

3.4. Indirect Proof of Principle on c.1213+5G>T [IVS6+5G>T] Pathogenicity

After conducting a classical sequencing approach of the *ARSB* gDNA and cDNA on the proband's father, a discrepant pattern was observed for the exonic rs1065757 polymorphism (c.1072G>A). Even though the individual was shown to be heterozygous for that SNP at gDNA level, when his cDNA was sequenced after RT-PCR, he seemed to be homozygous for the less common A allele rs1065757 (Figure 3). This suggests that one allele was most likely degraded, corroborating the *in silico* predictions.

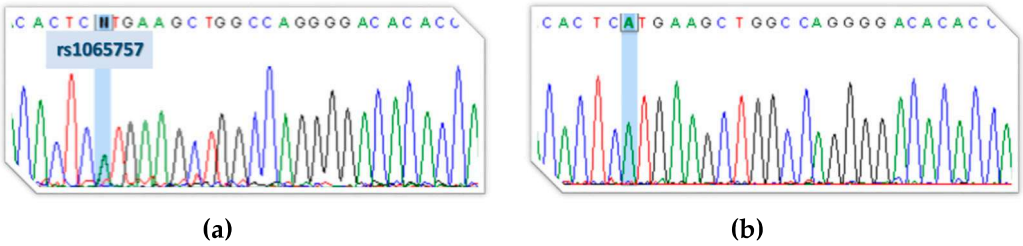


Figure 3. Indirect proof of principle on c.1213+5G>T [IVS6+5G>T] pathogenicity. Electropherograms highlighting the rs1065757 polymorphism (G>A) in the proband's father (Pf) gDNA (heterozygous; (**a**)) and cDNA (homozygous A; (**b**)). The discrepant pattern observed for the exonic polymorphism (rs1065757, c.1072G>A) provides indirect proof of an active nonsense-mediated mRNA decay (NMD) mechanism causing the degradation of the allele harboring the splicing mutation.

3.5. Functional Analyses

To further study the effect of the novel *ARSB* variant on splicing pattern, minigene assays were performed using constructs generated with the WT or mutant sequences (exon 6 plus its respective intronic flanking regions), in the pSPL3 vector. The results of RT-PCR analysis using vector-specific primers are depicted in Figure 4 and clearly show an effect of the +5 nucleotide substitution under analysis over the correct splicing of exon 6. In fact, while the WT amplicon spans approximately 350 bp, the one referring to the mutated minigene (harboring the c.1213+5G>T [IVS6+5G>T] nucleotide change), has a considerably lower molecular weight with less than 300 bp (Figure 4a). These results were further confirmed by Sanger sequencing. As expected, the WT amplicon revealed a transcript with the inclusion of exon 6 sequence (71 nucleotides). For the c.1213+5G>T [IVS6+5G>T] mutant, however, *ARSB* exon 6 got skipped. Therefore, the sequence resulting from RT-PCR of the mutated minigene, corresponds only to pSPL3 vector (Figure 4b).

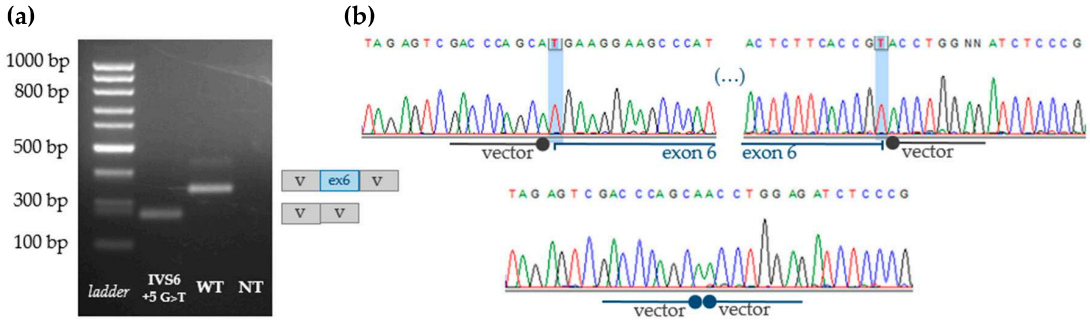


Figure 4. RT-PCR amplification and Sanger sequencing of WT and mutant splicing reporter minigenes using vector-specific primers. The results of RT-PCR analysis using vector specific primers are shown along with a diagram of the transcripts obtained in Hep3B cells after 24 h of incubation (**a**) and their sequencing results depicted in electropherograms (**b**). c.1213+5G>T [IVS6+5G>T]: mutant minigene; WT: wild-type; NT: non-transfected.

4. Discussion

After targeted NGS sequencing and variant calling analyses, the novel homozygous variant affecting the +5 position of *ARSB* intron 6 (c.1213+5G>T; IVS6+5G>T) as poped up as the most probable cause for disease. In fact, both bioinformatic predictors and literature support its pathogenecity. On one side the HSF bioinformatic tool predicted the disruption of the WT donor site most probably affecting splicing and, on the other, a bibliographic search of *ARSB* gene variants unveiled the existence of a MPS VI-causing mutation affecting the same residue and altering the normal splicing pattern (c.1213+5G>A [IVS6+5G>A]) [32], clearly pointed to a pathogenic effect over splicing. Actually, the guanine residue at the fifth position of the donor splice site consensus sequence is 75% conserved in humans [33] and any alteration over that residue may hold the potential to affect the normal splicing process. Moreover, segregation studies confirmed its presence in heretozygozity in both parents (Figure 1b). Thus, it seemed quite tempting to assume that this would be the variant underlying the patient's phenotype by affecting the normal *ARSB* splicing. Still, only after a proper cDNA analysis could we confirm its effect in splicing and, subsequently, its pathogenicity. Unfortunately, we only had access to an extremely degraded cDNA sample obtained from blood of one of her parents. Interestingly, the splicing pattern observed after cDNA amplification of that sample was absolutely normal (Figure 2). Still, taking into account that the original gDNA sample had been screened for mutations in 86 different genes related to lysosomal function and there were no more variants that could justify his phenotype (Supplementary Table S2), there was only one hypothesis that could justify the normal splicing pattern observed in the proband's father: an active nonsense-mediated mRNA decay (NMD) mechanism causing the degradation of the allele harboring the splicing mutation. However, its pathogenicity was yet to be proven.

Therefore, we conducted a classical sequencing approach of the *ARSB* gDNA and cDNA on the proband's father and ended up demonstrating that, while being heterozygous for an exonic SNP (rs1065757, c.1072G>A; Figure 3a) in the surroundings of the mutation, the same individual seemed to be homozygous for those exact same SNP (A) at cDNA level (Figure 3b). In accordance with these observations, when the proband's gDNA sequence was double-checked for the presence of the SNP, it was shown to be wild-type homozygous (G). This observation provided indirect proof of the mutation's effect on splicing, further suggesting that the mutant transcript(s) is degraded by NMD.

Still, much had yet to be proven concerning the effect of this novel mutation over the normal splicing of *ARSB*. It was, therefore, mandatory to further explore this novel mutation in order to fully characterize its effect at cDNA level. Having no further access to extra samples from either the proband herself or her mother, we designed a strategy to artificially evaluate the impact of this mutation at cDNA level by constructing WT and mutant minigenes to functionally investigate the splicing defects caused by the novel c.1213+5G>T *ARSB* mutation. Briefly, the relevant genomic segment (including exon 6 and its intronic boundaries) was cloned within a plasmid (pSPL3) specifically designed for splicing analysis, since its multiple cloning site is flanked by functional strong splice donor and acceptor sites.

After RT-PCR, it was possible to observe a clear effect of the novel c.1213+5G>T (IVS6+5G>T) variant over exon 6 constitutive splicing. In fact, the RT-PCR amplification product of the mutant minigene was significantly smaller than that seen for the WT minigene (Figure 4a). Direct sequencing of the amplicon further demonstrated the skipping of the full-length exon 6 sequence (71 nucleotides) in the mutant minigene, while those obtained for the WT minigene comprehended 71 nucleotides corresponding to the exon 6 sequence (Figure 4b). Exon 6 skipping results in an alteration of the *ARSB* mRNA open reading frame (ORF) with the introduction of 11 amino acids, which differ from the WT protein, ultimately resulting in the appearance of a premature stop codon (PTC). *In silico* translation of the mutant *ARSB* cDNA sequence results in the generation of a truncated protein with 141 amino acids less than the WT one. If generated, one such protein is not expected to be functional and, therefore, its underlying mutation is clearly pathogenic.

In general, these functional studies allowed us to establish the pathogenic potential of the novel c.1213+5G>T (IVS6+5G>T) mutation. Still, a number of questions may still be raised. For example,

it remains unclear whether this particular +5 change promotes the skipping of exon 6 alone or if it affects other exons as well. In fact, bioinformatic tools are clearly not sufficient when it comes to predict the exact effect of a particular change, even though they are usually quite reliable on evaluating whether it does affect splicing or not. For example, if we look at bioinformatic predictions concerning the other pathogenic mutation known to affect the +5 region of exon 6, the intronic mutation c.1213+5G>A [IVS6+5G>A] [32], that alteration would theoretically lead to incorrect splicing of exon 6. However, when the authors analyzed by RT-PCR the cDNA from the patient harboring that mutation, it was shown to produce two different aberrant transcripts: one with a deletion of exon 6 and one with a deletion of exons 5 and 6 [32]. One possible approach to understand whether the same happens with the novel c.1213+5G>T (IVS6+5G>T) mutation would be to design a larger minigene, including exon 5 and/or exon 7, to check whether additional alternative transcripts with further exons skipped would also be observed.

Ultimately, only a direct analysis of the proband's *ARSB* cDNA and/or protein product could provide complete evidence on the effect of this novel mutation over splicing. Nevertheless, the construction and transient expression of minigenes harboring the mutation under study allowed confirmation of its effect over the splicing process. Furthermore, the results obtained with reporter minigenes add up to those from the *ARSB* transcript analysis of the proband's father sample. Altogether, the two methods point out to the same general conclusion and provide solid indirect proof on the novel mutation's pathogenicity, even in the absence of an RNA/cDNA sample from the proband.

5. Conclusions

Here, we present the case of a molecular diagnosis of a patient with a general clinical suspicion of MPS.

In summary, the case report here presented is a perfect example on how complex and delicate the whole MGT process can be, even now, in the 'NGS era'. In fact, even though NGS holds a huge potential as an MGT tool, it is also responsible for the identification of a growing number of VUS in the same sample. Thus, functional studies are growing more and more necessary for proper molecular diagnosis. Minigenes, in particular, may be an interesting tool whenever an effect on splicing is predicted but no RNA/cDNA samples are available.

Supplementary Materials: The following are available online at http://www.mdpi.com/2075-4418/10/2/58/s1, Table S1: Primer sequences and PCR annealing temperatures for *ARSB* amplification; Table S2: List of variants identified in the studied patient using the NGS-targeted panel.

Author Contributions: Conceptualization, M.F.C., M.E. and S.A.; methodology, M.F.C., M.E., L.M., J.I.S., L.S., D.R. and S.A.; software, M.F.C., M.E., L.M., L.S. and S.A.; validation, M.E. and S.A.; writing—original draft preparation, M.F.C.; writing—review and editing, M.E., M.J.P. and S.A.; supervision, M.J.P. and S.A.; project administration, L.V. and S.A.; funding acquisition, L.V. and S.A. All authors have read and agreed to the published version of the manuscript.

Funding: This work was partially supported by the *Fundação Millennium bcp* (bcp/LIM/DGH/2014), N2020 (NORTE-01-0246-FEDER-000014) and *Fundação para a Ciência e Tecnologia* (FCT) IP (project: PTDC/SAU-GMG/117046/2010).

Acknowledgments: The authors wish to thank Souad Ouesleti, from the Biochemical Service, CHU Farhat Hached (Sousse, Tunisia) for referring the patient and collecting the necessary samples, along with the patient and her parents, for their support in this study. M.F.C. and J.I.S. were grantees from the FCT (SFRH/BPD/101965/2014; SFRH/BD/124372/2016).

Conflicts of Interest: The authors declare no conflict of interest.

References

1. Platt, F.M.; d'Azzo, A.; Davidson, B.L.; Neufeld, E.F.; Tifft, C.J. Author Correction: Lysosomal storage diseases. *Nat. Rev. Dis. Primers* **2018**, *4*, 36. [CrossRef] [PubMed]
2. Filocamo, M.; Morrone, A. Lysosomal storage disorders: Molecular basis and laboratory testing. *Hum. Genom.* **2011**, *5*, 156–169. [CrossRef] [PubMed]

3. Winchester, B. Lysosomal diseases: Diagnostic update. *J. Inherit. Metab. Dis.* **2014**, *37*, 599–608. [CrossRef] [PubMed]
4. Platt, F.M. Emptying the stores: Lysosomal diseases and therapeutic strategies. *Nat. Rev. Drug Discov.* **2018**, *17*, 133–150. [CrossRef]
5. Rehm, H.L. Disease-targeted sequencing: A cornerstone in the clinic. *Nat. Rev. Genet.* **2013**, *14*, 295–300. [CrossRef]
6. Selmer, K.K.; Gilfillan, G.D.; Strømme, P.; Lyle, R.; Hughes, T.; Hjorthaug, H.S.; Brandal, K.; Nakken, S.; Misceo, D.; Egeland, T.; et al. A mild form of Mucopolysaccharidosis IIIB diagnosed with targeted next-generation sequencing of linked genomic regions. *Eur. J. Hum. Genet.* **2012**, *20*, 58–63. [CrossRef]
7. Sperb-Ludwig, F.; Alegra, T.; Velho, R.V.; Ludwig, N.; Kim, C.A.; Kok, F.; Kitajima, J.P.; van Meel, E.; Kornfeld, S.; Burin, M.G.; et al. Exome sequencing for mucolipidosis III: Detection of a novel GNPTAB Gene Mutation in a Patient With a Very Mild Phenotype. *Mol. Genet. Metab. Rep.* **2015**, *2*, 34–37. [CrossRef]
8. Fernández-Marmiesse, A.; Morey, M.; Pineda, M.; Eiris, J.; Couce, M.L.; Castro-Gago, M.; Fraga, J.M.; Lacerda, L.; Gouveia, S.; Pérez-Poyato, M.S.; et al. Assessment of a targeted resequencing assay as a support tool in the diagnosis of lysosomal storage disorders. *Orphanet J. Rare Dis.* **2014**, *9*, 59. [CrossRef]
9. Yoshida, S.; Kido, J.; Matsumoto, S.; Momosaki, K.; Mitsubuchi, H.; Shimazu, T.; Sugawara, K.; Endo, F.; Nakamura, K. Prenatal diagnosis of Gaucher disease using next-generation sequencing. *Pediatr. Int.* **2016**, *58*, 946–949. [CrossRef]
10. Angelini, C.; Savarese, M.; Fanin, M.; Nigro, V. Next generation sequencing detection of late onset pompe disease. *Muscle Nerve* **2016**, *53*, 981–983. [CrossRef]
11. Di Fruscio, G.; Schulz, A.; De Cegli, R.; Savarese, M.; Mutarelli, M.; Parenti, G.; Banfi, S.; Braulke, T.; Nigro, V.; Ballabio, A. Lysoplex: An efficient toolkit to detect DNA sequence variations in the autophagy-lysosomal pathway. *Autophagy* **2015**, *11*, 928–938. [CrossRef] [PubMed]
12. Di Fruscio, G.; Banfi, S.; Nigro, V.; Ballabio, A. Next-Generation Sequencing Approaches to Define the Role of the Autophagy Lysosomal Pathway in Human Disease: The Example of LysoPlex. *Methods Mol. Biol.* **2017**, *1594*, 227–241. [CrossRef] [PubMed]
13. Song, H.K.; Sohn, Y.B.; Choi, Y.J.; Chung, Y.S.; Jang, J.H. A case report of pycnodysostosis with atypical femur fracture diagnosed by next-generation sequencing of candidate genes. *Medicine (Baltim.)* **2017**, *96*, e6367. [CrossRef] [PubMed]
14. Zeng, Q.; Fan, Y.; Wang, L.; Huang, Z.; Gu, X.; Yu, Y. Molecular defects identified by whole exome sequencing in a child with atypical mucopolysaccharidosis IIIB. *J. Pediatr. Endocrinol. Metab.* **2017**, *30*, 463–469. [CrossRef]
15. Tsai, A.C.; Hung, Y.W.; Harding, C.; Koeller, D.M.; Wang, J.; Wong, L.C. Next generation deep sequencing corrects diagnostic pitfalls of traditional molecular approach in a patient with prenatal onset of Pompe disease. *Am. J. Med. Genet. Part A* **2017**, *173*, 2500–2504. [CrossRef]
16. Zampieri, S.; Cattarossi, S.; Bembi, B.; Dardis, A. GBA Analysis in Next-Generation Era: Pitfalls, Challenges, and Possible Solutions. *J. Mol. Diagn.* **2017**, *19*, 733–741. [CrossRef]
17. Li, X.; Xiao, R.; Chen, B.; Yang, G.; Zhang, X.; Fu, Z.; Fu, J.; Zhuang, M.; Huang, Y. A novel mutation of SGSH and clinical features analysis of mucopolysaccharidosis type IIIA. *Medicine (Baltim.)* **2018**, *97*, e13758. [CrossRef]
18. Málaga, D.R.; Brusius-Facchin, A.C.; Siebert, M.; Pasqualim, G.; Saraiva-Pereira, M.L.; Souza, C.F.M.; Schwartz, I.V.D.; Matte, U.; Giugliani, R. Sensitivity, advantages, limitations, and clinical utility of targeted next-generation sequencing panels for the diagnosis of selected lysosomal storage disorders. *Genet. Mol. Biol.* **2019**, *42*, 197–206. [CrossRef]
19. Kobayashi, H. Recent trends in mucopolysaccharidosis research. *J. Hum. Genet.* **2019**, *64*, 127–137. [CrossRef]
20. Whitley, C.B.; Ridnour, M.D.; Draper, K.A.; Dutton, C.M.; Neglia, J.P. Diagnostic test for mucopolysaccharidosis. I. Direct method for quantifying excessive urinary glycosaminoglycan excretion. *Clin. Chem.* **1989**, *35*, 374–379. [CrossRef]
21. Gray, G.; Claridge, P.; Jenkinson, L.; Green, A. Quantitation of urinary glycosaminoglycans using dimethylene blue as a screening technique for the diagnosis of mucopolysaccharidoses: An evaluation. *Ann. Clin. Biochem.* **2007**, *44*, 360–363. [CrossRef] [PubMed]
22. Lawrence, R.; Brown, J.R.; Al-Mafraji, K.; Lamanna, W.C.; Beitel, J.R.; Boons, G.J.; Esko, J.D.; Crawford, B.E. Disease-specific non-reducing end carbohydrate biomarkers for mucopolysaccharidoses. *Nat. Chem. Biol.* **2012**, *8*, 197–204. [CrossRef] [PubMed]

23. Kubaski, F.; Osago, H.; Mason, R.W.; Yamaguchi, S.; Kobayashi, H.; Tsuchiya, M.; Orii, T.; Tomatsu, S. Glycosaminoglycans detection methods: Applications of mass spectrometry. *Mol. Genet. Metab.* **2017**, *120*, 67–77. [CrossRef] [PubMed]
24. Saville, J.T.; McDermott, B.K.; Fletcher, J.M.; Fuller, M. Disease and subtype specific signatures enable precise diagnosis of the mucopolysaccharidoses. *Genet. Med.* **2019**, *21*, 753–757. [CrossRef] [PubMed]
25. Ouesleti, S.; Coutinho, M.F.; Ribeiro, I.; Miled, A.; Mosbahi, D.S.; Alves, S. Update of the spectrum of mucopolysaccharidoses type III in Tunisia: Identification of three novel mutations and in silico structural analysis of the missense mutations. *World J. Pediatr.* **2017**, *13*, 374–380. [CrossRef]
26. Yeo, G.; Burge, C.B. Maximum entropy modeling of short sequence motifs with applications to RNA splicing signals. *J. Comput. Biol.* **2004**, *11*, 377–394. [CrossRef]
27. Cartegni, L.; Wang, J.; Zhu, Z.; Zhang, M.Q.; Krainer, A.R. ESEfinder: A web resource to identify exonic splicing enhancers. *Nucleic Acids Res.* **2003**, *31*, 3568–3571. [CrossRef]
28. Fairbrother, W.G.; Yeh, R.F.; Sharp, P.A.; Burge, C.B. Predictive identification of exonic splicing enhancers in human genes. *Science* **2002**, *297*, 1007–1013. [CrossRef]
29. Desmet, F.O.; Hamroun, D.; Lalande, M.; Collod-Béroud, G.; Claustres, M.; Béroud, C. Human Splicing Finder: An online bioinformatics tool to predict splicing signals. *Nucleic Acids Res.* **2009**, *37*, e67. [CrossRef]
30. den Dunnen, J.T.; Dalgleish, R.; Maglott, D.R.; Hart, R.K.; Greenblatt, M.S.; McGowan-Jordan, J.; Roux, A.F.; Smith, T.; Antonarakis, S.E.; Taschner, P.E. HGVS Recommendations for the Description of Sequence Variants: 2016 Update. *Hum. Mutat.* **2016**, *37*, 564–569. [CrossRef]
31. Bach, G.; Moskowitz, S.M.; Tieu, P.T.; Matynia, A.; Neufeld, E.F. Molecular analysis of Hurler syndrome in Druze and Muslim Arab patients in Israel: Multiple allelic mutations of the IDUA gene in a small geographic area. *Am. J. Hum. Genet.* **1993**, *53*, 330–338. [PubMed]
32. Karageorgos, L.; Brooks, D.A.; Harmatz, P.; Ketteridge, D.; Pollard, A.; Melville, E.L.; Parkinson-Lawrence, E.; Clements, P.R.; Hopwood, J.J. Mutational analysis of mucopolysaccharidosis type VI patients undergoing a phase II trial of enzyme replacement therapy. *Mol. Genet. Metab.* **2007**, *90*, 164–170. [CrossRef] [PubMed]
33. Roca, X.; Krainer, A.R.; Eperon, I.C. Pick one, but be quick: 5′ splice sites and the problems of too many choices. *Genes Dev.* **2013**, *27*, 129–144. [CrossRef] [PubMed]



© 2020 by the authors. Licensee MDPI, Basel, Switzerland. This article is an open access article distributed under the terms and conditions of the Creative Commons Attribution (CC BY) license (http://creativecommons.org/licenses/by/4.0/).

ANNEX 2 – REVIEW PAPERS

Authored by the PhD candidate

Review Paper#1 - Santos JI, Gonçalves M, Matos L, Moreira L, Carvalho S, Prata MJ, Coutinho MF, Alves S. Splicing Modulation as a Promising Therapeutic Strategy for Lysosomal Storage Disorders: The Mucopolysaccharidoses Example

Co-Authored by the PhD candidate

Review Paper#2 - Gonçalves M, Santos JI, Coutinho MF, Matos L, Alves S. Development of Engineered-U1 snRNA Therapies: Current Status.

Review Paper#3 - Carvalho S, Santos JI, Moreira L, Gonçalves M, David H, Matos L, Encarnação M, Alves S, Coutinho MF. Neurological Disease Modeling Using Pluripotent and Multipotent Stem Cells: A Key Step towards Understanding and Treating Mucopolysaccharidoses.

Review Paper#4 - Coutinho MF, Santos JI, S Mendonça L, Matos L, Prata MJ, S Jurado A, Pedroso de Lima MC, Alves S. Lysosomal Storage Disease-Associated Neuropathy: Targeting Stable Nucleic Acid Lipid Particle (SNALP)-Formulated siRNAs to the Brain as a Therapeutic Approach.

life

Review

Splicing Modulation as a Promising Therapeutic Strategy for Lysosomal Storage Disorders: The Mucopolysaccharidoses Example

Juliana Inês Santos [1,2,3,*], Mariana Gonçalves [1,4], Liliana Matos [1,3], Luciana Moreira [1,3], Sofia Carvalho [1,5], Maria João Prata [2,6], Maria Francisca Coutinho [1,3] and Sandra Alves [1,3]

1 Research and Development Unit, Department of Human Genetics, National Institute of Health Doutor Ricardo Jorge (INSA I.P.), Rua Alexandre Herculano, 321, 4000-055 Porto, Portugal; mariana.goncalves@insa.min-saude.pt (M.G.); liliana.matos@insa.min-saude.pt (L.M.); luciana.moreira@insa.min-saude.pt (L.M.); sofia.carvalho@insa.min-saude.pt (S.C.); francisca.coutinho@insa.min-saude.pt (M.F.C.); sandra.alves@insa.min-saude.pt (S.A.)
2 Biology Department, Faculty of Sciences, University of Porto, Rua do Campo Alegre, 4169-007 Porto, Portugal; mprata@ipatimup.pt
3 Center for the Study of Animal Science, CECA-ICETA, University of Porto, Praça Gomes Teixeira, Apartado 55142, 4051-401 Porto, Portugal
4 Centre for the Research and Technology of Agro-Environmental and Biological Sciences (CITAB), Inov4Agro, University of Trás-os-Montes and Alto Douro, 5000-801 Vila Real, Portugal
5 Faculty of Farmacy, University of Coimbra, 3000-548 Coimbra, Portugal
6 i3S-Institute of Research and Innovation in Health/IPATIMUP-Institute of Molecular Pathology and Immunology of the University of Porto, Rua Alfredo Allen, 208, 4200-135 Porto, Portugal
* Correspondence: juliana.santos@insa.min-saude.pt; Tel.: +351-223-401-100

check for updates

Citation: Santos, J.I.; Gonçalves, M.; Matos, L.; Moreira, L.; Carvalho, S.; Prata, M.J.; Coutinho, M.F.; Alves, S. Splicing Modulation as a Promising Therapeutic Strategy for Lysosomal Storage Disorders: The Mucopolysaccharidoses Example. *Life* **2022**, *12*, 608. https://doi.org/10.3390/life12050608

Academic Editor: Riccardo Autelli

Received: 16 March 2022
Accepted: 15 April 2022
Published: 19 April 2022

Publisher's Note: MDPI stays neutral with regard to jurisdictional claims in published maps and institutional affiliations.

Copyright: © 2022 by the authors. Licensee MDPI, Basel, Switzerland. This article is an open access article distributed under the terms and conditions of the Creative Commons Attribution (CC BY) license (https://creativecommons.org/licenses/by/4.0/).

Abstract: Over recent decades, the many functions of RNA have become more evident. This molecule has been recognized not only as a carrier of genetic information, but also as a specific and essential regulator of gene expression. Different RNA species have been identified and novel and exciting roles have been unveiled. Quite remarkably, this explosion of novel RNA classes has increased the possibility for new therapeutic strategies that tap into RNA biology. Most of these drugs use nucleic acid analogues and take advantage of complementary base pairing to either mimic or antagonize the function of RNAs. Among the most successful RNA-based drugs are those that act at the pre-mRNA level to modulate or correct aberrant splicing patterns, which are caused by specific pathogenic variants. This approach is particularly tempting for monogenic disorders with associated splicing defects, especially when they are highly frequent among affected patients worldwide or within a specific population. With more than 600 mutations that cause disease affecting the pre-mRNA splicing process, we consider lysosomal storage diseases (LSDs) to be perfect candidates for this type of approach. Here, we introduce the overall rationale and general mechanisms of splicing modulation approaches and highlight the currently marketed formulations, which have been developed for non-lysosomal genetic disorders. We also extensively reviewed the existing preclinical studies on the potential of this sort of therapeutic strategy to recover aberrant splicing and increase enzyme activity in our diseases of interest: the LSDs. Special attention was paid to a particular subgroup of LSDs: the mucopolysaccharidoses (MPSs). By doing this, we hoped to unveil the unique therapeutic potential of the use of this sort of approach for LSDs as a whole.

Keywords: lysosomal storage diseases (LSDs); mucopolysaccharidoses (MPSs); RNA-based therapies; antisense oligonucleotides (ASOs); splice-switching oligonucleotides (SSOs); U1 snRNA (small nuclear RNA)

1. Introduction

The somehow recent revolution in RNA biology has led to the recognition of the multiple roles that this molecule may assume within a cell through the identification of new

RNA classes that have previously unanticipated functions. This better understanding of basic RNA biology has been accompanied by a parallel revolution in the use of RNA-based strategies for therapeutic purposes [1]. All of a sudden, RNA-based drugs opened a whole new perspective on therapeutic approaches for previously untreatable diseases by entering the pharmacopoeia and greatly expanding the universe of druggable targets (Figure 1).

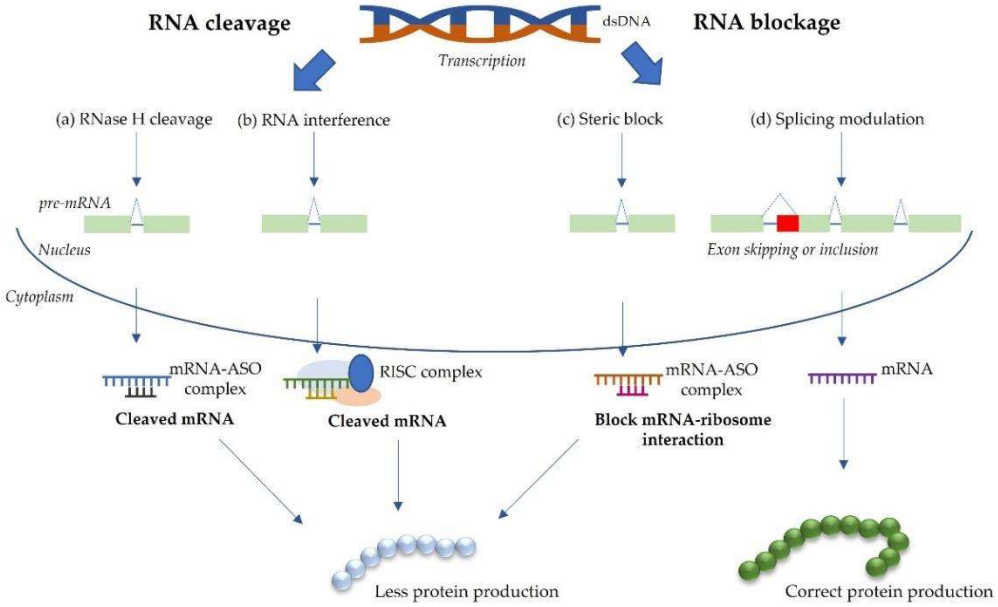


Figure 1. Schematic representation of the different mechanisms of action of antisense oligonucleotides (ASOs). ASOs can impact gene expression in different ways, either through RNA cleavage (**a**,**b**) or RNA blockage (**c**,**d**). RNA cleavage (or degradation) approaches include (**a**) RNAse H-mediated mRNA degradation and (**b**) RNA interference (RNAi), while RNA blockage approaches may promote (**c**) sterick block of ribosome binding and (**d**) splicing modulation. The green rectangles represent the coding exonic regions and the blue lines represent the non-coding intronic regions from the pre-mRNA. The red square represents the mutated region of the exon. The dashed lines that form a triangle represent the normal splicing pattern of the pre-mRNA. Abbreviations: ASO, antisense oligonucleotide; mRNA, messenger RNA; pre-mRNA, pre-messenger RNA; RISC, RNA-inducing silencing complex (Adapted from [2]).

Among this promising class of drugs, those that target the splicing process are probably the most widely studied and for which there are five approved drugs for two different diseases [3]. Splicing defects are particularly tempting as therapeutic targets because mutations in the consensus sequences at the borders of introns and exons are a common cause of human genetic diseases. Furthermore, those defects tend to result in the complete loss of function of the protein in question, thus underlying severe pathology [4].

Splicing defects in different genes have been identified as one of the underlying genetic causes of a huge number of genetic diseases of different etiologies. Among those disorders are countless rare diseases of monogenic origin, including the lysosomal storage diseases (LSDs) that were our major focus of interest. LSDs are a particular subset of genetic diseases that can benefit greatly from even the slightest increase in protein function [5]. The vast majority of LSDs are autosomal recessive, even though three X-linked diseases are also known. Still, few disease-specific therapies exist for this vast and heterogeneous group of disorders and even when they do exist, it is now well-recognized that there are some major drawbacks to the existing approaches, such as their inability to act on neurological symptoms [6]. Unfortunately, a great majority of LSDs have a significant neurological component, which is the dominating clinical effect of the disease in a number of disorders, although it is merely one element of a more generalized pathology in others [7]. Among the LSDs that are still lacking effective treatment, a major group is the mucopolysaccharidoses

(MPSs). The MPSs comprise a group of 11 disorders and each one is caused by defects in any of the enzymes that are involved in the stepwise degradation of glycosaminoglycans (GAGs), which lead to the progressive storage of those compounds. This storage, along with other pathogenic mechanisms, triggers several clinical consequences of wide phenotypic variability [8]. Interestingly, even patients that suffer from the same disease can present with extremely different phenotypes that are associated with enzyme activity levels: some patients, who have null or residual enzyme activity, present with early onset severe phenotypes; others, who retain significantly higher residual enzymatic activity, show a much more slowly progressing disorder with a later onset. This means that even a slight recovery in enzyme activity (which can be promoted by the recovery of the normal splicing) can be enough to have a clinical impact [9,10]. Of all MPS-causing mutations, a large percentage affect the pre-mRNA splicing process. Altogether, this makes MPSs excellent candidates for splicing correction therapeutics. Nevertheless, despite the immense potential that these approaches hold for this group of diseases, there are only a few works so far that have attempted splicing modulation approaches for these disorders.

In this work, we address this issue and comment not only on the potential of these drugs but also on the hurdles they must overcome. We start by explaining how splicing can be experimentally modulated for therapeutic purposes. In order to do so properly, we begin by briefly summarizing the normal splicing process and the possible consequences of its disruption. Then, we introduce the currently approved therapeutic approaches that modulate splicing and their mechanisms of action, even though they were not designed for LSDs. Finally, we bring the focus onto our diseases of interest: the MPSs. After an overview of their major clinical features and molecular bases, we outline the contribution of splicing defects to each of the individual diseases. Then, we discuss how some of them have been approached for therapeutic purposes and summarize the published preclinical studies that have assessed the feasibility of recovering pre-mRNA splicing mutations as a way to recover defective enzyme activity. Finally, we comment on the future of splicing therapeutics and the major issues that may hamper their transfer to the clinics and highlight a few strategies that could be used to overcome those hurdles.

2. Splicing: How It Works and How It Can Be Modulated

2.1. The Splicing Process: Machinery and Mechanisms

It is well known that eukaryotic gene(s) expression requires a series of highly regulated sequential steps in which non-coding introns are removed from the precursor messenger RNA (mRNA) molecule while the exons, or coding sequences, are joined together, which results in mRNA maturation being translated into protein. This well-known process is called splicing and is carried out by the spliceosome.

RNA splicing was initially discovered in the 1970s and it overturned years of research in the field of gene expression [11,12]. Its major effector, the spliceosome, functions in a complex and dynamic assembly–disassembly cycle in which five small nuclear ribonucleoprotein (snRNP) complexes (U1, U2, U4/U6 and U5) recognize and assemble on each intron to ultimately form a catalytically active spliceosome. An early event in the exon definition is the recognition of the 5′ donor splice site (ss) by the U1 snRNP, which is followed by the binding of splicing factor 1 (SF1) to the branch point and the binding of the U2 auxiliary factor heterodimer (U2AF 65/35) to the polypyrimidine tract (Py) and 3′ss, originating the E complex [13,14]. After that, SF1 is replaced by the U2 snRNP at the branch point, originating the A complex, which allows for the interaction between U1 snRNP and U2 snRNP across the exon [13,15]. Then, the U4, U5 and U6 snRNPs are recruited as a preassembled complex, which leads to the formation of the B complex. Afterward, the interaction between U4 and U6 is disrupted and the U6 snRNP base pairs with the 5′ss, thereby displacing U1 snRNP from its initial location and releasing it from the complex along with the U4 snRNP [16]. At the same time, U6 snRNP interacts extensively with U2 snRNP, which brings the 5′ss and the branch point into close proximity. This allows for the first step of splicing to take place, which originates the C complex, which contains the free

upstream exon and the intron–exon lariat intermediate [15]. This complex completes the second step of the splicing reaction and releases the intron and joins the exons together to form the mature mRNA, while the U2, U5 and U6 snRNPs are also released from the complex and recycled for future splicing reactions [15,17,18].

Although the spliceosome drives pre-mRNA processing with great complexity and fidelity, this is quite a flexible mechanism under the strong regulation by both *cis*- and *trans*-acting elements. The role of *cis*-acting regulatory sequences and RNA-binding protein splicing factors, which recognize and bind to those sites, compose a common mechanism for setting up and maintaining alternative splicing (AS) patterns. Heterogeneous nuclear ribonucleoproteins (hnRNPs) and serine and arginine-rich (SR/AR) proteins in the spliceosome regulate either splicing repression by binding intronic splicing silencers (ISS) and exonic splicing silencers (ESS) or splicing activation by binding intronic splicing enhancers (ISE) and exonic splicing enhancers (ESE) [14,15,19].

AS is a process through which a single precursor mRNA can generate a number of alternative mRNAs, thereby allowing for considerable proteomic diversity and complexity [20,21]. It is currently estimated that nearly 95% of human multi-exonic genes are alternatively spliced, thus giving rise to different protein isoforms. AS mechanisms include: exon skipping, intron retention, mutually exclusive exons and alternative donor 5′ss and acceptor 3′ss [19]. Furthermore, alternative polyadenylation sites and the alternation of the initial exons due to alternative promoter usage can also contribute to AS. In addition, AS can be regulated at the transcription level and in the chromatin structure (Figure 2).

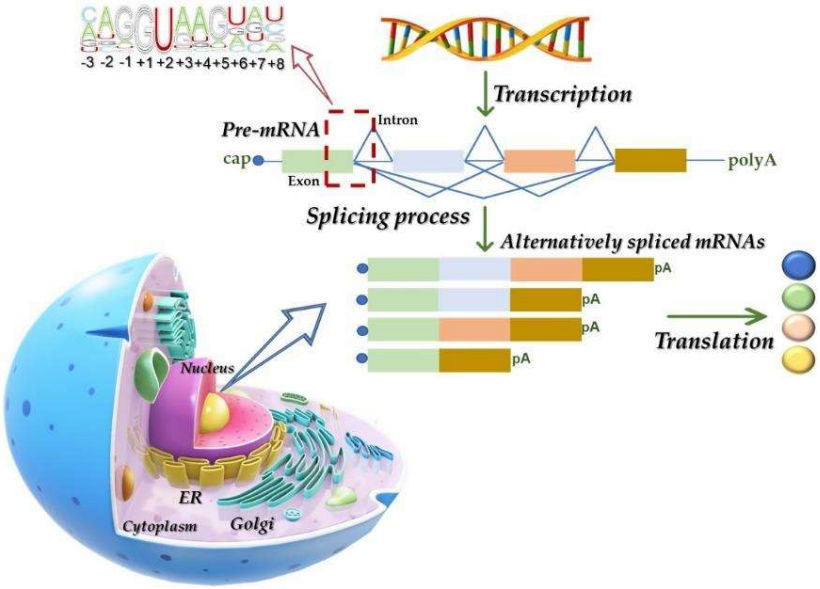


Figure 2. Simplified overview of the splicing process. The alternative splicing (AS) process generates mature mRNAs with different exon combinations, which results in the production of different protein isoforms from the same mRNA. Abbreviations: ER, endoplasmatic reticulum; mRNA, messenger RNA; pre-mRNA, precursor mRNA.

A detailed description of the AS process and regulation, which was beyond the scope of this review, can be found in a series of papers that have been published elsewhere [15,22–24]. A variety of therapeutic strategies, such as small molecules and antisense oligonucleotides (ASOs) as well as genome editing through the use of CRISPR/Cas9, have promising future interventions for the amelioration of the disease-causing effects of human mutations on the patterns of AS. Over the following sections, we briefly describe some of the interventions with a special focus on those that are currently approved for commercial use.

2.2. RNA-Based Approaches for Splice Modulation

In general, antisense-mediated splicing modulation is a tool that can be exploited in several ways to provide a potential therapy for rare genetic diseases [25]. It is an extremely versatile approach because it can not only promote the correction of cryptic splicing and the modulation of AS, but also the restoration of the open reading frame. Ultimately, it can even induce protein knockdown. This means that splicing modulation approaches can actually go far beyond the correction of individual splicing mutations (such as those that we focus on subsequent sections: see Section 4). Additionally, it may also rely on different effectors, or tools, from antisense oligonucleotides (ASOs) for splicing-switching to synthetic U1 snRNAs (small nuclear RNAs). The most widely known tools that are used to promote splicing correction/modulation are ASOs.

ASOs were first reported by Stephenson and Zamecnik in 1978 [26]. ASOs are short synthetic oligonucleotides (15–30 nucleic acid length) designed complementary to sense strand of mRNA and efficient laboratory tools that can regulate the expression of specific genes through an efficient modulation of the splicing process [27]. When designed to target the splice site or its auxiliary sequences, which leads to mRNA repair and the restoration of protein function and modifies the outcome of the splicing reaction, they are called splice-switching ASOs or splice-switching oligonucleotides (SSOs). These ASOs are able to sterically block relevant motifs in the pre-mRNA without promoting its degradation.

Numerous studies have investigated the therapeutic potential of ASOs in *in vitro* cell models, animal disease models and human clinical trials. Even though a complete overview of all of these studies clearly fell outside of the scope of this review, we briefly discuss the approved therapeutic strategies to treat diseases using ASOs. By doing so, we hope to unveil the full potential of this somewhat novel class of drug and show how life-changing these molecules can be for patients who harbor different genetic mutations, provided that a number of requirements are met.

The demonstration that an ASO drug can successfully promote the correction of its targets *in vivo* paved the way for the clinical trials of ASOs as a treatment for a variety of diseases, especially rare diseases such as Duchenne muscular dystrophy (DMD) and spinal muscular atrophy (SMA). Currently, there are a number of approved drugs for these pathologies, all of which are capable of manipulating the pre-mRNA splicing process: Eteplirsen (EXONDYS 51™, Sarepta Therapeutics, Cambridge, MA, USA) [28,29]; Golodirsen (Vyondys 53™, Sarepta Therapeutics, Cambridge, MA, USA) [30]; Viltolarsen (Viltepso®, NS Pharma, Paramus, NJ, USA) [31]; and Casimersen (Amondys 45™, Sarepta Therapeutics, Cambridge, MA, USA) [32] for the DMD and Nusinersen (Spinraza®, Biogen, Cambridge, MA, USA) [33,34] for SMA (Table 1).

DMD is an X-linked genetic disease that is characterized by the absence of the dystrophin protein in muscle fibers, which is manifested by progressive muscle degeneration and weakness. Approximately two thirds of DMD cases present deletion mutations in the *DMD* gene, which is composed of 79 exons (the largest known human gene) [35]. Becker muscular dystrophy (BMD) is a mild disease that is caused by dystrophin truncations and not by its absence. To produce mild phenotypes, such as BMD, a strategy that can generate a truncated but functional dystrophin protein would be a reliable tool. Thus, the skipping of exons to correct DMD-linked mutations can reduce the severity of the disease and produce a phenotype that is similar to that of BMD [36]. Eteplirsen, which is a 30-nucleotide phosphorodiamidate morpholino oligomer (PMO), binds to the 5′ss of exon 51, which leads to it being skipped (Figure 3b). Thus, an in-frame transcript is produced that allows for the formation of an internally truncated but functional dystrophin protein [36,37]. Eteplirsen can only be used for patients who are amenable to exon 51 skipping, which accounts for 13% of the DMD patient population [38]. In September 2016, this drug received approval from the US Food and Drug Administration (FDA), which made it the first ASO to be approved for DMD and the first approved exon skipping ASO to be used for humans [38].

Table 1. Antisense oligonucleotides (ASOs) that are approved for Duchenne muscular dystrophy (DMD) and spinal muscular atrophy (SMA) treatment.

Brand Name	Drug	Year of Approval	Target Molecule	Treatment Result	Target Disease
Spinraza®, Biogen	Nusinersen	2016	*SMN2* mRNA	Induces the inclusion of exon 7 in the *SMN2* mRNA	Spinal muscular atrophy
Exondys 51™, Sarepta Therapeutics	Eteplirsen	2016	Dystrophin mRNA	Induces the exclusion of exon 51 of dystrophin mRNA	Duchenne muscular dystrophy
Vyondys 53™, Sarepta Therapeutics	Golodirsen	2019	Dystrophin mRNA	Induces the exclusion of exon 53 of dystrophin mRNA	Duchenne muscular dystrophy
Viltepso®, NS Pharma	Viltolarsen	2020	Dystrophin mRNA	Induces the exclusion of exon 53 of dystrophin mRNA	Duchenne muscular dystrophy
Amondys 45™, Sarepta Therapeutics	Casimersen	2021	Dystrophin mRNA	Induces the exclusion of exon 45 of dystrophin mRNA	Duchenne muscular dystrophy

More recently, in 2019, another ASO drug was approved to treat this disease: Golodirsen. This is a 25-mer PMO that binds to the exon 53 of the *DMD* gene and causes it to be skipped, thereby avoiding the deleterious loss-of-function frameshifting mutations [30,39]. It was only approved for males with mutations that are amenable to exon 53 skipping. Then, in 2020, yet another drug for the treatment of DMD patients with the same characteristics was approved by the FDA: Viltolarsen, which is a 21-mer PMO that also binds to exon 53 and causes it to be skipped [31,40] (Figure 3c). In both cases, the skipping of this exon restores the reading frame and leads to the production of an internally truncated but partially functional dystrophin protein [41]. Both drugs are suitable for 8% of DMD patients. Finally, in 2021, an ASO from the PMO subclass was developed by Sarepta Therapeutics for the treatment of DMD in patients who have a mutation of the *DMD* gene that is amenable to exon 45 skipping: Casimersen. Casimersen was designed to bind to the exon 45 of the *DMD* gene pre-mRNA and leads to the production of an internally truncated but functional dystrophin protein [32] (Figure 3d).

Altogether, ASOs that address the primary genetic defect of DMD are among the first generation of therapies tailored to overcome specific genetic mutations in humans. They represent paradigm-forming approaches to medicine that may lead to life-changing treatments for those affected by this relentlessly progressive and fatal disease [42].

SMA is another disorder that has greatly benefited from the development of splice modulation therapeutics. SMA is an autosomal recessive neuromuscular disease that is caused by mutations and deletions in the survival motor neuron 1 (*SMN1*) gene, which results in the progressive loss of alpha motor neurons in the anterior horn of the spinal cord [43]. A second *SMN* gene exists in human genome: the *SMN2* that has a C to T mutation in exon 7. This single nucleotide change does not affect the protein sequence but it does affect the pre-mRNA splicing, which gives rise to an unstable isoform that is rapidly degraded [44,45] (Figure 4a).

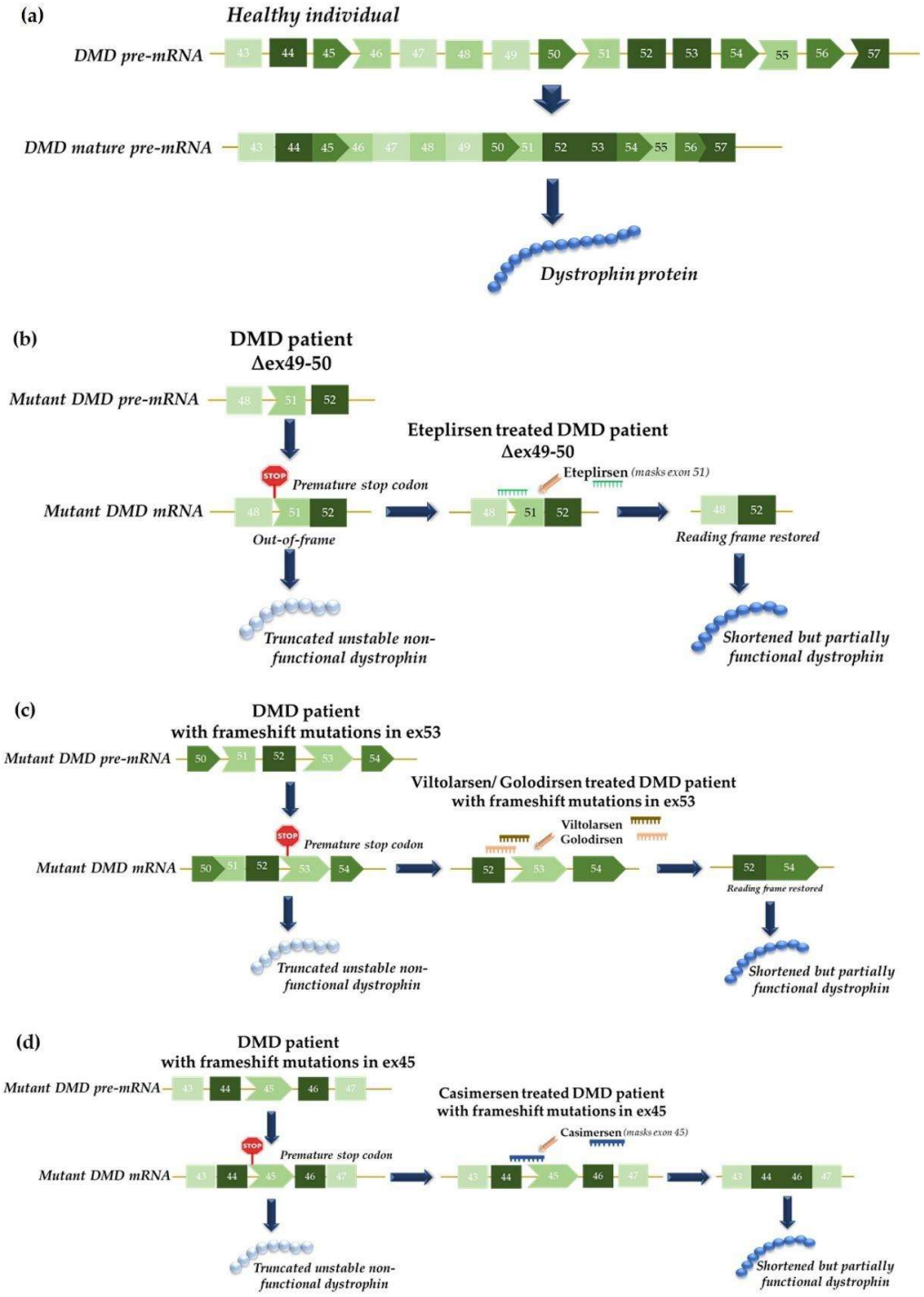


Figure 3. Mechanism of action of exon skipping therapy for Duchenne muscular dystrophy (DMD): (**a**) schematic representation of the normal splicing of the *DMD* gene in healthy individuals who produce normal dystrophin protein. In general, treatment of DMD with antisense oligonucleotides (ASOs) promotes selective exon skipping in order to restore the reading frame and produce a truncated but partly functional dystrophin protein. Different drugs are available for the different mutations that affect a number of *DMD* exons: (**b**) Eteplirsen, for DMD patients with deletions spanning exons 49 and 50; (**c**) Viltolarsen/Golodirsen, for DMD patients with frameshift mutations in exon 53; and (**d**) Casimersen, for DMD patients with frameshift mutations in exon 45. Abbreviations: Δ49-50, deletion of exons 49 and 50; DMD, Duchenne muscular dystrophy; mRNA, messenger RNA; pre-mRNA, precursor mRNA.

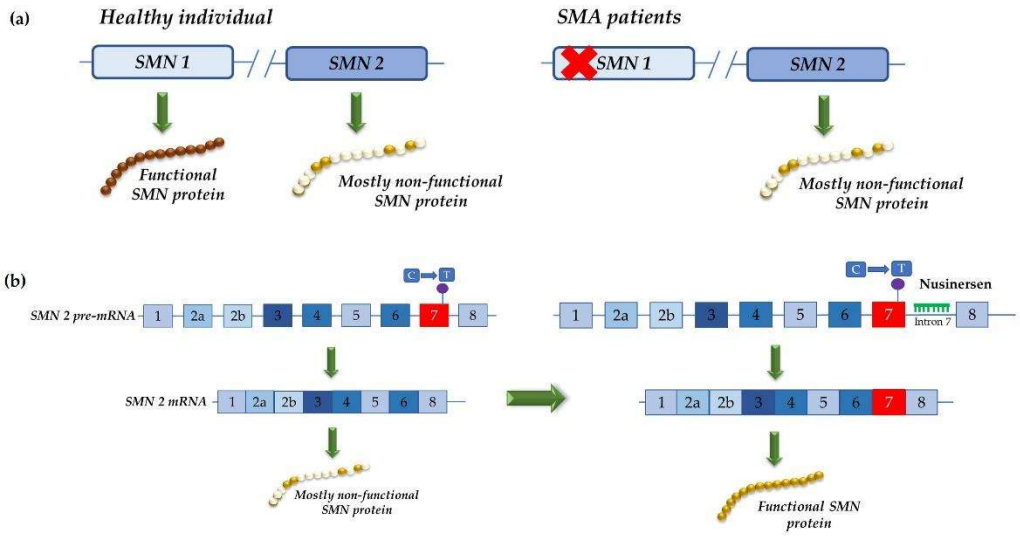


Figure 4. Mechanism of action of exon inclusion therapy for spinal muscular atrophy (SMA): (**a**) overview of the molecular basis of SMA. Humans have two *SMN* genes: *SMN1*, which gives rise to a functional SMN protein and *SMN2*, which has a C to T mutation in exon 7 that does not affect the protein sequence but does affect the pre-mRNA splicing, thereby giving rise to an unstable isoform that is rapidly degraded. In healthy individuals, the presence of a functional SMN protein that is encoded by the *SMN1* gene assures the assembly of the cellular machinery that is needed to process pre-mRNA. In SMA patients, mutations in the *SMN1* gene prevent the production of a functional SMN protein: (**b**) Nusinersen targets and blocks the intronic splicing silencer (ISS) in intron 7, which induces the inclusion of exon 7 in the *SMN2* mRNA. Abbreviations: C, cytosine; mRNA, messenger RNA; pre-mRNA, precursor mRNA; SMA, spinal muscular atrophy; SMN, survival motor neuron; T, thymine.

Taking this into account, Cartegni and colleagues showed that a 2′-O-methoxyethyl (2′MOE) phosphorothioate-modified ASO can efficiently correct *SMN2* exon 7 splicing both *in vitro* and *in vivo* [43,46,47]. By targeting and blocking the intron 7 ISS, Nusinersen induces the inclusion of exon 7 in the *SMN2* mRNA. This ASO was approved by the FDA in December 2016 [48] (Figure 4b). Together with the two other approved drugs for SMA replacement therapy, Nusinersen has provided a life-changing treatment option for SMA patients and their families. It extends life expectancy and allows patients to reach motor milestones that would previously have been unachievable [49].

The second major approach for the modulation of the splicing process, both *in vitro* and *in vivo*, is the use of synthetic U1 snRNAs designed to recognize mutant 5′ss, thus restoring complementarity. The first step of the splicing process requires the 5′ end of the U1 snRNA to interact by complementarity with the moderately conserved sequence of the 5′ss [20]. This implies that any mutation in this site may compromise the binding of the U1 snRNA and prevent spliceosome assembly, thus inhibiting the subsequent splicing process. Therefore, these sorts of variants usually cause disease.

Over the last decade, U1 snRNAs with a modified 5′ tail that base pair exactly to the mutant splice site have been used to correct 5′ss mutations, abolishing the skipping of some the exons that they originally caused. Another type of modified U1 snRNAs are the so-called exon-specific U1 snRNAs (ExSpe U1s), which have also been tested in different *in vitro* and *in vivo* approaches that have shown their therapeutic potential [20,50–52]. Recently, Balestra and colleagues published the *in vivo* proof of principle for the correction potential of compensatory U1 snRNAs in hereditary tyrosinemia type I [50]. Nevertheless, this approach is not yet available as a therapeutic option and more studies are needed before its translation into the clinic.

The combined use of ASOs and U1snRNAs is also under consideration. In fact, a combined treatment using ASOs and engineered U1 snRNAs has shown the highest

therapeutic efficacy for correcting mutation-induced splicing defects in Bardet–Biedl syndrome [51]. This recent observation has shown that there may be an advantage in the use of these two therapeutic approaches with complementary effects for the improvement of treatment efficacies.

Among the monogenic diseases, which may benefit from either sort of splice-modulation therapeutics are the LSDs, a group of life-threatening disorders, which are further addressed in the following sections.

2.3. Hurdles

Despite its promise, the development of RNA therapeutics has faced several major hurdles over recent decades, namely: (1) the rapid degradation of exogenous RNAs by ubiquitous endogenous RNases; (2) the challenging delivery of negatively charged RNA molecules across hydrophobic membranes; and (3) the strong immunogenicity of synthetic RNAs, which ends up causing cell toxicity and impairing translation. These hurdles have been substantially overcome with recent advancements in RNA biology, bioinformatics, separation science and nanotechnology, all of which have greatly facilitated the recent rapid development of RNA therapeutics as a whole [53].

However, there are several challenges that may still hinder the prompt clinical translation of some RNA drugs. Most of these challenges are common to all types of RNA drugs, but others are specific to those that are aimed at splicing modulation.

For example, the development of proper models to assess the sequence-dependent efficacy and safety of ASOs is still a pending issue [54]. This is particularly relevant for the splicing modulation approaches designed to correct specific disease-causing mutations that affect the normal splicing process, the so-called splicing mutations. Ideally, the preclinical development of that sort of drugs would require the development of animal models that carry the specific splicing mutations. Importantly, however, an alternative exists for a few specific approaches that does not require these mutation-specific models. In fact, for the therapies that rely on the promotion of the skipping of a specific exon, it is possible to use wild animals instead of mutation-specific models.

Then, there is the question of the species-specific sequence differences between orthologous genes. SSOs and U1snRNA-based therapies are sequence-specific approaches that aim to interfere with the splicing mechanism and they are specifically designed to recognize a certain target sequence in the human genome. Unfortunately, most of our sequences of interest are not completely conserved among different species. Therefore, the molecules designed to target a human sequence cannot be directly assessed in an animal model [55]. This means that for *in vivo* assessments, it is not usually possible to use exactly the same SSOs or U1snRNA sequences that are used for human cells. It is always necessary to design species-specific SSOs and U1snRNAs (i.e., specifically designed for animal sequences, which are orthologous to the human genes under study). This is actually the standard approach for *in vivo* ASO studies and most of the currently approved ASOs relied on the *in vivo* assessment of animal responses to slightly modified molecules, which were designed to match the orthologue sequences. This sort of *in vivo* studies may provide relevant safety and toxicity data, but it relies on the premise that the consensus splice site sequences in mice and humans are highly conserved and comparable. Still, some small changes in these patterns have been described [56].

The alternative would be to generate humanized animal models, an approach that is both time- and resource-consuming and may contribute to a substantial increase in the drug development time while requiring additional funding. Furthermore, the generation of a humanized animal model for every mutation that needs to be targeted is neither feasible nor ethical and may not always recapitulate the human molecular and/or physiological phenotypes [54,55].

The last and probably the major challenge that could hinder the broader clinical translation of this category of drugs is their inefficient delivery to the target tissues. This is not only true for splicing modulation but also for every other RNA-based approach. In general,

the delivery of ASOs and any other RNA-based drugs to target tissues is relatively poor after systemic delivery. Nevertheless, relevant increases in the efficiency of ASO delivery have been achieved over recent years through chemical modification and conjugation to other moieties, as well as the development of new chemical backbones. Furthermore, many teams have been working on the development of effective drug delivery systems, which ultimately enhance the delivery of drugs to the target sites of pharmacological action. Among these systems, lipid nanoparticles (LNPs) and/or adeno-associated viruses (AAVs) are probably the most well known (reviewed in [57]). Nevertheless, the latest advances in ASO technology have been coupled with the surprising finding that despite being highly charged and large, ASOs distribute widely throughout the CNS when they are delivered to the cerebral spinal fluid via intrathecal (IT) delivery, which is safe and well tolerated. This peculiarity (contrary to other RNA therapies, such as siRNAs and U1snRNAs vectors) has greatly enabled the application of ASOs as a therapeutic strategy for CNS disorders, many of which currently have no treatment [58]. Remarkably, IT ASO administration has already been implemented for the treatment of SMA and has produced safe and tolerable results [58,59]. An ASO that targets ALS and is delivered via IT was also recently administered to one patient [60].

Over the last decade, huge successes have also been documented for therapies that target hepatocytes and in which GalNAc conjugation and LNP technology allow for the targeted delivery of drugs with outstanding results, which has resulted in approval being granted for several clinical indications. These examples of how specific and well-designed drug delivery technologies can be used to overcome the targeting hurdles have provided a new impetus to the RNA-based therapeutics field, which will certainly contribute to fostering research and accelerating discoveries about extra-hepatic delivery (reviewed in [61]). Another drawback is the high exposure of certain organs upon the systemic delivery of AONs. For instance, after the intravenous injection of AONs, a significant proportion is absorbed by the liver and kidneys. This limits their biodistribution to other tissues and results in a toxic effect within these organs. Importantly, however, many of the liver and kidney injuries were found when using high and not clinically relevant doses of AONs. Obviously, the design and manufacture of efficient delivery systems is not the only hurdle. Their safety, both alone and in combination with RNA-based drugs, is also paramount [61].

3. Treatment Strategies for LSD Patients: MPSs in the Spotlight

3.1. Lysosomal Storage Diseases

Lysosomal storage diseases (LSDs) are a group of about 70 monogenic and hereditary diseases of lysosomal catabolism. The majority of them are inherited in an autosomal recessive manner, but three diseases are X-linked. These disorders have a combined incidence of around 1:7700 but, according to several authors, this figure may be as high as 1:3000 or even 1:1500 when all LSDs are considered [62,63]. LSDs occur when a mutation, or more than one mutation, occurs in genes that code for proteins that are important for lysosomal function (i.e., lysosomal proteins, in the majority cases), thus affecting their function. This results in lysosomal malfunction and the gradual storage of the undegraded/partially degraded substrates inside the lysosome, which ultimately results in cell dysfunction and death [64,65].

Frequently, LSDs present as pediatric neurodegenerative diseases [66]. However, as they are heterogeneous disorders, depending on the gene defect and on the biochemical nature of the stored substrates, lysosomal storage defects can cause skeletal dysmorphia, due to bone pathology, and central nervous sys-tem (CNS) defects, in addition to symptoms affecting many other organs..

LSD diagnosis is usually based on the clinical symptoms of patients, followed by the confirmation of increased storage and genetic alterations through several diagnostic tests, such as enzymatic analysis and gene sequencing. More recently, diagnosis through next

generation sequencing (NGS) has become routine, which greatly reduces the time from the initial presentation of symptoms to the diagnosis of the disease [67,68].

Based on the type of disorder and the age of diagnosis, LSDs can be classified into congenital or infantile, late-infantile, juvenile and adult types. Usually, the earlier the symptoms appear, the more severe the disease presentation.

Treatment strategies for LSDs include: enzyme replacement therapy (ERT), which consists of providing the missing/defective enzyme; substrate reducing therapy (SRT), in which the synthesis of the accumulated substrates is reduced; hematopoietic stem cell transplantation (HSCT), in which healthy matched donor cells are transplanted into the patient and the enzyme is then secreted continuously from the donor cells; and chaperone therapy, which encompasses the use of competitive inhibitors at sub-inhibitory concentrations to stabilize the mutant enzyme, thereby extending the half-life and improving catalysis. Even though treatments are available for 11 LSDs, most of these disorders are managed symptomatically and patients only receive supportive care due to the inability to treat neurological symptoms [64].

Most importantly, even when therapies are available, especially ERTs, they are only successful in the somatic tissues of the body and cannot cross the blood–brain barrier (BBB); therefore, they fail to treat neurological deficits, which are among the most debilitating symptoms of many LSDs. Once neurological damage has occurred, it is extremely difficult to revert the phenotype. Thus, obtaining the correct enzyme dose in the brain is a major therapeutic goal. About two thirds of LSDs have neurological involvement [59]. This is why small-molecule drugs are being developed to cross the BBB, even though, so far, none reliably reach the brain. However, gene therapies that directly target the CNS are promising.

3.2. Mucopolysaccharidoses

One of the subgroups in which neurological symptoms are the most prevalent is the mucopolysaccharidoses (MPSs), which represent approximately 30% of LSD cases [69]. Seven major MPSs are currently known (MPSI, II, III, IV, VI, VII and IX), which result from mutations in the genes that code for one of 11 acid hydrolases involved in the degradation of GAGs. Each individual enzyme deficiency underlies one particular MPS (for instance, four different deficiencies trigger an equivalent number of MPS III disorders) [70] (Table 2). As these lysosomal enzymes fail to fulfill their function, the compounds accumulate in cells and tissues, which then causes progressive damage and a variety of clinical multi-organ manifestations, such as cardiovascular disease, respiratory problems, skeletal abnormalities and premature death, but the spectrum and severity of the disease manifestations vary between and within the MPS types [8,71]. These compounds can also accumulate outside of the lysosomes, thereby activating inflammatory pathways and an innate immune response via the tool-like receptor 4 and the complement system. Aspects such as neuroinflammation, short bones and aortic fragmentation can also arise due to this inflammatory response [8].

MPSs are heterogeneous and multisystemic diseases and manifestations vary not only between the subtypes but also within the same subtype. These characteristics affect the quality of life and lifespan of the patients. Clinically, MPS patients can be classified as having a “visceral phenotype”, a “neurodegenerative phenotype” or a “skeletal phenotype”, depending on the subtype of the disease. In general, MPS types I, II, VI and VII present with coarse facies, visceromegaly (hepatosplenomegaly), hernia, upper airway obstruction, joint stiffness, heart disease and other skeletal deformities as the main group characteristics. Due to these manifestations, these MPSs are usually classified as the group with “visceral phenotype”. A short stature is present in MPS I, II and VII patients. Furthermore, corneal clouding is also very frequent in all of these subtypes, except for type II, in which hearing loss is marked [8]. MPS III patients belong to the group with “neurodegenerative phenotype”, in which the clinical manifestations of the groups that were referred to above are mild but there is a marked neurodegeneration, which usually starts between 3 and 5 years of age and is accompanied by behavioral disturbances and hyperactivity. Finally, the “skeletal phenotype” is a characteristic of MPS IV patients, who show skeletal dysplasia

and many other bone problems. They are mentally normal and have a short stature. MPS IX is not included in these three groups because the main clinical manifestation is the presence of joint swelling and synovial masses [8].

Table 2. Classification of mucopolysaccharidose (MPS) subtypes.

MPS Type	Common Name(s)	Associated Gene	Enzyme Deficiency	Number of Mutations	% of Splicing Mutations	Treatment Options Available
I	Hurler, Scheie and Hurler–Scheie syndromes	*IDUA*	Alpha-L-iduronidase	320	15.3	ERT, HSCT
II	Hunter syndrome	*IDS*	Iduronate-2-sulfatase	739	8.8	ERT, HSCT
IIIA	Sanfilippo syndrome type A	*SGSH*	Heparan-*N*-sulfatase	163	2.5	-
IIIB	Sanfilippo syndrome type B	*NAGLU*	*N*-acetylglucosaminidase	256	3.1	-
IIIC	Sanfilippo syndrome type C	*HGSNAT*	Acetyl CoA glucosamine *N*-acetyltransferase	91	17.6	-
IIID	Sanfilippo syndrome type D	*GNS*	*N*-acetyl-glucosamine-6-sulfatase	28	14.3	-
IVA	Morquio syndrome type A	*GALNS*	*N*-acetylgalactosamine-6-sulfate sulfatase	378	10.3	ERT, HSCT
IVB	Morquio syndrome type B	*GLB1*	β -galactosidase	265	8.3	-
VI	Maroteaux–Lamy syndrome	*ARSB*	Arylsulfatase B	229	5.7	ERT
VII	Sly syndrome	*GUSB*	β-glucuronidase	81	7.4	ERT
IX	Hyaluronidasedeficiency	*HYAL1*	Hyaluronidase	7	0	-

All subtypes are monogenic diseases that are transmitted in an autosomal recessive way except for MPS II, which is X-linked. In general, nonsense and frameshift mutations seem to lead to a more severe disease, while missense mutations are associated with more attenuated forms. Splicing mutations are generally associated with severe disease forms, but when the normal transcript is produced (even in small amounts), a milder phenotype can be present. This genotype–phenotype correlation can help to predict phenotype, which is very important for MPS I patients, for example, to ensure that the correct treatment option is applied. However, it is difficult to predict that the phenotype on an individual basis. This is why it is important to study the impact of each mutation at the cDNA and protein level, as well as develop new biomarkers for the assessment and follow-up of treated and untreated patients [72,73].

MPS type I is the most frequent form of MPS and results from mutations in the *IDUA* gene that codes for α-L-iduronidase (EC 3.2.1.76). A deficiency of this enzyme results in the lack of the degradation of dermatan and heparan sulphates (DS/ HS), which leads to their progressive accumulation. A wide range of phenotypic involvement exists, including three major recognized clinical entities: Hurler (MPS IH; OMIM #607014), which is the most severe; Scheie (MPS IS; OMIM #607016), which is milder; and Hurler–Scheie (MPS IH/S; OMIM #607015), which has an intermediate phenotype [74]. The incidence of MPS I is estimated to be approximately 1:100,000 births (reviewed in [73]). To date, at least 320 mutations in *IDUA* are known, of which 15.3% are splicing mutations ([75]; Table 2). The early initiation of treatment, as for all treatable LSDs, results in more favorable outcomes. For this subtype, treatment options include HSCT, which is the gold standard for severe forms of the disease and for young children in the early stages of Hurler syndrome, and ERT with recombinant laronidase (Aldurazyme®, Genzyme), either alone or in combination [73,76–78]. However, the diagnosis of MPS I is often difficult, particularly for patients with attenuated phenotypes, which results in the delayed introduction of treatment. Gene therapy for MPS I is still only in the preclinical stages of development [77].

MPS II, also known as Hunter syndrome (OMIM #309900), is caused by mutations in *IDS* gene, which result in a deficiency of iduronate-2-sulfatase activity (EC 3.1.6.13). This decreased activity leads to intracellular and extracellular accumulation of HS and DS in various organ systems, as in MPS I. This disease is the only MPS that is not inherited in an autosomal recessive manner but rather has an X-linked inheritance [73,79]. So far, at least 739 mutations in *IDS* are known, of which 8.8% are splicing mutations ([75]; Table 2). These genetic variations result in different phenotypes of the disease, which can be classified as severe or attenuated. The severe form affects about 60% of patients and has CNS involvement. The overall estimated incidence of MPS II is 1:162,000 live male births [79].

The two approved treatments for MPS II are ERT with recombinant human IDS infusions of idursulfase (Elaprase®, Shire) and HSCT, which has been shown to have neurological benefits in MPS II patients.

Sanfilippo syndrome, or MPS III, can be differentiated from the other types due to the predominance of CNS disease [59,80]. The main compound that is accumulated is HS. Depending on the mutated gene and, consequently, the associated enzyme deficiency, this type can be classified as: MPS IIIA (OMIM #252900), with mutations in the *SGSH* gene; IIIB (OMIM #252920), when the mutations are in *NAGLU*; IIIC (OMIM #252930), which is caused by mutations in the *HGSNAT* gene; or IIID (OMIM #252940), with mutations in *GNS*. To date, numerous mutations have been identified in each of the four genes, 2.5%, 3.1%, 17.6% and 14.3% of which affect the splicing process for subtypes A, B, C and D, respectively ([75]; Table 2). Somatic symptoms are mild, even though hepatosplenomegaly is often present but not usually diagnosed clinically, and cardiac problems are rare (reviewed in [81]). As HS accumulates primarily in the brain, classical ERT, which is the most successful strategy for other non-neurological LSDs, may not be effective. The BBB limits the availability of the enzyme in the brain and IT and intracerebroventricular (ICV) administrations are very invasive strategies that have a number of associated problems. Clinical trials have been conducted to investigate various methods for ERT delivery to the CNS; however, they have been shown not to promote neurocognitive benefits [82–84]. A recent clinical trial of MPS IIIA patients using IT administration for the defective enzyme showed a reduction in HS and GAG levels in the treated patients. Still, the primary neurocognitive endpoint was not met [83]. Currently, there are no available treatments for this syndrome. Most efforts are palliative and focus on regulating behavior (aggressiveness, hyperactivity, etc.) and sleep disturbances. However, a number of therapies are now being developed and evaluated, such as HSCT, gene therapy, SRT and anti-inflammatory therapies (reviewed in [80,85]).

MPS IV, also known as Morquio syndrome, is caused by the impaired degradation of keratan sulphate (KS). Two enzyme deficiencies are known to lead to this syndrome: N-acetylgalactosamine-6-sulphatase (GALNS; EC 3.1.6.4), which causes Morquio syndrome type A (OMIM #253000), and β-galactosidase (EC 3.2.1.23), which causes Morquio syndrome type B (OMIM #253010). To date, at least 378 mutations are known for MPS IVA, of which 10.3% are splicing mutations, and 265 are known for MPS IVB, 8.3% of which are known to affect the splicing process ([75]; Table 2). Both forms of MPS IV have skeletal dysplasia, very short stature, ligamentous laxity/joint hypermobility and odontoid hypoplasia as major characteristics. Most patients are mentally normal [70,86]. Nevertheless, neurological involvement can also occur in severe cases and can be life-threatening, with the affected individuals not normally surviving past the second or third decade of life. Those patients with milder forms of the disorder usually survive to adulthood, even though their life expectancy may be reduced [8]. ERT using recombinant human GALNS, elosulfase alfa (Vimizim®; BioMarin Pharmaceutical Inc) and HSCT are the treatment options for MPS IVA (reviewed in [87]). There are no therapies currently available for MPS IVB.

MPS type VI, or Maroteaux–Lamy syndrome (OMIM #253200), results from a deficiency of arylsulfatase B (N-acetylgalactosamine-4-sulfatase; EC 3.1.6.12), which is caused by mutations in the *ARSB* gene. This deficit results in the pathological accumulation of DS in most organs and systems. The incidence estimates range from 1:77,000 to 1:278,000 live births. Presently, 229 mutations in *ARSB* are known, of which 5.7% affect the normal

splicing process ([75]; Table 2). As with MPS IV, a purely somatic disease occurs with no cognitive involvement. Patients present within a spectrum of clinical severity: when they have a severe case of the disease, i.e., showing the onset of symptoms before 2 or 3 years of age and impaired mobility by 10 years of age, usually die in second or third decade of life; when the disease is attenuated, patients have a later onset of symptoms and tend to be diagnosed either in their teens or in early adulthood [88]. ERT with galsulfase (Naglazyme®, BioMarin Pharmaceutical Inc) is currently the recommended first-line treatment for MPS VI, although there have been various studies published on the positive effects of HSCT and the combination of the two treatments on MPS VI patients (reviewed in [89]).

MPS VII, also known as Sly syndrome (OMIM #253220), is a rare type of MPS that is characterized by the lack of the β-D-glucuronidase enzyme (EC 3.2.1.31) due to mutations in the *GUSB* gene. This deficiency causes an accumulation of DS, HS and chondroitin sulphate (CS) proteoglycans, which are mainly sulfated in the 4 (C4S) and 6 (C6S) positions, in multiple tissues. MPS VII patients are phenotypically heterogeneous but there are a few common features that can be recognized, including short stature, coarse facial features, corneal clouding, hydrocephalus, skeletal deformation and cardiac diseases, similar to those features that are observed in MPS I and II. Interestingly, a distinguishing feature is observed in this subtype: hydrops fetalis, which is an abnormal accumulation of bodily fluids in several tissues [90,91]. To date, 81 mutations have been identified in *GUSB*, 7.4% of which are splicing mutations ([75]; Table 2). For the non-neurological manifestations of MPS VII, ERT with vestronidase alfa (Mepsevii™, Ultragenyx, Novato, CA, USA), which was approved by the FDA in 2017, is the recommended therapeutic approach [92]. As for the other types of MPS, HSCT has also been studied in MPS VII patients but no definitive conclusions about its therapeutic efficacy have yet been drawn due to the limited data (reviewed in [93]).

Finally, MPS IX, also known as hyaluronidase (EC 3.2.1.35) deficiency (OMIM # 601492), is caused by mutations in the *HYAL1* gene, which results in the accumulation of hyaluronan. It is an ultra-rare type of MPS and, to date, only four patients have been reported worldwide: one patient in the original report was diagnosed in 1996 and the three other patients belonged to a second family, who were diagnosed in 2011 [94,95]. All reported patients with MPS IX presented with joint and skeletal problems. According to the data that were collected from these patients, there are only seven mutations that are known to be responsible for this disease, none of which affect the splicing process ([75], Table 2).

Altogether, excluding the ultra-rare MPS IX, which has no associated splicing defects, 3% to 18% of the currently described mutations are known to disrupt the normal pre-mRNA splicing, depending on the MPS type being considered. This reinforces the need for a deeper study on the effects of this type of mutation, but it also makes them great candidates for splice modulation approaches. While 11 different MPSs exist and only 5 of them have approved therapeutic approaches, the need for additional treatment options is real. It is also worth mentioning that, even for the diseases that do have treatments available, the currently approved drugs fail to address CNS lesions, thus allowing for the neuropathological progression of the disorder and the resultant neuropsychiatric manifestations [96]. In fact, the development and delivery of effective treatments for these neurological and psychiatric signs and symptoms are universal hurdles that are faced not only by MPSs, but also by virtually every other LSD. This is why so many different therapeutic approaches are either being developed or are under evaluation for this group of disorders, from substrate reduction to gene therapy [97]. Also included among those possibilities are patient-tailored, mutation-specific approaches, which take advantage of the current knowledge on the molecular basis of these disorders to design a drug which holds potential to surpass the molecular defect that underlies pathology in one particular patient. Ultimately, there is even room for the so-called N-of-1 therapeutics, in which a drug is specifically designed for the treatment of just one patient.

4. RNA-Based Therapeutic Approaches for MPS Mutations

Altogether, there are at least 226 MPS-causing mutations that affect the pre-mRNA splicing process [75]. These mutations can occur in *cis*-acting elements, including 5′ss and 3′ss, GU-AG canonical nucleotides, the Py tract, branch point sequence, ESE, ESS, ISE and ISS, which affects their interaction with *trans*-acting factors (SR family proteins and hnRNPs). These mutations can have a higher frequency worldwide, can be identified in a small number of families or they can be unique. While some notable exceptions have been recognized for a few LSDs [9], no MPS-related splicing mutations have yet been identified as being particularly prevalent among affected individuals and/or specific populations. Nevertheless, MPS-causing mutations are good candidates for splicing modulation approaches for several reasons, which we have already listed. Over the following sections, we summarize functional studies that have focused on MPS-causing mutations that affect splicing, as well as the studies that we are aware of that have attempted the correction and/or amelioration of MPS disease phenotypes through splice modulation.

4.1. Functional Studies of Splicing Mutations and Development of Therapeutic Approaches Using Antisense Oligonucleotides: The MPS II Example

So far, 739 MPS II causal mutations have been reported in the *IDS* gene (OMIM *309900), 65 of which have been described as affecting splicing (around 8.8%) [75]. In a study that was published in 2015, Matos et al. performed an extensive functional analysis on three *IDS* gene splicing mutations in order to better understand how and why splicing is altered and they subsequently addressed the *in vitro* correction of one of them using splicing-related ASOs [98,99]. Two of them, c.257 C>T and c.241 C>T, are located in exon 3 and activate a cryptic splice site in this exon. The third, c.1122 C>T, is located in exon 8 of *IDS* and is responsible for the creation of a new 5′ss, which leads to a shorter transcript than wild-type.

This is particularly relevant since only two of these disease-causing variants had previously been characterized at cDNA level and shown to disrupt the normal *IDS* splicing process: c.257 C>T and c.1122 C>T. The third, while previously reported, had only been analyzed at the gDNA level and incorrectly classified as a nonsense mutation [100]. Reporter minigenes were used as tools to perform these functional analyses. In fact, there is a significant number of papers on the efficacy of *in silico* predictors, which directly compare the bioinformatic results to those that were obtained with reporter minigenes, taking the latter as "controls", and only analyze patient RNA when available [101]. This is why the effects of intronic or exonic mutations on splicing should ideally be assessed both by *in silico* tools and through the construction and transient expression of minigenes that harbor the variants under analysis.

Moreover, the splicing regulation of exon 3 has also been addressed using mutant minigene analysis and overexpression/silencing assays. It was observed that SRSF2 and hnRNP E1 could be involved in the use and repression of the constitutive 3′ss of exon 3, respectively [98]. These two regulatory elements, SRSF2 and hnRNP E1, were overexpressed or silenced in the Hep3B cell line that was transfected with either wild-type (WT) or mutant minigenes. It was verified that the choice of the constitutive 3′ss of *IDS* may be dependent on an ESE site that is recognized by SRSF2, which is compromised by the presence of the mutation in this region and also affects the binding of the splicing silencers hnRNP E1 and E2. The correction of both mutations was not attempted because, in both cases, the full-length transcript leads to the production of aberrant proteins that arise from a missense (c.257 C>T) or a nonsense (c.241 C>T) mutation [98]. However, the studies that were performed may still be of use to the design of ASO therapeutic strategies that involve this exon.

For the c.1122 C>T mutation, which has a silent effect on the amino acidic sequence, the possibility of redirecting the transcript processing using modified ASOs was tested in patients' fibroblasts (Figure 5). Four ASOs were used, three 2′-O-methyl (2′OMe) and one locked nucleic acid (LNA), all of which were complementary to the region of the

newly created 5′ss in order to block the access of the splicing machinery to the mutant mRNA, thus preventing the formation of the mutant transcript. Quite unexpectedly, however, this treatment failed to abolish the abnormal transcript and instead resulted in the appearance of another aberrant splicing product that corresponded to the total skipping of exon 8. Furthermore, the transfection of these ASOs in control fibroblasts also led to the appearance of the aberrant transcript that was observed in the patients' cells, which showed that oligonucleotides masked an important *cis*-acting element for the 5′ss regulation of exon 8 [98].

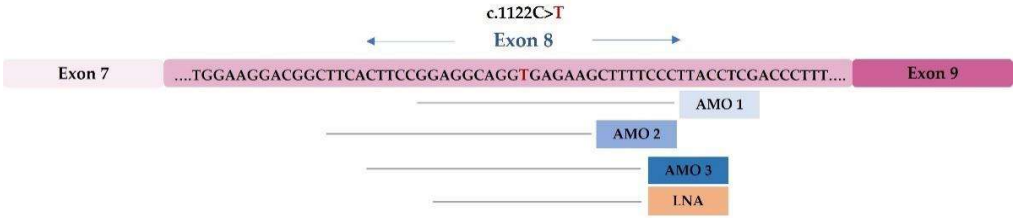


Figure 5. Antisense oligonucleotide (ASO) treatment for a MPS II-causing mutation: schematic representation of the *IDS* exon 8, in which the c.1122C>T nucleotide change is located (marked in red). The underlined sequences represent each blocking AMO or LNA that was designed for the different regions of the exon. Abbreviations: AMO, antisense morpholino; LNA, locked nucleic acid.

Overall, the importance of functional studies for understanding the pathogenic consequences of mis-splicing became evident from these results. Moreover, this study highlighted the difficulty in developing antisense therapies involving regions of genes that are under complex splicing regulation.

4.2. Development of Therapeutic Approaches Using Modified U1 snRNA Vectors: The MPS IIIC Example

In 2014, Matos et al. showed that a modified U1 snRNA could be a promising tool for the treatment of splicing mutations in MPS IIIC patients. This was actually the first published study that assessed the potential of modified U1 snRNAs to correct of splicing mutations, not only in MPSs but also in the larger LSD field [102].

That study included five patients who carried four different mutations: c.234+1G>A, c.633+1G>A and c.1542+4dupA, which affect the donor splice site, and c.372-2A>G, which affects an acceptor splice site of the *HGSNAT* gene. For the first three mutations, different modified U1 snRNAs were designed to recognize the mutated site (Figure 6).

Again, the *in vitro* assessment was started by checking whether the splicing patterns that were observed in patients' fibroblasts could be reproduced *in vitro* in an artificial system, which would allow for the subsequent functional analysis of each target mutation. In order to reproduce the splicing defects in a cellular model, several mutant minigenes were constructed and transfected in COS-7 cells. Post-transfection cDNA analysis and sequencing disclosed that the minigene-derived splicing patterns closely resembled the patterns that were observed in the control and patients' cDNAs, which were obtained from the fibroblasts that had been previously analyzed. This observation further supported that those minigenes were reliable tools for testing and optimizing the overexpression of the modified U1 snRNAs to correct the splicing defects. So, several U1 constructs were generated with different degrees of complementarity to each mutated donor splice site. However, the splicing correction was not observed when they were tested in these artificial systems in all cases.

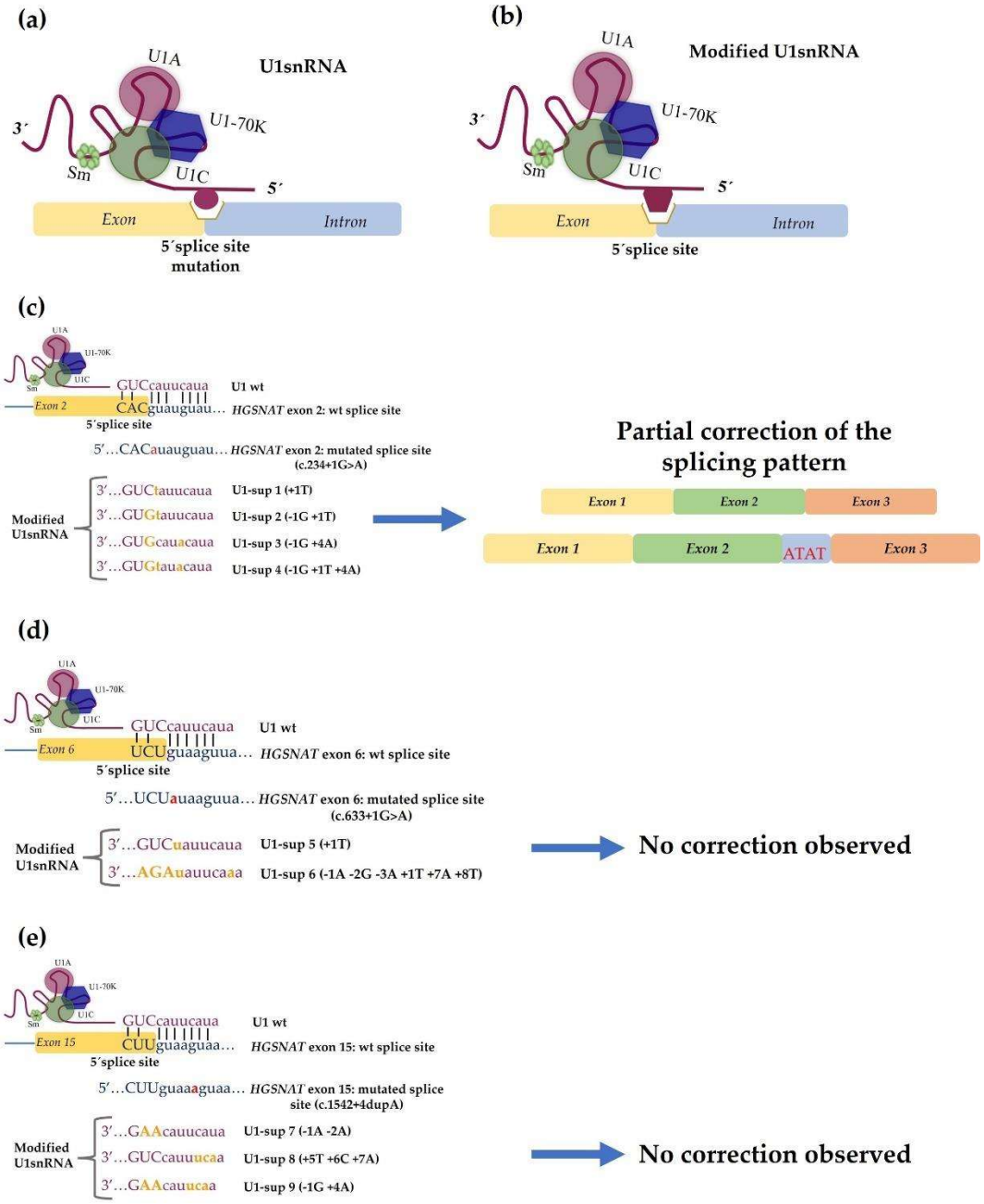


Figure 6. Therapeutic approach using modified U1 snRNA vectors: (**a**) the 5′ region of the U1 snRNA is involved in the recognition of the 5′ss. A mutation in this site compromises the binding of this molecule and the normal splicing process cannot occur; (**b**) a strategy for recovering the normal splicing process is the application of modified U1 snRNA to improve the recognition of the mutated 5′ss; (**c–e**) therapeutic approaches with different U1 snRNAs to correct the pathogenic effects of the splice site mutations in the *HGSNAT* gene (c.234+1G>A, c.633+1G>A and c.1542+4dupA). For the mutation described in (**c**), a partial recovery from the splicing defect was observed after treatment with the fully adapted U1 snRNA (U1-sup4). After sequence analysis, two different sequences were observed: one with a normal splicing pattern and another that included the first four base pairs of the intron 2 (ATAT). For the other two mutations at the 5′ss of the *HGSNAT* gene, no correction was observed after the application of the modified U1 snRNAs. Upper case letters show exonic nucleotides and lower case letters denote intronic nucleotides. Base pairing is indicated by vertical lines. The mutant nucleotide is highlighted in red and the changed nucleotides in the U1 sequence are illustrated in orange.

For the c.234+1G>A minigene, an expected band for the normal splicing was observed after co-expression with three of the five U1 snRNAs that were being tested; however, after sequence analysis, it was possible to observe that the fragment included exon 2 and the first four base pairs of intron 2 due to the use of an alternative downstream donor site (Figure 6c).

For the mutant c.633+1G>A minigene, an apparently normal band was detected with the overexpression of the U1 that matched all nucleotides of the mutated donor splice site. Yet again, the sequence analysis showed that, apart from exon 6, the first four nucleotides of the intron 6 were included. A band that corresponded to the skipping of exon 6 was also observed (Figure 6d).

In the c.1542+4dupA mutant minigene, when the co-transfection of the totally complementary U1 was performed, no correction was achieved, as the resulting fragment included not only exon 15 but also the first four nucleotides of intron 15. The inclusion of intronic nucleotides in all cases was due to the presence of a "gt" dinucleotide in positions +5 and +6 (Figure 6e).

Despite these results and taking into account that the minigenes only included partial intronic sequences that could lack some splicing regulatory sites and that they were assayed in non-human cells, modified U1 snRNAs were tested on patient-derived fibroblasts. For the c.234+1G>A mutation, a partial correction (almost 50%) was observed when the totally complementary U1 was transfected: one sequence demonstrated normal splicing and the other included the first four base pairs of intron 2 (as detected in the minigene approaches with COS-7 cells). However, no improvement in enzyme activity was observed. In the other patient fibroblasts (mutations c.633+1G>A and c.1542+4dupA), no effects of any modified U1 snRNAs were observed on the endogenous splicing process.

4.3. Identification and Characterization of Novel Splicing Defects and Assessment of Their Amenability for Splicing Correction Therapeutic Approaches: The MPS I Example

While there are only two publications on the design of innovative approaches for the correction of specific splicing defects in MPSs, to the best of our knowledge, many other MPS-causing mutations could also be amenable to splicing correction therapeutic approaches, as demonstrated by the significant number of splicing defects that have been (already) identified in this group of pathologies (Table 2). Moreover, as in DMD, other mutations besides the splicing mutations could be corrected with ASOs, namely the deletions and insertions that cause frameshift and for which exon skipping approaches could be applicable. Thus, many other studies could be designed to assess the feasibility of ameliorating the phenotypes of these multisystemic diseases by "simply" either correcting, skipping or partially recovering their underlying defects. The recent developments in the broader RNA therapeutics field, together with the growing number of splicing modulation therapeutics that have either been approved or are under development, will certainly contribute to increase the number of studies using this sort of approaches and extend the catalogue of genetic diseases to which they apply.

In our lab, for example, we are also addressing another MPS-causing mutation, which is known to disrupt splicing: the c.1650+5G>A mutation in the *IDUA* gene (Figure 7). This single nucleotide change leads to exon 11 skipping and, when present in homozygosity or compound heterozygosity, causes MPS I. Being a 5′ss mutation, this pathogenic variant could be an excellent target for mutation-specific U1 snRNA-mediated therapeutic approaches. Thus, we performed this antisense snRNA therapeutic strategy on fibroblasts of a MPS I patient harboring the 5′ss mutation c.1650+5G>A in compound heterozygosity with a nonsense mutation (c.1205 G>A; p.W402X) in intron 11, which leads to the exon 11 skipping of the *IDUA* gene. Briefly, we constructed three different U1 variants with increased complementarity to the mutated 5′ss. Unfortunately, when they were transfected in the patients' fibroblasts, no correction was achieved. Instead, it was still possible to observe the skipping of exon 11 (unpublished data).

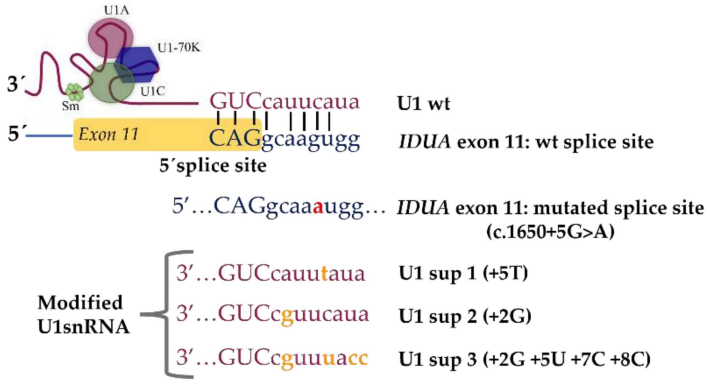


Figure 7. Therapeutic approach using modified U1 snRNA vectors. Different U1 snRNAs were designed to correct the pathogenic effects of the splice site mutation c.1650+5G>A in the *IDUA* gene. Upper case letters show exonic nucleotides and lower case letters denote intronic nucleotides. Base pairing is indicated by vertical lines. The mutant nucleotide is highlighted in red and the changed nucleotides in the U1 sequence are illustrated in orange.

The 5′ss is a very important sequence as it is a key factor in influencing not only the recognition of the donor splice site by U1, but also the overall success of the U1 therapeutic approach. This sequence can have a degenerative pattern feature and does not always conform to the consensus sequence (CAG/GURAG; R-purine) [103,104]. Therefore, not all positions of the sequence are equally important for enabling recognition by U1 and ensuring correct splicing. Various base pair combinations within the 5′ss can increase the U1 binding affinity [105].

Having this in mind, we are now performing further investigations. We started with one of the most obvious possibilities: the hypothesis that the absence of correction for the c.1650+5G>A mutation was caused by a low transfection efficacy. An interesting approach would be to test the therapeutic recovery of the mutation using a viral transduction technique. Viral vectors are considered significantly more efficient and less toxic than other delivery systems, namely cationic lipid transfection reagents such as Lipofectamine®. In fact, the viral transduction of U1 constructs in patients' fibroblasts has already been successfully applied for some diseases, allowing for the total or partial recovery of mis-spliced transcripts [106–108]. This is what we are currently testing in fibroblasts from MPS I patients carrying this splicing mutation. Other alternatives include testing the effects of modified U6 snRNA vectors in a similar way to that tested for the U1 snRNA vectors. Indeed, U6 snRNA has also been described as essential for proper splicing since its interaction with nucleotides at positions +4 to +6 of the splice donor site is necessary for the correct recognition of the exons at the 5′ss [109,110]. There is a published example in which only the co-application of adapted U1 and U6 isoforms corrected the splice defects that were caused by a +5 mutation [105].

Whatever the MPS we chose, the possibilities are numerous and diverse, as the catalogue of splicing defects known to cause it is vast (Table 2). Nevertheless, most of those variants are not particularly frequent among affected families. In fact, many of them are unique or rare. This could be an obstacle not only to the development of this sort of approaches, but also ultimately to making sure that those approaches that succeed eventually reach the clinic.

5. Challenges for the Development of Splice Modulation Approaches for MPSs

Regardless of these hurdles, MPSs, as with virtually any other LSD, are excellent candidates for splicing modulation for a number of reasons. First, they are monogenic diseases whose molecular bases have been under the lens of several teams around the world for many decades and knowledge about them has increased tremendously during this time. Second, and perhaps most importantly, it is assumed that a threshold enzyme

activity of approximately 10% is sufficient to prevent storage in LSDs [111,112]. This means that even a partial recovery could be sufficient to promote a clinically relevant effect.

Altogether, the possibilities are multiple and worth addressing. Still, there are at least two major issues that we need to address in order to ensure that this sort of therapeutic approach fulfils its full potential in the LSD field. The first, and most obvious, issue is the need for appropriate animal models in order to test these approaches *in vivo*.

5.1. Existence of Disease-Relevant Models

As important as cell models may be, a significant part of the efforts to demonstrate the therapeutic potential of any drug relies on studies with model organisms. The preclinical studies of adequate animal models are a major prerequisite, not only as proof of efficacy but also for safety and toxicity assessments, which are essential for the design of subsequent clinical trials. As previously discussed, the proper *in vivo* testing of splice modulation therapeutics requires the development of animal models that carry the specific splicing mutations. In fact, even though genetic models for MPSs encompass a wide range of biological systems [113–115] thanks to the numerous advances in mutagenesis techniques that have markedly improved the efficiency of model generation, knockout or transgenic mouse models that carry null mutations remain the gold standard within the field. It is important to notice, however, that while efforts should be made to develop suitable animal models, this may not be a straightforward task given the differences in the sequences that are involved in the overall splicing processes in different species [9]. Furthermore, the numerous species-specific differences that exist in orthologue-coding sequences may also hamper the process of animal model generation.

5.2. Design and Development of Effective Delivery Strategies

While the most obvious difficulty in terms of delivery is probably the BBB, which prevents patients with MPSs that involve the CNS from benefiting from several of the possible therapeutic approaches, including those which are already on the market, brain delivery may actually be feasible for some specific splicing modulation approaches. In fact, taking into account the latest findings on the wide distribution of ASOs after IT administration and its safety and tolerability, splicing modulation approaches that rely on ASOs hold a great promise for clinical translation. Nevertheless, the delivery of modified U1 snRNAs to the brain remains a pending issue. It is also important to note that brain delivery is far from being the only concern when it comes to promoting the clinical translation of this sort of approaches. There are other target tissues/organs that need to be taken into account when considering MPS-tailored approaches, namely the skeletal system. In fact, skeletal pathology is a huge burden in many MPSs and the currently available therapies fail to prevent or resolve it. The same is true for cardiovascular targeting, even though cardiovascular disease is not as prevalent in MPSs as skeletal pathology. Thus, both bone- and heart-targeting of therapeutic molecules are issues to be considered when designing splicing modulation approaches for MPS. Again, one possibility is to take advantage of the cell-specific receptors that can be targeted for uptake into these particularly impervious tissues [61].

5.3. Accurate Characterization of Disease-Causing Variants at mRNA Level

Finally, there is yet another issue that should not be forgotten: our efforts to correct specific pathogenic variants should also be accompanied by a serious attempt to characterize each novel disease-causing variant more accurately. While this may sound strange in a post-genomic era in which NGS allows for multiple genes to be sequenced in parallel, assuring a faster and more efficient identification of pathogenic variants while saving time and resources, the need for in-depth molecular characterization remains an issue [116]. In fact, even though NGS technologies have contributed to greatly to enlarging the catalogue of known disease-causing variants and have actually broadened the overall number of known genetic diseases (for example, the recently identified MPS type X was actually identified

through exome sequencing,), many of those variants need to be further investigated. This is particularly relevant for the mutations that affect splicing, which have to be functionally characterized and their impact evaluated at the molecular level. In fact, DNA variants that affect mRNA expression and processing are often missed or poorly characterized, not only because they are only analyzed at the genomic level but also because certain mRNA species tend to be subjected to degradation. A recent example in the field came from our own experience in the molecular characterization of LSD patients. For example, we recently demonstrated that an *NPC1* silent variant, which was previously classified as a non-pathological polymorphism (p.V562V), actually induces exon 11 skipping, which then leads to the appearance of a premature stop codon and underlies juvenile Niemann–Pick type C disease. This work relied on a series of molecular studies and led us to revisit other Portuguese patients who had been molecularly screened for the *NPC1* gene but for whom it was not possible to establish a definitive diagnosis. By doing so, we found a second patient with a clinical presentation of Niemann–Pick type C who harbored the silent p.V562V in heterozygosity with another known disease-causing mutation [117], thus highlighting the interest of reanalyzing existing test results in known disease genes **[116]**.

Plus, a better understanding of the fine mechanisms that regulate AS will also allow for a more effective targeting of those processes, thus contributing to the design and development of novel and more effective tools for therapeutic splicing modulation.

6. Concluding Remarks

Several lines of evidence support the *in vivo* effectiveness of RNA-based therapies in recovering aberrant splicing and, while exploratory, the studies on MPSs tend to follow this trend. Overall, the results that were reviewed in this paper further encourage the preclinical development and testing of this sort of approaches for this group of diseases, which so far either completely lack effective therapeutic options or have an urgent need for less expensive and more effective treatment. Still, in order for these approaches to reach the clinic and fulfill their therapeutic potential, several measures need to be undertaken both before and after the *in vitro* assessments. In fact, in an era in which a single genetic analysis allows us to sequence a huge number of genes and provide fast and reliable diagnoses, DNA variants that affect mRNA expression and processing are often still missed or their effects are poorly characterized. Thus, any efforts to address the therapeutic potential of splice modulation approaches should probably start earlier, with the proper molecular analysis of disease-causing pathogenic variants, in order to better characterize the incidence of splicing mutations and better understand their impacts at the molecular level. It is also mandatory to address the subsequent need for suitable animal models and better delivery systems for *in vivo* testing.

In addition, while not discussed in this review, there is another possible way to apply splicing modulation ASOs as a potential therapeutic approach for the treatment of MPSs: to deliberately skip or promote the skipping of disease-bearing exons. This is an approach that is somehow similar to that used for the treatment of DMD patients, which we briefly summarized in our introduction section (Figure 3). This would obviously require extra caution because the removal of whole exons or series of exons may be quite deleterious. Nevertheless, it could be feasible and even advantageous in some particular cases, as long as some key requirements are met. First, it would have to be checked whether the exon skipping under consideration would give rise to an in-frame protein product because it is mandatory to keep the remaining amino acid sequence intact. Then, it would also be necessary to check which protein domains would be affected by the change and how essential they are for protein function. Skipping an exon that codes for amino acids that are directly involved in the catalytic activity core of the enzyme, for example, may have a direct impact on protein function. Therefore, a careful bioinformatic analysis should be performed before considering this approach *in vitro*. Once attempted either in patient or model cell lines, a cautious analysis of the enzyme activity, location and expression should also be undertaken. While risky, this may be yet another route to targeting MPS diseases

using splicing modulation approaches. Nevertheless, to the best of our knowledge, no-one has ever attempted this sort of therapeutic approach for MPS diseases.

Author Contributions: Conceptualization, S.A.; NCBI Pubmed search, J.I.S., M.G., M.F.C. and L.M (Liliana Matos).; manuscript structure, J.I.S., M.F.C. and S.A.; original draft preparation, J.I.S. and M.F.C.; additional writing: M.G., L.M. (Liliana Matos), L.M. (Luciana Moreira), S.C. and S.A.; figures: J.I.S. and M.G.; critical review, J.I.S., M.F.C., L.M. (Liliana Matos), L.M. (Luciana Moreira), S.C., M.J.P. and S.A.; editing, J.I.S. and M.F.C.; funding acquisition, S.A. and M.F.C. All authors have read and agreed to the published version of the manuscript.

Funding: This research was partially funded by the FCT (FCT/PTDC/BBBBMD/6301/2014 and EXPL/BTM-SAL/0659/2021), the Portuguese Society for Metabolic Disorders (Sociedade Portuguesa de Doenças Metabólicas, SPDM—Bolsa SPDM de apoio à investigação Dr Aguinaldo Cabral 2018 (2019DGH1629/SPDM2018I&D) and 2019 (2020DGH1834)), the Sanfilippo Children's Foundation (SCF Incubator Grant 2019: 2019DGH1656/SCF2019I&D) and the MPS Society (2019DGH1642).

Institutional Review Board Statement: Not applicable.

Data Availability Statement: Not applicable.

Conflicts of Interest: The authors declare no conflict of interest.

References

1. Lieberman, J. Tapping the RNA world for therapeutics. *Nat. Struct. Mol. Biol.* **2018**, *25*, 357–364. [CrossRef] [PubMed]
2. Dhuri, K.; Bechtold, C.; Quijano, E.; Pham, H.; Gupta, A.; Vikram, A.; Bahal, R. Antisense Oligonucleotides: An Emerging Area in Drug Discovery and Development. *J. Clin. Med.* **2020**, *9*, 2004. [CrossRef]
3. Gagliardi, M.; Ashizawa, A.T. The Challenges and Strategies of Antisense Oligonucleotide Drug Delivery. *Biomedicines* **2021**, *9*, 433. [CrossRef] [PubMed]
4. Anna, A.; Monika, G. Splicing mutations in human genetic disorders: Examples, detection, and confirmation. *J. Appl. Genet.* **2018**, *59*, 253–268. [CrossRef] [PubMed]
5. Fernández-Pereira, C.; San Millán-Tejado, B.; Gallardo-Gómez, M.; Pérez-Márquez, T.; Alves-Villar, M.; Melcón-Crespo, C.; Fernández-Martín, J.; Ortolano, S. Therapeutic Approaches in Lysosomal Storage Diseases. *Biomolecules* **2021**, *11*, 1775. [CrossRef] [PubMed]
6. van Gool, R.; Tucker-Bartley, A.; Yang, E.; Todd, N.; Guenther, F.; Goodlett, B.; Al-Hertani, W.; Bodamer, O.A.; Upadhyay, J. Targeting neurological abnormalities in lysosomal storage diseases. *Trends Pharmacol. Sci.* **2021**, *in press*. [CrossRef]
7. Wraith, J.E.; Beck, M. Clinical Aspects and Clinical Diagnosis. In *Lysosomal Storage Disorders—A Practial Guide*; Metha, A., Winchester, B.E., Eds.; John Wiley and Sons: Hoboken, NJ, USA, 2012; pp. 13–19.
8. Giugliani, R. The Mucopolysaccharidoses. In *Lysosomal Storage Disorders—A Practical Guide*; Mehta, A.B., Ed.; Wiley-Blackwell: Oxford, UK, 2013; p. 208.
9. Dardis, A.; Buratti, E. Impact, Characterization, and Rescue of Pre-mRNA Splicing Mutations in Lysosomal Storage Disorders. *Genes* **2018**, *9*, 73. [CrossRef]
10. McBride, K.L.; Flanigan, K.M. Update in the Mucopolysaccharidoses. *Semin. Pediatr. Neurol.* **2021**, *37*, 100874. [CrossRef]
11. Berget, S.M.; Moore, C.; Sharp, P.A. Spliced segments at the 5′ terminus of adenovirus 2 late mRNA. *Proc. Natl. Acad. Sci. USA* **1977**, *74*, 3171–3175. [CrossRef]
12. Chow, L.T.; Gelinas, R.E.; Broker, T.R.; Roberts, R.J. An amazing sequence arrangement at the 5′ ends of adenovirus 2 messenger RNA. *Cell* **1977**, *12*, 1–8. [CrossRef]
13. Chen, M.; Manley, J.L. Mechanisms of alternative splicing regulation: Insights from molecular and genomics approaches. *Nat. Rev. Mol. Cell Biol.* **2009**, *10*, 741–754. [CrossRef] [PubMed]
14. De Conti, L.; Baralle, M.; Buratti, E. Exon and intron definition in pre-mRNA splicing. *Wiley Interdiscip Rev. RNA* **2013**, *4*, 49–60. [CrossRef] [PubMed]
15. Matera, A.G.; Wang, Z. A day in the life of the spliceosome. *Nat. Rev. Mol. Cell Biol.* **2014**, *15*, 108–121. [CrossRef] [PubMed]
16. Will, C.L.; Luhrmann, R. Spliceosome structure and function. *Cold Spring Harb. Perspect. Biol.* **2011**, *3*, a003707. [CrossRef] [PubMed]
17. Shi, Y. Mechanistic insights into precursor messenger RNA splicing by the spliceosome. *Nat. Rev. Mol. Cell Biol.* **2017**, *18*, 655–670. [CrossRef] [PubMed]
18. Yan, C.; Wan, R.; Shi, Y. Molecular Mechanisms of pre-mRNA Splicing through Structural Biology of the Spliceosome. *Cold Spring Harb. Perspect. Biol.* **2019**, *11*, a032409. [CrossRef] [PubMed]
19. Tazi, J.; Bakkour, N.; Stamm, S. Alternative splicing and disease. *Biochim. Biophys. Acta* **2009**, *1792*, 14–26. [CrossRef]
20. Sune-Pou, M.; Limeres, M.J.; Moreno-Castro, C.; Hernandez-Munain, C.; Sune-Negre, J.M.; Cuestas, M.L.; Sune, C. Innovative Therapeutic and Delivery Approaches Using Nanotechnology to Correct Splicing Defects Underlying Disease. *Front. Genet.* **2020**, *11*, 731. [CrossRef]

21. Kim, H.K.; Pham, M.H.C.; Ko, K.S.; Rhee, B.D.; Han, J. Alternative splicing isoforms in health and disease. *Pflugers Arch.* **2018**, *470*, 995–1016. [CrossRef]
22. Wang, Z.; Burge, C.B. Splicing regulation: From a parts list of regulatory elements to an integrated splicing code. *RNA* **2008**, *14*, 802–813. [CrossRef]
23. Wang, Y.; Liu, J.; Huang, B.O.; Xu, Y.M.; Li, J.; Huang, L.F.; Lin, J.; Zhang, J.; Min, Q.H.; Yang, W.M.; et al. Mechanism of alternative splicing and its regulation. *Biomed. Rep.* **2015**, *3*, 152–158. [CrossRef] [PubMed]
24. Dvinge, H. Regulation of alternative mRNA splicing: Old players and new perspectives. *FEBS Lett.* **2018**, *592*, 2987–3006. [CrossRef] [PubMed]
25. Arechavala-Gomeza, V.; Khoo, B.; Aartsma-Rus, A. Splicing modulation therapy in the treatment of genetic diseases. *Appl. Clin. Genet.* **2014**, *7*, 245–252. [CrossRef] [PubMed]
26. Stephenson, M.L.; Zamecnik, P.C. Inhibition of Rous sarcoma viral RNA translation by a specific oligodeoxyribonucleotide. *Proc. Natl. Acad. Sci. USA* **1978**, *75*, 285–288. [CrossRef] [PubMed]
27. Roberts, T.C.; Langer, R.; Wood, M.J.A. Advances in oligonucleotide drug delivery. *Nat. Rev. Drug Discov.* **2020**, *19*, 673–694. [CrossRef] [PubMed]
28. Syed, Y.Y. Eteplirsen: First Global Approval. *Drugs* **2016**, *76*, 1699–1704. [CrossRef] [PubMed]
29. Young, C.S.; Pyle, A.D. Exon Skipping Therapy. *Cell* **2016**, *167*, 1144. [CrossRef] [PubMed]
30. Heo, Y.A. Golodirsen: First Approval. *Drugs* **2020**, *80*, 329–333. [CrossRef]
31. Dhillon, S. Viltolarsen: First Approval. *Drugs* **2020**, *80*, 1027–1031. [CrossRef]
32. Shirley, M. Casimersen: First Approval. *Drugs* **2021**, *81*, 875–879. [CrossRef]
33. Finkel, R.S.; Chiriboga, C.A.; Vajsar, J.; Day, J.W.; Montes, J.; De Vivo, D.C.; Yamashita, M.; Rigo, F.; Hung, G.; Schneider, E.; et al. Treatment of infantile-onset spinal muscular atrophy with nusinersen: A phase 2, open-label, dose-escalation study. *Lancet* **2016**, *388*, 3017–3026. [CrossRef]
34. Finkel, R.S.; Mercuri, E.; Darras, B.T.; Connolly, A.M.; Kuntz, N.L.; Kirschner, J.; Chiriboga, C.A.; Saito, K.; Servais, L.; Tizzano, E.; et al. Nusinersen versus Sham Control in Infantile-Onset Spinal Muscular Atrophy. *N. Engl. J. Med.* **2017**, *377*, 1723–1732. [CrossRef] [PubMed]
35. Monaco, A.P.; Bertelson, C.J.; Liechti-Gallati, S.; Moser, H.; Kunkel, L.M. An explanation for the phenotypic differences between patients bearing partial deletions of the DMD locus. *Genomics* **1988**, *2*, 90–95. [CrossRef]
36. Kole, R.; Krieg, A.M. Exon skipping therapy for Duchenne muscular dystrophy. *Adv. Drug Deliv. Rev.* **2015**, *87*, 104–107. [CrossRef]
37. Mendell, J.R.; Rodino-Klapac, L.R.; Sahenk, Z.; Roush, K.; Bird, L.; Lowes, L.P.; Alfano, L.; Gomez, A.M.; Lewis, S.; Kota, J.; et al. Eteplirsen for the treatment of Duchenne muscular dystrophy. *Ann. Neurol.* **2013**, *74*, 637–647. [CrossRef]
38. Aartsma-Rus, A.; Krieg, A.M. FDA Approves Eteplirsen for Duchenne Muscular Dystrophy: The Next Chapter in the Eteplirsen Saga. *Nucleic Acid Ther.* **2017**, *27*, 1–3. [CrossRef]
39. FDA. Grants Accelerated Approval to First Targeted Treatment for Rare Duchenne Muscular Dystrophy Mutation. Available online: https://www.fda.gov/news-events/press-announcements/fda-grants-accelerated-approval-first-targeted-treatment-rare-duchenne-muscular-dystrophy-mutation (accessed on 15 March 2022).
40. FDA. Approves Targeted Treatment for Rare Duchenne Muscular Dystrophy Mutation. Available online: https://www.fda.gov/news-events/press-announcements/fda-approves-targeted-treatment-rare-duchenne-muscular-dystrophy-mutation (accessed on 15 March 2022).
41. Dzierlega, K.; Yokota, T. Optimization of antisense-mediated exon skipping for Duchenne muscular dystrophy. *Gene Ther.* **2020**, *27*, 407–416. [CrossRef]
42. Wilton, S.D.; Fletcher, S. Splice modification to restore functional dystrophin synthesis in Duchenne muscular dystrophy. *Curr. Pharm. Des.* **2010**, *16*, 988–1001. [CrossRef]
43. Hua, Y.; Sahashi, K.; Hung, G.; Rigo, F.; Passini, M.A.; Bennett, C.F.; Krainer, A.R. Antisense correction of SMN2 splicing in the CNS rescues necrosis in a type III SMA mouse model. *Genes Dev.* **2010**, *24*, 1634–1644. [CrossRef]
44. Faravelli, I.; Nizzardo, M.; Comi, G.P.; Corti, S. Spinal muscular atrophy–recent therapeutic advances for an old challenge. *Nat. Rev. Neurol.* **2015**, *11*, 351–359. [CrossRef]
45. Verma, A. Recent Advances in Antisense Oligonucleotide Therapy in Genetic Neuromuscular Diseases. *Ann. Indian Acad. Neurol.* **2018**, *21*, 3–8. [CrossRef] [PubMed]
46. Cartegni, L.; Krainer, A.R. Correction of disease-associated exon skipping by synthetic exon-specific activators. *Nat. Struct. Biol.* **2003**, *10*, 120–125. [CrossRef] [PubMed]
47. Hua, Y.; Sahashi, K.; Rigo, F.; Hung, G.; Horev, G.; Bennett, C.F.; Krainer, A.R. Peripheral SMN restoration is essential for long-term rescue of a severe spinal muscular atrophy mouse model. *Nature* **2011**, *478*, 123–126. [CrossRef] [PubMed]
48. Aartsma-Rus, A. FDA Approval of Nusinersen for Spinal Muscular Atrophy Makes 2016 the Year of Splice Modulating Oligonucleotides. *Nucleic Acid Ther.* **2017**, *27*, 67–69. [CrossRef]
49. Chaytow, H.; Faller, K.M.E.; Huang, Y.T.; Gillingwater, T.H. Spinal muscular atrophy: From approved therapies to future therapeutic targets for personalized medicine. *Cell Rep. Med.* **2021**, *2*, 100346. [CrossRef]

50. Balestra, D.; Scalet, D.; Ferrarese, M.; Lombardi, S.; Ziliotto, N.; Croes, C.C.; Petersen, N.; Bosma, P.; Riccardi, F.; Pagani, F.; et al. A Compensatory U1snRNA Partially Rescues FAH Splicing and Protein Expression in a Splicing-Defective Mouse Model of Tyrosinemia Type I. *Int. J. Mol. Sci.* **2020**, *21*, 2136. [CrossRef]
51. Breuel, S.; Vorm, M.; Brauer, A.U.; Owczarek-Lipska, M.; Neidhardt, J. Combining Engineered U1 snRNA and Antisense Oligonucleotides to Improve the Treatment of a BBS1 Splice Site Mutation. *Mol. Ther. Nucleic Acids* **2019**, *18*, 123–130. [CrossRef]
52. Daguenet, E.; Dujardin, G.; Valcarcel, J. The pathogenicity of splicing defects: Mechanistic insights into pre-mRNA processing inform novel therapeutic approaches. *EMBO Rep.* **2015**, *16*, 1640–1655. [CrossRef]
53. Damase, T.R.; Sukhovershin, R.; Boada, C.; Taraballi, F.; Pettigrew, R.I.; Cooke, J.P. The Limitless Future of RNA Therapeutics. *Front. Bioeng. Biotechnol.* **2021**, *9*, 628137. [CrossRef]
54. Arechavala-Gomeza, V.; Garanto, A. Antisense RNA Therapeutics: A Brief Overview. *Methods Mol. Biol.* **2022**, *2434*, 33–49. [CrossRef]
55. Vázquez-Domínguez, I.; Garanto, A. Considerations for Generating Humanized Mouse Models to Test Efficacy of Antisense Oligonucleotides. *Methods Mol. Biol.* **2022**, *2434*, 267–279. [CrossRef] [PubMed]
56. Abril, J.F.; Castelo, R.; Guigó, R. Comparison of splice sites in mammals and chicken. *Genome Res.* **2005**, *15*, 111–119. [CrossRef] [PubMed]
57. Godfrey, C.; Desviat, L.R.; Smedsrod, B.; Pietri-Rouxel, F.; Denti, M.A.; Disterer, P.; Lorain, S.; Nogales-Gadea, G.; Sardone, V.; Anwar, R.; et al. Delivery is key: Lessons learnt from developing splice-switching antisense therapies. *EMBO Mol. Med.* **2017**, *9*, 545–557. [CrossRef] [PubMed]
58. Schoch, K.M.; Miller, T.M. Antisense Oligonucleotides: Translation from Mouse Models to Human Neurodegenerative Diseases. *Neuron* **2017**, *94*, 1056–1070. [CrossRef]
59. Heon-Roberts, R.; Nguyen, A.L.A.; Pshezhetsky, A.V. Molecular Bases of Neurodegeneration and Cognitive Decline, the Major Burden of Sanfilippo Disease. *J. Clin. Med.* **2020**, *9*, 344. [CrossRef]
60. Anthony, K. RNA-based therapeutics for neurological diseases. *RNA Biol.* **2022**, *19*, 176–190. [CrossRef]
61. Hammond, S.M.; Aartsma-Rus, A.; Alves, S.; Borgos, S.E.; Buijsen, R.A.M.; Collin, R.W.J.; Covello, G.; Denti, M.A.; Desviat, L.R.; Echevarría, L.; et al. Delivery of oligonucleotide-based therapeutics: Challenges and opportunities. *EMBO Mol. Med.* **2021**, *13*, e13243. [CrossRef]
62. Fuller, M.; Meikle, P.J.; Hopwood, J.J. Epidemiology of lysosomal storage disorders: An overview. In *Fabry Disease: Perspectives from 5 Years of FOS*; Mehta, A., Beck, M., Sunder-Plassmann, G., Eds.; Oxford PharmaGenesis: Oxford, UK, 2006.
63. Fernández-Marmiesse, A.; Morey, M.; Pineda, M.; Eiris, J.; Couce, M.L.; Castro-Gago, M.; Fraga, J.M.; Lacerda, L.; Gouveia, S.; Pérez-Poyato, M.S.; et al. Assessment of a targeted resequencing assay as a support tool in the diagnosis of lysosomal storage disorders. *Orphanet J. Rare Dis.* **2014**, *9*, 59. [CrossRef]
64. Platt, F.M.; d'Azzo, A.; Davidson, B.L.; Neufeld, E.F.; Tifft, C.J. Lysosomal storage diseases. *Nat. Rev. Dis. Primers* **2018**, *4*, 27. [CrossRef]
65. Fecarotta, S.; Gasperini, S.; Parenti, G. New treatments for the mucopolysaccharidoses: From pathophysiology to therapy. *Ital. J. Pediatr.* **2018**, *44*, 124. [CrossRef]
66. Bellettato, C.M.; Scarpa, M. Pathophysiology of neuropathic lysosomal storage disorders. *J. Inherit. Metab. Dis.* **2010**, *33*, 347–362. [CrossRef] [PubMed]
67. Mokhtariye, A.; Hagh-Nazari, L.; Varasteh, A.R.; Keyfi, F. Diagnostic methods for Lysosomal Storage Disease. *Rep. Biochem. Mol. Biol.* **2019**, *7*, 119–128. [PubMed]
68. Zanetti, A.; D'Avanzo, F.; Bertoldi, L.; Zampieri, G.; Feltrin, E.; De Pascale, F.; Rampazzo, A.; Forzan, M.; Valle, G.; Tomanin, R. Setup and Validation of a Targeted Next-Generation Sequencing Approach for the Diagnosis of Lysosomal Storage Disorders. *J. Mol. Diagn.* **2020**, *22*, 488–502. [CrossRef] [PubMed]
69. Viana, G.M.; Priestman, D.A.; Platt, F.M.; Khan, S.; Tomatsu, S.; Pshezhetsky, A.V. Brain Pathology in Mucopolysaccharidoses (MPS) Patients with Neurological Forms. *J. Clin. Med.* **2020**, *9*, 396. [CrossRef]
70. Coutinho, M.F.; Lacerda, L.; Alves, S. Glycosaminoglycan storage disorders: A review. *Biochem. Res. Int.* **2012**, *2012*, 471325. [CrossRef]
71. Rapoport, D.M.; Mitchell, J.J. Pathophysiology, evaluation, and management of sleep disorders in the mucopolysaccharidoses. *Mol. Genet. Metab.* **2017**, *122S*, 49–54. [CrossRef]
72. Kubaski, F.; Osago, H.; Mason, R.W.; Yamaguchi, S.; Kobayashi, H.; Tsuchiya, M.; Orii, T.; Tomatsu, S. Glycosaminoglycans detection methods: Applications of mass spectrometry. *Mol. Genet. Metab.* **2017**, *120*, 67–77. [CrossRef]
73. Peters, H.; Ellaway, C.; Nicholls, K.; Reardon, K.; Szer, J. Treatable lysosomal storage diseases in the advent of disease-specific therapy. *Intern. Med. J.* **2020**, *50* (Suppl. 4), 5–27. [CrossRef]
74. Filocamo, M.; Tomanin, R.; Bertola, F.; Morrone, A. Biochemical and molecular analysis in mucopolysaccharidoses: What a paediatrician must know. *Ital. J. Pediatr.* **2018**, *44*, 129. [CrossRef]
75. HGMD. Available online: https://my.qiagendigitalinsights.com/ (accessed on 14 March 2022).
76. Giugliani, R.; Muschol, N.; Keenan, H.A.; Dant, M.; Muenzer, J. Improvement in time to treatment, but not time to diagnosis, in patients with mucopolysaccharidosis type I. *Arch. Dis. Child* **2020**, *106*, 674–679. [CrossRef]
77. Parini, R.; Deodato, F.; Di Rocco, M.; Lanino, E.; Locatelli, F.; Messina, C.; Rovelli, A.; Scarpa, M. Open issues in Mucopolysaccharidosis type I-Hurler. *Orphanet J. Rare Dis.* **2017**, *12*, 112. [CrossRef] [PubMed]

78. Kubaski, F.; de Oliveira Poswar, F.; Michelin-Tirelli, K.; Matte, U.D.S.; Horovitz, D.D.; Barth, A.L.; Baldo, G.; Vairo, F.; Giugliani, R. Mucopolysaccharidosis Type I. *Diagnostics* **2020**, *10*, 161. [CrossRef] [PubMed]
79. Hashmi, M.S.G.V. Mucopolysaccharidosis Type II. Available online: https://www.ncbi.nlm.nih.gov/books/NBK560829/ (accessed on 15 March 2022).
80. Pearse, Y.; Iacovino, M. A Cure for Sanfilippo Syndrome? A Summary of Current Therapeutic Approaches and their Promise. *Med. Res. Arch.* **2020**, *8*, 2045. [CrossRef] [PubMed]
81. Valstar, M.J.; Ruijter, G.J.; van Diggelen, O.P.; Poorthuis, B.J.; Wijburg, F.A. Sanfilippo syndrome: A mini-review. *J. Inherit. Metab. Dis.* **2008**, *31*, 240–252. [CrossRef]
82. Jones, S.A.; Breen, C.; Heap, F.; Rust, S.; de Ruijter, J.; Tump, E.; Marchal, J.P.; Pan, L.; Qiu, Y.; Chung, J.K.; et al. A phase 1/2 study of intrathecal heparan-N-sulfatase in patients with mucopolysaccharidosis IIIA. *Mol. Genet. Metab.* **2016**, *118*, 198–205. [CrossRef]
83. Wijburg, F.A.; Whitley, C.B.; Muenzer, J.; Gasperini, S.; Del Toro, M.; Muschol, N.; Cleary, M.; Sevin, C.; Shapiro, E.; Bhargava, P.; et al. Intrathecal heparan-N-sulfatase in patients with Sanfilippo syndrome type A: A phase IIb randomized trial. *Mol. Genet. Metab.* **2019**, *126*, 121–130. [CrossRef]
84. Whitley, C.B.; Vijay, S.; Yao, B.; Pineda, M.; Parker, G.J.M.; Rojas-Caro, S.; Zhang, X.; Dai, Y.; Cinar, A.; Bubb, G.; et al. Final results of the phase 1/2, open-label clinical study of intravenous recombinant human N-acetyl-α-d-glucosaminidase (SBC-103) in children with mucopolysaccharidosis IIIB. *Mol. Genet. Metab.* **2019**, *126*, 131–138. [CrossRef]
85. Seker Yilmaz, B.; Davison, J.; Jones, S.A.; Baruteau, J. Novel therapies for mucopolysaccharidosis type III. *J. Inherit. Metab. Dis.* **2021**, *44*, 129–147. [CrossRef]
86. Muenzer, J. Overview of the mucopolysaccharidoses. *Rheumatology* **2011**, *50* (Suppl. 5), v4–v12. [CrossRef]
87. Sawamoto, K.; Alvarez Gonzalez, J.V.; Piechnik, M.; Otero, F.J.; Couce, M.L.; Suzuki, Y.; Tomatsu, S. Mucopolysaccharidosis IVA: Diagnosis, Treatment, and Management. *Int. J. Mol. Sci.* **2020**, *21*, 1517. [CrossRef]
88. Harmatz, P.; Shediac, R. Mucopolysaccharidosis VI: Pathophysiology, diagnosis and treatment. *Front. Biosci. (Landmark Ed.)* **2017**, *22*, 385–406. [CrossRef] [PubMed]
89. Taylor, M.; Khan, S.; Stapleton, M.; Wang, J.; Chen, J.; Wynn, R.; Yabe, H.; Chinen, Y.; Boelens, J.J.; Mason, R.W.; et al. Hematopoietic Stem Cell Transplantation for Mucopolysaccharidoses: Past, Present, and Future. *Biol. Blood Marrow Transplant.* **2019**, *25*, e226–e246. [CrossRef] [PubMed]
90. Montano, A.M.; Lock-Hock, N.; Steiner, R.D.; Graham, B.H.; Szlago, M.; Greenstein, R.; Pineda, M.; Gonzalez-Meneses, A.; Coker, M.; Bartholomew, D.; et al. Clinical course of sly syndrome (mucopolysaccharidosis type VII). *J. Med. Genet.* **2016**, *53*, 403–418. [CrossRef] [PubMed]
91. Zhou, J.; Lin, J.; Leung, W.T.; Wang, L. A basic understanding of mucopolysaccharidosis: Incidence, clinical features, diagnosis, and management. *Intractable Rare Dis. Res.* **2020**, *9*, 1–9. [CrossRef]
92. Qi, Y.; McKeever, K.; Taylor, J.; Haller, C.; Song, W.; Jones, S.A.; Shi, J. Pharmacokinetic and Pharmacodynamic Modeling to Optimize the Dose of Vestronidase Alfa, an Enzyme Replacement Therapy for Treatment of Patients with Mucopolysaccharidosis Type VII: Results from Three Trials. *Clin. Pharm.* **2019**, *58*, 673–683. [CrossRef]
93. Sawamoto, K.; Stapleton, M.; Almeciga-Diaz, C.J.; Espejo-Mojica, A.J.; Losada, J.C.; Suarez, D.A.; Tomatsu, S. Therapeutic Options for Mucopolysaccharidoses: Current and Emerging Treatments. *Drugs* **2019**, *79*, 1103–1134. [CrossRef]
94. Triggs-Raine, B.; Salo, T.J.; Zhang, H.; Wicklow, B.A.; Natowicz, M.R. Mutations in HYAL1, a member of a tandemly distributed multigene family encoding disparate hyaluronidase activities, cause a newly described lysosomal disorder, mucopolysaccharidosis IX. *Proc. Natl. Acad. Sci. USA* **1999**, *96*, 6296–6300. [CrossRef]
95. Imundo, L.; Leduc, C.A.; Guha, S.; Brown, M.; Perino, G.; Gushulak, L.; Triggs-Raine, B.; Chung, W.K. A complete deficiency of Hyaluronoglucosaminidase 1 (HYAL1) presenting as familial juvenile idiopathic arthritis. *J. Inherit. Metab. Dis.* **2011**, *34*, 1013–1022. [CrossRef]
96. Sato, Y.; Okuyama, T. Novel Enzyme Replacement Therapies for Neuropathic Mucopolysaccharidoses. *Int. J. Mol. Sci.* **2020**, *21*, 400. [CrossRef]
97. Spahiu, L.; Behluli, E.; Peterlin, B.; Nefic, H.; Hadziselimovic, R.; Liehr, T.; Temaj, G. Mucopolysaccharidosis III: Molecular basis and treatment. *Pediatr. Endocrinol. Diabetes Metab.* **2021**, *27*, 201–208. [CrossRef]
98. Matos, L.; Gonçalves, V.; Pinto, E.; Laranjeira, F.; Prata, M.J.; Jordan, P.; Desviat, L.R.; Pérez, B.; Alves, S. Functional analysis of splicing mutations in the IDS gene and the use of antisense oligonucleotides to exploit an alternative therapy for MPS II. *Biochim. Biophys. Acta* **2015**, *1852*, 2712–2721. [CrossRef] [PubMed]
99. Matos, L.; Goncalves, V.; Pinto, E.; Laranjeira, F.; Prata, M.J.; Jordan, P.; Desviat, L.R.; Perez, B.; Alves, S. Data in support of a functional analysis of splicing mutations in the IDS gene and the use of antisense oligonucleotides to exploit an alternative therapy for MPS II. *Data Brief* **2015**, *5*, 810–817. [CrossRef] [PubMed]
100. Brusius-Facchin, A.C.; Schwartz, I.V.; Zimmer, C.; Ribeiro, M.G.; Acosta, A.X.; Horovitz, D.; Monlleo, I.L.; Fontes, M.I.; Fett-Conte, A.; Sobrinho, R.P.; et al. Mucopolysaccharidosis type II: Identification of 30 novel mutations among Latin American patients. *Mol. Genet. Metab.* **2014**, *111*, 133–138. [CrossRef] [PubMed]
101. Soukarieh, O.; Gaildrat, P.; Hamieh, M.; Drouet, A.; Baert-Desurmont, S.; Frebourg, T.; Tosi, M.; Martins, A. Exonic Splicing Mutations Are More Prevalent than Currently Estimated and Can Be Predicted by Using In Silico Tools. *PLoS Genet.* **2016**, *12*, e1005756. [CrossRef]

102. Matos, L.; Canals, I.; Dridi, L.; Choi, Y.; Prata, M.J.; Jordan, P.; Desviat, L.R.; Pérez, B.; Pshezhetsky, A.V.; Grinberg, D.; et al. Therapeutic strategies based on modified U1 snRNAs and chaperones for Sanfilippo C splicing mutations. *Orphanet J. Rare Dis.* **2014**, *9*, 180. [CrossRef]
103. Raponi, M.; Baralle, D. Can donor splice site recognition occur without the involvement of U1 snRNP? *Biochem. Soc. Trans.* **2008**, *36*, 548–550. [CrossRef]
104. Valadkhan, S.; Gunawardane, L.S. Role of small nuclear RNAs in eukaryotic gene expression. *Essays Biochem.* **2013**, *54*, 79–90. [CrossRef]
105. Schmid, F.; Hiller, T.; Korner, G.; Glaus, E.; Berger, W.; Neidhardt, J. A gene therapeutic approach to correct splice defects with modified U1 and U6 snRNPs. *Hum. Gene Ther.* **2013**, *24*, 97–104. [CrossRef]
106. Glaus, E.; Schmid, F.; Da Costa, R.; Berger, W.; Neidhardt, J. Gene therapeutic approach using mutation-adapted U1 snRNA to correct a RPGR splice defect in patient-derived cells. *Mol. Ther.* **2011**, *19*, 936–941. [CrossRef]
107. Hartmann, L.; Neveling, K.; Borkens, S.; Schneider, H.; Freund, M.; Grassman, E.; Theiss, S.; Wawer, A.; Burdach, S.; Auerbach, A.D.; et al. Correct mRNA processing at a mutant TT splice donor in FANCC ameliorates the clinical phenotype in patients and is enhanced by delivery of suppressor U1 snRNAs. *Am. J. Hum. Genet.* **2010**, *87*, 480–493. [CrossRef]
108. Schmid, F.; Glaus, E.; Barthelmes, D.; Fliegauf, M.; Gaspar, H.; Nürnberg, G.; Nürnberg, P.; Omran, H.; Berger, W.; Neidhardt, J. U1 snRNA-mediated gene therapeutic correction of splice defects caused by an exceptionally mild BBS mutation. *Hum. Mutat.* **2011**, *32*, 815–824. [CrossRef] [PubMed]
109. Kandels-Lewis, S.; Seraphin, B. Involvement of U6 snRNA in 5′ splice site selection. *Science* **1993**, *262*, 2035–2039. [CrossRef] [PubMed]
110. Lesser, C.F.; Guthrie, C. Mutations in U6 snRNA that alter splice site specificity: Implications for the active site. *Science* **1993**, *262*, 1982–1988. [CrossRef] [PubMed]
111. Schueler, U.H.; Kolter, T.; Kaneski, C.R.; Zirzow, G.C.; Sandhoff, K.; Brady, R.O. Correlation between enzyme activity and substrate storage in a cell culture model system for Gaucher disease. *J. Inherit. Metab. Dis.* **2004**, *27*, 649–658. [CrossRef]
112. Parenti, G. Treating lysosomal storage diseases with pharmacological chaperones: From concept to clinics. *EMBO Mol. Med.* **2009**, *1*, 268–279. [CrossRef]
113. Vuolo, D.; Do Nascimento, C.C.; D'Almeida, V. Reproduction in Animal Models of Lysosomal Storage Diseases: A Scoping Review. *Front. Mol. Biosci.* **2021**, *8*, 773384. [CrossRef]
114. Rigon, L.; De Filippis, C.; Napoli, B.; Tomanin, R.; Orso, G. Exploiting the potential of drosophila models in lysosomal storage disorders: Pathological mechanisms and drug discovery. *Biomedicines* **2021**, *9*, 268. [CrossRef]
115. Benetó, N.; Vilageliu, L.; Grinberg, D.; Canals, I. Sanfilippo Syndrome: Molecular Basis, Disease Models and Therapeutic Approaches. *Int. J. Mol. Sci.* **2020**, *21*, 7819. [CrossRef]
116. Hartley, T.; Lemire, G.; Kernohan, K.D.; Howley, H.E.; Adams, D.R.; Boycott, K.M. New Diagnostic Approaches for Undiagnosed Rare Genetic Diseases. *Annu. Rev. Genomics Hum. Genet.* **2020**, *21*, 351–372. [CrossRef]
117. Encarnacao, M.; Coutinho, M.F.; Cho, S.M.; Cardoso, M.T.; Ribeiro, I.; Chaves, P.; Santos, J.I.; Quelhas, D.; Lacerda, L.; Teles, E.L.; et al. NPC1 silent variant induces skipping of exon 11 (p.V562V) and unfolded protein response was found in a specific Niemann-Pick type C patient. *Mol. Genet. Genom. Med.* **2020**, *8*, e1451. [CrossRef]

International Journal of
Molecular Sciences

MDPI

Review

Development of Engineered-U1 snRNA Therapies: Current Status

Mariana Gonçalves [1,2,3,4], Juliana Inês Santos [1,2,3,5], Maria Francisca Coutinho [1,2,3], Liliana Matos [1,2,3,†] and Sandra Alves [1,2,3,*,†]

1 Research and Development Unit, Department of Human Genetics, National Institute of Health Doutor Ricardo Jorge, INSA I.P., Rua Alexandre Herculano, 321, 4000-055 Porto, Portugal; mariana.goncalves@insa.min-saude.pt (M.G.); juliana.santos@insa.min-saude.pt (J.I.S.); francisca.coutinho@insa.min-saude.pt (M.F.C.); liliana.matos@insa.min-saude.pt (L.M.)
2 Center for the Study of Animal Science, Institute of Sciences, Technologies and Agro-Environment, CECA-ICETA, University of Porto, Praça Gomes Teixeira, Apartado 55142, 4051-401 Porto, Portugal
3 Associate Laboratory for Animal and Veterinary Sciences, AL4AnimalS, Faculty of Veterinary Medicine, University of Lisboa, Avenida da Universidade Técnica, 1300-477 Lisboa, Portugal
4 Centre for the Research and Technology of Agro-Environmental and Biological Sciences, CITAB, Inov4Agro, University of Trás-os-Montes and Alto Douro, 5000-801 Vila Real, Portugal
5 Biology Department, Faculty of Sciences, University of Porto, Rua do Campo Alegre, 4169-007 Porto, Portugal
* Correspondence: sandra.alves@insa.min-saude.pt
† These authors contributed equally to this work.

Abstract: Splicing of pre-mRNA is a crucial regulatory stage in the pathway of gene expression. The majority of human genes that encode proteins undergo alternative pre-mRNA splicing and mutations that affect splicing are more prevalent than previously thought. Targeting aberrant RNA(s) may thus provide an opportunity to correct faulty splicing and potentially treat numerous genetic disorders. To that purpose, the use of engineered U1 snRNA (either modified U1 snRNAs or exon-specific U1s—ExSpeU1s) has been applied as a potentially therapeutic strategy to correct splicing mutations, particularly those affecting the 5′ splice-site (5′ss). Here we review and summarize a vast panoply of studies that used either modified U1 snRNAs or ExSpeU1s to mediate gene therapeutic correction of splicing defects underlying a considerable number of genetic diseases. We also focus on the pre-clinical validation of these therapeutic approaches both in vitro and in vivo, and summarize the main obstacles that need to be overcome to allow for their successful translation to clinic practice in the future.

Keywords: U1 snRNA (small nuclear RNA)-based therapies; modified U1 snRNAs; exon-specific U1 snRNAs (ExSpeU1s); 5′ splice-site (5′ss); splicing mutations; splicing correction

check for updates

Citation: Gonçalves, M.; Santos, J.I.; Coutinho, M.F.; Matos, L.; Alves, S. Development of Engineered-U1 snRNA Therapies: Current Status. *Int. J. Mol. Sci.* **2023**, *24*, 14617. https://doi.org/10.3390/ijms241914617

Academic Editors: Barbara Pascucci, Annalisa Masi and Maria Moccia

Received: 17 August 2023
Revised: 22 September 2023
Accepted: 25 September 2023
Published: 27 September 2023

Copyright: © 2023 by the authors. Licensee MDPI, Basel, Switzerland. This article is an open access article distributed under the terms and conditions of the Creative Commons Attribution (CC BY) license (https://creativecommons.org/licenses/by/4.0/).

1. Introduction

In most eukaryotic organisms, genes are transcribed as pre-messenger RNAs (pre-mRNAs) that contain both non-coding sequences, introns, and coding sequences, exons. During the splicing process, introns are removed, leaving just exons in the so-called mature messenger RNA (mRNA). The mature mRNA is then transferred to the cytoplasm and translated into proteins [1]. Briefly, the splicing of pre-mRNA(s) is carried out by a complex known as spliceosome, which is constituted by five small nuclear ribonucleoproteins (snRNPs): U1, U2, U4, U5, and U6, together with more than 150 other proteins. The spliceosome recognizes the intron-exon junctions and its function is to remove the introns in order to form a mature in-frame mRNA which may then be translated into a protein [2–4].

Overall, splicing is a very complex step in the mRNA processing which involves a variety of factors. The recognition of exon/intron boundaries for correct intron removal by the splicing machinery requires the presence of several sequence elements on pre-mRNA, including the 5′ splice-site (ss) and 3′ss, the branch point sequence (BPS), and the

polypyrimidine (Py) tract. In addition to these core splice-site motifs, other *cis*-regulatory elements that recruit specific RNA-binding proteins that either activate or repress the use of adjacent splice-sites contribute to the fine-tuning and specificity of this pre-mRNA processing event [5,6].

It is estimated that about 15% of all point mutations that result in genetic diseases in humans are caused by changes either in classical or auxiliary splicing sequence elements. Approximately 10% of those mutations affect 5′ and 3′ss, resulting most frequently in partial or whole exon skipping, and to a lesser extent in intron retention and cryptic splice-site activation [7–9]. Particularly, with respect to mutations affecting the 5′ss, these can reduce complementarity with the U1 small nuclear RNA (U1 snRNA), thus preventing spliceosome formation [10–13]. In fact, it is well-established that it is the U1 snRNP that initiates spliceosome assembly by binding to the 5′ss. This binding relies on a simple base pairing mechanism between the single-stranded terminal sequence of the U1 snRNA molecule and the moderately conserved stretch of nucleotides at the 5′ss marking the exon-intron boundary [14]. That is why the presence of point mutations in this stretch can easily disturb U1 snRNA binding to the pre-mRNA region. Therefore, restoring the complementarity through engineered modification of the U1 snRNA represents a valuable therapeutic approach to correct the abnormal splicing process, which results from that disruption. In fact, this approach has been explored by a number of independent teams and applied to a significant number of mutations affecting the 5′ss. For this purpose, the normal 5′ end sequence of the U1 snRNA cloned in a vector is altered to a sequence complementary to the target mutated region, the so-called modified U1 snRNA vectors. These are designed to bind to the mutant pre-mRNA(s) by increasing their complementarity with the mutated 5′ss thus allowing the restoration of normal splicing [15]. Over the last decade(s), these sort of modified U1 snRNAs have been largely tested not only in cellular models of genetic diseases but also in vivo [16,17]. The primary goal of this review is to offer an overview of the role of modified U1 snRNAs and of their second-generation version, the exon-specific U1 snRNAs (ExSpeU1s) as therapeutic tools. Here we summarize recent studies that used this approach to correct the splicing process. In addition, we also comment on the importance of the pre-clinical validation and summarize the main obstacles that this innovative RNA therapy faces in order to be translated into the clinic.

2. The U1 snRNA Structure/U1 snRNP Complex and 5′ Splice-Site Features

The U1 snRNP is one of the 5 snRNPs that constitute the spliceosome. This molecule is essential for the splicing process, and previous studies have shown that it is produced in larger quantities than any other snRNP, demonstrating its relevance. Mammalian U1 snRNP is comprised of a 164-nucleotide U1 snRNA, 7 Sm proteins (B or B′, D1, D2, D3, E, F, and G), which are shared with other snRNPs, and 3 U1-specific proteins (U1-A, U1-C, and U1-70K) (Figure 1a) [1,14,18].

In humans, one of the components of the U1 snRNP complex—the U1 snRNA, is encoded by a multigene family (known as *RNU1*) located on chromosome 1 (1p36) [19]. Imperfect copies of these U1 snRNA genes mapping to a separate location of chromosome 1 (1q12-21) were thought to be pseudogenes [20]. However, many of these "variant" (v)U1 snRNA genes produce fully processed transcripts, generating variant functional snRNAs. Studies in mice, frogs, and humans found expression changes of the canonical U1 and multiple U1 variant genes during cellular differentiation and development [21–24]. Furthermore, deletion of the chromosome region 1q12-21, involving all vU1 snRNA genes, causes severe neurological dysfunction reinforcing the notion that vU1 snRNAs may exert tissue-specific effects and be important for normal development. Therefore, the existence of a diverse population of vU1 snRNAs should not be ignored, as it can contribute to the fidelity and regulation of mRNA processing events in response to different environment stimuli, and have a significant impact on proteome diversity [25].

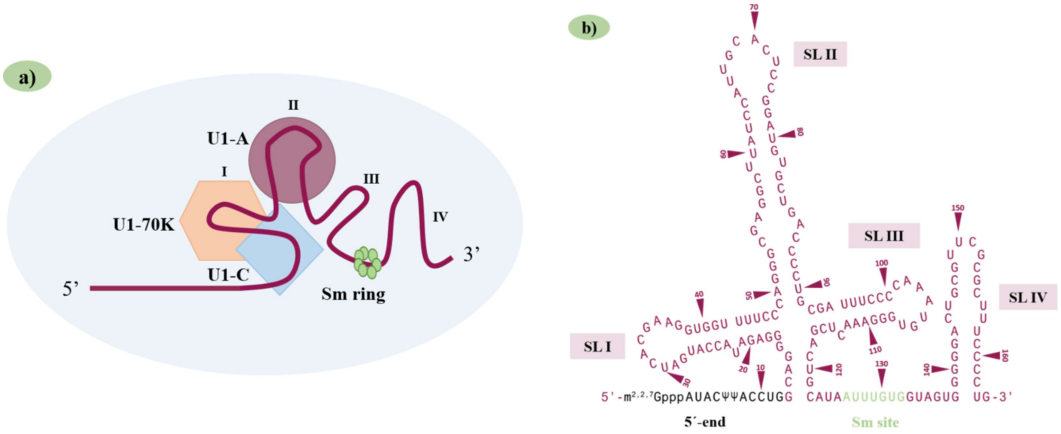


Figure 1. Illustrative figure of the U1 small nuclear ribonucleoprotein (U1 snRNP) complex and of the U1 small nuclear RNA (U1 snRNA) structure. (**a**) Summary of U1 snRNP topology. U1 snRNP (light blue) is composed of the U1 snRNA with 4 Stem-Loops (I-IV) (dark red line), 7 Sm proteins (green) and 3 U1 snRNP specific proteins: U1-70K (orange), U1-A (light burgundy) and U1-C (blue). (**b**) U1 snRNA sequence and structure. The $m^{2,2,7}G_{ppp}$ represents the snRNA-specific trimethyl cap structure. In U1 snRNA (164 nt), the 5′ end (black) binds to the 5′ splice-site and the downstream region contains the Stem-Loop (SL) I-III, followed by the Sm-site (green), and SL IV in the 3′end.

The U1 snRNA secondary structure consists of an unpaired 5′end, a four-way junction of 3 stem-loops (SL I-III) in a trefoil fold, a Sm site, and a fourth stem-loop at the 3′end (SL IV) (Figure 1b) [26]. This snRNA is transcribed in the nucleus by the RNA polymerase II (Figure 2a). Then, the pre-U1 snRNA moves to the cytoplasm (Figure 2b) where each of the 7 Sm proteins binds to a single base in the highly conserved Sm site (AUUUGUG) of the yet immature U1 snRNA, forming a ring structure in the following order: Sm-E, G, D3, B, D1, D2, and F. The formation of the ring structure is aided by the survival of the motor neuron (SMN) complex that is also involved in the assembly of snRNPs (Figure 2c,d). Following that, the U1 snRNA returns to the nucleus, where the U1-70K and the U1-A bind to SL I and II via specific motifs. The U1-C, on the other hand, does not bind to any U1 snRNA motif and is instead recruited to the U1 snRNP complex via protein:protein interaction with U1-70K and Sm-D3, ultimately resulting in the formation of the mature U1 snRNP (Figure 2e) [1,27]. This complex is now ready to start spliceosome assembly by binding to the 5′ss through base pairing between the 5′end of U1 snRNA (5′-$m^{2,2,7}G_{ppp}$AUACΨΨACCUG; Ψ—pseudouridine) and the moderately conserved stretch of nucleotides (CAG/GURAGU; R-purine) in the exon-intron junction (Figure 2f) [28]. However, not all base pairs at different 5′ss positions are equally important, and their contribution to splicing roughly correlates with their conservation. In eukaryotic organisms, in the 9 nucleotides consensus sequence (which can be expanded to include 11 base pairs), the most conserved 5′ss positions lie at the first two intronic positions (+1 and +2), which determine the 5′ss subtype. The GU subtype is present in 99% of the 5′ss, whereas the minor subtypes have a mismatch to U1 at either +1 or +2 and include the GC (0.9%) and the very rare AU 5′ss recognized by the spliceosome. The next most conserved 5′ss positions (>75% in humans) are -1G (the last exonic nucleotide) and +5G, which form strong G-C base pairing with the U1 snRNA, with three hydrogen bonds [18,29]. Consensus nucleotides −2A, +3A, +4A and +6U are also conserved but have a lesser although important contribution to 5′ss strength because their base pairing to U1 involves only the formation of two hydrogen bonds. The 5′ss positions +7 and +8 do not exhibit substantial conservation in humans, yet several lines of evidence indicate that these positions can base pair to U1 and contribute to 5′ss selection in mammals [29,30]. Thus, not all nucleotides located in the 5′ss region have an equal contribution to the splicing process: the more conserved, the greater their relevance (Figure 2f).

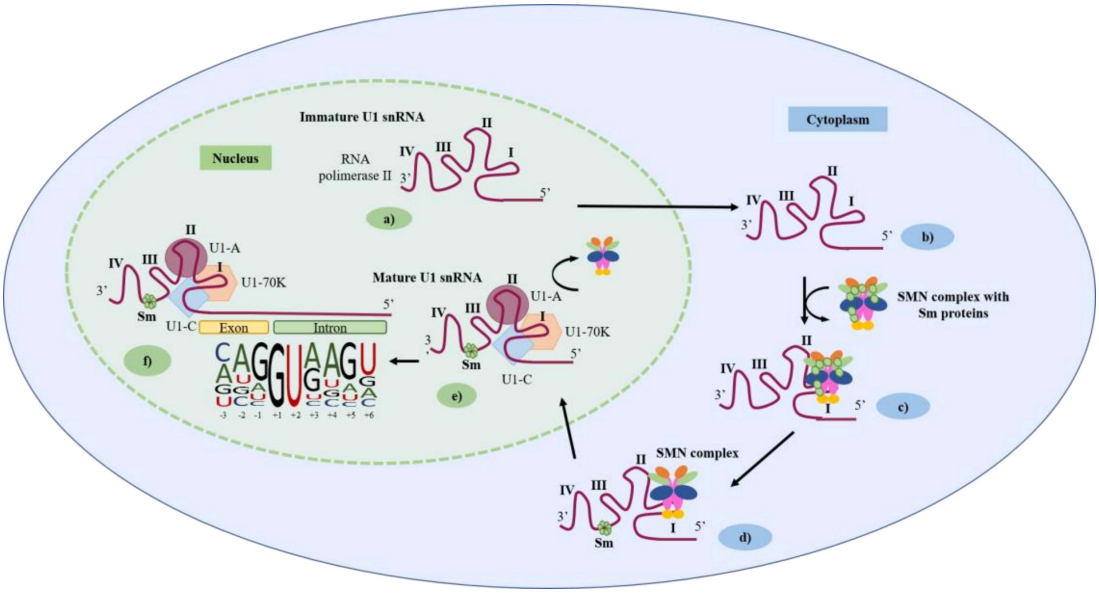


Figure 2. U1 small nuclear RNA (U1 snRNA) processing. The pre-U1 snRNA is transcribed in the nucleus by RNA polymerase II (**a**) and transported to the cytoplasm (**b**), where the formation of the Sm protein ring occurs (**c**,**d**). At this stage, however, the U1 snRNA is still immature. Then, the U1 snRNA returns to the nucleus, where the binding to the proteins U1-A, U1-70K and U1-C occurs and the U1 snRNA becomes mature (**e**). Finally, the mature U1 small nuclear ribonucleoprotein (U1 snRNP) initiates the spliceosome assembly through the binding to the pre-mRNA 5′ splice-site (9 nucleotides, CAG/GURAGU conserved between exons-introns) (**f**).

These different conservation levels in the 5′ss region turn it naturally diverse, with more than 9000 distinct sequences reported so far [29,31]. Relatively to the U1 snRNA sequence, approximately 40%, 22%, and 5% of the 5′ss include two, three, or four incompatibilities, respectively [32]. In fact, only about 5% of donor sites perfectly match the U1 snRNA consensus sequence, a value that could be substantially lower (0.85%) if only the most common canonical base pairing register is considered. However, the general helical U1 snRNA:5′ss duplex can accommodate alternative multiple non-canonical registers that include shifted base-pairing positions, bulged nucleotides on either the 5′ss or U1 snRNA strand, and asymmetric internal loops at different nucleotide positions, which contribute to increase complementarity and 5′ss selection. This reflects the huge flexibility and redundancy, that is allowed between the 5′ss-U1 snRNA base pairing to achieve efficient splicing at 5′ss [25,31,33]. In addition, this interaction is aided by several proteins such as U1-70K, U1-C, serine-arginine members and auxiliary elements, which may explain how the U1 snRNA is able to distinguish multiple pseudo-splice-sites [27,34,35].

Even though the U1 snRNP is known for its involvement in the splicing process, it does exert additional functions in the cell such as initiating transcription, protecting the mRNA from degradation, as well as protecting the pre-mRNA against premature polyadenylation [14,18,25].

3. The U1 snRNA Molecule as a Promising Therapeutic Tool for Splicing Correction

Together with the understanding of the constitutive splicing process and the perception of the crucial role U1 snRNAs play in it, came the realization that, by artificially generating and modifying U1 snRNAs, one could potentially correct aberrant splicing processes. To achieve this goal, two different generations of engineered U1 snRNAs are currently being explored: the modified U1 snRNAs and the ExSpeU1s (Figure 3). Here, we summarize the main results obtained in several studies where these two U1 generations were used to rescue aberrant splicing caused by different types of splicing mutations underlying different human genetic disorders (Table 1).

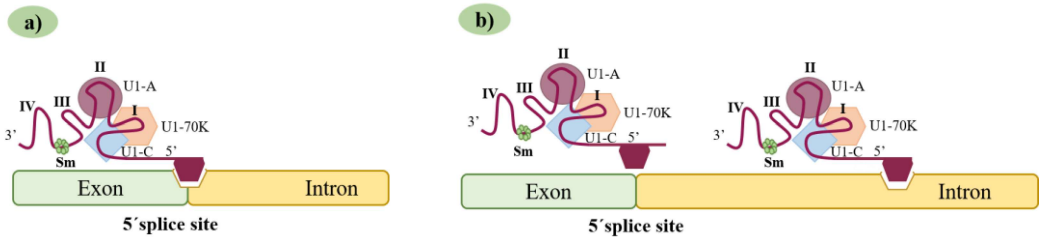


Figure 3. Schematic representation of U1 small nuclear RNA (U1 snRNA)-mediated therapeutic approaches for 5′splice-site (5′ss) mutations. (**a**) Mutation-adapted U1 snRNAs are designed to be complementary to the mutant 5′ss allowing a correct assembly of the spliceosome. (**b**) Exon-specific U1 snRNAs bind to a non-conserved intronic region promoting the use of the mutated 5′ss region through mechanisms not yet fully understood.

Table 1. Summary table of engineered U1 small nuclear RNA (U1 snRNA) and combined therapeutic approaches developed for different human genetic diseases.

	Genetic Disease	Gene	Type of Study	Splicing Variants *	Reference
Modified U1 snRNAs	Neurofibromatosis type 1	*NF1*	in vitro	c.288+5G>C	[36]
	Coagulation factor VII deficiency	*F7*	in vitro	9726+5G>A (c.805+5G>A)	[37,38]
			in vivo	859+5G>A (c.805+5G>A)	[39]
	Retinitis pigmentosa	*RHO*	in vitro	c.936G>A	[40]
		RPGR	in vitro	c.1245+3A>T	[41]
	Bardet-Biedl syndrome	*BBS1*	in vitro	c.479G>A	[42]
	Propionyl-CoA carboxylase deficiency	*PCCA*	in vitro	c.1209+3A>G	[43]
	Tyrosinaemia type 1	*FAH*	in vitro	c.1062+5G>A	[44]
	Fanconi anemia	*FANCC*	in vitro	c.165+1G>T	[45]
	Mucopolysaccharidosis type IIIC	*HGSNAT*	in vitro	c.234+1G>A; c.633+1G>A; c.1542+4dupA	[11]
	Shwachman-Diamond syndrome	*SBDS*	in vitro	c.258+2T>C	[46]
	Aromatic L-Amino Acid Decarboxylase deficiency	*AADC*	in vitro	IVS6+4A>T (c.714+4A>T)	[16]
			in vivo		
	ATP8B1 deficiency	*ATP8B1*	in vitro	c.2932-3C>A; c.2418+5G>A; c.279G>A; c.625_627+5delinsACAGTAAT	[10]
	CDKL5-deficiency	*CDKL5*	in vitro	c.99+1G>T c.99+5G>A c.463+1G>A c.744+1G>C c.2376+5G>A	[47]
	Tyrosinaemia type 1	*Fah*	in vivo	c.706G>A	[13]
Exon-Specific U1 snRNAs	Hemophilia B	*F9*	in vitro	c.392-9T>G; c.392-8T>G; c.519A>C; c.519A>G; c.519A>T c.520G>T; c.520+1G>A; c.520+2T>C	[48]
				p.V107V (c.459G>A); p.R116R (c.484C>A); p.A118V (c.491C>T); p. Q121H (c.501G>T)	[12]
				c.277+1G>A; c.277+1G>T, c.277+2T>C; c.277+2T>G; c.277+4A>G	[17]
			in vitro in vivo	c.519A>C	[49]

Table 1. *Cont.*

	Genetic Disease	Gene	Type of Study	Splicing Variants *	Reference
Exon-Specific U1 snRNAs	Cystic fibrosis	*CFTR*	in vitro	c.1766+3A>G; c.1766+3A>C; c.1766+5G>A; c.1766G>T; c.1766G>A; p.A566T (c.1696G>A); p.Y577Y (c.1731C>T)	[48]
			in vitro	711+3A>C (c.579+3A>C); 711+3A>G (c.579+3A>G); 711+5G>A (c.579+5G>A); 1863C>T (c.1731C>T); 1898+3A>G (c.1766+3A>G); 2789+5G>A (c.2657+5G>A); 3120G>A (c.2988G>A); TG13T3, TG13T5; TG12T5	[50]
	Spinal muscular atrophy	*SMN2*	in vitro	c.840C>T	[48]
			in vitro in vivo	c.840C>T	[51–53]
	ATP8B1 deficiency	*ATP8B1*	in vitro	c.625_627+5delinsACAGTAAT	[10]
	CDKL5-deficiency	*CDKL5*	in vitro	c.99+1G>T c.99+5G>A c.463+1G>A c.744+1G>C c.2376+5G>A	[47]
	Hemophilia A	*F8*	in vitro	c.602-32A>G; c.602-10T>G; c.669A>G; c.669A>T; c.670G>T; c.670+1G>T; c.670+1G>A; 670+2T>G; c.670+5G>A; c.670+6T>C	[54]
			in vitro	p.G2000A (c.5999G>C); p.Y2036Y (c.6108C>T); p.N2038S (c.6113A>G); c.6115+1G>A; c.6115+2T>C; c.6115+3G>T; c.6115+4A>G; c.6115+5G>A; c.6115+6T>A	[55]
	Netherton syndrome	*SPINK5*	in vitro	c.891C>T	[56]
	Fanconi anemia	*FANCA*	in vitro	c.790C>T	[57]
	Familial dysautonomia	*ELP1*	in vitro in vivo	c.2204+6T>C	[58,59]
	Autosomal dominant optic atrophy	*OPA1*	in vitro	c.1065+5G>A	[60]
	Phenylketonuria	*PAH*	in vitro	c.1199+17G>A; c. 1199+20G>C	[61]
	Shwachman-Diamond syndrome	*SBDS*	in vitro	c.258+2T>C	[46]
	Ornithine transcarbamylase deficiency	*Otc*	in vivo in vitro	c.386G>A	[62]
		OTC	in vitro	c.386G>A	[63]
Combined therapies	Bardet-Biedl syndrome	*BBS1*	in vitro	c.479G>A	[64]
				Exon 5 5′ss (position +5) #	[65]
	Autosomal dominant optic atrophy	*Opa1*	in vivo	c.1065+5G>A	[66]
	Hemophilia A	*F8*	in vitro	c.6115+5G>A	[55]

* All studied mutations were listed regardless of the outcome of the therapeutic approaches attempted. # Artificially generated variant that affects splicing but that has never been reported in a human patient so far.

3.1. First Generation of Synthetic U1 snRNAs: The Modified U1 snRNAs

The use of modified U1 snRNA vectors that are similar to the endogenous U1 snRNA and have the ability to bind to the target pre-mRNA can restore splicing. For this, the 5′ end of U1 snRNA must be modified to a sequence that complements the mutated target sequence (Figure 3a). These modifications are made by site-directed mutagenesis on a plasmid that contains the U1 snRNA sequence, a promoter, and a termination sequence.

The resulting modified U1 snRNA can then be transfected into cells, but it can also be inserted into adeno-associated viruses (AAVs) or lentiviruses and delivered both in vitro and in vivo [27,49,51].

In 1986, there was already evidence suggesting that the 5′ end of the U1 snRNA recognizes the 5′ss in mRNA precursors by complementary base pairing. In light of these facts, Zhuang and Weiner [67] tested for the first time whether modified U1 snRNAs can actually correct aberrant splicing patterns caused by mutations affecting the 5′ss. To do so, they checked whether the effect of point mutations in two alternative splice-sites of the adenovirus *E1A* gene was corrected by different modified U1 snRNAs. In normal conditions, the *E1A* pre-mRNA of the adenovirus is spliced into three mRNA species (13S, 12S, and 9S mRNAs) by the use of three alternative 5′ss. The presence of one point mutation at position +5 of the alternative 12S splice-site abolishes 12S mRNA synthesis. So, to try to correct the effect of that mutation, these authors constructed three modified U1 snRNAs using a plasmid vector and co-transfected it with the mutant *E1A* into HeLa cells. Remarkably, they verified that one of those U1 snRNAs was able to restore the 12S mRNA synthesis. In this same study, another point mutation was analyzed, in this case, it abolishes the production of the *E1A* 13S mRNA and is located at position +3 of the 13S 5′ss. Through the same protocol, three modified U1 snRNAs with three different matches to the 5′ss were designed. However, only a very weak mutation suppression was observed with one of those compensatory U1 snRNAs. These results further confirm that mutations, which reduce the match of a 5′ss to the U1 snRNA consensus sequence, usually impair splicing, and also suggest that this base pairing is necessary but not sufficient for the splicing of mRNA precursors. Most importantly, this discovery has unleashed numerous possibilities for the development of therapies for many diseases.

Subsequently, several studies in cellular models demonstrated that it was possible to correct disease-associated mutations in less conserved positions of the 5′ss. In fact, about a decade later, Baralle and colleagues [36] corrected a 5′ss variant causing the autosomal dominant disorder Neurofibromatosis type 1 (NF1). Their target was a substitution of a G for a C at the +5 position of the *NF1* intron 3 (c.288+5G>C). These authors used a minigene system containing the *NF1* exon 3 and its flanking intronic regions of both wild-type and mutant sequences. Transfection of the mutant minigene into Hep3B cells revealed that the G>C mutation in intron 3 drastically affects splicing leading to the skipping of exon 3, but when it was transfected together with an U1 snRNA fully complementary to the mutated site, the inclusion of the exon 3 was observed. To further prove this result, the authors also performed the co-transfection of the mutant minigene with a wild-type U1 snRNA vector and the recovery of the normal splicing process was not observed, highlighting that the correct splicing of exon 3 was due to the presence of the modified U1 snRNA molecule. Later, Pinotti and coworkers [38] also developed a U1 snRNA approach for the rescue of a 5′ss mutation causing Severe coagulation factor VII (FVII) deficiency. The target mutation in this study occurs at the +5 position of the *FVII* intron 7 [9726+5G>A (c.805+5G>A; according to current nomenclature)] and, results in the skipping of exon 7 leading to FVII deficiency. In an attempt to restore the normal splicing pattern, different complementary U1 snRNAs were designed and co-transfected with wild-type and mutant minigenes into COS-7 and Hep3B cell lines. The results showed that a totally complementary U1 snRNA improved the recognition of the correct 5′ss reducing exon skipping by 50% in both cell lines, an effect that showed to be dose-dependent. Afterward, the same authors [37] expanded this study, because although they had partially restored correct splicing using a totally modified U1 snRNA, the experimental settings did not allow for assessing its effect on protein levels and function, a key issue in the evaluation of the potential of a therapeutic approach. To solve this problem, the authors developed a full-length *FVII* splicing competent construct and co-transfected it together with the totally complementary U1 snRNA in COS-1 cells. As a result, a partial rescue of *FVII* splicing and FVII protein biosynthesis was observed. The result was dose-dependent, and it was the first time that a U1 snRNA-mediated rescue

of splicing impaired by mutations at 5′ss resulted in an appreciable increase in functional protein.

Another example of the potential of these therapies came from the work developed by Tanner and co-workers [40] that used an adapted U1 snRNA for correcting the effect of a mutation causing Retinitis pigmentosa (RP). The target mutation (c.936G>A) involves the last nucleotide of exon 4 of the rhodopsin gene (*RHO*) and leads to two aberrant transcripts, one presenting the total skipping of exon 4 and the other showing a 4-base pair (bp) deletion at the end of exon 4 due to the activation of a cryptic splice-site. As in the previous studies, the authors started by addressing the therapeutic potential of modified U1 snRNAs using two minigenes, one containing the wild-type sequence and another harboring the mutant sequence that was transfected into COS-7 cells. Besides that, in order to assess plasmid expression in photoreceptor cells, these minigenes were also transfected into mouse retinal explants. Once again, a U1 adapted to the mutation led to increased levels of exon recognition and significantly reduced exon skipping. Nevertheless, activation of the cryptic splice-site was still detected. This may be explained by the fact that the target mutation is not only weakening the constitutive splice-site but is simultaneously activating the cryptic one. Another important study of the same group, targeting the same disease but focusing attention on another pathogenic mutation, was carried out by Glaus et al. [41]. These authors showed the efficacy of a fully complementary U1 snRNA to overcome the exon skipping caused by a mutation at +3 position in intron 10 (c.1245+3A>T) of the retinitis pigmentosa GTPase regulator (*RPGR*) gene, which origins an X-linked form of RP. Contrary to previous studies, the evaluation of the efficacy of the modified U1 snRNAs was performed in patient fibroblasts and four different U1 snRNAs were generated. Primary control and patient fibroblasts were then transduced with lentiviral vectors expressing the four U1 snRNA variants and the use of the U1 snRNA fully complementary to the mutation resulted in a partial correction of exon skipping. The treatment also revealed the use of cryptic splice-sites and the authors suggested that this might be related to the base change involved (A to T) that strongly disturbs splicing, since in the +3 position the most frequent bases are A or G, while T and C are much less frequent.

By the same time these pivotal studies were published, the use of homozygosity mapping in a large consanguineous family allowed to identify yet another disease-associated splice-site mutation: the c.479G>A variant in exon 5 of the *BBS1* gene, causing Bardet–Biedl syndrome. This mutation gives rise to three transcripts, one with the inclusion of intron 5 in addition to the constitutively spliced exons, one presenting the exon 5 skipping and unexpectedly, the correct spliced transcript was found although at reduced expression levels. Fully aware of the potential of modified U1 snRNAs to correct this sort of abnormal splicing, the researchers who identified this novel mutation also developed modified U1 snRNAs to increase their binding affinity for the mutated transcript. They also generated several minigenes that were co-transfected with four different modified U1 snRNAs in COS-7 cells. Furthermore, to better evaluate the efficacy of this approach, the patient's fibroblasts carrying the c.479G>A variant were also transduced with lentiviruses containing the same adapted U1 snRNA sequences. The results revealed a significant increase in correctly spliced *BBS1* transcripts and, simultaneously, a reduction in transcripts lacking exon 5. Of note, the transcript with intron 5 retention was still observed [42].

Overall, there are many other genetic disorders for which the use of modified U1 snRNAs can be attempted for therapeutic purposes. For example, splicing defects have a significant role in Propionyl-CoA carboxylase deficiency, with the majority of mutations being located either in the 3′ss or the 5′ss. Thus, attempting splicing modulation seemed to be a promising approach to address some of those mutations, namely the c.1209+3A>G mutation, which causes the skipping of the exon 13 of the *PCCA* gene that encodes the protein, which is deficient in this syndrome. So, in 2011, Sánchez–Alcudia and co-workers [43] investigated the potential of modified U1 snRNAs to correct its effect. Initial studies were performed in Hep3B cells with minigenes, but the corresponding wild-type construct failed to recapitulate accurately the transcriptional profile observed in fibroblasts probably due

to the lack of the whole genomic sequence context. Therefore, patients' fibroblasts homozygous for the nucleotide change were used as a cellular model for transfection with U1 constructs with different compensatory modifications. Using this strategy, the authors observed that when three of the four adapted U1 snRNA vectors were transfected, a reversion of the splicing defect could be detected, but only with the fully modified U1 snRNA the levels of the normal spliced band with exon 13 reached ~100%. However, the correction of the splicing defect did not result in a significant increase in enzymatic activity, highlighting the existence of other factors still unknown that can affect the successful application of these therapies.

Another curious example comes from the work of Scalet and colleagues [44] that studied the splicing mutation c.1062+5G>A in the *FAH* gene, which causes Tyrosinemia type 1. This mutation involves the *FAH* exon 12 5′ss and prevents its usage, even when forced by a modified U1 snRNA designed to increase the mutant 5′ss recognition. Noticeably, these authors verified that in one patient the presence of a new somatic change involving the penultimate position of the exon 12 (c.1061C>A) in linkage with the c.1062+5G>A mutation, partially rescues the defective 5′ss. Interestingly, this combined genetic condition strongly favored the rescue by a modified U1 snRNA that promoted the inclusion of exon 12 with a robust synthesis of correct transcripts that reached up to 60%. Therefore, this study clearly demonstrates the complexity associated with the development of U1 snRNA therapies.

Overall, the studies reviewed so far have addressed the capacity of modified U1 snRNAs to restore the splicing process in the presence of mutations affecting less conserved regions of the 5′ss. However, there are also works reporting the correction of mutations affecting the more conserved positions of the 5′ss that is, those located at +1 or +2 sites. To the best of our knowledge, though, there are only three reports on the successful correction of this type of mutation: one for the Fanconi anemia C (FANCC) [45], other for the rare Lysosomal Storage Disease Mucopolysaccharidosis type IIIC (MPS IIIC) [11], and the third one for Shwachman–Diamond Syndrome [46].

In the first case, Hartmann and co-workers [45], showed a partial correction of a +1 mutation (c.165+1G>T) in the intron 2 of the *FANCC* gene, which is associated with a milder form of FANCC. This work was the first successful correction of a +1 mutation, which converts the highly conserved GT dinucleotide within the 5′ss of *FANCC* exon 2 to a TT dinucleotide resulting in aberrant splicing. The majority of the observed transcripts (73%) were non-functional due to exon skipping or the usage of cryptic splice donor sites. Unexpectedly, however, the presence of the mutant TT 5′ss also enabled a correct recognition of the normal exon-intron boundaries, leading to reduced amounts of normal transcripts (27%). Briefly, the authors used two different cellular systems, HeLa cells with a splicing reporter construct carrying the target mutation and patient-derived fibroblasts and demonstrated that transfection with two different TT-adapted U1 snRNA expression plasmids facilitated correct exon 2 recognition, thereby increasing the fraction of *FANCC* exon 2 in-frame spliced pre-mRNA. Finally, the use of lentiviral vectors as a delivery system to introduce the mutation-adapted U1 snRNAs into primary FANCC patient fibroblasts allowed the rescue of the pathological phenotype of these cells. Interestingly, the level of functional restoration of transduced cells differed between the two U1 snRNAs that were specifically adapted for the mutant *FANCC* exon 2 5′ss. The fully complementary U1 snRNA allowed to achieve a good correction level while the adapted U1 snRNA with only a single compensatory mutation was less efficient.

In the second case, the use of modified U1 snRNAs to correct *HGSNAT* gene splicing mutations was also attempted by Matos and collaborators [11] as an alternative therapeutic strategy for MPS IIIC. These authors tried to overcome the effect of three *HGSNAT* 5′ss mutations: c.234+1G>A, c.633+1G>A and c.1542+4dupA. The first two affect the position +1 of the donor splice-site causing the skipping of the corresponding exons. The c.234+1G>A mutation, leads to the skipping of exon 2 and the c.633+1G>A causes the skipping of exon 6. Regarding the c.1542+4dupA, this affects the position +4 of the 5′ss of exon 15 and origins two transcripts: one with the skipping of exon 15 and the other containing the exon

15 plus the five first nucleotides of intron 15 due to the presence of a cryptic splice-site at the beginning of this intron.

As many other authors did in the previously reported studies, a first optimization approach where the effect of different modified U1 snRNAs on the splicing process was tested on minigenes bearing each mutation, but no correction of the aberrant splicing was observed. In fact, even though the skipping of the respective exon was corrected, the transcript generated after treatment was still aberrant due to the use of cryptic "gt" donor sites situated at the intronic positions +5 and +6 (+1 mutations) or +6 and +7 (+4 dupA mutation) that was promoted, partially or completely, by some adapted U1 snRNAs. Still, taking into account that minigenes do not entirely reproduce the human-specific genomic context, the different U1 variants were also tested directly into patients' fibroblasts. In the case of the c.633+1G>A and c.1542+4dupA mutations, the correct endogenously splicing process was not recovered after the overexpression of the different modified U1 snRNAs. Remarkably, however, for the c.234+1G>A mutation, which was present in homozygosity in two patients, the overexpression of a modified U1 that completely matches the mutated 5′ss, did promote a partial correction (almost 50%) of the splicing process, together with the use of the cryptic "gt" site at intronic positions +5 and +6. This was an unexpected and surprisingly positive result since the majority of the mutations localized in the high conserved nucleotide positions +1 and +2 of the donor splice-site that were submitted to correction with modified U1 snRNAs were unable to be rescued.

Another example in which positive results were observed came from a recent study [46] involving a very common 5′ss variant that is present in more than 90% [68,69] of worldwide patients with Shwachman–Diamond syndrome, one of the most common inherited bone marrow failure syndromes. The c.258+2T>C variant at the 5′ss of *SBDS* gene exon 2 is associated with aberrant pre-mRNA splicing leading to exon 2 skipping but trace levels of correct transcripts (2%) are also detected by qPCR, which account for residual protein expression and explain the survival of affected patients [46].

Recently, the same team that assessed exon 2 inclusion efficiency in c.258+2T>C lymphoblastoid cells, also tested, in vitro, different therapeutic approaches for this mutation, which included the test of a panel of engineered U1 snRNAs either modified or exon-specific (see Section 3.2 for information about this kind of U1 snRNAs). *SBDS* minigenes (wild-type or mutated) were co-transfected with one modified U1 snRNA or three different ExSpeU1 variants in HEK293T cells. All modified U1 snRNAs strongly promoted the use of a proximal cryptic exonic 5′ss and two ExSpeU1s also promoted the use of an exonic cryptic 3′ss. However, the modified U1 led also to a slight increase in the relative proportion of the corrected transcripts meaning that forcing the definition of the defective exon by using a compensatory U1 snRNA, albeit with low efficacy, did promote the synthesis of correct transcripts [46].

Overall, the promising results obtained in vitro for the majority of disease-causing-variants, whose effect over splicing was total or partially corrected through the action of modified U1 snRNAs, prompted additional studies to assess the feasibility of this approach in vivo. Depending on the target mutation and on the phenotypic presentation of the associated disorder, different administration methods have been attempted, leading to either transient or continued expression of the therapeutic U1 snRNAs. In vivo, the administration of modified U1 snRNA vectors can be performed via hydrodynamic injection, which allows their transitory expression. To obtain continued expression of the modified U1 snRNAs, however, it is necessary to use viral vectors. Among these, the most used in in vivo studies are the AAVs [39,70]. Indeed, AAVs have many advantages, such as a wide biodistribution in tissues, being accepted by the animals, their capsid has low immunogenicity compared to other viruses and, finally, they have the necessary packaging capacity to incorporate the U1 snRNA sequence [71].

One of the first in vivo studies using a modified U1 snRNA was performed by Balestra et al. [39]. These authors performed both transient and stable expression of constructs with a splicing mutation that causes FVII deficiency in humans, which they intended to

correct. For the transient expression, they used plasmid constructs, while for the stable one, they used AAV vectors. Briefly, to obtain the desired correction, in the transient expression experiments, the plasmids carrying the human *FVII* splicing mutation and the modified U1 snRNA adapted to the mutation at position +5 of intron 7 [859+5G>A (c.805+5G>A; according to the current nomenclature)] were simultaneously administered by hydrodynamic injection. For the continued expression experiments, on the other hand, two AAV vectors of different serotypes, one containing the human *FVII* pre-mRNA and the other the adapted U1 snRNA were sequentially administered by intravenous (IV) injection. Remarkably, the authors demonstrated that, regardless of the expression method, the mutation-adapted U1 snRNA was able to rescue *FVII* gene splicing and improve clotting in C57BL/6 mice.

Later, Lee and co-workers also addressed the therapeutic potential of modified U1 snRNAs in vivo [16]. Having demonstrated in N2A cells that a totally modified U1 snRNA was able to improve the splicing of a minigene bearing the IVS6+4A>T (c.714+4A>T) mutation of the *AADC* gene, they checked whether a similar effect was observed on mouse sequences from an artificial splicing construct using the same cell model. Since they succeeded, they moved on to in vivo studies, showing a therapeutic effect in knock-in mice with Aromatic L-Amino Acid Decarboxylase (AADC) deficiency after intracerebroventricular (ICV) injection of the AAV9 carrying the fully modified U1 snRNA. The treatment had promising results with an improvement in the survival and in the brain dopamine and serotonin levels of the mice.

In another study, Balestra and colleagues [13] used a mouse model (FAH5961SB) for the Fumarylacetoacetate hydrolase (FAH) deficiency (also known as Tyrosinemia type 1) and demonstrated that a compensatory U1 snRNA expressed in AAV, and administered via the lateral tail vein was able to partially restore the normal splicing disrupted by a mutation at the last nucleotide of the mouse *Fah* gene exon 8 (c.706G>A). Importantly, there was no evidence of toxicity in this trial, even though the same was not true for the first in vivo study of Balestra et al. [39] for FVII coagulation deficiency, where the authors did observe some hepatotoxicity in mice expressing the human *F7* c.805+5G>A mutant after modified U1 snRNA overexpression, which was attributed to off-target effects.

3.2. A New Generation of Synthetic U1 snRNAs: The Exon-Specific U1 snRNAs

In addition to the modified U1 snRNA vectors whose modifications are based on the target 5′ss sequence, there is yet another U1 snRNA-based strategy being developed and applied. These new molecules are designated exon-specific U1 snRNAs (ExSpeU1s) (Figure 3b) and have been developed to increase the specificity and the ability to include the target exon while significantly reducing the possibility of occurring off-target effects [18,48]. These ExSpeU1s are designed to recognize very poorly conserved regions of a given intron, downstream of the 5′ss of a target exon [72]. This means they are specific to a certain exon, and that is why they are given the designation ExSpeU1s. Unlike antisense oligonucleotides (ASOs), these molecules do not block intronic elements, but promote spliceosome activation through the recruitment of splicing factors improving exon definition [52]. Thus, ExSpeU1s have a broader range of therapeutic applications when compared to their previously referred counterparts. Theoretically, ExSpeU1s can be used to correct exon skipping caused by mutations in either the 5′ss, 3′ss, polypyrimidine tract or exonic regulatory elements. In fact, these molecules proved to be quite efficient both in vitro and in vivo, and a significant number of studies developed ExSpeU1s to correct different types of splicing mutations associated with defective exon definition in several human disorders [18].

The overall potential of this approach was assessed for the first time back in 2012, in a work from Franco Pagani's lab by Alanis and collaborators [48]. This team used ExSpeU1s to rescue splicing mutations in three different genetic diseases. They started by characterizing natural mutations in *F9* exon 5, *CFTR* exon 12 and *SMN2* exon 7 associated with exon skipping in Hemophilia B, Cystic fibrosis (CF), and Spinal muscular atrophy (SMA), respectively and then tried its therapeutic splicing rescue by using different ExSpeU1s.

For each gene system (*F9* exon 5, *CFTR* exon 12 and *SMN2* exon 7), they identified an ExSpeU1 able to rescue splicing impaired by different types of mutations. More specifically, they showed that the ExSpeU1-mediated correction of different *F9* exon 5 mutations in the 5′ss (3 synonymous mutations in position −2: −2C, −2G and −2T; see Table 1) and in the polypyrimidine tract (2 intronic variants: −8G and −9G; see Table 1), results in complete restoration of secreted functional factor IX levels. However, for 5′ss mutations at the positions −1T, +1A and +2C (see Table 1), the ExSpeU1 did not correct the splicing defect. Regarding Cystic fibrosis, the 5′ss mutations in *CFTR* exon 12 showed a variable response to ExSpeU1, in this case, the rescue efficiency was optimal (~85%) for the +3G, intermediate (~50%) for the −1A, +3C and +5A and low (~20%) for the −1T (see mutations in Table 1). Furthermore, this ExSpeU1 allowed the almost complete splicing correction of two *CFTR* exon 12 mutations (see Table 1). Similarly, for SMA it was demonstrated in minigene assays and in the chromosomal context of normal cells (HEK293) that ExSpeU1s also improved *SMN2* exon 7 splicing. The SMA is a genetic neuromuscular disease caused by loss-of-function mutations in the *SMN1* gene, but humans have a paralogue gene called *SMN2*. One of the few nucleotide changes between *SMN1* and *SMN2* genes is a silent mutation within exon 7 (c.840C>T) that makes 80–90% of the transcripts derived from the *SMN2* gene skip exon 7. Thus, the modulation of *SMN2* exon 7 splicing has been on the basis of several therapeutic attempts for SMA. In fact, another study performed also by Pagani's team [53], showed that the same ExSpeU1s developed by Alanis et al. [48] for SMA significantly corrected endogenous *SMN2* exon 7 splicing and restored the levels of the resulting SMN protein in two cellular models (HEK293 Flp-In cells and lentiviral-infected SMA type I fibroblasts). Interestingly, the results demonstrate that the ExSpeU1 snRNA molecule not only corrects splicing but also increases mRNA levels and stabilizes the *SMN* pre-mRNA intermediate. This effect resulted in higher levels of *SMN* mRNAs when compared to those achieved in the treatment with an ASO that targets corresponding intronic sequences. The outcome of pre-mRNA processing can be explained because while the ASO acts as an antisense molecule masking an intronic splicing silencer (ISS), the ExSpeU1s recruits splicing factors on the defective upstream exon and decreases the mutation effect.

To evaluate the activity of ExSpeU1 in vivo, the authors also tested it in newborn mice carrying the *SMN2* transgene through AAV-mediated delivery. The RT-PCR showed an increase in exon 7 inclusion in the brain, heart, liver, kidney, and skeletal muscle. This result demonstrates that ExSpeU1 can be efficiently expressed in vivo in different mouse tissues and exert an effect on its natural human *SMN2* target [53].

In another study, also for SMA and conducted by the same lab [51], a transgenic mouse expressing an ExSpeU1 was bred and crossed with a severe SMA mouse model to assess the therapeutic potential of this specific sort of U1 snRNAs for erroneous splicing correction. The results showed an increase in the inclusion of *SMN2* exon 7, production of SMN protein, and a significant improvement in phenotype and survival. For the first time, a specific modification of a core spliceosomal component proved to be safe and effective in a severe SMA mouse model as a novel therapeutic strategy for this disorder. However, this was not the only contribution that came from this study when it comes to the overall ExSpeU1 state of the art. In fact, besides the in vivo analysis, the authors have also made an attempt to evaluate in vitro the structural requirements of these ExSpeU1 particles and showed that the U1 snRNP 70K protein and the stem-loop IV elements of the U1 snRNA mediate most of the splicing rescue activity through improvement of exon and intron definition.

Subsequently, this study was expanded and the team tested the viral delivery of the *SMN2* ExSpeU1 encoded by the adeno-associated virus AAV9. Overall, the virus increased *SMN2* exon 7 inclusion and SMN protein levels and rescued the phenotype of mild and severe SMA mice. Furthermore, the treatment improved the neuromuscular function and increased the life span from 10 to 219 days in severely affected mice. Quite remarkably, ExSpeU1 expression persisted for 1 month and was effective at around one five-hundredth of the concentration of the endogenous U1 snRNA. Moreover, when the same authors analyzed, through RNA-sequencing (RNA-seq), a human cellular model overexpressing

the ExSpeU1 more than 100-fold above the therapeutic level, no damaging effects were observed, i.e., it did not significantly alter global gene expression or splicing. Overall, the high efficacy in two SMA animal models, the lack of off-target effects on the human transcriptome and the long-lasting effect observed by these authors, further support the idea that ExSpeU1s delivered by AAV may be a valid therapeutic tool for splicing-related pathologies [52].

Overall, the pool of knowledge that has been accumulating over the last decade on the therapeutic potential of ExSpeU1 goes far beyond SMA. Other important clues on the applicability and translatability of the ExSpeU1 approach in rescuing exon skipping defects, came precisely from the study of yet another of the three original disorders addressed by Alanis and co-workers [48] in their proof of principle paper: Cystic fibrosis. In fact, when Donegà and colleagues [50] attempted an ExSpeU1-based approach to rescue a total of 10 different CF-causing splicing mutations, their overall results were extremely positive. The authors chose 10 relatively frequent splicing mutations that cause the skipping of 5 different exons (5, 10, 13, 16 and 18; see Table 1). Splicing mutations 711+3A>C/G (c.579+3A>C/G) and 711+5G>A (c.579+5G>A) are located in the 5′ss consensus of exon 5; 1863C>T (c.1731C>T) and 1898+3A>G (c.1766+3A>G) in an exonic regulatory element and in the 5′ss consensus of exon 13, respectively; 2789+5G>A (c.2657+5G>A) and 3120G>A (c.2988G>A) are located at the 5′ss consensus of exon 16 and 18, respectively, whereas TG13T3, TG13T5, TG12T5 are variants at the polypyrimidine tract of exon 10. Through a somehow classical, yet elegant, minigene-based splicing assay, the authors proved that all those mutations could be efficiently corrected in vitro by a panel of ExSpeU1s engineered to bind to intronic sequences downstream of each defective exon. Most importantly, they also showed that the ExSpeU1-mediated splicing correction at the RNA level did correlate with a recovery of the full-length CFTR protein for some of those variants. Additionally, from the panel of mutations analyzed in this study, those involving exon 13 skipping were shown to be less prone to an efficient ExSpeU1-mediated correction. Therefore, the authors further analyzed exon 13 splicing, focusing attention on intronic regulatory elements within the ExSpeU1 binding region and performing a detailed mechanistic analysis, which eventually disclosed why exon 13 was the most challenging to rescue. In summary, this was the first time that an exon rescue strategy was shown to work with such efficiency in a single gene on several exon-skipping mutations and different exons [50], but soon evidence started to gather on the overall potential of ExSpeU1s as therapeutic molecules, with a number of other diseases and mutations adding up to the targets catalog. For example, the effect of different ExSpeU1s and modified U1 snRNAs was evaluated for mutations in the *ATP8B1* gene. ATP8B1 deficiency is a severe autosomal recessive liver disease characterized by a continuous phenotypical spectrum from intermittent to progressive Familial intrahepatic cholestasis. The differences in disease severity may be caused by variations in the structure and/or function of the ATP8B1 protein resulting from the type of mutation. As in other trials described throughout this review, Van der Woerd and co-workers [10] also used a minigene system to evaluate splicing effects caused by variants at exon-intron boundaries, as well as to test the ability of complementary modified U1 snRNAs and ExSpeU1s to rescue aberrant splicing. The first ones have been shown to completely restore splicing for two 5′ss *ATP8B1* mutations (c.279G>A; c.625_627+5delinsACAGTAAT) and to improve the normal splicing process for the first time of one mutation located at the position −3 of the 3′ss (c.2932-3C>A). However, for the c.2418+5G>A splicing correction was not achieved. Furthermore, the authors evaluated five ExSpeU1s that bind at different intronic positions downstream of *ATP8B1* exon 7 for mutation c.625_627+5delinsACAGTAAT. Although very effective in correcting exon skipping, the ExSpeU1 treatment also resulted in partial retention of the short downstream intron.

In another study, Balestra and colleagues [47] also evaluated the capability of modified U1 snRNA and ExSpeU1 variants to correct mutations affecting +1 and +5 nucleotides at the 5′ss, which are predicted to cause *CDKL5* exon skipping. Mutations in the *CDKL5* gene lead to the CDKL5-deficiency disorder, a rare neurological condition characterized

by the onset of seizures in the first weeks of life and severe intellectual disability. In this study, the authors used the two variants of U1 snRNA, the modified U1 snRNA, and the second-generation ExSpeU1. However, both failed to restore exon definition in the presence of nucleotide changes occurring at position +1 (c.99+1G>T; c.463+1G>A; c.744+1G>C) in multiple exons of *CDKL5* gene. On the other hand, both generations of U1 snRNA variants completely rescued exon definition in the presence of the mutations c.99+5G>A and c.2376+5G>A located in the exon 3 and 16 contexts, respectively. Nevertheless, since the modified U1 snRNA improved *CDKL5* splicing in a dose-dependent manner and the ExSpeU1 completely restored proper exon definition at the lowest dose tested, only the ExSpeU1 was considered for protein assays. The results showed that this molecule fully restores CDKL5 protein synthesis, subcellular distribution and kinase activity further supporting its therapeutic potential.

Adding up to the catalog of severe genetic diseases, which may be caused by splicing mutations potentially amenable to U1 snRNA-based therapies, are a number of hereditary bleeding disorders, such as Hemophilias A and B. The first of those disorders was precisely Hemophilia B. In fact, back in 2016, Pagani's Lab [12] addressed a series of exonic splicing mutations (synonymous, missense and nonsense) in exon 5 of the *F9* (*FIX*) gene that causes Coagulation factor IX disease, also known as Hemophilia B. These authors studied the impact of those mutations on mRNA splicing and/or protein biology as well as their possible therapeutic rescue by the ExSpeU1 approach. Through expression studies with splicing-cassette minigenes and full-length protein constructs, the authors identified two synonymous substitutions (p.V107V; p.R116R) causing exon skipping and two missense mutations (p.A118V; p.Q121H) with partial effects on splicing and coagulation factor IX (FIX) secretion, but in which the spliced-corrected proteins maintain normal FIX coagulant activity as potential targets for a splicing-switching therapy. Furthermore, they tested different ExSpeU1 molecules binding intronic sequences downstream of *FIX* exon 5 and found an active ExSpeU1 (U1-fix9), which completely rescued aberrant exon skipping caused by different exonic mutations, through an SRSF2-mediated mechanism. Interestingly, the same team had already shown in previous work [48] that this ExSpeU1 recovered exon skipping caused by 5 mutations located at the polypyrimidine tract or at the 5′ss of *FIX* exon 5. So, together both studies identified different splicing mutations causing Hemophilia B, which may likely have a therapeutic benefit from splicing correction by a unique ExSpeU1 molecule.

In general, the evaluation of the safety and efficacy of this kind of therapy is limited by the availability of cellular and animal models specific to a given mutation. Remarkably however, Barbon and co-workers [49] were actually able to assess the efficacy of the ExSpeU1 fix9 (U1-fix9) reported above in cellular and mouse models that were generated using a specific transposon system to integrate splicing-competent human *FIX* minigenes either wild-type or carrying the c.519A>C splicing mutation in *FIX* exon 5 into the genome of HEK293 cells and C57BL/6 mice. Both models were then used to test, in a genomic DNA context, the efficacy of the U1-fix9, delivered with an AAV8 vector to overcome the effect of the splicing variant found in patients with Hemophilia B. The results showed the correction of the splicing pattern of human *FIX* mRNA, which translated into an increase in FIX protein expression levels.

Still on Hemophilia-related pathologies a very interesting study was conducted by Balestra et al. [54] that challenged the efficacy of a U1 snRNA-mediated strategy for splicing mutations occurring at the 3′ss, 5′ss or within exon 5 of the *F8* (*FVIII*) gene (see Table 1) and associated with different severity degrees of Coagulation factor VIII (FVIII) deficiency (Hemophilia A). The *F8* exon 5 is a singular model in which the original 5′ss has several cryptic 5′ss nearby, a scenario that becomes even more complex in the presence of nucleotide alterations at the 5′ss. So, taking this model and using minigenes, the authors demonstrated for the first time that a unique ExSpeU1 targeting an intronic region downstream of exon 5 was able to redirect the use of the canonical 5′ss (~80%) in the presence of several mutations located at 3′ss, 5′ss or within the exon. Once again, a more detailed investigation of the

rescued transcripts from +1 and +2 intronic variants showed that the ExSpeU1 promoted the use of adjacent cryptic 5′ss, leading to frameshifted transcript forms, which eventually compromised the correction attempt.

A similar approach was later developed by the same team for the correction of several *F8* gene mutations affecting the splicing of exon 19 (see Table 1) [55]. This exon was chosen as a model because it is poorly defined, which points towards the existence of functional regulatory elements promoting its proper inclusion. An extended panel of disease-causing exon 19 variants was challenged by a correction approach with engineered U1 snRNAs. First, the authors used a *F8* exon 19 minigene and tested in vitro the effect of one complementary U1 snRNA and three ExSpeU1s in the rescue of the c.6115+4A>G variant, which was previously associated with total exon skipping. The most efficient, which was one of the ExSpeU1s, was then used to correct the other exon 19 splicing affecting variants and was very efficient in the rescue of all exonic variants as well as of three intronic variants (exon inclusion ranging from +18% to +68%). Only for three mutations, c.6115+1G>A, +2T>C and +5G>A, the use of the ExSpeU1 led to the activation of a cryptic 5′ss, which resulted in partial intron 19 retention. However, the co-delivery of the ExSpeU1 with a modified U6 snRNA partially rescued (from 0 to 3%) the effect of one of those variants (c.6115+5G>A; see Section 3.3 for combined therapeutic strategies).

Overall, these studies demonstrate that a single ExSpeU1 can efficiently rescue different mutations involving the same exon adding up to the pool of knowledge on the plasticity of single ExSpeU1s and making these molecules particularly attractive for the correction of rare genetic variants. In fact, the development of this kind of approach has a great therapeutic potential for rare diseases, particularly for splicing mutations that are relatively frequent among patients with a specific rare disease. That is the case of the work conducted by Dal Mas et al. [56] in which an ExSpeU1 approach was tested to correct the splicing defect caused by a frequent synonymous variant (c.891C>T) in the *SPINK5* gene, which resulted in Netherton syndrome (NS), a rare severe autosomal-recessive genodermatosis. This variant is located in the position +9 of exon 11 and induces its skipping. Briefly, different ExSpeU1s targeting the intronic region downstream of the exon 11 constitutive 5′ss were tested through minigene splicing assays and rescued with different efficacies the skipping of the exon 11. Then, the most active ExSpeU1 was tested in keratinocytes from a NS patient bearing the target variant. Its lentiviral-mediated transduction allowed to recover the correct *SPINK5* transcript and also the corresponding functional protein.

Similar approaches have been attempted for different diseases over the last decade, even though their results have not always been as promising as the previously reported. For example, virtually at the same time the previously referred ExSpeU1 proved to be efficient both at mRNA and protein level for that particular NS-causing variant, other ExSpeU1 failed to correct the effect of yet another 5′ss mutation (c.790C>T) in a patient with Fanconi anemia [57].

In another work, Pagani's team [58] tested the therapeutic effect of ExSpeU1s in Familial dysautonomia (FD), a rare neurodegenerative genetic disease with no treatment, caused in more than 99% of the patients by a homozygous intronic point mutation (c.2204+6T>C) in the *ELP1* gene, which causes different degrees of exon 20 skipping in various tissues. In a first approach, the team tested eleven ExSpeU1s binding different regions of intron 20 through co-transfection with a mutant T>C minigene in neuronal SH-SY5Y cells and found that seven of the ExSpeU1s allowed a significant recovery of the splicing defect. Then, to better understand exon 20 splicing inhibition and to select the best U1 molecule to test both in the patient's cells and in mice, different functional splicing assays were performed, and the results showed that two ExSpeU1s were the most effective on splicing recovery, being able to overcome the negative effect of different inhibitory splicing factors. Subsequently, to evaluate the effect of ExSpeU1 in FD patient's fibroblasts, its lentivirus-mediated expression was performed, and the results showed a huge increase in the percentage of exon 20 inclusion consistent with a recovery of ~80% at the protein level. Next, the therapeutic potential of the ExSpeU1s was assessed in a transgenic mouse model that carries the *ELP1*

splicing mutation and has the same tissue-specific mis-splicing observed in FD patients, but which does not exhibit any symptoms. The intraperitoneal (IP) delivery of ExSpeU1s-AAV9 particles successfully increased the production of the human *ELP1* full-length transcript and protein in several mouse tissues, demonstrating that the ExSpeU1 approach would be a potential therapeutic option for FD.

Later, in another study, to understand if the *ELP1* exon 20 splicing rescues achieved with the specific AAV9-ExSpeU1 in the FD asymptomatic mouse model is translated in an amelioration of the disease phenotype and life span, the same group tested this modified U1 molecule in a phenotypic humanized mouse model that exhibits the major disease symptoms and reproduced the human splicing defect. The postnatal systemic and ICV treatment with the AAV9-ExSpeU1 in these mice allowed an effective correction of the *ELP1* splicing and increased the production of a functional protein in several tissues. Furthermore, the treatment rescued FD mice's motor, cardiac, and renal functions, and reduced animal mortality in the first month of life. Then, to evaluate possible off-target effects caused by the presence of the ExSpeU1, the authors did RNA-seq analyses in human cells overexpressing the specific U1 and in the dorsal root ganglia of treated mice, and did not observe significant changes in gene expression and alternative splicing, a result that together with the potentially long-lasting splicing correction provided by the systemic treatment of AAV9-ExSpeU1 make this a promising therapeutic strategy for FD [59].

Remarkably, the engineered U1 snRNA vectors can also be tested in N-of-1 treatment approaches and be developed for variants that are present in a single patient/family or only in a few patients. One such example is a very recently developed study by Jüschke et al. [60] focused on patients with Autosomal dominant optic atrophy (ADOA), an ocular disorder frequently caused by mutations in the *OPA1* gene, and in which haploinsufficiency is the main genetic pathomechanism. They identified a family with ADOA harboring a novel 5′ss mutation, c.1065+5G>A, in intron 10 that causes exon 10 skipping and leads to a reduction of ~50% of OPA1 protein expression. Similarly, to what Balestra et al. had executed in 2019 for CDKL5-deficiency disorder, these authors also tested the effect of the two different generations of synthetical U1 snRNAs. Briefly, in order to correct the mutation-induced splicing defect, the team designed five different modified U1s: a U1 variant with full complementarity to the mutated 5′ss of exon 10 and four ExSpeU1s adapted to different regions downstream of the 5′ss in intron 10. Their lentiviral transduction in patient-derived fibroblasts showed that only the ExSpeU1 directed to the position +18 in intron 10 was able to significantly reduce the transcripts with exon 10 skipping and simultaneously increase the expression level of normal transcripts in a dose-dependent manner. Furthermore, a tendency towards increased OPA1 protein expression was associated with the treatment with this ExSpeU1. So, the authors hypothesized that the increased amount of correctly spliced *OPA1* transcripts may be sufficient to surpass the haploinsufficiency and lead to an amelioration of the phenotype and to a slower disease progression. To the best of our knowledge, there is not any published data on the in vivo effect of this ExSpeU1 yet. Still, the in vitro results shared so far seem quite promising.

As in the previous study, Martinez–Pizarro and collaborators [61] also studied two very rare intronic variants (c.1199+17G>A and c.1199+20G>C) located in intron 11 of the *PAH* gene, which cause exon 11 skipping and origin one of the most common inherited disorders of amino acid metabolism, Phenylketonuria. Again, several ExSpeU1s were tested as therapeutic tools for the mentioned variants involving intronic positions downstream of the 5′ss, also allowing us to gain more insights into the cellular functions of the natural U1 snRNP. Through different functional splicing studies, the authors identified a novel region in intron 11 that functions as an intronic splicing enhancer (ISE) for the exon 11, which has a weak 3′ss and a suboptimal 5′ss. This ISE has a binding motif for U1 snRNA and RNA affinity assays showed that U1-70K binds to this region in the wild-type sequence. However, this binding is abolished in the presence of the two intronic variants which reduce the complementarity to U1 snRNA. Overall, this shows that the splicing regulatory element in intron 11 is relevant for the regulation of correct splicing at the canonical 5′ss. Further

evidence of the role of this ISE for exon 11 inclusion was obtained by the results of splicing therapeutic approaches using different ExSpeU1s in co-transfection with mutant minigenes. Only the ExSpeU1s which were totally complementary to the +17G>A or +20G>C mutations did increase exon 11 inclusion. This demonstrates that in this context the binding of each specific U1 to the intronic sites possibly compensates for the defect by recruiting the U1-70K protein (identified as a mediator in the splicing rescue by ExSpeU1s, see [51]), thus allowing to restore the interactions that define exon 11 and achieve a therapeutic effect. Of note, this work extended the knowledge about the mechanism of action of the natural U1 snRNPs showing that in some contexts it can act as a splicing stimulator particularly when it binds to an intronic region downstream of the natural 5′ss.

In summary, the ability of different engineered U1 snRNAs to rescue splicing has been proven in both cellular and animal models of different human genetic disorders. However, the existence of species-specific splicing profiles can constitute a challenge to the development and validation of these therapies. This is elegantly presented in two recent studies developed by the same group [62,63], both targeting a splicing variant (c.386G>A) in the *OTC* gene, the gene mutated in Ornithine transcarbamylase deficiency (OTCD). The presence of the c.386G>A variant in the last base of exon 4 leads to aberrant splicing but with a substantially different impact between humans and mice. In mice, this variant causes exon 4 skipping and the use of a cryptic intronic 5′ss at position +49, but the correct transcript is still present in appreciable amounts. In turn, in humans, the same variant also leads to exon 4 skipping but that is the major similarity between both systems. Indeed, in humans, that same variant leads to the use of a cryptic 5′ss at the +5 position and only trace levels of the normal transcript are found.

In the first report [62], through in vitro studies using mouse *otc* minigenes transiently expressed in mouse hepatoma cells, the authors identified an ExSpeU1, which led to an increase in the levels of the correct transcript. The same was observed in vivo upon delivery via an AAV8 of the same ExSpeU1 to a mouse model carrying the c.386G>A variant (*spf*^{ash} mouse). In a second study [63], the same group dissected the molecular mechanisms mediating the differences in the pathogenic splicing patterns between mice and humans in the presence of the c.386G>A variant and how it can influence susceptibility to RNA-based therapies. Actually, they tested in vitro several engineered U1 snRNAs for the human sequence and none of those U1 snRNAs improved the selection of the authentic mutated 5′ss, because while decreasing exon skipping, they further promoted the usage of the adjacent cryptic 5′ss. The authors elegantly demonstrated that it can be attributed to the key role of subtle intronic changes downstream of the authentic 5′ss, which lead to differential binding of splicing factors and dictated the different splicing patterns between the two species. Altogether, these two studies highlight the importance of carefully investigating species-specific molecular mechanisms for translational purposes.

Another important challenge is related to the ineffectiveness, as reported in several studies [47,54,72], of the ExSpeU1 approach for mutations affecting the conserved GT dinucleotide at positions +1 and +2 of the 5′ss region, where the correction attempts also resulted in the activation of cryptic donor sites. Nevertheless, a pivotal study by Scalet and colleagues [17] targeting several splicing mutations in the *F9* gene causing Hemophilia B (Factor IX deficiency), proved that an ExSpeU1 can indeed rescue aberrant splicing caused by a variant located at the position +2 of the 5′ss. Initially, through minigene expression in mammalian cells, it was demonstrated that five naturally occurring variants in the 5′ss region of exon 3 (c.277+1G>A, c.277+1G>T, c.277+2T>C, c.277+2T>G and c.277+4A>G) induce complete exon 3 skipping. So, in an attempt to restore exon 3 definition a modified U1 snRNA totally complementary to the exon 3 5′ss and an ExSpeU1 targeting the downstream intron between positions +6 and +14 were designed and tested. As expected, for variant c.277+4A>G located in a less conserved position of the 5′ss, both modified U1 snRNA and ExSpeU1 promoted the inclusion of exon 3 (~60% of correct transcripts). Regarding the variants in the conserved +1 and +2 positions, the ExSpeU1 reduced the level of transcripts with exon 3 skipping but also led to the use of an exonic cryptic 5′ss

located eight nucleotides upstream of the mutant 5′ss, which origins a frameshift transcript. However, surprisingly, the engineered ExSpeU1 also triggered the usage of the 5′ss affected by the c.277+2T>C mutation, allowing a significant recovery of correct transcripts (~20%). For both variants, the splicing rescue also produced a considerable increase in secreted FIX protein levels. Overall, this study broadens the spectrum of mutations, that are potentially amenable to ExSpeU1 treatment, thus adding a new perspective to the rescue of mutations that alter the conserved 5′ss GT dinucleotide.

3.3. When Modified U1 snRNAs Meet Other Therapeutic Molecules: Combined Therapeutic Strategies

While modified U1 snRNAs hold a therapeutic potential on their own, there are also approaches that combine modified U1 snRNAs with other therapeutic molecules. This is the case of a combined treatment for Bardet–Biedl syndrome recently developed by Breuel and colleagues [64] in which a modified U1 snRNA (to correct the exon skipping) and ASOs (to block intron retention) were used in an attempt to correct the effect of a mutation in the last base of exon 5 of the *BBS1* gene (c.479G>A), which leads to both exon 5 skipping and intron 5 retention. In fact, the team was able to prove that the combined use of these two splicing modulation molecules improved the efficacy of the splice correction and increased the amount of correctly spliced *BBS1* transcripts compared to single treatments.

However, this was not the only combined therapy including modified U1 snRNAs to be attempted. In fact, some years before, Schmid and co-workers [65] also used a combined treatment for the same disorder in which modified U1 snRNAs and U6 snRNAs with different compensatory mutations were tested for the correction of a mutation located at position +5 of *BBS1* gene intron 5 (see Table 1). Unlike the single treatment with a modified U1 snRNA, this combined treatment led to an almost complete correction of the splicing defect caused by the target mutation, showing that the sequence complementarity between U6 and the three splice donor site positions (+4, +5, and +6) was indeed relevant for the succeeded outcome. Nevertheless, the authors point out that the single use of modified U6 snRNA isoforms did not result in significant improvements.

A similar approach combining the modified U1 snRNAs and U6 snRNAs was also very recently developed by the same group [66] for the correction of the previously referred 5′ss *OPA1* mutation, c.1065+5G>A, which underlies a severe ocular disorder. These authors tested this combined therapy in a mouse model carrying the *Opa1* c.1065+5G>A 5′ss mutation (Opa1$^{enu/+}$), which causes the same splicing defect observed in the patient's fibroblasts. Briefly, three AAV2/8 vectors expressing different combinations of totally complementary (tc) or wild-type (wt) U1 and U6 sequences were produced: U1.wt/U6.wt, U1.tc/U6.wt and U1.tc/U6.tc. Importantly, the subretinal delivery of either the U1.tc/U6.wt or the U1.tc/U6.tc via AAV2/8 showed therapeutic efficacy and increased the *Opa1* wild-type transcripts expression in the eye. As no significant differences between the two treatments were observed on the transcript level, the effect on the protein was only tested using the U1.tc/U6.wt variant. The results showed a significant increase in Opa1 protein expression after treatment. Of notice, the expression of the engineered U1.tc/U6.wt did not induce obvious short-term side effects on the splicing of visual-associated genes as well on retinal morphology and functionality.

4. Factors to Consider in the Effectiveness and Use of Engineered U1 snRNA Vectors

Similar to any other therapeutic approach, the use of engineered U1 snRNAs also has some limitations. The fundamental limitation of both modified U1 snRNAs and ExSpeU1s is the possibility of unforeseen off-target effects in addition to a relatively low efficiency [35]. Theoretically, this seemed especially dangerous for the classical single base modified U1 snRNAs, which are designed to act over highly conserved regions. This meant that, ultimately, a modified U1 snRNA could be so similar to an endogenous U1 snRNA that it would bind to virtually any 5′ss. Plus, it would be more likely to activate cryptic splice-sites, thus affecting mRNA length and stability [18,70]. Intriguingly, however, recent in vivo

assessments on the specificity of both modified U1 snRNAs [13] and ExSpeU1s [52,59] have provided similar results regarding their specificity. While somehow unexpected, these are encouraging results regarding the therapeutic potential of these molecules.

Overall, off-target effects are difficult to predict. That is why screening procedures must be undertaken as early as possible in the drug development pipeline in order to reduce the occurrence of non-specific bonds. In fact, to be able to predict the effect of any specific engineered U1 snRNA vector, experimental studies are required. Some relevant insights on the general effects of the classical modified U1 snRNAs and the novel ExSpeU1s have further highlighted their potential and specificity. Regarding the classical modified U1 snRNAs, when Balestra and co-workers [13] evaluated changes in the alternative splicing profile and in the global expression levels in liver specimens from mutation-specific FAH deficient mice treated with an AAV8-delivered modified U1 snRNA, negligible effects were observed. In fact, only a small proportion of the 13,000 investigated genes displayed an altered expression profile, and that percentage was even lower when only protein-coding genes were considered (one over- and three under-expressed genes). Similarly, recent transcriptome studies by Donadon et al. [52] and Romano and co-workers [59] have demonstrated that ExSpeU1s have high specificity for their target pre-mRNA, leading to minimal global changes in gene expression and splicing. Overall, the studies performed so far support the idea that the use of both modified U1 snRNAs and ExSpeU1s may be justified if the therapeutic benefits outweigh the drawbacks already indicated.

Last but not least, one of the most significant challenges in the therapeutic use of engineered U1 snRNA vectors, regardless of their generation, is their delivery to the target tissues/organs. This is actually a challenge faced by many other RNA-based therapeutics, such as small interfering RNAs (siRNAs) or even ASOs. In fact, even though successful delivery schemes have already been designed and implemented for some of these therapeutic molecules to reach a few specific organs (e.g.,: the eye, liver and even the central nervous system), systemic delivery is still an issue for many of them. Modified U1 snRNAs and ExSpeU1s in particular, are among those in need of additional delivery studies. Taking into account most of the data published so far, viral vectors will certainly be the first to reach clinical trials, as AAVs have been used as the principal delivery method in most of the in vivo studies developed. However, despite the changes made to these viral vectors, the potential for immune reactions to be triggered remains a significant limitation to their use and does raise a number of concerns. Still, it is worth mentioning that different AAV serotypes with specific tissue tropisms have been described, including serotypes that are able to transduce the blood-brain barrier (BBB) [73] a feature that makes them particularly suitable to deliver therapeutic agents for diseases that present neurological symptoms. Furthermore, AAV vectors have been shown to mediate long-term in vivo expression with little or no acute toxicity. These two observations are probably among the major reasons why AAV vectors have been extensively used not only in pre-clinical studies for different rare genetic diseases such as Lysosomal Storage Disorders, but also in numerous clinical trials for this group of diseases [74]. It should also be noted that the AAVs are nonpathogenic as they generally do not integrate into the host genome. Thus, in this respect, AAVs are safer than other types of viral vectors [75]. Overall, it is reasonable to assume that AAVs may as well be used for modified U1 snRNAs and the ExSpeU1s targeted delivery with equally promising results. Nevertheless, viral vector delivery is not the only possibility to take into account when designing a U1 snRNA-based therapeutic approach. Alternatives include delivering these molecules using nanoparticles, which will necessitate new research and development before this therapeutic strategy can be used in humans [18]. However, to the best of our knowledge, this type of approach has never been attempted for engineered U1 snRNAs.

While falling slightly out of the scope of this review, it should also be noticed that there is yet another U1 snRNA-related therapeutic approach, which can be attempted. It relies on the use of chimeric snRNA molecules carrying antisense sequences against the 3′ss of target exons for exon skipping purposes. This sort of approach was designed to

counteract the fact that ASOs alone require periodic administration. To circumvent this problem, some teams made efforts to produce constructs, which would be able to express in vivo, in a stable fashion, large amounts of chimeric RNAs containing the therapeutic antisense sequences [76]. Those constructs are suitable for administration via traditional gene delivery vehicles, thus holding the potential to reduce the frequency of dosing [77].

To the best of our knowledge, this sort of approach was mainly tested as a possible therapeutic for Duchenne muscular dystrophy (DMD), which is probably the most well-known and in-depth studied muscular dystrophy of them all, in the RNA therapeutics field.

The rationale behind many of the studies that tested novel therapeutic approaches for DMD over the last decades was to convert severe DMD forms into milder ones through targeted exon skipping using antisense sequences against splice junctions and/or exonic splicing enhancers (ESEs) to induce the exclusion of certain exon(s) from the mature mRNA, while preserving the reading frame. Most teams are working with chemically modified ASOs, whose safety and efficacy are now largely documented, with several approved drugs reaching the market [78]. Others, however, have attempted to administer the therapeutic antisense sequences as part of a snRNA namely U1 [76,79–82] but also U7 [83–87]. Ultimately, one such approach may provide persistent expression, in vivo stability, and correct compartmentalization.

Indeed, chimeric U1 snRNA antisense molecules, i.e., ASOs raised in the U1 snRNA backbone, were shown to effectively induce the desired exon skipping not only in human DMD myoblasts [76,81,82] but also in DMD mouse models, namely the mdx mouse [79,80,88]. In both cases, the chimeric molecules were delivered as part of lentiviral or AAV vectors and provided high skipping activity and efficient rescue of dystrophin synthesis. Altogether, these results further highlight the therapeutic potential of U1 snRNAs, even though from a completely different perspective from that focused on this revision. This is particularly relevant since it has already been reported that the single-stranded 5′ terminus of U1 can be replaced by unrelated sequences as long as 50 nucleotides without noticeable effects not only over their stability but also on their capacity to assemble into snRNP particles. That makes it an effective vector for the stable expression of ASOs and for the inhibition of the splicing reaction [89]. Moreover, this approach can be appropriately designed to mediate either a single or multi-exon skipping [78,85]. To the best of our knowledge, however, none of the U1 snRNA antisense molecules has reached clinical trials. Still, there is an ongoing phase 1/2 clinical trial using a U7 snRNA-based approach for the correction of DMD exon 2 duplications (NCT04240314) [78].

5. Conclusions

Based on all the work here reviewed, there is a growing body of evidence on the potential of both modified U1 snRNAs and ExSpeU1s to mediate gene therapeutic correction of splicing defects underlying different genetic diseases. Remarkably, those positive results have been observed not only in vitro but also in vivo in different animal models. The first tests on animals started with modified U1 snRNAs and were evidenced by successful studies using ExSpeU1s.

It may be worth mentioning that a significant part of the studies relying on the use of both modified U1 snRNAs and ExSpeU1s was developed in the labs of Mirko Pinotti (University of Ferrara, Italy) and of Franco Pagani (Centre for Genetic Engineering and Biotechnology in Trieste, Italy) [12,13,38,44,48,51,58,59], where the whole pipeline to address their therapeutic potential in vitro and in vivo, seems to be well-implemented. However, it is important to stress that many other teams, in different labs, have been able to replicate the same sort of methods, achieving similar results for other disease-causing mutations [11,16,41,61,66]. This adds up to the overall therapeutic potential of engineered U1s, by demonstrating the replicability of the method and the robust correction levels it may promote. However, as with any other method, this approach also has some limitations. The most obvious and relevant one is the possibility of generating off-target effects. However,

if this is a serious concern for modified U1 snRNAs, the emergence of the ExSpeU1s largely bypassed this issue by increasing its specificity and stability. Last but not least, the delivery of these molecules in vivo is a topic that also requires significant focus. In fact, targeted delivery of these molecules has been largely neglected as an object of study. However, this is a matter that requires further optimization and development to better test these molecules.

Author Contributions: Conceptualization, L.M. and S.A.; NCBI Pubmed search, M.G., J.I.S. and L.M.; manuscript structure, M.G., L.M. and S.A., original draft preparation, M.G.; additional writing, J.I.S., L.M., M.F.C. and S.A.; figures, M.G.; critical review, M.G., J.I.S., M.F.C., L.M. and S.A.; editing, J.I.S. and L.M.; funding acquisition, L.M. and S.A. All authors have read and agreed to the published version of the manuscript.

Funding: This work was financially supported with funding from FCT/MCTES (UIDB/00211/2020) through national funds, and also partially supported by the MPS Society project (2019DGH1642) and the LA/P/0059/2020—Laboratório Associado para a Ciência Animal e Veterinária/Associate Laboratory for Animal and Veterinary Sciences (AL4animalS).

Institutional Review Board Statement: Not applicable.

Data Availability Statement: Not applicable.

Conflicts of Interest: The authors declare no conflict of interest.

References

1. Singh, R.N.; Singh, N.N. A Novel Role of U1 SnRNP: Splice Site Selection from a Distance. *Biochim. Biophys. Acta Gene Regul. Mech.* **2019**, *1862*, 634–642. [CrossRef]
2. Shi, Y. The Spliceosome: A Protein-Directed Metalloribozyme. *J. Mol. Biol.* **2017**, *429*, 2640–2653. [CrossRef]
3. Schmidt, V.; Kirschner, K.M. Alternative Pre-MRNA Splicing. *Acta Physiol.* **2018**, *222*, e13053. [CrossRef] [PubMed]
4. Yan, C.; Wan, R.; Shi, Y. Molecular Mechanisms of Pre-MRNA Splicing through Structural Biology of the Spliceosome. *Cold Spring Harb. Perspect. Biol.* **2019**, *11*, a032409. [CrossRef] [PubMed]
5. Wan, R.; Bai, R.; Shi, Y. Molecular Choreography of Pre-MRNA Splicing by the Spliceosome. *Curr. Opin. Struct. Biol.* **2019**, *59*, 124–133. [CrossRef] [PubMed]
6. Suñé-Pou, M.; Limeres, M.J.; Moreno-Castro, C.; Hernández-Munain, C.; Suñé-Negre, J.M.; Cuestas, M.L.; Suñé, C. Innovative Therapeutic and Delivery Approaches Using Nanotechnology to Correct Splicing Defects Underlying Disease. *Front. Genet.* **2020**, *11*, 731. [CrossRef]
7. Baralle, D.; Buratti, E. RNA Splicing in Human Disease and in the Clinic. *Clin. Sci.* **2017**, *131*, 355–368. [CrossRef]
8. Anna, A.; Monika, G. Splicing Mutations in Human Genetic Disorders: Examples, Detection, and Confirmation. *J. Appl. Genet.* **2018**, *59*, 253–268. [CrossRef]
9. Montes, M.; Sanford, B.L.; Comiskey, D.F.; Chandler, D.S. RNA Splicing and Disease: Animal Models to Therapies. *Trends Genet.* **2019**, *35*, 68–87. [CrossRef]
10. van der Woerd, W.L.; Mulder, J.; Pagani, F.; Beuers, U.; Houwen, R.H.J.; van de Graaf, S.F.J. Analysis of Aberrant Pre-Messenger RNA Splicing Resulting from Mutations in ATP8B1 and Efficient in Vitro Rescue by Adapted U1 Small Nuclear RNA. *Hepatology* **2015**, *61*, 1382–1391. [CrossRef]
11. Matos, L.; Canals, I.; Dridi, L.; Choi, Y.; Prata, M.J.; Jordan, P.; Desviat, L.R.; Pérez, B.; Pshezhetsky, A.V.; Grinberg, D.; et al. Therapeutic Strategies Based on Modified U1 Snrnas and Chaperones for Sanfilippo c Splicing Mutations. *Orphanet J. Rare Dis.* **2014**, *9*, 180. [CrossRef]
12. Tajnik, M.; Rogalska, M.E.; Bussani, E.; Barbon, E.; Balestra, D.; Pinotti, M.; Pagani, F. Molecular Basis and Therapeutic Strategies to Rescue Factor IX Variants That Affect Splicing and Protein Function. *PLoS Genet.* **2016**, *12*, e1006082. [CrossRef]
13. Balestra, D.; Scalet, D.; Ferrarese, M.; Lombardi, S.; Ziliotto, N.; Croes, C.C.; Petersen, N.; Bosma, P.; Riccardi, F.; Pagani, F.; et al. A Compensatory U1snRNA Partially Rescues FAH Splicing and Protein Expression in a Splicing-Defective Mouse Model of Tyrosinemia Type I. *Int. J. Mol. Sci.* **2020**, *21*, 2136. [CrossRef] [PubMed]
14. Buratti, E.; Baralle, D. Novel Roles of U1 SnRNP in Alternative Splicing Regulation. *RNA Biol.* **2010**, *7*, 412–419. [CrossRef] [PubMed]
15. Matos, L.; Santos, J.I.; Coutinho, M.F.; Alves, S. How to Design U1 SnRNA Molecules for Splicing Rescue. In *Methods in Molecular Biology*; Humana Press Inc.: New York, NY, USA, 2022; Volume 2434, pp. 89–102.
16. Lee, N.-C.; Lee, Y.-M.; Chen, P.-W.; Byrne, B.J.; Hwu, W.-L. Mutation-Adapted U1 SnRNA Corrects a Splicing Error of the Dopa Decarboxylase Gene. *Hum. Mol. Genet.* **2016**, *25*, ddw323. [CrossRef] [PubMed]
17. Scalet, D.; Maestri, I.; Branchini, A.; Bernardi, F.; Pinotti, M.; Balestra, D. Disease-Causing Variants of the Conserved +2T of 5′ Splice Sites Can Be Rescued by Engineered U1snRNAs. *Hum. Mutat.* **2019**, *40*, 48–52. [CrossRef]

18. Coutinho, M.F.; Matos, L.; Santos, J.I.; Alves, S. RNA Therapeutics: How Far Have We Gone? *Cell* **2019**, *46*, 133–177.
19. Naylor, S.L.; Zabel, B.U.; Manser, T.; Gesteland, R.; Sakaguchi, A.Y. Localization of Human U1 Small Nuclear RNA Genes to Band P36.3 of Chromosome 1 by in Situ Hybridization. *Somat. Cell Mol. Genet.* **1984**, *10*, 307–313. [CrossRef]
20. Lindgren, V.; Bernstein, L.B.; Weiner, A.M.; Francke1, U. Human Ul Small Nuclear RNA Pseudogenes Do Not Map to the Site of the Ul Genes in Lp36 but Are Clustered in Lql2–q22. *Mol. Cell. Biol.* **1985**, *5*, 2172–2180.
21. Lund, E.; Dahlberg, J.E. True Genes for Human U1 Small Nuclear RNA. Copy Number, Polymorphism, and Methylation. *J. Biol. Chem.* **1984**, *259*, 2013–2021. [CrossRef]
22. Lund, E.; Bostock, C.J.; Dahlberg, J.E. The Transcription of Xenopus Laevis Embryonic U1 SnRNA Genes Changes When Oocytes Mature into Eggs. *Genes Dev.* **1987**, *1*, 47–56. [CrossRef]
23. O'Reilly, D.; Dienstbier, M.; Cowley, S.A.; Vazquez, P.; Drozdz, M.; Taylor, S.; James, W.S.; Murphy, S. Differentially Expressed, Variant U1 SnRNAs Regulate Gene Expression in Human Cells. *Genome Res.* **2013**, *23*, 281–291. [CrossRef] [PubMed]
24. Vazquez-Arango, P.; Vowles, J.; Browne, C.; Hartfield, E.; Fernandes, H.J.R.; Mandefro, B.; Sareen, D.; James, W.; Wade-Martins, R.; Cowley, S.A.; et al. Variant U1 SnRNAs Are Implicated in Human Pluripotent Stem Cell Maintenance and Neuromuscular Disease. *Nucleic Acids Res.* **2016**, *44*, 10960–10973. [CrossRef]
25. Guiro, J.; O'Reilly, D. Insights into the U1 Small Nuclear Ribonucleoprotein Complex Superfamily. *Wiley Interdiscip. Rev. RNA* **2015**, *6*, 79–92. [CrossRef]
26. Pomeranz Krummel, D.A.; Oubridge, C.; Leung, A.K.W.; Li, J.; Nagai, K. Crystal Structure of Human Spliceosomal U1 SnRNP at 5.5 Resolution. *Nature* **2009**, *458*, 475–480. [CrossRef] [PubMed]
27. Blazquez, L.; Fortes, P. U1 SnRNP Control of 3′-End Processing and the Therapeutic Application of U1 Inhibition Combined with RNA Interference. *Curr. Mol. Med.* **2013**, *13*, 1203–1216. [CrossRef] [PubMed]
28. Kondo, Y.; Oubridge, C.; van Roon, A.M.M.; Nagai, K. Crystal Structure of Human U1 SnRNP, a Small Nuclear Ribonucleoprotein Particle, Reveals the Mechanism of 5′ Splice Site Recognition. *Elife* **2015**, *4*, e04986. [CrossRef]
29. Roca, X.; Krainer, A.R.; Eperon, I.C. Pick One, but Be Quick: 5′ Splice Sites and the Problems of Too Many Choices. *Genes Dev.* **2013**, *27*, 129–144. [CrossRef] [PubMed]
30. Freund, M.; Hicks, M.J.; Konermann, C.; Otte, M.; Hertel, K.J.; Schaal, H. Extended Base Pair Complementarity between U1 SnRNA and the 5′ Splice Site Does Not Inhibit Splicing in Higher Eukaryotes, but Rather Increases 5′ Splice Site Recognition. *Nucleic Acids Res.* **2005**, *33*, 5112–5119. [CrossRef]
31. Tan, J.; Ho, J.X.J.; Zhong, Z.; Luo, S.; Chen, G.; Roca, X. Noncanonical Registers and Base Pairs in Human 5′ Splice-Site Selection. *Nucleic Acids Res.* **2016**, *44*, 3908–3921. [CrossRef]
32. Carmel, I.; Tal, S.; Vig, I.; Ast, G. Comparative Analysis Detects Dependencies among the 5′ Splice-Site Positions. *RNA* **2004**, *10*, 828–840. [CrossRef] [PubMed]
33. Malard, F.; Mackereth, C.D.; Campagne, S. Principles and Correction of 5′-Splice Site Selection. *RNA Biol.* **2022**, *19*, 943–960. [CrossRef] [PubMed]
34. Fredericks, A.; Cygan, K.; Brown, B.; Fairbrother, W. RNA-Binding Proteins: Splicing Factors and Disease. *Biomolecules* **2015**, *5*, 893–909. [CrossRef] [PubMed]
35. Hwu, W.L.; Lee, Y.M.; Lee, N.C. Gene Therapy with Modified U1 Small Nuclear RNA. *Expert. Rev. Endocrinol. Metab.* **2017**, *12*, 171–175. [CrossRef] [PubMed]
36. Baralle, M. Identification of a Mutation That Perturbs NF1 Agene Splicing Using Genomic DNA Samples and a Minigene Assay. *J. Med. Genet.* **2003**, *40*, 220–222. [CrossRef]
37. Pinotti, M.; Balestra, D.; Rizzotto, L.; Maestri, I.; Pagani, F.; Bernardi, F. Rescue of Coagulation Factor VII Function by the U1+5A SnRNA. *Blood* **2009**, *113*, 6461–6464. [CrossRef]
38. Pinotti, M.; Rizzotto, L.; Balestra, D.; Lewandowska, M.A.; Cavallari, N.; Marchetti, G.; Bernardi, F.; Pagani, F. U1-SnRNA–Mediated Rescue of MRNA Processing in Severe Factor VII Deficiency. *Blood* **2008**, *111*, 2681–2684. [CrossRef]
39. Balestra, D.; Faella, A.; Margaritis, P.; Cavallari, N.; Pagani, F.; Bernardi, F.; Arruda, V.R.; Pinotti, M. An Engineered U1 Small Nuclear RNA Rescues Splicing- Defective Coagulation F7 Gene Expression in Mice. *J. Thromb. Haemost.* **2014**, *12*, 177–185. [CrossRef]
40. Tanner, G.; Glaus, E.; Barthelmes, D.; Ader, M.; Fleischhauer, J.; Pagani, F.; Berger, W.; Neidhardt, J. Therapeutic Strategy to Rescue Mutation-Induced Exon Skipping in Rhodopsin by Adaptation of U1 SnRNA. *Hum. Mutat.* **2009**, *30*, 255–263. [CrossRef]
41. Glaus, E.; Schmid, F.; Da Costa, R.; Berger, W.; Neidhardt, J. Gene Therapeutic Approach Using Mutation-Adapted U1 SnRNA to Correct a RPGR Splice Defect in Patient-Derived Cells. *Mol. Ther.* **2011**, *19*, 936–941. [CrossRef]
42. Schmid, F.; Glaus, E.; Barthelmes, D.; Fliegauf, M.; Gaspar, H.; Nürnberg, G.; Nürnberg, P.; Omran, H.; Berger, W.; Neidhardt, J. U1 SnRNA-Mediated Gene Therapeutic Correction of Splice Defects Caused by an Exceptionally Mild BBS Mutation. *Hum. Mutat.* **2011**, *32*, 815–824. [CrossRef]
43. Sánchez-Alcudia, R.; Pérez, B.; Pérez-Cerdá, C.; Ugarte, M.; Desviat, L.R. Overexpression of Adapted U1snRNA in Patients' Cells to Correct a 5′ Splice Site Mutation in Propionic Acidemia. *Mol. Genet. Metab.* **2011**, *102*, 134–138. [CrossRef] [PubMed]
44. Scalet, D.; Sacchetto, C.; Bernardi, F.; Pinotti, M.; van de Graaf, S.F.J.; Balestra, D. The somatic FAH C. 1061C>A change counteracts the frequent FAH c. 1062+ 5G>A mutation and permits U1snRNA-based splicing correction. *J. Hum. Genet.* **2018**, *63*, 683–686. [CrossRef] [PubMed]

45. Hartmann, L.; Neveling, K.; Borkens, S.; Schneider, H.; Freund, M.; Grassman, E.; Theiss, S.; Wawer, A.; Burdach, S.; Auerbach, A.D.; et al. Correct MRNA Processing at a Mutant TT Splice Donor in FANCC Ameliorates the Clinical Phenotype in Patients and Is Enhanced by Delivery of Suppressor U1 SnRNAs. *Am. J. Hum. Genet.* **2010**, *87*, 480–493. [CrossRef]
46. Peretto, L.; Tonetto, E.; Maestri, I.; Bezzerri, V.; Valli, R.; Cipolli, M.; Pinotti, M.; Balestra, D. Counteracting the Common Shwachman–Diamond Syndrome-Causing SBDS c.258+2T>C Mutation by RNA Therapeutics and Base/Prime Editing. *Int. J. Mol. Sci.* **2023**, *24*, 4024. [CrossRef] [PubMed]
47. Balestra, D.; Giorgio, D.; Bizzotto, M.; Fazzari, M.; Ben Zeev, B.; Pinotti, M.; Landsberger, N.; Frasca, A. Splicing Mutations Impairing CDKL5 Expression and Activity Can Be Efficiently Rescued by U1snRNA-Based Therapy. *Int. J. Mol. Sci.* **2019**, *20*, 4130. [CrossRef]
48. Fernandez Alanis, E.; Pinotti, M.; Dal Mas, A.; Balestra, D.; Cavallari, N.; Rogalska, M.E.; Bernardi, F.; Pagani, F. An Exon-Specific U1 Small Nuclear RNA (SnRNA) Strategy to Correct Splicing Defects. *Hum. Mol. Genet.* **2012**, *21*, 2389–2398. [CrossRef]
49. Barbon, E.; Ferrarese, M.; van Wittenberghe, L.; Sanatine, P.; Ronzitti, G.; Collaud, F.; Colella, P.; Pinotti, M.; Mingozzi, F. Transposon-Mediated Generation of Cellular and Mouse Models of Splicing Mutations to Assess the Efficacy of SnRNA-Based Therapeutics. *Mol. Ther. Nucleic Acids* **2016**, *5*, e392. [CrossRef]
50. Donegà, S.; Rogalska, M.E.; Pianigiani, G.; Igreja, S.; Amaral, M.D.; Pagani, F. Rescue of Common Exon-Skipping Mutations in Cystic Fibrosis with Modified U1 SnRNAs. *Hum. Mutat.* **2020**, *41*, 2143–2154. [CrossRef] [PubMed]
51. Rogalska, M.E.; Tajnik, M.; Licastro, D.; Bussani, E.; Camparini, L.; Mattioli, C.; Pagani, F. Therapeutic Activity of Modified U1 Core Spliceosomal Particles. *Nat. Commun.* **2016**, *7*, 11168. [CrossRef]
52. Donadon, I.; Bussani, E.; Riccardi, F.; Licastro, D.; Romano, G.; Pianigiani, G.; Pinotti, M.; Konstantinova, P.; Evers, M.; Lin, S.; et al. Rescue of Spinal Muscular Atrophy Mouse Models with AAV9-Exon-Specific U1 SnRNA. *Nucleic Acids Res.* **2019**, *47*, 7618–7632. [CrossRef] [PubMed]
53. Dal Mas, A.; Rogalska, M.E.; Bussani, E.; Pagani, F. Improvement of SMN2 Pre-MRNA Processing Mediated by Exon-Specific U1 Small Nuclear RNA. *Am. J. Hum. Genet.* **2015**, *96*, 93–103. [CrossRef] [PubMed]
54. Balestra, D.; Maestri, I.; Branchini, A.; Ferrarese, M.; Bernardi, F.; Pinotti, M. An Altered Splicing Registry Explains the Differential ExSpeU1-Mediated Rescue of Splicing Mutations Causing Haemophilia A. *Front. Genet.* **2019**, *10*, 974. [CrossRef]
55. Lombardi, S.; Leo, G.; Merlin, S.; Follenzi, A.; McVey, J.H.; Maestri, I.; Bernardi, F.; Pinotti, M.; Balestra, D. Dissection of Pleiotropic Effects of Variants in and Adjacent to F8 Exon 19 and Rescue of MRNA Splicing and Protein Function. *Am. J. Hum. Genet.* **2021**, *108*, 1512–1525. [CrossRef]
56. Dal Mas, A.; Fortugno, P.; Donadon, I.; Levati, L.; Castiglia, D.; Pagani, F. Exon-Specific U1s Correct SPINK 5 Exon 11 Skipping Caused by a Synonymous Substitution That Affects a Bifunctional Splicing Regulatory Element. *Hum. Mutat.* **2015**, *36*, 504–512. [CrossRef] [PubMed]
57. Mattioli, C.; Pianigiani, G.; De Rocco, D.; Bianco, A.M.R.; Cappelli, E.; Savoia, A.; Pagani, F. Unusual Splice Site Mutations Disrupt FANCA Exon 8 Definition. *Biochim. Biophys. Acta (BBA)-Mol. Basis Dis.* **2014**, *1842*, 1052–1058. [CrossRef]
58. Donadon, I.; Pinotti, M.; Rajkowska, K.; Pianigiani, G.; Barbon, E.; Morini, E.; Motaln, H.; Rogelj, B.; Mingozzi, F.; Slaugenhaupt, S.A.; et al. Exon-Specific U1 SnRNAs Improve ELP1 Exon 20 Definition and Rescue ELP1 Protein Expression in a Familial Dysautonomia Mouse Model. *Hum. Mol. Genet.* **2018**, *27*, 2466–2476. [CrossRef] [PubMed]
59. Romano, G.; Riccardi, F.; Bussani, E.; Vodret, S.; Licastro, D.; Ragone, I.; Ronzitti, G.; Morini, E.; Slaugenhaupt, S.A.; Pagani, F. Rescue of a Familial Dysautonomia Mouse Model by AAV9-Exon-Specific U1 SnRNA. *Am. J. Hum. Genet.* **2022**, *109*, 1534–1548. [CrossRef]
60. Jüschke, C.; Klopstock, T.; Catarino, C.B.; Owczarek-Lipska, M.; Wissinger, B.; Neidhardt, J. Autosomal Dominant Optic Atrophy: A Novel Treatment for OPA1 Splice Defects Using U1 SnRNA Adaption. *Mol. Ther. Nucleic Acids* **2021**, *26*, 1186–1197. [CrossRef]
61. Martínez-Pizarro, A.; Dembic, M.; Pérez, B.; Andresen, B.S.; Desviat, L.R. Intronic PAH Gene Mutations Cause a Splicing Defect by a Novel Mechanism Involving U1snRNP Binding Downstream of the 5′ Splice Site. *PLoS Genet.* **2018**, *14*, e1007360. [CrossRef]
62. Balestra, D.; Ferrarese, M.; Lombardi, S.; Ziliotto, N.; Branchini, A.; Petersen, N.; Bosma, P.; Pinotti, M.; van de Graaf, S.F.J. An Exon-Specific Small Nuclear U1 Rna (Exspeu1) Improves Hepatic Otc Expression in a Splicing-Defective Spf/Ash Mouse Model of Ornithine Transcarbamylase Deficiency. *Int. J. Mol. Sci.* **2020**, *21*, 8735. [CrossRef] [PubMed]
63. Sacchetto, C.; Peretto, L.; Baralle, F.; Maestri, I.; Tassi, F.; Bernardi, F.; van de Graaf, S.F.J.; Pagani, F.; Pinotti, M.; Balestra, D. OTC Intron 4 Variations Mediate Pathogenic Splicing Patterns Caused by the c.386G>A Mutation in Humans and Spfash Mice, and Govern Susceptibility to RNA-Based Therapies. *Mol. Med.* **2021**, *27*, 157. [CrossRef]
64. Breuel, S.; Vorm, M.; Bräuer, A.U.; Owczarek-Lipska, M.; Neidhardt, J. Combining Engineered U1 SnRNA and Antisense Oligonucleotides to Improve the Treatment of a BBS1 Splice Site Mutation. *Mol. Ther. Nucleic Acids* **2019**, *18*, 123–130. [CrossRef] [PubMed]
65. Schmid, F.; Hiller, T.; Korner, G.; Glaus, E.; Berger, W.; Neidhardt, J. A Gene Therapeutic Approach to Correct Splice Defects with Modified U1 and U6 SnRNPs. *Hum. Gene Ther.* **2013**, *24*, 97–104. [CrossRef]
66. Swirski, S.; May, O.; Ahlers, M.; Wissinger, B.; Greschner, M.; Jüschke, C.; Neidhardt, J. In Vivo Efficacy and Safety Evaluations of Therapeutic Splicing Correction Using U1 SnRNA in the Mouse Retina. *Cells* **2023**, *12*, 955. [CrossRef] [PubMed]
67. Zhuang, Y.; Weiner, A.M. A Compensatory Base Change in U1 SnRNA Suppresses a 5′ Splice Site Mutation. *Cell* **1986**, *46*, 827–835. [CrossRef]

68. Boocock, G.R.B.; Morrison, J.A.; Popovic, M.; Richards, N.; Ellis, L.; Durie, P.R.; Rommens, J.M. Mutations in SBDS Are Associated with Shwachman-Diamond Syndrome. *Nat. Genet.* **2003**, *33*, 97–101. [CrossRef]
69. Bezzerri, V.; Cipolli, M. Shwachman-Diamond Syndrome: Molecular Mechanisms and Current Perspectives. *Mol. Diagn. Ther.* **2019**, *23*, 281–290. [CrossRef]
70. Blázquez, L.; Fortes, P. U1 Interference (U1i) for Antiviral Approaches. In *Advances in Experimental Medicine and Biology*; Springer: New York, NY, USA, 2015; Volume 848, pp. 51–69.
71. Imbert, M.; Dias-Florencio, G.; Goyenvalle, A. Viral Vector-Mediated Antisense Therapy for Genetic Diseases. *Genes* **2017**, *8*, 51. [CrossRef]
72. Balestra, D.; Scalet, D.; Pagani, F.; Rogalska, M.E.; Mari, R.; Bernardi, F.; Pinotti, M. An Exon-Specific U1snRNA Induces a Robust Factor IX Activity in Mice Expressing Multiple Human FIX Splicing Mutants. *Mol. Ther. Nucleic Acids* **2016**, *5*, e370. [CrossRef]
73. Manfredsson, F.P.; Rising, A.C.; Mandel, R.J. AAV9: A Potential Blood-Brain Barrier Buster. *Mol. Ther.* **2009**, *17*, 403–405. [CrossRef]
74. Kido, J.; Sugawara, K.; Nakamura, K. Gene Therapy for Lysosomal Storage Diseases: Current Clinical Trial Prospects. *Front. Genet.* **2023**, *14*, 1064924. [CrossRef] [PubMed]
75. Parenti, G.; Pignata, C.; Vajro, P.; Salerno, M. New Strategies for the Treatment of Lysosomal Storage Diseases (Review). *Int. J. Mol. Med.* **2013**, *31*, 11–20. [CrossRef] [PubMed]
76. De Angelis, F.G.; Sthandier, O.; Berarducci, B.; Toso, S.; Galluzzi, G.; Ricci, E.; Cossu, G.; Bozzoni, I. Chimeric SnRNA Molecules Carrying Antisense Sequences against the Splice Junctions of Exon 51 of the Dystrophin Pre-MRNA Induce Exon Skipping and Restoration of a Dystrophin Synthesis in Δ48–50 DMD Cells. *Proc. Natl. Acad. Sci. USA* **2002**, *99*, 9456–9461. [CrossRef]
77. Hatch, S.T.; Smargon, A.A.; Yeo, G.W. Engineered U1 SnRNAs to Modulate Alternatively Spliced Exons. *Methods* **2022**, *205*, 140–148. [CrossRef]
78. Happi Mbakam, C.; Lamothe, G.; Tremblay, J.P. Therapeutic Strategies for Dystrophin Replacement in Duchenne Muscular Dystrophy. *Front. Med.* **2022**, *9*, 859930. [CrossRef] [PubMed]
79. Denti, M.A.; Rosa, A.; D'Antona, G.; Sthandier, O.; De Angelis, F.G.; Nicoletti, C.; Allocca, M.; Pansarasa, O.; Parente, V.; Musarò, A.; et al. Body-Wide Gene Therapy of Duchenne Muscular Dystrophy in the *Mdx* Mouse Model. *Proc. Natl. Acad. Sci. USA* **2006**, *103*, 3758–3763. [CrossRef]
80. Denti, M.A.; Rosa, A.; D'Antona, G.; Sthandier, O.; De Angelis, F.G.; Nicoletti, C.; Allocca, M.; Pansarasa, O.; Parente, V.; Musarò, A.; et al. Chimeric Adeno-Associated Virus/Antisense U1 Small Nuclear RNA Effectively Rescues Dystrophin Synthesis and Muscle Function by Local Treatment of Mdx Mice. *Hum. Gene Ther.* **2006**, *17*, 565–574. [CrossRef] [PubMed]
81. Incitti, T.; De Angelis, F.G.; Cazzella, V.; Sthandier, O.; Pinnarò, C.; Legnini, I.; Bozzoni, I. Exon Skipping and Duchenne Muscular Dystrophy Therapy: Selection of the Most Active U1 SnRNA Antisense Able to Induce Dystrophin Exon 51 Skipping. *Mol. Ther.* **2010**, *18*, 1675–1682. [CrossRef]
82. Cazzella, V.; Martone, J.; Pinnarò, C.; Santini, T.; Twayana, S.S.; Sthandier, O.; D'amico, A.; Ricotti, V.; Bertini, E.; Muntoni, F.; et al. Exon 45 Skipping through U1-SnRNA Antisense Molecules Recovers the Dys-NNOS Pathway and Muscle Differentiation in Human DMD Myoblasts. *Mol. Ther.* **2012**, *20*, 2134–2142. [CrossRef]
83. Brun, C.; Suter, D.; Pauli, C.; Dunant, P.; Lochmüller, H.; Burgunder, J.-M.; Schümperli, D.; Weis, J. U7 SnRNAs Induce Correction of Mutated Dystrophin Pre-MRNA by Exon Skipping. *Cell. Mol. Life Sci.* **2003**, *60*, 557–566. [CrossRef]
84. Goyenvalle, A.; Vulin, A.; Fougerousse, F.; Leturcq, F.; Kaplan, J.-C.; Garcia, L.; Danos, O. Rescue of Dystrophic Muscle Through U7 SnRNA-Mediated Exon Skipping. *Science* **2004**, *306*, 1796–1799. [CrossRef]
85. Goyenvalle, A.; Wright, J.; Babbs, A.; Wilkins, V.; Garcia, L.; Davies, K.E. Engineering Multiple U7snRNA Constructs to Induce Single and Multiexon-Skipping for Duchenne Muscular Dystrophy. *Mol. Ther.* **2012**, *20*, 1212–1221. [CrossRef]
86. Goyenvalle, A.; Babbs, A.; van Ommen, G.J.B.; Garcia, L.; Davies, K.E. Enhanced Exon-Skipping Induced by U7 SnRNA Carrying a Splicing Silencer Sequence: Promising Tool for DMD Therapy. *Mol. Ther.* **2009**, *17*, 1234–1240. [CrossRef] [PubMed]
87. Benchaouir, R.; Meregalli, M.; Farini, A.; D'Antona, G.; Belicchi, M.; Goyenvalle, A.; Battistelli, M.; Bresolin, N.; Bottinelli, R.; Garcia, L.; et al. Restoration of Human Dystrophin Following Transplantation of Exon-Skipping-Engineered DMD Patient Stem Cells into Dystrophic Mice. *Cell Stem Cell* **2007**, *1*, 646–657. [CrossRef] [PubMed]
88. Denti, M.A.; Incitti, T.; Sthandier, O.; Nicoletti, C.; De Angelis, F.G.; Rizzuto, E.; Auricchio, A.; Musarò, A.; Bozzoni, I. Long-Term Benefit of Adeno-Associated Virus/Antisense-Mediated Exon Skipping in Dystrophic Mice. *Hum. Gene Ther.* **2008**, *19*, 601–608. [CrossRef] [PubMed]
89. Martone, J.; De Angelis, F.G.; Bozzoni, I. U1 SnRNA as an Effective Vector for Stable Expression of Antisense Molecules and for the Inhibition of the Splicing Reaction. *Methods Mol. Biol.* **2012**, *867*, 239–257. [CrossRef]

Disclaimer/Publisher's Note: The statements, opinions and data contained in all publications are solely those of the individual author(s) and contributor(s) and not of MDPI and/or the editor(s). MDPI and/or the editor(s) disclaim responsibility for any injury to people or property resulting from any ideas, methods, instructions or products referred to in the content.

biomedicines

MDPI

Review

Neurological Disease Modeling Using Pluripotent and Multipotent Stem Cells: A Key Step towards Understanding and Treating Mucopolysaccharidoses

Sofia Carvalho [1,2,3,4], Juliana Inês Santos [1,2,3,5], Luciana Moreira [1,2,3], Mariana Gonçalves [1,2,3,6], Hugo David [1,2,3,5], Liliana Matos [1,2,3], Marisa Encarnação [1,2,3], Sandra Alves [1,2,3,†] and Maria Francisca Coutinho [1,2,3,*,†]

1 Research and Development Unit, Department of Human Genetics, National Institute of Health Doutor Ricardo Jorge, INSA I.P., Rua Alexandre Herculano, 321, 4000-055 Porto, Portugal; sofia.carvalho@insa.min-saude.pt (S.C.); juliana.santos@insa.min-saude.pt (J.I.S.); luciana.moreira@insa.min-saude.pt (L.M.); mariana.goncalves@insa.min-saude.pt (M.G.); hugo.david@insa.min-saude.pt (H.D.); liliana.matos@insa.min-saude.pt (L.M.); marisa.encarnacao@insa.min-saude.pt (M.E.); sandra.alves@insa.min-saude.pt (S.A.)
2 Center for the Study of Animal Science-Instituto de Ciências, Tecnologias e Agroambiente da Universidade do Porto, CECA-ICETA, University of Porto, Praça Gomes Teixeira, Apartado 55142, 4051-401 Porto, Portugal
3 Associate Laboratory for Animal and Veterinary Sciences, AL4AnimalS, Faculdade de Medicina Veterinária Avenida da Universidade Técnica, 1300-477 Lisboa, Portugal
4 Faculty of Pharmacy, University of Coimbra, Polo das Ciências da Saúde, Azinhaga de SantaComba, 3000-548 Coimbra, Portugal
5 Biology Department, Faculty of Sciences, University of Porto, Rua do Campo Alegre, 4169-007 Porto, Portugal
6 Centre for the Research and Technology of Agro-Environmental and Biological Sciences, CITAB, Inov4Agro, University of Trás-os-Montes and Alto Douro, 5000-801 Vila Real, Portugal
* Correspondence: francisca.coutinho@insa.min-saude.pt
† These authors contributed equally to this work.

Abstract: Despite extensive research, the links between the accumulation of glycosaminoglycans (GAGs) and the clinical features seen in patients suffering from various forms of mucopolysaccharidoses (MPSs) have yet to be further elucidated. This is particularly true for the neuropathology of these disorders; the neurological symptoms are currently incurable, even in the cases where a disease-specific therapeutic approach does exist. One of the best ways to get insights on the molecular mechanisms driving that pathogenesis is the analysis of patient-derived cells. Yet, not every patient-derived cell recapitulates relevant disease features. For the neuronopathic forms of MPSs, for example, this is particularly evident because of the obvious inability to access live neurons. This scenario changed significantly with the advent of induced pluripotent stem cell (iPSC) technologies. From then on, a series of differentiation protocols to generate neurons from iPSC was developed and extensively used for disease modeling. Currently, human iPSC and iPSC-derived cell models have been generated for several MPSs and numerous lessons were learnt from their analysis. Here we review most of those studies, not only listing the currently available MPS iPSC lines and their derived models, but also summarizing how they were generated and the major information different groups have gathered from their analyses. Finally, and taking into account that iPSC generation is a laborious/expensive protocol that holds significant limitations, we also hypothesize on a tempting alternative to establish MPS patient-derived neuronal cells in a much more expedite way, by taking advantage of the existence of a population of multipotent stem cells in human dental pulp to establish mixed neuronal and glial cultures.

Keywords: mucopolysaccharidoses; disease modeling; in vitro models; induced pluripotent stem cells (iPSCs); dental pulp stem cells (DPSCs)

check for updates

Citation: Carvalho, S.; Santos, J.I.; Moreira, L.; Gonçalves, M.; David, H.; Matos, L.; Encarnação, M.; Alves, S.; Coutinho, M.F. Neurological Disease Modeling Using Pluripotent and Multipotent Stem Cells: A Key Step towards Understanding and Treating Mucopolysaccharidoses. *Biomedicines* **2023**, *11*, 1234. https://doi.org/10.3390/biomedicines11041234

Academic Editors: Luigi Michele Pavone and Valeria De Pasquale

Received: 8 March 2023
Revised: 18 April 2023
Accepted: 19 April 2023
Published: 21 April 2023

Copyright: © 2023 by the authors. Licensee MDPI, Basel, Switzerland. This article is an open access article distributed under the terms and conditions of the Creative Commons Attribution (CC BY) license (https://creativecommons.org/licenses/by/4.0/).

1. Introduction

Lysosomal storage disorders (LSDs) are a group of rare diseases caused by mutations in genes that encode lysosomal enzymes, lysosomal membrane proteins, or transporters, and in a few cases caused by other cell proteins that are important for lysosomal function. This triggers an accumulation of undegraded substrates, which ultimately results in a broad range of clinical symptoms. Overall, those symptoms may be highly debilitating and affect multiple organs/systems, including the central nervous system (CNS) [1]. Among the LSDs, which may present with severe neurological phenotypes are mucopo-lysaccharidoses (MPSs), which are caused by impaired degradation of glycosaminoglycans (GAGs), with consequent intralysosomal accumulation of undegraded products [2]. Quite remarkably, none of the available therapies for this sub-group of disorders are effective against the neurological symptoms. Instead, they are limited to treating non-neurological symptoms [3]. Thus, there is an urgent need for the development of new ones that can tackle the neuronal pathogenesis. A crucial step towards the development of those approaches is the existence of suitable disease models, which can be used to further understand the pathophysiological mechanisms that underlie the phenotype and to adequately test those therapeutic strategies in vitro. Here, we review some of those models and the major results that other groups have published on the pathophysiological mechanisms underlying this particular subset of LSDs. To start with, we will highlight the different patient samples they used and the protocols they relied on. Particular attention will be given to the potential of induced pluripotent stem cells (iPSCs) to mimic disease-relevant phenotypes, and to the methods others have used to assess them. Finally, we will also mention a few studies, which have provided in vitro proof of principle on the potential of ex vivo genetically corrected iPSC-derived cells for therapeutic purposes.

Overall, the results reviewed here strongly support the utility of iPSCs for the study of MPSs. Still, iPSC generation is a laborious and expensive protocol. Furthermore, the use of iPSCs has a number of limitations, which should not be ignored. That is why in our lab we are addressing the question of whether alternative sources of stem cells (SCs) may exist, holding a similar potential for disease modeling in these rare yet life-threatening genetic disorders. In fact, recent studies have shown that dental pulp provides a niche for diverse arrays of mesenchymal stem cells (MSCs), and they are now being established in our laboratory for the study of LSDs, particularly MPSs. This approach is non-invasive, cost-effective, and can be established in any laboratory with standard cell culture conditions. Additionally, as we will briefly highlight in this manuscript, it may provide another potentially effective approach for investigating cellular and gene expression changes that occur in these monogenic diseases.

2. Mucopolysaccharidoses

Among the LSDs in need for better and more effective therapeutic options are the mucopolysaccharidoses (MPSs). The MPS subgroup includes seven different disease types, all of them accumulating glycosaminoglycans (GAGs) as the primary substrate. A brief overview of each individual disorder is given below.

MPS I is one of the most common forms of MPS and the first MPS type treated with enzyme replacement therapy (ERT; available since 2003) [4]. At a clinical level, MPS I may be divided into three subtypes: Hurler (OMIM #607014), Hurler–Scheie (OMIM #607015), and Scheie (OMIM #607016) depending on the disease severity [5]. Regardless of the clinical presentation, *IDUA* is the affected gene in this disorder. Mutations in this gene, which encodes for α-L-iduronidase (IDUA; EC 3.2.1.76), lead to an enzyme deficiency that ultimately results in heparan and dermatan sulfate (HS and DS, respectively) accumulation [6]. Currently, there are two possible therapeutic options for MPS I, ERT and hematopoietic stem cell transplantation (HSCT), which is only used in the most severe form of the disease and, preferably in the first years of life [7]. Regarding ERT, there is only one recombinant enzyme approved for MPS I: laronidase (Aldurazyme®, Genzyme). As every other ERT, this recombinant enzyme is injected into the blood circulation, which leads to

the correction of the enzyme deficiency in various organs and tissues, except for the brain, since it does not cross the blood brain barrier (BBB) [8,9].

MPS II (OMIM #309900), or Hunter syndrome, is the only X-linked MPS disease; all the other MPSs are autosomal. Two forms of the disease may be distinguished, neuronopathic and non-neuronopathic, whereby the most severe forms are CNS-associated [10]. Both forms are caused by mutations in the *IDS* gene, which encodes the enzyme iduronate 2-sulfatase (IDS; EC 3.1.6.13), leading to the accumulation of two substrates: HS and DS. Regarding MPS II therapeutics, ERT with idursulfase (Elaprase®, Takeda Pharmaceutical Company) is the first choice for patients with this condition [11].

MPS type III, also known as Sanfilippo syndrome, may be subdivided into four subtypes: IIIA (OMIM #252900), IIIB (OMIM #252920), IIIC (OMIM #252930), and IIID (OMIM #252940). Each particular subtype is associated with a unique enzymatic defect. MPS IIIA is caused by the deficiency of the enzyme heparan-N-sulfatase (SGSH, EC 3.10.1.1); MPS IIIB, in turn, is caused by defects in the enzyme N-acetylglucosaminidase (NAGLU, EC 3.2.1.50); in MPS IIIC the protein involved is the transmembrane enzyme, acetyl-CoA:Glucosamine N-acetyltransferase (HGSNAT, EC 2.3.1.78); and, finally, MPS IIID is caused by defects in N-acetyl-glucosamine-6-sulfatase (GNS, EC 3.1.6.14). All MPS III subtypes are associated with a severe deterioration of neurological function [12], which results in a number of clinical symptoms either directly or indirectly related to a CNS dysfunction [13,14]. Unfortunately, there is no approved treatment for these neurological diseases. On the one hand, while it has already been attempted by several different teams, HSCT has proven virtually no benefit over the neurocognitive symptoms [15–19]. On the other hand, ERT is hard to apply, since classically formulated enzymes do not penetrate the CNS. Moreover, in the case of MPS IIIC, for example, ERT is not an option, since the deficient enzyme is a transmembrane protein. There are, however, teams attempting brain-specific delivery of both ERT and chemical compounds for MPS type III. In general, there are three strategies to increase the delivery (reviewed in [20]): enzymatic modulation, route(s) of administration [21–23], and increase in enzyme dosage. In addition, cellular and genetic therapies represent approaches that have gained importance when it comes to BBB delivery (reviewed in [24]).

There are two different forms of MPS IV, each one caused by a single enzymatic defect: N-acetyl-galactosamine-6-sulfatase (GALNS; EC 3.1.6.4) deficiency underlies MPS IVA (OMIM #253000) while β-galactosidase (EC 3.2.1.23) defects cause MPS IVB (OMIM #253010). The involved genes are *GALNS* and *GLB1*, respectively. Unlike MPS III, which is almost exclusively a neurological syndrome, the skeleton is the main affected system in MPS IV, with the substrates (keratan sulfate (KS) and chondroitin-6-sulfate (C6S)) accumulating predominantly in the cartilage and bones [25]. The only FDA-approved treatment for MPS IV is elosulfase alfa (Vimizim®; BioMarin Pharmaceutical Inc.) which is used to treat MPS IVA patients. All other options are symptomatic and mostly consist of surgical approaches to prevent spinal cord damage or other skeletal issues, for example spinal decompression surgery [26].

Yet another form of MPS, usually coined Maroteaux–Lamy Syndrome, is MPS type VI (OMIM #253220), caused by mutations in the *ARSB* gene [27]. Even though being a multisystemic condition, MPS VI does not affect intelligence, and, as in the Morquio syndrome, the skeleton is the most affected system [28]. To counteract the DS storage promoted by the deficiency of arylsulfatase B (EC 3.1.6.12) activity, galsulfase (Naglazyme®, BioMarin Pharmaceutical Inc.) is the drug approved for and currently employed in patients. HSCT may also be possible; however, additional safety studies are needed [29–31].

MPS type VII (OMIM #253220), or Sly syndrome, is an extremely rare form of MPS, which occurs with an estimated frequency of 0.02 [32–35] to 0.29 [36] per 100,000 live births (reviewed in [37]). Several systems/organs are involved in this disease with clinical features affecting organs as diverse as the eyes, lungs, heart, musculoskeletal system, spleen, etc. There may also be a neurological involvement as testified by recurrent observations of limited vocabulary and mental retardation in several MPS VII patients [38]. Overall,

these symptoms are caused by an ubiquitous accumulation of several different GAGs, namely DS, HS, and CS, as a consequence of the deficient activity of β-glucuronidase (GUS: β-D-glucuronoside glucuronosohydrolase, EC 3.2.1.31), which is encoded by the *GUSB* gene [39]. The approved drug for this pathology is vestronidase alfa (Mepsevii™, Ultragenyx Pharmaceutical Inc.), which is indicated in both pediatric and adult cases [40].

Finally, MPS IX, or Natowicz disease (OMIM #601492), is an ultra-rare disorder. The first report was published in 1996, with the described patient presenting a number of clinical manifestations associated to joint and skeletal systems [41]. This disorder is caused by a deficiency in the enzyme hyaluronidase 1 (HYAL1; EC 3.2.1.35) due to mutations in the *HYAL1* gene, which leads to the accumulation of yet another substrate: hyaluronan. Due to the rareness of the disorder, very few mutations have been reported to date, and a possible treatment is very challenging [42].

In general, even though the molecular bases and biochemical defects underlying MPS diseases are well defined, knowledge is still lacking on the pathophysiological mechanisms that actually trigger the appearance of different symptoms in the different organs and systems. Furthermore, even though over the last few decades much has been learnt from the study of individual patients and, particularly, from the generation and extensive characterization of bona fide in vivo models, truth is, we still do not fully understand the whole physiological cascade, which underlies some of MPSs' most challenging phenotypes, namely those which affect the CNS. This is particularly relevant since no therapeutic exists to ameliorate them. Still, finding an in vitro model that could recapitulate the disease-relevant features is also challenging since live neurons are inaccessible cells. Indeed, for almost a century, patient-derived fibroblasts were gold standard for in vitro studies of MPSs, as for all other LSDs. These cells are relatively easy to access, since a simple skin biopsy is enough to obtain them and, remarkably, they do display the cellular phenotype that actually coined these diseases as "storage" disorders: the presence of undegraded or partially degraded substrates. Nevertheless, fibroblasts may also fail to recapitulate disease-relevant features, which are only evident in other particular cell types of higher pathological significance, such as neurons. A viable option is to generate the neurons from a patient-derived cell line, which involves extracting cells from the patient and differentiating them into neuronal cells. Indeed, there are two possible ways to perform this process: iPSCs and mesenchymal stem cells (MSCs) from the patient.

3. Modeling Mucopolysaccharidoses with Induced Pluripotent Stem Cells (iPSCs)

Human iPSC generation in particular started its journey in 2007, when Yamanaka et al. [43] first generated those cells from human somatic fibroblasts using a remarkable method, which relies on the retroviral transduction of four independent transcription factors into patients' fibroblasts: Oct-3/4, Sox2, Klf4, and c-Myc. Remarkably, the cells that resulted from this experiment showed numerous similarities with human embryonic stem cells (hESCs), including morphology, proliferative capacity, gene expression patterns, and in vitro differentiation potential. Ever since this hallmark report was published, the search for novel and improved protocols for cell reprogramming advanced at an outstanding pace, with various optimizations being published in order to generate virtually every cell of interest from iPSCs of different origins [44].

Over the past few years, in vitro models derived from iPSCs have been unraveling some enigmatic aspects of MPSs. In particular, the subtypes that present neurological involvement appear as the ones with the greatest need for additional knowledge and new therapeutic solutions.

Here, we will review numerous studies attempting not only MPS-derived iPSC generation, but also their subsequent differentiation into relevant cell types. We have divided those studies into four major groups, each one of them having a dedicated section in this review (Figure 1). First, we will address the papers in which only iPSCs were generated, briefly discussing the methods used to characterize them. Then, we will focus on those papers where iPSCs were further differentiated into either neural precursor cells or totally differentiated neurons, highlighting the disease modeling potential of those lines by

showing the numerous pathophysiological insights one can get with a few simple cellular assays. Then, we will go through the papers where those cells were used for in vitro drug screening, commenting not only on the results obtained but also on the advantages or disadvantages of the use of those particular cells for therapy development. Finally, in the last iPSC-devoted section, we will refer to a few studies where the therapeutic potential of these particular SCs was addressed. Meaning: we will summarize the papers where, instead of generating iPSCs to further understand one particular disorder or genotype or to serve as a drug-screening platform, the authors have actually created them for gene therapy.

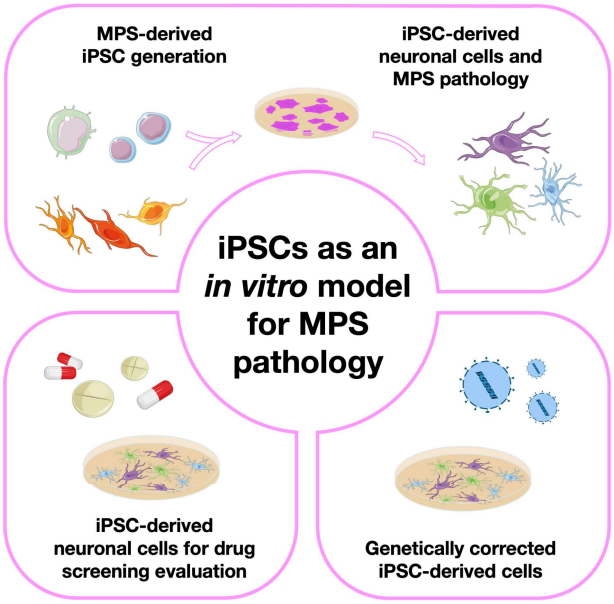


Figure 1. The four major types of studies involving the generation and characterization of induced pluripotent stem cells (iPSCs) as in vitro models for Mucopolysaccharidoses (MPSs), grouped together according to their ultimate aims: (1) papers on iPSC generation and characterization; (2) papers describing their subsequent differentiation into different types of neuronal cells; (3) papers on the use of iPSCs and their derived cell models for drug screening; and (4) papers on the use of genetically corrected iPSCs for therapeutic purposes.

3.1. The Basic Studies: iPSC Generation from Different MPS Patient-Derived Cell Sources

The first MPS-derived iPSCs were generated in 2011 when Thomas Lemonnier and colleagues [45] reprogrammed fibroblasts from two patients suffering from MPS IIIB into pluripotent stem cells (PSCs). As in any other iPSC generation report, the resulting SCs were extensively analyzed and characterized. In this particular study, the authors confirmed a positive expression of three particular markers (SSEA4, Nanog, and TRA-1-60) and the differentiation ability of those cells, thus proving their pluripotent nature. Additionally, the authors have also provided information on the karyotype presented by those cells. This is a relevant assessment whenever a novel iPSC line is generated but it should also be considered later on, when using the same iPSC line after several passages, or after having one particular iPSC cell line in culture for a long period. In fact, long-term iPSC culture has already been shown to have a number of drawbacks, as cells tend to accumulate chromosomal abnormalities and changes in gene expression or cellular functions [46–48]. Eventually, this increases the risk of tumorigenicity. Altogether, those genomic alterations represent a source of potential risks to many final applications of iPSCs making it is crucial to monitor the genomic integrity of iPSC lines [49]. That is why iPSC karyotype analysis is such an important step in the validation of this type of cell models, and nowadays considered a routine procedure by all the groups working with iPSC technology [45].

However, these were not the only published MPS IIIB-derived iPSCs reported in the literature so far. Two other MPS IIIB patient-derived iPSC lines were generated from

skin fibroblasts by Vallejo-Diez et al. in 2018 [50]. In that particular study, additional pluripotency markers besides the previously referred Nanog and TRA-1-60 were also assessed: Oct-3/4, Sox2, and TRA-1-81 were also analyzed. As in the previous study, the karyotype was also assessed, and the associated mutation confirmed. However, the authors actually went one step further in terms of SC characterization, analyzing the differentiation ability of the generated iPSCs. Cells derived from embryoid bodies were differentiated into three germ layers and specific markers were evaluated. The same characterization was carried out for MPS IIIA-derived cells, where the same team was the first to create patient-derived iPSCs for that particular disease [51].

Regarding MPS IIIC, Noelia Benetò et al. also generated iPSC lines, but this time using a slightly different protocol from the previously described ones. Instead of using patient-derived cell lines, these authors created isogenic *HGSNAT*-mutated lines from healthy iPSCs using CRISPR/Cas9. This technology allows to create such lines from human cells, which have the genetic background of the wild-type cells but differ by the genetic modification of interest. These isogenic pairs are powerful tools for understanding gene function. While circumventing confounding effects of the genetic background, they allow for genotype–phenotype correlation studies [52]. To prove the reliability of this model, the authors measured HGSNAT enzyme activity and assessed the differentiation capacity of the generated SCs. This last parameter was studied by inducing the formation of embryoid bodies and their subsequent differentiation into three germ layers. The formation of these structures is a characteristic of pluripotent SCs and serves as a platform for the intended differentiations [53].

Still, even though the neurological involvement is a major hallmark of the Sanfilippo syndrome, almost every other MPS may present with severe neurological symptoms. Type I and II in particular even have specifically recognized clinical forms where the CNS is strongly affected, presenting with major clinical symptoms. Thus, these disorders would also strongly benefit from the development of appropriate neuronal cell models to study them. Furthermore, the models would also allow for tissue- or cell-specific drug screening assays. Generating iPSC lines from those disorders is a rational step towards that first goal, and that is probably one of the reasons why iPSC lines from both disorders have also been created and subsequently published in the past few years.

Regarding MPS type II, in 2016, Eszter Varga et al. collected peripheral blood mononuclear cells (PBMCs) from 1-, 3-, and 7-year old phenotypically affected patients [54–56] and from an unaffected 39-year old woman with a carrier mutation [57]. Then, all patients' PBMCs were subjected to induction of the pluripotent stage, resulting in disease-specific iPSCs, which were extensively characterized as required for the technology itself.

Last but not least, MPS type I has also been modeled with the help of this revolutionary technology. In 2019, Lito S. et al. [58] and Suga M et al. [59] reprogrammed and characterized dermal fibroblasts and PBMCs, respectively, into iPSC lines. The fibroblast-derived pluripotent cells were obtained from a patient with the Hurler form of the disease, whereas PBMCs were collected from a patient suffering from Scheie.

3.2. Moving One Step Further: Generation of Neuronal Models from MPS-Derived iPSCs

As we already referred to, the neurological involvement, which places such a tremendous burden on patients suffering from several forms of MPS, may be further explored by differentiating iPSCs into different types of neuronal or pre-neuronal populations. In fact, most works published until now are not only focused on reprogramming different types of patient-derived cells (namely fibroblasts and PBMCs) but also on the differentiation step, searching for disease-relevant features in those cells. Ultimately, these models may also allow for the discovery of novel hallmarks related or non-related to neuropathology. Considering the intrinsic nature of all MPSs, lysosomal pathology is probably the most crucial parameter to study, since the enzymatic defect will primarily affect these organelles.

Thus, when it comes to disease-phenotype assessments, some markers have been particularly relevant in the LSD field, namely the lysosome-associated membrane proteins

1 and 2 (LAMP-1 and LAMP-2). These two proteins are heavily investigated since they represent the major components of the lysosome membrane. For example, in the study involving the first MPS-derived iPSCs [45], which were generated from MPS IIIB patients' samples, the accumulation of storage lesions was intensively analyzed through LAMP-1 and Golgi matrix protein 130 (GM130) detection. A prominent fluorescence of both markers was detected in patient-derived iPSCs, and the vesicles observed using microscopy were revealed to have a heterogenous content. This was actually the first study to describe Golgi-complex impairment in the MPS pathology. Most importantly, beyond iPSC generation, this group also investigated the differentiation into neural stem cells (NSCs) by adding specific growth factors to the original iPSC culture, namely fibroblast growth factor 2 (FGF2) and endothelial growth factor (EGF). When this protocol was initiated, the development of neurospheres became evident and after 2 weeks of non-adherent growth, the authors measured both the expression of Nestin (a neural progenitor marker) and total GAG storage, observing increased storage levels. Interestingly, the higher LAMP-1 and GM130 expression previously seen in iPSCs did not translate to the floating neurospheres. However, the gene expression profile showed significant alterations in several pathways including the Wnt signal transduction pathway and transforming growth factor β (TGFβ) signaling, as well as genes encoding proteins associated with cell adhesion, Golgi apparatus, and lysosomes. Curiously, higher LAMP-1 and GM130 fluorescence was seen again as soon as neurosphere adhesion was performed, and during the final process of neuronal differentiation. This observation was also accompanied by vesicle storage positive for LAMP-1 and Ganglioside GM3. These results reflect the existence of a modest cellular pathology during the neurodifferentiation of this iPSC model. This study was the first comprehensive characterization of MPS-affected neuronal cells in vitro [45].

To the best of our knowledge, the second report on the differentiation of MPS-derived iPSCs into neuronal cells was the work of Bruyerè and collaborators, in 2015 [60], where these authors correlated two independent models of the disease: one in vitro and another in vivo. For the in vitro studies they used patient- and control-derived iPSCs, further differentiated into neural precursor cells (NPCs), while for the in vivo differences they used a mouse model. Their goal was to investigate how HS saccharide accumulation impacts focal adhesions (FAs). They saw that activation of FAs occurred when neural cells from healthy individuals were submitted to exogenous soluble HS fragments. Consequently, this activation becomes constitutive in MPS IIIB, since those fragments are accumulated. Constitutive activation of FA, in turn, affects the polarization as well as the oriented migration of those cells [60].

Later, in 2015, Canals et al. [61] performed the differentiation of MPS IIIC-derived iPSCs into neuronal cells. Their goal was to verify if early functional alterations could be visible before the appearance of disease-related phenotypes. Briefly, iPSC lines generated spherical neural masses (SNMs), whose expression patterns included PAX6, Nestin, and Sox2. The existence of active neurons was also proven by the presence of microtubule-associated protein 2 (MAP2) and synapsin (SYP), which are dendritic and synaptic markers, respectively. In addition to the formation of mature neurons, an astrocytic-related marker, glial fibrillary acidic protein (GFAP), was noticed. That observation further reinforced the neurogenic capacity of these cells. Regarding the neuronal cultures generated, as expected, GAG accumulation was shown to have a progressive pattern, becoming significant only after 9 weeks. These observations document a marked difference between the patients' fibroblasts and iPSC-derived neurons: the patients' fibroblasts presented a double amount of accumulated GAGs, right from the first cell culture, when compared to iPSCs-derived neurons. Network activities were also evaluated to verify whether there were differences between Sanfilippo- and control-iPSC-derived neurons. Through calcium imaging, the spontaneous activity of Sanfilippo-derived neurons was shown to gradually decrease between 6 and 9 weeks. Concerning degradation of effective connectivity, which was determined by identifying causal influences among neurons through generalized transfer entropy, an information theory method that allows drawing a functional map of neuronal

interactions in the network, the authors reported that, quite differently from the controls analyzed, in the Sanfilippo neurons strong connections were only established within a subset of neurons, the rest of them remaining disconnected or poorly connected [61].

At a technical level, the authors used two different protocols, one relying on neuronal induction medium without any extra supplementation, and another where that medium was supplemented with N2 and B27, two chemically defined supplements recommended for growth and survival of neuronal cells, and observed significant differences in the time it took for them to generate neurons. In fact, while it took several weeks in neuronal induction medium for mature neurons to arise, when supplementing that same medium with N2 and B27, it took only 3–5 weeks to distinguish synapses between neurons. Moreover, the neuronal activity and effective connectivity analyses they performed were nicely designed and described, and could be applicable to virtually any other neurodegenerative disease in which iPSC-based models are available [61].

Five years later, Benetó et al. [62] took advantage of the existence of a few previously reported iPSC lines to generate neuronal and astrocytic models of Sanfilippo syndrome type C for disease modeling and drug development: two isogenic MPS IIIC mutant lines [61], one wild-type control (from a healthy donor), and one MPS IIIC-derived line [53]. Again, all four lines were differentiated into neurons and astrocytes through lentiviral transduction and promoting the overexpression of neurogenin 2 (Ngn2) in the case of neurons (named iNs) and Sox2/Nuclear Factor one B (NfIb) in the case of astrocytes (named iAs). To confirm cell identity, the authors performed a characterization of the specific markers. In the generated neurons, they detected an increase in neural stem cell markers, namely tubulin β-3 (TUBB3), SYP, MAP2, and neuron-specific class III β-tubulin (Tuj1). In the astrocytes, they observed that the expression of astrocytic-specific genes namely GFAP, aldehyde dehydrogenase 1 family member L1 (ALDH1L1), calcium-binding protein B (S100B), and vimentin (VIM) increased during the astrocytic differentiation. In addition, disease-relevant features were assessed through LAMP-2 staining and HS quantification. In the LAMP-2 immunocytochemistry assays, the authors clearly saw an intensity increase in all disease lines compared to the wild-type one. In the case of HS accumulation, they only presented results for neurons, where, as expected, increased substrate storage could be observed [62].

Still in Sanfilippo syndrome, for its most frequent type MPS IIIA, a comprehensive study was carried out by R. J. Lehmann et al. in 2021 [63], to investigate the ability of fibroblasts-derived iPSCs to differentiate into a neuronal cell line and discover intrinsic mechanisms of the disease. After properly characterizing the pluripotent phase, the authors performed a neurodifferentiation protocol. Two main parameters were assessed: the FGF2 signaling pathway and the neurogenesis process. Interestingly, in the beginning of this study a curious fact was noticed: when the FGF2 supplement was added to the medium, the proliferation rate of the MPS IIIA iPSC-derived NPC culture increased significantly. Remarkably, however, even with the supplementary FGF2, the signaling pathway of this factor is still reduced when compared to controls. So, understanding this event became a priority for this team. In fact, the FGF2 signaling pathway only occurs when this factor binds to a possible receptor. Since FGF2 also binds to HS, this may suggest that this GAG plays a key role in neurogenesis and in the homeostasis of the CNS. Taking this into account, the subsequent step was to investigate the relationship between the accumulated HS in MPS IIIA and the lower proliferation rate. They verified that the affinity of HS MPS IIIA to FGF2 was similar to the HS present in the control, meaning that the accumulation does not alter the affinity. So, a possible explanation for decreased FGF2 signaling is that since the FGF2 binds to the accumulated HS, it does not interact with the proper receptors (cell-surface HS and fibroblast growth factor receptors), thus affecting not only cell proliferation without supplementary FGF2 but also the signaling pathway. To investigate the disorder's impact on the neurogenesis process, control and disease cells were analyzed regarding both morphological parameters and expression patterns. At a structural level, the formation of cell body aggregation and cell extensions was seen in both cell lines. However, as already

seen by other authors in SC models for other neurological disorders, in MPS IIIA cells, those characteristics were less frequent. Regarding the expression profiles, the genes evaluated were *Nestin*, *TUBB3*, hyperphosphorylated neurofilament (*NF-H*), and neuron-specific enolase (*NSE*). In general, the increase/decrease pattern during the four weeks of neuronal induction was consistent between the controls and the disease cell lines; nonetheless, the disease cells showed consistently lower levels of all markers. This pattern was seen both in the absolute values themselves and in differences during the period of the procedure. Attention was also paid to the model's capacity to recapitulate disease-relevant features. So, the same parameters, which were initially assessed in fibroblasts, were also analyzed after the neurodifferentiation protocol. Not surprisingly, the MPS IIIA cells exhibited higher levels of HS, a consequence of lower enzyme activity compared to the controls, further validating the disease modeling value of this kind of cells [63].

As previously stated, though, other MPSs apart from the Sanfilippo syndrome may benefit from the development of disease-specific neuronal cell models, and from the pathophysiological insights one may gain from them. Thus, some of the most striking reports on iPSC-derived neuronal and astrocytic models for MPSs actually came from MPS II. In 2019, Kobolák et al. [64] even proposed a novel neuropathology model using this approach and observed similar results regarding the impact of HS as the ones described above for MPS IIIA. They used the iPSCs originally published in a number of publications already reviewed in the previous section [54–57] that were differentiated into NPCs and terminally differentiated (TD) neuronal cells. Briefly, those iPSCs were derived from two affected siblings. As expected, both individuals shared the same nonsense mutation. Also included in this study were their mother (a carrier for the same causal mutation) and an unrelated patient with a different mutation (missense). Finally, the authors also included cells from an unrelated non-carrier, which were used as a control. At the neurodifferentiation stage, neither the patient-derived nor the healthy cells had differences in the expression of specific neuronal markers. Briefly, for NPCs the authors assessed Nestin, Sox1, and PAX6; for terminally differentiated neuronal cells, on the other hand, they checked TUBB3, MAP2, and neurofilament 200 KDa (NF200). An exhaustive characterization of those cells was conducted, showing that mature neurons exhibited postsynaptic density protein 95 (PSD95) expression, an indicator of activated synapses. Astrocytes, on the other hand, were shown to be positive for GFAP and aquaporin 4 (AQP4) markers [64]. Interestingly, according to these authors' results, the proliferation capacity of NPCs seems to be a distinctive factor between the controls and the patients' cells, once, after 8 passages, the proliferative capacity of the MPS II-derived cells slowed down or even stopped and the PAX6 and Sox1 expression decreased, independently of bFGF and EGF presence in the cell culture. Meanwhile, the control-derived NPCs maintained the proliferation rate up until passage 12. Actually, the authors considered this event to be related to the overall MPS II brain pathology: in normal conditions HS binds to growth factors at a proper rate, not harming their proper function. However, in the case of storage, the accumulated HS usually binds to growth factors at a higher rate, including to the one with a key role in NPC proliferation, FGF2. This link prevents the accomplishment of the transcription factor function. As a response, the cells start to differentiate into neurons, occurring in the appearance of anticipated neurites when compared with control cells [64].

One of the essential aims of this work was to verify if some of the disease hallmarks were already present in the NPC stage. Thus, the authors performed several analyses and, remarkably, they realized that GAG accumulation was not evident. Interestingly however, it was even reduced compared to both controls (carrier and non-carrier). They hypothesized that this phenomenon could be related to the lower levels of the early endosomal marker RAB5 (which is translated in a lower endocytosis level), as well as to the normal levels of the late endosomal marker RAB7 and the lysosomal marker cathepsin D, in addition to the higher LAMP-2 expression. The existence of those factors is reflected in functional exocytosis by patients' cells: GAGs and GAG fragments are expelled to the extracellular space, which could explain the appearance of GAG accumulation in cerebrospinal fluid.

This whole pattern changed, however, when mature neurons and astrocytes were analyzed. In fact, for those mature neurons and astrocytes differentiated from cells harboring the frameshift/PTC mutation, GAG accumulation was (quite) evident. Importantly, however, the levels of Rab7, Rab5, and LAMP-2, were still similar to those observed in controls, indicating a non-influence of the endosomal–lysosomal system on substrate accumulation. It should also be stressed that for the cells harboring the missense mutation all assessed parameters were comparable to those seen in the controls. While somehow unexpected, these results highlight the intrinsic potential of these sort of cell-based patient-derived models as they allow for more accurate comparisons between the effect of different disease-causing mutations of several subcellular parameters, ultimately allowing for more precise genotype–phenotype correlation. Also noteworthy, regardless of the analyzed genotype all terminally differentiated neuronal cells (neurons and astrocytes) showed a significant increase in the autophagy marker LC3-I, revealing the involvement of this pathway in disease cytopathology. Additionally, an accumulation of autophagosomes, as well as a lower ratio of LC3-II/LC3-I, was also detected [64].

Regardless of the cell differentiation status, a common point in the cytopathology of MPS II from NPCs and TDs was the presence of ER stress with the occurrence of dilated ER cisterns. In NPCs, the authors observed a significantly higher level of XBP1, a well-known ER stress marker. For TDs, even more events related to this stress were observed, namely depletion of ER luminal Ca^{2+} storage, higher ion concentration in the cytoplasm, and a higher sensitivity to apoptosis. Concerning cell death, they noticed a higher rate of apoptosis in astrocytes rather than other TDs. It is known that this cell type plays an important role in supporting the differentiation and survival of cortical neurons. Therefore, if they are not functional, cell death and neurodegeneration may occur [64].

Furthermore, for MPS I, a few studies exist where iPSCs were differentiated into NSCs and from which curious insights were gathered. An interesting study was performed in 2018, by Swaroop et al. [65], where after generating iPSCs and NSCs from all MPS I subtypes, the authors addressed the question of whether those three subtypes could be distinguished from each other, while extensively characterizing each one of them. In the characterization step, they observed a normal iPSC and NSC morphology, karyotype, and growth rate in all three. Still, differences among the MPS I subtypes were quite evident, when it came to the diseases' hallmarks. Regarding enzyme activity, for example, all NSC-MPS I types exhibited a lower rate when compared to controls. However, the levels observed in the Hurler-derived cells were remarkably lower than in the others. The same happened when DS and HS accumulation and lysosomal enlargement were evaluated: the values for the Hurler subtype were much higher. Also noteworthy, when the authors compared those cell lines using differential expression (DE), about 3036 genes were found to be significantly changed between patients and controls. Remarkably, however, out of those, 42% were exclusive to the Hurler syndrome. Not surprisingly, those genes were involved in GAG homeostasis, dysregulation of the lysosomal pathway, and autophagy [65]. Overall, these results strongly support the idea that one can nicely characterize and distinguish different forms of the same disorder by evaluating iPSC-derived models, as they recapitulate the severity seen in patients at the subcellular level [65].

Four years later, another interesting study was conducted by Lito S. et al. [66] focusing on the most severe form of the disease alone (Hurler). In that paper, in addition to reprogramming dermal fibroblasts into iPSCs and generating NSCs, the authors went one step beyond and created an isogenic control from these iPSCs by re-establishing *IDUA* expression to avoid any type of variability that could emerge from the comparison with control iPSC lines derived from other individuals. Then, those isogenic cells were also differentiated into NSCs. As a matter of fact, these cells showed a total functional enzyme, both in the iPSCs phase as well as when differentiated into NSCs. Through comparison with isogenic cells, they could see the most evident hallmark of these disorders: GAG accumulation. Furthermore, at the end of a three-week-long neuronal differentiation protocol (where FGF2 and EGF were removed from the media), they saw a higher migration of rescued-

enzyme NSCs as well as neurite outgrowth when compared to deficient iPSC-derived NSCs in vitro. In turn, proliferation capacity during three weeks of neurodifferentiation, did not change significantly between the two cell conditions. They hypothesized that due to the strong binding properties of CS and HS when accumulation occurs, these storage products bind to molecules responsible for neurite outgrowth and cell migration, preventing their binding to the proper receptors, and accomplishing the right function. Furthermore, these aspects were accompanied by an evaluation of gene expression patterns. Biological processes associated with the pathways of TGFβ and focal adhesions, PI3K-AKT signaling, Hippo signaling, the RAP1 signaling pathway, extracellular matrix interaction, and calcium signaling were altered with around 173 downregulated and 167 upregulated genes. In general, these migration defects and gene expression changes seen in patients affected by monogenic diseases are associated with a cause–effect relationship, where the genotype presents as a cause and the phenotype as an effect. However, based on these results, the authors proposed that the reverse may also occur, presenting a bidirectional pattern [66].

3.3. iPSC-Derived Neuronal Cells for Drug Screening/Therapy Evaluation

As we already referred to, MPS iPSC-derived neuronal cells have been generated not only to model MPS and study their pathology. Indeed, one of their crucial goals is to work as a platform to test future therapeutics. Thus, several research and development groups, some of them already mentioned in the previous sections, have been using those cells to test a number of compounds that may allegedly hold promise for the treatment of this LSD class.

Starting, again, with the Sanfilippo syndrome, one of the studies referred before [62], besides intending the development of neuronal and astrocytic models derived from MPS IIIC iPSCs, also aimed at testing an SRT approach that had already given positive results in MPS IIIC fibroblasts [67]. That was the work of Benetó and co-workers, back in 2015, and the approach they wanted to test consisted of the use of an siRNA against one of the genes responsible for GAG biosynthesis (the *EXTL2* gene) as a genetically triggered SRT. Still, while its application in the generated neuronal and astrocyte cells revealed a great success in the reduction in mRNA levels of this gene (about 75%), when the HS levels were analyzed in neurons, no difference in substrate accumulation could be detected. Curiously, this parameter was not measured in astrocytes, and it is actually a future perspective of this the group to test it as well. A few years ago, this team also reported an siRNA-driven SRT approach against *EXTL3* (another gene involved in GAG biosynthesis) with positive results in fibroblast disease cells [67], and they proposed to assess its effect in the same neuronal and astrocytic models, but, to the best of our knowledge, no follow-up studies have been published so far. Altogether, however, the results they published so far, further highlight the need to develop suitable cell models for drug testing, by clearly demonstrating that there may be significant differences between the results obtained in vitro in fibroblasts vs. neurons using the exact same therapeutic molecule. In fact, fibroblasts are the classical human cellular model in LSDs, but there are significant metabolic differences between fibroblasts and neural cell types. Furthermore, fibroblasts are dividing cells, while neurons are not. This means that even though fibroblasts accumulate undegraded materials, storage can be underestimated due to dilution by cell division, when compared to that in non-dividing cells [62].

One year later, Huang W. et al. [68] published a comprehensive work, which went all the way from the iPSC generation and characterization to the generation of (iPSC-derived) MPS IIIB neuronal cells. While it goes far beyond the scope of this review to go through the extensive characterization analyses and pathophysiological assessments the authors performed on both types of cells, we would like to briefly highlight the therapeutic assessments they made in vitro using these models. Briefly, they examined the effects of three possible therapeutic agents: ERT with recombinant NAGLU (rhNAGLU), δ-tocopherol (DT), and hydroxypropyl-β-cyclodextrin (HPBCD). When rhNAGLU was applied to NSCs, a dose-dependent decrease in enlarged lysosomes was readily observed; the same happened when testing DT and HPBCD in addition to a dose-dependent reduction in the

lipidic accumulation. In fact, those two compounds have already shown positive results in Niemann–Pick disease type C and, more recently, also in other LSDs [69–71]. Due to this observation, both compounds were also evaluated in MPS II iPSC-derived NSCs by Hong et al. [72]. In the case of DT, the results showed a reduction in lipid accumulation after three days, but in a dose-dependent manner; in turn, when evaluating the lysosomal accumulation, only a 7% reduction was revealed. The HPBCD results were not so encouraging, since it had virtually no effect on primary and secondary accumulation. As previously anticipated, however, when NSCs were treated with a recombinant enzyme for MPS II (rhIDS), a marked reduction in lipid accumulation was also observed.

Curiously, the effect of rhIDS enzyme was also the target of a study presented in 2018 by Rybová et al. [73]. This study also contemplated reprogramming MPS II PBMCs into iPSCs and their subsequent differentiation into NPCs, neurons, astrocytes, and oligodendrocytes. Having properly characterized all those cells, the authors moved on to evaluate the effect of rhIDS on GAG levels. Remarkably, however, their results showed that despite achieving 10-fold higher enzyme activity levels, the treatment could not reverse the exponential growth of GAG levels, even though some decrease could be seen [73].

3.4. Genetically Corrected MPS-Derived iPSCs

Finally, we will also mention a few studies, which have provided in vitro proof of principle on the potential of ex vivo genetically corrected iPSCs for therapeutic purposes.

The proof-of-concept study on the therapeutic use of iPSCs for autologous HSCT was published in 2015, by Griffin and co-workers, who attempted ex vivo gene therapy using patient iPSC-derived NSCs to reverse brain pathology in MPS VII [74]. Those authors assessed the engraftment potential of MPS VII NSCs genetically corrected with a transposon vector, by transplanting those cells into a previously reported mouse model for the disease, the so-called NOD/SCID/MPS VII model. Briefly, they intraventricularly injected genetically corrected GFP-labeled NSCs into different neonatal mouse populations, either suffering or not suffering from MPS VII. Remarkably, the authors observed similar levels of cell distribution in both pathological and non-pathological contexts, demonstrating that engraftment properties are not influenced by the disease. Importantly, transplanted cells survived and remained in the immature stage (Nestin-positive) for over 4 months. However, the proliferation rate reduced dramatically with the total disappearance of proliferation markers after 4 weeks following transplantation. It is worth mentioning, that the authors chose to work with neonatal mice for these initial assessments because they provide a more hospitable environment for engraftment relative to the adult brain. Then, to test whether similar results could be obtained in older animals, they injected ex vivo corrected MPS VII iPSC-NSCs in diseased mice' adult brains. Again, the immature stage remained with a Nestin-positive pattern. In the adult mice, however, the authors also addressed a number of pathological aspects, in order to address the therapeutic potential of this approach. In fact, they did detect GUSB activity but only near the injection site of the hemisphere receiving corrected cells. Additionally, they also verified a high reduction in neuroinflammation after only 1 month following transplantation in that same region. Basically, they showed that xenotransplantation of ex vivo corrected MPS VII-derived NSCs into a mouse homolog of the human disease can reverse pathologic lesions surrounding the engrafted cells. However, more relevant than the particular results they saw in this disease and their accurate analysis, are the innovation potential they hold and the new avenues they open by showing that genetically corrected iPSC-derived NSCs may indeed have the potential to treat MPSs [74].

Then, in 2018, Clarke et al. described a somewhat similar approach, attempting to use genetically corrected NSCs derived from iPSCs as a transplantation approach to the treatment of MPS IIIB [75]. Briefly, *Naglu*$^{-/-}$ mouse embryonic fibroblasts were reprogrammed into iPSCs and later differentiated in NSCs. Those cells were then corrected ex vivo, through lentiviral transduction of the full-length human *NAGLU* cDNA. This led to an obvious overexpression of the gene in the corrected NSCs, which resulted in a

4-fold increase in enzyme activity and in a 14-fold higher level of secreted NAGLU when compared to wild-type cells. Importantly, before they attempted HSCT of those genetically corrected cells, the authors confirmed in vitro whether secreted NAGLU could enter *Naglu*$^{-/-}$ cells in an M6P-dependent way, and verified that corrected cells were indeed able to "cross-correct" enzyme-deficient ones. Additionally, they also addressed whether there was a difference in lysosomal enlargement between genetically corrected NSCs and unmodified *Naglu*$^{-/-}$-derived NSCs. Curiously, they could not see any differences. However, when both cell lines were allowed to differentiate into mature neural cells, the ones derived from genetically corrected NSCs did show a significant decrease. Only then did the authors move to in vivo studies. Basically, they repeated virtually the same experiments previous teams had performed before: ex vivo genetically modified cells were injected into newborn *Naglu*$^{-/-}$ mice to understand whether they would promote an amelioration of the animals' phenotype. However, there is one remarkable aspect about this study that should be highlighted: this team evaluated two independent protocols, intracerebroventricular (ICV) and intraparenchymal (directly in the striatum), and the pathological aspects they analyzed were microglial activation, astrocytosis, and lysosomal dysfunction/storage material. These aspects were analyzed using immunostaining of CD68, GFAP, and LAMP-1, respectively [75].

Again, we will not review in detail all their observations, but we would like to stress that, from this team's observations regarding the two administration routes attempted, intraparenchymal was the one shown to have better engraftment. Still, it should be stressed that, at 2 months of age, there was high variability in the pathophysiology results in both ICV and intraparenchymal approaches. Importantly, however, the follow-up results after long-term transplantation of the corrected NSCs into *Naglu*$^{-/-}$ mice were much more conclusive. The evaluation of the long-term effect was performed after 9 months following transplantation via the intraparenchymal administration route. In general, NAGLU activity was detected in the majority of engrafted animals. Furthermore, all pathological hallmarks evaluated were more pronounced in non-transplanted *Naglu*$^{-/-}$ mice. In grafted *Naglu*$^{-/-}$ mice, however, CD68 and GFAP levels were significantly lower in some regions of the brain. A similar pattern was observed after LAMP-1 staining, which correlated with a significant decrease in storage material. Furthermore, transplanted mice displayed a reduction in astrocyte activation, accompanied by a complete prevention of microglial activation not only within the area of engrafted cells but also on its neighboring regions. Quite remarkably, beneficial effects were observed along the rostrocaudal axis of the brain. Altogether, this study provided evidence that the transplantation of genetically corrected iPSC-derived NSCs, may indeed represent a potential treatment for MPS IIIB, and this is particularly relevant since no approved therapeutic approach exists for this neurological MPS [75,76].

The latest ex vivo gene therapy experience to be performed in MPS models is extremely recent. It was published in 2022 [76] and took advantage of results for MPS IIIB we just reviewed [75]. In fact, the same team, which originally published the proof of principle on the potential of ex vivo corrected NSCs to positively impact the brain neuropathology in *Naglu*$^{-/-}$ mice, later extended that study by using a modified Naglu enzyme with the fusion protein IFGII (named NAGLU-IGFII) for the ex vivo correction of the NSCs. This modified/chimeric enzyme, had already been described to allow a greater cellular uptake via IGFII binding sites on the M6PR. Again, the overall process of NSC generation was performed, as well as lentiviral transduction of the *NAGLU-IGFII* sequence. Having confirmed that the modified NAGLU-IGFII enzyme could also be secreted and taken up, just like the unmodified enzyme they had previously reported [75], the authors moved on to in vivo studies. Briefly, they engrafted modified cells into the brain of newborn mice and evaluated the long-term therapeutic effect of that approach, 9 months post-transplantation. First, they confirmed the remaining capability of engrafted NSCs to generate different subtypes of CNS-associated cells through positive staining of several markers: NeuN and MAP2 for neurons; GFAP for astrocytes; and O4 for oligodendrocytes. Once more, the success of the engraftment could be better since there was a high variability in the enzyme

activity between sections of the brain in different animals. However, the range of enzyme activity was increased by 10%, compared to *Naglu*$^{-/-}$ mice, which could be promising since it is reported that sometimes only an increase of 1–5% is sufficient for a proper enzyme activity correction. In the case of pathophysiological events, glial activation and storage accumulation, measured, respectively, through the staining of CD68/GFAP and LAMP-1, revealed a pattern similar to that of wild-type animals. Both effects were more pronounced closer to injection sites [76]. Furthermore, the authors also assessed a parameter which had not yet been looked at in previous studies: the downregulation of MAP2. MAP2 is now known to have a relevant/significant role in the microtubule stabilization of dendritic processes. Its downregulation is heavily associated with dementia in Alzheimer's disease. Dementia is also a primary symptom in MPS IIIB and, remarkably, when *Naglu*$^{-/-}$ mice were stained for MAP2, the results showed that MAP2 was reduced when compared to wild type. Nine months post-transplantation this downregulation was actually reversed, with treated animals presenting MAP2 levels similar to those observed in *Naglu*$^{+/-}$ mice. Moreover, the accumulation of aggregates of synaptophysin, which is a known indicator of axonal damage in inflammatory conditions, was higher in *Naglu*$^{-/-}$ mice than in wild-type and engrafted animals [76].

Overall, even though the efficacy of this therapeutic approach must be improved to reach all brain sections and counteract the Sanfilippo-associated neuroimmune response throughout the whole brain, truth is that, once more, this team has gathered evidence on the possibility of ex vivo gene therapy, with remarkable ameliorated MPS IIIB phenotypic aspects. Moreover, this was the first report documenting a significant reduction in the neuronal marker MAP2 and accumulation of synaptophysin-positive aggregates, both well-known to be related to neuropathophysiology [76].

Then again, even MPSs, which already benefit from the existent ERTs, may ultimately benefit from this sort of approach. Therefore, ex vivo gene therapy experiments have also been performed in MPS I. In fact, in 2019, Miki et al. [77] generated iPSCs from *Idua*$^{-/-}$ mouse embryonic fibroblasts. Then, the authors performed the ex vivo correction of those cells using CRISPR/Cas9 technology and verified that the resulting levels of enzyme activity were significantly restored with values comparable to the wild-type iPSCs. While exploratory and not yet attempted in vivo, these results further validate the overall potential of iPSCs and iPSC-derived cells for gene therapy in MPSs.

Table 1 summarizes works performed in MPSs using iPSC technology.

Table 1. A summary of the works performed in Mucopolysaccharidoses (MPSs) to date using induced pluripotent stem cell (iPSC) technology.

Disorder	Affected Gene	Defective Enzyme	Stored Substrate	Subtype	Generation of MPS-Derived iPSCs				Drug Screening	Ex Vivo Gene Therapy
					Source	iPSC	NPC	Mature Neurons		
MPS I	*IDUA*	α-L-iduronidase	DS and HS	Hurler	Fibroblasts	[58,65,66]	[65,66]			
					Mouse embryonic fibroblasts	[77]				[77]
				Hurler/Scheie	Fibroblasts	[65]	[65]			
				Scheie	Fibroblasts	[59]				
					PBMCs	[65]	[65]			
MPS II	*IDS*	Iduronate-2-sulfatase	DS and HS		Fibroblasts	[63,72]	[63,72]		[72]	
					PBMCs	[54–56,73,78]	[64,73]	[64,73]	[73]	
MPS III	*SGSH*	Sulfamidase	HS	A	Fibroblasts	[51]				
	NAGLU	α-N-acetylgluc-osaminidase		B	Fibroblasts	[45,50,60,68]	[45,60,68]	[68]	[68]	
					Mouse embryonic fibroblasts	[75,76]	[75,76]			[75,76]
	HGSNAT	N-acetyltransferase		C	Fibroblasts	[53,61]	[61,62]	[61,62]	[61,62]	
MPS VII	*GUSB*	β-Glucuronidase	DS, HS, and CS		Mouse embryonic fibroblasts	[74]	[74]			[74]

4. A Hypothetical Alternative Approach to Model Mucopolysaccharidoses

Regardless of their ultimate purpose, the rationale followed in virtually all the studies reviewed so far is the same: first, differentiated cells from patients with the target disease are reprogrammed into iPSCs and, then, differentiated again but into disease-relevant cell lines, thus creating a viable cell model for neuronopathic MPS. This technology, as described above, is undoubtedly contributing to increase the knowledge on the pathophysiology of MPSs with neurological involvement and, consequently, with no treatment available. Nevertheless, while iPSC technology proves to be quite valuable and promising, it also involves some disadvantages. Those positive and negative considerations are recapitulated in Figure 2.

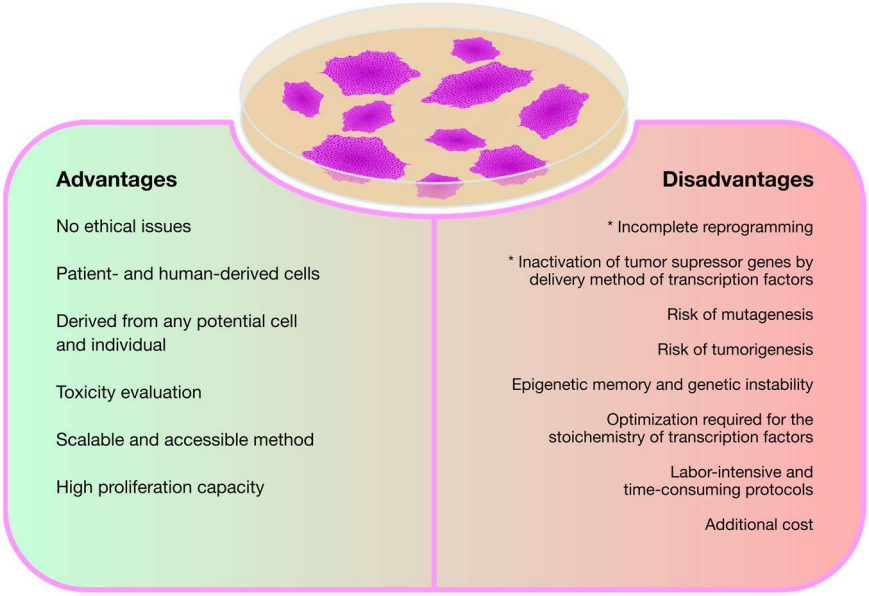


Figure 2. Advantages and limitations of iPSCs. Even though extensively reported in the literature, the issues marked with (*) have been largely solved thanks to the most recent technical improvements of the iPSC generation protocols.

That is why alternative protocols and additional sources of SCs should also be considered, especially those which are naturally-occurring (Figure 3).

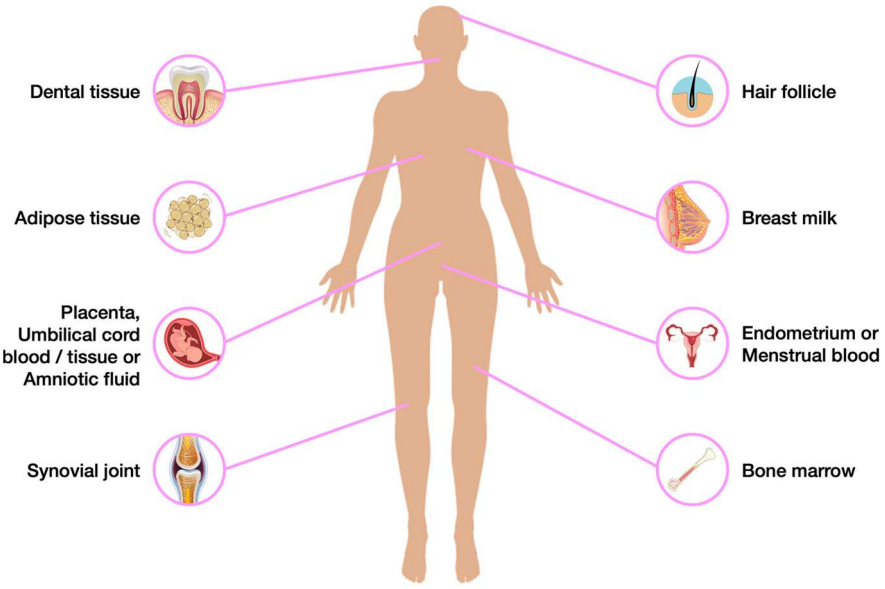


Figure 3. Different sources of mesenchymal stem cells (MSCs).

An excellent option would be to take advantage of patients' MSCs, reducing the possibility of errors and avoiding the long, laborious, and expensive pluripotency induction phase. In fact, those cells represent a suitable alternative since they can be differentiated into any of the three germ layers: endodermal, mesodermal, and ectodermal, as long as they are cultured in proper media. To be considered an MSC, the cell needs to fulfill a number of criteria (Figure 4).

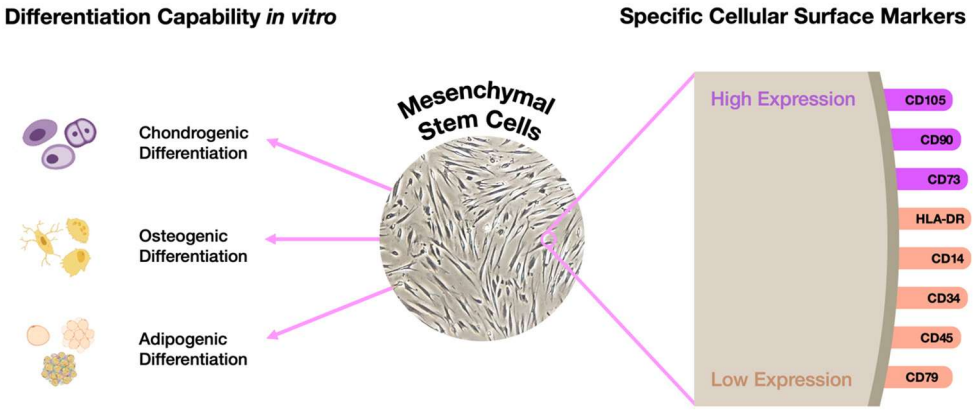


Figure 4. Minimal requirements for identification of mesenchymal stem cells (MSCs).

Bone marrow mesenchymal stem cells (BMMSCs) are the most often used ones. However, the patients' wellness remains an essential issue, due to invasive procedures [79,80].

An interesting study [81] in 2000 introduced a possible new source of SC to the world: the dental pulp. The dental pulp is an oral non-mineralized tissue with various cell types, localized in the central pulp cavity, and mostly comprises soft tissue with nervous/vascular lymphatic elements [82]. Inside it, we may find the so-called dental pulp stem cells (DPSCs). Those cells have an ectodermal origin derived from neural crest cells [83], more specifically from peripheral nerve-associated glia [84]. In that original study [81], those recently discovered SCs were compared to BMMSCs, and the evidence the authors gathered showed that those DPSCs exhibit a higher proliferation rate when compared to BMMSCs, while expressing the same pluripotency markers. Thus, this pivotal study became a launching pad for the subsequent exploration of these cells. The impossibility of generating adipocytes in the original study was the only lack in classifying DPSCs as MSCs. However, over the following years, more evidence was gathered proving their stemness. Ultimately, in 2002, the same group that originally assessed their MSC features, was actually able to promote the adipogenic differentiation of those cells, using a more specific induction medium. They also confirmed that human DPSCs are capable of self- renewal after an in vivo transplant [85].

After a few years of constant research, a terminology was established that is still used today, which allows us to distinguish between the different SC populations that reside inside the dental tissue (Figure 5). Indeed, depending on the source of the oral cavity from which they are extracted, five different types of SCs may be distinguished: DPSCs, stem cells from deciduous teeth (SHEDs) [86], stem cells from apical papilla (SCAPs) [87], periodontal ligament stem cells (PDLSCs) [87], and dental follicle stem cells (DFSCs—precursor cells of PDLSCs) [87–89]. Collectively, for their confirmed MSC properties, these cells may be denominated as dental mesenchymal stem cells (DMSCs).

In addition to the different oral cavity source, we can distinguish those SCs by their proliferation rate and potential to differentiate into the several cells. Regarding the proliferation rate, the follicle-derived ones seem to have the highest, closely followed by SHEDs, SCAPs, PSLSCs, and DPSCs [90–97]. In Table 2, we review some experiments performed so far, to identify the best cell type for each kind of differentiation.

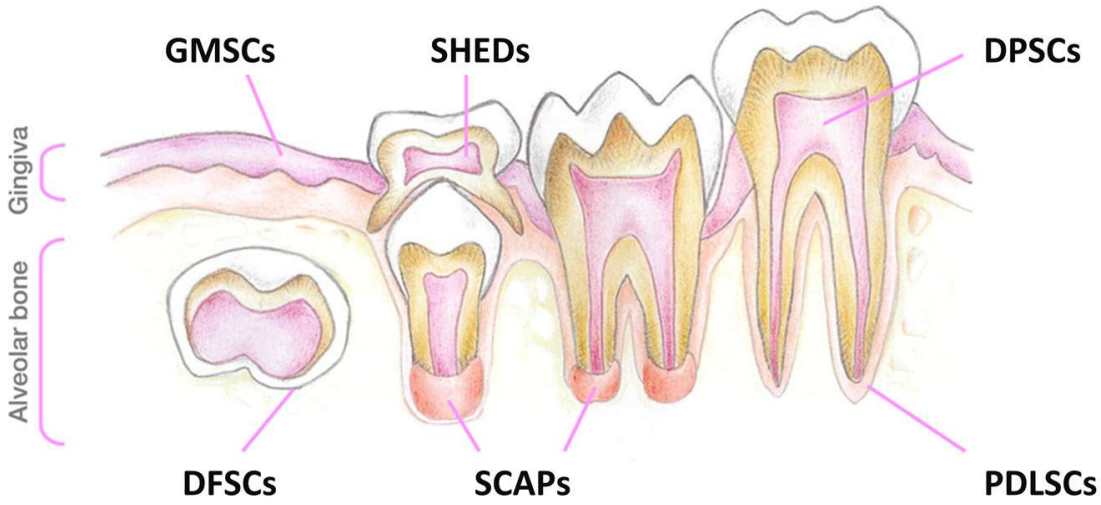


Figure 5. Schematic drawing illustrating the sources of dental mesenchymal stem cells (DMSCs) in the oral cavity. Abbreviations: GMSCs, gingiva-derived MSCs; DFPCs, dental follicle progenitor cells; SHED, stem cells from exfoliated deciduous teeth; SCAPs, stem cells from the apical papilla; DPSCs, dental pulp stem cells; PDLSCs, periodontal ligament stem cells.

We are now in 2023, and the existence of these different SC populations has now been known for over 20 years. So, DPSC and SHEDs in particular, have been generated from pulp for some time. Nevertheless, the majority of the studies involving those cells have focused on their differentiation into chondrocytes for dental repair, with the eventual goal of re-growing teeth from multipotent DMSC [85,98]. Also addressed by a few teams is the potential they hold for stroke therapy. The first study to investigate DPSCs in an animal model of stroke dates back to 2009 and used a mechanical extraction method to obtain cells from human third molars. The cells extracted from those teeth were shown to efficiently express the nuclear receptor related 1 protein, which is essential for the dopaminergic system of the brain, and to promote, when transplanted, functional motor recovery [99]. After this pivotal study was performed, a few others followed, always relying on the use of SCs from different dental pulp sources, and being tested in vivo in rat models of focal cerebral ischemia via the transient occlusion of the middle cerebral artery. While it falls completely out of the scope of this review to summarize all those studies, it is worth mentioning that most of them showed really promising results (reviewed in [100]). Curiously, those cells have been shown to enhance post-stroke functional recovery through a non-neural replacement mechanism, i.e., via DPSC-dependent paracrine effects ([101]; reviewed in [100]). This is probably one of the reasons why these sorts of cells have been addressed for their therapeutic potential in many other disorders, affecting various different organs such as kidney (acute renal injury [102,103] and nephritis [104]); lungs (acute lung injury [105]); brain (Parkinson's disease [106,107], Alzheimer's disease [108], cerebral ischemia [109,110]); spinal cord (spinal cord injury [111–114]); liver (liver fibrosis [115–117]); heart (acute myocardial infarction [118,119]); muscle (muscular dystrophy [120–122]); bone (calvarial defect [104,123–125], and osteoporosis [126]); skin (wound injury [127,128]); pancreas (diabetes [129,130]); eye (glaucoma [131], cornea trauma [132]); and immune system (rheumatoid arthritis [133], autoimmune encephalomyelitis [134], and systemic lupus erythematosus (reviewed in [135,136]).

Table 2. Published results on the multilineage differentiation potential of several DMSC populations.

Type of Differentiation	Dental Stem Cell Population	Confirmation	References
Osteogenic	DPSC, PDLSC, SHED, SCAP, DFSC	Alizarin red staining	[91,97,137–140]
	DPSC, PDLSC, SHED, DFSC, SCAP	ALP activity	[91,137,140]
	DPSC, PDLSC, SHED, DFSC, SCAP	qRT-PCR (*RunX2*, *ALP*, *COL-1*, *OSX*, *OCN*, *OPN*, *SPP1*, *BMP2*)	[91,137,138]
	DPSC, DFSC, SCAP	RT-PCR (*RunX2*, *ON*, *OCN*)	[139]
	DPSC, PDLSC, DFSC	Western blot (RunX2, ALP, OSX, OPN)	[91]
Chondrogenic	DPSC, PDLSC, DFSC, SCAP	Alcian Blue	[91,139]
	DPSC, PDLSC, DFSC	qRT-PCR (*SOX2*, *COL-2*, *ACAN*)	[91]
	DPSC, DFSC, SCAP	RT-PCR (*ACAN*, *COL1α-1*, *COL1α-2*)	[139]
Adipogenic	DPSC, PDLSC, DFSC, SCAP	Oil Red O staining	[91,138–140]
	DPSC, PDLSC, DFSC, SCAP	qRT-PCR (*APN*, *C/EBPα*, *FABP4*, *PPARG*, *LPL*)	[91,138]
	DPSC, DFSC, SCAP	RT-PCR (*ap2*, *PPARG*)	[139]
Neurogenic	DPSC, PDLSC	Giemsa staining	[140]
	DPSC, SHED, DFSC, SCAP	Immunostaining (MAP2, TUBB3, NF-M, NG-F, Thy1)	[138,140]
	DPSC, SHED, DFSC, SCAP	qRT-PCR (*MAP2*, *TUBB3*,*NF-M*, *NF-H*, *GFAP*, *Nestin*	[138,141]
	DPSC, PDLSC	RT-PCR (*DCX*, *NCAM*, *NCAD*, *NROUND1*)	[140]

Osteogenic markers: OPN—osteopontin; OCN—osteocalcin; OSX—osterix; ALP—alkaline phosphatase; COL1A1—collagen 1A1; SPP1—secreted phosphoprotein 1. Chondrogenic markers: COL-2—collagen 2; ACAN—aggrecan. Adipogenic markers: APN—adiponectin; C/EBPα-CCAAT enhancer binding protein alpha; FABP4—fatty acid-binding protein-4; PPARG—peroxisome proliferator-activated receptor gamma; LPL—lipoprotein lipase; ap2—adipocyte protein 2. Neurogenic markers: MAP2—Microtubule-associated protein 2; TUBB3—tubulin beta 3; NF-M—Neurofilament medium-chain; NG-F—nerve growth factor; NF-H—neurofilament heavy chain; GFAP—glial fibrillary acidic protein; DCX—doublecortin; NCAM—neural cell adhesion molecule; NCAD—neural cadherin; NROUND1—neurogenic differentiation 1.

Additionally, if it is true that, for most of these injuries, the evidence gathered so far comes from in vivo studies alone, when it comes to the use of DMSCs in oral diseases, the scenario is significantly different, with two clinical studies on pulp regeneration having been launched within the past several years that have achieved breakthroughs in humans (reviewed in [135]). Overall, the results are so good and the possibilities so vast that soon a commercial interest was found in this type of cells. In fact, due to their easy accessibility and favorable therapeutic applications, cell/tissue banking in the dental field is now a reality in several countries, with some of the most well-known ones being BioEDEN (Austin, TX, USA), Store-a-Tooth (Lexington, KY, USA), Cell Technology (Japan), or the Tooth Bank (Brownsburg, IN, USA) (reviewed in [96,142]). Additionally, as exciting as these results and perspectives may sound per se, we believe that the overall potential of these SCs goes far beyond their properties for tissue repair and regeneration. We think, as other authors have also highlighted before, these cells also hold an exceptional potential for neurogenetic disease cell modeling and basic research. In fact, the neural crest origin of DMSCs makes them an excellent proxy to study NSCs in a lab setting, and a useful source of primary cells for modeling virtually any neurological disorder at the molecular level [143]. Therefore, it will be of utmost value to better characterize different populations of patient-derived DMSCs to understand to what extent these cells will mimic the subcellular phenotype seen in iPSC-derived NSCs, for example, or even in other, more elaborate cell models, such as engineered neuronal and glial cells. Given our interest in LSDs, their monogenic nature, and the extremely high prevalence of severe neurological phenotypes in this group of disorders, we considered DMSCs an excellent model to study these disorders. Additionally, over the past few years, several successful neurodifferentiation protocols have already been described (reviewed in [144]) and the generated cells characterized by several different teams (Table 2). Still, there is clearly room for improvement, both in terms of protocol standardization and of the subsequent characterization of differentiated cell lines. Indeed, there are many differences between the different protocols, some subtle and others more

obvious [145,146]. For example, besides the adherent growth of cells, also non-adherent conditions can be applied for the formation of neurospheres that will further differentiate into neuron-like cells [147,148]. There are even some published comparisons between different neurodifferentiation conditions, but more consistent data and a higher number of studies remain mandatory for more robust conclusions to be drawn. Only then will the modeling potential of DMSCs and their derived counterparts be fully unveiled.

Interestingly, while their modeling potential has never been addressed for LSDs, as advantageous as it may sound, truth is that DPSCs are not totally unknown in the field. In fact, back in 2015, Jackson et al. [149] suggested that human MSCs derived from bone marrow and dental pulp could work as an alternative to the use of hematopoietic stem cells in standard transplantation approaches for the treatment of MPSs. Similarly to what has been discussed in the last section, in which we summarized the studies published so far on MPSs using iPSCs, in this particular publication, it was the therapeutic potential of the MSCs per se, which was analyzed. Actually, none of the MSCs analyzed were derived from MPS patients. Instead, all studies were performed on MSCs obtained from healthy donors. This meant that neither the BMMSCs nor the DPSCs they established had any MPS-related enzymatic defect. Instead, all analyzed cell lines (MSCs and HSCs) were able to produce the different MPS-associated enzymes in the cell layer and secrete low levels of each and every one of them into the surrounding media, the same being true for the used HSCs. However, MSCs were found to produce significantly higher levels of the majority of MPS enzymes assayed when compared to HSCs, a result that can be considered particularly relevant for therapeutic purposes.

However, these authors achieved more than just characterizing the normal levels of MPS-related enzymes secreted by different types of wild type SCs, namely BMMSCs, DPSCs, and HSCs. They also attempted to overexpress, through lentiviral transduction, four different lysosomal enzymes in those same cell lines, to check whether their secretion levels were somewhat similar. Importantly, the evidence they gathered further supported the idea that MSCs had higher secretion and production levels of MPS enzymes when compared to HSCs. Also noteworthy, the lentiviral transduction was more efficient in MSCs compared to HSCs.

Then, the authors moved on to investigate, in vitro, the cross-correction potential of MPS enzymes secreted from those two different sorts of MSCs in MPS patient-derived fibroblasts, and, after confirming the reduction in GAG accumulation, they also verified that this cross-correction was reached in an M6P-dependent way.

Finally, they also addressed the differentiation ability of the MSCs tested, verifying that both transduced and non-transduced cells maintained that capacity, with only slight differences in the neurogenic process, which appeared to have a slower differentiation pattern in transduced MSCs. As expected, however, MSCs derived from dental pulp had a premature upregulation of mature neuronal markers, when compared to those derived from bone marrow.

Altogether, these results provided the in vitro proof of principle of the therapeutic potential of DPSCs and BMSCs as an isolated therapy, or even a combined therapy with the standard HSCTs. To the best of our knowledge, no follow-up studies or in vivo assessments have yet been published on this subject, even though its overall results seem extremely promising.

To the best of our knowledge, MPS patient-derived DPSCs have never been used for differentiation into specific cell types even though they represent a natural source of SCs that may be used to investigate human diseases, especially the infantile forms of these disorders (Figure 6). In fact, taking into account that the most severe forms of MPSs are pediatric, there is one particular population of SCs in the dental pulp that seems particularly suitable to study them: SHEDs. Among their numerous advantages, which include a high proliferation rate and the greater tendency to generate both skeletal and brain cells, SHED collection does not require the active removal of teeth, only their natural fall, and this is certainly an advantage for children who may already be dealing with undue stress and pain.

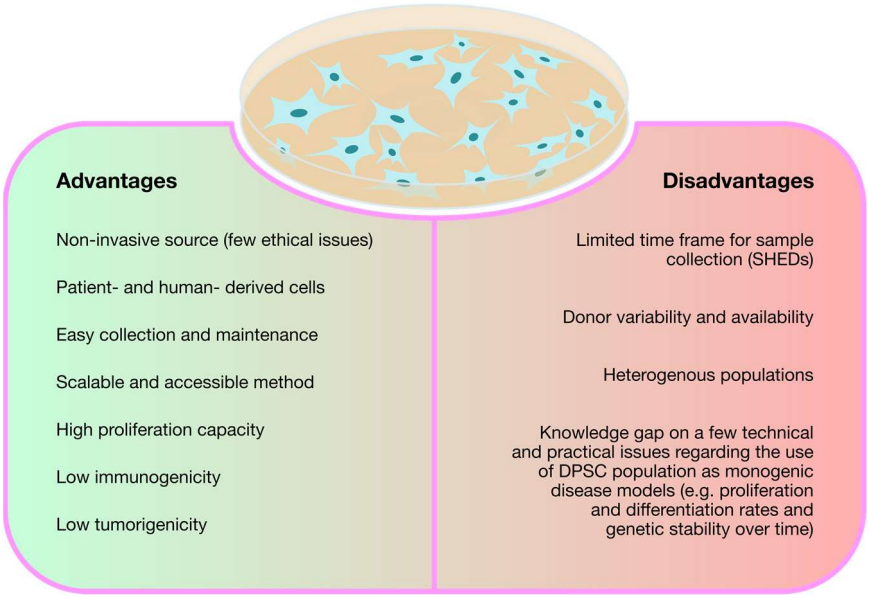


Figure 6. Advantages and limitations of dental pulp stem cells (DPSCs).

It is also worth mentioning, that while this review focuses on the insights one can get on the neuropathology of MPSs by studying iPSCs, and we have only commented on the neuronal differentiation potential of SCs from different sources, such as the DPSC, their differentiation capacity to osteogenic fates is also known and successful protocols have been published. This is quite relevant for MPS disease modeling because some of these diseases present with a marked skeletal phenotype, which fails to be corrected by the currently available therapies. Thus, by implementing the method envisaged here, one may also pave the way for additional applications of DPSCs. For example, we may easily foresee their differentiation into chondrocytes, one of the major components of cartilage and primary site of accumulation in several LSDs.

In general, the higher the number of genotypes we collect, the larger the spectrum of future applications our DPSC-derived LSD neuronal cultures may have not only in our lab but also for other researchers in the field. In addition, with the advances of new gene editing technologies, such as CRISPR/Cas, base editing, prime editing, and the "older" transcription activator-like effector nucleases (TALEN) and zinc finger nucleases (ZFN), the possibility to generate pairs of isogenic lines that facilitate the study of the function of a given gene and the role that different mutations play in the pathophysiological mechanisms of the respective diseases arose. This approach has been increasingly applied to iPSC lines and could also be very useful in the case of our DPSC-derived cell lines. However, the value of these cutting-edge technologies goes far beyond the generation of isogenic cell lines to account for individual variability and allow more precise conclusions regarding gene function or mutation-specific effects in one particular phenotype. They bring along invaluable possibilities, and greatly expand the catalogue of methods which may be used not only for basic but also for translational research. In the specific case of the CRISPR/Cas technology, for example, it has become a relevant platform due to its simple configuration, using advanced algorithms and web-based tools, that allow to analyze its efficiency in recognizing the sequence of interest as well as possible off-targets. Therefore, many advances have been made not only in disease modeling but also in its potential application to gene therapy, namely in combination with stem cells [150]. Recently, Ahumada-Ayala et al. [151] reviewed a number of studies on therapeutic approaches using CRISPR/Cas, namely in hematological, hemato-oncological, cardiovascular, neurological, infectious, and musculoskeletal diseases. Some of these studies show the importance of CRISPR as a promising therapeutic approach, but also show the challenges that still need to be overcome, such as safety concerns arising from toxicity due to the double-strand

breaks, chromosome loss, and genomic instability, the potential for off-targets, as well as bioethical implications. Nevertheless, given the rapid advances in these cutting-edge technologies, there is hope that gene editing platforms such as CRISPR/Cas can be used for correction of genetic mutations and restoration of functional deficiencies, offering a therapeutic alternative for life-threatening diseases.

Still another naturally occurring source of SCs are human urine-derived stem cells (USCs), a type of MSCs with proliferation and multi-potent differentiation potential that can be readily obtained from voided urine using a non-invasive protocol and with minimal ethical restriction. These cells express surface markers of MSCs, but not of hematopoietic stem cells, express the stemness-related genes *Nanog* and *Oct3/4*, and show telomerase activity, not forming teratomas in vivo after being subcutaneously implanted in nude mice [152–155]. When cultured in appropriate media, USCs may differentiate into endothelial, osteogenic, chondrogenic, adipogenic, skeletal myogenic, and neurogenic lineages. Interestingly, USCs may be established from individuals of any age, despite Gao et al. having shown that those isolated from children (5 to 14 years old) show higher proliferation, lower tendency to senescence, and stronger osteogenic capacity than those from middle-aged (30 to 40 years old) and elderly (65 to 75 years old) individuals [154]. This property allows to significantly expand the cohort of patients accessible to be studied. Overall, USCs are yet another alternative source of SCs that can be used as a valuable in vitro model to study genetic diseases, with potential applications in regenerative medicine, cell therapy, diagnostic testing, and drug screening [156].

Finally, it is important to stress that even though in this review we have only focused attention on cell models, the unquestionable role that animal models continue to play in disease modeling cannot be forgotten. Indeed, despite the cellular models here described displaying numerous advantages for both basic and translational research, namely the fact that they cover the genetic diversity needed to fully model human genetic diseases, in vivo models are fundamental not only to explore and interpret the pathophysiology of the disease in the context of the whole organism, but also the cognitive and behavioral aspects. This is particularly important in diseases with marked/severe neuronal involvement such as MPSs. In fact, only animal models allow for a comprehensive analysis of the CNS as a whole, starting with the molecular and cellular examinations all the way up to the macroscopic anatomical and behavioral observations. As reviewed by Megagiannis et al. [157], it is necessary to go through the animal model phase in order to evaluate if a new therapeutic approach is safe and effective at all levels, including in the behavior and in social interaction. In particular, the latest evaluation is impossible to obtain using in vitro models. However, even the type of animal model that will be used for a certain disease must be taken into account, as its pathophysiological pathways may differ from those in humans, especially in the species further down the phylogenetic tree. For example, symptoms related to the complexity of cognitive function and behaviors in humans are difficult to model in rodent species, and therefore their interpretation must be handled with great care and caution [157]. Differences between species may impede the therapeutic translation to humans. In this regard, the use of higher order animal models can be invaluable, and gene editing can also play a key role in this case by generating specific mutants. Choosing the models for their genetic and evolutionary relevancy to humans represents an important step in adequate disease modeling. Therefore, it is the combination of animal models together with relevant cellular models derived from human patients that offer a closer look at human cells that may ultimately serve as a platform both for unraveling the pathophysiological mechanisms underlying the disease and for translating new therapeutic approaches into preclinical testing.

5. Conclusions

Disease models are essential tools to both identify and study the pathological mechanisms that underlie the development of a disease. They are also a pre-requisite for proper drug development. Indeed, it is essential to have a relevant study model, which reproduces

the pathological features of the disease to design and evaluate new therapeutic strategies. This need goes all the way, from the early in vitro assessments to the investigative in vivo pre-clinical studies.

Over the last few decades, amazing advances have been made in the attempt to model the neuropathology of MPSs in vitro, mostly relying on the establishment and subsequent differentiation of disease-specific human iPSCs. This is certainly true for the larger LSD field, where multiple studies have identified neural progenitor cell-migration and differentiation defects, substrate accumulation, axon-growth and myelination defects, impaired calcium homeostasis, and altered electrophysiological properties, all using patient-derived iPSCs (reviewed in [158]). So, not even 20 years after iPSC generation was first described and attempted, their potential to provide mechanistic insights to unravel the pathophysiology associated with neurodevelopment in these rare pathologies is well-established. However, several challenges do remain. That is why we consider it may be useful to contemplate additional sources of patient-derived pluripotent or multipotent cell lines, namely those which are naturally occurring, such as the dental pulp SCs derived from human permanent and deciduous teeth. Those cells may even allow for subsequent differentiation into mixed neuronal and glial cultures, which may be analyzed with virtually the exact same methods many authors perform to address neuropathology in MPS-derived iPSCs. Finally, regardless of the original source of the SCs we are considering, in an era where personalized medicine and mutation-specific therapeutic approaches are gaining momentum, those SC-derived models will also constitute optimal platforms for in vitro drug testing.

Author Contributions: Conceptualization, S.A. and M.F.C.; NCBI Pubmed search, S.C., J.I.S., M.F.C. and S.A.; manuscript structure, S.C., M.F.C. and S.A.; original draft preparation, S.C. and M.F.C.; additional writing: J.I.S., M.G., H.D., L.M. (Luciana Moreira), L.M. (Liliana Matos), M.E. and S.A.; digital figures: H.D. and M.G.; analogue figure: M.F.C.; critical review, S.C., J.I.S., M.G., H.D., L.M. (Luciana Moreira), L.M. (Liliana Matos), M.E., M.F.C. and S.A.; editing, S.C., J.I.S. and M.F.C.; funding acquisition, S.A. and M.F.C. All authors have read and agreed to the published version of the manuscript.

Funding: This work was partially supported by the Portuguese Society for Metabolic Disorders, SPDM (*Bolsa SPDM de apoio à investigação Dr. Aguinaldo Cabral 2018*; 2019DGH1629/SPDM2018I&D), Sanfilippo Children's Foundation (2019DGH1656/SCF2019I&D), and *Fundação para a Ciência e a Tecnologia*, FCT: EXPL/BTM-SAL/0659/2021; UIDB/00211/2020—*Centro de Estudos de Ciência Animal*/Center for the Study of Animal Science; LA/P/0059/2020—*Laboratório Associado para Ciência Animal e Veterinária*/Associate Laboratory for Animal and Veterinary Sciences.

Conflicts of Interest: The authors declare no conflict of interest.

References

1. Scerra, G.; De Pasquale, V.; Scarcella, M.; Caporaso, M.G.; Pavone, L.M.; D'Agostino, M. Lysosomal Positioning Diseases: Beyond Substrate Storage. *Open Biol.* **2022**, *12*, 220155. [CrossRef] [PubMed]
2. Leal, A.F.; Benincore-Flórez, E.; Rintz, E.; Herreño-Pachón, A.M.; Celik, B.; Ago, Y.; Alméciga-Díaz, C.J.; Tomatsu, S. Mucopolysaccharidoses: Cellular Consequences of Glycosaminoglycans Accumulation and Potential Targets. *Int. J. Mol. Sci.* **2023**, *24*, 477. [CrossRef] [PubMed]
3. Sahin, O.; Thompson, H.P.; Goodman, G.W.; Li, J.; Urayama, A. Mucopolysaccharidoses and the Blood–Brain Barrier. *Fluids Barriers CNS* **2022**, *19*, 76. [CrossRef] [PubMed]
4. De Ponti, G.; Donsante, S.; Frigeni, M.; Pievani, A.; Corsi, A.; Bernardo, M.E.; Riminucci, M.; Serafini, M. MPSI Manifestations and Treatment Outcome: Skeletal Focus. *Int. J. Mol. Sci.* **2022**, *23*, 11168. [CrossRef]
5. Clarke, L.A. Mucopolysaccharidosis Type I. Available online: https://www.ncbi.nlm.nih.gov/books/NBK1162/ (accessed on 3 January 2023).
6. Medline Plus. Mucopolysacchaidosis Type I. Available online: https://medlineplus.gov/genetics/condition/mucopolysaccharidosis-type-i/ (accessed on 3 January 2023).
7. Giugliani, R.; Muschol, N.; Keenan, H.A.; Dant, M.; Muenzer, J. Improvement in Time to Treatment, but Not Time to Diagnosis, in Patients with Mucopolysaccharidosis Type I. *Arch. Dis. Child.* **2021**, *106*, 674–679. [CrossRef]
8. NIH. GARD Mucopolysaccharidosis Type I. Available online: https://rarediseases.info.nih.gov/diseases/10335/mucopolysaccharidosis-type-i (accessed on 3 January 2023).

9. Williams, I.M.; Pineda, R.; Neerukonda, V.K.; Stagner, A.M. Mucopolysaccharidosis Type I–Associated Corneal Disease: A Clinicopathologic Study. *Am. J. Ophthalmol.* **2021**, *231*, 39–47. [CrossRef]
10. NORD Mucopolysaccharidosis Type II. Available online: https://rarediseases.org/rare-diseases/mucopolysaccharidosis-type-ii-2/ (accessed on 3 January 2023).
11. Verma, S.; Pantoom, S.; Petters, J.; Pandey, A.K.; Hermann, A.; Lukas, J. A Molecular Genetics View on Mucopolysaccharidosis Type II. *Mutat. Res./Rev. Mutat. Res.* **2021**, *788*, 108392. [CrossRef]
12. Kong, W.; Yao, Y.; Zhang, J.; Lu, C.; Ding, Y.; Meng, Y. Update of Treatment for Mucopolysaccharidosis Type III (Sanfilippo Syndrome). *Eur. J. Pharmacol.* **2020**, *888*, 173562. [CrossRef]
13. Valstar, M.J.; Ruijter, G.J.G.; van Diggelen, O.P.; Poorthuis, B.J.; Wijburg, F.A. Sanfilippo Syndrome: A Mini-Review. *J. Inherit. Metab. Dis.* **2008**, *31*, 240–252. [CrossRef]
14. Bodamer, O.A.; Giugliani, R.; Wood, T. The Laboratory Diagnosis of Mucopolysaccharidosis III (Sanfilippo Syndrome): A Changing Landscape. *Mol. Genet. Metab.* **2014**, *113*, 34–41. [CrossRef]
15. NORD. Mucopolysaccharidosis Type III. Available online: https://rarediseases.org/rare-diseases/mucopolysaccharidosis-type-iii/ (accessed on 3 January 2023).
16. Köhn, A.F.; Grigull, L.; du Moulin, M.; Kabisch, S.; Ammer, L.; Rudolph, C.; Muschol, N.M. Hematopoietic Stem Cell Transplantation in Mucopolysaccharidosis Type IIIA: A Case Description and Comparison with a Genotype-Matched Control Group. *Mol. Genet. Metab. Rep.* **2020**, *23*, 100578. [CrossRef] [PubMed]
17. Hoogerbrugge, P.M.; Brouwer, O.F.; Bordigoni, P.; Cornu, G.; Kapaun, P.; Ortega, J.J.; O'Meara, A.; Souillet, G.; Frappaz, D.; Blanche, S.; et al. Allogeneic Bone Marrow Transplantation for Lysosomal Storage Diseases. *Lancet* **1995**, *345*, 1398–1402. [CrossRef] [PubMed]
18. Shapiro, E.G.; Lockman, L.A.; Balthazor, M.; Krivit, W. Neuropsychological Outcomes of Several Storage Diseases with and without Bone Marrow Transplantation. *J. Inherit. Metab. Dis.* **1995**, *18*, 413–429. [CrossRef] [PubMed]
19. Sivakumur, P.; Wraith, J.E. Bone Marrow Transplantation in Mucopolysaccharidosis Type IIIA: A Comparison of an Early Treated Patient with His Untreated Sibling. *J. Inherit. Metab. Dis.* **1999**, *22*, 849–850. [CrossRef]
20. Sato, Y.; Okuyama, T. Novel Enzyme Replacement Therapies for Neuropathic Mucopolysaccharidoses. *Int. J. Mol. Sci.* **2020**, *21*, 400. [CrossRef]
21. Beard, H.; Chidlow, G.; Neumann, D.; Nazri, N.; Douglass, M.; Trim, P.J.; Snel, M.F.; Casson, R.J.; Hemsley, K.M. Is the Eye a Window to the Brain in Sanfilippo Syndrome? *Acta Neuropathol. Commun.* **2020**, *8*, 194. [CrossRef]
22. Belur, L.R.; Romero, M.; Lee, J.; Podetz-Pedersen, K.M.; Nan, Z.; Riedl, M.S.; Vulchanova, L.; Kitto, K.F.; Fairbanks, C.A.; Kozarsky, K.F.; et al. Comparative Effectiveness of Intracerebroventricular, Intrathecal, and Intranasal Routes of AAV9 Vector Administration for Genetic Therapy of Neurologic Disease in Murine Mucopolysaccharidosis Type I. *Front. Mol. Neurosci.* **2021**, *14*, 618360. [CrossRef]
23. Grover, A.; Crippen-Harmon, D.; Nave, L.; Vincelette, J.; Wait, J.C.M.; Melton, A.C.; Lawrence, R.; Brown, J.R.; Webster, K.A.; Yip, B.K.; et al. Translational Studies of Intravenous and Intracerebroventricular Routes of Administration for CNS Cellular Biodistribution for BMN 250, an Enzyme Replacement Therapy for the Treatment of Sanfilippo Type B. *Drug Deliv. Transl. Res.* **2020**, *10*, 425–439. [CrossRef]
24. Christensen, C.L.; Ashmead, R.E.; Choy, F.Y.M. Cell and Gene Therapies for Mucopolysaccharidoses: Base Editing and Therapeutic Delivery to the CNS. *Diseases* **2019**, *7*, 47. [CrossRef]
25. Politei, J.; Schenone, A.B.; Guelbert, N.; Fainboim, A.; Szlago, M. Morquio Disease (Mucopolysaccharidosis Type IV-A): Clinical Aspects, Diagnosis and New Treatment with Enzyme Replacement Therapy. *Arch. Argent. Pediatr.* **2015**, *113*, 359–364.
26. NORD. Mucopolysaccharidosis Type IV. Available online: https://rarediseases.org/rare-diseases/morquio-syndrome/ (accessed on 3 January 2023).
27. HGMD. Available online: https://www.hgmd.cf.ac.uk/ac/index.php (accessed on 3 January 2023).
28. NORD. Maroteaux Lamy Syndrome. Available online: https://rarediseases.org/rare-diseases/maroteaux-lamy-syndrome/ (accessed on 3 January 2023).
29. Valayannopoulos, V.; Nicely, H.; Harmatz, P.; Turbeville, S. Mucopolysaccharidosis VI. *Orphanet J. Rare Dis.* **2010**, *5*, 5. [CrossRef] [PubMed]
30. Tomanin, R.; Karageorgos, L.; Zanetti, A.; Al-Sayed, M.; Bailey, M.; Miller, N.; Sakuraba, H.; Hopwood, J.J. Mucopolysaccharidosis Type VI (MPS VI) and Molecular Analysis: Review and Classification of Published Variants in the ARSB Gene. *Hum. Mutat.* **2018**, *39*, 1788–1802. [CrossRef] [PubMed]
31. Harmatz, P.R.; Shediac, R. Mucopolysaccharidosis VI: Pathophysiology, Diagnosis and Treatment. *Front. Biosci.-Landmark* **2017**, *22*, 385–406. [CrossRef] [PubMed]
32. Josahkian, J.A.; Trapp, F.B.; Burin, M.G.; Michelin-Tirelli, K.; de Magalhães, A.P.P.S.; Sebastião, F.M.; Bender, F.; De Mari, J.F.; Brusius-Facchin, A.C.; Leistner-Segal, S.; et al. Updated Birth Prevalence and Relative Frequency of Mucopolysaccharidoses across Brazilian Regions. *Genet. Mol. Biol.* **2021**, *44*, 1–6. [CrossRef] [PubMed]
33. Poup, H.; Ledvinová, J.; Berná, L.; Dvo, L.; Ko, V.; Elleder, M. The Birth Prevalence of Lysosomal Storage Disorders in the Czech Republic: Comparison with Data in Different Populations. *J. Soc. Stud. Inborn Errors Metab.* **2010**, *33*, 387–396.
34. Federhen, A.; Pasqualim, G.; de Freitas, T.F.; Gonzalez, E.A.; Trapp, F.; Matte, U.; Giugliani, R. Estimated Birth Prevalence of Mucopolysaccharidoses in Brazil. *Am. J. Med. Genet. Part A* **2020**, *182*, 469–483. [CrossRef]

35. Khan, S.A.; Peracha, H.; Ballhausen, D.; Wiesbauer, A.; Rohrbach, M.; Gautschi, M.; Mason, R.W.; Giugliani, R.; Suzuki, Y.; Orii, K.E.; et al. Epidemiology of Mucopolysaccharidoses. *Mol. Genet. Metab.* **2017**, *121*, 227–240. [CrossRef]
36. Applegarth, D.A.; Toone, J.R.; Brian Lowry, R. Incidence of Inborn Errors of Metabolism in British Columbia, 1969-1996. *Pediatrics* **2000**, *105*, 109. [CrossRef]
37. Celik, B.; Tomatsu, S.C.; Tomatsu, S.; Khan, S.A. Epidemiology of Mucopolysaccharidoses Update. *Diagnostics* **2021**, *11*, 273. [CrossRef]
38. Montaño, A.M.; Lock-Hock, N.; Steiner, R.D.; Graham, B.H.; Szlago, M.; Greenstein, R.; Pineda, M.; Gonzalez-Meneses, A.; çoker, M.; Bartholomew, D.; et al. Clinical Course of Sly Syndrome (Mucopolysaccharidosis Type VII). *J. Med. Genet.* **2016**, *53*, 403–418. [CrossRef]
39. Tomatsu, S.; Montano, A.M.; Dung, V.C.; Grubb, J.H.; Sly, W.S. Mutations and Polymorphisms in GUSB Gene in Mucopolysaccharidosis VII (Sly Syndrome). *Hum. Mutat.* **2009**, *30*, 511–519. [CrossRef] [PubMed]
40. NORD. Mucopolysaccharidosis Type VII. Available online: https://rarediseases.org/rare-diseases/sly-syndrome/ (accessed on 3 January 2023).
41. Of, A.; Report, C. Clinical and Biochemical Manifestations of Hyaluronidase Deficiency. *N. Engl. J. Med. Fig.* **1996**, *335*, 1029–1033.
42. MPS Society. MPS IX. Available online: https://www.mpssociety.org.uk/mps-ix (accessed on 3 January 2023).
43. Takahashi, K.; Tanabe, K.; Ohnuki, M.; Narita, M.; Ichisaka, T.; Tomoda, K.; Yamanaka, S. Induction of Pluripotent Stem Cells from Adult Human Fibroblasts by Defined Factors. *Cell* **2007**, *131*, 861–872. [CrossRef] [PubMed]
44. Malik, N.; Rao, M.S. A Review of the Methods for Human IPSC Derivation. *Methods Mol. Biol.* **2013**, *997*, 23–33.
45. Lemonnier, T.; Blanchard, S.; Toli, D.; Roy, E.; Bigou, S.; Froissart, R.; Rouvet, I.; Vitry, S.; Heard, J.M.; Bohl, D. Modeling Neuronal Defects Associated with a Lysosomal Disorder Using Patient-Derived Induced Pluripotent Stem Cells. *Hum. Mol. Genet.* **2011**, *20*, 3653–3666. [CrossRef]
46. Liu, G.; David, B.T.; Trawczynski, M.; Fessler, R.G. Advances in Pluripotent Stem Cells: History, Mechanisms, Technologies, and Applications. *Stem Cell Rev. Rep.* **2020**, *16*, 3–32. [CrossRef]
47. Hong, S.G.; Dunbar, C.E.; Winkler, T. Assessing the Risks of Genotoxicity in the Therapeutic Development of Induced Pluripotent Stem Cells. *Mol. Ther.* **2013**, *21*, 272–281. [CrossRef]
48. Doss, M.X.; Sachinidis, A. Current Challenges of iPSC-Based Disease Modeling and Therapeutic Implications. *Cells* **2019**, *8*, 403. [CrossRef]
49. Brouwer, M.; Zhou, H.; Nadif Kasri, N. Choices for Induction of Pluripotency: Recent Developments in Human Induced Pluripotent Stem Cell Reprogramming Strategies. *Stem Cell Rev. Rep.* **2016**, *12*, 54–72. [CrossRef]
50. Vallejo-Diez, S.; Fleischer, A.; Martín-Fernández, J.M.; Sánchez-Gilabert, A.; Bachiller, D. Generation of Two Induced Pluripotent Stem Cells Lines from a Mucopolysaccharidosis IIIB (MPSIIIB) Patient. *Stem Cell Res.* **2018**, *33*, 180–184. [CrossRef]
51. Vallejo, S.; Fleischer, A.; Martín, J.M.; Sánchez, A.; Palomino, E.; Bachiller, D. Generation of Two Induced Pluripotent Stem Cells Lines from Mucopolysaccharidosis IIIA Patient: IMEDEAi004-A and IMEDEAi004-B. *Stem Cell Res.* **2018**, *32*, 110–114. [CrossRef] [PubMed]
52. Ben Jehuda, R.; Shemer, Y.; Binah, O. Genome Editing in Induced Pluripotent Stem Cells Using CRISPR/Cas9. *Stem Cell Rev. Reports* **2018**, *14*, 323–336. [CrossRef] [PubMed]
53. Benetó, N.; Cozar, M.; García-Morant, M.; Creus-Bachiller, E.; Vilageliu, L.; Grinberg, D.; Canals, I. Generation of Two Compound Heterozygous HGSNAT-Mutated Lines from Healthy Induced Pluripotent Stem Cells Using CRISPR/Cas9 to Model Sanfilippo C Syndrome. *Stem Cell Res.* **2019**, *41*, 101616. [CrossRef] [PubMed]
54. Varga, E.; Nemes, C.; Bock, I.; Varga, N.; Fehér, A.; Dinnyés, A.; Kobolák, J. Generation of Mucopolysaccharidosis Type II (MPS II) Human Induced Pluripotent Stem Cell (IPSC) Line from a 1-Year-Old Male with Pathogenic IDS Mutation. *Stem Cell Res.* **2016**, *17*, 482–484. [CrossRef]
55. Varga, E.; Nemes, C.; Bock, I.; Varga, N.; Fehér, A.; Kobolák, J.; Dinnyés, A. Generation of Mucopolysaccharidosis Type II (MPS II) Human Induced Pluripotent Stem Cell (IPSC) Line from a 3-Year-Old Male with Pathogenic IDS Mutation. *Stem Cell Res.* **2016**, *17*, 479–481. [CrossRef]
56. Varga, E.; Nemes, C.; Bock, I.; Varga, N.; Fehér, A.; Kobolák, J.; Dinnyés, A. Generation of Mucopolysaccharidosis Type II (MPS II) Human Induced Pluripotent Stem Cell (IPSC) Line from a 7-Year-Old Male with Pathogenic IDS Mutation. *Stem Cell Res.* **2016**, *17*, 463–465. [CrossRef]
57. Varga, E.; Nemes, C.; Kovács, E.; Bock, I.; Varga, N.; Fehér, A.; Dinnyés, A.; Kobolák, J. Generation of Human Induced Pluripotent Stem Cell (IPSC) Line from an Unaffected Female Carrier of Mucopolysaccharidosis Type II (MPS II) Disorder. *Stem Cell Res.* **2016**, *17*, 514–516. [CrossRef]
58. Lito, S.; Burda, P.; Baumgartner, M.; Sloan-Béna, F.; Táncos, Z.; Kobolák, J.; Dinnyés, A.; Krause, K.H.; Marteyn, A. Generation of Human Induced Pluripotent Stem Cell Line UNIGEi001-A from a 2-Years Old Patient with Mucopolysaccharidosis Type IH Disease. *Stem Cell Res.* **2019**, *41*, 101604. [CrossRef]
59. Suga, M.; Kondo, T.; Imamura, K.; Shibukawa, R.; Okanishi, Y.; Sagara, Y.; Tsukita, K.; Enami, T.; Furujo, M.; Saijo, K.; et al. Generation of a Human Induced Pluripotent Stem Cell Line, BRCi001-A, Derived from a Patient with Mucopolysaccharidosis Type I. *Stem Cell Res.* **2019**, *36*, 101406. [CrossRef]

60. Bruyère, J.; Roy, E.; Ausseil, J.; Lemonnier, T.; Teyre, G.; Bohl, D.; Etienne-Manneville, S.; Lortat-Jacob, H.; Heard, J.M.; Vitry, S. Heparan Sulfate Saccharides Modify Focal Adhesions: Implication in Mucopolysaccharidosis Neuropathophysiology. *J. Mol. Biol.* **2015**, *427*, 775–791. [CrossRef]
61. Canals, I.; Soriano, J.; Orlandi, J.G.; Torrent, R.; Richaud-Patin, Y.; Jiménez-Delgado, S.; Merlin, S.; Follenzi, A.; Consiglio, A.; Vilageliu, L.; et al. Activity and High-Order Effective Connectivity Alterations in Sanfilippo C Patient-Specific Neuronal Networks. *Stem Cell Rep.* **2015**, *5*, 546–557. [CrossRef] [PubMed]
62. Benetó, N.; Cozar, M.; Castilla-Vallmanya, L.; Zetterdahl, O.G.; Sacultanu, M.; Segur-Bailach, E.; García-Morant, M.; Ribes, A.; Ahlenius, H.; Grinberg, D.; et al. Neuronal and Astrocytic Differentiation from Sanfilippo C Syndrome IPSCs for Disease Modeling and Drug Development. *J. Clin. Med.* **2020**, *9*, 644. [CrossRef] [PubMed]
63. Lehmann, R.J.; Jolly, L.A.; Johnson, B.V.; Lord, M.S.; Kim, H.N.; Saville, J.T.; Fuller, M.; Byers, S.; Derrick-Roberts, A.L.K. Impaired Neural Differentiation of MPS IIIA Patient Induced Pluripotent Stem Cell-Derived Neural Progenitor Cells. *Mol. Genet. Metab. Rep.* **2021**, *29*, 100811. [CrossRef] [PubMed]
64. Kobolák, J.; Molnár, K.; Varga, E.; Bock, I.; Jezsó, B.; Téglási, A.; Zhou, S.; Lo Giudice, M.; Hoogeveen-Westerveld, M.; Pijnappel, W.P.; et al. Modelling the Neuropathology of Lysosomal Storage Disorders through Disease-Specific Human Induced Pluripotent Stem Cells. *Exp. Cell Res.* **2019**, *380*, 216–233. [CrossRef]
65. Swaroop, M.; Brooks, M.J.; Gieser, L.; Swaroop, A.; Zheng, W. Patient IPSC-Derived Neural Stem Cells Exhibit Phenotypes in Concordance with the Clinical Severity of Mucopolysaccharidosis I. *Hum. Mol. Genet.* **2018**, *27*, 3612–3626. [CrossRef]
66. Lito, S.; Sidibe, A.; Ilmjarv, S.; Burda, P.; Baumgartner, M.; Wehrle-Haller, B.; Krause, K.H.; Marteyn, A. Induced Pluripotent Stem Cells to Understand Mucopolysaccharidosis. I: Demonstration of a Migration Defect in Neural Precursors. *Cells* **2020**, *9*, 2593. [CrossRef]
67. Canals, I.; Benetó, N.; Cozar, M.; Vilageliu, L.; Grinberg, D. EXTL2 and EXTL3 Inhibition with SiRNAs as a Promising Substrate Reduction Therapy for Sanfilippo C Syndrome. *Sci. Rep.* **2015**, *5*, 13654. [CrossRef]
68. Huang, W.; Cheng, Y.S.; Yang, S.; Swaroop, M.; Xu, M.; Huang, W.; Zheng, W. Disease Modeling for Mucopolysaccharidosis Type IIIB Using Patient Derived Induced Pluripotent Stem Cells. *Exp. Cell Res.* **2021**, *407*, 112785. [CrossRef]
69. Marín, T.; Contreras, P.; Castro, J.F.; Chamorro, D.; Balboa, E.; Bosch-Morató, M.; Muñoz, F.J.; Alvarez, A.R.; Zanlungo, S. Vitamin E Dietary Supplementation Improves Neurological Symptoms and Decreases C-Abl/P73 Activation in Niemann-Pick C Mice. *Nutrients* **2014**, *6*, 3000–3017. [CrossRef]
70. Long, Y.; Xu, M.; Li, R.; Dai, S.; Beers, J.; Chen, G.; Soheilian, F.; Baxa, U.; Wang, M.; Marugan, J.; et al. Induced Pluripotent Stem Cells for Disease Modeling and Evaluation of Therapeutics for Niemann-Pick Disease Type A. *Stem Cells Transl. Med.* **2014**, *5*, 1644–1655. [CrossRef]
71. Cheng, Y.S.; Yang, S.; Hong, J.; Li, R.; Beers, J.; Zou, J.; Huang, W.; Zheng, W. Modeling Cns Involvement in Pompe Disease Using Neural Stem Cells Generated from Patient-Derived Induced Pluripotent Stem Cells. *Cells* **2021**, *10*, 8. [CrossRef]
72. Hong, J.; Cheng, Y.S.; Yang, S.; Swaroop, M.; Xu, M.; Beers, J.; Zou, J.; Huang, W.; Marugan, J.J.; Cai, X.; et al. IPS-Derived Neural Stem Cells for Disease Modeling and Evaluation of Therapeutics for Mucopolysaccharidosis Type II. *Exp. Cell Res.* **2022**, *412*, 113007. [CrossRef] [PubMed]
73. Rybová, J.; Ledvinová, J.; Sikora, J.; Kuchař, L.; Dobrovolný, R. Neural Cells Generated from Human Induced Pluripotent Stem Cells as a Model of CNS Involvement in Mucopolysaccharidosis Type II. *J. Inherit. Metab. Dis.* **2018**, *41*, 221–229. [CrossRef] [PubMed]
74. Griffin, T.A.; Anderson, H.C.; Wolfe, J.H. Ex Vivo Gene Therapy Using Patient IPSC-Derived NSCs Reverses Pathology in the Brain of a Homologous Mouse Model. *Stem Cell Reports* **2015**, *4*, 835–846. [CrossRef] [PubMed]
75. Clarke, D.; Pearse, Y.; Kan, S.H.; Le, S.Q.; Sanghez, V.; Cooper, J.D.; Dickson, P.I.; Iacovino, M. Genetically Corrected IPSC-Derived Neural Stem Cell Grafts Deliver Enzyme Replacement to Affect CNS Disease in Sanfilippo B Mice. *Mol. Ther.-Methods Clin. Dev.* **2018**, *10*, 113–127. [CrossRef]
76. Pearse, Y.; Clarke, D.; Kan, S.; Le, S.Q.; Sanghez, V.; Luzzi, A.; Pham, I.; Nih, L.R.; Cooper, J.D.; Dickson, P.I.; et al. Brain Transplantation of Genetically Corrected Sanfilippo Type B Neural Stem Cells Induces Partial Cross-Correction of the Disease. *Mol. Ther.-Methods Clin. Dev.* **2022**, *27*, 452–463. [CrossRef]
77. Miki, T.; Vazquez, L.; Yanuaria, L.; Lopez, O.; Garcia, I.M.; Ohashi, K.; Rodriguez, N.S. Induced Pluripotent Stem Cell Derivation and Ex Vivo Gene Correction Using a Mucopolysaccharidosis Type 1 Disease Mouse Model. *Stem Cells Int.* **2019**, *2019*, 6978303. [CrossRef]
78. Řeboun, M.; Rybová, J.; Dobrovolný, R.; Včelák, J.; Veselková, T.; Štorkánová, G.; Mušálková, D.; Hřebíček, M.; Ledvinová, J.; Magner, M.; et al. X-Chromosome Inactivation Analysis in Different Cell Types and Induced Pluripotent Stem Cells Elucidates the Disease Mechanism in a Rare Case of Mucopolysaccharidosis Type Ll in a Female. *Folia Biol.* **2016**, *62*, 82–89.
79. Huang, G.T.J.; Gronthos, S.; Shi, S. Critical Reviews in Oral Biology & Medicine: Mesenchymal Stem Cells Derived from Dental Tissues vs. Those from Other Sources: Their Biology and Role in Regenerative Medicine. *J. Dent. Res.* **2009**, *88*, 792–806.
80. Berebichez-Fridman, R.; Montero-Olvera, P.R. Sources and Clinical Applications of Mesenchymal Stem Cells State-of-the-Art Review. *Sultan Qaboos Univ. Med. J.* **2018**, *18*, e264–e277. [CrossRef]
81. Gronthos, S.; Mankani, M.; Brahim, J.; Robey, P.G.; Shi, S. Postnatal Human Dental Pulp Stem Cells (DPSCs) in Vitro and in Vivo. *Proc. Natl. Acad. Sci. USA* **2000**, *97*, 13625–13630. [CrossRef] [PubMed]

82. Nuti, N.; Corallo, C.; Chan, B.M.F.; Ferrari, M.; Gerami-Naini, B. Multipotent Differentiation of Human Dental Pulp Stem Cells: A Literature Review. *Stem Cell Rev. Rep.* **2016**, *12*, 511–523. [CrossRef] [PubMed]
83. Koussoulakou, D.S.; Margaritis, L.H.; Koussoulakos, S.L. A Curriculum Vitae of Teeth: Evolution, Generation, Regeneration. *Int. J. Biol. Sci.* **2009**, *12*, 329–334. [CrossRef] [PubMed]
84. Kaukua, N.; Shahidi, M.K.; Konstantinidou, C.; Dyachuk, V.; Kaucka, M.; Furlan, A.; An, Z.; Wang, L.; Hultman, I.; Ährlund-Richter, L.; et al. Glial Origin of Mesenchymal Stem Cells in a Tooth Model System. *Nature* **2014**, *513*, 551–554. [CrossRef] [PubMed]
85. Gronthos, S.; Brahim, J.; Li, W.; Fisher, L.W.; Cherman, N.; Boyde, A.; Denbesten, P.; Robey, P.G.; Shi, S. Stem Cell Properties of Human Dental Pulp Stem Cells. *J. Dent. Res.* **2002**, *81*, 531–535. [CrossRef]
86. Miura, M.; Gronthos, S.; Zhao, M.; Lu, B.; Fisher, L.W.; Robey, P.G.; Shi, S. SHED: Stem Cells from Human Exfoliated Deciduous Teeth. *Proc. Natl. Acad. Sci. USA* **2003**, *100*, 5807–5812. [CrossRef]
87. Al Madhoun, A.; Sindhu, S.; Haddad, D.; Atari, M.; Ahmad, R.; Al-Mulla, F. Dental Pulp Stem Cells Derived From Adult Human Third Molar Tooth: A Brief Review. *Front. Cell Dev. Biol.* **2021**, *9*, 717624. [CrossRef]
88. Handa, K.; Saito, M.; Yamauchi, M.; Kiyono, T.; Sato, S.; Teranaka, T.; Narayanan, A.S. Cementum Matrix Formation in Vivo by Cultured Dental Follicle Cells. *Bone* **2002**, *31*, 606–611. [CrossRef]
89. Morsczeck, C.; Götz, W.; Schierholz, J.; Zeilhofer, F.; Kühn, U.; Möhl, C.; Sippel, C.; Hoffmann, K.H. Isolation of Precursor Cells (PCs) from Human Dental Follicle of Wisdom Teeth. *Matrix Biol.* **2005**, *24*, 155–165. [CrossRef]
90. Yildirim, S.; Zibandeh, N.; Genc, D.; Ozcan, E.M.; Goker, K.; Akkoc, T. The Comparison of the Immunologic Properties of Stem Cells Isolated from Human Exfoliated Deciduous Teeth, Dental Pulp, and Dental Follicles. *Stem Cells Int.* **2016**, *2016*, 4682875. [CrossRef]
91. Qu, G.; Li, Y.; Chen, L.; Chen, Q.; Zou, D.; Yang, C.; Zhou, Q. Comparison of Osteogenic Differentiation Potential of Human Dental-Derived Stem Cells Isolated from Dental Pulp, Periodontal Ligament, Dental Follicle, and Alveolar Bone. *Stem Cells Int.* **2021**, *2021*, 6631905. [CrossRef] [PubMed]
92. Kunimatsu, R.; Nakajima, K.; Awada, T.; Tsuka, Y.; Abe, T.; Ando, K.; Hiraki, T.; Kimura, A.; Tanimoto, K. Comparative Characterization of Stem Cells from Human Exfoliated Deciduous Teeth, Dental Pulp, and Bone Marrow–Derived Mesenchymal Stem Cells. *Biochem. Biophys. Res. Commun.* **2018**, *501*, 193–198. [CrossRef]
93. Park, J.Y.; Jeon, H.J.; Kim, T.Y.; Lee, K.Y.; Park, K.; Lee, E.S.; Choi, J.M.; Park, C.G.; Jeon, S.H. Comparative Analysis of Mesenchymal Stem Cell Surface Marker Expression for Human Dental Mesenchymal Stem Cells. *Regen. Med.* **2013**, *8*, 453–466. [CrossRef] [PubMed]
94. Guo, L.; Li, J.; Qiao, X.; Yu, M.; Tang, W.; Wang, H.; Guo, W.; Tian, W. Comparison of Odontogenic Differentiation of Human Dental Follicle Cells and Human Dental Papilla Cells. *PLoS ONE* **2013**, *8*, e62332. [CrossRef]
95. Bakopoulou, A.; Leyhausen, G.; Volk, J.; Tsiftsoglou, A.; Garefis, P.; Koidis, P.; Geurtsen, W. Comparative Analysis of in Vitro Osteo/Odontogenic Differentiation Potential of Human Dental Pulp Stem Cells (DPSCs) and Stem Cells from the Apical Papilla (SCAP). *Arch. Oral Biol.* **2011**, *56*, 709–721. [CrossRef] [PubMed]
96. Shi, S.; Miura, M.; Seo, B.M.; Robey, P.G.; Bartold, P.M.; Gronthos, S. The Efficacy of Mesenchymal Stem Cells to Regenerate and Repair Dental Structures. *Orthod. Craniofacial Res.* **2005**, *8*, 191–199. [CrossRef]
97. Eleuterio, E.; Trubiani, O.; Sulpizio, M.; Di Giuseppe, F.; Pierdomenico, L.; Marchisio, M.; Giancola, R.; Giammaria, G.; Miscia, S.; Caputi, S.; et al. Proteome of Human Stem Cells from Periodontal Ligament and Dental Pulp. *PLoS ONE* **2013**, *8*, e71101. [CrossRef]
98. Bueno, D.F.; Sunaga, D.Y.; Kobayashi, G.S.; Aguena, M.; Raposo-Amaral, C.E.; Masotti, C.; Cruz, L.A.; Pearson, P.L.; Passos-Bueno, M.R. Human Stem Cell Cultures from Cleft Lip/Palate Patients Show Enrichment of Transcripts Involved in Extracellular Matrix Modeling By Comparison to Controls. *Stem Cell Rev. Rep.* **2011**, *7*, 446–457. [CrossRef]
99. Yang, K.L.; Chen, M.F.; Liao, C.H.; Pang, C.Y.; Lin, P.Y. A Simple and Efficient Method for Generating Nurr1-Positive Neuronal Stem Cells from Human Wisdom Teeth (TNSC) and the Potential of TNSC for Stroke Therapy. *Cytotherapy* **2009**, *11*, 606–617. [CrossRef]
100. Gancheva, M.R.; Kremer, K.L.; Gronthos, S.; Koblar, S.A. Using Dental Pulp Stem Cells for Stroke Therapy. *Front. Neurol.* **2019**, *10*, 422. [CrossRef]
101. Leong, W.K.; Henshall, T.L.; Arthur, A.; Kremer, K.L.; Lewis, M.D.; Helps, S.C.; Field, J.; Hamilton-Bruce, M.A.; Warming, S.; Manavis, J.; et al. Human Adult Dental Pulp Stem Cells Enhance Poststroke Functional Recovery Through Non-Neural Replacement Mechanisms. *Stem Cells Transl. Med.* **2012**, *1*, 177–187. [CrossRef] [PubMed]
102. Hattori, Y.; Kim, H.; Tsuboi, N.; Yamamoto, A.; Akiyama, S.; Shi, Y.; Katsuno, T.; Kosugi, T.; Ueda, M.; Matsuo, S.; et al. Therapeutic Potential of Stem Cells from Human Exfoliated Deciduous Teeth in Models of Acute Kidney Injury. *PLoS ONE* **2015**, *10*, e0140121.
103. Barros, M.A.; Martins, J.F.P.; Maria, D.A.; Wenceslau, C.V.; De Souza, D.M.; Kerkis, A.; Câmara, N.O.S.; Balieiro, J.C.C.; Kerkis, I. Immature Dental Pulp Stem Cells Showed Renotropic and Pericyte-Like Properties in Acute Renal Failure in Rats. *Cell Med.* **2015**, *7*, 95–108. [CrossRef] [PubMed]
104. Ma, L.; Makino, Y.; Yamaza, H.; Akiyama, K.; Hoshino, Y.; Song, G.; Kukita, T.; Nonaka, K.; Shi, S.; Yamaza, T. Cryopreserved Dental Pulp Tissues of Exfoliated Deciduous Teeth Is a Feasible Stem Cell Resource for Regenerative Medicine. *PLoS ONE* **2012**, *7*, e51777. [CrossRef]

105. Wakayama, H.; Hashimoto, N.; Matsushita, Y.; Matsubara, K.; Yamamoto, N.; Hasegawa, Y.; Ueda, M.; Yamamoto, A. Factors Secreted from Dental Pulp Stem Cells Show Multifaceted Benefits for Treating Acute Lung Injury in Mice. *Cytotherapy* **2015**, *17*, 1119–1129. [CrossRef]
106. Fujii, H.; Matsubara, K.; Sakai, K.; Ito, M.; Ohno, K.; Ueda, M.; Yamamoto, A. Dopaminergic Differentiation of Stem Cells from Human Deciduous Teeth and Their Therapeutic Benefits for Parkinsonian Rats. *Brain Res.* **2015**, *1613*, 59–72. [CrossRef]
107. Simon, C.; Gan, Q.F.; Kathivaloo, P.; Mohamad, N.A.; Dhamodharan, J.; Krishnan, A.; Sengodan, B.; Palanimuthu, V.R.; Marimuthu, K.; Rajandas, H.; et al. Deciduous DPSCs Ameliorate MPTP-Mediated Neurotoxicity, Sensorimotor Coordination and Olfactory Function in Parkinsonian Mice. *Int. J. Mol. Sci.* **2019**, *20*, 568. [CrossRef]
108. Mita, T.; Furukawa-Hibi, Y.; Takeuchi, H.; Hattori, H.; Yamada, K.; Hibi, H.; Ueda, M.; Yamamoto, A. Conditioned Medium from the Stem Cells of Human Dental Pulp Improves Cognitive Function in a Mouse Model of Alzheimer's Disease. *Behav. Brain Res.* **2015**, *293*, 189–197. [CrossRef]
109. Inoue, T.; Sugiyama, M.; Hattori, H.; Wakita, H.; Wakabayashi, T.; Ueda, M. Stem Cells from Human Exfoliated Deciduous Tooth-Derived Conditioned Medium Enhance Recovery of Focal Cerebral Ischemia in Rats. *Tissue Eng. Part A* **2013**, *19*, 24–29. [CrossRef]
110. Yamagata, M.; Yamamoto, A.; Kako, E.; Kaneko, N.; Matsubara, K.; Sakai, K.; Sawamoto, K.; Ueda, M. Human Dental Pulp-Derived Stem Cells Protect against Hypoxic-Ischemic Brain Injury in Neonatal Mice. *Stroke* **2013**, *44*, 551–554. [CrossRef]
111. Matsubara, K.; Matsushita, Y.; Sakai, K.; Kano, F.; Kondo, M.; Noda, M.; Hashimoto, N.; Imagama, S.; Ishiguro, N.; Suzumura, A.; et al. Secreted Ectodomain of Sialic Acid-Binding Ig-like Lectin-9 and Monocyte Chemoattractant Protein-1 Promote Recovery after Rat Spinal Cord Injury by Altering Macrophage Polarity. *J. Neurosci.* **2015**, *35*, 2452–2464. [CrossRef] [PubMed]
112. Nicola, F.D.C.; Marques, M.R.; Odorcyk, F.; Arcego, D.M.; Petenuzzo, L.; Aristimunha, D.; Vizuete, A.; Sanches, E.F.; Pereira, D.P.; Maurmann, N.; et al. Neuroprotector Effect of Stem Cells from Human Exfoliated Deciduous Teeth Transplanted after Traumatic Spinal Cord Injury Involves Inhibition of Early Neuronal Apoptosis. *Brain Res.* **2017**, *1663*, 95–105. [CrossRef] [PubMed]
113. Taghipour, Z.; Karbalaie, K.; Kiani, A.; Niapour, A.; Bahramian, H.; Nasr-Esfahani, M.H.; Baharvand, H. Transplantation of Undifferentiated and Induced Human Exfoliated Deciduous Teeth-Derived Stem Cells Promote Functional Recovery of Rat Spinal Cord Contusion Injury Model. *Stem Cells Dev.* **2012**, *21*, 1794–1802. [CrossRef] [PubMed]
114. Yang, C.; Li, X.; Sun, L.; Guo, W.; Tian, W. Potential of Human Dental Stem Cells in Repairing the Complete Transection of Rat Spinal Cord. *J. Neural Eng.* **2017**, *14*, 026005. [CrossRef] [PubMed]
115. Kim, H.J.; Cho, Y.A.; Lee, Y.M.; Lee, S.Y.; Bae, W.J.; Kim, E.C. PIN1 Suppresses the Hepatic Differentiation of Pulp Stem Cells via Wnt3a. *J. Dent. Res.* **2016**, *95*, 1415–1424. [CrossRef]
116. Yamaza, T.; Alatas, F.S.; Yuniartha, R.; Yamaza, H.; Fujiyoshi, J.K.; Yanagi, Y.; Yoshimaru, K.; Hayashida, M.; Matsuura, T.; Aijima, R.; et al. In Vivo Hepatogenic Capacity and Therapeutic Potential of Stem Cells from Human Exfoliated Deciduous Teeth in Liver Fibrosis in Mice. *Stem Cell Res. Ther.* **2015**, *6*, 171. [CrossRef]
117. Hirata, M.; Ishigami, M.; Matsushita, Y.; Ito, T.; Hattori, H.; Hibi, H.; Goto, H.; Ueda, M.; Akihito, Y. Multifaceted Therapeutic Benefits of Factors Derived From Dental Pulp Stem Cells for Mouse Liver Fibrosis. *Stem Cells Transl. Med.* **2016**, *5*, 1416–1424. [CrossRef]
118. Yamaguchi, S.; Shibata, R.; Yamamoto, N.; Nishikawa, M. Dental Pulp-Derived Stem Cell Conditioned Medium Reduces Cardiac Injury Following Ischemia-Reperfusion. *Sci. Rep.* **2015**, *5*, 16295. [CrossRef]
119. Gandia, C.; Arminan, A.; Verdugo, J.M.; Lledó, E.; Ruiz, A.; Minana, M.; Torrijos, J.; Paya, R.; Mirabet, V.; Uberos, F.; et al. Human Dental Pulp Stem Cells Improve Left Ventricular Function, Induce Angiogenesis, and Reduce Infarct Size in Rats with Acute Myocardial Infarction. *Stem Cells* **2008**, *26*, 638–645. [CrossRef]
120. Martínez-Sarrà, E.; Montori, S.; Gil-Recio, C.; Núñez-Toldrà, R.; Costamagna, D.; Rotini, A.; Atari, M.; Luttun, A.; Sampaolesi, M. Human Dental Pulp Pluripotent-like Stem Cells Promote Wound Healing and Muscle Regeneration. *Stem Cell Res. Ther.* **2017**, *8*, 175. [CrossRef]
121. Kerkis, I.; Ambrosio, C.E.; Kerkis, A.; Martins, D.S.; Zucconi, E.; Fonseca, S.A.S.; Cabral, R.M.; Maranduba, C.M.C.; Gaiad, T.P.; Morini, A.C.; et al. Early Transplantation of Human Immature Dental Pulp Stem Cells from Baby Teeth to Golden Retriever Muscular Dystrophy (GRMD) Dogs: Local or Systemic? *J. Transl. Med.* **2008**, *6*, 35. [CrossRef] [PubMed]
122. Pisciotta, A.; Riccio, M.; Carnevale, G.; Lu, A.; De Biasi, S.; Gibellini, L.; La Sala, G.B.; Bruzzesi, G.; Ferrari, A.; Huard, J.; et al. Stem Cells Isolated from Human Dental Pulp and Amniotic Fluid Improve Skeletal Muscle Histopathology in Mdx/SCID Mice. *Stem Cell Res. Ther.* **2015**, *6*, 156. [CrossRef] [PubMed]
123. Feitosa, M.L.; Fadel, L.; Beltrão-Braga, P.C.; Wenceslau, C.V.; Kerkis, I.; Kerkis, A.; Birgel Júnior, E.H.; Martins, J.F.; Martins, D.D.; Miglino, M.A.; et al. Successful Transplant of Mesenchymal Stem Cells in Induced Osteonecrosis of the Ovine. *Acta Cir. Bras.* **2010**, *25*, 416–422. [CrossRef]
124. Novais, A.; Lesieur, J.; Sadoine, J.; Slimani, L.; Baroukh, B.; Saubaméa, B.; Schmitt, A.; Vital, S.; Poliard, A.; Hélary, C.; et al. Priming Dental Pulp Stem Cells from Human Exfoliated Deciduous Teeth with Fibroblast Growth Factor-2 Enhances Mineralization Within Tissue-Engineered Constructs Implanted in Craniofacial Bone Defects. *Stem Cells Transl. Med.* **2019**, *8*, 844–857. [CrossRef]
125. Asutay, F.; Polat, S.; Gül, M.; Subaşi, C.; Kahraman, S.A.; Karaöz, E. The Effects of Dental Pulp Stem Cells on Bone Regeneration in Rat Calvarial Defect Model: Micro-Computed Tomography and Histomorphometric Analysis. *Arch. Oral Biol.* **2015**, *60*, 1729–1735. [CrossRef]

126. Kong, F.; Shi, X.; Xiao, F.; Yang, Y.; Zhang, X.; Wang, L.S.; Wu, C.T.; Wang, H. Transplantation of Hepatocyte Growth Factor-Modified Dental Pulp Stem Cells Prevents Bone Loss in the Early Phase of Ovariectomy-Induced Osteoporosis. *Hum. Gene Ther.* **2018**, *29*, 271–282. [CrossRef]
127. Nishino, Y.; Yamada, Y.; Ebisawa, K.; Nakamura, S.; Okabe, K.; Umemura, E.; Hara, K.; Ueda, M. Stem Cells from Human Exfoliated Deciduous Teeth (SHED) Enhance Wound Healing and the Possibility of Novel Cell Therapy. *Cytotherapy* **2011**, *13*, 598–605. [CrossRef]
128. Nishino, Y.; Ebisawa, K.; Yamada, Y.; Okabe, K.; Kamei, Y.; Ueda, M. Human Deciduous Teeth Dental Pulp Cells with Basic Fibroblast Growth Factor Enhance Wound Healing of Skin Defect. *J. Craniofac. Surg.* **2011**, *22*, 438–442. [CrossRef]
129. Izumoto-Akita, T.; Tsunekawa, S.; Yamamoto, A.; Uenishi, E.; Ishikawa, K.; Ogata, H.; Iida, A.; Ikeniwa, M.; Hosokawa, K.; Niwa, Y.; et al. Secreted Factors from Dental Pulp Stem Cells Improve Glucose Intolerance in Streptozotocin-Induced Diabetic Mice by Increasing Pancreatic β-Cell Function. *BMJ Open Diabetes Res. Care* **2015**, *3*, e000128. [CrossRef]
130. Kanafi, M.M.; Rajeshwari, Y.B.; Gupta, S.; Dadheech, N.; Nair, P.D.; Gupta, P.K.; Bhonde, R.R. Transplantation of Islet-like Cell Clusters Derived from Human Dental Pulp Stem Cells Restores Normoglycemia in Diabetic Mice. *Cytotherapy* **2013**, *15*, 1228–1236. [CrossRef]
131. Mead, B.; Hill, L.J.; Blanch, R.J.; Ward, K.; Logan, A.; Berry, M.; Leadbeater, W.; Scheven, B.A. Mesenchymal Stromal Cell-Mediated Neuroprotection and Functional Preservation of Retinal Ganglion Cells in a Rodent Model of Glaucoma. *Cytotherapy* **2016**, *18*, 487–496. [CrossRef] [PubMed]
132. Syed-Picard, F.; Du, Y.; Lathrop, K.; Mann, M.; Funderburgh, M.; Funderburgh, J. Dental Pulp Stem Cells: A New Cellular Resource for Corneal Stromal Regeneration. *Stem Cells Transl. Med.* **2015**, *4*, 276–285. [CrossRef] [PubMed]
133. Ishikawa, J.; Takahashi, N.; Matsumoto, T.; Yoshioka, Y.; Yamamoto, N.; Nishikawa, M.; Hibi, H.; Ishigro, N.; Ueda, M.; Furukawa, K.; et al. Factors Secreted from Dental Pulp Stem Cells Show Multifaceted Benefits for Treating Experimental Rheumatoid Arthritis. *Bone* **2016**, *83*, 210–219. [CrossRef] [PubMed]
134. Shimojima, C.; Takeuchi, H.; Jin, S.; Parajuli, B.; Hattori, H.; Suzumura, A.; Hibi, H.; Ueda, M.; Yamamoto, A. Conditioned Medium from the Stem Cells of Human Exfoliated Deciduous Teeth Ameliorates Experimental Autoimmune Encephalomyelitis. *J. Immunol.* **2016**, *196*, 4164–4171. [CrossRef]
135. Sui, B.; Wu, D.; Xiang, L.; Fu, Y.; Kou, X.; Shi, S. Dental Pulp Stem Cells: From Discovery to Clinical Application. *J. Endod.* **2020**, *46*, S46–S55. [CrossRef]
136. Shi, X.; Mao, J.; Liu, Y. Pulp Stem Cells Derived from Human Permanent and Deciduous Teeth: Biological Characteristics and Therapeutic Applications. *Stem Cells Transl. Med.* **2020**, *9*, 445–464. [CrossRef]
137. Winning, L.; El Karim, I.A.; Lundy, F.T. A Comparative Analysis of the Osteogenic Potential of Dental Mesenchymal Stem Cells. *Stem Cells Dev.* **2019**, *28*, 1050–1058. [CrossRef]
138. Ullah, I.; Subbarao, R.B.; Kim, E.J.; Bharti, D.; Jang, S.J.; Park, J.S.; Shivakumar, S.B.; Lee, S.L.; Kang, D.; Byun, J.H.; et al. In Vitro Comparative Analysis of Human Dental Stem Cells from a Single Donor and Its Neuronal Differentiation Potential Evaluated by Electrophysiology. *Life Sci.* **2016**, *154*, 39–51. [CrossRef]
139. Patil, R.; Kumar, B.M.; Lee, W.J.; Jeon, R.H.; Jang, S.J.; Lee, Y.M.; Park, B.W.; Byun, J.H.; Ahn, C.S.; Kim, J.W.; et al. Multilineage Potential and Proteomic Profiling of Human Dental Stem Cells Derived from a Single Donor. *Exp. Cell Res.* **2014**, *320*, 92–107. [CrossRef]
140. Wu, T.; Xu, W.; Chen, H.; Li, S.; Dou, R.; Shen, H.; Liu, X.; Liu, X.; Hong, Y.; He, J. Comparison of the Differentiation of Dental Pulp Stem Cells and Periodontal Ligament Stem Cells into Neuron-like Cells and Their Effects on Focal Cerebral Ischemia. *Acta Biochim. Biophys. Sin.* **2020**, *52*, 1016–1029. [CrossRef] [PubMed]
141. Morsczeck, C.; Völlner, F.; Saugspier, M.; Brandl, C.; Reichert, T.E.; Driemel, O.; Schmalz, G. Comparison of Human Dental Follicle Cells (DFCs) and Stem Cells from Human Exfoliated Deciduous Teeth (SHED) after Neural Differentiation in Vitro. *Clin. Oral Investig.* **2010**, *14*, 433–440. [CrossRef] [PubMed]
142. Yoshida, S.; Tomokiyo, A.; Hasegawa, D.; Hamano, S.; Sugii, H.; Maeda, H. Insight into the Role of Dental Pulp Stem Cells in Regenerative Therapy. *Biology* **2020**, *9*, 160. [CrossRef] [PubMed]
143. Victor, A.K.; Reiter, L.T. Dental Pulp Stem Cells for the Study of Neurogenetic Disorders. *Hum. Mol. Genet.* **2017**, *26*, R166–R171. [CrossRef] [PubMed]
144. Sramkó, B.; Földes, A.; Kádár, K.; Varga, G.; Zsembery, Á.; Pircs, K. The Wisdom in Teeth: Neuronal Differentiation of Dental Pulp Cells. *Cell. Reprogram.* **2023**, *25*, 32–44. [CrossRef]
145. Kadar, K.; Kiraly, M.; Porcsalmy, B.; Molnar, B.; Racz, G.Z.; Blazsek, J.; Kallo, K.; Szabo, E.L.; Gera, I.; Gerber, G.; et al. Differentiation Potential of Stem Cells from Human Dental Origin—Promise for Tissue Engineering. *J. Physiol. Pharmacol.* **2009**, *60* (Suppl. 7), 167–175.
146. Al-Maswary, A.A.; O'Reilly, M.; Holmes, A.P.; Walmsley, A.D.; Cooper, P.R.; Scheven, B.A. Exploring the Neurogenic Differentiation of Human Dental Pulp Stem Cells. *PLoS ONE* **2022**, *17*, e0277134. [CrossRef]
147. Gonmanee, T.; Arayapisit, T.; Vongsavan, K.; Phruksaniyom, C.; Sritanaudomchai, H. Optimal Culture Conditions for Neurosphere Formation and Neuronal Differentiation from Human Dental Pulp Stem Cells. *J. Appl. Oral Sci.* **2021**, *29*, 1–11. [CrossRef]
148. Rafiee, F.; Pourteymourfard-Tabrizi, Z.; Mahmoudian-Sani, M.R.; Mehri-Ghahfarrokhi, A.; Soltani, A.; Hashemzadeh-Chaleshtori, M.; Jami, M.S. Differentiation of Dental Pulp Stem Cells into Neuron-like Cells. *Int. J. Neurosci.* **2020**, *130*, 107–116. [CrossRef]

149. Jackson, M.; Derrick Roberts, A.; Martin, E.; Rout-Pitt, N.; Gronthos, S.; Byers, S. Mucopolysaccharidosis Enzyme Production by Bone Marrow and Dental Pulp Derived Human Mesenchymal Stem Cells. *Mol. Genet. Metab.* **2015**, *114*, 584–593. [CrossRef]
150. Mollashahi, B.; Latifi-Navid, H.; Owliaee, I.; Shamdani, S.; Uzan, G.; Jamehdor, S.; Naserian, S. Research and Therapeutic Approaches in Stem Cell Genome Editing by CRISPR Toolkit. *Molecules* **2023**, *28*, 1982. [CrossRef]
151. Ahumada-Ayala, M.; Aguilar-López, R.; González-Stoylov, N.; Palacio-Sosa, E.; Cervantes-Barragán, D.E.; Fernández-Hernández, L. Editing the Human Genome with CRISPR/Cas: A Review of Its Molecular Basis, Current Clinical Applications, and Bioethical Implications. *Rev. Investig. Clin.* **2023**, *75*, 13–28. [CrossRef] [PubMed]
152. Bharadwaj, S.; Liu, G.; Shi, Y.; Wu, R.; Yang, B.; He, T.; Fan, Y.; Lu, X.; Zhou, X.; Liu, H.; et al. Multipotential Differentiation of Human Urine-Derived Stem Cells: Potential for Therapeutic Applications in Urology. *Stem Cells* **2013**, *31*, 1840–1856. [CrossRef] [PubMed]
153. Falzarano, M.S.; D'Amario, D.; Siracusano, A.; Massetti, M.; Amodeo, A.; La Neve, F.; Maroni, C.R.; Mercuri, E.; Osman, H.; Scotton, C.; et al. Duchenne Muscular Dystrophy Myogenic Cells from Urine-Derived Stem Cells Recapitulate the Dystrophin Genotype and Phenotype. *Hum. Gene Ther.* **2016**, *27*, 772–783. [CrossRef]
154. Gao, P.; Han, P.; Jiang, D.; Yang, S.; Cui, Q.; Li, Z. Effects of the Donor Age on Proliferation, Senescence and Osteogenic Capacity of Human Urine-Derived Stem Cells. *Cytotechnology* **2017**, *69*, 751–763. [CrossRef] [PubMed]
155. Falzarano, M.S.; Rossi, R.; Grilli, A.; Fang, M.; Osman, H.; Sabatelli, P.; Antoniel, M.; Lu, Z.; Li, W.; Selvatici, R.; et al. Urine-Derived Stem Cells Express 571 Neuromuscular Disorders Causing Genes, Making Them a Potential in Vitro Model for Rare Genetic Diseases. *Front. Physiol.* **2021**, *12*, 716471. [PubMed]
156. Falzarano, M.S.; Ferlini, A. Urinary Stem Cells as Tools to Study Genetic Disease: Overview of the Literature. *J. Clin. Med.* **2019**, *8*, 627. [CrossRef]
157. Megagiannis, P.; Suresh, R.; Rouleau, G.A.; Zhou, Y. Reversibility and Therapeutic Development for Neurodevelopmental Disorders, Insights from Genetic Animal Models. *Adv. Drug Deliv. Rev.* **2022**, *191*, 114562. [CrossRef] [PubMed]
158. Sabitha, K.R.; Chandran, D.; Shetty, A.K.; Upadhya, D. Delineating the Neuropathology of Lysosomal Storage Diseases Using Patient-Derived Induced Pluripotent Stem Cells. *Stem Cells Dev.* **2022**, *31*, 221–238. [CrossRef]

Disclaimer/Publisher's Note: The statements, opinions and data contained in all publications are solely those of the individual author(s) and contributor(s) and not of MDPI and/or the editor(s). MDPI and/or the editor(s) disclaim responsibility for any injury to people or property resulting from any ideas, methods, instructions or products referred to in the content.

International Journal of
Molecular Sciences

MDPI

Review

Lysosomal Storage Disease-Associated Neuropathy: Targeting Stable Nucleic Acid Lipid Particle (SNALP)-Formulated siRNAs to the Brain as a Therapeutic Approach

Maria Francisca Coutinho [1,2,*], Juliana Inês Santos [1,3], Liliana S. Mendonça [4,5], Liliana Matos [1,2], Maria João Prata [3,6], Amália S. Jurado [7], Maria C. Pedroso de Lima [4] and Sandra Alves [1,2]

1 Research and Development Unit, Department of Human Genetics, National Institute of Health Doutor Ricardo Jorge (INSA I.P), Rua Alexandre Herculano, 321, 4000-055 Porto, Portugal; juliana.santos@insa.min-saude.pt (J.I.S.); liliana.matos@insa.min-saude.pt (L.M.); sandra.alves@insa.min-saude.pt (S.A.)
2 Center for the Study of Animal Science, CECA-ICETA, University of Porto, Praça Gomes Teixeira, Apartado 55142, 4051-401 Porto, Portugal
3 Biology Department, Faculty of Sciences, University of Porto, Rua do Campo Alegre, 4169-007 Porto, Portugal; mprata@ipatimup.pt
4 CNC—Center for Neuroscience and Cell Biology, University of Coimbra, 3004-504 Coimbra, Portugal; liliana.mendonca@cnc.uc.pt (L.S.M.); mdelima@ci.uc.pt (M.C.P.d.L.)
5 CIBB—Center for Innovative Biomedicine and Biotechnology, University of Coimbra, 3004-504 Coimbra, Portugal
6 i3S—Institute of Research and Innovation in Health/IPATIMUP—Institute of Molecular Pathology and Immunology of the University of Porto, Rua Alfredo Allen, 208 4200-135 Porto, Portugal
7 University of Coimbra, CNC—Center for Neuroscience and Cell Biology, Department of Life Sciences, Calçada Martim de Freitas, 3000-456 Coimbra, Portugal; asjurado@ci.uc.pt
* Correspondence: francisca.coutinho@insa.min-saude.pt; Tel.: +351-(223)-401-113

Received: 6 July 2020; Accepted: 6 August 2020; Published: 10 August 2020



Abstract: More than two thirds of Lysosomal Storage Diseases (LSDs) present central nervous system involvement. Nevertheless, only one of the currently approved therapies has an impact on neuropathology. Therefore, alternative approaches are under development, either addressing the underlying enzymatic defect or its downstream consequences. Also under study is the possibility to block substrate accumulation upstream, by promoting a decrease of its synthesis. This concept is known as substrate reduction therapy and may be triggered by several molecules, such as small interfering RNAs (siRNAs). siRNAs promote RNA interference, a naturally occurring sequence-specific post-transcriptional gene-silencing mechanism, and may target virtually any gene of interest, inhibiting its expression. Still, naked siRNAs have limited cellular uptake, low biological stability, and unfavorable pharmacokinetics. Thus, their translation into clinics requires proper delivery methods. One promising platform is a special class of liposomes called stable nucleic acid lipid particles (SNALPs), which are characterized by high cargo encapsulation efficiency and may be engineered to promote targeted delivery to specific receptors. Here, we review the concept of SNALPs, presenting a series of examples on their efficacy as siRNA nanodelivery systems. By doing so, we hope to unveil the therapeutic potential of these nanosystems for targeted brain delivery of siRNAs in LSDs.

Keywords: lysosomal storage diseases (LSDs); neuropathy; substrate reduction therapy (SRT); RNA interference (RNAi); siRNA nanodelivery systems; stable nucleic acid lipid particles (SNALPs)

1. Introduction

When, in 1998, Fire and Mello published their first discovery of double-stranded RNAs, which were able to trigger gene-silencing in *Caenorhabditis elegans*, thus acting as gene function regulators [1], no one realized we were looking at one of the last great advances in cell biology. Shortly thereafter, however, similar observations came from plants [2] and mammals [3,4]. The grounds were thus seeded for the establishment of the concept of RNA interference (RNAi) as a post-transcriptional regulatory mechanism that triggers gene-silencing through the action of small RNA molecules, coined small interfering RNAs (siRNAs). Soon, it became clear that this pathway could be elicited not only by the action of endogenous siRNAs, but also by chemically synthesized (RNA) molecules, exogenously introduced into the cells, as soon as they matched a series of criteria [5] (reviewed in [6]). Since then, RNAi has rapidly become one of the most powerful and widely used tools for the study of gene function, providing researchers with a potent and specific way to promote gene-silencing. However, RNAi's true potential as a gene-silencing tool for therapeutic purposes is still being unveiled. Promisingly, RNAi-induced gene-silencing holds potential to hijack the inhibitory effects of conventional pharmaceuticals, which are mainly achieved by blocking their targets' function. Additionally, it may also target a plethora of disease-related molecules that were previously considered "non-druggable", as for example proteins that do not have enzymatic function, or whose conformation makes them (or their active sites) hardly accessible to conventional drugs [7].

Over recent years, the therapeutic potential of RNAi has been extensively assessed and clinical trials are ongoing for several disorders. Here, we discuss its application in a substrate reduction therapy for a group of genetic disorders characterized by intralysosomal accumulation of undegraded materials, where brain pathology remains a challenge even though some therapeutic approaches are available mainly for systemic pathology. As it happens with many other disorders, translation of one such approach into the clinical setting largely depends on the development of appropriate systems for targeted delivery, which allow for proper biodistribution and promote more favorable pharmacokinetics. Therefore, the development of such systems is of utmost importance. Here, we will review some of the latest advances on different nanotechnological platforms for siRNA delivery, with special focus on the so-called stable nucleic acid lipid particles (SNALPs), one of the most widely used lipidic nanocarriers presently, which combines a high nucleic acid encapsulation efficiency with the capacity of being engineered in order to promote targeting to specific cell surface receptors. Special attention will also be given to the targeting approaches towards the most problematic organ to treat—the brain. By doing so, we hope to unveil the therapeutic potential of these siRNA nanodelivery systems for targeted brain delivery in a series of rare but life-threatening genetic pathologies, which have been our research focus over recent decades, the so-called Lysosomal Storage Diseases (LSDs).

2. Lysosomal Storage Disorders

LSDs are inherited metabolic disorders that affect the biological function of lysosomes. In general, LSDs result from mutations in genes that code for lysosomal enzymes, transport proteins, activator proteins, or other gene products that are necessary for proper lysosomal function. Those mutations lead to substrate accumulation within the cell, which ultimately cause lysosomal enlargement, cellular dysfunction and systemic clinical symptoms (reviewed in [8]). Currently, there are almost 70 known LSDs and, even though the individual disorders are considered rare, their collective incidence may be as high as 1 in every 5000–8000 live births [9,10] (reviewed in [8,11]). These disorders are known for more than a century now, but their underlying pathophysiological mechanisms are yet to be fully understood. Traditionally, LSDs are grouped according to the nature of the primary storage material (reviewed in [12]). This classification relies on the biochemical data collected for early disease diagnosis and, according to it, LSDs are divided into sphingolipidoses, mucopolysaccharidoses (MPSs), glycoproteinoses, neuronal ceroid lipofuscinoses (NCLs) and glycogen storage diseases, among others. Although it has several limitations, this categorization has reached our days and it is still the most informative classification for those disorders resulting from a block of a single enzymatic step in

a particular catabolic pathway. Nevertheless, it failed to accommodate other sorts of LSDs, such as those involving defects in the post-translational processing of lysosomal enzymes (e.g., mucolipidosis types II and/or III [13,14]) or the ones resulting from lysosomal membrane and transport defects (e.g., cystinosis [15]). For these cases, only the elucidation of their molecular basis allowed for a proper understanding and subsequent classification. Thus, the traditional LSDs categorization ended up being refined over the decades, in order to reflect the accumulating molecular knowledge, and accordingly, several diseases have been re-allocated to more appropriate sub-groups. Currently, the accepted classification relies on the molecular defects in the lysosomal system, as well as on the accumulating substrates. One such categorization focuses attention on both function and pathogenetic mechanisms, thus contributing to the development of logical forms of therapy (reviewed in [16]).

In general, LSDs clinical presentation often involves bone, muscle, liver, kidney, and spleen. Adding to lysosomal disease complexity and broad systemic involvement of multiple tissues and organs is the extensive neurological impairment that affects nearly two thirds of the cases. Determining whether lysosomal storage per se is a fundamental cause of neuronal dysfunction remains a challenge, and an important question to be answered. Neurons from different lysosomal diseases have been shown to present significant storage pathology quite early and yet survived for decades before accumulation eventually became cytotoxic. Still, this does not necessarily mean that those neurons remain functionally normal. Both the metabolic compromise and the presence of axonal, dendritic, and synaptic abnormalities, most likely, affect not only neurons, but also the neural networks in which they are involved. As a result, those networks are not optimally functioning even from early time points in the storage process. Eventually, the presence of such malfunctioning neurons is expected to reach a tipping-point at a systemic level, leading to clinical disease even in the absence of obvious neurodegeneration. Such clinical deficits would then be solidified and, most likely, worsened with the eventual death of neurons involved in those neural circuits (reviewed in [12]).

In recent years, biochemical and cell biology studies of LSDs have revealed an ample spectrum of abnormalities in a variety of cellular functions. These include defects in signaling pathways, calcium homeostasis, lipid biosynthesis and degradation and intracellular trafficking [17], but certainly there is still much to be learned on this subject. Interestingly, the more we become elucidated on the pathogenic cascades underlying lysosomal disease, the more intricate becomes the nature of the so-called "greater-lysosomal system" and its crucial role in cell homeostasis [18,19] (reviewed in [12]).

Whatever the mechanistic/physiological cascade triggering pathology, the burden of disease is tremendous, in most cases. LSDs critically affect well-being, life quality, and survival at all ages. Furthermore, even though our knowledge of the molecular and biochemical bases of these disorders has been increasing over the years, for most patients there is still no specific or curative therapy available [20].

The Unmet Need—Defeating Central Nervous System Pathology

Of the about 70 described LSDs, more than two thirds are associated with cognitive or motor deterioration, demonstrating central nervous system (CNS) involvement [11,21,22]. This neurodegeneration may start early in life or not manifest until later, depending on the individual LSD and on the nature and/or extent of the enzymatic deficit. Still, once triggered, the progression of neurodegenerative signs is unrelenting (reviewed in [22]). The typical developmental pattern seen in virtually every "neuronopathic" LSD is one of regression. After a period of apparently uneventful progress, development slows, and peers start to acquire skills at an increasingly faster rate. Eventually, development reaches a plateau and acquired skills are then lost following the common pattern where the most recently acquired skills are lost first and the losses then progress in such a way that eventually the child becomes totally dependent on his/her caregivers (reviewed in [23]). Typically, diagnosis occurs post-symptomatically, when patients begin to show developmental decline after a period of normal development (reviewed in [8]). Some of the most common CNS manifestations include delayed

development, spasticity in movement, hypotonia, macular cherry red spots, and seizures [24,25] (reviewed in [8]).

In general, the symptomatology of the so-called "neuropathic" LSDs is similar and, in the most severe cases, peripheral disease may remain subclinical because CNS deterioration is more progressive and severe than that of peripheral organs (reviewed in [8]). One representative example of this curious pattern is the phenotype of the so-called MPSs. MPSs are LSDs in which the major accumulating substrate is glycosaminoglycans (GAGs; previously known as mucopolysaccharides). This accumulation results from defects in the GAG catabolism. In fact, each MPS disorder is caused by a deficiency in the activity of a single, specific lysosomal enzyme required for GAG degradation (reviewed in [26]). These disorders are biochemically characterized by an accumulation of partially degraded GAGs within the lysosomes, and their subsequent accumulation in urine, blood, and cerebrospinal fluid (CSF) [27–30] (reviewed in [31]). As every other LSD, the MPSs are chronic and progressive syndromes that produce in multiple organ systems a spectrum of signs and symptoms that can differ substantially across different MPSs. In overall presentation, MPS I, II, and VII have many similar clinical features, even though hydrops fetalis is not generally seen in MPS I or II [32–34] (reviewed in [31]). Among patients who present the first symptoms after the neonatal period, the ones who suffer from the severe forms of MPS I, II, and VII have both somatic and cognitive involvement [31]. Still, there is a subtype of MPSs, which is characterized by an extremely severe neurological phenotype, although exhibiting little or no somatic involvement: the MPS III or Sanfilippo syndrome (reviewed in [26,35]). The characteristic feature in MPS III is that of a child who presents with normal development until the age of 12 to 18 months and then fails to develop normal speech. Initially, this is usually thought to be due to middle ear disease and deafness, but even when these problems are mitigated, speech fails to improve. Furthermore, developmental problems tend to increase during that period. Children with this disorder have only mild somatic abnormalities, which may hinder the diagnosis of an MPS disease. Still, once the children develop a challenging behavior that is typical of MPS III, the diagnosis becomes easier for an experienced physician. Such behavior is characterized by severe insomnia and extreme hyperactivity, which makes disease management extremely difficult. As the disease progresses, patients may also develop autistic behavior (reviewed in [35]). Then, skills are lost, and the children become unsteady and fall frequently, tending to develop neurological dysphagia. By their mid-teenage years most affected patients are dependent on their caregivers for all needs, before death occurs towards the end of the second or early in the third decade of life (reviewed in [23,35]).

Another classical example of the large phenotypic spectrum that characterizes LSDs is that of sphingolipidoses. Sphingolipidoses are a group of LSDs characterized by a defective metabolism of sphingolipids, which results in a decrease of the ceramide pool in lysosomes. Some of the most common and well-known LSDs, such as Gaucher disease (GD) or Fabry disease (FD), are sphingolipidoses, but this group includes a large number of other disorders: Metachromatic Leukodystrophy (MLD), Krabbe disease, Niemann Pick disease, GM1 and GM2 gangliosidosis. In sphingolipidoses, lysosomal lipid storage occurs both in the CNS and visceral tissues but CNS pathology is a common hallmark for all of them [11,36]. For GD, a prototype LSD, for example, even though there is a vast heterogeneity of disease manifestations among affected individuals, three major clinical entities/sub-types may be recognized (GD types 1, 2 and 3), with two of them being neuronopathic forms: type 2 GD and type 3 GD [37]. Briefly, type 2 GD is a lethal neuronopathic form, characterized by hypertonic posturing, strabismus, trismus, and retroflexion of the head shortly after birth. Visceral manifestations are also common, with massive hepatosplenomegaly and lung involvement. Type 3 GD is both a more heterogeneous and a more attenuated neuronopathic form, presenting in childhood with the pathognomonic sign of supranuclear horizontal gaze palsy [38].

Many other LSDs and sub-groups of LSDs may be listed that follow this general clinical pattern, where the most severe forms of the disease are the ones presenting CNS involvement, while the milder forms appear to be mostly somatic. Still, in recent years, pathophysiological boundaries have blurred between LSDs and other disorders including late-onset neurodegenerative diseases such as Alzheimer's

and Parkinson's [12]. In fact, it is now well-established that heterozygous and homozygous mutations in *GBA1*, the gene involved in GD, are the highest genetic risk factor for Parkinson's disease (PD). Moreover, a significant percent of PD patients have a mutation in one or more genes that cause a LSD, as recently shown by a whole exome study in PD patients [39,40]. This suggests that lysosomal loss of function is likely involved in PD pathology. It also sheds a different light over the general idea that there is an absence of neurological symptoms in the mildest forms of LSDs.

Finally, we cannot review the LSDs-associated neurological burden without referring to a particular group of LSDs known as NCLs or Batten disease, which are collectively considered to be the most common inherited neurodegenerative disorder of childhood. These are probably the neurological LSDs for excellence, but they may well also be those which remain most elusive. There are currently 13 genes known to cause NCLs. Most have an autosomal recessive inheritance pattern, but autosomal dominant inheritance can be seen in one of the adult-onset forms, CLN4. The mechanism of pathogenesis has been characterized for some disorders. For example, deficiency of the lysosomal enzyme palmitoyl-protein thioesterase 1 in the classic infantile form results in the inability to remove long-chain fatty acids from proteins, which impairs their normal breakdown. For other disorders, the pathogenesis remains unclear [41]. Indeed, even though the molecular basis of NCLs are now established, very little is known about the normal function of the disease-causing gene products. Therefore, it has also been quite a challenge to draw conclusions about how these are compromised by the disease-causing mutations identified so far. The characteristic pathology common to all these disorders is the accumulation of autofluorescence storage material within the lysosome and the widespread death of neurons. At a clinical level NCLs typically involve visual failure, medically refractory epilepsy and relentless declines in motor and cognitive skills, invariably ending in premature death. Each NCL is caused by mutations in a different gene, the so-called CLN genes. The first presentation of disease, which has been reviewed in detail elsewhere [42], varies between the different forms of NCL. Briefly, this tends to be a slowing in development followed by developmental regression in CLN1 disease, seizures in CLN2 disease, and loss of vision in CNL3 disease, just to sum up the most relevant ones. Typically, for individuals presenting early in life, disease progression is faster than that seen in those presenting later. However, there may be periods of plateau preceding subsequent deterioration [43].

Currently, effective treatments have been developed for a small number of LSDs, but the CNS pathology remains practically beyond reach. Up to now, almost all therapeutic approaches have been hindered by an inability to cross the blood-brain barrier (BBB) without invasive administration (intrathecal (IT) or intracerebroventricular (ICV)). Furthermore, even when (or if) the therapeutic molecules enter the brain, it is difficult to ensure therapeutic levels of enzyme distributed evenly throughout the entire parenchyma (reviewed in [8]). This is particularly relevant for enzyme replacement therapy (ERT), which remains the gold standard for LSDs treatment. In reality, no ERT is yet available that can cross the BBB to treat the primary CNS burden in the majority of LSDs (reviewed in [8]). CLN2 was the first and only LSD with an approved therapy directly targeted to the brain; all the other therapies address systemic non-neurological manifestations [44]. Still, even the successful CLN2 brain-targeted ERT is ICV administered, thus circumventing the inability of systemically administered recombinant enzymes to cross the BBB. Considering the previously referred MPS diseases, for example, there is now several available recombinant enzymes for MPS I, II, IVA, VI, and VII somatic manifestations. Also, for the sphingolipidoses subgroup of LSDs, several recombinant enzymes have reached the market with ERTs approved for GD and FD. Still, even when recombinant enzymes are available, there are some adverse events that may be associated with ERT, including infusion-related hypersensitivity reactions that can be characterized by flushing, headache, pyrexia, or urticaria. Furthermore, there is also a significant number of patients who develop IgE anti-drug antibodies [45–50]. In some cases, this leads to life-threatening anaphylactic reactions, which justify the need for ERT to be administered in a facility with appropriate medical support [51]. Therefore, there is still much to be done in order to improve the existing treatments and develop new and more effective therapies, which are able to cope with the neurological burden of these diseases (reviewed in [20]).

For ERT, for example, there are several possibilities being exploited from enzyme modification to ICV injection of the developed formulae. With regard to chemical modification of the lysosomal enzymes, deglycosylation has been the most widely tested as a method of increasing the serum half-life and, consequently, the therapeutic effect of lysosomal enzymes [52] (reviewed in [8]). Another chemical modification, which may be attempted to improve ERT efficacy is the covalent attachment of polyethylene glycol (PEG). PEGylation has also been employed to modify some undesirable properties for enzyme delivery, while allowing for the protein to maintain its activity [53] (reviewed in [8]). In fact, the simple addition of PEG to the therapeutic enzyme may be sufficient to significantly enhance its half-life, while increasing its size and aqueous solubility [54] (reviewed in [8]). There are some first (linear PEG) and second (branched PEG) generation PEGylated molecules already approved for clinical use, but not in the LSDs field. Adagen® and Oncaspar®, are two first-generation PEGylated molecules used in leukemia treatment, while PEGIntron®, a second generation PEGylated drug is currently administered to treat hepatitis C (reviewed in [8]). Still, to the best of our knowledge, this technique has not yet been reported for lysosomal enzymes. The most promising method to expand ERT to neuronopathic LSDs by chemical modification involves the generation of a chimera through the fusion of the therapeutic enzyme with targeting peptides. Fusion of the recombinant enzyme to peptides, which are specifically recognized by cell surface receptors at the BBB endothelium, may actively increase cellular uptake and promote targeted brain delivery. Thus, over the last decade, there has been several teams creating either fusion proteins or conjugates with lysosomal enzymes for brain-driven ERT, although the in vivo success has been quite variable. For MPS diseases, for example, this approach has been extensively evaluated. Recently, Pardridge and co-workers have generated a fusion protein for the treatment of MPS IIIA, by adding a peptide targeting the human insulin receptor to a recombinant sulfamidase (the enzyme deficient in that pathology), which was intravenously (IV) injected into one male Rhesus monkey at a dose of 19 µg/kg. Importantly, 140 min post-injection, high amounts of the fusion protein were found in the total brain homogenate [55] (reviewed in [8]). Interesting results were also reported for MPS I, by another team developing different chimeras for the human alpha-L-iduronidase (IDUA), the enzyme deficient in that disorder [56].

Direct targeting of the CNS through ICV injections of recombinant enzymes is also being exploited. This method of treatment takes advantage of protein transport to the brain through the CSF via strategically placed catheters into the lateral ventricle. Although ICV injection is an established drug administration route for chemotherapy and antibiotics, in use for more than 50 years, it is typically a defined course of treatment administered by slow push bolus. Conversely, ERT is a lifelong treatment, which is anticipated to require ICV infusions administered on a dosing frequency based on the recombinant enzyme's half-life. The chronic nature of one such treatment regimen poses unique challenges in achieving successful drug delivery and safe administration [57]. Still, the need for a treatment, which is indeed effective for the CNS manifestations of LSDs, has prompted several teams to evaluate its potential/feasibility. Thus, this sort of approach was attempted in vivo for several LSDs, including MLD, Sandhoff, CLN2 and MPS IIIB [58–61], suggesting its feasibility, although still being associated with a high risk of infection. For CLN2 in particular, the recombinant form of the enzyme whose activity is impaired in the disorder (recombinant human tripeptidyl peptidase 1, rhTPP1, commercially known as cerliponase alfa-Brineura®) has shown efficacy and tolerability in mouse and canine models of the disease when ICV delivered. Later, assessments of the CNS distribution of the enzyme in healthy cynomolgus monkeys demonstrated that rhTPP1 was able to reach deep brain structures such as the thalamus, midbrain, and striatum. Overall, the results from those studies in healthy animals and CLN2 disease models have helped the design of clinical trials in terms of administration, infusion times, and frequencies, as well as dosages. Soon cerliponase alfa reached clinical trials and its ICV injection lead to significant reductions in the rate of decline of motor and language functions in comparison with a natural history population. Based on the aforementioned clinical trial results, cerliponase alfa is now available in Europe for patients of all ages and in the USA for patients aged 3 years or over. Importantly, the enzyme is infused after antihistamine administration

to reduce hypersensitivity reactions. In general, the procedure has been accepted by patients and families, and as yet, no patients have withdrawn from treatment for efficacy or safety reasons [62]. Still, it should be noticed that there are several risks which are known to be associated with ICV administration including infection, intracerebral hemorrhage, device failure, catheter malpositioning or obstruction, and CSF leakage [57]. Furthermore, both systemic and ICV enzyme delivery require weekly to monthly infusions as a lifelong treatment. Therefore, there is a real need for new and effective therapies to bypass the neurological dysfunction associated with LSDs.

Technology is evolving, though. Although ERT had initially set the trend, and even though many teams are still focused on making the best out of it, several other approaches have started being exploited for LSDs treatment. Some of them were granted orphan drug designations and a few have actually reached the market. Currently, four small molecules have already been approved for the treatment of different LSDs. Their mechanisms of action target the facilitation of subcellular transport [e.g., cysteamine (Cystagon®) for cystinosis] and the reduction of storage (miglustat (Zavesca®) and eliglustat (Cerdelga®), both approved for the treatment of GD). In 2018, the first pharmacological chaperone for an LSD has also reached the market: migalastat (Galafold®), which stabilizes misfolded forms of the enzyme alpha-galactosidase A, got FDA approval for the treatment of adults with confirmed FD and an amenable *GLA* variant [44].

The plethora of innovative ideas on pharmacological approaches is growing at an incredible rate and different mechanisms of action are being exploited from mutation-specific approaches such as stop-codon read-through [63–65] and splicing modulation with antisense oligonucleotides [66–68] to more generic approaches, such as the use of anti-inflammatory or neuroprotective drugs, which address endpoints of the LSDs pathophysiological cascade [69]. Not all these approaches hold potential to address brain pathology, but the neurological dysfunction has not been forgotten. Several strategies are being developed and evaluated. Ex vivo and in vivo gene therapy approaches and a variety of nanoparticle-based systems are currently under investigation in different labs having in view different diseases, and numerous studies have been conducted to optimize the different parameters required for proper treatment of LSDs with CNS involvement. A broad overview of all these investigations and the results of their application fall out of the scope of this review, but they have been extensively dissected elsewhere (see [8]). Also under consideration is a molecular approach based on RNAi to selectively down-regulate genes involved in the biosynthesis of accumulating substrates. This approach has been referred to as genetic substrate reduction therapy (gSRT) and is accumulating evidence on its feasibility in vitro over recent years [70] (reviewed in [71]). In the next section, we will further elaborate on this therapeutic approach and its supporting rationale, which will be grounded in the review of studies highlighting its potential towards clinical application.

3. RNA Interference (RNAi)—An Overview of the Silencing Machinery

The term RNAi was coined to describe a naturally and evolutionarily conserved mechanism of specific post-transcriptional gene-silencing, which can be mediated by different small RNA effector molecules, including endogenous microRNA (miRNA) and exogenous siRNA or short hairpin RNA (shRNA) [72] (reviewed in [7]). The endogenous siRNA pathway starts with the cytoplasmic cleavage of long double-stranded RNA (dsRNA) by an enzyme called Dicer. As a result, the fragments known as siRNAs are produced, which are then incorporated into the multiprotein RNA-induced silencing complex (RISC). At RISC, the sense (passenger) strand of siRNA is cleaved by the catalytic subunit of Argonaute 2 (AGO2), whereas the antisense strand serves to guide the RISC towards the complementary target mRNA sequence that is cleaved by AGO2 generating two mRNA fragments. The activated antisense strand-RISC complex can be recycled and can then move on to destroy additional target mRNA molecules. Ultimately, this process results in reduced gene expression at the levels of the target mRNA and the encoded protein (Figure 1; reviewed in [6,7,73]).

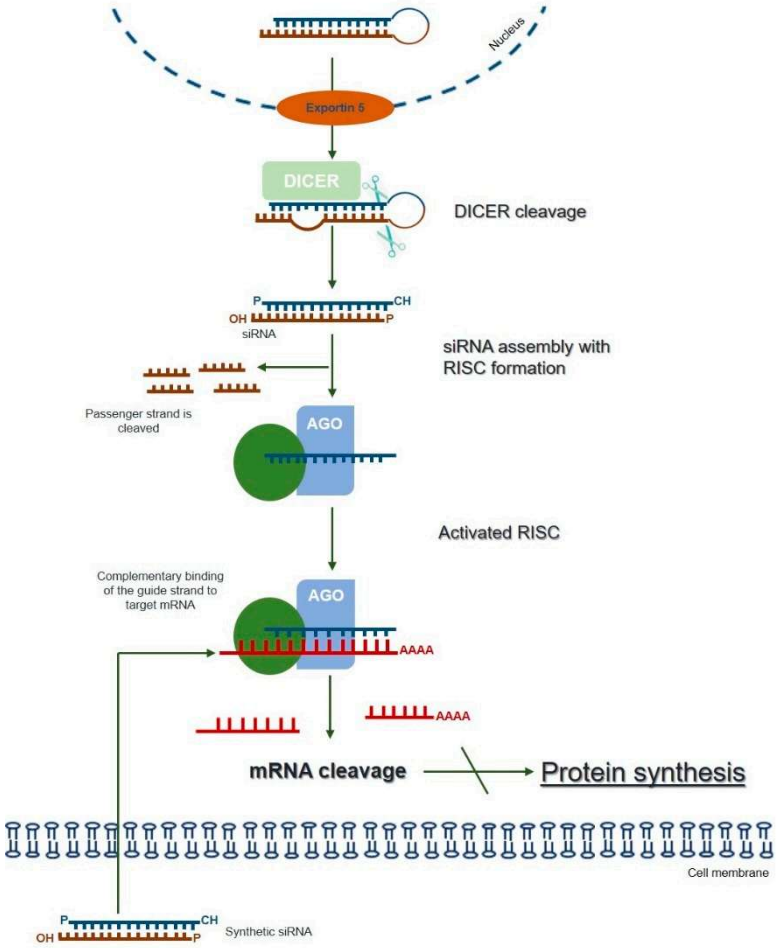


Figure 1. The mechanism of RNA interference (adapted from [7,73]). Long dsRNAs are produced within the nucleus and exported to the cytoplasm through exportin 5. Once they reach the cytoplasm, dsRNAs are cleaved by an enzyme called Dicer. The resulting fragments, consisting of a guide (antisense) strand and a passenger (sense) strand, are called small interfering RNAs (siRNAs). The siRNAs are then incorporated into the RNA-induced silencing complex (RISC), resulting in the cleavage of the sense strand of RNA by Argonaute 2 (AGO2), whereas the antisense strand guides RISC towards the complementary mRNA, which is cleaved into two mRNA fragments leading to the silencing of the target gene. The activated antisense–RISC complex can then be recycled for degradation of additional target mRNA molecules (see text for details). The RNAi-mediated gene-silencing can be triggered by synthetically produced siRNAs directly introduced into the cell, circumventing the Dicer-cleavage step. This shortcut reduces the potential for an innate immune interferon response.

As mentioned above, this powerful gene-silencing process can be induced by exogenous siRNA through direct supply of synthetic siRNAs. Synthetic siRNAs have a well-defined structure mimicking that observed in vivo, which consists of a short (usually 21-bp) dsRNA with phosphorylated 5′ ends and hydroxylated 3′ ends with two overhanging nucleotides [3]. Alternative synthetic molecules do exist, including both shRNAs and miRNAs, which may also be chemically produced and elicit RNAi (reviewed in [7]). Compared to siRNA, an shRNA expression vector is more cost-effective than the bulk manufacturing of siRNA [74] while providing a more durable gene-silencing, as it is constantly synthesized in host cells [7]. On the other hand, endogenous miRNAs require only to be partially complementary to their target mRNAs 3′ untranslated region (3′-UTR), regulating the expression of their targets via all four ago proteins (AGO1-4), unlike the other molecules, which rely on AGO2 alone [75] (reviewed in [7]). Thus, one single miRNA may affect hundreds of different genes [74],

thus exhibiting much more off-target effects than the other two types of molecules. siRNAs are, by far, the most popular RNAi-inducer molecules, with the great majority of studies relying on this sort of dsRNAs to promote targeted gene-silencing. Over the years, a series of empirical and rational guidelines started accumulating from the analysis of hundreds of functional siRNAs, paving the way to the current number of consensual rules one should follow in order to design an effective siRNA molecule [5]. There are also many websites and companies that either offer reliable methods for the design of effective siRNAs or design them on demand, which is understandable because given the small size of siRNAs, their chemical synthesis is not only relatively easy, but also rapid and scalable, so that several companies deliver them in ready-to-transfect format. This is, therefore, a simple, easy-to-handle RNAi-effector for virtually every lab need (reviewed in [6]). Nevertheless, as any other existing strategy, the use of siRNAs has also a series of drawbacks among which are the poor cellular uptake and instability under biological conditions that result in low bioavailability of naked siRNAs. In fact, unmodified siRNAs are quite stable under a variety of conditions in vitro but the same is not observed in vivo (Figure 2). When systemic delivery strategies are used, siRNAs are exposed to nuclease degradation being rapidly cleared from circulation, with consequent accumulation in kidney and fast excretion into urine [76–78]. In addition to circulating nuclease degradation and renal clearance, a major barrier to successful in vivo delivery of siRNAs is the uptake by the reticuloendothelial system (RES), whose physiological function is to clear foreign pathogens and remove cellular debris and apoptotic cells [79] (reviewed in [80]). Despite the phagocytosis role as a significant immunological barrier, not only in the bloodstream, but also in the extracellular matrix of tissues, unfortunately it does not act exclusively against viruses, bacteria, and fungi, being now well known that phagocytes are also highly efficient at removing several therapeutic macromolecules, including siRNAs [73].

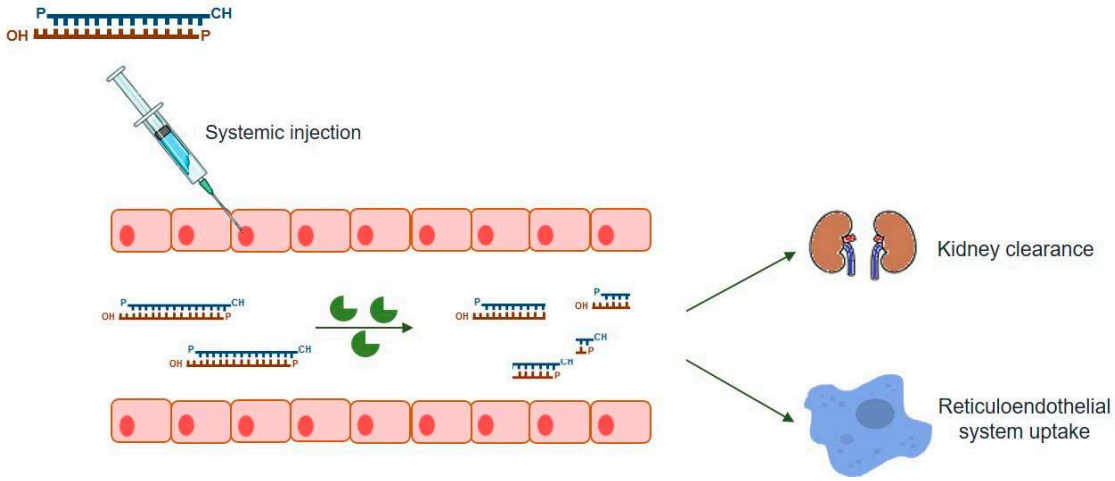


Figure 2. Barriers to the systemic delivery of siRNAs nanoparticles. In vivo, siRNAs systemic delivery faces several barriers, namely: stability in the blood stream; transport across the vascular endothelial barrier; diffusion through the extracellular matrix and endosomal escape. Upon systemic administration, nano-sized carriers might be rapidly cleared from bloodstream by the reticuloendothelial system (RES) and phagocytosed by the mononuclear phagocyte system (e.g., macrophages and liver Kupffer cells). These clearance processes, mediated by the interaction of the nanoparticles with blood components (e.g., immunoglobulins of the complement system), result in higher particle accumulations in RES organs, such as liver and spleen, relative to non-RES organs; therefore, decreasing the amount of nanoparticles that reaches organs such as the brain.

Furthermore, studies developed by different teams have also demonstrated that siRNA molecules are not as safe as initially predicted (reviewed in [80]). Humans have evolved several host-defense mechanisms against dsRNAs, as they are feature of certain viral infections, which may hinder the use of synthetic naked siRNAs in vivo (reviewed in [73]). Evidence exists that high levels of siRNAs may

trigger innate immune response via interaction with RNA-binding proteins such as Toll-like receptors (TLRs) and protein kinase receptor (PKR). Importantly, this process was shown to be both sequence- and length-dependent [81] (reviewed in [7,80]), implying that it can be, if not avoided, significantly reduced if the siRNA design takes this issue into account. It should be stressed that despite the promise of RNAi as a gene-specific process, the truth is that it can sometimes induce undesirable non-specific off-target effects, which raised the need to mitigate it through siRNA redundancy and/or chemical modification [21,82,83] (reviewed in [84]).

Still, the major hindrance in the development of RNAi therapies, as it happens with other approaches relying on nucleic acids, is the specific and efficient delivery of these molecules to their target cells. Since they are negatively charged and relatively large molecules, siRNAs do not readily cross the cell membrane, thus requiring endocytosis as the major route of entry into the cell, unless viral delivery is attempted (reviewed in [7]). The intracellular trafficking of siRNAs via the endocytic route usually begins in early endosomes. Then, those endosomes fuse with sorting endosomes, which in turn transfer their contents into acidified late endosomes (pH ~ 5.0–6.2). Subsequently, the late endosomes fuse with lysosomes that are further acidified (pH ~ 4.5), which contain several nucleases that may easily promote siRNA degradation. Thus, siRNAs that fail to be released from these acidic vesicles will ultimately be degraded [85] (reviewed in [7]). In addition, siRNAs need to escape to the cytosol, where RISC operates, so that they can exert their action, meaning that the endosomal membrane constitutes an important barrier that must be overcome. Owing to this, siRNA delivery strategies that take advantage of endocytosis must provide for endosomal escape (reviewed in [6,7]).

The successful therapeutic application of siRNAs requires the development of clinically suitable, safe, and effective delivery systems, and, therefore, the abovementioned issues should be considered to be key elements towards their rational design. As important as the effective silencing action, is the assurance that siRNAs are specifically delivered to their target cells at the desired concentration (reviewed in [86]).

4. RNAi as a Potential Therapeutic Approach for LSDs

Proof-of-principle on the potential of RNA-degrading technologies as effective tools to achieve significant reduction of the levels of accumulated substrate(s) in LSDs cell lines was first achieved by Diaz-Font et al., after assessing the potential of an artificially induced RNAi mechanism to reduce storage in one of the most common and well-known LSD: GD [87]. GD is a pan-ethnic LSD due to a deficiency in the lysosomal enzyme beta-glucocerebrosidase (GCase), which results in its inability to degrade glucosylceramide adequately. In the early 80s, purification of GCase and the subsequent cloning of the gene that codes for this enzyme (*GBA*) led to the pioneer works of enzyme replacement setting the grounds for ERT [88]. Later, SRT was also evaluated as a management therapy for GD, showing potential to also impact the neurological manifestations of the disorder [89]. Currently, there are two different small molecules approved for GD substrate reduction: miglustat, Zavesca® (an amino sugar; reviewed in [90]) and eliglustat tartrate, Cerdelga® (a longer-chain ceramide mimetic; reviewed in [91]). Still, in 2006, Diaz-Font and co-workers have also evaluated the potential of a siRNA-mediated strategy to promote substrate reduction in GD, thus establishing the concept of gSRT. In that work, the authors designed different siRNAs targeting the human *GCS* gene, transfected them into HeLa cells, having observed a clear reduction of *GCS* mRNA levels. They also confirmed inhibition at the protein level by assessing the enzyme GCS activity. Altogether, the results seemed promising and completely in line with the hypothesis that RNAi would be an effective method for genetic inhibition of GCS [87] (reviewed in [71]). By acting at the post-transcriptional stage of gene expression, siRNAs have a high degree of safety, as they do not interact with DNA, thus avoiding the mutation and teratogenicity risks of other gene therapy approaches, such as those involving plasmid DNA delivery [80]. Furthermore, a siRNA-based approach for SRT could also hold potential to overcome some of the well-known side effects of currently approved SRT drugs.

Importantly, GD is one of the few LSDs with approved formulae for both ERT and SRT, and chaperone therapy is also being tested for GD type 1. Although there are LSDs for which no therapy is yet available, a significant number of these disorders have at least one approved therapy. However, most approved drugs have a series of drawbacks, as reported in the previous section.

The MPSs subgroup of LSDs is among those in debt of either specific therapies (for several diseases that lack treatment approaches), or more efficient ones (for those with approved formulae presenting the above-referred limitations). Fortunately, the major biochemical pathways that give rise to GAGs (the substrates accumulating in this subgroup of diseases) are well known and almost all the involved genes have been cloned. Therefore, it seemed reasonable to design a similar RNAi-based substrate reduction approach for MPSs by targeting for degradation one (or more) of the enzymes responsible for GAGs biosynthesis. The underlying rationale for this idea prompted several investigators to target genes of the biosynthetic pathway that produce the different GAGs that accumulate in MPS diseases. Once again, their objective was to decrease GAGs synthesis by silencing specific genes, so that they would actively reduce substrate accumulation to slow down the pathology. This is particularly relevant as previous attempts to apply SRT for MPS diseases, particularly MPS III, had been focused on the use of non-specific inhibitors of GAG synthesis [92,93].

The first study aimed at impairing GAGs synthesis in MPS cells by using siRNAs was published early in this decade, by Dziedzic and co-workers [94]. This team transfected MPS type IIIA fibroblasts with four siRNAs targeting genes from the initial steps of GAGs' biosynthetic cascade (*XYLT1*, *XYLT2*, *GALTI*, and *GALTII*). By real-time PCR, the authors observed a significant decrease in the mRNA levels of all targeted genes, which was accompanied by a significant reduction of their target protein levels. To further investigate the effects of the induced gene-silencing, the authors measured the incorporation of ^{35}S sulphate in siRNA-transfected cells, to assess de novo synthesized amount of GAGs, having observed a considerable impairment in GAGs synthesis [94]. Later, they examined whether treating patients' fibroblasts with two of those siRNAs together would be more effective than using single siRNAs in terms of GAGs synthesis inhibition. It was found that inhibition of GAGs synthesis in cells treated with two siRNAs was generally more effective than using single siRNAs; nevertheless, the differences were not statistically significant. Thus, the authors concluded that the potential benefit from the use of two siRNAs over the use of a single siRNA would be limited in the light of the cost-benefit ratio and possible stronger side effects of the putative therapy [95] (reviewed in [71]).

By the same time, Kaidonis and co-workers used RNAi technology to inhibit the expression of the *EXTL2* and *EXTL3* genes involved in the synthesis of heparan sulphate (HS), the glycosaminoglycan that accumulates specifically in MPS III [96]. Through a reporter gene assay, these authors showed that shRNAs directed to *EXTL2* significantly reduced endogenous target gene expression, while decreasing HS synthesis and reducing lysosomal storage of this GAG in an MPS IIIA cell line. Similar results were reached for at least one of the shRNAs designed to target *EXTL3*. Of note that this team has also assessed the incorporation of the studied shRNAs into a stable lentiviral expression system, with promising results in a reporter gene assay [96] (reviewed in [71]).

Later, Chmielarz and colleagues compared the effects of different treatment methods on the regulation of GAGs storage in various cell lines established from MPS I, MPS IIIA, and MPS IIIB patients [97]. Taking advantage of the existence of an approved ERT for MPS I, these authors addressed the effect of (i) ERT alone (laronidase; Aldurazyme®), (ii) different "anti-GAG" siRNAs alone, and (iii) the combination of both treatments on the above-referred cell lines. As anticipated, ERT was more effective than the siRNA treatment alone in reducing GAGs storage in all studied cell lines. Surprisingly, however, when a combined treatment was employed (ERT + "anti-GAG" siRNAs), results varied depending on the analyzed cell line(s), among which the combinatory effect of these two therapeutic approaches could be more or less pronounced than that obtained with either method alone. This was a particularly relevant observation, as it demonstrated that the efficacy of a combination of ERT and the use of siRNA depend on specific features of each cell line, thus highlighting that

a combined therapy might potentially result in various effects in different patients [97] (reviewed in [71]).

More recently, Canals and his team [98] have also assessed the potential of four other siRNAs to act as gSRT triggers in MPS. They elected as targets the two genes that Kaidonis and co-workers, five years earlier, were able to inhibit, *EXTL2* and *EXTL3*, which code for two key proteins involved in the chain elongation of HS. However, instead of addressing the effect of gene-silencing in MPS IIIA, as the previous team did, Canals et al. analyzed MPS IIIC, another neurological MPS, in which HS specifically accumulates. After transfecting the siRNAs into fibroblasts from two different MPS IIIC patients, and assessing the effects from day 3 to day 14 after transfection, the authors observed a target mRNA inhibition of around 90%. Additionally, they have examined the downstream effect of that reduction, by quantifying the cell incorporation levels of a ^{35}S sodium sulphate medium. The results were also promising showing that fibroblasts exhibited 30% to 60% decrease in the incorporation of ^{35}S sulphate, 3 days post-transfection. Moreover, patients' fibroblasts showed a significant reduction in HS accumulation, after a 3-day treatment with a siRNA for *EXTL2*, as revealed by an immunocytochemistry assay [98] (reviewed in [71]). Curiously, when the exact same molecules were tested in induced pluripotent stem cells (iPSC)-derived neurons, the same pattern was not seen [99,100]. This recent observation highlights the need for proper cell models for drug testing. In fact, only after an extensive in vitro assessment of the drug's effect, should it be tested in vivo.

Altogether, these findings highlight the feasibility of a gSRT approach for MPS diseases, clearly demonstrating that positive effects on the levels of GAGs accumulation may be achieved whatever the step of the biosynthetic pathway one might target. This is very meaningful as it opens prospects for the use of a single compound to treat a series of pathologies (reviewed in [71]). Ultimately, the same principle may be applied for virtually all LSDs even though there are currently no reports attempting gSRT in other LSDs sub-groups. However, there are many hurdles that still need to be overcome since the therapeutic potential of one such approach depends on a series of factors apart from the efficacy of the siRNA itself. For example, the greater the residual enzymatic activity a patient retains, the greater is the likelihood for the patient to benefit from this approach (reviewed in [101]).

5. RNAi-Based Therapy Challenges

Most siRNA-based drugs currently being tested in clinical trials are directly administered to pathology-bearing regions, to avoid the complexity of systemic delivery. Still, the introduction of systemic routes for siRNA delivery is mandatory for this technology to achieve its full therapeutic potential. That is why many different teams worldwide have been focusing attention on this issue pursuing the development of suitable delivery systems for siRNAs to reach their sites of action. There are several possibilities being evaluated, from chemical modifications of the siRNA structure alone to specific siRNA nanodelivery systems. Whatever the case, an effective delivery system must fulfil a series of criteria, including biocompatibility, biodegradability, and non-immunogenicity, in order to enable multi-administration treatment modalities, which are crucial for improved clinical outcomes (reviewed in [102,103]). An ideal siRNA delivery platform should i) provide protection from blood nucleases and prolonged blood circulation, while avoiding rapid renal and/or hepatic clearance, ii) exhibit high siRNA loading abilities and be internalized by endocytosis, and finally iii), rely in siRNA with an endosome escape ability to reach the cytosol and enter the RNAi machinery, thus activating the RNAi pathway (reviewed in [6,80,104]).

5.1. Some Examples of Small Interfering RNAs (siRNAs) Delivery Systems

Early strategies for solving the dual problems associated with the intracellular delivery of siRNAs and their rapid excretion involved incorporation of siRNAs into lipid nanoparticles (LNPs), which are smaller and more homogeneous analogues of lipoplexes used for laboratory transfection [105–107] (reviewed in [108]). Lipoplexes (and other nanoparticles used for siRNA delivery) accumulate in the liver and other filtering organs, which limits their effectiveness in penetrating other tissues [107,109]

(reviewed in [108]). Moreover, it has been shown that the administration of siRNAs via LNP delivery vehicles results in pro-inflammatory effects, because lipid-based vehicles can become entrapped in endosomes [110], where the TLR will recognize various moieties in dsRNAs, modified siRNAs or even their degradation products [111], eliciting an undesirable innate inflammatory response. Therefore, in most circumstances, the siRNA administration requires pre-treatment regimens, including antihistamines, non-steroidal anti-inflammatories, and even relatively high doses of glucocorticoids [112–114] (reviewed in [115]).

Many efforts were made to develop a class of nanoparticles that could circumvent these limitations. A plethora of polymers such as polyethylenimine (PEI), cyclodextrin, chitosan, dendrimers, and metal cores was used to develop novel and more stable nanoparticles, while ensuring those entities remained biodegradable, biocompatible, and non-toxic (reviewed in [7]). PEI, for example, is a synthetic polymer with extensive branches and dense cationic charge, which facilitates its complexation with siRNAs and protects them from RNAse degradation. This polymer has a high content of protonable amino groups, allowing it to act as a proton sponge to induce the release of siRNAs to the cytoplasm [78] (reviewed in [7]). Given these properties, PEI nanoparticles were initially viewed as promising vectors for siRNA delivery. Nevertheless, some wariness limits the PEI use in vivo, such as the weak electrostatic cohesion between PEI and siRNAs [116] (reviewed in [7]). To overcome this issue, the low molecular weight PEI was combined with other synthetic polymeric constructs such as PEG, and encouragingly the development of PEG-grafted nanocarriers led to significant advances in terms of vector efficiency [117]. The hydrophilic nature of PEG provides an aqueous shield around the nanoparticle surface, decreasing the extent of opsonization and, consequently, the recognition by the RES, thus resulting in an increase of the nanoparticle blood residence time (reviewed in [7,103]). Still, as works with PEG-grafted nanoparticles grew, the limitations involving these particles also started to accumulate. Early reports in clinical setting demonstrated that upon subsequent administrations of PEG-grafted nanocarriers (PEGylated LNPs in particular), an immune response could be elicited, leading to a rapid blood clearance of the nanoparticles, which inexorably compromised their clinical utility [118,119] (reviewed in [103]). It became further known that PEGylation also exerts a negative effect on cellular internalization and endosomal escape, significantly hindering the cellular uptake of LNPs and the escape of their entrapped siRNAs, because it limits the contact between membranes [120,121] (reviewed in [103]). Recently, however, the use of internalizing ligands has also contributed to the emergence of novel lipid-based nanoparticles with remarkable transfection efficacy [103]. Among them is a subclass of lipid-based nanoparticles called SNALPs, one of the most widely used LNPs presently [80].

5.2. Stable Nucleic Acid Lipid Particles (SNALPs)

SNALPs are among the most promising nucleic acid delivery nanosystems for in vivo application and have emerged as one of the leading lipid-based siRNA formulations under clinical development. Typically, SNALPs have a mean size of 100 nm and a neutral charge, comprising, three important components: an ionizable cationic lipid, a neutral helper lipid and a PEG-derivatized lipid (Figure 3). These PEG stabilized LNPs have been originally developed by Tekmira Pharmaceuticals Corporation, currently Arbutus Biopharma (http://www.arbutusbio.com/our-science/lnp-delivery-platform.php) and have been gaining momentum as more and more data on their in vivo efficacy accumulate. The underlying rationale for the development of these particles was to combine the potential of a fusogenic and ionizable cationic lipid, crucial for efficient encapsulation of siRNAs at acidic pH, with that of helper lipids (1,2-distearoyl-sn-glycero-3-phosphocholine (DSPC) and cholesterol), to stabilize the lipid bilayer, and add PEG-derivatized lipids, which would provide an aqueous shield around the nanoparticle surface, thus promoting prolonged blood circulation. Currently used cationic lipids include DODAP, DLinDMA and, more recently, DLin-KC2-DMA, whereas diacylglycerols (DAGs) are the most frequently used PEG-derivatized lipids (reviewed in [103]).

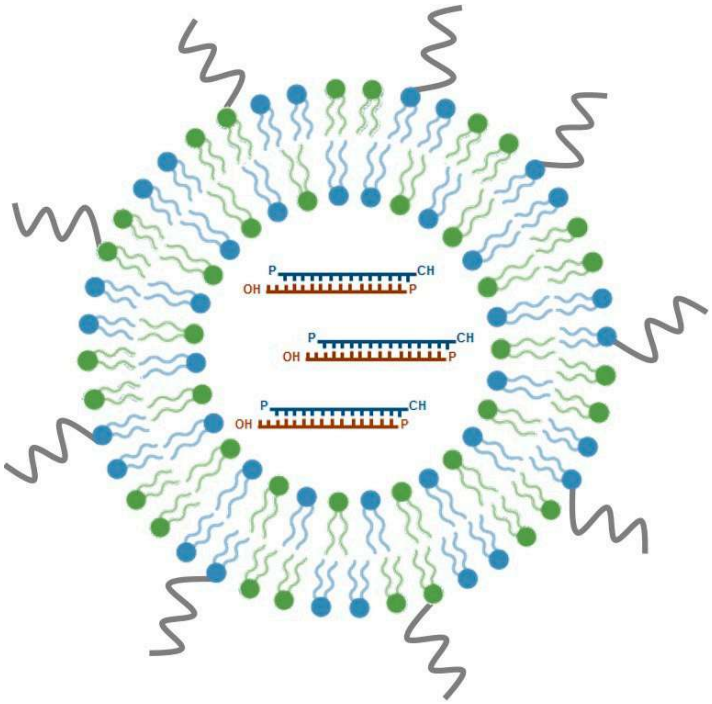


Figure 3. Schematic representation of stable nucleic acid lipid particles (SNALPs). SNALPs are a particular class of lipid nanoparticles (LNPs), which comprise cationic lipids (in blue), non-ionic lipids (in green), and polyethylene glycol (in grey; see text for details). SNALPs are nanoparticles, displaying optimal physico-chemical features for in vivo delivery of therapeutic nucleic acids, such as siRNAs. siRNAs are enclosed in the hydrophilic core of the nanoparticle. These siRNA-lipid particles show considerably enhanced cellular internalization and endosomal escape of siRNA. Several SNALP-formulated siRNA therapeutic molecules have reached clinical trials and are currently being evaluated for efficacy. The most well-known example is Patisiran®, the first FDA-approved siRNA drug.

Over the last 15 years, many data on the efficacy of SNALP-formulated siRNAs for targeted gene-silencing in different models in vivo, were produced. The first study to demonstrate a specific silencing effect of SNALP-formulated siRNAs was performed by Morrissey and co-workers [122], and involved the targeting of the hepatitis B virus (HBV) in an in vivo mouse model of HBV replication. The SNALP-formulated anti-*HBV* siRNAs were administered by IV injection into mice carrying replicating HBV, according to a dose regimen of three daily IV injections of 3 mg/kg/day, and its efficacy was compared to naked siRNAs. A reduction of serum HBV levels by at least one order of magnitude was observed, and, most importantly, this reduction was specific, dose-dependent, and lasted for up to 7 days after administration. Furthermore, the application of SNALP-formulated siRNAs resulted in a clear increase of the half-life in plasma and liver, when compared with naked siRNAs. Although they are unmodified, naked siRNAs were rapidly eliminated from the plasma compartment (elimination/circulation half-life (T1/2) of ~2min), chemically modified siRNAs had a slightly increased half-life (T1/2 ~ 49 min). Whatever the case, the half-life values of naked siRNAs were dramatically different from those observed when the same siRNA was given as a SNALP-formulated drug (T1/2 ~ 6.5 h). Similarly, SNALP-formulated siRNAs exhibited lower toxicity and immunostimulatory side effects than their unformulated counterparts [123] (reviewed in [73,103]).

Shortly thereafter, Zimmermann and colleagues [124] came up with the first report on the efficacy of SNALP-formulated siRNAs systemic delivery in non-rodent species. This team encapsulated siRNAs against apolipoprotein B (ApoB) in SNALPs and administered that formulation by IV injection to cynomolgus monkeys at doses of 1 or 2.5 mg/kg. Apo B is essential for the assembly and secretion of very-low-density lipoprotein (VLDL) and low-density lipoprotein (LDL), which are required for the transport and metabolism of cholesterol. Elevated ApoB and/or LDL levels are long known to

correlate with increased risk of coronary artery disease [125]. To address the therapeutic potential of SNALP-formulated anti-*ApoB* siRNAs, Zimmermann et al. evaluated the pharmacokinetics, efficacy, and safety of that formulation, finding out that a single SNALP-formulated siRNA injection resulted in dose-dependent silencing of ApoB mRNA expression in the liver (where it is predominantly expressed), with maximal silencing of more than 90%. Results were visible as early as 48 h post-administration and persisted for 11 days at the highest administered dose [124]. Interestingly, the silencing effect of SNALP-formulated siRNAs was over 100-fold more potent than that observed for cholesterol-conjugated anti-*ApoB* siRNAs, which the authors had already proven to be efficient for in vivo silencing of ApoB in rodents [124,126]. It was also shown that the degree and persistence of RNAi-mediated silencing in cynomolgus monkeys far exceeded the results obtained with rodents. The authors proposed that the longer duration observed in primates could either relate to species differences in the efficiency and stability of the RISC or to the mitotic state of the hepatocytes analyzed. Finally, treatment efficacy was confirmed by measuring the expected downstream effects of ApoB mRNA reduction: both plasma ApoB-100 protein and serum cholesterol levels decreased. Overall, results were consistent with an immediate, potent, and lasting biological effect of SNALP-formulated anti-ApoB siRNAs, supporting RNAi-based therapeutics as a potential new class of molecular pharmaceutical drugs and further validating SNALPs as efficient siRNA nanodelivery systems [124] (reviewed in [73,103]).

By the same time, the team of Geisbert focused efforts on assessing the potential of RNAi against a lethal Ebola virus (EBOV) challenge, with similar success. The EBOV infection causes a frequently fatal hemorrhagic fever (HF) that is currently refractory to the available antiviral therapeutics. Therefore, RNAi came up as a possible treatment option, as it held potential to specifically target the EBOV genome inhibiting its expression. Proof-of-principle on this was achieved when guinea pigs were treated with four different siRNAs targeting the polymerase (L) gene of the Zaire species of EBOV (ZEBOV), formulated in SNALPs, either before or after lethal ZEBOV challenge. Complete post-exposure protection against a lethal ZEBOV was revealed, both in guinea pigs [127] and Rhesus monkeys [128] injected with SNALP-formulated siRNAs, specifically designed to target different regions of the non-infectious ZEBOV RNA genome. In these two works, the animals were subjected to repeated administration of the SNALP-formulated siRNAs according to different dose regimens: for guinea pigs, the authors used 1 mg/kg per dose on days 1 to 6 after viral infection [127]; for macaques, the authors used 2 mg/kg per dose on days 1, 3, and 5 after challenge with ZEBOV [128]. Complete post-exposure protection against the virus clearly showed that the RNAi-based therapeutic approach employed could hold promise for the treatment of people infected not only with ZEBOV HF but probably also with other emerging viral infections [128] (reviewed in [73,103]).

Another outstanding study, on the efficacy of in vivo silencing promoted by SNALP-formulated siRNAs aimed at confirming the RNAi-mediated mechanism of action of siRNA-based cancer therapeutics in mice was performed by Judge and colleagues. To establish proof that systemically administered siRNAs could elicit RNAi-mediated anticancer efficacy in the absence of significant immune activation the authors selected two cell cycle protein kinases known to be cancer targets with well characterized mechanisms for direct tumor cell killing: kinesin spindle protein (KSP) and polo-like kinase 1 (PLK1) [129]. Previously, it had been shown that inhibition of both KSP and PLK1 rapidly resulted in mitotic arrest and apoptosis induction [130–132], making these two kinases ideal targets for RNAi silencing in tumor cells. In the work of Judge and co-workers, mice bearing established Hep3B orthotopic liver tumors were subjected to IV administration of 2 mg/kg of SNALP-formulated anti-*PLK1* siRNA twice a week for three weeks. An equivalent dose of SNALP-formulated anti-*KSP* siRNA was used in a hepatic Neuro2a tumor mouse model. Both experiments resulted in significant suppression of tumor growth, but not in its complete eradication. Still, it is important to note that this treatment schedule was devoid of immune responses. Since the well-designed methodological approach followed by the authors allowed to discriminate siRNA-mediated specific effects on gene expression from off-target effects, Judge et al. succeed to demonstrate that systemic administration

of SNALP-formulated siRNAs can actually trigger RNA-mediated cleavage of target mRNAs within solid tumors, silencing their expression at a magnitude sufficient to induce mitotic disruption and subsequent apoptosis of tumor cells [129] (reviewed [103]).

The success obtained in these different works prompted additional studies on the use of RNAi as a therapeutic tool, which soon will boost the clinical evaluation of SNALP-formulated siRNAs. From the above-referred formulations, a significant number has moved into clinical trials and its therapeutic potential has been further evaluated, namely for those addressing hypercholesterolemia, Ebola virus infection, and liver cancer (reviewed in [73,103]).

Currently, patisiran (ONPATTRO^{TM}) is the only commercially available siRNA drug formulated into SNALPs. Patisiran is an RNAi therapeutic agent that specifically inhibits hepatic synthesis of transthyretin (TTR) by targeting a genetically conserved sequence in the 3′ untranslated region of mutant and wild-type TTR mRNA. Clinical trials performed in both healthy adult volunteers and patients with hereditary TTR-mediated amyloidosis (hATTR), have shown that patisiran was able to consistently and specifically reduce serum TTR protein levels and tissue TTR protein deposits (known as amyloid), the hallmark of the pathology. Interestingly, the siRNA oligonucleotide molecule that ended up gaining approval for the treatment of hATTR in adults with stage 1 or 2 polyneuropathy was tested in two independent phase I trials, which involved drug encapsulation into two different lipid-based nanocarriers: ALN-TTR01 and ALN-TTR02 (patisiran). ALN-TTR01 was encapsulated in the first-generation version of LNP carriers, while ALN-TTR02 was encapsulated in a SNALP. The results from both trials were published in 2013 in the New England Journal of Medicine [112]. To summarize the published reports, each of the two formulations was studied in a single-dose, placebo-controlled phase I trial. Both formulations showed rapid, dose-dependent, and durable RNAi-mediated reduction in blood TTR levels. Yet, ALN-TTR02 was much more potent than ALN-TTR01, hence being the chosen formulae, which moved on into phases II and III [113,133,134] clinical trials. In all the reported studies, patisiran reduced serum TTR protein levels, regardless of age, race, sex or TTR mutation, and exhibited linear and time-independent pharmacokinetics with multiple-dosing. Most importantly, the drug did show therapeutic effect, significantly improving the pathological manifestations and quality of life of the patients (aged 24 to 83 years) with hATTR neuropathy that participated in the phase III study, as compared with placebo. The most frequent adverse events reported were peripheral edema and infusion-related reactions (reviewed in [135]). Taking together all these positive results, on August 2018, patisiran received its first global approval for the treatment of the polyneuropathy of hATTR in adults in the USA (https://www.drugs.com/history/onpattro.html) and, subsequently, in Europe, becoming the first, and so far the only, approved RNAi therapeutic agent.

Overall, the studies reviewed above aimed at developing efficient methods for siRNA systemic delivery. Yet, for gene-silencing-based drugs such as siRNAs to pave their way into the clinical practice, another important issue to deal with is how to endow the delivery system with targeting capacity.

5.3. Ligand-Mediated SNALP Targeting

The nanotechnological platforms for siRNA delivery have been widely tested in the oncobiology field, with data on the efficacy of different drug delivery systems arriving at a tremendous velocity. RNAi technology has been the gold standard to achieve down-regulation of several overexpressed genes in cancer. In this context, improved targeting specificity and enhanced delivery efficacy have deserved a special attention. Some of the recent studies in this domain explore the application of SNALPs. Although SNALPs can exhibit passive accumulation into tumors, due to their large fenestrated endothelium, which results in an enhanced permeability and retention effect [136] (reviewed in [137,138]), big improvements can be achieved through the covalent attachment of internalizing targeting ligands that will specifically interact with their receptors usually overexpressed on the surface of target cells (Figure 4) [103]. It is understandable that several teams, including our own, have invested on the development of different tumor-targeted SNALPs, by coupling specific moieties to the surface of those PEGylated lipid nanocarriers.

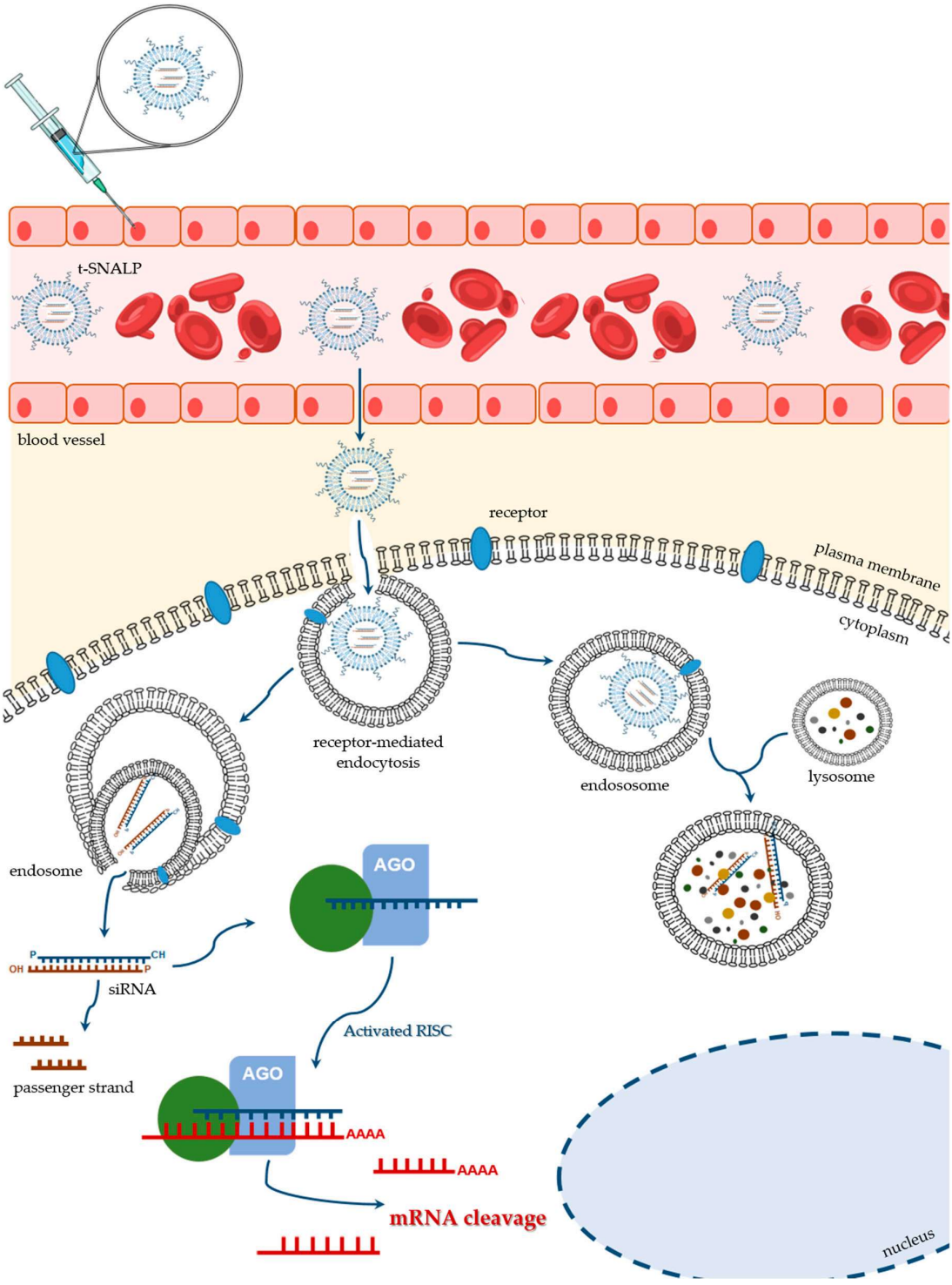


Figure 4. Schematic representation of the ligand-mediated SNALP targeting for delivery of therapeutic siRNAs. After being injected into the bloodstream, t-SNALPs must cross the endothelial barrier and diffuse through the extracellular matrix. When reaching their target cells, the engineered ligands, which are covalently attached to the SNALP surface, interact specifically with their receptors on the plasma membrane. That interaction will result in the t-SNALP internalization through receptor-mediated endocytosis, for example. Once inside the cell, siRNAs must escape the endocytic pathway (right side of the picture) and avoid lysosomal destruction. Instead, siRNAs need to be unpacked and released into the cytoplasm, where they can be incorporated into the RNAi machinery (left side of the picture) and actively promote the silencing of their target gene(s).

In this regard, we have assessed the efficacy of transferrin receptor (TrfR)-targeted SNALPs encapsulating gene-silencing tools for chronic myeloid leukemia (CML) treatment [139]. CML is a hematopoietic stem cell disease, whose molecular trigger is the *BCR-ABL* oncogene. This gene encodes the Bcr-Abl protein, which is a constitutively active tyrosine kinase, responsible for the malignant transformation in the disease [140]. Thus, *BCR-ABL* seemed a good target for the application of gene-silencing approaches, using either siRNAs or antisense oligonucleotides (ASOs). The question was then how tumor cells could be targeted to selectively deliver the gene-silencing tools. We chose to couple transferrin (Trf) to th e surface of SNALPs encapsulating either anti-*BCR-ABL* siRNA or anti-*BCR-ABL* ASOs. Trf is an 80 kDa glycoprotein that undergoes internalization by endocytosis mediated by TrfR, a cell membrane associated glycoprotein (reviewed in [141,142]), which is known to be overexpressed in tumor cells [143,144]. After extensively characterizing the developed targeted Trf-SNALPs in terms of size, encapsulation yield, amount of coupled Trf protein and size stability over time, having registered very satisfactorily reproducible results, we moved on to address the selective internalization of the Trf-SNALPs, and clearly demonstrated that it occurred through TrfR-mediated endocytosis. Finally, the capacity of those formulations to achieve the desired therapeutic effect was also evaluated and a significant correlation between the reduction of *BCR-ABL* mRNA levels and the expected decrease of Bcr-Abl protein expression and cytotoxicity was observed [139]. Following these findings, we performed further studies aiming at generating Trf-SNALPs co-encapsulating anti-*BCR-ABL* siRNAs and imatinib. Imatinib is the first-line treatment for CML, which operates by effectively blocking Bcr-Abl activity (reviewed in [145,146]). Since many CML patients present with resistance and intolerance to imatinib, siRNAs and imatinib were co-encapsulated at different molar ratios. The developed Trf-SNALPs enabled the encapsulation of both siRNAs and imatinib at molar ratios that allowed reaching therapeutic doses, which clearly resulted in increased anti-tumoral activity [147]. This sort of approach is particularly attractive, since it allows triple targeting, while using a single therapeutic agent: the developed Trf-SNALPs are targeted to TrfR at the cancer cell surface, addressing two different molecular targets, BCR-ABL mRNA (through the use of siRNAs) and Bcr-Abl protein (through the use of imatinib) [147].

Similar efforts were conducted to design siRNA-containing SNALPs targeted to cancer cells and their tumor microenvironment. Actually, the aggressiveness of a tumor does not rely on the cancer cells alone, but rather on the cross-talk between cancer cells and other cells from the tumor microenvironment such as the endothelial cells (reviewed in [148]). To achieve such goal, we have covalently attached the F3 peptide to those nanoparticles with the rationale to target not only the cancer cells, but also angiogenesis. In fact, the F3 peptide is internalized upon specific binding to nucleolin, a receptor that is overexpressed on the surface of both cancer cells and tumor blood vessel cells [149,150]. Overall, our work culminated in the development of F3-SNALPs, whose general features were adequate for systemic delivery and led to a significant improvement in their internalization by both cancer and endothelial cells from angiogenic blood vessels, which was further correlated with effective gene-silencing [151,152]. Soon after, we have also assessed the therapeutic potential of those F3-SNALPs, upon encapsulation of a siRNA against *PLK1* [153] in prostate cancer (PC3) and angiogenic endothelial (HMEC-1) cells, having observed a significant decrease in cell viability, which was mediated by a marked *PLK1* silencing, both at the mRNA and protein levels. We have evaluated the anti-*PKL1* F3-SNALPs effect on the sensitization of cancer cells to conventional chemotherapy (paclitaxel), having observed the ability of anti-*PKL1* F3-SNALPs to render cancer cells sensitive to paclitaxel, thus potentially contributing to lower undesired side effects and resistance of cancer cells to conventional chemotherapy [153]. In another work, we have also designed a F3 peptide-targeted liposomal strategy, involving sterically stabilized pH-sensitive liposomes targeting the cell surface nucleolin, and exploited its potential for delivery of doxorubicin (DXR) to cancer cells and the tumor microenvironment (endothelial cells) in breast cancer, with similar success [154]. Later, the same liposomal strategy was successfully applied for the simultaneous delivery of a synergistic combination of the pro-apoptotic csc-ceramide (C6-Cer), an inhibitor of PI3K/Akt signaling, and DXR, aiming at promoting tumor cell

death towards breast cancer treatment [155,156]. Finally, since an effective treatment for breast cancer would require targeting both cancer stem cells (CSCs) and non-stem cancer cells (n-SCCs), as the second may also originate CSCs through epithelial-to-mesenchymal transition [157], Fonseca et al. showed that F3-functionalized pH-sensitive liposomes were able to target simultaneously nucleolin-overexpressing CSCs and non-SCCs [156].

We have developed similar targeted approaches using peptides coupled to liposomal systems towards overexpressed tumoral receptors for treatment of other cancer types such as glioblastoma (GBM). For that purpose, chlorotoxin (CTX), a scorpion-derived peptide reported to bind selectively to glioma cells, while showing no affinity for non-neoplastic cells, was covalently coupled to SNALPs encapsulating either siRNAs or ASOs [158], the latter being designed to inhibit miR-21 which is overexpressed in the majority of tumors, including GBM. We have shown that targeted SNALP-mediated miR-21 silencing in cultured GBM cells promoted tumor suppressor expression and caspase activity, and reduced tumor cell proliferation [158]. Biodistribution analysis of IV-administered CTX-coupled SNALPs into GBM-bearing mice has revealed that these targeted nanoparticles preferentially accumulate within intracranial tumors, while sparing healthy tissue [158]. Moreover, systemic delivery of CTX-coupled SNALPs-formulated anti-*miR-21* oligonucleotides led to efficient release of the encapsulated nucleic acids into the brain tumors, which was associated with a significant and specific miR-21 silencing, resulting in increased mRNA and protein levels of its target, RhoB (Rho-related GTP-binding protein RhoB), while showing no signs of immunogenicity [159]. Importantly, CTX-coupled SNALP-mediated miR-21 knockdown combined with oral administration of the tyrosine kinase inhibitor sunitinib resulted in significant decrease in tumor size, cell proliferation and angiogenesis, enhanced apoptosis, and improvement of animal survival. No evidence of acute cardio- and hepatoxicity, potentially induced by the treatment as side-effect, was found, thus revealing that this multimodal approach holds great promise towards GBM therapy [159].

Overall, the reported studies highlight not only the potential of targeted lipid-based nanosystems, including SNALPs, to promote efficient and specific intracellular delivery for a whole new generation of molecular drugs, but also the importance of choosing the most adequate target receptor for each disorder and, consequently, the moiety to be coupled to the nanocarrier surface in each case. This sort of technology may also bring a hope for several diseases that urgently need innovative and effective therapies, such as the life-threatening LSDs.

6. General Considerations on the Pre-Clinical Development of RNAi-Based Substrate Reduction Approaches for LSDs

Currently, there is a lack of studies on the development of delivery strategies for siRNA-triggered SRT, even though this is a critical issue that must be carefully addressed whenever designing a therapeutic approach based on the use of siRNAs or other antisense technologies. This is not surprising, since delivery optimization is often left till the later stages of pre-clinical development (often following rigorous sequence optimization). However, it is fundamental to address this issue earlier as it is instrumental to a successful clinical translation [160]. This is especially meaningful for neurological diseases, as the BBB is one of the major challenges for targeted drug delivery. As it happens with many other disorders, translation of any siRNA-based approach for neurological LSDs into the clinical setting largely depends on the development of appropriate delivery systems, which allow for proper biodistribution and promote more favorable pharmacokinetics, while ensuring that the drug reaches specifically its therapeutic target.

Characterized by their favorable features for successful in vivo application, including prolonged blood-circulation times, SNALPs are highly bioavailable and may represent excellent nanodelivery systems for siRNA-based drugs, as referred in the previous section. Furthermore, SNALPs surface may be engineered with internalizing ligands targeting specific receptors, expressed in different cell types, including brain cells, which may allow for the simultaneous systemic and brain delivery. In fact, there are several types of receptors, expressed on the capillary endothelium of the brain, such as

Trf, LDL, insulin, and nicotinic acetylcholine (nACh) receptors, and any moiety targeting one of these receptors may hold potential to promote receptor-mediated endocytosis (RME) of therapeutic compounds [161]. Still, caution is needed when choosing the moiety to be tested in each case. Trf, for example, is an ion transporting protein interacting with receptors ubiquitously expressed in various tissues (reviewed in [142]) and has been shown to promote cell uptake of lipid-based nanosystems in a multitude of cells, including neurons [162–167]. Moreover, we have proposed that Trf can trigger the cytoplasmic delivery of the carried nucleic acids by destabilizing the endosomal membrane, enhancing transfection [162,163,168]. Trf-associated cationic liposomes were initially assessed with great success, in our laboratory, for their potential to deliver plasmid DNA in a plethora of cells, including cultured cancer cells and primary neuronal cultures, as well as into the rat brain upon intracranial injection [166,167]. Later, their capacity for siRNA delivery was also assessed, with very promising results [168]. In fact, when we complexed Trf-associated cationic liposomes with siRNAs, at different lipid/siRNA (+/−) charge ratios, and assessed the cellular internalization of the resulting Trf-lipoplexes, confocal microscopy analysis showed fast uptake via endocytosis. Furthermore, in GFP-expressing glioblastoma cells, Trf-lipoplexes showed enhanced gene-silencing with minimum cytotoxicity in comparison to Trf-free lipoplexes [168]. Evidence was provided for the feasibility of Trf-lipoplexes to promote efficient down-regulation of the transcription factor c-Jun without detectable off-target effects, both in neuronal cell lines [168] and primary cultures of cortical neurons [169,170], which resulted in significant neuronal protection and repair from glutamate-induced damage or oxygen/glucose deprivation [168,170]. Importantly, upon stereotactic injection of anti-*c-Jun* siRNAs formulated into Trf-lipoplexes in a rat model of excitotoxic brain lesion, efficient and specific gene-silencing was achieved with minimum toxicity, leading to significant improvement in neuronal survival and attenuation of the inflammatory reaction, characterized by microglia activation and gliosis, caused by the induced excitotoxic damage [170]. Seemingly, whereas Trf would be an auspicious ligand to promote therapeutic delivery in LSDs, Trf-SNALPs would be an attractive choice of nanoparticles for targeted siRNA delivery in these multisystemic neurodegenerative disorders.

Other potential ligands for targeted delivery of "anti-LSDs" drugs are the rabies virus glycoprotein (RVG)-derived peptides, which hold promise to facilitate drug delivery into the CNS. Son et al. have even described RVG as a potential "magical bullet" for the targeting of genes to the brain [171]. Knowing that the RVG is a 505 amino acid glycoprotein responsible for the neurotrophic nature of the rabies virus infection, peptide derivatives of RVG, such as rabies virus derived peptide (RDP) and RVG-29, are emerging as promising targeting ligands for brain delivery (reviewed in [172]). The RDP is a 39 amino acid derivative of residues 300–357 of RVG that functions as an important nerve binding region [173]. It retains the neurotrophic penetrating properties of RVG, acting as a facilitating ligand for neural cell entry of a conjugated payload. Although there is still conflicting evidence in the literature regarding which receptor of the BBB is used by RVG and its derivatives, several studies point out an interaction between RVG and nicotinic acetylcholine receptor (nAChR). This interaction is thought to be the major responsible for BBB-crossing properties of RVG, but there is evidence on its association with other neural cell-specific molecules, such as neural cell adhesion molecule (NCAM) and Neurotrophin receptor p75 (p75NTR) (reviewed in [172,174]). Furthermore, interactions of RVG with carbohydrates, gangliosides, and lipids, also hold a stake in its entry into the CNS (reviewed in [174]). Whatever the case, the exact mechanism by which the RVG peptide traverses the BBB and enters cells is yet to be elucidated [175]. However, no doubts exist: nAChR is an ubiquitous receptor in the CNS, and, therefore, any moiety targeting it holds potential for whole-brain delivery [172]. That is why one such receptor would be potentially adequate for "anti-LSDs" drug delivery, as it may target the neurological phenotype of these diseases. Moreover, RDP may be chemically modified to present more favorable pharmacokinetics. For example, the rabies virus peptide derivative RVG-9r, one of the most widely used RDPs, results from the combination of a short peptide, derived from the RVG that specifically binds nAChRs of neuronal cells, with a sequence of 9 arginines added to its carboxy terminus, which enhances cell uptake and cargo release into the cytoplasm. When complexed with siRNAs, RVG-9r

allowed specific delivery of siRNAs to GFP-expressing neuronal cells in vitro, resulting in efficient gene-silencing. In in vivo studies it was demonstrated that following IV injection into GFP transgenic mice, RVG-9r-bound siRNAs were successfully targeted to neuronal cells and promoted efficient and brain-specific gene-silencing [176]. Kumar et al. have also shown that intravascular delivery of RVG-9r-bound antiviral siRNAs in mice was able to confer efficient protection against fatal viral encephalitis. Not accidentally, the same pathway that allows for the transport of RVG throughout the CNS (axonal retrograde transport; [177]) is also responsible for the passage of other neurotoxins, such as the tetanus toxin [178] justifying why the Tet-1 peptide from the tetanus toxin has been looked as a targeting peptide for the delivery of therapeutic nucleic acids to neural cells, in an in vivo study in mice [179]. Likewise, the capacity of the Human Immunodeficiency Virus (HIV) gp120 protein to bind nAChR and the ability of α-bungarotoxin and HIV Tat proteins to cross the BBB, further suggest that peptides derived from other viruses that infect the brain (including HIV, the herpes simplex virus, and flaviviruses) may also be explored as targeting agents for siRNA delivery [175]. To the best of our knowledge, however, so far, these possibilities have not yet been tested. Contrarily, evidence collected on the use of RVG and its derivatives is far more compelling, as reflected in the much higher number of studies using those moieties [173,176]. Therefore, we consider that using one of the RVG peptide derivatives, namely RVG-9r, is particularly tempting for brain delivery of siRNA drugs towards gSRT in LSDs.

It cannot be ignored that there are many other possible ways to promote siRNA brain delivery and several moieties that could be tested for the same purpose as for example lactoferrin [180], folic acid [181,182], glutamate [183], mannose [184] and recombinant IL-1 receptor antagonist [185], among others (reviewed in [186]).

In this regard, our team has shown that covalent coupling of RVG-9r to SNALPs encapsulating siRNAs targeting mutant ataxin-3, which was stably expressed in cultured neuronal cells, promoted specific gene-silencing [187]. Most importantly, IV injection of the RVG-9r-targeted SNALPs-formulated siRNAs into Machado-Joseph transgenic mice expressing mutant ataxin-3 led to efficient silencing of the pathogenic protein, which resulted in drastic reduction of the neuropathology and associated motor behavior abnormalities [187]. Nevertheless, an improved cellular internalization is not necessarily synonymous of an efficient gene-silencing (reviewed in [103,188]), which implies that targeted SNALP-formulated siRNAs must be tested for their efficacy in vivo, even when the effect of the naked molecule has already been extensively analyzed in vitro. Ideally, the effect of these targeted SNALP-formulated therapeutic molecules should be addressed at different levels: mRNA; protein and substrate accumulation and/or excretion. As other authors have already pointed out, in vitro and in vivo models are complementary, and their use must be done heeding limitations of each model. Cell culture models are useful for proof-of-concept studies if an adequate cell type is selected. Currently, the possibility of deriving diverse cell types from affected patients' iPSCs offers an interesting alternative for siRNA drug testing in different cellular environments. Although in general delivery studies in cell culture have provided very useful data on cellular uptake mechanisms, the results cannot be directly extrapolated to in vivo studies, which are indeed irreplaceable [160].

It is also important to stress, that although we focused this review on SNALPs alone, several other platforms may be used to translate the therapeutic potential of RNAi and deliver its effectors to different organs and tissues. Recombinant adeno-associated vectors (AAV), for example, are among those platforms. In fact, various noncoding RNAi effectors such as shRNAs, miRNAs and siRNA decoys can be expressed from recombinant AAV and there is a significant number of pre-clinical studies evaluating this possibility, which have been extensively reviewed elsewhere [189]. Still, we can anticipate that viral delivery renders the toxicology studies of a product more complex than a classic formulation, which may hinder translational studies with AAV-mediated RNAi vectors. Also, in the nanotechnology field attempts to develop effective delivery systems that protect the siRNA from nuclease degradation, deliver it to target cells, and release it into their cytoplasm, without creating adverse effects are countless. There is an ever-growing number of hypotheses being tested that go far

beyond those reviewed here, including dendrimers, inorganic nanoparticles, exosomes, extracellular vesicles, and even red blood cells. Interestingly, some of these approaches are actually being attempted in the LSDs field, but not for siRNA delivery. For example, both AAV vectors [190] and extracellular vesicles [191] have been tested for their potential to treat CLN2 Batten disease acting as drug carriers for gene therapy or ERT, respectively.

Finally, there is one last issue that deserves attention to improve siRNA delivery into its target tissues: administration. Currently, there are several possible approaches, from IV injection to more direct delivery methods, including ICV or IT injection. The systemic route for delivery into the CNS includes diffusion [192] and RME [193,194] and requires the development of a siRNA nanodelivery system, which is able to cross the BBB, such as the RVG-targeted SNALPs we have been referring to. So far, however, the most widely used methods to bypass the BBB are the direct brain parenchyma injections, which allow for the use of non-targeted nanocarriers or chemically modified naked therapeutic molecules.

Commonly, delivery optimization is often left until the latter stages of pre-clinical development, a practice that can considerably delay the successful clinical translation of molecular therapies (reviewed in [160]). The LSDs field is no exception t, with a scarce number of in vitro proof-of-principle studies on different molecular approaches to either overcome or minimize pathology [66,94–98,195]; barely contributed to enrich the knowledge of the development of proper therapeutic delivery methods. As far as we know, there are no studies on the development of targeted SNALPs for brain delivery of siRNAs designed to decrease substrate biosynthesis in LSDs, but the potential of one such approach does seem undeniable. Among other important advantages, one such approach would virtually allow for the generation of multifunctional siRNA mixtures that could be applied to different diseases, as they share the same accumulating substrates, thus reducing therapy costs and increasing the number of patients that could benefit from available therapeutic options.

7. Concluding Remarks and Future Perspectives

Since the discovery of the Nobel prize-winning mechanism of RNAi, 20 years ago, this technology has become not only a major gene-silencing tool in the lab for the experimental manipulation of gene expression, but also a promising therapeutic approach. Since it is a naturally occurring post-transcriptional process, this silencing mechanism has several advantages when compared to other technologies. That recognition triggered major investments in RNAi-based drug development by large pharmaceutical and biotechnological companies, which culminated in the first U.S. FDA approval of one such drug in 2018 (reviewed in [6]).

In general, the clinical application of this sort of drugs largely depends on the development of appropriate delivery systems, which are able to ameliorate the unfavorable pharmacokinetics of RNAi effectors (siRNAs), while enhancing their biodistribution properties. Throughout these decades, many different types of nanomaterials have been developed for siRNA delivery, and based on the extensive evaluation of their properties, lipid-based nanoparticles have probably become the most popular ones. Among them, PEG-grafted nanocarriers and, particularly, SNALPs, have gained momentum (reviewed in [80,103]) in such a way that SNALPs represent one of the most widely adopted RNAi delivery technology to date. At present, human applications of SNALP-formulated siRNAs are yet almost exclusively confined to targets within the liver, where siRNA nanodelivery systems naturally accumulate. Extra-hepatic targets remain a challenge [196], but expectantly as we have here reviewed, there are several in vivo studies addressing these targets, whose positive results hold promise for a wider application of SNALPs in other disorders, including those that affect the CNS. LSDs are certainly among those disorders, as they may benefit from brain-targeted gSRT, an approach that can circumvent one of the most urgent unmet medical needs for these patients: CNS pathology and the relentless neurodegeneration, which ultimately results in premature death.

Author Contributions: Conceptualization, M.F.C, M.C.P.d.L. and S.A.; NCBI Pubmed search: M.F.C. and J.I.S.; manuscript structure: M.F.C., A.S.J., M.C.P.d.L. and S.A.; original draft preparation: M.F.C.; additional writing: M.C.P.d.L.; figures, M.F.C. and J.I.S; critical review, M.F.C., J.I.S., L.S.M., L.M., M.J.P., A.S.J., M.C.P.d.L. and S.A.; editing, M.F.C and J.I.S.; funding acquisition, M.F.C. and S.A. All authors have read and agreed to the published version of the manuscript.

Funding: This work was supported by the Portuguese Society for Metabolic Disorders (Sociedade Portuguesa de Doenças Metabólicas, SPDM—Bolsa SPDM de apoio à investigação Dr. Aguinaldo Cabral 2018; 2019DGH1629/SPDM2018I&D) and Sanfilippo Children's Foundation (SCF Incubator Grant 2019; 2019DGH1656/SCF2019I&D). Additional support came from the European Regional Development Fund (ERDF), through the Centro 2020 Regional Operational Programme (project CENTRO-01-0145-FEDER-000008: BrainHealth 2020), and the COMPETE 2020—Operational Programme for Competitiveness and Internationalisation and Portuguese national funds via FCT—Fundação para a Ciência e a Tecnologia (projects POCI-01-0145-FEDER-016390: CANCEL STEM and POCI-01-0145-FEDER-007440; UIDB/04539/2020). L.S.M. is funded by FCT/MCTES National Funds under project CEECIND/04242/2017.

Conflicts of Interest: The authors declare no conflict of interest.

Abbreviations

AGO2	Argonaute 2
ApoB	Apolipoprotein B
ASOs	Antisense oligonucleotides
BBB	Blood-brain barrier
C6-Cer	C6-ceramide
CML	Chronic myeloid leukemia
CNS	Central nervous system
CSCs	Cancer stem cells
CSF	Cerebrospinal fluid
CTX	Chlorotoxin
DAGs	Diacylglycerols
DSPC	1,2-distearoyl-sn-glycero-3-phosphocholine
dsRNA	Double-stranded RNA
DXR	Doxorubicin
EBOV	Ebola virus
ERT	Enzyme replacement therapy
FD	Fabry disease
GAGs	Glycosaminoglycans
GD	Gaucher disease
GBM	Glioblastoma
gSRT	Genetic substrate reduction therapy
hATTR	Hereditary TTR-mediated amyloidosis
HBV	Hepatitis B virus
HF	Hemorrhagic fever
HIV	Human immunodeficiency virus
HMEC-1	Angiogenic endothelial cells
HS	Heparan sulphate
ICV	Intracerebroventricular
iPSCs	Induced pluripotent stem cells
IT	Intrathecal
IV	Intravenous
KSP	Kinesin spindle protein
LNPs	Lipid nanoparticles
LDL	Low-density lipoprotein
LSDs	Lysosomal storage disorders
miRNA	microRNA
MLD	Metachromatic Leukodystrophy
MPSs	Mucopolysaccharidoses
mRNA	messenger RNA

NCAM	Neural cell adhesion molecule
NCLs	Neuronal Ceroid Lipofuscinoses
nACh	Nicotinic acetylcholine
nAChR	Nicotinic acetylcholine receptor
n-SCC	Non-stem cancer cells
PD	Parkinson's disease
PLK1	Polo-like kinase 1
PEG	Polyethylene glycol
PEI	Polyethylenimine
PC3	Prostate cancer cells
PKR	Protein kinase receptor
P75NTR	Neurotrophin receptor 75
RDP	Rabies virus derived peptide
RVG	Rabies virus glycoprotein
RVG-9r	Rabies virus peptide derivative
RME	Receptor-mediated endocytosis
rhTPP1	Recombinant human tripeptidyl peptidase 1
RES	Reticuloendothelial system
RNAi	RNA interference
RISC	RNA-induced silencing complex
shRNA	Short hairpin RNA
siRNAs	small interfering RNAs
SNALP	Stable nucleic acid lipid particle
SRT	Substrate reduction therapy
TLRs	Toll-like receptors
Trf	Transferrin
TrfR	Transferrin receptor
TTR	Transthyretin
$T_{1/2}$	Elimination/circulation half-time
U.S. FDA	United States Food and drug administration
VLDL	Very-low-density lipoprotein
ZEBOV	Zaire species of EBOV
3′-UTR	3′ untranslated region

References

1. Fire, A.; Xu, S.; Montgomery, M.K.; Kostas, S.A.; Driver, S.E.; Mello, C.C. Potent and specific genetic interference by double-stranded RNA in Caenorhabditis elegans. *Nature* **1998**, *391*, 806–811. [CrossRef] [PubMed]
2. Hamilton, A.J.; Baulcombe, D.C. A species of small antisense RNA in posttranscriptional gene silencing in plants. *Science* **1999**, *286*, 950–952. [CrossRef] [PubMed]
3. Elbashir, S.M.; Harborth, J.; Lendeckel, W.; Yalcin, A.; Weber, K.; Tuschl, T. Duplexes of 21-nucleotide RNAs mediate RNA interference in cultured mammalian cells. *Nature* **2001**, *411*, 494–498. [CrossRef] [PubMed]
4. Elbashir, S.M.; Lendeckel, W.; Tuschl, T. RNA interference is mediated by 21- and 22-nucleotide RNAs. *Genes Dev.* **2001**, *15*, 188–200. [CrossRef]
5. Sandy, P.; Ventura, A.; Jacks, T. Mammalian RNAi: A practical guide. *Biotechniques* **2005**, *39*, 215–224. [CrossRef]
6. Coutinho, M.F.; Matos, L.; Santos, J.I.; Alves, S. RNA Therapeutics: How Far Have We Gone? *Adv. Exp. Med. Biol.* **2019**, *1157*, 133–177. [CrossRef]
7. Deng, Y.; Wang, C.C.; Choy, K.W.; Du, Q.; Chen, J.; Wang, Q.; Li, L.; Chung, T.K.; Tang, T. Therapeutic potentials of gene silencing by RNA interference: Principles, challenges, and new strategies. *Gene* **2014**, *538*, 217–227. [CrossRef]
8. Kelly, J.M.; Bradbury, A.; Martin, D.R.; Byrne, M.E. Emerging therapies for neuropathic lysosomal storage disorders. *Prog. Neurobiol.* **2017**, *152*, 166–180. [CrossRef]

9. Wraith, J.E. Lysosomal disorders. *Paediatr. Child Health* **2011**, *21*, 76–79. [CrossRef]
10. Gritti, A. Gene therapy for lysosomal storage disorders. *Expert Opin. Biol.* **2011**, *11*, 1153–1167. [CrossRef]
11. Platt, F.M.; d'Azzo, A.; Davidson, B.L.; Neufeld, E.F.; Tifft, C.J. Author Correction: Lysosomal storage diseases. *Nat. Rev. Dis. Primers* **2018**, *4*, 36. [CrossRef] [PubMed]
12. Micsenyi, M.C.; Walkley, S.U. The lysosomal system: Physiology and pathology. In *Lysosomal Storage Disorders—A Practial Guide*, 1st ed.; Mehta, A., Winchester, B., Eds.; Wiley-Blackwell: West Sussex, UK, 2012; pp. 3–12.
13. Raas-Rothschild, A.; Cormier-Daire, V.; Bao, M.; Genin, E.; Salomon, R.; Brewer, K.; Zeigler, M.; Mandel, H.; Toth, S.; Roe, B.; et al. Molecular basis of variant pseudo-hurler polydystrophy (mucolipidosis IIIC). *J. Clin. Investig.* **2000**, *105*, 673–681. [CrossRef] [PubMed]
14. Tiede, S.; Storch, S.; Lübke, T.; Henrissat, B.; Bargal, R.; Raas-Rothschild, A.; Braulke, T. Mucolipidosis II is caused by mutations in GNPTA encoding the alpha/beta GlcNAc-1-phosphotransferase. *Nat. Med.* **2005**, *11*, 1109–1112. [CrossRef] [PubMed]
15. Anikster, Y.; Lucero, C.; Guo, J.; Huizing, M.; Shotelersuk, V.; Bernardini, I.; McDowell, G.; Iwata, F.; Kaiser-Kupfer, M.I.; Jaffe, R.; et al. Ocular nonnephropathic cystinosis: Clinical, biochemical, and molecular correlations. *Pediatr. Res.* **2000**, *47*, 17–23. [CrossRef] [PubMed]
16. Winchester, B. Laboratory diagnosis of Lysosomal Storage Diseases. In *Lysosomal Storage Disorders—A Practial Guide*, 1st ed.; Metha, A., Winchester, B., Eds.; Wiley-Blackwell: West Sussex, UK, 2012; pp. 20–28.
17. Lieberman, A.P.; Puertollano, R.; Raben, N.; Slaugenhaupt, S.; Walkley, S.U.; Ballabio, A. Autophagy in lysosomal storage disorders. *Autophagy* **2012**, *8*, 719–730. [CrossRef] [PubMed]
18. Walkley, S.U. Pathogenic cascades in lysosomal disease-Why so complex? *J. Inherit. Metab. Dis.* **2009**, *32*, 181–189. [CrossRef]
19. Sardiello, M.; Palmieri, M.; di Ronza, A.; Medina, D.L.; Valenza, M.; Gennarino, V.A.; Di Malta, C.; Donaudy, F.; Embrione, V.; Polishchuk, R.S.; et al. A gene network regulating lysosomal biogenesis and function. *Science* **2009**, *325*, 473–477. [CrossRef]
20. Cox, T. Current Treatments. In *Lysosomal Storage Disorders—A Practial Guide*, 1st ed.; Mehta, A.B., Winchester, B., Eds.; Wiley-Blackwell: West Sussex, UK, 2012; pp. 153–165.
21. Schultz, N.; Marenstein, D.R.; De Angelis, D.A.; Wang, W.Q.; Nelander, S.; Jacobsen, A.; Marks, D.S.; Massagué, J.; Sander, C. Off-target effects dominate a large-scale RNAi screen for modulators of the TGF-β pathway and reveal microRNA regulation of TGFBR2. *Silence* **2011**, *2*, 3. [CrossRef]
22. Begley, D.; Scarpa, M. Central Nervous System Aspects, Neurodegeneration and the Blood-Brain Barrier. In *Lysosomal Storage Disorders—A Practical Guide*, 1st ed.; Mehta, A.B., Winchester, B., Eds.; Wiley-Blackwell: West Sussex, UK, 2012; pp. 166–173.
23. Wraith, J.E.; Beck, M. Clinical Aspects and Clinical Diagnosis. In *Lysosomal Storage Disorders—A Practial Guide*, 1st ed.; Metha, A., Winchester, B., Eds.; Wiley-Blackwell: West Sussex, UK, 2012; pp. 13–19.
24. Heese, B.A. Current strategies in the management of lysosomal storage diseases. *Semin. Pediatr. Neurol.* **2008**, *15*, 119–126. [CrossRef]
25. Bley, A.E.; Giannikopoulos, O.A.; Hayden, D.; Kubilus, K.; Tifft, C.J.; Eichler, F.S. Natural history of infantile G(M2) gangliosidosis. *Pediatrics* **2011**, *128*, 1233–1241. [CrossRef]
26. Coutinho, M.F.; Lacerda, L.; Alves, S. Glycosaminoglycan storage disorders: A review. *Biochem. Res. Int.* **2012**, *2012*, 471325. [CrossRef] [PubMed]
27. Federico, A.; Capece, G.; Cecio, A.; D'Auria, N.; Di Iorio, G.; Ronsisvalle, L.; Di Natale, P. Sanfilippo B syndrome (MPS III B): Case report with analysis of CSF mucopolysaccharides and conjunctival biopsy. *J. Neurol.* **1981**, *225*, 77–83. [CrossRef] [PubMed]
28. Tomatsu, S.; Gutierrez, M.A.; Ishimaru, T.; Peña, O.M.; Montaño, A.M.; Maeda, H.; Velez-Castrillon, S.; Nishioka, T.; Fachel, A.A.; Cooper, A.; et al. Heparan sulfate levels in mucopolysaccharidoses and mucolipidoses. *J. Inherit. Metab. Dis.* **2005**, *28*, 743–757. [CrossRef] [PubMed]
29. Tomatsu, S.; Okamura, K.; Maeda, H.; Taketani, T.; Castrillon, S.V.; Gutierrez, M.A.; Nishioka, T.; Fachel, A.A.; Orii, K.O.; Grubb, J.H.; et al. Keratan sulphate levels in mucopolysaccharidoses and mucolipidoses. *J. Inherit. Metab. Dis.* **2005**, *28*, 187–202. [CrossRef]
30. Munoz-Rojas, M.V.; Vieira, T.; Costa, R.; Fagondes, S.; John, A.; Jardim, L.B.; Vedolin, L.M.; Raymundo, M.; Dickson, P.I.; Kakkis, E.; et al. Intrathecal enzyme replacement therapy in a patient with mucopolysaccharidosis type I and symptomatic spinal cord compression. *Am. J. Med. Genet. A* **2008**, *146A*, 2538–2544. [CrossRef]

31. Muenzer, J. Overview of the mucopolysaccharidoses. *Rheumatology (Oxford)* **2011**, *50*, 4–12. [CrossRef]
32. Neufeld, E.U.; Muenzer, J. The Mucopolysaccharidoses. In *The Metabolic Basis of Inherited Disease*; Scriver, C.R., Ed.; McGraw-Hill: New York, NY, USA, 2001; pp. 3421–3452.
33. Muenzer, J.; Wraith, J.E.; Clarke, L.A. Mucopolysaccharidosis I: Management and treatment guidelines. *Pediatrics* **2009**, *123*, 19–29. [CrossRef]
34. Martin, R.; Beck, M.; Eng, C.; Giugliani, R.; Harmatz, P.; Muñoz, V.; Muenzer, J. Recognition and diagnosis of mucopolysaccharidosis II (Hunter syndrome). *Pediatrics* **2008**, *121*, 377–386. [CrossRef] [PubMed]
35. Heon-Roberts, R.; Nguyen, A.L.A.; Pshezhetsky, A.V. Molecular Bases of Neurodegeneration and Cognitive Decline, the Major Burden of Sanfilippo Disease. *J. Clin. Med.* **2020**, *9*, 344. [CrossRef]
36. Paciotti, S.; Albi, E.; Parnetti, L.; Beccari, T. Lysosomal Ceramide Metabolism Disorders: Implications in Parkinson's Disease. *J. Clin. Med.* **2020**, *9*, 594. [CrossRef]
37. Aerts, J.M.F.G.; Kuo, C.L.; Lelieveld, L.T.; Boer, D.E.C.; van der Lienden, M.J.C.; Overkleeft, H.S.; Artola, M. Glycosphingolipids and lysosomal storage disorders as illustrated by gaucher disease. *Curr. Opin. Chem. Biol.* **2019**, *53*, 204–215. [CrossRef] [PubMed]
38. Elstein, D.; Zimran, A. Gaucher Disease. In *Lysosomal Storage Disorders—A Practical Guide*, 1st ed.; Mehta, A.B., Winchester, B., Eds.; Wiley-Blackwell: West Sussex, UK, 2012; pp. 49–57.
39. Robak, L.A.; Jansen, I.E.; van Rooij, J.; Uitterlinden, A.G.; Kraaij, R.; Jankovic, J.; Heutink, P.; Shulman, J.M.; IPDGC. Excessive burden of lysosomal storage disorder gene variants in Parkinson's disease. *Brain* **2017**, *140*, 3191–3203. [CrossRef] [PubMed]
40. Blumenreich, S.; Barav, O.B.; Jenkins, B.J.; Futerman, A.H. Lysosomal Storage Disorders Shed Light on Lysosomal Dysfunction in Parkinson's Disease. *Int. J. Mol. Sci.* **2020**, *21*, 4966. [CrossRef] [PubMed]
41. Sun, A. Lysosomal storage disease overview. *Ann. Transl. Med.* **2018**, *6*, 476. [CrossRef] [PubMed]
42. Mole, S.E.; Anderson, G.; Band, H.A.; Berkovic, S.F.; Cooper, J.D.; Kleine Holthaus, S.M.; McKay, T.R.; Medina, D.L.; Rahim, A.A.; Schulz, A.; et al. Clinical challenges and future therapeutic approaches for neuronal ceroid lipofuscinosis. *Lancet. Neurol.* **2019**, *18*, 107–116. [CrossRef]
43. Cooper, D.C.; Williams, R.E. Neuronal Ceroid Lipofuscinoses. In *Lysosomal Storage Disorders—A Practical Guide*, 1st ed.; Mehta, A.B., Winchester, B., Eds.; Wiley-Blackwell: West Sussex, UK, 2012; pp. 3–12.
44. Garbade, S.F.; Zielonka, M.; Mechler, K.; Kölker, S.; Hoffmann, G.F.; Staufner, C.; Mengel, E.; Ries, M. FDA orphan drug designations for lysosomal storage disorders—A cross-sectional analysis. *PLoS ONE* **2020**, *15*, e0230898. [CrossRef]
45. Wraith, J.E.; Beck, M.; Lane, R.; van der Ploeg, A.; Shapiro, E.; Xue, Y.; Kakkis, E.D.; Guffon, N. Enzyme replacement therapy in patients who have mucopolysaccharidosis I and are younger than 5 years: Results of a multinational study of recombinant human alpha-L-iduronidase (laronidase). *Pediatrics* **2007**, *120*, 37–46. [CrossRef]
46. Clarke, L.A.; Wraith, J.E.; Beck, M.; Kolodny, E.H.; Pastores, G.M.; Muenzer, J.; Rapoport, D.M.; Berger, K.I.; Sidman, M.; Kakkis, E.D.; et al. Long-term efficacy and safety of laronidase in the treatment of mucopolysaccharidosis I. *Pediatrics* **2009**, *123*, 229–240. [CrossRef]
47. Muenzer, J.; Wraith, J.E.; Beck, M.; Giugliani, R.; Harmatz, P.; Eng, C.M.; Vellodi, A.; Martin, R.; Ramaswami, U.; Gucsavas-Calikoglu, M.; et al. A phase II/III clinical study of enzyme replacement therapy with idursulfase in mucopolysaccharidosis II (Hunter syndrome). *Genet. Med.* **2006**, *8*, 465–473. [CrossRef]
48. Harmatz, P.; Giugliani, R.; Schwartz, I.; Guffon, N.; Teles, E.L.; Miranda, M.C.; Wraith, J.E.; Beck, M.; Arash, L.; Scarpa, M.; et al. Enzyme replacement therapy for mucopolysaccharidosis VI: A phase 3, randomized, double-blind, placebo-controlled, multinational study of recombinant human N-acetylgalactosamine 4-sulfatase (recombinant human arylsulfatase B or rhASB) and follow-on, open-label extension study. *J. Pediatr.* **2006**, *148*, 533–539. [CrossRef]
49. Muenzer, J.; Beck, M.; Giugliani, R.; Suzuki, Y.; Tylki-Szymanska, A.; Valayannopoulos, V.; Vellodi, A.; Wraith, J.E. Idursulfase treatment of Hunter syndrome in children younger than 6 years: Results from the Hunter Outcome Survey. *Genet. Med.* **2011**, *13*, 102–109. [CrossRef] [PubMed]
50. Muenzer, J.; Beck, M.; Eng, C.M.; Giugliani, R.; Harmatz, P.; Martin, R.; Ramaswami, U.; Vellodi, A.; Wraith, J.E.; Cleary, M.; et al. Long-term, open-labeled extension study of idursulfase in the treatment of Hunter syndrome. *Genet. Med.* **2011**, *13*, 95–101. [CrossRef] [PubMed]

51. Burton, B.K.; Whiteman, D.A.; Investigators, H. Incidence and timing of infusion-related reactions in patients with mucopolysaccharidosis type II (Hunter syndrome) on idursulfase therapy in the real-world setting: A perspective from the Hunter Outcome Survey (HOS). *Mol. Genet. Metab.* **2011**, *103*, 113–120. [CrossRef] [PubMed]
52. Meng, Y.; Sohar, I.; Wang, L.; Sleat, D.E.; Lobel, P. Systemic administration of tripeptidyl peptidase I in a mouse model of late infantile neuronal ceroid lipofuscinosis: Effect of glycan modification. *PLoS ONE* **2012**, *7*, e40509. [CrossRef]
53. Veronese, F.M. Peptide and protein PEGylation: A review of problems and solutions. *Biomaterials* **2001**, *22*, 405–417. [CrossRef]
54. Harris, J.M.; Chess, R.B. Effect of pegylation on pharmaceuticals. *Nat. Rev. Drug Discov.* **2003**, *2*, 214–221. [CrossRef]
55. Boado, R.J.; Lu, J.Z.; Hui, E.K.; Pardridge, W.M. Insulin receptor antibody-sulfamidase fusion protein penetrates the primate blood-brain barrier and reduces glycosoaminoglycans in Sanfilippo type A cells. *Mol. Pharm.* **2014**, *11*, 2928–2934. [CrossRef]
56. Wang, D.; El-Amouri, S.S.; Dai, M.; Kuan, C.Y.; Hui, D.Y.; Brady, R.O.; Pan, D. Engineering a lysosomal enzyme with a derivative of receptor-binding domain of apoE enables delivery across the blood-brain barrier. *Proc. Natl. Acad. Sci. USA* **2013**, *110*, 2999–3004. [CrossRef]
57. de Los Reyes, E.; Lehwald, L.; Augustine, E.F.; Berry-Kravis, E.; Butler, K.; Cormier, N.; Demarest, S.; Lu, S.; Madden, J.; Olaya, J.; et al. Intracerebroventricular Cerliponase Alfa for Neuronal Ceroid Lipofuscinosis Type 2 Disease: Clinical Practice Considerations From US Clinics. *Pediatr. Neurol.* **2020**. [CrossRef]
58. Stroobants, S.; Gerlach, D.; Matthes, F.; Hartmann, D.; Fogh, J.; Gieselmann, V.; D'Hooge, R.; Matzner, U. Intracerebroventricular enzyme infusion corrects central nervous system pathology and dysfunction in a mouse model of metachromatic leukodystrophy. *Hum. Mol. Genet.* **2011**, *20*, 2760–2769. [CrossRef]
59. Tsuji, D.; Akeboshi, H.; Matsuoka, K.; Yasuoka, H.; Miyasaki, E.; Kasahara, Y.; Kawashima, I.; Chiba, Y.; Jigami, Y.; Taki, T.; et al. Highly phosphomannosylated enzyme replacement therapy for GM2 gangliosidosis. *Ann. Neurol.* **2011**, *69*, 691–701. [CrossRef] [PubMed]
60. Kan, S.H.; Aoyagi-Scharber, M.; Le, S.Q.; Vincelette, J.; Ohmi, K.; Bullens, S.; Wendt, D.J.; Christianson, T.M.; Tiger, P.M.; Brown, J.R.; et al. Delivery of an enzyme-IGFII fusion protein to the mouse brain is therapeutic for mucopolysaccharidosis type IIIB. *Proc. Natl. Acad. Sci. USA* **2014**, *111*, 14870–14875. [CrossRef] [PubMed]
61. Kan, S.H.; Le, S.; Vincellete, J.; Bullens, S.; Brown, J. Intracerebroventricular enzyme replacement therapy with glycosylation-independent lysosomal targeted NAGLU leads to widespread enzymatic activity, reduction of lysosomal storage and of secondary defects in brain of mice with Sanfilippo syndrome type B. *Mol. Genet. Metab.* **2014**, *111*, S59. [CrossRef]
62. Specchio, N.; Pietrafusa, N.; Trivisano, M. Changing Times for CLN2 Disease: The Era of Enzyme Replacement Therapy. *Clin. Risk Manag.* **2020**, *16*, 213–222. [CrossRef] [PubMed]
63. Brooks, D.A.; Muller, V.J.; Hopwood, J.J. Stop-codon read-through for patients affected by a lysosomal storage disorder. *Trends Mol. Med.* **2006**, *12*, 367–373. [CrossRef] [PubMed]
64. Luddi, A.; Crifasi, L.; Capaldo, A.; Piomboni, P.; Costantino-Ceccarini, E. Suppression of galactocerebrosidase premature termination codon and rescue of galactocerebrosidase activity in twitcher cells. *J. Neurosci. Res.* **2016**, *94*, 1273–1283. [CrossRef]
65. Banning, A.; Schiff, M.; Tikkanen, R. Amlexanox provides a potential therapy for nonsense mutations in the lysosomal storage disorder Aspartylglucosaminuria. *Biochim. Biophys. Acta Mol. Basis Dis.* **2018**, *1864*, 668–675. [CrossRef]
66. Matos, L.; Gonçalves, V.; Pinto, E.; Laranjeira, F.; Prata, M.J.; Jordan, P.; Desviat, L.R.; Pérez, B.; Alves, S. Functional analysis of splicing mutations in the IDS gene and the use of antisense oligonucleotides to exploit an alternative therapy for MPS II. *Biochim. Biophys. Acta.* **2015**, *1852*, 2712–2721. [CrossRef]
67. Matos, L.; Duarte, A.J.; Ribeiro, D.; Chaves, J.; Amaral, O.; Alves, S. Correction of a Splicing Mutation Affecting an Unverricht-Lundborg Disease Patient by Antisense Therapy. *Genes* **2018**, *9*, 455. [CrossRef]
68. Matos, L.; Vilela, R.; Rocha, M.; Santos, J.I.; Coutinho, M.F.; Gaspar, P.; Prata, M.J.; Alves, S. Development of an Antisense Oligonucleotide-Mediated Exon Skipping Therapeutic Strategy for Mucolipidosis II: Validation at RNA Level. *Hum. Gene* **2020**, *31*, 775–783. [CrossRef]

69. Crivaro, A.N.; Mucci, J.M.; Bondar, C.M.; Ormazabal, M.E.; Ceci, R.; Simonaro, C.; Rozenfeld, P.A. Efficacy of pentosan polysulfate in in vitro models of lysosomal storage disorders: Fabry and Gaucher Disease. *PLoS ONE* **2019**, *14*, e0217780. [CrossRef] [PubMed]
70. Gabig-Cimińska, M.; Jakóbkiewicz-Banecka, J.; Malinowska, M.; Kloska, A.; Piotrowska, E.; Chmielarz, I.; Moskot, M.; Węgrzyn, A.; Węgrzyn, G. Combined Therapies for Lysosomal Storage Diseases. *Curr. Mol. Med.* **2015**, *15*, 746–771. [CrossRef]
71. Coutinho, M.F.; Santos, J.I.; Matos, L.; Alves, S. Genetic Substrate Reduction Therapy: A Promising Approach for Lysosomal Storage Disorders. *Diseases* **2016**, *4*, 33. [CrossRef] [PubMed]
72. Wang, Z.; Rao, D.D.; Senzer, N.; Nemunaitis, J. RNA interference and cancer therapy. *Pharm. Res.* **2011**, *28*, 2983–2995. [CrossRef] [PubMed]
73. Whitehead, K.A.; Langer, R.; Anderson, D.G. Knocking down barriers: Advances in siRNA delivery. *Nat. Rev. Drug Discov.* **2009**, *8*, 129–138. [CrossRef]
74. Aagaard, L.; Rossi, J.J. RNAi therapeutics: Principles, prospects and challenges. *Adv. Drug Deliv. Rev.* **2007**, *59*, 75–86. [CrossRef]
75. John, B.; Enright, A.J.; Aravin, A.; Tuschl, T.; Sander, C.; Marks, D.S. Human MicroRNA targets. *PloS Biol.* **2004**, *2*, e363. [CrossRef]
76. van de Water, F.M.; Boerman, O.C.; Wouterse, A.C.; Peters, J.G.; Russel, F.G.; Masereeuw, R. Intravenously administered short interfering RNA accumulates in the kidney and selectively suppresses gene function in renal proximal tubules. *Drug Metab. Dispos.* **2006**, *34*, 1393–1397. [CrossRef]
77. Alexis, F.; Pridgen, E.; Molnar, L.K.; Farokhzad, O.C. Factors affecting the clearance and biodistribution of polymeric nanoparticles. *Mol. Pharm.* **2008**, *5*, 505–515. [CrossRef]
78. Guo, P.; Coban, O.; Snead, N.M.; Trebley, J.; Hoeprich, S.; Guo, S.; Shu, Y. Engineering RNA for targeted siRNA delivery and medical application. *Adv. Drug Deliv. Rev.* **2010**, *62*, 650–666. [CrossRef]
79. Mosser, D.M.; Edwards, J.P. Exploring the full spectrum of macrophage activation. *Nat. Rev. Immunol.* **2008**, *8*, 958–969. [CrossRef] [PubMed]
80. Xu, C.F.; Liu, Y.; Shen, S.; Zhu, Y.H.; Wang, J. Targeting glucose uptake of glioma cells by siRNA delivery with polymer nanoparticle. *J. Control. Release* **2015**, *213*, 23–24. [CrossRef] [PubMed]
81. Hornung, V.; Guenthner-Biller, M.; Bourquin, C.; Ablasser, A.; Schlee, M.; Uematsu, S.; Noronha, A.; Manoharan, M.; Akira, S.; de Fougerolles, A.; et al. Sequence-specific potent induction of IFN-alpha by short interfering RNA in plasmacytoid dendritic cells through TLR7. *Nat. Med.* **2005**, *11*, 263–270. [CrossRef] [PubMed]
82. Birmingham, A.; Anderson, E.M.; Reynolds, A.; Ilsley-Tyree, D.; Leake, D.; Fedorov, Y.; Baskerville, S.; Maksimova, E.; Robinson, K.; Karpilow, J.; et al. 3′ UTR seed matches, but not overall identity, are associated with RNAi off-targets. *Nat. Methods* **2006**, *3*, 199–204. [CrossRef]
83. Jackson, A.L.; Burchard, J.; Schelter, J.; Chau, B.N.; Cleary, M.; Lim, L.; Linsley, P.S. Widespread siRNA "off-target" transcript silencing mediated by seed region sequence complementarity. *RNA* **2006**, *12*, 1179–1187. [CrossRef]
84. Jackson, A.L.; Linsley, P.S. Recognizing and avoiding siRNA off-target effects for target identification and therapeutic application. *Nat. Rev. Drug Discov.* **2010**, *9*, 57–67. [CrossRef]
85. Zhang, B.; Mallapragada, S. The mechanism of selective transfection mediated by pentablock copolymers; part II: Nuclear entry and endosomal escape. *Acta. Biomater.* **2011**, *7*, 1580–1587. [CrossRef]
86. Gomes, M.J.; Martins, S.; Sarmento, B. siRNA as a tool to improve the treatment of brain diseases: Mechanism, targets and delivery. *Ageing Res. Rev.* **2015**, *21*, 43–54. [CrossRef]
87. Diaz-Font, A.; Chabás, A.; Grinberg, D.; Vilageliu, L. RNAi-mediated inhibition of the glucosylceramide synthase (GCS) gene: A preliminary study towards a therapeutic strategy for Gaucher disease and other glycosphingolipid storage diseases. *Blood Cells Mol. Dis.* **2006**, *37*, 197–203. [CrossRef]
88. Zimran, A.; Elstein, D. Management of Gaucher disease: Enzyme replacement therapy. *Pediatr. Endocrinol. Rev.* **2014**, *12*, 82–87.
89. Cox, T.; Lachmann, R.; Hollak, C.; Aerts, J.; van Weely, S.; Hrebícek, M.; Platt, F.; Butters, T.; Dwek, R.; Moyses, C.; et al. Novel oral treatment of Gaucher's disease with N-butyldeoxynojirimycin (OGT 918) to decrease substrate biosynthesis. *Lancet* **2000**, *355*, 1481–1485. [CrossRef]
90. Venier, R.E.; Igdoura, S.A. Miglustat as a therapeutic agent: Prospects and caveats. *J. Med. Genet.* **2012**, *49*, 591–597. [CrossRef] [PubMed]

91. Nabizadeh, A.; Amani, B.; Kadivar, M.; Toroski, M.; Asl, A.A.; Bayazidi, Y.; Mojahedian, M.; Davari, M. The Clinical Efficacy of Imiglucerase versus Eliglustat in Patients with Gaucher's Disease Type 1: A Systematic Review. *J. Res. Pharm. Pr.* **2018**, *7*, 171–177. [CrossRef]
92. Wegrzyn, G.; Jakóbkiewicz-Banecka, J.; Gabig-Cimińska, M.; Piotrowska, E.; Narajczyk, M.; Kloska, A.; Malinowska, M.; Dziedzic, D.; Gołebiewska, I.; Moskot, M.; et al. Genistein: A natural isoflavone with a potential for treatment of genetic diseases. *Biochem. Soc. Trans.* **2010**, *38*, 695–701. [CrossRef] [PubMed]
93. Derrick-Roberts, A.L.; Marais, W.; Byers, S. Rhodamine B and 2-acetamido-1,3,6-tri-O-acetyl-4-deoxy-4-fluoro-D-glucopyranose (F-GlcNAc) inhibit chondroitin/dermatan and keratan sulphate synthesis by different mechanisms in bovine chondrocytes. *Mol. Genet. Metab.* **2012**, *106*, 214–220. [CrossRef]
94. Dziedzic, D.; Wegrzyn, G.; Jakóbkiewicz-Banecka, J. Impairment of glycosaminoglycan synthesis in mucopolysaccharidosis type IIIA cells by using siRNA: A potential therapeutic approach for Sanfilippo disease. *Eur. J. Hum. Genet.* **2010**, *18*, 200–205. [CrossRef] [PubMed]
95. Dziedzic, D.; Narajczyk, M.; Gabig-Cimińska, M.; Jakóbkiewicz-Banecka, J. Simultaneous siRNA-mediated silencing of pairs of genes coding for enzymes involved in glycosaminoglycan synthesis. *Acta Biochim. Pol.* **2012**, *59*, 293–298. [CrossRef]
96. Kaidonis, X.; Liaw, W.C.; Roberts, A.D.; Ly, M.; Anson, D.; Byers, S. Gene silencing of EXTL2 and EXTL3 as a substrate deprivation therapy for heparan sulphate storing mucopolysaccharidoses. *Eur. J. Hum. Genet.* **2010**, *18*, 194–199. [CrossRef]
97. Chmielarz, I.; Gabig-Cimińska, M.; Malinowska, M.; Banecka-Majkutewicz, Z.; Węgrzyn, A.; Jakobkiewicz-Banecka, J. Comparison of siRNA-mediated silencing of glycosaminoglycan synthesis genes and enzyme replacement therapy for mucopolysaccharidosis in cell culture studies. *Acta. Biochim. Pol.* **2012**, *59*, 697–702. [CrossRef]
98. Canals, I.; Benetó, N.; Cozar, M.; Vilageliu, L.; Grinberg, D. EXTL2 and EXTL3 inhibition with siRNAs as a promising substrate reduction therapy for Sanfilippo C syndrome. *Sci. Rep.* **2015**, *5*, 13654. [CrossRef]
99. Benetó, N.; Cozar, M.; García-Morant, M.; Creus-Bachiller, E.; Vilageliu, L.; Grinberg, D.; Canals, I. Generation of two compound heterozygous HGSNAT-mutated lines from healthy induced pluripotent stem cells using CRISPR/Cas9 to model Sanfilippo C syndrome. *Stem Cell Res.* **2019**, *41*, 101616. [CrossRef] [PubMed]
100. Benetó, N.; Cozar, M.; Castilla-Vallmanya, L.; Zetterdahl, O.G.; Sacultanu, M.; Segur-Bailach, E.; García-Morant, M.; Ribes, A.; Ahlenius, H.; Grinberg, D.; et al. Neuronal and Astrocytic Differentiation from Sanfilippo C Syndrome iPSCs for Disease Modeling and Drug Development. *J. Clin. Med.* **2020**, *9*, 644. [CrossRef] [PubMed]
101. Platt, F.M. Emptying the stores: Lysosomal diseases and therapeutic strategies. *Nat. Rev. Drug Discov.* **2018**, *17*, 133–150. [CrossRef] [PubMed]
102. Vaishnaw, A.K.; Gollob, J.; Gamba-Vitalo, C.; Hutabarat, R.; Sah, D.; Meyers, R.; de Fougerolles, T.; Maraganore, J. A status report on RNAi therapeutics. *Silence* **2010**, *1*, 14. [CrossRef]
103. Gomes-da-Silva, L.C.; Fonseca, N.A.; Moura, V.; Pedroso de Lima, M.C.; Simões, S.; Moreira, J.N. Lipid-based nanoparticles for siRNA delivery in cancer therapy: Paradigms and challenges. *ACC Chem. Res.* **2012**, *45*, 1163–1171. [CrossRef]
104. Tatiparti, K.; Sau, S.; Kashaw, S.K.; Iyer, A.K. siRNA Delivery Strategies: A Comprehensive Review of Recent Developments. *Nanomaterials* **2017**, *7*, 77. [CrossRef]
105. Akinc, A.; Zumbuehl, A.; Goldberg, M.; Leshchiner, E.S.; Busini, V.; Hossain, N.; Bacallado, S.A.; Nguyen, D.N.; Fuller, J.; Alvarez, R.; et al. A combinatorial library of lipid-like materials for delivery of RNAi therapeutics. *Nat. Biotechnol.* **2008**, *26*, 561–569. [CrossRef]
106. Semple, S.C.; Akinc, A.; Chen, J.; Sandhu, A.P.; Mui, B.L.; Cho, C.K.; Sah, D.W.; Stebbing, D.; Crosley, E.J.; Yaworski, E.; et al. Rational design of cationic lipids for siRNA delivery. *Nat. Biotechnol.* **2010**, *28*, 172–176. [CrossRef]
107. Shi, B.; Keough, E.; Matter, A.; Leander, K.; Young, S.; Carlini, E.; Sachs, A.B.; Tao, W.; Abrams, M.; Howell, B.; et al. Biodistribution of small interfering RNA at the organ and cellular levels after lipid nanoparticle-mediated delivery. *J. Histochem. Cytochem.* **2011**, *59*, 727–740. [CrossRef]
108. Wittrup, A.; Lieberman, J. Knocking down disease: A progress report on siRNA therapeutics. *Nat. Rev. Genet.* **2015**, *16*, 543–552. [CrossRef]

109. Akinc, A.; Querbes, W.; De, S.; Qin, J.; Frank-Kamenetsky, M.; Jayaprakash, K.N.; Jayaraman, M.; Rajeev, K.G.; Cantley, W.L.; Dorkin, J.R.; et al. Targeted delivery of RNAi therapeutics with endogenous and exogenous ligand-based mechanisms. *Mol. Ther.* **2010**, *18*, 1357–1364. [CrossRef] [PubMed]
110. Gooding, M.; Browne, L.P.; Quinteiro, F.M.; Selwood, D.L. siRNA delivery: From lipids to cell-penetrating peptides and their mimics. *Chem. Biol. Drug Des.* **2012**, *80*, 787–809. [CrossRef] [PubMed]
111. Czech, M.P.; Aouadi, M.; Tesz, G.J. RNAi-based therapeutic strategies for metabolic disease. *Nat. Rev. Endocrinol.* **2011**, *7*, 473–484. [CrossRef]
112. Coelho, T.; Adams, D.; Silva, A.; Lozeron, P.; Hawkins, P.N.; Mant, T.; Perez, J.; Chiesa, J.; Warrington, S.; Tranter, E.; et al. Safety and efficacy of RNAi therapy for transthyretin amyloidosis. *N. Engl. J. Med.* **2013**, *369*, 819–829. [CrossRef]
113. Suhr, O.B.; Coelho, T.; Buades, J.; Pouget, J.; Conceicao, I.; Berk, J.; Schmidt, H.; Waddington-Cruz, M.; Campistol, J.M.; Bettencourt, B.R.; et al. Efficacy and safety of patisiran for familial amyloidotic polyneuropathy: A phase II multi-dose study. *Orphanet J. Rare Dis.* **2015**, *10*, 109. [CrossRef] [PubMed]
114. Robbins, M.; Judge, A.; MacLachlan, I. siRNA and innate immunity. *Oligonucleotides* **2009**, *19*, 89–102. [CrossRef]
115. Crooke, S.T.; Witztum, J.L.; Bennett, C.F.; Baker, B.F. RNA-Targeted Therapeutics. *Cell Metab.* **2018**, *27*, 714–739. [CrossRef]
116. Xie, F.Y.; Woodle, M.C.; Lu, P.Y. Harnessing in vivo siRNA delivery for drug discovery and therapeutic development. *Drug Discov. Today* **2006**, *11*, 67–73. [CrossRef]
117. Schiffelers, R.M.; Mixson, A.J.; Ansari, A.M.; Fens, M.H.; Tang, Q.; Zhou, Q.; Xu, J.; Molema, G.; Lu, P.Y.; Scaria, P.V.; et al. Transporting silence: Design of carriers for siRNA to angiogenic endothelium. *J. Control. Release* **2005**, *109*, 5–14. [CrossRef]
118. Ishida, T.; Atobe, K.; Wang, X.; Kiwada, H. Accelerated blood clearance of PEGylated liposomes upon repeated injections: Effect of doxorubicin-encapsulation and high-dose first injection. *J. Control. Release* **2006**, *115*, 251–258. [CrossRef]
119. Ishida, T.; Ichihara, M.; Wang, X.; Yamamoto, K.; Kimura, J.; Majima, E.; Kiwada, H. Injection of PEGylated liposomes in rats elicits PEG-specific IgM, which is responsible for rapid elimination of a second dose of PEGylated liposomes. *J. Control. Release* **2006**, *112*, 15–25. [CrossRef] [PubMed]
120. Song, L.Y.; Ahkong, Q.F.; Rong, Q.; Wang, Z.; Ansell, S.; Hope, M.J.; Mui, B. Characterization of the inhibitory effect of PEG-lipid conjugates on the intracellular delivery of plasmid and antisense DNA mediated by cationic lipid liposomes. *Biochim. Biophys. Acta* **2002**, *1558*, 1–13. [CrossRef]
121. Mishra, S.; Webster, P.; Davis, M.E. PEGylation significantly affects cellular uptake and intracellular trafficking of non-viral gene delivery particles. *Eur. J. Cell Biol.* **2004**, *83*, 97–111. [CrossRef] [PubMed]
122. Morrissey, D.V.; Blanchard, K.; Shaw, L.; Jensen, K.; Lockridge, J.A.; Dickinson, B.; McSwiggen, J.A.; Vargeese, C.; Bowman, K.; Shaffer, C.S.; et al. Activity of stabilized short interfering RNA in a mouse model of hepatitis B virus replication. *Hepatology* **2005**, *41*, 1349–1356. [CrossRef] [PubMed]
123. Morrissey, D.V.; Lockridge, J.A.; Shaw, L.; Blanchard, K.; Jensen, K.; Breen, W.; Hartsough, K.; Machemer, L.; Radka, S.; Jadhav, V.; et al. Potent and persistent in vivo anti-HBV activity of chemically modified siRNAs. *Nat. Biotechnol.* **2005**, *23*, 1002–1007. [CrossRef] [PubMed]
124. Zimmermann, T.S.; Lee, A.C.; Akinc, A.; Bramlage, B.; Bumcrot, D.; Fedoruk, M.N.; Harborth, J.; Heyes, J.A.; Jeffs, L.B.; John, M.; et al. RNAi-mediated gene silencing in non-human primates. *Nature* **2006**, *441*, 111–114. [CrossRef]
125. Cannon, C.P.; Braunwald, E.; McCabe, C.H.; Rader, D.J.; Rouleau, J.L.; Belder, R.; Joyal, S.V.; Hill, K.A.; Pfeffer, M.A.; Skene, A.M.; et al. Intensive versus moderate lipid lowering with statins after acute coronary syndromes. *N. Engl. J. Med.* **2004**, *350*, 1495–1504. [CrossRef]
126. Soutschek, J.; Akinc, A.; Bramlage, B.; Charisse, K.; Constien, R.; Donoghue, M.; Elbashir, S.; Geick, A.; Hadwiger, P.; Harborth, J.; et al. Therapeutic silencing of an endogenous gene by systemic administration of modified siRNAs. *Nature* **2004**, *432*, 173–178. [CrossRef]
127. Geisbert, T.W.; Hensley, L.E.; Kagan, E.; Yu, E.Z.; Geisbert, J.B.; Daddario-DiCaprio, K.; Fritz, E.A.; Jahrling, P.B.; McClintock, K.; Phelps, J.R.; et al. Postexposure protection of guinea pigs against a lethal ebola virus challenge is conferred by RNA interference. *J. Infect. Dis.* **2006**, *193*, 1650–1657. [CrossRef]

128. Geisbert, T.W.; Lee, A.C.; Robbins, M.; Geisbert, J.B.; Honko, A.N.; Sood, V.; Johnson, J.C.; de Jong, S.; Tavakoli, I.; Judge, A.; et al. Postexposure protection of non-human primates against a lethal Ebola virus challenge with RNA interference: A proof-of-concept study. *Lancet* **2010**, *375*, 1896–1905. [CrossRef]
129. Judge, A.D.; Robbins, M.; Tavakoli, I.; Levi, J.; Hu, L.; Fronda, A.; Ambegia, E.; McClintock, K.; MacLachlan, I. Confirming the RNAi-mediated mechanism of action of siRNA-based cancer therapeutics in mice. *J. Clin. Investig.* **2009**, *119*, 661–673. [CrossRef] [PubMed]
130. Tao, W.; South, V.J.; Zhang, Y.; Davide, J.P.; Farrell, L.; Kohl, N.E.; Sepp-Lorenzino, L.; Lobell, R.B. Induction of apoptosis by an inhibitor of the mitotic kinesin KSP requires both activation of the spindle assembly checkpoint and mitotic slippage. *Cancer Cell* **2005**, *8*, 49–59. [CrossRef] [PubMed]
131. Liu, X.; Erikson, R.L. Polo-like kinase (Plk)1 depletion induces apoptosis in cancer cells. *Proc. Natl. Acad. Sci. USA* **2003**, *100*, 5789–5794. [CrossRef] [PubMed]
132. Steegmaier, M.; Hoffmann, M.; Baum, A.; Lénárt, P.; Petronczki, M.; Krssák, M.; Gürtler, U.; Garin-Chesa, P.; Lieb, S.; Quant, J.; et al. BI 2536, a potent and selective inhibitor of polo-like kinase 1, inhibits tumor growth in vivo. *Curr. Biol.* **2007**, *17*, 316–322. [CrossRef]
133. Adams, D.; Coelho, T.; Conceicao, I.; Cruz, M.W.n.; Schmidt, H.; Buades, J.; Campistol, J.; Pouget, J.; Berk, J.; Polydefkis, M.; et al. Phase 2 Open-Label Extension (OLE) Study of Patisiran, an Investigational RNA interference (RNAi) Therapeutic for the Treatment of Hereditary ATTR Amyloidosis with Polyneuropathy (S27.004). *Neurology* **2017**, *88*, S27.004.
134. Adams, D.; Suhr, O.B.; Dyck, P.J.; Litchy, W.J.; Leahy, R.G.; Chen, J.; Gollob, J.; Coelho, T. Trial design and rationale for APOLLO, a Phase 3, placebo-controlled study of patisiran in patients with hereditary ATTR amyloidosis with polyneuropathy. *BMC Neurol.* **2017**, *17*, 181. [CrossRef]
135. Hoy, S.M. Patisiran: First Global Approval. *Drugs* **2018**, *78*, 1625–1631. [CrossRef]
136. Iyer, A.K.; Khaled, G.; Fang, J.; Maeda, H. Exploiting the enhanced permeability and retention effect for tumor targeting. *Drug Discov. Today* **2006**, *11*, 812–818. [CrossRef]
137. Fang, J.; Nakamura, H.; Maeda, H. The EPR effect: Unique features of tumor blood vessels for drug delivery, factors involved, and limitations and augmentation of the effect. *Adv. Drug Deliv. Rev.* **2011**, *63*, 136–151. [CrossRef]
138. Danhier, F. To exploit the tumor microenvironment: Since the EPR effect fails in the clinic, what is the future of nanomedicine? *J. Control. Release* **2016**, *244*, 108–121. [CrossRef]
139. Mendonça, L.S.; Firmino, F.; Moreira, J.N.; Pedroso de Lima, M.C.; Simões, S. Transferrin receptor-targeted liposomes encapsulating anti-BCR-ABL siRNA or asODN for chronic myeloid leukemia treatment. *Bioconjug. Chem.* **2010**, *21*, 157–168. [CrossRef] [PubMed]
140. Savona, M.; Talpaz, M. Getting to the stem of chronic myeloid leukaemia. *Nat. Rev. Cancer* **2008**, *8*, 341–350. [CrossRef] [PubMed]
141. Ponka, P.; Lok, C.N. The transferrin receptor: Role in health and disease. *Int. J. Biochem. Cell Biol.* **1999**, *31*, 1111–1137. [CrossRef]
142. Li, H.; Qian, Z.M. Transferrin/transferrin receptor-mediated drug delivery. *Med. Res. Rev.* **2002**, *22*, 225–250. [CrossRef] [PubMed]
143. Daniels, T.R.; Delgado, T.; Rodriguez, J.A.; Helguera, G.; Penichet, M.L. The transferrin receptor part I: Biology and targeting with cytotoxic antibodies for the treatment of cancer. *Clin. Immunol.* **2006**, *121*, 144–158. [CrossRef] [PubMed]
144. Daniels, T.R.; Delgado, T.; Helguera, G.; Penichet, M.L. The transferrin receptor part II: Targeted delivery of therapeutic agents into cancer cells. *Clin. Immunol.* **2006**, *121*, 159–176. [CrossRef]
145. Savage, D.G.; Antman, K.H. Imatinib mesylate–a new oral targeted therapy. *N. Engl. J. Med.* **2002**, *346*, 683–693. [CrossRef]
146. Walz, C.; Sattler, M. Novel targeted therapies to overcome imatinib mesylate resistance in chronic myeloid leukemia (CML). *Crit. Rev. Oncol. Hematol.* **2006**, *57*, 145–164. [CrossRef]
147. Mendonça, L.S.; Moreira, J.N.; de Lima, M.C.; Simões, S. Co-encapsulation of anti-BCR-ABL siRNA and imatinib mesylate in transferrin receptor-targeted sterically stabilized liposomes for chronic myeloid leukemia treatment. *Biotechnol. Bioeng.* **2010**, *107*, 884–893. [CrossRef]
148. Hanahan, D.; Weinberg, R.A. Hallmarks of cancer: The next generation. *Cell* **2011**, *144*, 646–674. [CrossRef]

149. Christian, S.; Pilch, J.; Akerman, M.E.; Porkka, K.; Laakkonen, P.; Ruoslahti, E. Nucleolin expressed at the cell surface is a marker of endothelial cells in angiogenic blood vessels. *J. Cell Biol.* **2003**, *163*, 871–878. [CrossRef] [PubMed]
150. Porkka, K.; Laakkonen, P.; Hoffman, J.A.; Bernasconi, M.; Ruoslahti, E. A fragment of the HMGN2 protein homes to the nuclei of tumor cells and tumor endothelial cells in vivo. *Proc. Natl. Acad. Sci. USA* **2002**, *99*, 7444–7449. [CrossRef] [PubMed]
151. Gomes-da-Silva, L.C.; Fernández, Y.; Abasolo, I.; Schwartz, S.; Ramalho, J.S.; Pedroso de Lima, M.C.; Simões, S.; Moreira, J.N. Efficient intracellular delivery of siRNA with a safe multitargeted lipid-based nanoplatform. *Nanomedicine (London)* **2013**, *8*, 1397–1413. [CrossRef] [PubMed]
152. Gomes-da-Silva, L.C.; Santos, A.O.; Bimbo, L.M.; Moura, V.; Ramalho, J.S.; Pedroso de Lima, M.C.; Simões, S.; Moreira, J.N. Toward a siRNA-containing nanoparticle targeted to breast cancer cells and the tumor microenvironment. *Int. J. Pharm.* **2012**, *434*, 9–19. [CrossRef] [PubMed]
153. Gomes-da-Silva, L.C.; Ramalho, J.S.; Pedroso de Lima, M.C.; Simões, S.; Moreira, J.N. Impact of anti-PLK1 siRNA-containing F3-targeted liposomes on the viability of both cancer and endothelial cells. *Eur. J. Pharm. Biopharm.* **2013**, *85*, 356–364. [CrossRef]
154. Moura, V.; Lacerda, M.; Figueiredo, P.; Corvo, M.L.; Cruz, M.E.; Soares, R.; de Lima, M.C.; Simões, S.; Moreira, J.N. Targeted and intracellular triggered delivery of therapeutics to cancer cells and the tumor microenvironment: Impact on the treatment of breast cancer. *Breast Cancer Res. Treat.* **2012**, *133*, 61–73. [CrossRef]
155. Fonseca, N.A.; Gomes-da-Silva, L.C.; Moura, V.; Simões, S.; Moreira, J.N. Simultaneous active intracellular delivery of doxorubicin and C6-ceramide shifts the additive/antagonistic drug interaction of non-encapsulated combination. *J. Control. Release* **2014**, *196*, 122–131. [CrossRef]
156. Fonseca, N.A.; Rodrigues, A.S.; Rodrigues-Santos, P.; Alves, V.; Gregório, A.C.; Valério-Fernandes, Â.; Gomes-da-Silva, L.C.; Rosa, M.S.; Moura, V.; Ramalho-Santos, J.; et al. Nucleolin overexpression in breast cancer cell sub-populations with different stem-like phenotype enables targeted intracellular delivery of synergistic drug combination. *Biomaterials* **2015**, *69*, 76–88. [CrossRef]
157. Chaffer, C.L.; Marjanovic, N.D.; Lee, T.; Bell, G.; Kleer, C.G.; Reinhardt, F.; D'Alessio, A.C.; Young, R.A.; Weinberg, R.A. Poised chromatin at the ZEB1 promoter enables breast cancer cell plasticity and enhances tumorigenicity. *Cell* **2013**, *154*, 61–74. [CrossRef]
158. Costa, P.M.; Cardoso, A.L.; Mendonça, L.S.; Serani, A.; Custódia, C.; Conceição, M.; Simões, S.; Moreira, J.N.; Pereira de Almeida, L.; Pedroso de Lima, M.C. Tumor-targeted Chlorotoxin-coupled Nanoparticles for Nucleic Acid Delivery to Glioblastoma Cells: A Promising System for Glioblastoma Treatment. *Mol. Nucleic Acids* **2013**, *2*, e100. [CrossRef]
159. Costa, P.M.; Cardoso, A.L.; Custódia, C.; Cunha, P.; Pereira de Almeida, L.; Pedroso de Lima, M.C. MiRNA-21 silencing mediated by tumor-targeted nanoparticles combined with sunitinib: A new multimodal gene therapy approach for glioblastoma. *J. Control. Release* **2015**, *207*, 31–39. [CrossRef] [PubMed]
160. Godfrey, C.; Desviat, L.R.; Smedsrod, B.; Pietri-Rouxel, F.; Denti, M.A.; Disterer, P.; Lorain, S.; Nogales-Gadea, G.; Sardone, V.; Anwar, R.; et al. Delivery is key: Lessons learnt from developing splice-switching antisense therapies. *Embo. Mol. Med.* **2017**, *9*, 545–557. [CrossRef] [PubMed]
161. Gabathuler, R. Approaches to transport therapeutic drugs across the blood-brain barrier to treat brain diseases. *Neurobiol. Dis.* **2010**, *37*, 48–57. [CrossRef] [PubMed]
162. Simões, S.; Slepushkin, V.; Gaspar, R.; de Lima, M.C.; Düzgüneş, N. Gene delivery by negatively charged ternary complexes of DNA, cationic liposomes and transferrin or fusigenic peptides. *Gene Ther.* **1998**, *5*, 955–964. [CrossRef]
163. Simões, S.; Slepushkin, V.; Pires, P.; Gaspar, R.; de Lima, M.P.; Düzgüneş, N. Mechanisms of gene transfer mediated by lipoplexes associated with targeting ligands or pH-sensitive peptides. *Gene Ther.* **1999**, *6*, 1798–1807. [CrossRef]
164. Simões, S.; Slepushkin, V.; Pretzer, E.; Dazin, P.; Gaspar, R.; Pedroso de Lima, M.C.; Düzgüneş, N. Transfection of human macrophages by lipoplexes via the combined use of transferrin and pH-sensitive peptides. *J. Leukoc. Biol.* **1999**, *65*, 270–279. [CrossRef]
165. Tros de Ilarduya, C.; Düzgüneş, N. Efficient gene transfer by transferrin lipoplexes in the presence of serum. *Biochim. Biophys. Acta* **2000**, *1463*, 333–342. [CrossRef]

166. da Cruz, M.T.; Simões, S.; de Lima, M.C. Improving lipoplex-mediated gene transfer into C6 glioma cells and primary neurons. *Exp. Neurol.* **2004**, *187*, 65–75. [CrossRef]
167. da Cruz, M.T.; Cardoso, A.L.; de Almeida, L.P.; Simões, S.; de Lima, M.C. Tf-lipoplex-mediated NGF gene transfer to the CNS: Neuronal protection and recovery in an excitotoxic model of brain injury. *Gene* **2005**, *12*, 1242–1252. [CrossRef]
168. Cardoso, A.L.; Simões, S.; de Almeida, L.P.; Pelisek, J.; Culmsee, C.; Wagner, E.; Pedroso de Lima, M.C. siRNA delivery by a transferrin-associated lipid-based vector: A non-viral strategy to mediate gene silencing. *J. Gene Med.* **2007**, *9*, 170–183. [CrossRef]
169. Cardoso, A.L.; Simões, S.; de Almeida, L.P.; Plesnila, N.; Pedroso de Lima, M.C.; Wagner, E.; Culmsee, C. Tf-lipoplexes for neuronal siRNA delivery: A promising system to mediate gene silencing in the CNS. *J. Control. Release* **2008**, *132*, 113–123. [CrossRef] [PubMed]
170. Cardoso, A.L.; Costa, P.; de Almeida, L.P.; Simões, S.; Plesnila, N.; Culmsee, C.; Wagner, E.; de Lima, M.C. Tf-lipoplex-mediated c-Jun silencing improves neuronal survival following excitotoxic damage in vivo. *J. Control. Release* **2010**, *142*, 392–403. [CrossRef] [PubMed]
171. Son, S.; Hwang, D.W.; Singha, K.; Jeong, J.H.; Park, T.G.; Lee, D.S.; Kim, W.J. RVG peptide tethered bioreducible polyethylenimine for gene delivery to brain. *J. Control. Release* **2011**, *155*, 18–25. [CrossRef] [PubMed]
172. Huey, R.; Hawthorne, S.; McCarron, P. The potential use of rabies virus glycoprotein-derived peptides to facilitate drug delivery into the central nervous system: A mini review. *J. Drug Target.* **2017**, *25*, 379–385. [CrossRef] [PubMed]
173. Fu, A.; Zhao, Z.; Gao, F.; Zhang, M. Cellular uptake mechanism and therapeutic utility of a novel peptide in targeted-delivery of proteins into neuronal cells. *Pharm. Res.* **2013**, *30*, 2108–2117. [CrossRef] [PubMed]
174. Oswald, M.; Geissler, S.; Goepferich, A. Targeting the Central Nervous System (CNS): A Review of Rabies Virus-Targeting Strategies. *Mol. Pharm.* **2017**, *14*, 2177–2196. [CrossRef]
175. Cantin, E.M.; Rossi, J.J. Molecular medicine: Entry granted. *Nature* **2007**, *448*, 33–34. [CrossRef]
176. Kumar, P.; Wu, H.; McBride, J.L.; Jung, K.E.; Kim, M.H.; Davidson, B.L.; Lee, S.K.; Shankar, P.; Manjunath, N. Transvascular delivery of small interfering RNA to the central nervous system. *Nature* **2007**, *448*, 39–43. [CrossRef]
177. Lewis, P.; Fu, Y.; Lentz, T.L. Rabies virus entry at the neuromuscular junction in nerve-muscle cocultures. *Muscle Nerve* **2000**, *23*, 720–730. [CrossRef]
178. Hislop, J.N.; Islam, T.A.; Eleftheriadou, I.; Carpentier, D.C.; Trabalza, A.; Parkinson, M.; Schiavo, G.; Mazarakis, N.D. Rabies virus envelope glycoprotein targets lentiviral vectors to the axonal retrograde pathway in motor neurons. *J. Biol. Chem.* **2014**, *289*, 16148–16163. [CrossRef]
179. Kwon, E.J.; Lasiene, J.; Jacobson, B.E.; Park, I.K.; Horner, P.J.; Pun, S.H. Targeted nonviral delivery vehicles to neural progenitor cells in the mouse subventricular zone. *Biomaterials* **2010**, *31*, 2417–2424. [CrossRef] [PubMed]
180. Huang, R.; Ke, W.; Liu, Y.; Wu, D.; Feng, L.; Jiang, C.; Pei, Y. Gene therapy using lactoferrin-modified nanoparticles in a rotenone-induced chronic Parkinson model. *J. Neurol. Sci.* **2010**, *290*, 123–130. [CrossRef] [PubMed]
181. Lu, Y.J.; Wei, K.C.; Ma, C.C.; Yang, S.Y.; Chen, J.P. Dual targeted delivery of doxorubicin to cancer cells using folate-conjugated magnetic multi-walled carbon nanotubes. *Colloids Surf. B. Biointerfaces* **2012**, *89*, 1–9. [CrossRef] [PubMed]
182. Gao, J.Q.; Lv, Q.; Li, L.M.; Tang, X.J.; Li, F.Z.; Hu, Y.L.; Han, M. Glioma targeting and blood-brain barrier penetration by dual-targeting doxorubincin liposomes. *Biomaterials* **2013**, *34*, 5628–5639. [CrossRef] [PubMed]
183. Li, Z.; Loh, X.J. Recent advances of using polyhydroxyalkanoate-based nanovehicles as therapeutic delivery carriers. *Nanomed. Nanobiotechnol.* **2016**, *9*, e1429. [CrossRef] [PubMed]
184. Byeon, H.J.; Thao, l.Q.; Lee, S.; Min, S.Y.; Lee, E.S.; Shin, B.S.; Choi, H.G.; Youn, Y.S. Doxorubicin-loaded nanoparticles consisted of cationic- and mannose-modified-albumins for dual-targeting in brain tumors. *J. Control. Release* **2016**, *225*, 301–313. [CrossRef]
185. Shevtsov, M.A.; Nikolaev, B.P.; Yakovleva, L.Y.; Dobrodumov, A.V.; Zhakhov, A.V.; Mikhrina, A.L.; Pitkin, E.; Parr, M.A.; Rolich, V.I.; Simbircev, A.S.; et al. Recombinant interleukin-1 receptor antagonist conjugated to superparamagnetic iron oxide nanoparticles for theranostic targeting of experimental glioblastoma. *Neoplasia* **2015**, *17*, 32–42. [CrossRef]

186. Meng, J.; Agrahari, V.; Youm, I. Advances in Targeted Drug Delivery Approaches for the Central Nervous System Tumors: The Inspiration of Nanobiotechnology. *J. Neuroimmune Pharm.* **2017**, *12*, 84–98. [CrossRef]
187. Conceição, M.; Mendonça, L.; Nóbrega, C.; Gomes, C.; Costa, P.; Hirai, H.; Moreira, J.N.; Lima, M.C.; Manjunath, N.; Pereira de Almeida, L. Intravenous administration of brain-targeted stable nucleic acid lipid particles alleviates Machado-Joseph disease neurological phenotype. *Biomaterials* **2016**, *82*, 124–137. [CrossRef]
188. Santos, A.O.; da Silva, L.C.; Bimbo, L.M.; de Lima, M.C.; Simões, S.; Moreira, J.N. Design of peptide-targeted liposomes containing nucleic acids. *Biochim. Biophys. Acta* **2010**, *1798*, 433–441. [CrossRef]
189. Borel, F.; Kay, M.A.; Mueller, C. Recombinant AAV as a platform for translating the therapeutic potential of RNA interference. *Mol. Ther.* **2014**, *22*, 692–701. [CrossRef] [PubMed]
190. Kleine Holthaus, S.M.; Smith, A.J.; Mole, S.E.; Ali, R.R. Gene Therapy Approaches to Treat the Neurodegeneration and Visual Failure in Neuronal Ceroid Lipofuscinoses. *Adv. Exp. Med. Biol.* **2018**, *1074*, 91–99. [CrossRef] [PubMed]
191. Haney, M.J.; Zhao, Y.; Jin, Y.S.; Batrakova, E.V. Extracellular Vesicles as Drug Carriers for Enzyme Replacement Therapy to Treat CLN2 Batten Disease: Optimization of Drug Administration Routes. *Cells* **2020**, *9*, 1273. [CrossRef]
192. Banks, W.A.; Farr, S.A.; Butt, W.; Kumar, V.B.; Franko, M.W.; Morley, J.E. Delivery across the blood-brain barrier of antisense directed against amyloid beta: Reversal of learning and memory deficits in mice overexpressing amyloid precursor protein. *J. Pharm. Exp. Ther.* **2001**, *297*, 1113–1121.
193. Lee, H.J.; Boado, R.J.; Braasch, D.A.; Corey, D.R.; Pardridge, W.M. Imaging gene expression in the brain in vivo in a transgenic mouse model of Huntington's disease with an antisense radiopharmaceutical and drug-targeting technology. *J. Nucl. Med.* **2002**, *43*, 948–956.
194. Kozlu, S.; Caban, S.; Yerlikaya, F.; Fernandez-Megia, E.; Novoa-Carballal, R.; Riguera, R.; Yemisci, M.; Gursoy-Ozdemir, Y.; Dalkara, T.; Couvreur, P.; et al. An aquaporin 4 antisense oligonucleotide loaded, brain targeted nanoparticulate system design. *Pharmazie* **2014**, *69*, 340–345.
195. Matos, L.; Canals, I.; Dridi, L.; Choi, Y.; Prata, M.J.; Jordan, P.; Desviat, L.R.; Pérez, B.; Pshezhetsky, A.V.; Grinberg, D.; et al. Therapeutic strategies based on modified U1 snRNAs and chaperones for Sanfilippo C splicing mutations. *Orphanet J. Rare Dis.* **2014**, *9*, 180. [CrossRef]
196. Di Paolo, D.; Brignole, C.; Pastorino, F.; Carosio, R.; Zorzoli, A.; Rossi, M.; Loi, M.; Pagnan, G.; Emionite, L.; Cilli, M.; et al. Neuroblastoma-targeted nanoparticles entrapping siRNA specifically knockdown ALK. *Mol. Ther.* **2011**, *19*, 1131–1140. [CrossRef]



© 2020 by the authors. Licensee MDPI, Basel, Switzerland. This article is an open access article distributed under the terms and conditions of the Creative Commons Attribution (CC BY) license (http://creativecommons.org/licenses/by/4.0/).

ANNEX 3 – BOOK CHAPTERS

Co-Authored by the PhD candidate

Book Chapter#1 - Matos L, Santos JI, Coutinho MF, Alves S. How to Design U1 snRNA Molecules for Splicing Rescue.

Book Chapter#2 - Coutinho MF, Matos L, Santos JI, Alves S. RNA Therapeutics: How Far Have We Gone?



Chapter 5

How to Design U1 snRNA Molecules for Splicing Rescue

Liliana Matos, Juliana I. Santos, Mª. Francisca Coutinho, and Sandra Alves

Abstract

Mutations affecting constitutive splice donor sites (5′ss) are among the most frequent genetic defects that disrupt the normal splicing process. Pre-mRNA splicing requires the correct identification of a number of *cis*-acting elements in an ordered fashion. By disrupting the complementarity of the 5′ss with the endogenous small nuclear RNA U1 (U1 snRNA), the key component of the spliceosomal U1 ribonucleoprotein, 5′ss mutations may result in exon skipping, intron retention or activation of cryptic splice sites. Engineered modification of the U1 snRNA seemed to be a logical method to overcome the effect of those mutations. In fact, over the last years, a number of in vitro studies on the use of those modified U1 snRNAs to correct a variety of splicing defects have demonstrated the feasibility of this approach. Furthermore, recent reports on its applicability in vivo are adding up to the principle that engineered modification of U1 snRNAs represents a valuable approach and prompting further studies to demonstrate the clinical translatability of this strategy.

Here, we outline the design and generation of U1 snRNAs with different degrees of complementarity to mutated 5′ss. Using the *HGSNAT* gene as an example, we describe the methods for a proper evaluation of their efficacy in vitro, taking advantage of our experience to share a number of tips on how to design U1 snRNA molecules for splicing rescue.

Key words U1 snRNA-based therapy, Splicing modulation, 5′ss mutations, Aberrant exon skipping, Modified U1 snRNA, Mucopolysaccharidosis IIIC

1 Introduction

The U1 small nuclear ribonucleoprotein (U1 snRNP) is a key molecule involved in an early event of the splicing process. Like other snRNPs involved in the overall splicing regulation process, it contains a small RNA complexed with several proteins, namely seven Smith antigen (Sm) proteins and three U1-specific proteins (U1A, U1C, and U170K) [1]. U1 snRNA, the RNA component of the U1 snRNP is a 164 nucleotides-long molecule whose 5′ end interacts by complementarity with the 5′ splice donor site (5′ss). That interaction between the single stranded 5′ tail of the U1 snRNA molecule and the moderately conserved stretch of nucleotides that constitutes the 5′ss (CAG/GURAGU, where R is a

Virginia Arechavala-Gomeza and Alejandro Garanto (eds.), *Antisense RNA Design, Delivery, and Analysis*, Methods in Molecular Biology, vol. 2434, https://doi.org/10.1007/978-1-0716-2010-6_5, © The Editor(s) (if applicable) and The Author(s) 2022

purine) marks the exon-intron boundary and initiates spliceosome assembly [2]. About 40%, 22%, and 5% of normal 5′ss contain two, three, or four mismatches towards the U1 snRNA, respectively [3, 4]. This variable degree of degeneration is among the major factors that significantly contribute to hinder a clear prediction of the effect of mutations flanking the canonical GU site. Furthermore, there is a number of additional elements, which may influence the splice site selection and need to be taken into account such as splicing silencer and enhancer motifs, the presence of alternative splice sites, secondary structures, and regulatory proteins [5]. Therefore, a straightforward prediction of the effect of mutations flanking the canonical GU site without a direct assessment of the mature mRNA produced can be quite challenging. Interestingly, however, it is also the variable degree of degeneration of 5′ss and the surprising heterogeneity existing among human spliceosomal snRNA, which allows for splicing correction using modified exogenous U1 snRNAs.

Overall, the rationale on the use of modified U1 snRNAs to correct splicing defects is as simple as it can be: as 5′ss mutations alter the 5′ss recognition by the endogenous U1 snRNA, exogenous U1 snRNAs may be engineered through complementary base pairing in order to correctly recognize the mutated allele and initiate spliceosome assembly, thus suppressing the mutation effect.

So far, the effects of modified U1 snRNAs have been tested in vitro in a number of cellular platforms from patient-derived cells to model cell lines overexpressing the splicing defects under study, and their potential to either fully or partially correct those mutations was demonstrated for a number of different diseases [5, 6]. Importantly, the application of this sort of modified U1 snRNAs in animal models has also been addressed in recent studies, with a few promising results reported to date [7–10] (*see* **Note 1**).

Globally, mutations affecting constitutive 5′ss represent roughly 8% of all known genetic disease-causing variants. Their pathogenicity derives from the reduced complementarity of the U1 snRNA to the 5′ss. 5′ss mutations mostly result in exon skipping but their effect over splicing may vary. Currently, there are a number of in silico tools that may help predict disease-causing effects, but cDNA analysis remains mandatory for a proper assessment of their consequence over splicing. For example, mutations affecting RNA splicing represent more than 20% of the mutant alleles in Mucopolysaccharidosis type IIIC (MPS IIIC; *HGSNAT* gene), a rare lysosomal storage disorder that causes severe neurodegeneration. Many of these mutations are located in the conserved splice donor or acceptor sites, while few are found in the nearby nucleotides. For three mutations that affect the donor site, we have previously developed different modified U1 snRNAs with compensatory changes that may allow for proper recognition of the mutated 5′ss, in an attempt to rescue the normal splicing process.

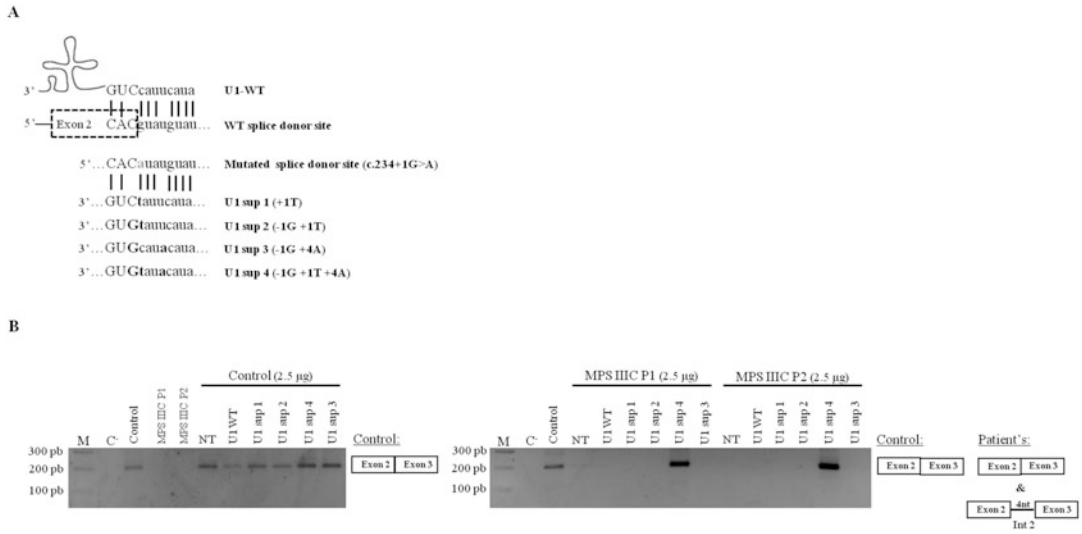


Fig. 1 Modified U1 snRNA therapeutic approach to correct the pathogenic effect of a 5′ splice site mutation on the *HGSNAT* gene. (**a**) Schematic illustration of base pairing between the wild-type U1 (U1-WT) and the 5′ss of wild-type and mutant exon 2 of the *HGSNAT* gene. The mutation position in the 5′ss is marked in grey and it is in italics. The different U1 snRNAs used for the mutated 5′ss of *HGSNAT* (designated as U1-sup, for suppressor) are also shown. The U1 sequence modifications are illustrated in bold. (**b**) RT-PCR analysis of the endogenous splicing pattern of control and MPS IIIC patients derived fibroblasts after transfection with different U1 isoforms. The constitutive splicing of exon 2 of the *HGSNAT gene* was not altered in control fibroblasts after overexpression of U1-WT or any of the modified U1 constructs. In the MPS IIIC patients 1 (MPS IIIC P1) and 2 (MPS IIIC P2), bearing the homozygous mutation c.234+1G>A, only the fully adapted U1 (U1-sup4) resulted in partial correction of exon 2 skipping

For the c.234+1G>A mutation, a totally complementary U1 snRNA allowed for partial correction of exon 2 aberrant splicing in patients' fibroblasts (Fig. 1) [11]. Here, we take advantage of our experience on the development of modified U1 snRNAs to compensate for those *HGSNAT* mutations, to present a practical overview on how to design U1 snRNA molecules for splicing rescue.

In summary, we present an overview of the experimental design for in vitro testing the potential of modified U1 snRNA vectors to correct aberrant splicing caused by 5′ss mutations. Briefly, we show: (a) how to design in silico U1's with different degrees of complementarity to each mutated 5′ss by introducing a number of sequence changes, and (b) how the different U1 vectors harboring those alterations are obtained by site-directed mutagenesis of the original wild-type (WT) human U1 snRNA-harboring pG3U1 vector [12], a derivative of pHU1 [13]. We also describe how these molecules are transfected into patients' fibroblasts and how their effectiveness on splicing redirection can be assessed by post-transfection cDNA analysis and sequencing. Finally, we elaborate on the relevance of further addressing the treatment's effect at protein level.

2 Materials

2.1 Generating Modified U1 snRNA Vectors Adapted to the 5′ss of Interest

1. The *Homo sapiens* U1 snRNA gene sequence is required to design primers for site-directed mutagenesis PCR and can be found in the Ensembl database (ENSG00000104852).
2. The sequence of the 5′ss of interest for splicing rescue can be found in Ensembl or other reference sequence databases (in this particular chapter we used the *Homo sapiens HGSNAT* gene sequence, ENSG00000165102).
3. pG3U1 vector [12] a derivative of pHU1 [13] (*see* **Note 2**).
4. Sense and antisense mutagenic primers.
5. PCR mutagenesis kit.
6. PCR thermocycler.
7. Chemically *Escherichia coli* competent cells (Homemade or commercial; usually are included in the PCR mutagenesis kits).
8. Water bath.
9. Thermomixer.
10. Ice.
11. Super optimal broth with catabolite repression (SOC) medium (commercially available).
12. Luria-Bertani (LB) agar medium (commercially available; sterilize by autoclaving) plates with selection antibiotic (100 μg/mL, ampicillin; *see* **Note 3**).
13. Sterile bacterial cell spreaders.
14. Plasmid DNA miniprep purification kit.
15. LB liquid medium (commercially available; sterilize by autoclaving).
16. Ampicillin.
17. 15 mL conical centrifuge tubes.
18. Sterile tips.
19. Orbital shaking incubator.
20. pG3U1 forward primer (U1-seq Fw—5′ CACGAAG GAGTTCCCGTG 3′).
21. Sterile flasks (1 L).
22. Endotoxin-free maxiprep plasmid DNA purification kit.
23. 40% Glycerol (sterilize by autoclaving).
24. 2 mL polypropylene conical tubes.

2.2 In Vitro Therapeutic Evaluation of Modified U1 snRNA Vectors in Human Fibroblasts

2.2.1 Transfection of Modified U1 snRNA Vectors in Human Fibroblasts

1. Human Dermal Fibroblasts from patients harboring the mutation under analysis (e.g. fibroblasts from patients' with MPS IIIC, carrying the c.234+1G>A mutation in homozigosity) and WT Human Dermal Fibroblasts to use as control.
2. Dulbecco's Modified Eagle's Medium (DMEM) + Glutamax supplemented with 10% Fetal Bovine Serum (FBS), 5% penicillin/streptomycin (PenStrep) antibiotics, and 5% amphotericin B (Fungizone®).
3. Phosphate buffered saline 1x (PBS).
4. Trypsin-EDTA.
5. CO_2 incubator.
6. 15 mL conical centrifuge tubes.
7. Refrigerated centrifuge.
8. Neubauer chamber (hemocytometer).
9. Inverted Microscope.
10. Hand cell counter.
11. T-75 cm^2 cell culture flasks.
12. 6-well cell culture plates.
13. Opti-MEM™ Reduced Serum Medium.
14. Transfection reagent.
15. 1.5 and 2 mL polypropylene conical tubes.
16. Modified U1 snRNA constructs (*see* Subheading 2.1).

2.2.2 Analysis of Splicing Rescue by RT-PCR

1. RNA isolation kit.
2. Refrigerated centrifuge.
3. 1.5 mL polypropylene conical tubes.
4. Spectrophotometer for nucleic acids measurement.
5. cDNA synthesis kit.
6. Taq DNA polymerase.
7. Oligo$(dT)_{18}$ primer mix (if required).
8. Gene-specific primers (e.g. *HGSNAT* primers—Exon 2 Fw: 5′ ACATGCAGAGCTGAAGATGGA 3′; Exon 3 Rv: 5′ GATA GATCCGTGCTGGGTG 3′).
9. Ice.
10. RNase free water.
11. PCR thermocycler.
12. Agarose gel with ethidium bromide for electrophoresis.

13. DNA Ladder (molecular weight size marker).
14. UV transilluminator.
15. Sterile scalpel blades.
16. PCR products purification kits.

3 Methods

3.1 Generating the Modified U1 snRNA Vectors

To design the primers for producing the desired modified human U1 snRNA vectors, it is first necessary to know the sequences of the 5′ss under study, both WT and mutant. Then, it is necessary to analyze the complementarity of those sequences with that of U1 snRNA. Next, several modified U1 snRNA vectors can be designed and constructed to have different complementarities to the target sequences (Fig. 2). To generate those constructs, the plasmid pG3U1 [12] (kindly provided by Prof. Dr. Belén Pérez) a derivative of pHU1 [13], containing the coding sequence of the human U1 can be used as template for site-directed mutagenesis PCR reactions (*see* **Note 2**). Depending on the number of mutations to insert in the U1 snRNA vector sequence, different mutagenic primer pairs need to be designed.

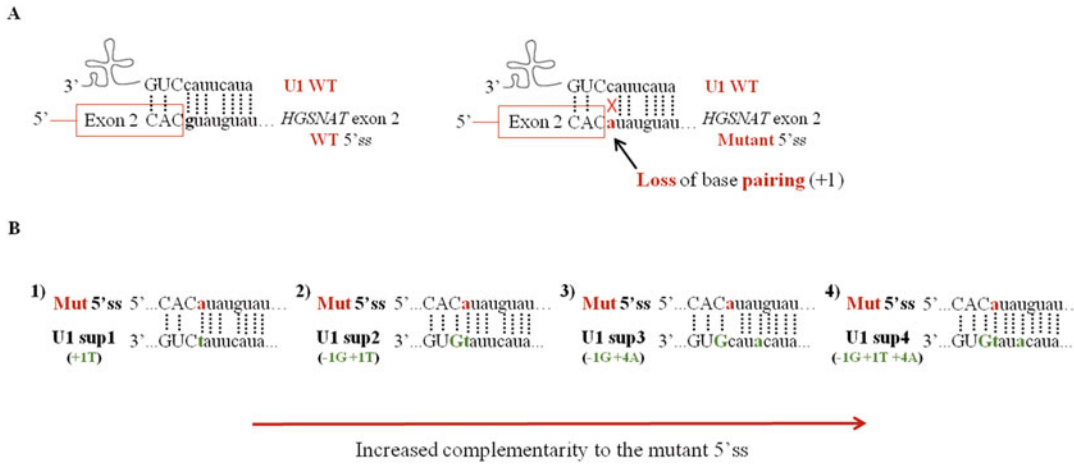


Fig. 2 Design and construction of modified U1 snRNA vectors. (**a**) Schematic representation of base pair interactions between the U1 snRNA and the wild-type and mutant 5′ss of *HGSNAT* exon 2, respectively. (**b**) Illustration of the strategy followed to increase the complementarity of U1 snRNA with the mutated 5′ss of *HGSNAT* gene. U1 complementarity was increased stepwise, and to try to compensate for the *HGSNAT* mutation at +1 position, four different U1-adaptations were designed [U1 sup1 (+1T); U1 sup2 (−1G +1T); U1 sup3 (−1G +4A); U1 sup4 (−1G +1T +4A)]. Upper case letters show exonic nucleotides, whereas the lower case letters denote intronic nucleotides. Base pairing is indicated by vertical lines and its loss by an *X*. The mutant nucleotide is highlighted in red and the changed nucleotides in the U1 sequence are illustrated in green

3.1.1 Engineering Modified U1 snRNA Vectors Adapted to the 5′ss of Interest

1. According to the different modifications to be introduced in the U1 snRNA vector sequence, design sense and antisense primers with the desired mutation(s) to be introduced by site-directed mutagenesis (*see* **Note 4**).
2. Using the mutagenic primers, perform the site-directed mutagenesis of the WT U1 snRNA vector using the mutagenesis kit (*see* **Note 5**). Briefly, mix the U1 snRNA plasmid DNA (~40 ng) with primers, buffer, dNTPs (according to the kit), apyrogenic water, a High Fidelity Taq polymerase and subject the mixture to recommended PCR conditions from the mutagenesis kit. The number of PCR cycles varies according to the type of the desired mutation(s) (*see* **Note 6)**; and the number (*n*) of min of the PCR extension step depends on the plasmid length, *n* is calculated as 1 min/kb; *see* **Note 7**. After the PCR reaction is completed, add 1 μL (10 U) of *Dpn*I restriction enzyme to the amplified products and incubate for 1 h at 37 °C to digest the parental dsDNA.
3. Use 1–4 μL of the *Dpn*I treated DNA reaction to transform *E. coli* competent cells. Briefly, thaw on ice a 50 μL aliquot of competent cells and add 1–4 μL of the digested reaction. Swirl the tube gently to mix and incubate on ice for 30 min. In a water bath or dry thermomixer, heat pulse the tube at 42 °C for 45 s and then place the reaction tube on ice for 2 min. Add room temperature SOC medium (5× the volume of competent cells) and incubate for 1 h with shaking at 600 rpm in a dry thermomixer (*see* **Note 8**). After incubation spread the appropriate volume (*see* **Note 9**) of transformation reaction on pre-warmed (37 °C) LB-agar plates containing ampicillin (100 μg/mL) and incubate at 37 °C for 16–18 h (*see* **Note 10**).
4. To obtain plasmid DNA minipreps, prepare minicultures of selected bacterial colonies to allow their growth. Add 3 mL (*see* **Note 11**) of LB medium containing ampicillin (100 μg/mL) to a 15 mL tube and using a sterilized pipette tip pick a colony and add it into the medium by pipetting up and down (or, simply, place the pipet tip into the medium). Repeat the procedure for 3–5 colonies. Incubate the tubes in an orbital shaking incubator at 220 rpm and 37 °C for 16–18 h. To purify the plasmid DNA prepare DNA minipreps using a plasmid miniprep purification kit (*see* **Note 12**). Select the mutant (s) U1 snRNA plasmid(s) by Sanger sequencing analysis (U1-seq Fw primer) using ~100 ng of purified miniprep.
5. Once the desired modified U1 snRNA construct(s) are selected, propagate them in maxicultures to obtain a high quantity of the modified construct(s) that can be used for transfection. First, prepare a miniculture of each case according to **step 4** (*see* **Note 13**). Then add 100–150 mL of LB medium

containing ampicillin (100 μg/mL) to a sterilized flask(s) (*see* **Note 11**) and innoculate all the bacterial growth from the miniculture(s). Incubate the flask(s) in an orbital shaking incubator at 37 °C and 220 rpm for 16–18 h. Using an endotoxin-free maxiprep plasmid DNA purification kit, maxiprep the plasmid(s) containing the modified U1 snRNA construct (s) and perform its sequencing analysis for validation.

3.2 In Vitro Therapeutic Evaluation of Modified U1 snRNA Vectors in Human Fibroblasts

Even though we must always find a balance between the best possible experimental design and the resources available, adequate controls may never be forgotten. Still, there is a minimum standard for cell culture experiments that must always be met if we want to draw strong conclusions out of them. Therefore, adequate controls to the variables under test should always be included (*see* **Note 14**).

3.2.1 Modified U1 snRNA Vectors Transfection in Human Fibroblasts

1. Grow both WT control and patient fibroblasts in T-75 flasks with DMEM + Glutamax medium supplemented with 10% FBS, 5% antibiotics, and 5% amphotericin B, in an incubator at 37 °C with 95% humidity and 5% CO_2 following standard cell culture procedures.
2. On the day before transfection, detach the cells by trypsinization. Briefly, discard the growth medium and wash cells with 3 mL of PBS buffer. Then, discard the PBS and add 2 mL of trypsin-EDTA. Subsequently, incubate cells with the solution for 5 min at 37 °C. After this period, check in an inverted microscope that cells are detached and add 4 mL of fresh medium to inactivate trypsin-EDTA action.
3. Harvest the cells to a 15 mL tube and centrifuge at 500 × *g* for 5 min to eliminate any traces of trypsin.
4. Discard the supernatant and resuspend cells in 4 mL of fresh medium.
5. Count cells in suspension with an hemocytometer (Neubauer chamber). Pipette a small volume of cell suspension (approximately 15 μL) to both hemocytometer chambers and count the cells present in all four external quadrants of each chamber by observing it in an inverted microscope. Considering the dimensions of the chamber (1 mm × 1 mm × 0.1 mm), each quadrant has a total volume of 0.1 mm^3, which equals 10^{-4} mL. Therefore, the total number of cells in the original suspension can be calculated with the following equation:

$$N = \frac{\sum n}{8} \times 10^4$$

where N is the total number of cells per milliliter, n is the number of cells counted in each quadrant of the Neubauer chamber and the 10^4 factor allows for the correction of the total number of cells in 1 mL of cell suspension.

6. For modified U1 snRNA vectors transfection, seed a total of ~2.5–3 × 10^5 fibroblast cells into 6-well plates and grow cells in DMEM + Glutamax medium supplemented with 10% FBS, 5% antibiotics and 5% amphotericin B, in an incubator at 37 °C with 95% humidity and 5% CO_2.
7. On the next day (cells at 80–90% confluence), transfect the cells with quantities between 1 and 3.5 μg of the modified U1 snRNA constructs using a transfection reagent according to the manufacturer's protocol (*see* **Notes 15** and **16**).
8. 24–48 h after transfection, harvest cells by trypsinization. Discard the growth medium of each plate well and wash cells with 1 mL of PBS buffer. Discard the PBS, add 500 μL of trypsin-EDTA to each well and incubate for 5 min at 37 °C. Then, check by microscopy that cells are rounding up and add 1 mL of DMEM + Glutamax medium to inactivate trypsin-EDTA. Harvest cells to 2 mL tubes and centrifuge at 500 × *g* for 5 min at 4 °C; discard the supernatant; wash cells with 1 mL of PBS buffer and centrifuge again. Proceed to RNA extraction or store the pellet(s) at −80 °C for future use.

3.2.2 Analysis of Splicing Rescue by RT-PCR

1. Extract total RNA from the transfected human fibroblasts using a RNA extraction kit according to the manufacturer's protocol. Then, perform RNA quantification using a spectrophotometer.
2. For reverse transcription, use a cDNA synthesis kit following the manufacturer's protocol, and start with 1–2 μg of total RNA. The cDNA synthesis reaction can be stored at −20 °C or used immediately for PCR amplification.
3. Perform a PCR in standard conditions using a Taq polymerase supplemented with its buffer, dNTPs, gene-specific primers for a final concentration of 0.4 μM each (e.g. *HGSNAT* primers), 2 μL of cDNA, and RNase free water to a final volume of 50 μL.
4. To evaluate the splicing rescue, analyze the amplification products through agarose gel electrophoresis in an agarose gel stained with 5 μL of ethidium bromide (*see* **Note 17**). Choose a DNA ladder according to the size of the amplified band. After separation, visualize the gel using an UV transilluminator. As an example, Fig. 1 shows the results of the partial correction of *HGSNAT* exon 2 splicing after expression of a modified U1 snRNA (totally complementary to the 5′ss of exon 2) in patients' fibroblasts.
5. Assess the identity of the obtained band(s) by sequencing analysis (*see* **Note 18**). For this purpose, purify the PCR products directly with a PCR clean-up kit if there is only one amplified band or when multiple bands are present excise each band from the gel and purify them using a gel band

purification kit. Whatever the case, follow the indications present in the manufacturer's protocol.

6. Subject the purified bands to standard automated sequencing using gene-specific primers for the amplification (e.g. *HGSNAT* primers). Compare the obtained sequence (s) with the reference sequence of the gene of interest (retrieved from the Ensembl database) using the Clustal Omega bioinformatic tool (https://www.ebi.ac.uk/Tools/msa/clustalo/), in order to analyze the effect of the modified U1 snRNA's in rescuing the normal splicing pattern.

3.2.3 Assessment of the Effect of U1 snRNA-Induced Splicing Rescue at Protein Level

While not included in this chapter, for it is case-specific, the effect of modified U1 snRNAs-treatment at protein level is mandatory whenever we want to proceed to in vivo studies in order to address the true therapeutic potential of a given U1 snRNA molecule.

Ideally, as soon as we get an RT-PCR pattern that confirms splicing correction to some extent, and that rescue is confirmed by band excision and Sanger sequencing, the overall effect of that rescue at protein level should also be checked. There is a variety of methods we can choose in order to address this issue, from the direct quantification of enzymatic activity (whenever the gene product under analysis has a catalytic activity) to that of the protein itself (through Western blot).

Usually, the method of choice depends on two major factors: the protein itself and the assays available *in house* to assess it. Virtually every method from Western blot to immunofluorescence may be informative and provide extra support to the conclusions drawn from the RT-PCR. Therefore, as a take-home message, we would recommend that, whenever designing U1 snRNA molecules for splicing rescue, the effect should be checked not only at cDNA level, but also at protein level.

4 Notes

1. This chapter is exclusively focused on mutation-adapted U1 snRNAs. Nevertheless, it is important to refer that there is a novel, second generation, of engineered U1 snRNAs, which may be used for therapeutic purposes: the so-called Exon-Specific U1 snRNAs (ExSpeU1). These ExSpeU1s are complementary to non-conserved sequences downstream of mutant 5′ss. In theory, ExSpeU1 is expected to decrease the potential of off-target effects of U1 snRNA-based therapies, while allowing for a single ExSpeU1 to rescue multiple splicing defects that affect a single exon [4–6].
2. The pG3U1 vector [12] {Susani, 2004, TCIRG1-dependent recessive osteopetrosis: mutation analysis, functional

identification of the splicing defects, and in vitro rescue by U1 snRNA} was used, but the human U1 snRNA sequence can be cloned in other standard expression vector(s).

3. Store LB-agar plates with antibiotics at 4 °C in the dark.
4. Mutagenic primers can be designed using the web-based QuikChange Primer Design Program, available online at www.agilent.com/store/primerDesignProgram.jsp (we recommend to read the "help" section of the program). However, it is important to take into account a number of considerations:
   (a) both mutagenic primers must contain the desired mutation(s) and anneal to the same sequence on opposite strands of the plasmid;
   (b) each primer should have between 25 and 45 bases in length with a melting temperature (Tm) of ≥78 °C;
   (c) the desired mutation(s) should be located in the middle of the primer (~12–15 nucleotides of the correct sequence on both sides);
   (d) the primers should have a minimum GC content of 40% and should terminate in one or more C or G bases;
   (e) the primers do not need to be 5′ phosphorylated and purification may either be performed by liquid chromatography (HPLC) or by polyacrylamide gel electrophoresis (PAGE).
5. To modify the pG3U1 we recommend to use the QuikChange™ II mutagenesis kit (Agilent). However, other site-directed mutagenesis commercial kits can be used. The kit should be chosen according to the plasmid length and the type of mutations to introduce.
6. According to the type of mutation(s) to be inserted in the U1 snRNA WT sequence, the number of PCR cycles varies. For point mutations (1 nucleotide change) use 12 cycles; for single aminoacid changes (3 nucleotides) use 16 cycles and for multiple amino acid deletions or insertions (≥4 nucleotides) use 18 cycles.
7. The number (*n*) of min of PCR extension step recommended is usually 1 min/kb. However, using the QuikChange™ II mutagenesis kit (Agilent) we usually increment the time for 2 min/kb. For the pG3U1 plasmid length, 8 min should work, but from our experience adding one more min to this step (in this case 9 min for extension) gives the best results.
8. If a thermomixer is not available, follow the site-directed mutagenesis kit manufacturer's recommendations concerning shaking of transformation reactions.

9. The entire volume of transformation reaction can be plated on a single LB-agar plate. However, depending on the transformation efficiency this may originate a huge number of colonies which are then difficult to select. Therefore, we recommend to use more than one plate and spread different volumes to increase the probability to obtain individualized colonies (e.g. 200 and 100 μL). When plaquing lower volumes a small quantity (1:1) of SOC medium can be added to the transformation reaction to dilute and help to spread the transformation product.
10. If colonies cannot be selected immediately, store plate(s) at 4 °C.
11. The total volume of the tube should allow a volume of air that is 5× the volume of LB medium (e.g. 3 mL of LB medium in a 15 mL tube; 5 mL of LB medium in a 25 mL tube, etc.).
12. Before starting the miniprep(s) procedure, a sample of bacterial culture can be preserved in a "glycerolate" for future use. For a final volume of 1 mL, add a part of bacterial culture and a part of sterilized glycerol to a 2 mL tube for a final concentration of ~10–15% of glycerol. Vortex immediately and store at −80 °C.
13. To avoid the need to pick another bacterial colony from an LB-agar plate, the glycerolate(s) (*see* **Note 12**) can be used to prepare a new miniculture. Briefly, defrost the glycerolate on ice, scrape it lightly with a pipette tip or aspirate few microliters and pipet them up and down into a tube containing the desired volume of LB medium and ampicillin (100 μg/mL). Incubate the tube(s) in an orbital shaking incubator as recommended in **step 4** of Subheading 3.1.1.
14. In the transfection experiments here referred (*see* **step 7** of Subheading 3.2.1) we included two negative controls: one where only the transfection reagent was added to the cells and other where the minigene expressing the WT U1 sequence was transfected on cells.
15. For liposome-based transfection of fibroblasts, Lipofectamine® 2000 (Invitrogen) or other commercial lipofection reagent can also be tested. To further increase transfection efficacy, the modified U1's can also be inserted into the cells by the electroporation technique. For both methods we recommend to optimize the amount of transfection reagent according to the quantity of modified U1 and number of cells to transfect.
16. To assess transfection efficiency, transfect fibroblasts with a control plasmid encoding GFP or RFP and monitor fluorescence by microscopy. Also, the cell uptake of the modified U1's can be confirmed by PCR with specific primers (U1 Fw—5′ A TCGAAATTAATACGACTCA 3′ and U1 Rv—5′ CTGGGA AAACCACCTTCGT 3′). Otherwise, clone the WT human U1

snRNA cassette from pG3U1 vector in a plasmid encoding GFP and monitor fluorescence and U1 expression simultaneously.

17. Adjust the agarose gel percentage according to the molecular weight of the target amplified products.
18. In RT-PCR analysis after U1 snRNA's transfection, the size of the amplified band(s) seen on the agarose gel can give an idea of whether the aberrantly spliced exon under study is included in the cDNA or not. However, it is necessary to sequence the amplified band(s) from control and patient fibroblasts treated with the different modified U1 snRNAs, to confirm the correct splicing pattern.

Acknowledgments

The authors would like to acknowledge Prof. Dr. Belén Pérez (Molecular Biology Department, Faculty of Sciences, University Autonoma of Madrid, Spain) for kindly provide the pG3U1 vector. In addition, the authors would like to acknowledge BioMedCentral, Part of Springer Nature for allowing the reproduction in this chapter of an adapted version of a figure originally published in Matos, L. et al. Therapeutic strategies based on modified U1 snRNAs and chaperones for Sanfilippo C splicing mutations. Orphanet J Rare Dis 9, 180 (2014). https://doi.org/10.1186/s13023-014-0180-y. Copyright © 2014, Springer Nature. This work was partially supported by *Fundação para a Ciência e Tecnologia* (FCT) IP (project: FCT/PTDC/BBBBMD/6301/2014) and by *The National MPS Society* (project: 2019DGH1642).

References

1. van der Feltz C, Anthony K, Brilot A, Pomeranz Krummel DA (2012) Architecture of the spliceosome. Biochemistry 51(16): 3321–3333. https://doi.org/10.1021/bi201215r
2. Buratti E, Baralle D (2010) Novel roles of U1 snRNP in alternative splicing regulation. RNA Biol 7(4):412–419
3. Carmel I, Tal S, Vig I, Ast G (2004) Comparative analysis detects dependencies among the 5′ splice-site positions. RNA 10(5):828–840. https://doi.org/10.1261/rna.5196404
4. Pinotti M, Bernardi F, Dal Mas A, Pagani F (2011) RNA-based therapeutic approaches for coagulation factor deficiencies. J Thromb Haemost 9(11):2143–2152. https://doi.org/10.1111/j.1538-7836.2011.04481.x
5. Coutinho MF, Matos L, Santos JI, Alves S (2019) RNA therapeutics: how far have we gone? Adv Exp Med Biol 1157:133–177. https://doi.org/10.1007/978-3-030-19966-1_7
6. Hwu WL, Lee YM, Lee NC (2017) Gene therapy with modified U1 small nuclear RNA. Expert Rev Endocrinol Metab 12(3): 171–175. https://doi.org/10.1080/17446651.2017.1316191
7. Balestra D, Faella A, Margaritis P, Cavallari N, Pagani F, Bernardi F, Arruda VR, Pinotti M (2014) An engineered U1 small nuclear RNA rescues splicing defective coagulation F7 gene expression in mice. J Thromb Haemost 12(2): 177–185. https://doi.org/10.1111/jth.12471

8. Lee NC, Lee YM, Chen PW, Byrne BJ, Hwu WL (2016) Mutation-adapted U1 snRNA corrects a splicing error of the dopa decarboxylase gene. Hum Mol Genet 25(23):5142–5147. https://doi.org/10.1093/hmg/ddw323
9. Lee B, Kim YR, Kim SJ, Goh SH, Kim JH, Oh SK, Baek JI, Kim UK, Lee KY (2019) Modified U1 snRNA and antisense oligonucleotides rescue splice mutations in SLC26A4 that cause hereditary hearing loss. Hum Mutat 40(8): 1172–1180. https://doi.org/10.1002/humu.23774
10. Breuel S, Vorm M, Bräuer AU, Owczarek-Lipska M, Neidhardt J (2019) Combining engineered U1 snRNA and antisense oligonucleotides to improve the treatment of a BBS1 splice site mutation. Mol Ther Nucl Acids 18: 123–130. https://doi.org/10.1016/j.omtn.2019.08.014
11. Matos L, Canals I, Dridi L, Choi Y, Prata MJ, Jordan P, Desviat LR, Pérez B, Pshezhetsky AV, Grinberg D, Alves S, Vilageliu L (2014) Therapeutic strategies based on modified U1 snRNAs and chaperones for Sanfilippo C splicing mutations. Orphanet J Rare Dis 9:180. https://doi.org/10.1186/s13023-014-0180-y
12. Susani L, Pangrazio A, Sobacchi C, Taranta A, Mortier G, Savarirayan R, Villa A, Orchard P, Vezzoni P, Albertini A, Frattini A, Pagani F (2004) TCIRG1-dependent recessive osteopetrosis: mutation analysis, functional identification of the splicing defects, and in vitro rescue by U1 snRNA. Hum Mutat 24(3):225–235. https://doi.org/10.1002/humu.20076
13. Lund E, Dahlberg JE (1984) True genes for human U1 small nuclear RNA. Copy number, polymorphism, and methylation. J Biol Chem 259(3):2013–2021

Open Access This chapter is licensed under the terms of the Creative Commons Attribution 4.0 International License (http://creativecommons.org/licenses/by/4.0/), which permits use, sharing, adaptation, distribution and reproduction in any medium or format, as long as you give appropriate credit to the original author(s) and the source, provide a link to the Creative Commons license and indicate if changes were made.

The images or other third party material in this chapter are included in the chapter's Creative Commons license, unless indicated otherwise in a credit line to the material. If material is not included in the chapter's Creative Commons license and your intended use is not permitted by statutory regulation or exceeds the permitted use, you will need to obtain permission directly from the copyright holder.



RNA Therapeutics: How Far Have We Gone?

7

Maria Francisca Coutinho, Liliana Matos, Juliana Inês Santos, and Sandra Alves

Abstract

In recent years, the RNA molecule became one of the most promising targets for therapeutic intervention. Currently, a large number of RNA-based therapeutics are being investigated both at the basic research level and in late-stage clinical trials. Some of them are even already approved for treatment. RNA-based approaches can act at pre-mRNA level (by splicing modulation/correction using antisense oligonucleotides or U1snRNA vectors), at mRNA level (inhibiting gene expression by siRNAs and antisense oligonucleotides) or at DNA level (by editing mutated sequences through the use of CRISPR/Cas). Other RNA approaches include the delivery of *in vitro* transcribed (IVT) mRNA or the use of oligonucleotides aptamers. Here we review these approaches and their translation into clinics trying to give a brief overview also on the difficulties to its application as well as the research that is being done to overcome them.

Keywords

Antisense oligonucleotides · Aptamers · CRISPR-Cas gene editing · Modified mRNA replacement therapy · siRNA-based drugs · U1snRNA vectors

Abbreviations

2′-F	2′-fluoro
2′-MOE	2′-O-methoxyethyl
2′-O-CH2Py(4)	2′-O-methyl-4-pyrimidine
2′-OMe	2′-O-methyl
AADC	Aromatic L-amino Acid Decarboxylase
AAVs	Adeno-associated Viruses;
AGO	Argonaute
AMD	Age-related Macular Degeneration
AONs	Antisense Oligonucleotides
ASGPR	Asialoglycoprotein receptor
ASGR	Asialoglycoprotein Receptor
BBB	Blood Brain Barrier
BMD	Becker Muscular Dystrophy
CNS	Central Nervous System
CPPs	Cell-penetrating Peptides
CRISPR	Clustered Regulatory Interspaced Short Palindromic Repeats

M. F. Coutinho · L. Matos · J. I. Santos · S. Alves (✉)
Department of Human Genetics, National Institute of Health Doutor Ricardo Jorge, Porto, Portugal
e-mail: sandra.alves@insa.min-saude.pt

© Springer Nature Switzerland AG 2019
L. Romão (ed.), *The mRNA Metabolism in Human Disease*, Advances in Experimental Medicine and Biology 1157, https://doi.org/10.1007/978-3-030-19966-1_7

sandra.alves@insa.min-saude.pt

CRISPR-Cas 9	CRISPR-associated protein 9 (Cas9)
CSF	Cerebrospinal Fluid
DLin-MC3-DMA	Anionic lipid dilinol eylmethyl-4-dimethyl-aminoburyate
DMD	Duchenne Muscular Dystrophy
dsRNAs	double-stranded RNAs
ExSpeU1s	Exon-Specific U1 snRNAs
FH	Familial Hypercholesterolemia
GalNAc	N-acetylgalactosamine
GPCRs	G Protein-coupled Receptors
HCV	Hepatitis C Virus
hFVII	Human Factor VII
hTTRA	Hereditary Transthyretin Amyloidosis
I2S	Iduronate 2-sulfatase
IVT	*in vitro* transcribed
LDL-C	Low-density Lipoprotein Cholesterol
LNAs	Locked Nucleic Acids
LNPs	Lipid-based Nanoparticles
miRNAs	microRNAs
mNIS+7	Modified Neurologic Impairment Score +7
mRNA	messenger RNA
NDA	New Drug Application
PCK9	Proprotein Convertase Subtilisin/Kexin Type 9
PD	Pharmacodynamics
PILs	Pegylated immunoliposomes
PIWI	P-element induced wimpy testis
PK	Pharmacokinetics
PMOs	Phosphoroamidate Morpholino Oligomers
PNAs	Peptide Nucleic Acids
PS	Phosphorothioate
RIS	RNA-induced silencing complex
RNAi	RNA interference
RNP	Ribonucleoprotein
RTK	Human Receptor Tyrosine Kinase
SELEX	Systematic Evolution of Ligands by Exponential enrichment
sgRNA	single guide RNA
shRNA	short hairpin RNA
siRNAs	small interference RNAs
SLNs	Solid Lipid Nanoparticles
Sm	Smith antigen
SMA	Spinal Muscular Atrophy
SNALPs	Nucleic-acid-lipid-particles
SSOs	Splice Switching Oligonucleotides
TLRs	Toll-like Receptors
TTR	Transthyretin
U.S. FDA	U.S. Food and Drug Administration

7.1 Introduction

The RNA molecule has traditionally been viewed as an intermediate between DNA and protein. Recently though, this reductive view has been abandoned as more classes and functions of RNA have been discovered as well as therapeutic applications involving this molecule are being developed. RNA therapeutics can either mimic or antagonize the endogenous RNA functions and have several advantages. They can act even on targets that were previously "undraggable" and, most importantly, they are easy to design, cost effective, stable and easy to combine with other drugs presenting also low immunogenicity. Despite these advantages, the use of RNAs as drugs requires the overcoming of two major obstacles: the poor pharmacological properties of RNA, which is rapidly degraded by RNases and the difficulties in its delivery to the target organs and tissues. In this chapter we present the major RNA-based therapeutics currently under research, discussing the challenges to their translation into the clinic and the recent advances in delivery strategies. RNA tools such as ribozymes, riboswitches and SINE-UP strategy are no less important but will not be discussed in this chapter.

sandra.alves@insa.min-saude.pt

7.2 Antisense Oligonucleotides

7.2.1 Brief Overview

Antisense oligonucleotides (AONs) are short synthetic oligonucleotides that bind to RNA through standard Watson-Crick base pairing and can modulate the function of their target RNA [1, 2]. AONs can function in various ways (Fig. 7.1). For example, AONs can mediate targeted gene knockdown through the recruitment of endogenous RNAse H to degrade mRNA at sites of DNA:RNA hybridization caused by AON binding (Fig. 7.1a). They can also be designed to bind to translation initiation sites on mRNAs in cytosol to block translation (Fig. 7.1b). Another approach uses single-stranded AONs to modulate miRNAs expression; these AONs directly bind target miRNAs to inhibit their function (anti-miRs), and thus depress their target gene (Fig. 7.1c). Moreover, AONs can also be used to modulate pre-mRNA splicing in the target gene bypassing the disease-causing mutation (Fig. 7.1d) [3, 4]. These AONs are designated Splice Switching Oligonucleotides (SSOs) and are single stranded 15–25 nucleotides long, which direct pre-mRNA splicing to a new pathway by binding sequence elements and sterically blocking access to the transcript by the spliceosome and other splicing factors [1, 5–7].

The modification of gene expression, using a synthetic single stranded DNA, resulting in inhibition of mRNA translation was demonstrated for the first time by Paterson and colleagues in 1977 in a cell-free system [8]. Almost a year later, Zamecnik and Stephenson showed that in chicken fibroblast tissue culture containing Rous Sarcoma virus, the addition of a synthetic 13-mer oligonucleotide complementary to the 3′ end of the virus, could inhibit its replication and the subsequent transformation of fibroblasts into sarcoma cells [9]. Since then, remarkable progress

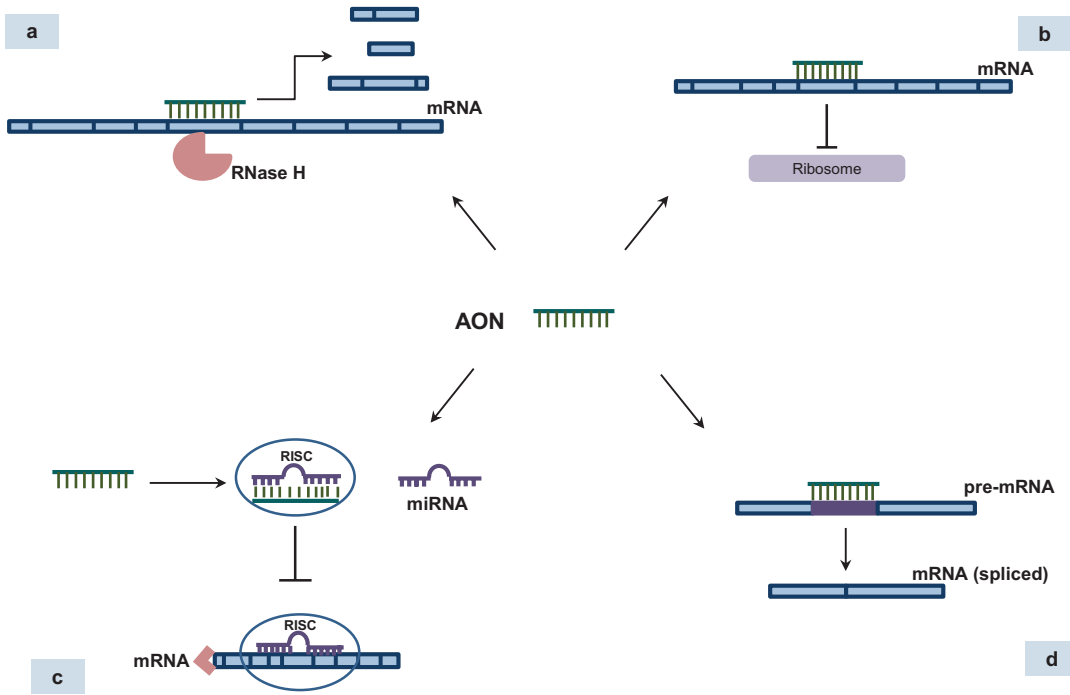


Fig. 7.1 Antisense mechanisms of RNA-based drugs. Antisense oligonucleotides (AONs) impact in gene expression through four different mechanisms: (**a**) RNase H-mediated mRNA degradation; (**b**) steric block of ribosome binding; (**c**) complementary binding to target microRNAs (miRNAs) in order to inhibit their function (antagomirs); and (**d**) splicing modulation

sandra.alves@insa.min-saude.pt

has been made in oligonucleotide drug development and currently, antisense technology is a powerful tool that can be used for target validation and to correct or alter RNA expression for therapeutic benefit [1, 10–12].

Initially, AONs were just synthetic unmodified DNA or RNA molecules, which despite delivering some promising results, would prove to be quite ineffective in biological systems due to their susceptibility to degradation by nucleases, poor affinity for their target mRNA, multiple off-target effects, inability to cross the cell membrane given their negative charge, and weak binding to plasma proteins, leading to rapid clearance by the kidney [1, 3, 13]. Therefore, a wide variety of chemically modified analogues of nucleotides have been developed since then. These chemical modifications were made in the oligonucleotides, generating three categories of AONs, commonly known as generations, with different chemical and pharmacological properties.

7.2.2 Antisense Oligonucleotides Chemistry

Several characteristics need to be fulfilled for the clinical application of antisense oligonucleotides. First, the sequence of the antisense oligonucleotide must be specific enough to avoid off-targets. Other important aspects to be taken into account are the chemistry of the AON and its resistance to degradation by nucleases in order not only to maintain the integrity of the molecule but also to ensure that it is present in an amount, which is sufficient for a true efficacy. In addition, ideal AON should have good pharmacokinetic (PK) and pharmacodynamic (PD) properties and, above all, should not be toxic. Finally, and a very fundamental thing to check, is whether the designed AONs are possible to deliver to target tissues or organs. To try to cope with these desired AON properties, several chemical modifications have been made to the backbone, ribose sugar moiety or nucleobase components, which have a profound effect on the enhanced stability, binding strength and specificity to the target RNA sequence [13] (Fig. 7.2).

The first generation of AONs is characterized by alterations in the backbone, the most common being the phosphorothioate (PS) backbone, accomplished by the replacement of one of the non-bridging oxygen atoms by a sulphur atom. AONs bearing PS linkages are compatible with recruitment of RNase H, which cleaves the target of AONs. This modification allows for an improved nuclease resistance, as well as strong binding to plasma proteins, reducing renal clearance, but still presents poor binding affinity, low specificity and poor cellular uptake [1, 7, 10, 13–15]. Despite these disadvantages, PS oligonucleotides are still the most commonly used AONs and were the first antisense-based drug approved for clinical use in 1998 with fomivirsen (Vitravene®) used for repression of cytomegalovirus mRNA translation [16]. It gained U.S. FDA (U.S. Food and Drug Administration) approval for intraocular treatment of cytomegalovirus retinitis in immunosuppressed patients in 1998 [16] and was discontinued later due to commercial considerations.

In order to surpass the downsides of the first generation oligonucleotides, a second generation was developed through modifications at the 2′ position of the ribose. The most widely studied second generation AONs are 2′-O-methyl (2′-OMe) and 2′-O-Methoxyethyl (2′-MOE), which present higher nuclease resistance and higher affinity for the target RNA, while also reducing non-specific protein binding and toxicity [7, 10, 13, 15]. These second generation AONs, however, do not support RNase H-mediated cleavage of the target mRNA, which impairs their usage for purposes of gene downregulation [1, 14, 17]. This limitation has been minimized with the development of "gapmer" structures where 2′ sugar-modified residues are present on either side of a central "gap" region comprising 8–10 PS-modified nucleotides. The external sugar modified residues thus increase affinity and nuclease resistance, while the internal "gap" region allows RNase H-mediated cleavage of the target RNA [1, 6, 18, 19].

sandra.alves@insa.min-saude.pt

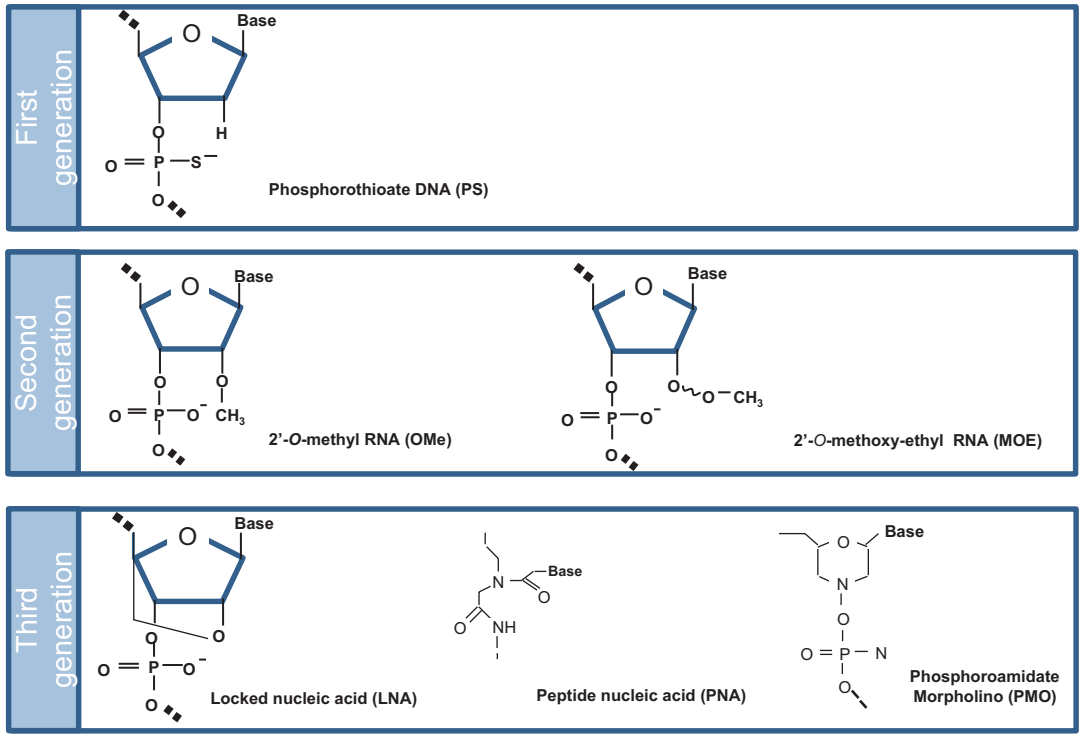


Fig. 7.2 Chemical modifications of antisense oligonucleotides. First generation antisense oligonucleotides (AONs) are characterized by phosphorothioate (PS) backbone; second generation AONs contain a methyl or methoxyethyl group at the 2′ position of the ribose; finally, third generation AONs are characterized by modifications of the furanose ring structure

Finally, the third generation of oligonucleotides is characterized by modifications of the furanose ring of the nucleotide, with the most common being peptide nucleic acids (PNAs), locked nucleic acids (LNAs) and phosphoroamidate morpholino oligomers (PMOs) [12, 14]. These modifications further increase nuclease and protease resistance, target affinity, specificity and *in vivo* stability of antisense drugs, while reduce non-specific interactions with proteins [1, 13, 14, 20, 21]. Nevertheless, PNAs and PMOs present poor cellular uptake, low water solubility and are rapidly cleared from the blood due to their uncharged nature [1, 10, 20, 22] whereas LNAs appear to generate higher toxicity than other chemical modifications, questioning their safety for therapeutic applications [1, 20].

7.2.3 Recent Successful Applications of Antisense Oligonucleotides

The therapeutic application of AONs is very promising. A huge amount of preclinical data has been produced in recent years and many studies have even undergone clinical trials (Table 7.1). Of those, four drugs with different AON chemistries and treatment targets reached, or almost reached clinical practice [12] (Fig. 7.3). One of them is Mipomersen (Kynamro®; Genzyme) that was approved by the U.S. FDA in 2013 for the treatment of familial hypercholesterolemia (FH). Mipomersen is a gapmer of 20 nucleotides and has a sequence complementary to a segment of the Apo b-100 mRNA. Its binding creates a

sandra.alves@insa.min-saude.pt

Table 7.1 Summary table of clinical trials for Antisense Oligonucleotides (AONs)

Chemistry	Drug	Target/organ	Dose/route	Indication	Key observations	References
Commercialized						
2′-H (PS backbone)	Fomivirsen	HCMV *UL122*, Eye	330 μg/eye once every 4 weeks, ITV	CMV retinitis	(1) Effective for CMV retinitis in AIDS patients	[23–25]
2′-MOE (PS backbone)	Mipomersen	*APOB*, Liver	200 mg once weekly, SC	HoFH	(1) Reduction of apoB100 containing lipoprotein particles; (2) Target-related ALT elevations; (3) Clinically meaning full tolerability issues	[26–29]
2′-MOE, fully modified (PS backbone)	Nusinersen	*SMN2* (Intron 7), CNS	12 mg once every 4 months, IT	SMA	(1) Correction of SMN2 splicing defect; (2) Two phase 3 studies terminated early for significant benefit; (3) No drug related adverse events	[30–33]
PMO	Eteplirsen	*DMD* (Exon 51), Muscle	30 mg/kg once weekly, IV	DMD	(1) Increased production of dystrophin; (2) Interpretation of results controversial	[34, 35]
Phase 3						
2′-H	Alicaforsen	*ICAM1*, Colon	240 mg once daily, Enema	Chronic pouchitis	Phase 2 findings included reduction in Pouchitis Disease Activity Index and endoscopy subscore	NCT02525523 [36]
2′-H	Mongersen	*SMAD7*, Intestine	160 mg once daily, Oral	Crohn's disease	Phase 3 failed to demonstrate benefit in patients with Crohn's Disease	NCT02596893 [37] NCT02601300
2′-MOE	Inotersen	*TTR*, Liver	300 mg once weekly, SC	Hereditary ATTR	Phase 3 findings included (1) significant benefit in inotersen-treated patients in both neuropathic disease progression and quality of life measures compared to placebo-treated patients, (2) reduction of mutant and normal TTR, (3) thrombocytopenia (1 fatal bleeding event) and (4) renal events	NCT01737398 [38] (Ionis Pharmaceuticals, press release, Nov 2, 2017)
2′-MOE	Volanesorsen	*APOC3*, Liver	300 mg once weekly, SC	FCS	Phase 3 findings included (1) consistent reduction of triglycerides, (2) mean reduction in triglycerides of 1712 mg/dLin FCS patients, (3) reduced abdominal pain and pancreatitis, and (4) FCS-related thrombocytopenia	NCT02211209 [39–42]

sandra.alves@insa.min-saude.pt

PMO	SRP-4045	*DMD* (Exon 45), Muscle	30 mg/kg once weekly, IV	DMD	Not published	NCT02500381
PMO	Golodirsen (SRP-4053)	*DMD* (Exon 53), Muscle	30 mg/kg once weekly, IV	DMD	On clinical hold due to serious adverse event	NCT02500381
Phase 2						
2′-MOE	IONIS-FXI$_{Rx}$/BAY 2306001	*F11*, Liver	100–300 mg once weekly, SC	Clotting disorders	Phase 2 findings included (1) reduction of Factor XI protein, and (2) reduction of thrombotic events without increase in bleeding	NCT02553889 NCT01713361 [43]
2′-MOE	IONIS-PTP1B$_{Rx}$	*PTPN1*, Liver	200 mg once weekly, SC	T2D	Phase 2 findings included (1) reduction of HbA1c, (2) improved leptin and diponectin levels, and (3) decreased body weight	NCT00455598
2′-MOE	IONIS-GCCR$_{Rx}$	*NR3C1*, Liver	60–420 mg once weekly, SC	T2D	Phase 1 findings included (1) improvement in lipid profile, and (2) attenuation of dexamethasone-induced hepatic insulin resistance	NCT01968265 [44]
2’-MOE	IONIS-GCGR$_{Rx}$	*GCGR*, Liver	50–200 mg once weekly, SC	T2D	Phase 2 findings included (1) attenuation of glucagon-induced increase in blood glucose levels, and (2) reduction of HbA1c	NCT02583919 [45]
2′-MOE	IONIS-FGF$_{R4}$	*FGFR4*, Liver	100–200 mg once weekly, SC	Obesity	Not published	NCT02463240
2′-MOE	IONIS-HTT$_{Rx}$	*HTT*, CNS	10–120 mg once every 4 weeks, IT	Huntington’s disease	In progress	NCT02519036
2′-MOE	IONIS-DGAT2$_{Rx}$	*DGAT2*, Liver	once weekly, SC	NASH	In progress	NCT03334214
2′-MOE	Apatorsen	*HSPB1*, Tumor Cells	200–1000 mg once weekly, IV	Cancer	Phase 1 findings included decrease in tumor markers and decline in CTCs	NCT01454089 [46]
2′-MOE	ATL1102	*ITGA4*, Immune Cells	200 mg twice weekly, SC	MS	Phase 2 findings included reduction in new active lesions	[47]
2′-MOE	Atesidorsen/ ATL1103	*GHR*, Liver	6 mg/kg twice weekly, SC	Acromegaly	Not published	ACTRN12615000289516

(continued)

sandra.alves@insa.min-saude.pt

Table 7.1 (continued)

Chemistry	Drug	Target/organ	Dose/route	Indication	Key observations	References
2′-MOE	IONIS-PKK$_{Rx}$	*KLKB1*, Liver	200 mg once weekly, SC	HAE, chronic migraine	In progress	NCT03108469
2′-MOE	IONIS-HBV$_{Rx}$	*HBV S*, Liver	SC	HBV, chronic atypical	In progress	NCT02981602
cET	AZD9150/IONISSTAT3-2.5$_{Rx}$	*STAT3*, Cancer and Stromal Cells	2–4 mg/kg once weekly, IV	Cancer	Phase 1 findings included (1) reduction of STAT3, (2) reduction in serum IL6, and (3) reduction in tumor burden	NCT02549651 NCT01563302 [48]
cET	AZD5312/ IONISAR-2.5$_{Rx}$	*AR*, Cancer Cells	150–1150 mg once weekly, IV	Prostate cancer	Phase 1 findings included declines in PSA and circulating tumor cells in some patients	NCT02144051 [49]
LNA	Miravirsen	*MIR122*, Liver	3–7 mg/kg once weekly, SC	HCV	Phase 2 findings included inhibition of miR-122 function.	NCT01200420 [50, 51]
2′-MOE, GalNAc	IONIS-APO(a)-L$_{Rx}$	*LPA*, Liver	10–40 mg once weekly, SC	CVD	Phase 1 findings included reduction of Lp(a)	NCT03070782 [52]
2′-MOE, GalNAc	IONIS-ANGPTL3-L$_{Rx}$	*ANGPTL3*, Liver	10–60 mg once weekly, SC	Dyslipidemias	Phase 1 findings included reduction of ANGPTL3, LDL cholesterol and triglycerides	NCT02709850 [53]
2′-MOE, GalNAc	IONIS-APOCIII-L$_{Rx}$	*APOC3*, Liver	once weekly, SC	CVD	In progress	NCT02900027
2′-MOE, GalNAc	GSK3389404/ IONIS-HBV-L$_{Rx}$	*HBV S*, Liver	30–120 mg single dose/once weekly, SC	Chronic HBV	In progress	NCT03020745
Undisclosed, GalNac	AZD4076/RG-125	*MIR107*, Liver	SC	Diabetic NASH	In progress	NCT02826525
Undisclosed	RG-012	*MIR21*, Kidney	110–220 mg once weekly, SC	Alport syndrome	In progress	NCT02855268
Phase 1						
2′-MOE	Eluforsen	Lung/ respiratory epithelium	Intranasal (three times weekly for 4 weeks)	Cystic fibrosis	Phase findings included (1) eluforsen was well tolerated (2) improved CFTR function	NCT02564354; [54]
2′-MOE	BIIB067/ IONISSOD1$_{Rx}$	*SOD1*, CNS	IT	Familial ALS	In progress	NCT02623699

sandra.alves@insa.min-saude.pt

LNA	MRG-106	*MIR155*, Cancer Cells	75–900 mg once weekly, ITM/SC/IV	Hematological malignancies	Phase findings included (1) improvements in cutaneous lesions, and (2) transcriptional changes consistent with target activity	NCT02580552 [55]
LNA	ISTH0036	*TGFB2*, Eye	6.75–225 μg single dose, IVT	Glaucoma	Phase 1 findings included (1) dose-response trend observed in post-operative intraocular pressure, and (2) no adverse events	NCT02406833 [56]
PO, 2′-OMe, ENA	DS-5141b	*DMD* (Exon 45), Muscle	0.1–6.0 mg/kg once weekly, SC	DMD	In progress	NCT02667483
2′-MOE, GalNAc	IONIS-FB-L_{Rx}	*CFB*, Liver	10–40 mg once every 2 weeks, SC	Ocular disease	Phase 1 findings included (1) dose-dependent reduction in factor B levels accompanied by similar reduction in factor B function and complement split factor Bb, and (2) no drug related adverse events	ACTRN12616000335493 [57]
2′-MOE, GalNAc	IONIS-AGT-L_{Rx}	*AGT*, Liver	once weekly, SC	Treatment resistant Hypertension	In progress	NCT03101878
2′-MOE, GalNAc	IONIS-PKK-L_{Rx}	*KLKB1*, Liver	SC	HAE, chronic migraine	In progress	NCT03263507
Discontinued						
2′-OMe	Drisapersen	*DMD* (Exon 51), Muscle	6 mg/kg once weekly, SC	DMD	Rejected by FDA	[58, 59] (Biomarin Pharmaceutical, press release, May 31, 2016)
2′-MOE	Custirsen	*CLU*, Tumor Cells	640 mg once weekly, IV	Prostate cancer and NSCLC	Failure to meet primary endpoints in phase 3 trials	NCT01578655 NCT01630733 [60] (OncoGeneX, press release, Nov 10, 2016)
2′-MOE	IONIS-APO(a)$_{Rx}$	*LPA*, Liver	300 mg once weekly, SC	CVD	Replaced with GalNac conjugate	[61]
2′-MOE	ISIS 388626	*SLC5A2*, Kidney	50–200 mg once weekly, SC	T2D	Availability of small-molecule inhibitors of SGLT2	[62]

(continued)

sandra.alves@insa.min-saude.pt

Table 7.1 (continued)

Chemistry	Drug	Target/organ	Dose/route	Indication	Key observations	References
2′-MOE	ISIS 333611	*SOD1*, CNS	0.15–3.0 mg single dose, IT	Familial ALS	Replaced by more potent compound	[63]
2′-MOE	ISIS 104838	*TNF*, Immune Cells	0.1–6 mg/kg IV, 200 mg once weekly, SC	Inflammatory disease	Inadequate activity	[64]
2′-MOE	ISIS 113715	*PTPN1*, Liver	100–600 mg once weekly, SC	T2D	Replaced by more potent compound	
cET, 2′-MOE	IONIS-DMPK$_{2.5Rx}$	*DMPK*, Muscle	100–600 mg once weekly, SC	DM1	Inadequate activity	NCT02312011 [65]
LNA	EZN-4176	*AR*, Cancer Cells	0.5–10 mg/kg once weekly, IV	Prostate cancer	ALT elevations	NCT01337518 [66]
Undisclosed, GalNac	RG-101	*MIR122*, Liver	SC	HCV	Cases of hyperbilirubinemia	EudraCT 2016-002069-77 (Regulus, press release, Jun 12, 2017)

Abbreviations: **Chemistry:** *2′ – H* 2′- deoxy, *2′ – MOE* 2′ –O- methoxy ethyl, *PMO* phosphorodiamidate morpholino oligomer, *cET* (S)- constrained ethyl, *LNA* locked nucleic acid, *GalNAc* N-Acetilgalactosamine, ENA, 2′ –O, 4′ –C- ethylene-bridged nucleic acid. **Target/organ:** *HCMV UL122* Human cytomegalovirus with IE-2, *APOB* apolipoprotein B, *SMN2* survival of motor neuron 2, *CNS* central nervous system, *DMD* dystrophin, *ICAM1* intercellular adhesion molecule, *SMAD7* SMAD family member, *TTR* transthyretin, *APOC3* apolipoprotein 3, *PTPN1* protein tyrosine phosphatase, non-receptor type1, *NR3C1* nuclear receptor subfamily 3, group C member 1 (glucocorticoid receptor), *GCGR* glucagon receptor, *FGFR4* fibroblast growth factor receptor 4, *HTT* huntingtin, *DGAT* diacylglycerol O-acyltransferase 2, *HSPB1* heat shock protein family B (small) member 1 (heat shock protein27), *ITGA4* integrin subunit alpha 4, *GHR* growth hormone receptor, *KLKB1* kallikrein B1, *HBV S* hepatitis surface antigen (HBsAg), *STAT3* signal transducer and activator of transcription 3, *AR* androgen receptor, *MIR* microRNA, *LPA* lipoprotein (a), *ANGPTL3* angiopoietin like 3, *SOD1* superoxide dismutase 1, *TGFB2* transforming growth factor beta 2, *CFB* complement factor B, *AGT* angiotensinogen, *CLU* clusterin, Solute Carrier Family 5 Member 2, *TNF* tumor necrosis factor alpha, *DMPK* DM1 protein kinase. **Dose/route:** *IVT* intravitreal, *SC* subcutaneous, *IT* intrathecal, *IV* intravenous. **Indication:** *CMV* cytomegalovirus, *HoFH* homozygous familial hypercholesterolemia, *SMA* spinal muscular atrophy, *ATTR* transthyretin amyloidosis, *FCS* familial chylomicronemia, *T2D* type 2 diabetes, *NASH* non-alcoholic steatohepatitis, *MS* multiple sclerosis, *HAE* hereditary angiodema, *HCV* hepatitis C virus, *CVD* cardiovascular disease, *ALS* amyotrophic lateral sclerosis, *NSCLC* non-small cell lung cancer, *DM1* myotonic dystrophy type 1. **Key observations:** *ALT* alanine aminotransferase, *HbA1c* hemoglobin A1c, *CTC* circulating tumor cells, *PSA* prostate specific antigen, *FDA* food and drug administration, *SGLT2* sodium-glucose co-transporter 2, *ALT* alanine aminotransferase

sandra.alves@insa.min-saude.pt

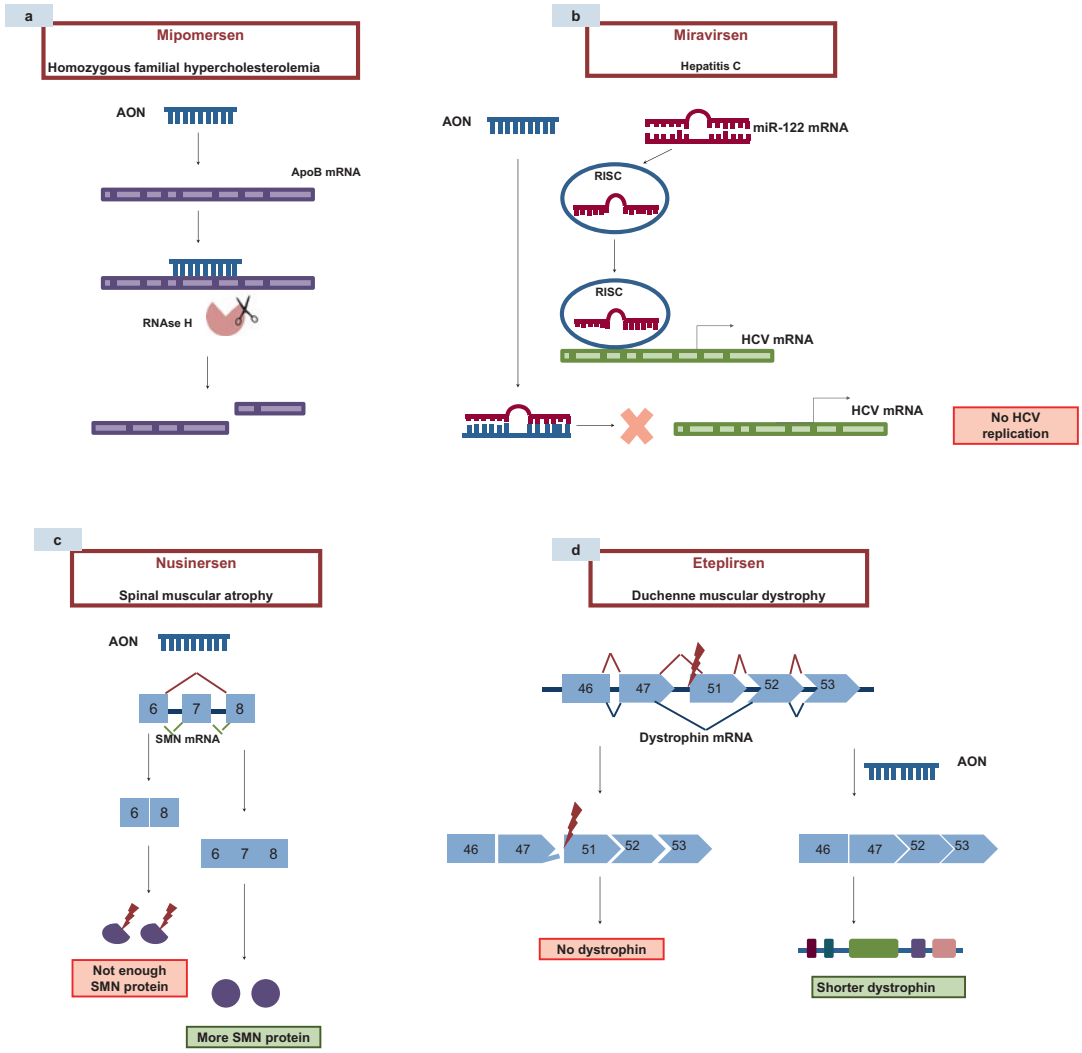


Fig. 7.3 Antisense drugs for clinical practice. Currently, four drugs with different AON chemistries and mechanisms of action have either obtained U.S. FDA approval (Mipomersen, Nusinersen and Eteplirsen) and reached clinical practice, or are seeking accelerated approval soon, with significant pre-clinical data supporting their rapid translation into clinic (Miraversen). (**a**) Mipomersen (Kynamro®; Genzyme), a 2′-MOE-modified AON approved by the U.S. FDA in 2013 for the treatment of familial hypercholesterolemia (FH); (**b**) Miravirsen (SPC3649, Santaris Pharma), an antagomir to miR-122, seeking approval for hepatitis C treatment; (**c**) Nusinersen (Spinraza®, Biogen), a fully modified 2′-MOE AON, approved by U.S. FDA in 2016 for the treatment of spinal muscular atrophy (SMA) and, (**d**) Eterplirsen® (EXONDYS 51TM, Sarepta), a PMO approved by the U.S. FDA in 2016 for the use in Duchenne muscular dystrophy (lightning symbol means the existence of a pathogenic alteration)

DNA:RNA hybrid that is substrate for the enzyme RNase H thus inducing the cleavage of the human Apo b-100 mRNA. The drug has a PS backbone, with 2′-MOE-modified ends, which when compared with earlier antisense technologies, provides greater biological stability and higher affinity to the target mRNA [12, 67]. When administered subcutaneously at a dose of 200 mg per week, it was shown to reduce ApoB-100 production and low-density lipoprotein cholesterol (LDL-C) in a dose-dependent fashion [68]. In general, the results achieved with Mipomersen

sandra.alves@insa.min-saude.pt

point to its efficacy, safety, and tolerability, demonstrating its suitability for use in the target patient population, and providing a tangible tool for use in the management of FH and severe hypercholesterolemia [11, 12, 68]. However, mild-to-moderate injection site reactions, flu-like symptoms and hepatic effects (despite transient and generally reversible) limited its utilization and therefore its commercial success [11].

AONs complementary to mature miRNAs (antagomirs) are also being developed to counteract miRNAs implicated in disease pathogenesis. An example is Miravirsen (SPC3649, Santaris Pharma), an antagomir to miR-122, a liver-specific microRNA that the hepatitis C virus (HCV) requires for replication. Miravirsen is designed to recognize and sequester miR-122, making it unavailable to HCV. As a result, viral replication is inhibited, and the level of HCV infection is reduced [12]. Positive results were observed in a phase II study. The use of Miravirsen in patients with chronic HCV genotype 1 infection showed prolonged dose-dependent reductions in HCV RNA levels without evidence of viral resistance [50]. The updated results revealed no long-term safety issues among 27 Miravirsen-treated patients [51, 69]. Moreover, there was a prolonged decrease in miR-122 plasma levels in patients dosed with Miravirsen but the plasma levels of other miRNAs were not significantly affected by antagonizing miR-122 [69, 70].

The above examples use AONs to alter gene expression, either directly or indirectly, to change disease progression. Another precise method to alter gene expression is to manipulate pre-mRNA splicing using SSOs. This is the case of Nusinersen (Spinraza®, Biogen), a fully modified 2′-MOE AON, approved by U.S. FDA in 2016 for the treatment of spinal muscular atrophy (SMA). SMA is an autosomal recessive neuromuscular disease caused by progressive loss of alfa-motor neurons in the anterior horn of the spinal cord [12, 71]. The most severe form, infant onset or type 1, is the most common one, representing 50% of all SMA cases. Type 2 is less severe, but also very debilitating. These infants never walk, and as they grow the disease progresses and patients begin to lose the capacity of lift even their arms. In humans, a parolog gene of SMA exists, the *SMN2* gene that differs of the *SMN1* by 5–11 nucleotides. However, in the majority of the *SMN2* transcripts the exon 7 is lacking, resulting in a truncated protein, which is rapidly degraded [72]. Nusinersen induces the inclusion of exon 7 in the *SMN2* mRNA by targeting and blocking an intron 7 internal splice site. This action increases SMN protein production, thus improving its function [73]. Intrathecal injection of Nusinersen (every 4 months) allows therapeutic delivery directly into the cerebrospinal fluid (CSF) bathing the spinal cord, the site of motor neuron degeneration and, substantially prolonging survival of type 1 infants, while also resulting in improvements in all measures evaluated [32]. Similar benefit was demonstrated in patients with later onset type 2 SMA [33]. More remarkable, treatment of type 1 pre-symptomatic infants with Nusinersen has been demonstrated to result, in many cases, in achievement of motor milestones at the age expected for healthy infants. Moreover, 92% of the infants treated prior to the development of symptoms were able to sit without support, a milestone never achieved by a type 1 SMA infant before Nusinersen treatment was introduced and 50% were able to walk without support [74].

Another SSO, already in the market is Eterplirsen® (EXONDYS 51™, Sarepta) that was approved by the U.S. FDA in 2016 for use in Duchenne muscular dystrophy (DMD) patients, a severe, childhood-onset disease that results mostly from deletions within the dystrophin gene. DMD is a progressive, neuromuscular disease, occurring mainly in males (1 in 3500–5000 males born worldwide) [75, 76]. It is caused by an absence of the protein dystrophy, a membrane-associated protein that forms a network with sarcolemmal glycoproteins by linking the cytoskeleton actin in muscle fibers within the first few extracellular matrix [77], which results in altered myocyte integrity, muscle wasting and relentlessly progressive weakness. Becker muscular dystrophy (BMD) is a milder disease

sandra.alves@insa.min-saude.pt

caused by dystrophin truncations (due to "in frame" deletions) rather than its absence. A viable strategy for generating truncated, but functional, dystrophin protein involves the skipping of exons to correct DMD-linked mutations (which includes 83% of mutations in DMD) [78]. This can reduce the severity of the disease and produce a milder phenotype, similar to that of BMD. Eteplirsen, the first PMO drug ever approved, binds to the exon/intron splice site at the beginning of exon 51, resulting in its skipping, giving origin to an in frame transcript, which prevents the unwanted degradation of the mutant transcripts by the nonsense-mediated mRNA decay (NMD) pathway, and allowing the production of an internally deleted but functional dystrophin protein [79]. Eterplirsen is applicable for approximately 14% of patients with DMD mutations. It is administered via intravenous infusion and was found to be well tolerated, with no adverse effects, in several clinical trials [79]. In addition, over 3 years of follow-up, Eterplirsen-treated patients showed a slower rate of decline in ambulation assessed by the 6-min walk test compared to untreated matched historical controls from two DMD natural history cohorts: the Leuven Neuromuscular Reference Center (LNMRC) and the Italian Telethon registry [80]. Previously, the ability of Eteplirsen to induce expression of dystrophin had been demonstrated by an observed increase of dystrophin-positive fibers in skeletal muscle of DMD patients [35]. Recently, Kinane and coworkers compared the pulmonary function data from DMD patients, who received Eteplirsen in studies 201/202 (included 12 patients treated with Eteplirsen over 5 years) with the natural history data published. This study verified that the deterioration of respiratory muscle function with Eteplirsen treatment as measured by forced vital capacity was half of that seen in natural history. Maximum expiratory pressure and maximum inspiratory pressure also declined more slowly in Eteplirsen treated patients compared to natural history, thus demonstrating its potential to preserve respiratory function in patients with DMD [81].

7.2.4 Antisense Oligonucleotides Delivery

One of the major issues for the use of AONs for therapeutic purposes is the efficient delivery to their target site. AONs need to reach the target tissue and, once there, they must reach the appropriate intracellular compartment [2, 7]. Parenteral injection, such as intravenous infusion or subcutaneous injection is the main method at the moment of delivery of PS modified single-stranded AONs formulated in a simple saline solution [15, 21]. However, even though AON activity has been observed in many tissues such as lung, stomach, bladder, and heart, AONs predominantly accumulate in liver, kidney, bone marrow, adipocytes, and lymph nodes [21]. Therefore, delivery problems must be considered in terms of sets of barriers to movement of AON within the body. Tissue barriers to delivery include the vascular endothelial barrier, first-pass renal excretion (which strongly affects PK and bio-distribution of AONs), and the blood brain barrier (BBB) that AONs cannot cross due to their size and charge, limiting their access to the central nervous system (CNS), in the case of CNS diseases. The one exception to this is intrathecal injection of single-stranded AONs with specific chemical modifications into the CSF, which allows AONs into the CNS [21].

Two main strategies are being developed to improve AON delivery: viral and non-viral delivery. Despite viral vectors are efficient systems for the delivery of genetic material and for the capability to infect a large number of cell types, they also showed some constraints, such as immunogenicity, tumorogenicity risks, limited loading capacity and scaling-up problems [7]. However, adeno-associated viruses (AAVs), which are non-integrative vectors and therefore present a low risk of genomic insertions, have been used in *in vitro* cells and in animal models to efficiently deliver AONs sequences embedded into modified snRNA systems (modified U1 snRNAs and modified U7 snRNAs). Indeed, promising therapeutic results were obtained with this strategy to induce exon-skipping in diseases like Leber Congenital

sandra.alves@insa.min-saude.pt

Amaurosis [82] and DMD [83–87] and exon-inclusion in SMA [88, 89] (for a more extended review on this subject see [90]). Non-viral delivery also represents a good alternative and the conjugation of free AONs with non-viral delivery carriers can be achieved by different strategies. One option is to conjugate AONs (or their carrier) to a ligand that interacts selectively with a cell surface receptor. Ideally, one such receptor should be expressed only in the tissue to be targeted. Additionally, it should also be abundantly expressed, rapidly and extensively internalized, and have a high affinity to its ligands, so that they become readily available. Some receptors used to target AONs include integrins, G protein-coupled receptors (GPCRs), human receptor tyrosine kinase (RTK), scavenger receptors, asialoglycoprotein receptor (ASGR), Toll-like receptors (TLRs) and folate receptor [91–97], as reviewed in [98]. However, receptors fulfilling all the above-referred criteria are not available for the majority of tissues and, once the AONs reach the cell surface of the target cell, they must be internalized by endocytosis and packed into a vesicle, termed endosome. Then, the endosomes fuse with lysosomes, organelles rich in hydrolases, which ultimately degrade a high portion of the internalized AONs. In fact, one strategy to improve delivery of AONs is the use of short cell-penetrating peptides (CPPs), sequences of short cationic and/or amphipathic peptides (fewer than 30 amino acids) that translocate small drugs/cargo across cell membranes. CPPs are attached to their cargo through covalent linkages or through the formation of noncovalent nanoparticle complexes [99] that can promote uptake of macromoleclues via endocytosis. CPPs covalently conjugated to AONs were already used for therapeutic purposes in DMD [100–105] Myotonic Dystrophy type I [106] and SMA [107, 108]. However, CPPs have a limited endosomal escape and overcoming the rate-limiting step of endosomal escape into the cytoplasm remains a major challenge to their successful use. Several studies tried to overcome this and some relevant results have been obtained. For instance, specific synthetic endosomal escape domains (EEDs) significantly enhanced cytoplasmic delivery in the absence of cytotoxicity [109] and a CPP-adaptor system capable of efficient intracellular delivery was also recently developed [110]. Another possibility is to incorporate AONs into nanoparticles (NPs) that based on their size and materials, will determine the AON biodistribution and interaction. In fact, the progress of nanotechnology has provided several nanosystems with the aim to increase the drug targeting efficacy. The most common types used for drug delivery are solid lipid nanoparticles (SLNs), polymer nanoparticles, lipid-based nanoparticles (LNPs) and carbon-based nanomaterials [110]. For example, cationic core-shell NPs named T1 and ZM2 (a type of polymer nanoparticles) were used to conjugate AONs for exon skipping application in preclinical studies in DMD mice [110, 111]. As these obstacles of delivery are overcome, the advantages of antisense technology will warrant that antisense oligonucleotide therapeutics will be one of the most promising clinical approaches to genetic diseases in the future.

7.3 U1 snRNA-Mediated Therapy

7.3.1 Brief Overview

Since its discovery in the early days of splicing research, U1 snRNA has been recognized as a crucial player in the first stages of the splicing process [112–114]. U1 snRNA is a 164 nucleotides long molecule with a well-defined structure consisting of four stem-loops, which primarily exerts its function in the form of a ribonucleoprotein (RNP) complex (termed U1 snRNP) containing seven Smith antigen (Sm) proteins and three U1-specific proteins U1A, U1C and U1-70K [115] (Fig. 7.4a). It is now well-established that U1 snRNP initiates spliceosome assembly by binding to the 5′ splice donor site (ss) through base pairing between the single stranded 5′ tail of the U1 snRNA molecule and the moderately conserved stretch of nucleotides at the 5′ss (CAG/GURAGU; R-purine) marking the exon-intron boundary [116]. However, not all base pairs at different 5′ss positions are equally important, and their contribution to splicing

sandra.alves@insa.min-saude.pt

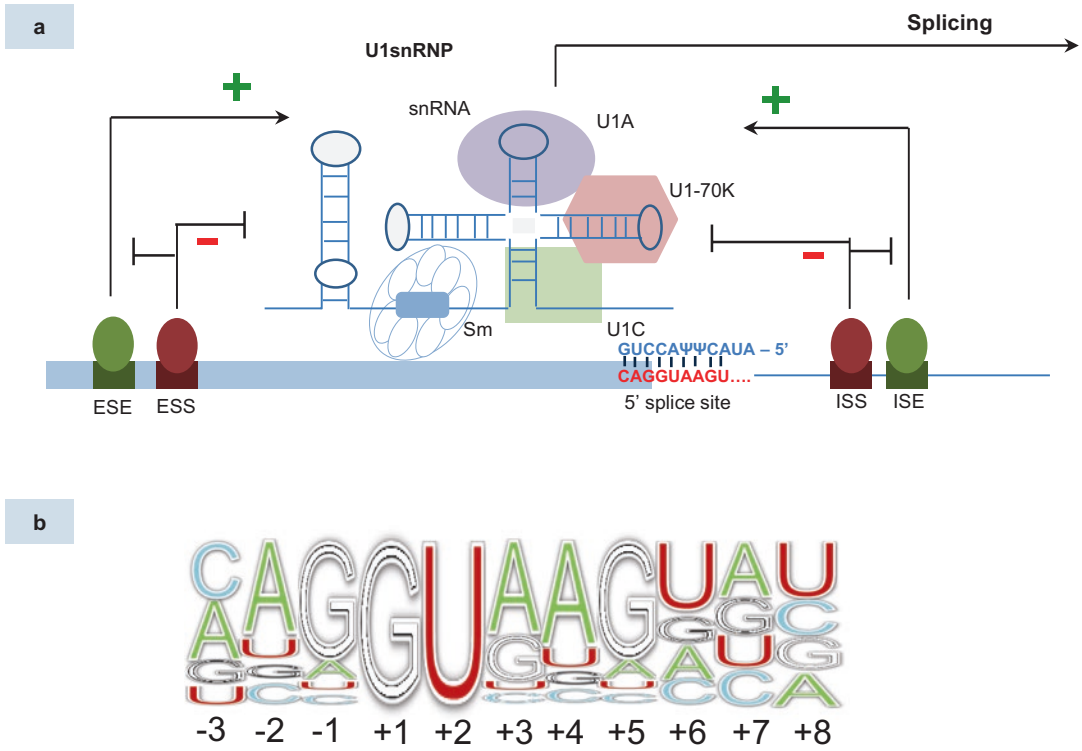


Fig. 7.4 Role of U1 small nuclear ribonucleoproteins (snRNPs) in splicing. (**a**) The 5′ end of U1 snRNA base pairs to the 5′ splice site (ss) in order to define a functional splice donor site. This process is positively and negatively modulated by different splicing factors, which bind to exonic and intronic splicing enhancer and silencer motifs (ESE, ISE, ESS and ISS, respectively). (**b**) The 5′ss motif. The height of each nucleotide corresponds to its conservation at the corresponding positon (−3 to −1 are exonic positions, while +1 to +8 correspond to intronic positions). The most conserved 5′ss positions are +1 and +2, which determine the 5′ss subtype: the GU subtype accounts for ~99% of 5'ss. Minoritary subtypes have a mismatch to U1 at either +1 or +2 and include the GC and the very rare AU 5′ss. The next most conserved 5′ ss positions are -1G and +5G, which form strong G-C base pairs with U1 through three hydrogen bonds. Consensus nucleotides −2A, +3A, +4A, and + 6U are also conserved but have a lesser although important contribution to 5'ss strength because their base pairing to U1 involves only the formation of two hydrogen bonds. The 5'ss positions +7 and +8 do not exhibit substantial conservation in humans, yet several lines of evidence indicate that these positions can base-pair to U1 and contribute to splicing

roughly correlates with their conservation (Fig. 7.4b). In the 9 nucleotides consensus sequence the most conserved 5′ss positions lie at the first two intronic nucleotides (+1 and +2), and the sequence GU at these positions accounts for ~99% of all 5′ss. The next most conserved 5′ss positions are −1G and +5G, which form strong G-C base pairing with U1 [117]. Once the donor site does not always conform to the consensus sequence, but can instead have a degenerate pattern feature, it is understandable that many other additional elements such as splicing silencer and enhancer motifs, the presence of alternative splice sites, secondary structures and regulatory proteins can influence the splice site selection (Fig. 7.4a) [117, 118].

U1 snRNA is classically known for its role in pre-mRNA splicing events. However, the finding that U1 snRNA levels far exceed other spliceosomal associated snRNA levels led to the notion that it may have additional roles in the cell apart from splicing regulation [115, 119]. Indeed, emerging evidence suggests that U1 snRNA plays a key role in transcription initiation and in the protection of pre-mRNAs from degradation, as also has a regulatory function in the 3′-end for-

sandra.alves@insa.min-saude.pt

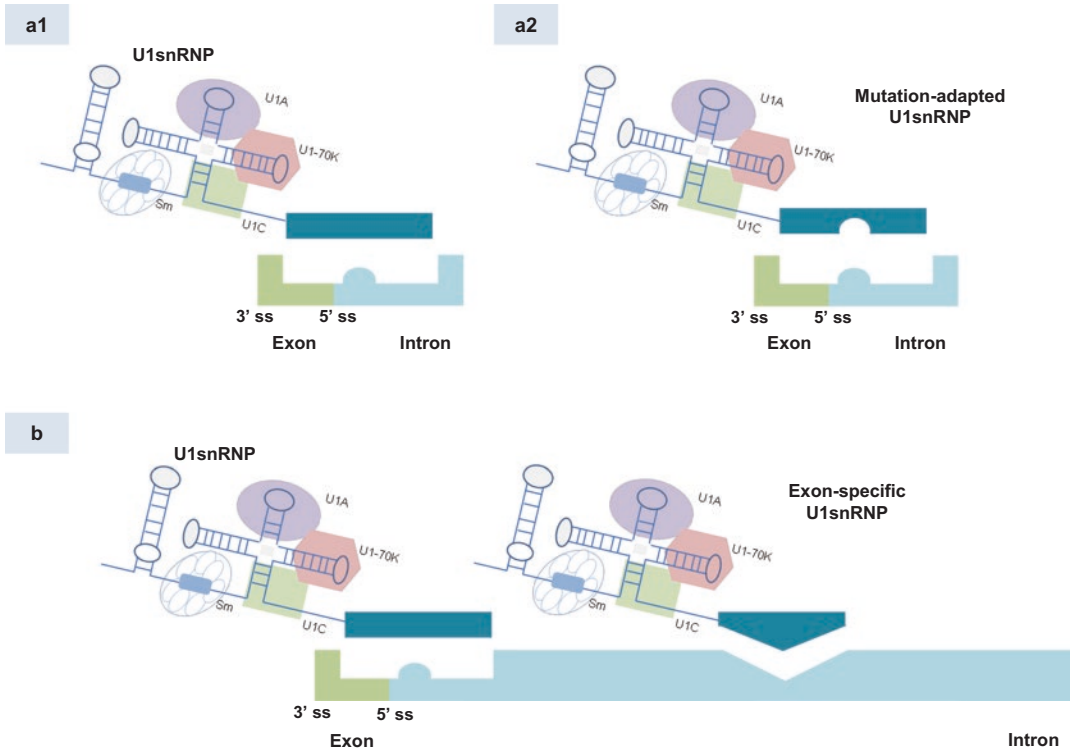


Fig. 7.5 U1 snRNA-mediated therapy for mutations affecting 5′ splice site (ss). (**a1**) A wild-type endogenous U1 small nuclear ribonucleoprotein (snRNP) does not bind to 5′ss due to the presence of a 5′ss mutation. (**a2**) An exogenous U1 snRNP (first generation particle) is modified in 5′ tail with a compensatory alteration (semi-circle) that allows for base-pairing with the mutated 5′ss and the restoration of exon recognition and inclusion. (**b**) The presence of a 5′ss mutation does not allow the correct 5′ss recognition by U1 snRNP but an exon-specific U1 snRNP (second generation particle) with an engineered 5′ tail which binds a downstream non-conserved intronic region can activate the mutated 5′ss, through a mechanism not yet fully understood, allowing the correct exon recognition and inclusion

mation, protecting pre-mRNA transcripts against premature polyadenylation and contributing to the regulation of alternative polyadenylation [115, 119–121].

Splicing mutations at the 5′ss, which are frequent among defects that cause human disease, compromise U1 snRNA binding and can prevent spliceosome assembly and subsequent splicing, which results in exon skipping, intron retention or activation of cryptic splice sites [117, 122]. The most deleterious mutations at a 5′ss are those affecting the nearly invariant GU dinucleotide at the positions +1 and +2. For the remaining nine positions the effects on splicing are less understood. Indeed, nucleotide substitutions in the less conserved positions can cause splicing defects in several but not all 5′ss, suggesting that this 5′ss positions and/or the general context define at what level splicing is changed [117, 123].

7.3.2 Two Generations of Engineered U1 snRNAs to Correct Splicing Defects

As donor splice site mutations disrupt the complementarity of the donor site with the endogenous U1 snRNA, restoring the complementarity through engineered modification of the U1 snRNA represents a valuable approach (Fig. 7.5a1, a2). In fact, in the mid-80s, Zhuang and Weiner [124] demonstrated for the first time that modified U1 snRNAs were able to suppress 5′ss mutations. Since then, the physiological role

sandra.alves@insa.min-saude.pt

of the U1 snRNA to promote exon inclusion in the presence of 5′ss mutations affecting different positions of the donor site, has been extensively exploited as a possible therapy for numerous diseases. Significant correction levels have been achieved for mutations located in less conserved 5′ss positions in diseases like Neurofibromatosis type 1 [125], Coagulation factor VII deficiency [126, 127], Retinitis pigmentosa [128, 129], Propionic acidemia [130], Phenylketonuria [131] and Bardet-Biedl syndrome [132, 133]. Furthermore, recent studies have also demonstrated the feasibility of this approach in the more conserved GU region. In fact, partial correction of splicing defects caused by mutations in the +1 position of 5′ss was observed, not only in a Fanconi anemia case [134], but also in Sanfilippo C disease patient cells [135]. Also, for a mutation in the +2 position causing Hemophilia B, the treatment with a modified U1 snRNA led to an increase in the proportion of correct transcripts (~20%) [136]. In general, though, results of U1 snRNA therapeutic approaches can vary depending on the nature of the mutation and on the overall genomic context.

Until now, modified U1s effects *in vivo* were only addressed in two studies. In the first one, Balestra and co-workers [137] showed the rescue of the expression of a splicing-defective human factor VII (hFVII) mutant by a mutation-adapted U1 snRNA which improved hFVII circulating levels in mice, highlighting the potential of this strategy as a therapy for FVII coagulation deficiency. In the second study, Lee et al. [138] demonstrated the therapeutic effect of a mutation-adapted U1 snRNA in a knock-in mouse model of Aromatic L-amino acid decarboxylase (AADC) deficiency.

In common with other rescue strategies based on targeting RNA by complementarity, modified U1 snRNAs have to deal with potential off-target effects. This is particularly dangerous for modified U1 snRNAs with only one base change from the natural U1 snRNA, which might activate normally silent cryptic donor splice sites and induce aberrant splicing in other genes [139]. The consequences of such unwanted side reactions are hard to predict and depend on the function of the spliced transcript. However, the binding site sequence screening and mapping against the human genome to rule out sequence homologies should extensively decrease nonspecific events although their total exclusion cannot be guaranteed [140]. Therefore, experimental analysis should be performed whenever possible to test the effect of the U1 treatment on non-target transcripts. In mutation-adapted U1 snRNA *in vitro* approaches to correct 5′ splicing defects in Retinitis pigmentosa [129] and Bardet-Biedl syndrome [133], this type of test was performed and no missplicing events were found in the non-target transcripts. Also, in the *in vivo* U1 snRNA therapeutic strategy for AADC deficiency, the treatment was well tolerated and no toxic effects were seen within the study period [138]. However, in the *in vivo* study for hFVII deficiency [137], the authors observed hepatotoxicity, most probably caused by the binding of the engineered U1 to similar consensus 5′ss in other genes.

It was previously shown that U1 snRNAs do not necessarily have to bind at the 5′ss to promote exon definition. Some atypical 5′ss are recognized by U1 snRNA shifted by one nucleotide [141] and U1 snRNAs complementary to intronic sequences downstream of the 5′ss were originally reported to enhance the recognition of 5′ss in model gene systems [142, 143]. Given this, to reduce the possible interaction of modified U1 snRNAs with non-target 5′ss, a second generation of engineered U1s called Exon-Specific U1 snRNAs (ExSpeU1s) was developed. The ExSpeU1s have engineered 5′ tails that direct their loading into non-conserved intronic regions downstream of the 5′ss of a specific exon, and are expected to improve specificity and reduce potential off-target events [139, 144] (Fig. 7.5b). In different cellular models (i.e. minigene assays, patient's cells or iPSC's), a number of ExSpeU1s has been successfully applied, allowing an efficient rescue of exon skipping caused by various types of splicing mutations in Hemophilia B [144, 145], Cystic Fibrosis [144], SMA [144, 146, 147], Fanconi anemia [148] and Netherton syndrome [149]. The ExSpeU1 strategy has also been investigated in mouse models. For SMA, Dal Mas et al. [146], reported that AAV-mediated

sandra.alves@insa.min-saude.pt

delivery of ExSpeU1 corrects splicing, increasing the inclusion of *SMN2* exon 7 in different tissues/organs. In another study, Rogalska and colleagues [150] created a mouse expressing a particular ExSpeU1 and, after crossing it with a severely affected SMA mouse, observed increased inclusion of the missing exon, followed by SMN protein production and increased mice lifespan. Possible gene expression side effects were also addressed and, from a panel of 12,414 analysed genes, only 12 had altered expression after treatment.

ExSpeU1 molecules have also successfully rescued splicing in a transgenic mouse model of Familial Dysautonomia, a rare genetic disease with no treatment [151]. For Hemophilia B, another ExSpeU1 was explored in mice expressing two natural *F9* splicing defective variants at 5′ss or 3′ss, and efficiently rescued human *F9* splicing in liver resulting in an increase of the target protein and coagulation activity [152]. This study, as the pivotal one developed by Fernandez Alanis et al. with the ExSpeU1 strategy [144], interestingly showed that a single ExSpeU1 can be used to correct exon-skipping mutations at the consensus 5′ss (apart from canonical GU dinucleotide), the polypyrimidine tract, and even at exonic regulatory elements, thus extending the applicability of ExSpeU1s to panels of mutations and cohorts of patients with the same genetic disorder.

Despite the promising results obtained with ExSpeU1s in different studies, its precise mechanism of action for splicing correction is not totally clear. Pagani and co-workers demonstrated that ExSpeU1s are assembled as U1-like particles and that their splicing rescue activity is dependent on the U1-70K protein and on the loop IV structure of the U1 snRNA; not on the recruitment of endogenous U1 snRNP to the upstream 5′ss [150]. This may indicate that ExSpeU1s promote correct exon recognition through the recruitment of splicing factors that subsequently activate the mutated 5′ss [144, 146, 149–152]. However, it is important to stress that the splicing stimulator activity of ExSpeU1s was also responsible for the activation of a cryptic 5′ss in an approach attempted to correct a splicing defect causing Intrahepatic Cholestasis, which resulted in the production of an additional splice transcript with intron retention [153].

Globally, both mutation-adapted U1 snRNA and exon-specific U1 snRNA constitute a novel therapeutic strategy to correct splicing defects associated to defective exon definition in several human disorders. Once the U1 snRNA-mediated approaches act at pre-mRNA level, they have the main advantage of maintaining the regulated expression of the targeted gene in the normal chromosomal context [139, 154]. Also, given that the U1 snRNA gene used for splicing rescue includes promoter and regulatory sequences, it has the capability of guaranteeing long term correction of the genetic defect [139]. Despite these advantages, U1 snRNA-mediated therapies may also face some problems such as the presence of off-target effects and low efficacies. Therefore, in a near future, it will be imperative not only to develop a specific method or tool to search for off-target effects, but also to adjust the expression levels of U1 snRNA therapeutic particles in preclinical *in vivo* studies [154].

7.3.3 Engineered U1 snRNAs Delivery

U1 snRNA-mediated therapies also have to deal with the challenge of an efficient delivery to a target tissue. In the *in vivo* studies already developed, one of the most successful gene therapy systems available nowadays – AAV vectors – has been chosen as the method for U1 snRNA-engineered particles delivery into mice [137, 138, 146, 150, 151]. AAV vectors allow a highly efficient delivery to various tissues following systemic injection, even though dependent on the viral serotype used [90, 155]. Also, the low packaging capacity of AAV vectors is quite adequate for U1 snRNA-based approaches given the small cassette size to package [90]. However, despite the modifications that have been introduced in viruses, the potential for antiviral immunity and phenotoxicity of the transgene are still major limitations to the use of viral vectors for therapy.

sandra.alves@insa.min-saude.pt

Possible alternatives to viruses are liposomes and nanoparticle delivery [155].

Among the several RNA tools enabling the rescue of splicing, both mutation-adapted U1 snRNA and ExSpeU1 snRNA therapeutic strategies have already shown their efficacy to repair different types of splicing defects at least in animal models of disease. Still, further developments will be necessary for this therapeutic approach to be translated to human trials.

7.4 siRNA-Based Drugs

7.4.1 Brief Overview

The last decade of the twentieth century has also witnessed the discovery of a new mechanism of gene regulation whose therapeutic potential is still being unveiled: RNA interference (RNAi). Interestingly, the first experimental observation of this mechanism came up from a failed genetic experiment aimed at developing more attractive petunia flowers. In fact, in 1990, Jorgensen and co-workers attempted to genetically engineer flower pigmentation genes, to be inserted into the target plant genome. To their surprise, however, instead of generating more colorful flowers, they ended up producing a generation of plants that had virtually lost all pigmentation, thus becoming white. This observation prompted additional studies to check the expression levels of endogenous genes involved in the natural pigmentation biosynthetic pathway and most of them were strongly reduced. Thus, a concept of co-suppression, whereby sequence-related genes could negatively regulate each other, was born [156, 157]. Still, little was known on its underlying mechanism. The first major breakthrough came from the pivotal studies by Andrew Fire and Craig Mello. By introducing various forms of long RNA molecules into *C. elegans*, their team observed that those with a double-stranded presentation (double stranded RNAs, dsRNAs) were the actual inducers of the silencing phenomenon, which was then coined RNAi [158]. Thus, the work by Fire and Mello, which earned them the 2006 Nobel Prize of Medicine, has not only represented a major advance in the understanding of RNAi basic mechanism, but also provided a simple and reproducible method by which long dsRNAs could be used to induce specific gene silencing in lower organisms commonly used in genetic research, such as *C. elegans* [159] and *D. melanogaster* [160]. In the meantime, other teams kept their focus in plant systems, aiming at a better understanding of the role that RNAi and additional silencing processes assume in plant homeostasis. Soon it became clear that gene silencing operating at the RNA level has roles in adaptative protection against viruses [161], genome defense against mobile DNA elements [162, 163] and developmental regulation of gene expression (reviewed in [164]). A second component of RNA silencing, in addition to dsRNAs, was then identified and coined short interfering RNAs, which resulted from the processing of dsRNAs into 21–26 nt counterparts [165]. Interestingly, those short interfering RNA molecules could be sorted into two classes depending on their size, and soon it became clear that each of those classes assumed different functions. The long ones (24–26 nt) were dispensable for sequence specific mRNA degradation, but essential for systemic silencing and methylation of homologous DNA [164]. Another interesting contribution to the deeper understanding of the overall RNA silencing process came from a work of Cogoni and co-workers, who described a new biological function for RNA silencing in *Neurospora* called quelling, which can be activated upon the introduction of transgenic DNA. These authors observed that quelling targets preferentially transgenes arranged in large tandem arrays and its effectors are also short interfering RNAs [166], reviewed in [167]. Altogether, these works unveiled an unexpected complexity in the RNA silencing process in plants, prompting additional studies to check whether the same would also apply in animals. By this time, however, no one foresaw that the RNAi mechanism would also work in mammalian systems because long dsRNAs were already known to induce a strong interferon response. The first demonstrations that RNAi also works in humans came from the work of two

sandra.alves@insa.min-saude.pt

independent groups in Germany, one operating at the Max Planck Institute, and the other at the University of Bayreuth, and a third one in the United States, operating at the NIH, Bethesda. The team at the Max Plank Institute showed that synthetic versions of short dsRNA molecules were able to trigger a strong gene silencing effect in mammalian cells without inducing the interferon response. Moreover, they tested a series of design features for those short dsRNAs including length, blunt or sticky ends and chemical modifications, finding that structurally defined 21–23 base-pair small RNAs, with 2 nucleotide unpaired overhangs at the 3′ ends, were the most efficient mediators of RNAi [168, 169]. This fundamental work was published in Nature in 2001, and became the scientific content for a key patent in the field called "Tuschl II". In parallel, the NIH team came up with another demonstration that synthetic siRNAs can induce gene-specific inhibition of expression in *C. elegans* and in cell lines from humans and mice. They did it by systematically comparing the level of gene expression decrease caused by siRNAs *versus* that caused by single stranded AONs [170]. Their work, published in PNAS, was another step to open a path toward the use of siRNAs as a reverse genetic and therapeutic tool in mammalian cells, as the authors themselves have stated. Around the same time, at the University of Bayreuth, Kreutzer and Limmer had also reasoned that short fragments of dsRNA would putatively mediate a RNAi response similar to the one originally described by Fire and Mello and, even though their findings have never been published, they did file key patents around the discovery. Additional studies on the subject ended up unveiling the endogenous RNA silencing pathway that was being fed by small dsRNAs, from now on called small interfering RNAs (siRNAs). It also became evident that the same pathway is also able to process microRNAs (miRNAs), as previously seen (Fig. 7.1c). Here, we will focus solely on the RNAi process triggered by siRNAs.

The siRNA pathway starts with the cytoplasmic cleavage of long dsRNAs by an enzyme called Dicer. As a result, short dsRNA duplexes are formed. Then, those dsRNAs are incorporated into the RNA-induced silencing complex (RISC), where the strands are separated, and one strand guides RISC to the complementary region of target mRNA (Fig. 7.6). The heart of RISC is the Argonaute (AGO) proteins. In humans there are 8 AGO proteins, 4 from AGO clade (AGO1-4) and 4 from P-element induced wimpy testis (PIWI) clade (PIWI1-4; [171]). Still, not all AGO proteins are cleavage competent. In fact, AGO2 is the sole executer that accomplishes siRNA-induced silencing. Thus, whenever the siRNA strand loaded into RISC has complete sequence complementarity with its target mRNA sequence, it triggers site-specific mRNA cleavage, which ultimately results in a reduced expression of that mRNA and of the target protein (Fig. 7.4; reviewed in [172]). This exact same process can also be induced by direct exogenous supply of synthetic siRNAs. Over the years, a series of empirical and rational guidelines started accumulating from the analysis of hundreds of functional siRNAs. There are now a number of guidelines one should follow in order to design an effective siRNA, which have been well reviewed elsewhere [173]. There are also many websites and companies that either offer reliable methods for the design of effective siRNAs or even design them on demand. Because of their small size, the chemical synthesis of siRNAs is relatively easy and nowadays, several companies offer them delivered in ready-to-transfect format. This is, therefore, a simple, easy-to-handle RNAi-effector for virtually every lab need.

Since the half-life of siRNA is short, an alternative RNAi-effector molecule has also been developed: short hairpin RNAs (shRNAs), which are not directly transfected into their target cells. Instead, shRNAs are transcribed in the nucleus from an exogenous DNA expression vector bearing a palindromic sequence with a spacer in between, whose transcript folds into a short dsRNA with a terminal loop. The shRNA transcript is processed by Drosha, an RNase III endonuclease. The resulting pre-shRNA is exported to the cytoplasm, where it can then be processed by another RNase III, called Dicer, and incorporated into RISC, thus triggering the same RNAi process previously described (reviewed in [172]). In

sandra.alves@insa.min-saude.pt

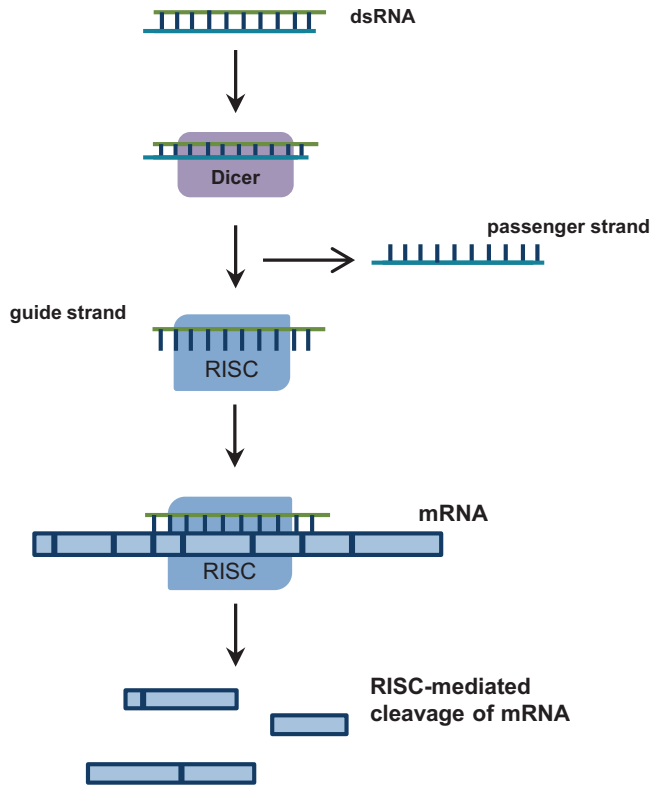


Fig. 7.6 The RNA interference (RNAi) mechanism. Entry of double-stranded RNA (dsRNA) into eukaryotic cells results in targeted RNA-induced silencing complex (RISC)-mediated cleavage of messenger RNA (mRNA) through activation of the endogenous RNAi mechanism: dsRNAs are recognized and cleaved into shorter fragments by Dicer, and subsequently loaded into a multiprotein conglomerate called RISC, which facilitates the separation of the two RNA strands. Once the double-stranded RNA is separated, one strand gets degraded while the other associated with RISC acts as a template for RISC-mediated cleavage of complementary RNA, thus reducing protein translation

general, shRNAs are harder to complex/internalize. Still, by delivering DNA instead of the effector RNA molecule, they take advantage of the cell's transcription machinery to produce specific shRNA transcripts, they allow for high potency sustainable effects using low-copy numbers. One such approach results in less off-target effects, putatively ensuring greater safety. Additionally, a shRNA expression vector does also cost less than the bulk manufacturing of siRNAs (reviewed in [174]).

Once all cells have the RNAi machinery and, in principle, any gene can be knocked down, soon siRNAs became invaluable tools in the lab, enabling the easy genetic knockdown of any sequence. RNAi was rapidly exploited as a tool to promote unbiased genome-wide screening to search for relevant genes involved in specific biological processes, first in invertebrate cells [170, 175–177] and latter in mammalian cells [178–182]. In fact, this knockdown technique provides a valuable tool for the functional annotation of mammalian genes [183, 184], for the creation of knockout animals [185] and for the identification of new drug targets (reviewed in [186]), but these are far from being the major application of this technology. In fact, RNAi has been regarded as one of the major breakthroughs in the field of molecular medicine, and its potential as a therapeutic effector has been largely tested over the last decades.

The need to optimize the technique and take it from bench to clinic is also prompting extra research efforts to gain a deeper understanding of

sandra.alves@insa.min-saude.pt

the overall RNAi mechanism. For example, in order to function, siRNAs need to escape to the cytosol, where the RISC works. Thus, release from the endosome is an important barrier. Understanding the mechanism(s) that promotes and limits endosomal release may help to optimize this limiting step. This remains, though, a major area of investigation for all nucleic acid therapeutics [11].

7.4.2 Recent Successful Applications of siRNA-Based Drugs

Being a naturally occurring post-transcriptional gene silencing process, this mechanism has several advantages when compared to other AON technologies, and that recognition triggered major investments in RNAi-based drug development by large pharmaceutical and biotechnological companies [187]. The potential of siRNA therapeutics was first demonstrated by Song and co-workers 15 years ago, when injection of *Fas* siRNAs protected mice from autoimmune hepatitis. Fas-mediated apoptosis is implicated in a broad spectrum of liver diseases, where inhibiting hepatocyte death can be life-saving. These authors investigated the silencing effect of siRNA duplexes targeting the gene encoding the Fas receptor (*Fas*), to protect mice from liver failure and fibrosis in two models of autoimmune hepatitis. Intravenous injection of *Fas* siRNA specifically reduced both *Fas* mRNA and Fas protein expression levels in mouse hepatocytes, and the effects persisted without diminution for 10 days [188]. This pioneer work has not only shown that siRNA-directed Fas silencing could work *in vivo* and be of therapeutic effect for preventing and/or treating acute and chronic liver injury [188], but also provided the proof-of-principle on the potential of the overall RNAi technology to treat or prevent disease (reviewed in [189]). Since then, drug development has been rapid, with siRNAs facing virtually the same obstacles as AONs. Fortunately, some of the AON strategies could be adapted to siRNA therapeutics, thus accelerating siRNA preclinical drug development and clinical evaluation. In general, RNAi clinical trials are progressing well. Clinical Phase I and II studies of siRNA therapeutics have demonstrated potent (as high as 98%) and persistent (lasting for weeks) gene knockdown effects, especially in liver, with some signs of clinical improvement and without unacceptable toxicity (reviewed in [189]). There are also several trials in Phase III development (Table 7.2; reviewed in [11]).

Early this year Alnylam has announced U.S. FDA acceptance of New Drug Application (NDA) and Priority Review Status for Patisiran, an investigational RNAi therapeutic for the treatment of hereditary transthyretin amyloidosis (hATTR) [225]. Almost at the same time, the company presented new clinical results from the APOLLO Phase III study of this drug at the 16th International Symposium on Amyloidosis. The APOLLO Phase III trial was a randomized, double-blind, placebo-controlled, global study designed to evaluate the efficacy and safety of Patisiran in hATTR amyloidosis patients with polyneuropathy. The primary endpoint of the study was the change from baseline in modified Neurologic Impairment Score +7 (mNIS+7) relative to placebo at 18 months. According to the general manager of the transthyretin (TTR) program at Alnylam, "*the clinical results presented further highlight the robust profile of Patisiran and provide evidence supporting Patisiran as a potentially transformative treatment approach for patients with hATTR amyloidosis*". Also the results obtained in the cardiac subpopulation, which corresponded to approximately 50% of the patients enrolled in the APOLLO study, revealed significant improvements in measures of cardiomyopathy, the leading cause of death in patients with hATTR amyloidosis, relative to placebo [201]. Finally, in August 2018, the drug got its U.S. FDA approval, and is now commercialized under the designation Onpattro™ [226].

Hopefully, the approval of the first RNAi therapeutic will pave the way for approval of other targets (reviewed in [227]), especially if we take into account that there are several other siRNA drugs under evaluation, which have recently advanced for phase III development (Table 7.2; reviewed in [11]). The most relevant examples

sandra.alves@insa.min-saude.pt

Table 7.2 Summary table of clinical trials for Small interfering RNAs (siRNAs)

Chemistry	Drug	Target/organ	Dose/route	Indication	Key observations	References
Phase 3						
PS, 2′-OMe, 2′-F (LNP)	Patisiran (ALN-TTR02)	*TTR*, Liver	0.3 mg/kg once every 3 weeks, IV (Pretreatment w/ glucocorticoids, antihistamines and analgesics)	Hereditary ATTR	Phase 3 findings included (1) significant improvement with patisiran compared to placebo in neuropathy and quality of life metrics, (2) infusion-related reactions, and (3) peripheral edema	NCT01960348 (Coelho [190, 191]) (Alnylam Pharmaceuticals, press release, Sept 20, 2017)
2′-MOE (None)	QPI-1002 (15NP)	*TP53*, Kidney	0.5–10 mg/kg, IV	Delayed graft function; AKI following cardiac surgery	Phase 2 findings in renal transplant patients included improved (1) dialysis-free survival time, and (2) reduced number dialysis in first 30 days	NCT02610296 NCT02610283 [192, 193]
Unmodified (None)	SYL1001	*TRPV1*, Eye	11.25 g/mL/drop, Eye drops	Ocular pain; dry eye syndrome	Phase 2 findings included analgesic trend that was not significant compared to placebo	NCT03108664 [194]
2′-MOE (None)	QPI-1007	*CASP2*, Eye	1.5 mg, IVT	Acute NAION, acute primary angle closure glaucoma	Phase 1 findings included conjunctival hemorrhage	NCT02341560 [195, 196]
PS, 2′-OMe, 2′-F, GalNAc (None)	Fitusiran (ALN-AT3SC)	*SERPINC1*, Liver	80 mg once monthly, SC	Severe Hemophilia A or B	Phase 1/2 open-label and open-label extension findings in patients included (1) mean 80% target reduction and reduced bleeding, and (2) 1 death due to thromboembolic event	NCT03417245 NCT03417102 NCT02035605 NCT02554773 [197, 198]
PS, 2′-OMe, 2′-F,GalNAc (None)	Inclisiran (ALN-PCSSC)	*PCSK9*, Liver	300 mg once every 3–6 months, SC	ASCVD, HC, HoFH, HeFH	Phase 2 findings included (1) mean 53% reduction of LDL-C, (2) injection site reactions, and (3) ALT elevations	NCT03400800 NCT03399370 NCT03397121 [199, 200]

(continued)

sandra.alves@insa.min-saude.pt

Table 7.2 (continued)

Chemistry	Drug	Target/organ	Dose/route	Indication	Key observations	References
PS, 2′-OMe, 2′-F, GalNAc (None)	Givosiran, (ALN-AS1)	*ALAS1*, Liver	2.5 mg/kg once monthly, SC	Acute hepatic porphyrias	Phase 1 findings in ASHE and AIP patients included (1) dose-dependent reduction of target, (2) 63% reduction in annualized AIP attack rate, (3) injection site reactions, and (4) myalgia	NCT03338816 [201], press release, Nov 7, 2017) NCT02452372
Phase 2						
Undisclosed (PLGA polymer)	siG12D-LODER	mutant *KRAS*, Tumor	0.025-3 mg, Surgical implant	Pancreatic ductal adenocarcinoma	Phase 2 findings included (1) suggestion of improved median survival, and (2) cholangitis and neutropenia	NCT01676259 NCT01188785 [202, 203]
Unmodified (None)	Bamosiran (SYL 040012)	*ADRB2*, Eye	300-900 mg/eye/day, Eye drops	Ocular hypertension; open angle glaucoma	Phase 1/2 findings included (1) reduction of intraocular pressure, and (2) no drug related adverse events	NCT02250612 [204, 205]
Undisclosed (LNP)	TKM-080301 (TKM-PLK1)	*PLK1*, Liver	0.15-0.9 mg/kg, IV	Solid tumors with liver involvement; neuroendocrine tumors; adrenocortical carcinoma	Phase 1/2 findings included (1) some evidence of antitumor activity, (2) infusion reaction-like inflammatory response, (3) ALT elevations, and (4) acute respiratory failure	NCT01437007 NCT01262235 NCT02191878 [206]
Undisclosed (None)	RXI-109	*CTGF*, Skin/ Eye	1-10 mg, ID/IVT	Hypertrophic scars; keloids, and subretinal fibrosis	Phase 1 findings included modest target reduction	NCT02246465 NCT02079168 NCT02599064 [207]
2′-OMe (cationic lipoplex)	Atu027	*PKN3*, Vascular endothelium	0.001-0.336 mg/kg, IV (administered w/ gemcitabine)	Advanced solid tumors; pancreatic ductal carcinoma	Phase 1/2 findings included possible anti-tumor effects	NCT00938574 NCT01808638
2′-OMe (None)	PF-655	*DDIT4*, Eye	0.05-3 mg/eye, IVT	AMD	Phase 1/2 findings included (1) no evidence of benefit in AMD patients, and (2) increased intraocular pressure	NCT01445899 [208]

sandra.alves@insa.min-saude.pt

PS, 2′-OMe, 2′-F, GalNAc	Cemdisiran (ALN-CC5)	*C5*, Liver	600 mg once every 4 weeks, SC	Complement mediated diseases (aHUS, PNH)	Open-label phase 1 findings included (1) sustained control of hemolysis with up to 67% reduction in eculizumab dose, (2) 99% reduction of C5, (3) injection site reactions, and (4) 1/6 (17%) Gr 3 LFT	NCT03303313 NCT02352493 [209]
PS, 2′-OMe, 2′-F, GalNAc (None)	Lumisiran (ALN-GO1)	*HAO1*, Liver	1.0 mg/kg, SC	1st Hyperoxaluria type 1	Phase 1 findings in healthy volunteers included (1) increased plasma and urine glycolate, and (2) injection site pain	NCT02706886 [210]
3 siRNAs Undisclosed (LNP)	ARB-1467 (TKM-HBV)	*HBV*, Liver	2 mg/mL, IV in combination w/ nucleoside analogues (Pretreatment w/ medication to mitigate infusion-related reactions)	HBV infection	Phase 1 findings in patients included dose-dependent additive HBsAg reduction	NCT02631096 [211]
Phase 1						
PS, 2′-OMe, 2′-F, GalNAc (None)	ALN-TTR$_{SC}$02	*TTR*, Liver	5-300 mg, SC	Hereditary ATTR	Phase 1 findings in healthy volunteers included (1) dose dependent reduction in plasma TTR	NCT02797847 (Alnylam Pharmaceuticals, press release Dec 16, 2016)
Undisclosed (LNP, vitamin A)	ND-L02-s0201	*SERPINH1* Liver	0.03-0.6 mg/kg/wk, IV (Pretreat w/ antihistamines)	Hepatic fibrosis	Phase 1b findings included (1) no doselimiting toxicities, and (2) infusion reactions.	NCT02227459 [212]
Undisclosed (siRNAelectroporated PBMCs)	APN401	*CBLB*, Tumors	5-50 3 10^5 cells /kg, IV	Melanoma, pancreatic cancer, renal cell cancer	(1) Immune modulation shown by in vitro increase in IFN-g and IL-2 with CD3/CD28 stimulation, and (2) infusion reaction like adverse events	NCT02166255 NCT03087591 [213, 214]

(continued)

sandra.alves@insa.min-saude.pt

Table 7.2 (continued)

Chemistry	Drug	Target/organ	Dose/route	Indication	Key observations	References
Undisclosed (liposome)	siRNA-EphA2-DOPC	*EPHA2*, Tumors	IV	Advanced cancers	Not published	NCT01591356
2 siRNAs, Undisclosed (LNP)	ALN-VSP02	KIF11 and *VEGFA*, Liver/Tumors	0.1-1.5 mg/kg, IV (Pretreatment w/ glucocorticoids, antihistamines, and analgesics)	Advanced solid tumors with liver involvement	Phase 1/2 findings included (1) evidence of antitumor activity, and (2) infusion reactions, dose-limiting thrombocytopenia, and complement split product Bb increase	NCT01158079 [215, 216]
Undisclosed (LNP)	ALN-PCS02	*PCSK9*, Liver	0.4 mg /kg, IV (Pretreatment w/ glucocorticoids, antihistamines, and analgesics)	HC	Phase 1 findings included (1) reductions in PCSK9 of up to 84% and LDL cholesterol plasma levels of up to 50% after a single IV dose, and (2) infusion reactions	NCT01437059 [217]
Undisclosed (None)	TD101	*KRT6A*, Nails/Skin	0.1-17 mg, Intra-lesion	PC	Limited data from one patient	NCT00716014 [218]
Undisclosed (gold NP)	NU-0129	*BCL2L12*, Cancer	IV	Glioblastoma multiforme	Not published	NCT03020017
Discontinued						
Unmodified (None)	Bevasiranib (Cand5)	*VEGFA*, Eye	IVT	Macular degeneration, diabetic macular edema	Terminated in Phase 3 due to lack of efficacy.	NCT00499590 (Health, press release Mar 2009)
Unmodified (None)	AGN211745	*FLT1*, Eye	0.100-1 mg, IVT	AMD w/choroidal neo-vascularization	Terminated after Phase 2 due to lack of efficacy	NCT00395057
Undisclosed, GalNAc (None)	ALN-HBV	*HBV*, Liver	0.1-3.0 mg/kg, SC	Non-cirrhotic chronic HBV	Replaced by more potente compound	NCT02826018

sandra.alves@insa.min-saude.pt

2′-OMe, 2′-F, GalNAc (None)	Revusiran (ALN-TTRSC)	*TTR*, Liver	500 mg once weekly, SC	TTR-mediated cardiac amyloidosis	Terminated due to imbalance of mortality in the drug arm compared to placebo, adverse events included ISRs and LFT elevations	NCT02319005 [219, 220]
Unmodified (SNALP)	PRO-040201 (TKM-ApoB)	*APOB*, Liver	IV	HC	Terminated after phase 1due to infusion reactions	NCT00927459 [221]
Undisclosed (RONDEL™ cyclodextrin insert polymer, adamantane-PEG-transferrin)	CALAA-01	*RRM2*, Tumors	3-30 mg/m^2, IV	Solid tumors	Terminated in phase 1due to dose-limiting toxicities, including infusion reaction-like adverse events, elevated creatinine and LFTs, and dose-dependent thrombocytopenia	NCT00689065 [222]
Undisclosed (LNP)	DCR-MYC	*MYC*, Tumors	0.1-0.85 mg/kg, IV	Multiple cancers	No evidence of clinical activity	NCT02110563 NCT02314052 (Dicerna Pharmaceuticals, press release Sept 26, 2016)
Undisclosed (LNP)	DCR-PH1	*AGXT*, Liver	0.005-0.05 mg/kg, IV	Primary hyperoxaluria type 1		NCT02795325
PS, 2′-OMe, 2′-F, GalNAc (None)	ALN-AAT	*SERPINA1*, Liver	0.1-6.0 mg/kg, SC	Alpha-1 Antitrypsin deficiency	Terminated after phase 1/2 due to LFT elevations.	NCT02503683
Undisclosed, cholesterol (MLPCDM-GalNAc)	ARC-520	*HBV*, Liver	4 mg/kg, IV (Pretreatment w/ antihistamine and acetaminophen)	Chronic HBV	Terminated due to toxicities in NHPs, but had favorable tolerability in clinic	NCT02349126 (Arrowhead Pharmaceuticals, press release Nov 29, 2016)
Undisclosed, cholesterol (MLPCDM-GalNAc)	ARC-521	*HBV*, Liver	0.6-6.0 mg/kg, IV (Pretreatment w/ antihistamine and acetaminophen)	Chronic HBV	Terminated due to toxicities in NHPs, but had favorable tolerability in clinic.	NCT02797522 [223] (Arrowhead Pharmaceuticals, press release Nov 29, 2016)

(continued)

sandra.alves@insa.min-saude.pt

Table 7.2 (continued)

Chemistry	Drug	Target/organ	Dose/route	Indication	Key observations	References
UNA, cholesterol (MLP-CDM-GalNAc)	ARC-AAT	*SERPINA1*, Liver	0.38-8.0 mg/kg, IV (Pretreatment not disclosed, but assumed same as other ARC drugs)	Alpha-1 antitrypsin deficiency	Terminated due to toxicities in NHPs, but had favorable tolerability in clinic and dose-dependent reductions in sérum AAT up to 90%	NCT02363946 [224] (Arrowhead Pharmaceuticals, press release Nov 29, 2016)
Undisclosed (LNP)	ALN-TTR01	*TTR*, Liver	1 mg/kg, IV (Pretreatment w/ glucocorticoids, anti-histamines and analgesics)	Hereditary ATTR	Terminated due to greater potency of patisiran (ALN-TTR02)	NCT01148953 [190]

Abbreviations: **Chemistry:** *PS* phosphorothioate, *2′ –Ome* 2′ –methoxy, *2′ – F* 2′ – fluoro, *2′ – MOE* 2′ –O- methoxy ethyl, *GalNAc* N-Acetilgalactosamine, *PLGA* poly(lactic-co-glycolic) acid, *LNP* lipid nanoparticle, *NP* nanoparticle, *PEG* polyethylene glycol, *SNALPs* stable nucleic acid-lipid paricles, *MLP* melittin-like protein, *CDM* carboxy-dimethylmaleamide, *UNA* unlocked nucleic acid. **Target/ organ:** *TTR* transthyretin, *TP53* tumor protein 53, *TRPV1* transient receptor potential cation chanel subfamily V member 1, *CASP2* caspase2, *SERPINC1* serpin family C member 1, *PCSK9* proprotein convertase subtilisin/kexin type 9, *ALAS1* 5′-aminolevulinate synthase 1, *KRAS* KRAS proto-oncogene, *ADRB2* adrenoreceptor beta 2, *PLK1* Serine/threonine-protein kinase, *CTGF* connective tissue growth factor, *PKN3* protein kinase N3, *DDIT4* DNA damage inducible transcript 4, *C5* complement C5, *HAO1* hydroxyacid oxidase 1, *HBV* Hepatitis B Virus, *SERPINH1* serpin family H member 1, *CBLB* Cbl proto-oncogene B, *EPHA2* ephrin receptor A2, *KIFF11* kinesin family member 11, *VEGFA* vascular endothelial growth factor, *KRT6A* keratin 6A, *BCL2L 12* BCL2 like 12, *FLT1* fms related tyrosine kinase 1, *APOB* apolipoprotein B, *RRM2* ribonucleotide reductase regulatory subunit M2, *MYC* MYC proto-oncogene, *AGXT* alanine-glyoxylate and serine-pyruvate aminotransferase, *SERPINA1* serpin family A member 1. **Dose/route:** *IV* intravenous, *IVT* intravitreal, *SC* subcutaneous, *ID* intradermal. **Indication:** *ATTR* transthyretin amyloidosis, *AKI* acute kidney injury, *NAION* non-arteritic anterior ischemic optic neuropathy, *ASCVD* atherosclerotic cardiovascular disease, *HC* hypercholesterolemia, *HoFH* homozygous familial hypercholesterolemia, *HeFH* heterozygous familial hypercholesterolemia, *AMD* age-related macular degeneration, *aHUS* atypical hemolytic-uremic syndrome, *PNH* paroxysmal nocturnal hemoglobinuria, *HBV* Hepatitis B Virus, *ATTR* transthyretin amyloidosis, *HC* hypercholesterolemia, *PC* pachyonychia congenital, *AMD* age-related macular degeneration. **Key observations:** *ALT* alanine aminotransferase, *ASHE* asymptomatic high excreters, *AIP* acute intermittent porphyria, *AMD* age-related macular degeneration, *C5* complement C5, *LFT* liver function tests, *TTR* transthyretin amyloidosis, *IFN-g* interferon gamma, *IL-2* interleukin 2, *PCSK9* Proprotein convertase subtilisin/kexin type 9, *LDL* Low-density lipoprotein, *ISR* injection site reaction, *NHP* non-human primate, *AAT* Alpha-1-antitrypsin

sandra.alves@insa.min-saude.pt

include Revusiran, which is a second siRNA drug under evaluation as a treatment option for patients with familial amyloid cardiomyopathy by reducing plasma TTR levels [220]; QPI-1002, which is being developed for the treatment of delayed graft function for kidney transplants [192]; Fitusiran, a potent siRNA drug under study for patients with hemophilia, which aims at ameliorating the disorder by reducing the plasma levels of anti-thrombin [198], and Inclisiran, which targets proprotein convertase subtilisin/kexin type 9 (PCK9) to reduce the risk of cardiovascular disease [200], as reviewed in [11].

7.4.3 Delivery of siRNA-Based Drugs

Intracellular delivery of double-stranded siRNAs is more challenging than delivery of single stranded AONs [186]. Still, it is also worth mentioning that, as suggested by the best estimates, only a few hundred cytosolic siRNAs per cell are needed for efficient and sustained gene knockdown [228, 229]. This happens because the guide strand of the siRNA remains stable within the RISC for weeks, even though it gets diluted with every cell division [230]. Thus, the same siRNA molecule can target multiple transcripts, knocking down gene expression in slowly dividing or non-dividing cells over the same period. Overall, as noticed by several authors, this actually contributes to turn the delivery obstacle into a less formidable one than that faced by other antisense mechanisms, which act on a one-to-one basis [230] (reviewed in [229]).

Still, knowing that the translation of siRNAs from the bench to the clinic would be hindered by their limited cellular uptake, low biological stability and unfavorable pharmacokinetics, the development of appropriate delivery methods became mandatory to proceed with preclinical studies. Therefore, different approaches have been (and are being) attempted to ensure safer and long-lasting delivery methods for siRNA-based drugs, for both systemic and targeted delivery. Most of these developments were made in parallel with siRNA drug development and only through the combined efforts of several independent teams were these drugs modified in ways that allowed their clinical evaluation, with the promising results highlighted in the previous section. Whatever the case, an effective delivery system must fulfill a series of criteria, which have already been listed by Tatiparti et al. amongst other author: be stable at the body temperature and pH variations, have an endocytosis promoting shape, cannot be toxic, must exhibit high siRNA loading abilities and have a size that avoids rapid renal and hepatic clearance [231]. In general, all the delivery systems developed for gene therapy may also be adapted for siRNA delivery [232].

7.4.4 Non-targeted Delivery

Early strategies for solving the dual problems of intracellular delivery and rapid excretion involved incorporating siRNAs into LNPs – smaller, more homogeneous analogues of lipoplexes used for laboratory transfection [233–235], (reviewed in [189]). LPNs were first shown to be effective in targeting the hepatitis B virus (HBV) in mice, where the LPN-formulated siRNA was given in 3 daily injections of 3 mg/Kg/day. This treatment regimen resulted in a decrease of HBV levels by 1–2 orders of magnitude [236], as reviewed in [237]. Nevertheless, these complexes (and other nanoparticle strategies for siRNA delivery) accumulate in the liver and other filtering organs, which limits their effectiveness in penetrating other tissues [235, 238] (reviewed in [189]). Furthermore, the administration of siRNAs with LNP delivery vehicles is quite pro-inflammatory. In fact, lipid-based vehicles can become entrapped in endosomes [237], where the Toll-like receptors (TLR) will recognize various moieties in dsRNAs, modified siRNAs or even from their degradation products [239], eliciting an undesirable innate inflammatory response. So, in most circumstances the siRNAs require pretreatment regimens including antihistamines, non-steroidal anti-inflammatories and even relatively high doses of glucocorticoids [190, 191, 240] (reviewed in [11]).

sandra.alves@insa.min-saude.pt

Still, recent developments by several independent teams have demonstrated the feasibility of systemic administration of either chemically modified or complexed siRNAs. In fact, even though unmodified siRNAs do not distribute broadly to tissues after systemic administration (reviewed in [11]), simple chemical modifications of the 2′-position of the ribose and substitution of phosphorothioate linkages, such as the ones described for AONs in the first section of this chapter (2′-OMe and 2′-MOE), and 2′-fluoro (2′-F), protect siRNAs from nuclease digestion, thus prolonging their half-lives, both in serum and other body fluids [236, 241] (reviewed in [189]). 2′-modifications can also prevent recognition by innate immune receptors by blocking the binding to TLR [242–244] and reduce off-target effects that could arise from the suppression of partially complementary sequences [245] (reviewed in [189]). As already referred, these modifications had been previously designed for use in AONs and not siRNAs and, even though they did show effective in improving stability, specificity and immunogenic properties, they do not improve potency. Recently, however, two novel, siRNA-optimized 2′-O modifications, were shown to increase *in vivo* activity of siRNAs, not only by increasing their potency but also their *in vivo* duration compared to their unmodified counterparts when delivered using LNPs: 2′-O-benzyl and 2′-O-methyl-4-pyrimidine (2′-O-CH2Py(4); [246]). Several teams have also been assessing different complexation methods with functional peptides [247] and/or different vectors: exosomes [248] including lipid nanocarriers such as pegylated immunoliposomes (PILs; [249]), stable-nucleic-acid-lipid-particles (SNALPs; [250]), or polyhydroxyalkanoate-based nanovehicles [251], reviewed in [252]. Also under consideration are siRNA delivery strategies that use viral particles. The viral delivery of siRNAs is composed of two main strategies: siRNAs are either chemically synthesized and loaded into a viral capsule, or they can be expressed from the DNA of a recombinant virus (reviewed in [253]).

Meanwhile, second generation LPNs were also developed. Constructed with the anionic lipid dilinol eylmethyl-4-dimethylaminoburyate (DLin-MC3-DMA), they mediate potent gene knockdown at reduced doses compared with first generation LNPs, while improving delivery [190, 217]. Partisiran (previously termed ALN-TTR02; ChemIDplus-Partisiran), for example, is exemplary of a minimally chemically modified siRNA delivered primarily to the liver in a second generation liposome formulation.

7.4.5 Targeted Delivery

Overall, there has been a huge progress over the last decade concerning not only non-targeted but also targeted delivery of siRNA drugs. In fact, siRNAs can also be targeted for uptake in selected tissues or cell types by taking advantage of high-affinity antibody or antibody fragments [254–256], aptamers (nucleic acids selected for high-affinity binding; [257–259] or receptor ligands [260–264], which bind to specific cell surface receptors and mediate cell-specific uptake. The targeting moieties can be either directly conjugated to siRNAs (bound non-covalently) or incorporated into LPNs or other nanoparticles (reviewed in [189]). In general, targeted uptake has the advantages of being effective at a lower dose while exhibiting lower toxicity, which may potentially occur from knockdown effects in unintended tissues. It is also a tool of great advantage for the treatment of non-systemic diseases. The easiest organ to target is the liver, which is a filtering organ that traps nanoparticles. It is also the primary site of synthesis of many circulating proteins. That is why it has been the target organ in most early clinical attempts at translating RNAi (reviewed in [186]). Furthermore, several diseases, which directly affect this organ may benefit from a straightforward liver targeting method. The most successful possibility under study includes a series of more drastic chemical modifications, where siRNAs have a trivalent N-acetylgalactosamine (GalNAc) moiety conjugated to the 3′ terminus of one of the strands [220, 264] (reviewed in [11]). GalNAc mediates hepatocyte uptake through the hepatocyte-

sandra.alves@insa.min-saude.pt

restricted asialoglycoprotein receptor (ASGPR), thus being a suitable mediator for whole-liver delivery [265] (reviewed in [189]). Uptake by this receptor is primarily through clathrin-dependent endocytosis [97]. Examples of GalNAc-modified siRNAs include Revusiran and Fitusiran (ChemIDplus-Revusiran; ChemIDplus-Fitusiran (reviewed in [11]). Also, local delivery to the CNS, a region that is difficult to deliver drugs to due to the BBB, is being addressed, with promising results. First preliminary evidence that *in vivo* downregulation of specific genes by RNAi could work at the CNS level came from studies in rats and mice using invasive local delivery methods (reviewed in [266]). Lately, however, evidence is accumulating on the successful brain delivery of si/shRNAs using specifically designed vectors and/or modifications that include the use of enzyme-sensitive LPNs [267], carbosilane dendrimers [268], cholesterol modifications [269], and recombinant fusion proteins [270]. Also, the pharmaceutical industry is investing in developing BBB-directed vectors. One of those examples is a family of vectors that take advantage on the existence of specific receptors and transport systems, which are highly expressed at the BBB to provide essential substances to brain cells. These vectors comprise a full-length protein (Melanotransferrin) and may be used to facilitate receptor mediated drug delivery into the brain to treat CNS disorders [271]. Recently, the application of this new peptide vector to siRNA and ongoing studies addressing the brain delivery of Iduronate 2-sulfatase (I2S) for the treatment of Hunter Syndrome, a rare X-linked lysosomal storage disorder, was discussed and its results in knockout mice were quite promising [272].

7.5 CRISPR-Cas Gene Editing

In addition to the most well known RNA-based therapeutics (antisense drugs and siRNA-based drugs) several other mechanisms of action are also potential strategies. Recently, a new gene editing technology, Clustered Regulatory Interspaced Short Palindromic Repeats (CRISPR) and the CRISPR-associated protein 9 (Cas9) (CRISPR-Cas 9) system, has received unprecedented acceptance in the scientific community for a variety of genetic applications (reviewed in [273]) (Fig. 7.7a). Even though this technology lies beyond the scope of this chapter, it does deserve some attention, as it may become a leading method for gene editing and even RNA-based therapeutics, in the long term.

Similarly to what had already happened with RNAi, the CRISPR-Cas system was not specifically developed as a method for gene editing. Instead, it is a naturally occurring prokaryotic immune defense strategy against non-self DNA based invasions (e.g., viruses, plasmids), which was recently discovered in bacteria and archaea [273–276], and latter adapted for bench applications [277, 278]. Also like RNAi, the specificity of CRISPR-Cas relies on the antisense pairing of RNAs (here termed single guide RNA, sgRNA) to specific genes but instead of binding directly to RNA, sgRNAs bind to chromosomal DNA. Another relevant difference between the RNAi and CRISPR technologies has to do with the transiency of their effect. In fact, unlike siRNAs, sgRNAs induce stable changes in gene expression, which are invaluable for *in vivo* gene screening. Thus, genomic targeting through CRISPR-Cas creates indels that can be adapted for stable eukaryotic genome engineering, namely Cas-mediated gene knockdown (reviewed in [186, 273]). In general, the application of CRISPR/Cas9 for DNA editing as well as for mammalian gene editing was established in the 2012–2013 period and, in just 3 years, this technique has revolutionized the entire gene editing field. Currently, CRISPR-Cas gene knockdown in zygotes provides a fast method for the development of different animal models, when compared to homologous recombination. Nevertheless, it does hold a series of drawbacks and raises a number of concerns, particularly when its therapeutic potential is considered. In fact, since this technique has the ability to modify the genome, its ethical and safe concerns are enormous. Furthermore (and like every other

sandra.alves@insa.min-saude.pt

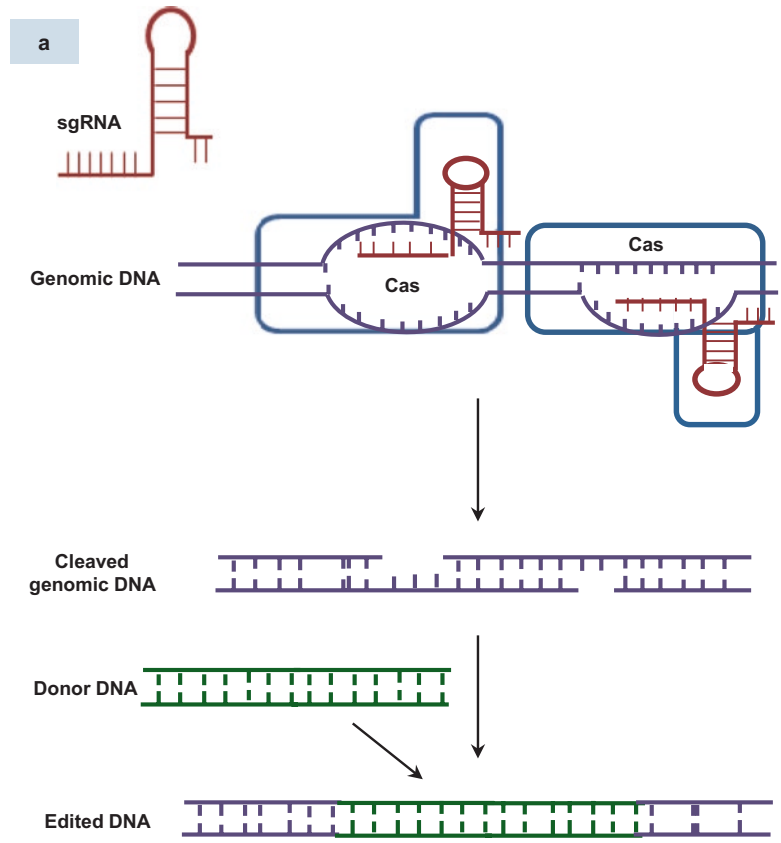


Fig. 7.7 Additional RNA-based drug mechanisms. **(a)** CRISPR/Cas9: CRISPR/Cas9 induces double strand breaks (DBS) when targeted to a specific genomic site by an appropriate guide RNA (sgRNA). This property may be used for mutation correction, by adding a donor DNA sequence that has homologous overlaps to the DBS (typically 100–1000 bp of overlap is used), thus promoting homologous repair of the cleaved genomic DNA; **(b)** Modified mRNAs: This approach consists in introducing chemically modified, stabilized mRNAs into cells to be translated to protein. Once internalized, sense-RNA drugs can be used for transient *in vivo* transcription (IVT) of mRNAs to replace mutated proteins or for vaccination without the risk of genomic alteration; **(c)** Aptamers: Aptamers take advantage of their selection for high-affinity binding to molecular ligands, often in the nanomolar or subnanomolar range. They can be compared to nucleic acid antibodies, having many of the advantages of conventional protein antibodies. They can be either agonists or antagonists, linked for bifunctional targeting and conjugated to other RNAs, small-molecule drugs, toxins or peptides. However, unless modified, they are rapidly excreted and do not activate immune functions, as other antibodies do

antisense technology), CRISPR-Cas holds potential for both on- and off-target effects. Moreover, by creating double-stranded DNA breaks, the Cas endonuclease can also lead to oncogenic gene translocations and trigger a DNA damage response, ultimately causing cell-cycle arrest or even cell death. Finally, depending on the repair pathway which is activated, gene editing may be imprecise [186]. Still, it must be noticed that in the 5 years following the publication of the method, several improvements to reduce off-target effects and provide a better control of the whole mechanism, while enhancing its efficiency have been developed and reported (reviewed in [186, 279]). It should also be mentioned that CRISPR/Cas9 is certainly a more versatile technique than RNAi, has it may not only induce indels but also repress or activate gene expression and cause both heritable and non-heritable genomic changes [280–

sandra.alves@insa.min-saude.pt

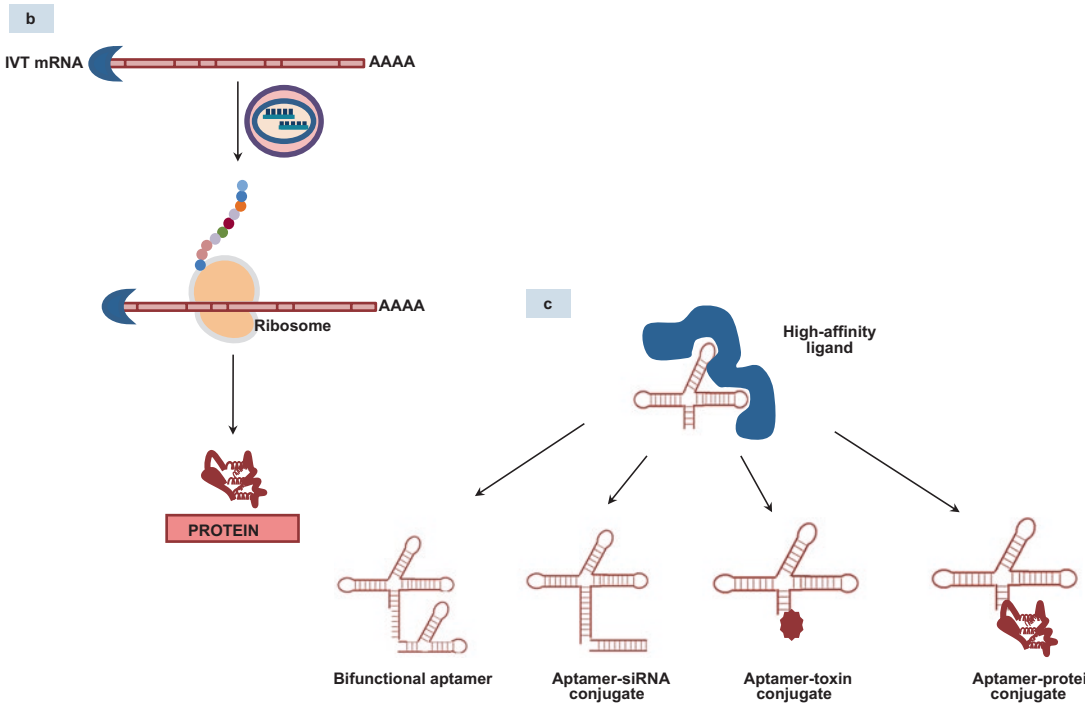


Fig. 7.7 (continued)

282]. In fact, CRISPR/Cas9 can be adapted to upregulate gene expression in different ways: the first, most obvious approach consists in using this technology to stably introduce constitutive active promoter elements to a gene, thus stably enhancing its expression. Alternatively, a modified Cas9 (fused to a transcriptor activator protein) may be targeted to any gene of interest, driving a transient enhancement in gene expression known as CRISPR activation (CRISPRa; [273]). In addition, the emergence of newer gene editing tools such as the Cpf1 enzyme, which is a single RNA-guided endonuclease, will eventually strengthen the portfolio of applications that may be achieved by CRISPR mediated genome engineering [283]. Therefore, it is becoming clear that clinical CRISPR-Cas studies will also be a trend in research over the next years, starting with *ex vivo* editing of differentiated cells, which may then be infused into patients. Furthermore, as other authors have already stated, it will also greatly benefit from the accumulated knowledge on other non-RNA-based gene editing tools, such as zinc-finger nucleases and on the delivery methods previously developed for AON- and siRNA-based drugs.

7.6 Messenger RNA as a Novel Therapeutic Approach

Another RNA-based approach is to introduce chemically modified stabilized mRNAs into cells, where those exogenous mRNAs will eventually be translated to protein (Fig. 7.7b). In fact, *in vitro* transcribed (IVT) mRNA has recently come into focus as a potential new drug class to deliver genetic information. Such synthetic mRNAs can be engineered to transiently express proteins by structurally resembling natural mRNAs [186, 284]. One advantage of mRNA-based therapy over viral gene delivery is that mRNA does not transit to the nucleus, thereby mitigating insertional mutagenesis risks. Moreover, mRNA provides transient, half-life-

sandra.alves@insa.min-saude.pt

dependent protein expression, while avoiding constitutive gene activation and maintaining dose responsiveness. Because of these advantages, IVT mRNA treatment is an emerging class of therapy, with multiple mRNA-based cancer immunotherapies and vaccines currently in clinical trials [284–286]. However, the fact that IVT mRNA, despite its strong resemblance to naturally occurring mRNA, can be recognized by the innate immune system may play an important part in its applicability. For vaccination approaches, the inflammatory cytokine production resulting from mRNA-induced immune stimulation might add to the effectiveness of the evoked immune response. For non-immunotherapy approaches, however, the story is different and so far, cancer immunotherapy is the only field in which mRNA based therapeutics have reached clinical trials [287–294]. Nevertheless, the potential of IVT mRNA is currently being explored for a variety of applications, ranging from inherited or acquired disorders to regenerative medicine, all of which remain at the preclinical stage [295, 296]. In fact, an increasing number of preclinical studies has evaluated mRNA-based therapy for a wide range of diseases such as surfactant B deficiency, myocardial infarction [297] sensory nerve disorders [298], fulminant hepatitis [299] hemophilia B [300, 301], congenital lung disease [302], cancer [303], liver and lung fibrosis [304], and methylmalonic acidemia [305]. However, the main hurdle in implementation of mRNA for therapeutics, the systemic delivery of mRNA molecules to target cells, remains a challenge. Better understanding of the factors that determine translational efficiency as well as RNA recognition by innate immune receptors, has improved the intracellular stability and functionality of mRNA transfected to cells. Still, when aiming to harness mRNA molecules for gene therapy purposes, this progress was insufficient. The need for mRNA protection from degradation in extracellular compartments, as well as for enabling its entry to the cell, has raised the demand for suitable delivery platforms [285, 295]. A possible solution for this challenge relies in the rapidly evolving field of nucleic acid-loaded NPs. In fact, the progress in the field of NPs-mediated RNAi-based therapy, has led to similar development of nanocarriers for mRNA. Particularly, the widely investigated family of LNPs was proposed to be such appropriate mRNA nanocarriers [296, 305, 306]. Moreover, the use of polyplex nanomicelles has also been explored [298, 299]. In order to achieve high efficacy *in vivo* some IVT mRNA specific formulation adjustments should be done in a near future. These adjustments are more important when systemic administration is required. Moreover, in order to expand the variety of mRNA-based therapies, cell specific targeted delivery systems are also needed especially in diseases involving a certain organ, which is inaccessible by standard LNPs, as well as in many types of solid tumors [296]. In conclusion, innovative design of nanocarriers for IVT mRNAs delivery will help to increase their potential and turn them into a valid therapeutic approach.

7.7 Aptamer-Based Drugs

Another potential class of RNA therapeutics are oligonucleotide aptamers (see Fig. 7.7c). The term aptamer comes from the Latin word "*aptus*", which means "to fix", as a clear reference to the lock and key relationship of aptamers and their targets [307, 308].

Aptamers are short (20–70 bases) single stranded oligonucleotides (ssRNA/ssDNA), which bind to their targets through 3D conformational complementarities with high affinity and specificity. Unlike the previously referred strategies, aptamers can be tailored selectively against a variety of targets, from nucleotides to amino acids, proteins, small molecules or even live cells [309]. Still, proteins are the major targets in aptamer research (reviewed in [310]). Oligonucleotide aptamers have affinity and specificity capacities, which are comparable to those of monoclonal antibodies, whilst having minimal immunogenicity, high production, low cost and high stability. These oligonucleotides can be selected trough an *in vivo* process called Systematic Evolution of Ligands by Exponential

sandra.alves@insa.min-saude.pt

enrichment (SELEX), which dates back to 1990. This method was originally described and performed by Szostak and Gold [307, 308]. The whole process starts with the synthesis of a screening library formed by a large number of randomly combinatorial ssDNA and/or ssRNAs. Each one of those random ssDNA/ssRNAs has one conserved sequence at each end. That sequence allows primer binding and amplification. The random library is then incubated with the target proteins, under proper conditions. Then, through a partition step, the sequences that had bind to target proteins are separated from those that did not bind. In the third step, the binding sequences are eluted and amplified with primers complementary to their conserved sequences, either by PCR (for ssDNA) or RT-PCR (for ssRNA). All these steps form a single SELEX cycle. This selection process is then repeated for about 7–20 rounds of incubation, partitioning and amplification. Ultimately, this results in the identification of a small number of binding sequences with high affinity and specificity for further processing and optimization. Generally, the binding sequences are then transformed into bacteria (*E. coli*) for further sequencing and characterization (reviewed in [310]). Naturally, in the post-SELEX process, the synthesized aptamers (as every other AON) can be chemically modified for therapeutic purposes, to stabilize and protect them against nucleases *in vivo*. Recent advances in SELEX technology, with the introduction of chemically modified bases and the use of deep sequencing to analyze enriched RNAs in early rounds of selection, have greatly reduced the time needed and the likelihood of identifying high-affinity aptamers (reviewed in [186]).

Over approximately 10 years, starting in 2005, when the first aptamer Pegaptanib (PubChem, Pegaptanib) was approved for wet age-related macular degeneration (AMD) therapy by U.S. FDA, oligonucleotide aptamers were growing more and more popular. Until 2016, when the last estimates were published online, there had been over 900 aptamers developed against various targets for diagnostic and therapeutic purposes [311]. Nevertheless, drug development of aptamers is currently not very active, with big pharmacological companies being much more focused on the technologies reviewed in the previous sections of this chapter. Still, it is worth mentioning that these oligonucleotides could substitute for some applications of therapeutic antibodies, with lower risk of developing immunological responses. They could also be used for targeted intracellular delivery of other molecules, including RNA-based drugs.

7.8 Conclusion

Over the last decades, an exceptional increase on the understanding of the versatile roles of RNAs has sparked the development of new classes of RNA-based drugs. Therapeutic RNA-based applications are emerging, in different fields, from inherited genetic diseases, oncology, viral infections and diabetes to neurological, cardiovascular, bone-related and ocular diseases. Over the last years in particular, much effort has been focused on the development of RNA-based therapeutics. Currently, even though there are a number of RNA-based therapeutic strategies, which may be attempted in order to either correct or modulate gene expression, there has been a clear prevalence of studies focused on splicing modification and gene expression inhibition using different types of AONs. Actually, the first AON-based drugs were recently approved, closely followed by the first siRNA-based therapeutic drug, which was approved last year. Still, there is a strong need to optimize the delivery steps of RNA-based technologies and to improve the drug-like properties of therapeutic nucleic acids. Expanding the range of targeted cells and tissues will require the development of robust strategies for cytosolic delivery, thus overcoming the two major hurdles of getting across the plasma membrane and out of the endosome.

In conclusion, as the first generation of nucleic acid therapeutics become drugs, the barrier for investing in RNA-based therapeutics will be lowered, and more resources will become available for exploring other mechanisms of action for RNA-based drugs apart from splicing modulation and single-gene knockdown. As already

sandra.alves@insa.min-saude.pt

pointed out by other authors, the flexibility of RNA design should allow for the facile construction of potent multifunctional drugs that have more than one mode of action and disrupt multiple targets. One such multifunctional drug may hold the promise of substituting for drug cocktails in a future not so distant. There is also the largely unexplored potential of targeting other RNA species and disrupting their functions. Therefore, in the near future, RNA-based drugs may become an increasing component of the pharmacopoeia, greatly expanding the universe of druggable targets and providing affordable treatment options for previously untreatable diseases. Ultimately, this kind of drugs may hold potential to actually cure genetic diseases [186].

References

1. Bennett CF, Swayze EE (2010) RNA targeting therapeutics: molecular mechanisms of antisense oligonucleotides as a therapeutic platform. Annu Rev Pharmacol Toxicol 50:259–293
2. Godfrey C et al (2017) Delivery is key: lessons learnt from developing splice-switching antisense therapies. EMBO Mol Med 9(5):545–557
3. McClorey G, Wood MJ (2015) An overview of the clinical application of antisense oligonucleotides for RNA-targeting therapies. Curr Opin Pharmacol 24:52–58
4. Rossor AM, Reilly MM, Sleigh JN (2018) Antisense oligonucleotides and other genetic therapies made simple. Pract Neurol 18(2):126–131
5. Bauman JA et al (2010) Anti-tumor activity of splice-switching oligonucleotides. Nucleic Acids Res 38(22):8348–8356
6. Kole R, Krainer AR, Altman S (2012) RNA therapeutics: beyond RNA interference and antisense oligonucleotides. Nat Rev Drug Discov 11(2):125–140
7. Sardone V et al (2017) Antisense oligonucleotide-based therapy for neuromuscular disease. Molecules 22(4):E563
8. Paterson BM, Roberts BE, Kuff EL (1977) Structural gene identification and mapping by DNA-mRNA hybrid-arrested cell-free translation. Proc Natl Acad Sci USA 74(10):4370–4374
9. Zamecnik PC, Stephenson ML (1978) Inhibition of Rous sarcoma virus replication and cell transformation by a specific oligodeoxynucleotide. Proc Natl Acad Sci USA 75(1):280–284
10. Schoch KM, Miller TM (2017) Antisense oligonucleotides: translation from mouse models to human neurodegenerative diseases. Neuron 94(6):1056–1070
11. Crooke ST et al (2018) RNA-targeted therapeutics. Cell Metab 27(4):714–739
12. Oberemok VV et al (2018) A half-century history of applications of antisense oligonucleotides in medicine, agriculture and forestry: we should continue the journey. Molecules 23(6):1302
13. Khvorova A, Watts JK (2017) The chemical evolution of oligonucleotide therapies of clinical utility. Nat Biotechnol 35(3):238–248
14. Chan JH, Lim S, Wong WS (2006) Antisense oligonucleotides: from design to therapeutic application. Clin Exp Pharmacol Physiol 33(5–6):533–540
15. Chery J (2016) RNA therapeutics: RNAi and antisense mechanisms and clinical applications. Postdoc J 4(7):35–50
16. Roehr B (1998) Fomivirsen approved for CMV retinitis. J Int Assoc Phys AIDS Care 4(10):14–16
17. Kurreck J (2003) Antisense technologies. Improvement through novel chemical modifications. Eur J Biochem 270(8):1628–1644
18. Rigo F, Seth P, Bennett C (2014) Antisense oligonucleotide-based therapies for diseases caused by pre-mRNA processing defects. In: Yeo G (ed) Systems biology of RNA binding proteins, advances in experimental medicine and biology. Springer, New York, pp 303–352
19. Monia BP et al (1993) Evaluation of 2′-modified oligonucleotides containing 2′-deoxy gaps as antisense inhibitors of gene expression. J Biol Chem 268(19):14514–14522
20. Evers MM, Toonen LJ, van Roon-Mom WM (2015) Antisense oligonucleotides in therapy for neurodegenerative disorders. Adv Drug Deliv Rev 87:90–103
21. Geary RS et al (2015) Pharmacokinetics, biodistribution and cell uptake of antisense oligonucleotides. Adv Drug Deliv Rev 87:46–51
22. Aartsma-Rus A (2012) Overview on AON design. Methods Mol Biol 867:117–129
23. Vitravene Study G (2002) A randomized controlled clinical trial of intravitreous fomivirsen for treatment of newly diagnosed peripheral cytomegalovirus retinitis in patients with AIDS. Am J Ophthalmol 133(4):467–474
24. Vitravene Study G (2002) Randomized dose-comparison studies of intravitreous fomivirsen for treatment of cytomegalovirus retinitis that has reactivated or is persistently active despite other therapies in patients with AIDS. Am J Ophthalmol 133(4):475–483
25. Vitravene Study G (2002) Safety of intravitreous fomivirsen for treatment of cytomegalovirus retinitis in patients with AIDS. Am J Ophthalmol 133(4):484–498
26. Duell PB et al (2016) Long-term mipomersen treatment is associated with a reduction in cardiovascular events in patients with familial hypercholesterolemia. J Clin Lipidol 10(4):1011–1021
27. Raal FJ et al (2010) Mipomersen, an apolipoprotein B synthesis inhibitor, for lowering of LDL cholesterol concentrations in patients with homozygous

sandra.alves@insa.min-saude.pt

familial hypercholesterolaemia: a randomised, double-blind, placebo-controlled trial. Lancet 375(9719):998–1006
28. Raal FJ et al (2016) Pediatric experience with mipomersen as adjunctive therapy for homozygous familial hypercholesterolemia. J Clin Lipidol 10(4):860–869
29. Santos RD et al (2015) Mipomersen, an antisense oligonucleotide to apolipoprotein B-100, reduces lipoprotein(a) in various populations with hypercholesterolemia: results of 4 phase III trials. Arterioscler Thromb Vasc Biol 35(3):689–699
30. Chiriboga CA et al (2016) Results from a phase 1 study of nusinersen (ISIS-SMN(Rx)) in children with spinal muscular atrophy. Neurology 86(10):890–897
31. Finkel RS et al (2016) Treatment of infantile-onset spinal muscular atrophy with nusinersen: a phase 2, open-label, dose-escalation study. Lancet 388(10063):3017–3026
32. Finkel RS et al (2017) Nusinersen versus sham control in infantile-onset spinal muscular atrophy. N Engl J Med 377(18):1723–1732
33. Mercuri E et al (2018) Nusinersen versus sham control in later-onset spinal muscular atrophy. N Engl J Med 378(7):625–635
34. Cirak S et al (2011) Exon skipping and dystrophin restoration in patients with Duchenne muscular dystrophy after systemic phosphorodiamidate morpholino oligomer treatment: an open-label, phase 2, dose-escalation study. Lancet 378(9791):595–605
35. Mendell JR et al (2013) Eteplirsen for the treatment of Duchenne muscular dystrophy. Ann Neurol 74(5):637–647
36. Miner P et al (2004) An enema formulation of alicaforsen, an antisense inhibitor of intercellular adhesion molecule-1, in the treatment of chronic, unremitting pouchitis. Aliment Pharmacol Ther 19(3):281–286
37. Monteleone G et al (2015) Mongersen, an oral SMAD7 antisense oligonucleotide, and Crohn's disease. N Engl J Med 372(12):1104–1113
38. Ackermann EJ et al (2016) Suppressing transthyretin production in mice, monkeys and humans using 2nd-generation antisense oligonucleotides. Amyloid 23(3):148–157
39. Digenio A et al (2016) Antisense-mediated lowering of plasma apolipoprotein C-III by Volanesorsen improves dyslipidemia and insulin sensitivity in type 2 diabetes. Diabetes Care 39(8):1408–1415
40. Gaudet D et al (2017) The APPROACH study: a randomized, double-blind, placebo-controlled, phase 3 study of volanesorsen administered subcutaneously to patients with familial chylomicronemia syndrome (FCS). J Clin Lipidol 11:814–815
41. Gaudet D et al (2014) Targeting APOC3 in the familial chylomicronemia syndrome. N Engl J Med 371(23):2200–2206
42. Gaudet D et al (2015) Antisense inhibition of apolipoprotein C-III in patients with hypertriglyceridemia. N Engl J Med 373(5):438–447
43. Buller HR et al (2015) Factor XI antisense oligonucleotide for prevention of venous thrombosis. N Engl J Med 372(3):232–240
44. Bhanot S et al (2013) ISIS-GCCRRX, a novel glucocorticoid (GC) receptor antisense drug reduces cholesterol and triglycerides and attenuates dexamethasone induced hepatic insulin resistance without systemic GC antagonism in normal subjects. Diabetologia 56:S282
45. Morgan E, et al (2014) ISIS-GCGRRx, an antisense glucagon receptor antagonist, caused rapid, robust, and sustained improvements in glycemic control without changes in BW, BP, lipids, or hypoglycemia in T2DM patients on stable metformin therapy. Diabetes 56(11):2183–2195
46. Chi KN et al (2016) A phase I dose-escalation study of apatorsen (OGX-427), an antisense inhibitor targeting heat shock protein 27 (Hsp27), in patients with castration-resistant prostate cancer and other advanced cancers. Ann Oncol 27(6):1116–1122
47. Limmroth V et al (2014) CD49d antisense drug ATL1102 reduces disease activity in patients with relapsing-remitting MS. Neurology 83(20):1780–1788
48. Hong D et al (2015) AZD9150, a next-generation antisense oligonucleotide inhibitor of STAT3 with early evidence of clinical activity in lymphoma and lung cancer. Sci Transl Med 7(314):314ra185
49. Chowdhury S et al (2016) A phase I dose escalation, safety and pharmacokinetic (PK) study of AZD5312 (IONISARRx), a first-in-class Generation 2.5 antisense oligonucleotide targeting the androgen receptor (AR). Eur J Cancer 69:S145
50. Janssen HL et al (2013) Treatment of HCV infection by targeting microRNA. N Engl J Med 368(18):1685–1694
51. van der Ree MH et al (2014) Long-term safety and efficacy of microRNA-targeted therapy in chronic hepatitis C patients. Antivir Res 111:53–59
52. Viney NJ et al (2016) Antisense oligonucleotides targeting apolipoprotein(a) in people with raised lipoprotein(a): two randomised, double-blind, placebo-controlled, dose-ranging trials. Lancet 388(10057):2239–2253
53. Graham MJ et al (2017) Cardiovascular and metabolic effects of ANGPTL3 antisense oligonucleotides. N Engl J Med 377(3):222–232
54. Sermet-Gaudelus I et al (2018) Antisense oligonucleotide eluforsen improves CFTR function in F508del cystic fibrosis. J Cyst Fibros S1569–1993(18)30914–7
55. Querfeld C et al (2017) Ph 1 trial evaluating MRG-106, a microrna-155 inhibitor, administered by intratumoral, subcutaneous, or intravenous delivery in cutaneous T-cell lymphoma (CTCL) patients. Hematol Oncol 35:275
56. Pfeiffer N et al (2017) First-in-human phase I study of ISTH0036, an antisense oligonucleotide selectively targeting transforming growth factor beta 2 (TGF-β2), in subjects with open-angle glaucoma

sandra.alves@insa.min-saude.pt

undergoing glaucoma filtration surgery. PLoS One 12(11):e0188899
57. McCaleb M et al (2017) Systemic pharmacodynamic efficacy of a complement factor B antisense oligonucleotide in preclinical and phase 1 clinical studies. Invest Ophthalmol Vis Sci 58:1952
58. Goemans NM et al (2016) Long-term efficacy, safety, and pharmacokinetics of drisapersen in Duchenne muscular dystrophy: results from an open-label extension study. PLoS One 11(9):e0161955
59. Voit T et al (2014) Safety and efficacy of drisapersen for the treatment of Duchenne muscular dystrophy (DEMAND II): an exploratory, randomised, placebo-controlled phase 2 study. Lancet Neurol 13(10):987–996
60. Saad F et al (2011) Randomized phase II trial of Custirsen (OGX-011) in combination with docetaxel or mitoxantrone as second-line therapy in patients with metastatic castrate-resistant prostate cancer progressing after first-line docetaxel: CUOG trial P-06c. Clin Cancer Res 17(17):5765–5773
61. Tsimikas S et al (2015) Antisense therapy targeting apolipoprotein(a): a randomised, double-blind, placebo-controlled phase 1 study. Lancet 386(10002):1472–1483
62. van Meer L et al (2016) Renal effects of antisense-mediated inhibition of SGLT2. J Pharmacol Exp Ther 359(2):280–289
63. Miller TM et al (2013) An antisense oligonucleotide against SOD1 delivered intrathecally for patients with SOD1 familial amyotrophic lateral sclerosis: a phase 1, randomised, first-in-man study. Lancet Neurol 12(5):435–442
64. Sewell KL et al (2002) Phase I trial of ISIS 104838, a 2′-methoxyethyl modified antisense oligonucleotide targeting tumor necrosis factor-alpha. J Pharmacol Exp Ther 303(3):1334–1343
65. Mignon L et al (2016) ISIS-DMPKRx in healthy volunteers: a placebo-controlled, randomized, single ascending-dose phase 1 Study. Neurology 86(16 Supplement):P3.166
66. Bianchini D et al (2013) First-in-human Phase I study of EZN-4176, a locked nucleic acid antisense oligonucleotide to exon 4 of the androgen receptor mRNA in patients with castration-resistant prostate cancer. Br J Cancer 109(10):2579–2586
67. Toth PP (2011) Antisense therapy and emerging applications for the management of dyslipidemia. J Clin Lipidol 5(6):441–449
68. Visser ME et al (2012) Mipomersen, an apolipoprotein B synthesis inhibitor, lowers low-density lipoprotein cholesterol in high-risk statin-intolerant patients: a randomized, double-blind, placebo-controlled trial. Eur Heart J 33(9):1142–1149
69. Nguyen DD, Chang S (2017) Development of novel therapeutic agents by inhibition of oncogenic microRNAs. Int J Mol Sci 19(1):E65
70. van der Ree MH et al (2016) Miravirsen dosing in chronic hepatitis C patients results in decreased microRNA-122 levels without affecting other microRNAs in plasma. Aliment Pharmacol Ther 43(1):102–113
71. Hua Y et al (2010) Antisense correction of SMN2 splicing in the CNS rescues necrosis in a type III SMA mouse model. Genes Dev 24(15):1634–1644
72. Lefebvre S et al (1997) Correlation between severity and SMN protein level in spinal muscular atrophy. Nat Genet 16(3):265–269
73. Hua Y et al (2008) Antisense masking of an hnRNP A1/A2 intronic splicing silencer corrects SMN2 splicing in transgenic mice. Am J Hum Genet 82(4):834–848
74. De Vivo DC et al (2017) Interim efficacy and safety results from the phase 2 NURTURE study evaluating nusinersen in presymptomatic infants with spinal muscular atrophy. Neurology 88:S46.003.75
75. Mendell JR et al (2012) Evidence-based path to newborn screening for Duchenne muscular dystrophy. Ann Neurol 71(3):304–313
76. Emery AE (1991) Population frequencies of inherited neuromuscular diseases–a world survey. Neuromuscul Disord 1(1):19–29
77. Ervasti JM (2007) Dystrophin, its interactions with other proteins, and implications for muscular dystrophy. Biochim Biophys Acta 1772(2):108–117
78. Kole R, Krieg AM (2015) Exon skipping therapy for Duchenne muscular dystrophy. Adv Drug Deliv Rev 87:104–107
79. Lim KR, Maruyama R, Yokota T (2017) Eteplirsen in the treatment of Duchenne muscular dystrophy. Drug Des Devel Ther 11:533–545
80. Mendell JR et al (2016) Longitudinal effect of eteplirsen versus historical control on ambulation in Duchenne muscular dystrophy. Ann Neurol 79(2):257–271
81. Kinane TB et al (2018) Long-term pulmonary function in Duchenne muscular dystrophy: comparison of Eteplirsen-treated patients to natural history. J Neuromuscul Dis 5(1):47–58
82. Garanto A et al (2016) In vitro and in vivo rescue of aberrant splicing in CEP290-associated LCA by antisense oligonucleotide delivery. Hum Mol Genet 25(12):2552–2563
83. Denti MA et al (2006) Body-wide gene therapy of Duchenne muscular dystrophy in the mdx mouse model. Proc Natl Acad Sci USA 103(10):3758–3763
84. Denti MA et al (2008) Long-term benefit of adeno-associated virus/antisense-mediated exon skipping in dystrophic mice. Hum Gene Ther 19(6):601–608
85. Goyenvalle A et al (2009) Enhanced exon-skipping induced by U7 snRNA carrying a splicing silencer sequence: promising tool for DMD therapy. Mol Ther 17(7):1234–1240
86. Goyenvalle A et al (2012) Engineering multiple U7snRNA constructs to induce single and multiexon-skipping for Duchenne muscular dystrophy. Mol Ther 20(6):1212–1221
87. Vulin A et al (2012) Muscle function recovery in golden retriever muscular dystrophy after AAV1-U7 exon skipping. Mol Ther 20(11):2120–2133

sandra.alves@insa.min-saude.pt

88. Geib T, Hertel KJ (2009) Restoration of full-length SMN promoted by adenoviral vectors expressing RNA antisense oligonucleotides embedded in U7 snRNAs. PLoS One 4(12):e8204
89. Odermatt P et al (2016) Somatic therapy of a mouse SMA model with a U7 snRNA gene correcting SMN2 splicing. Mol Ther 24(10):1797–1805
90. Imbert M, Dias-Florencio G, Goyenvalle A (2017) Viral vector-mediated antisense therapy for genetic diseases. Genes (Basel) 8(2):E51
91. Krause DS, Van Etten RA (2005) Tyrosine kinases as targets for cancer therapy. N Engl J Med 353(2):172–187
92. Cornelio DB, Roesler R, Schwartsmann G (2007) Gastrin-releasing peptide receptor as a molecular target in experimental anticancer therapy. Ann Oncol 18(9):1457–1466
93. Low PS, Kularatne SA (2009) Folate-targeted therapeutic and imaging agents for cancer. Curr Opin Chem Biol 13(3):256–262
94. McGettrick AF, O'Neill LA (2010) Localisation and trafficking of Toll-like receptors: an important mode of regulation. Curr Opin Immunol 22(1):20–27
95. Millard M, Odde S, Neamati N (2011) Integrin targeted therapeutics. Theranostics 1:154–188
96. Canton J, Neculai D, Grinstein S (2013) Scavenger receptors in homeostasis and immunity. Nat Rev Immunol 13(9):621–634
97. D'Souza AA, Devarajan PV (2015) Asialoglycoprotein receptor mediated hepatocyte targeting – strategies and applications. J Control Release 203:126–139
98. Juliano RL (2016) The delivery of therapeutic oligonucleotides. Nucleic Acids Res 44(14):6518–6548
99. McClorey G, Banerjee S (2018) Cell-penetrating peptides to enhance delivery of oligonucleotide-based therapeutics. Biomedicine 6(2):E51
100. Yin H et al (2008) Cell-penetrating peptide-conjugated antisense oligonucleotides restore systemic muscle and cardiac dystrophin expression and function. Hum Mol Genet 17(24):3909–3918
101. Yin H et al (2009) A fusion peptide directs enhanced systemic dystrophin exon skipping and functional restoration in dystrophin-deficient mdx mice. Hum Mol Genet 28(4):699
102. Wu B et al (2008) Effective rescue of dystrophin improves cardiac function in dystrophin-deficient mice by a modified morpholino oligomer. Proc Natl Acad Sci USA 105(39):14814–14819
103. Betts C et al (2012) Pip6-PMO, a new generation of peptide-oligonucleotide conjugates with improved cardiac exon skipping activity for DMD treatment. Mol Ther Nucleic Acids 1:e38
104. Gao X et al (2014) Effective dystrophin restoration by a novel muscle-homing peptide-morpholino conjugate in dystrophin-deficient mdx mice. Mol Ther 22(7):1333–1341
105. Jirka SMG et al (2014) Peptide conjugation of 20-O-methyl phosphorothioate antisense oligonucleotides enhances cardiac uptake and exon skipping in mdx mice. Nucleic Acid Ther 24:25–36
106. Leger AJ et al (2013) Systemic delivery of a Peptide-linked morpholino oligonucleotide neutralizes mutant RNA toxicity in a mouse model of myotonic dystrophy. Nucleic Acid Ther 23(2):109–117
107. Hammond SM et al (2016) Systemic peptide-mediated oligonucleotide therapy improves long-term survival in spinal muscular atrophy. Proc Natl Acad Sci USA 113(39):10962–10967
108. Shabanpoor F et al (2017) Identification of a peptide for systemic brain delivery of a morpholino oligonucleotide in mouse models of spinal muscular atrophy. Nucleic Acid Ther 27(3):130–143
109. Lönn P et al (2016) Enhancing endosomal escape for intracellular delivery of macromolecular biologic therapeutics. Sci Rep 6:32301
110. Salerno JC et al (2016) Novel cell-penetrating peptide-adaptors effect intracellular delivery and endosomal escape of protein cargos. J Cell Sci 129(12):2473–2474
111. Falzarano MS, Passarelli C, Ferlini A (2014) Nanoparticle delivery of antisense oligonucleotides and their application in the exon skipping strategy for Duchenne muscular dystrophy. Nucleic Acid Ther 24(1):87–100
112. Lerner MR et al (1980) Are snRNPs involved in splicing? Nature 283(5743):220–224
113. Rogers J, Wall R (1980) A mechanism for RNA splicing. Proc Natl Acad Sci USA 77(4):1877–1879
114. Mount SM et al (1983) The U1 small nuclear RNA-protein complex selectively binds a 5′ splice site in vitro. Cell 33(2):509–518
115. West S (2012) The increasing functional repertoire of U1 snRNA. Biochem Soc Trans 40(4):846–849
116. Buratti E, Baralle D (2010) Novel roles of U1 snRNP in alternative splicing regulation. RNA Biol 7(4):412–419
117. Roca X, Krainer AR, Eperon IC (2013) Pick one, but be quick: 5′ splice sites and the problems of too many choices. Genes Dev 27(2):129–144
118. Raponi M, Baralle D (2008) Can donor splice site recognition occur without the involvement of U1 snRNP? Biochem Soc Trans 36.(Pt 3:548–550
119. Guiro J, O'Reilly D (2015) Insights into the U1 small nuclear ribonucleoprotein complex superfamily. Wiley Interdiscip Rev RNA 6(1):79–92
120. Spraggon L, Cartegni L (2013) U1 snRNP-dependent suppression of polyadenylation: physiological role and therapeutic opportunities in Cancer. Int J Cell Biol 2013:846510
121. Valadkhan S, Gunawardane LS (2013) Role of small nuclear RNAs in eukaryotic gene expression. Essays Biochem 54:79–90
122. Buratti E et al (2007) Aberrant 5′ splice sites in human disease genes: mutation pattern, nucleotide structure and comparison of computational tools that predict their utilization. Nucleic Acids Res 35(13):4250–4263

sandra.alves@insa.min-saude.pt

123. Roca X et al (2008) Features of 5′-splice-site efficiency derived from disease-causing mutations and comparative genomics. Genome Res 18(1):77–87
124. Zhuang Y, Weiner AM (1986) A compensatory base change in U1 snRNA suppresses a 5′ splice site mutation. Cell 46(6):827–835
125. Baralle M et al (2003) Identification of a mutation that perturbs NF1 agene splicing using genomic DNA samples and a minigene assay. J Med Genet 40(3):220–222
126. Pinotti M et al (2008) U1-snRNA-mediated rescue of mRNA processing in severe factor VII deficiency. Blood 111(5):2681–2684
127. Pinotti M et al (2009) Rescue of coagulation factor VII function by the U1+5A snRNA. Blood 113(25):6461–6464
128. Tanner G et al (2009) Therapeutic strategy to rescue mutation-induced exon skipping in rhodopsin by adaptation of U1 snRNA. Hum Mutat 30(2):255–263
129. Glaus E et al (2011) Gene therapeutic approach using mutation-adapted U1 snRNA to correct a RPGR splice defect in patient-derived cells. Mol Ther 19(5):936–941
130. Sánchez-Alcudia R et al (2011) Overexpression of adapted U1snRNA in patients' cells to correct a 5′ splice site mutation in propionic acidemia. Mol Genet Metab 102(2):134–138
131. Martínez-Pizarro A et al (2018) Intronic PAH gene mutations cause a splicing defect by a novel mechanism involving U1snRNP binding downstream of the 5′ splice site. Plos Genet 14:e1007360
132. Schmid F et al (2011) U1 snRNA-mediated gene therapeutic correction of splice defects caused by an exceptionally mild BBS mutation. Hum Mutat 32(7):815–824
133. Schmid F et al (2013) A gene therapeutic approach to correct splice defects with modified U1 and U6 snRNPs. Hum Gene Ther 24(1):97–104
134. Hartmann L et al (2010) Correct mRNA processing at a mutant TT splice donor in FANCC ameliorates the clinical phenotype in patients and is enhanced by delivery of suppressor U1 snRNAs. Am J Hum Genet 87(4):480–493
135. Matos L et al (2014) Therapeutic strategies based on modified U1 snRNAs and chaperones for Sanfilippo C splicing mutations. Orphanet J Rare Dis 9:180
136. Scalet D et al (2019) Disease-causing variants of the conserved +2T of 5′ splice sites can be rescued by engineered U1snRNAs. Hum Mutat 40(1):48–52
137. Balestra D et al (2014) An engineered U1 small nuclear RNA rescues splicing defective coagulation F7 gene expression in mice. J Thromb Haemost 12(2):177–185
138. Lee NC et al (2016) Mutation-adapted U1 snRNA corrects a splicing error of the dopa decarboxylase gene. Hum Mol Genet 25(23):5142–5147
139. Pinotti M et al (2011) RNA-based therapeutic approaches for coagulation factor deficiencies. J Thromb Haemost 9(11):2143–2152
140. Wally V, Murauer EM, Bauer JW (2012) Spliceosome-mediated trans-splicing: the therapeutic cut and paste. J Invest Dermatol 132(8):1959–1966
141. Roca X, Krainer AR (2009) Recognition of atypical 5′ splice sites by shifted base-pairing to U1 snRNA. Nat Struct Mol Biol 16(2):176–182
142. Cohen JB et al (1994) Suppression of mammalian 5′ splice-site defects by U1 small nuclear RNAs from a distance. Proc Natl Acad Sci USA 91(22):10470–10474
143. Hwang DY, Cohen JB (1997) U1 small nuclear RNA-promoted exon selection requires a minimal distance between the position of U1 binding and the 3′ splice site across the exon. Mol Cell Biol 17(12):7099–7107
144. Fernandez Alanis E et al (2012) An exon-specific U1 small nuclear RNA (snRNA) strategy to correct splicing defects. Hum Mol Genet 21(11):2389–2398
145. Tajnik M et al (2016) Molecular basis and therapeutic strategies to rescue factor IX variants that affect splicing and protein function. PLoS Genet 12(5):e1006082
146. Dal Mas A et al (2015) Exon-specific U1s correct SPINK5 exon 11 skipping caused by a synonymous substitution that affects a bifunctional splicing regulatory element. Hum Mutat 36(5):504–512
147. Nizzardo M et al (2015) Spinal muscular atrophy phenotype is ameliorated in human motor neurons by SMN increase via different novel RNA therapeutic approaches. Sci Rep 5:p. 11746
148. Mattioli C et al (2014) Unusual splice site mutations disrupt FANCA exon 8 definition. Biochim Biophys Acta 1842(7):1052–1058
149. Dal Mas A et al (2015) Improvement of SMN2 pre-mRNA processing mediated by exon-specific U1 small nuclear RNA. Am J Hum Genet 96(1):93–103
150. Rogalska ME et al (2016) Therapeutic activity of modified U1 core spliceosomal particles. Nat Commun 7:11168
151. Donadon I et al (2018) Exon-specific U1 snRNAs improve ELP1 exon 20 definition and rescue ELP1 protein expression in a familial dysautonomia mouse model. Hum Mol Genet 27(14):2466–2476
152. Balestra D et al (2016) An exon-specific U1snRNA induces a robust factor IX activity in mice expressing multiple human FIX splicing mutants. Mol Ther Nucleic Acids 5(10):e370
153. van der Woerd WL et al (2015) Analysis of aberrant pre-messenger RNA splicing resulting from mutations in ATP8B1 and efficient in vitro rescue by adapted U1 small nuclear RNA. Hepatology 61(4):1382–1391
154. Hwu WL, Lee YM, Lee NC (2017) Gene therapy with modified U1 small nuclear RNA. Expert Rev Endocrinol Metab 12(3):171–175

sandra.alves@insa.min-saude.pt

155. Suñé-Pou M et al (2017) Targeting splicing in the treatment of human disease. Genes (Basel) 8(3):E87
156. Napoli C, Lemieux C, Jorgensen R (1990) Introduction of a chimeric chalcone synthase gene into petunia results in reversible co-suppression of homologous genes in trans. Plant Cell 2(4):279–289
157. van der Krol AR et al (1990) Flavonoid genes in petunia: addition of a limited number of gene copies may lead to a suppression of gene expression. Plant Cell 2(4):291–299
158. Fire A et al (1998) Potent and specific genetic interference by double-stranded RNA in Caenorhabditis elegans. Nature 391(6669):806–811
159. Montgomery MK, Xu S, Fire A (1998) RNA as a target of double-stranded RNA-mediated genetic interference in Caenorhabditis elegans. Proc Natl Acad Sci USA 95(26):15502–15507
160. Kennerdell JR, Carthew RW (1998) Use of dsRNA-mediated genetic interference to demonstrate that frizzled and frizzled 2 act in the wingless pathway. Cell 95(7):1017–1026
161. Voinnet O (2001) RNA silencing as a plant immune system against viruses. Trends Genet 17(8):449–459
162. Ketting RF et al (1999) Mut-7 of C. elegans, required for transposon silencing and RNA interference, is a homolog of Werner syndrome helicase and RNaseD. Cell 99(2):133–141
163. Wu-Scharf D et al (2000) Transgene and transposon silencing in Chlamydomonas reinhardtii by a DEAH-box RNA helicase. Science 290(5494):1159–1162
164. Hamilton A et al (2002) Two classes of short interfering RNA in RNA silencing. EMBO J 21(17):4671–4679
165. Hamilton AJ, Baulcombe DC (1999) A species of small antisense RNA in posttranscriptional gene silencing in plants. Science 286(5441):950–952
166. Cogoni C et al (1996) Transgene silencing of the al-1 gene in vegetative cells of Neurospora is mediated by a cytoplasmic effector and does not depend on DNA-DNA interactions or DNA methylation. EMBO J 15(12):3153–3163
167. Cecere G, Cogoni C (2009) Quelling targets the rDNA locus and functions in rDNA copy number control. BMC Microbiol 9:44
168. Elbashir SM et al (2001) Duplexes of 21-nucleotide RNAs mediate RNA interference in cultured mammalian cells. Nature 411(6836):494–498
169. Elbashir SM, Lendeckel W, Tuschl T (2001) RNA interference is mediated by 21- and 22-nucleotide RNAs. Genes Dev 15(2):188–200
170. Caplen NJ et al (2000) dsRNA-mediated gene silencing in cultured Drosophila cells: a tissue culture model for the analysis of RNA interference. Gene 252(1–2):95–105
171. Hutvagner G, Simard MJ (2008) Argonaute proteins: key players in RNA silencing. Nat Rev Mol Cell Biol 9(1):22–32
172. Deng Y et al (2014) Therapeutic potentials of gene silencing by RNA interference: principles, challenges, and new strategies. Gene 538(2):217–227
173. Sandy P, Ventura A, Jacks T (2005) Mammalian RNAi: a practical guide. BioTechniques 39(2):215–224
174. Aagaard L, Rossi JJ (2007) RNAi therapeutics: principles, prospects and challenges. Adv Drug Deliv Rev 59(2–3):75–86
175. Fraser AG et al (2000) Functional genomic analysis of C. elegans chromosome I by systematic RNA interference. Nature 408(6810):325–330
176. Lum L et al (2003) Identification of Hedgehog pathway components by RNAi in Drosophila cultured cells. Science 299(5615):2039–2045
177. Boutros M et al (2004) Genome-wide RNAi analysis of growth and viability in Drosophila cells. Science 303(5659):832–835
178. Paddison PJ et al (2004) A resource for large-scale RNA-interference-based screens in mammals. Nature 428(6981):427–431
179. Silva JM et al (2008) Profiling essential genes in human mammary cells by multiplex RNAi screening. Science 319(5863):617–620
180. Schlabach MR et al (2008) Cancer proliferation gene discovery through functional genomics. Science 319(5863):620–624
181. Brass AL et al (2008) Identification of host proteins required for HIV infection through a functional genomic screen. Science 319(5865):921–926
182. Luo J et al (2009) A genome-wide RNAi screen identifies multiple synthetic lethal interactions with the Ras oncogene. Cell 137(5):835–848
183. Mittal V (2004) Improving the efficiency of RNA interference in mammals. Nat Rev Genet 5(5):355–365
184. Hannon GJ, Rossi JJ (2004) Unlocking the potential of the human genome with RNA interference. Nature 431(7006):371–378
185. Rytlewski JA, Beronja S (2015) RNAi in the mouse: rapid and affordable gene function studies in a vertebrate system. Wiley Interdiscip Rev Dev Biol 4(1):45–57
186. Lieberman J (2018) Tapping the RNA world for therapeutics. Nat Struct Mol Biol 25(5):357–364
187. Hayden EC (2014) RNA interference rebooted. Nature 508(7497):443
188. Song E et al (2003) RNA interference targeting Fas protects mice from fulminant hepatitis. Nat Med 9(3):347–351
189. Wittrup A, Lieberman J (2015) Knocking down disease: a progress report on siRNA therapeutics. Nat Rev Genet 16(9):543–552
190. Coelho T et al (2013) Safety and efficacy of RNAi therapy for transthyretin amyloidosis. N Engl J Med 369(9):819–829
191. Suhr OB et al (2015) Efficacy and safety of patisiran for familial amyloidotic polyneuropathy: a phase II multi-dose study. Orphanet J Rare Dis 10:109

sandra.alves@insa.min-saude.pt

192. Demirjian S et al (2017) Safety and tolerability Study of an intravenously administered small interfering ribonucleic acid (siRNA) post on-pump cardiothoracic surgery in patients at risk of acute kidney injury. Kidney Int Rep 2(5):836–843
193. Peddi V, Ratner L, Cooper M, Gaber O, Feng S, Tso P, Bowers V, Naraghi R, Budde K, Polinsky M et al (2014) Treatment with QPI-1002, a short interfering (SI) RNA for the prophylaxis of delayed graft function. Transplantation 98:153
194. Benitez-Del-Castillo JM et al (2016) Safety and efficacy clinical trials for SYL1001, a novel short interfering RNA for the treatment of dry eye disease. Invest Ophthalmol Vis Sci 57(14):6447–6454
195. Antoszyk A, Katz B, Singh R, Gurses-Ozden R, Erlich S, Rothenstein D, Sharon N, Hodge J, Levin L, Miller N et al (2013) A phase I open label, dose escalation trial of QPI-1007 delivered by a single intravitreal (IVT) injection to subjects with low visual acuity and acute non-arteritic anterior ischemic optic neuropathy (NAION). Invest Ophthalmol Vis Sci 54(4575):4575
196. Solano EC et al (2014) Toxicological and pharmacokinetic properties of QPI-1007, a chemically modified synthetic siRNA targeting caspase 2 mRNA, following intravitreal injection. Nucleic Acid Ther 24(4):258–266
197. Pasi KJ et al (2016) Fitusiran, an investigational RNAi therapeutic targeting antithrombin for the treatment of hemophilia: updated results from phase 1 and phase 2 extension studies in patients with inhibitors. Blood 128:1397
198. Ragni, et al (2016) Fitusiran, an investigational RNAi therapeutic targeting antithrombin for the treatment of hemophilia: updated results from a phase 1 and phase 1/2 extension study in patients without inhibitors. Blood 128:2572
199. Fitzgerald K et al (2017) A highly durable RNAi therapeutic inhibitor of PCSK9. N Engl J Med 376(1):41–51
200. Ray KK et al (2017) Inclisiran in patients at high cardiovascular risk with elevated LDL cholesterol. N Engl J Med 376(15):1430–1440
201. Drugs.com. Alnylam announces FDA acceptance of New Drug Application (NDA) and priority review status for patisiran, an investigational RNAi therapeutic for the treatment of hereditary ATTR (hATTR) amyloidosis. 2018 10 Aug 2018. Available from: https://www.drugs.com/nda/patisiran_180201.html
202. Golan T et al (2015) RNAi therapy targeting KRAS in combination with chemotherapy for locally advanced pancreatic cancer patients. Oncotarget 6(27):24560–24570
203. Zorde Khvalevsky E et al (2013) Mutant KRAS is a druggable target for pancreatic cancer. Proc Natl Acad Sci USA 110(51):20723–20728
204. Gonzalez, et al (2014) Phase 2 of bamosiran (SYL040012), a novel RNAi based compound for the treatment of increased intraocular pressure associated to glaucoma. Invest Ophthalmol Vis Sci 55(13):564
205. Moreno-Montanes J et al (2014) Phase I clinical trial of SYL040012, a small interfering RNA targeting beta-adrenergic receptor 2, for lowering intraocular pressure. Mol Ther 22(1):226–232
206. Demuere et al (2016) A phase I/II study of TKM-080301, a PLK1-targeted RNAi in patients with adrenocortical cancer (ACC). J Clin Oncol 34:2547
207. Libertine, et al. (2015) Update on phase 2 clinical trial results of RXI-109 treatment to reduce the formation of hypertrophic dermal scars. J Am Acad Dermatol 72:AB273
208. Nguyen QD et al (2012) Dose-ranging evaluation of intravitreal siRNA PF-04523655 for diabetic macular edema (the DEGAS study). Invest Ophthalmol Vis Sci 53(12):7666–7674
209. Hill, et al (2016) A subcutaneously administered investigational RNAi Therapeutic (ALN-CC5) targeting complement C5 for treatment of PNH and complement-mediated diseases: preliminary phase 1/2 study results in patients with PNH. Blood 128:3891
210. Hulton, et al. (2016) A phase 1/2 trial of ALN-GO1, an investigational RNAi therapeutic for primary hyperoxaluria type 1 (PH1). Pediatr Nephrol 31:1763
211. Sterinu-Cercel et al (2017) A phase 2a study evaluating the multi-dose activity of ARB-1467 in HBeAg-Positive and –negative virally suppressed subjects with hepatitis B. J Hepatol p 66:S688–S689
212. Lawitz E et al (2015) Safety, pharmacokinetics, and biologic activity of ND-L02-s0201, a novel targeted lipid-nanoparticle to deliver HSP47 siRNA for the treatment of patients with advanced liver fibrosis: interim results from clinical phase 1b/2 studies. S Hepatology 62(909A):S688–S689
213. Salzberg et al (2016) Adoptive cellular immunotherapy with APN401, autologous Cbl-b-silenced peripheral blood mononuclear cells, in patients with solid tumors. J Clin Oncol 34:e14541
214. Triozzi, et al. (2015) Phase I clinical trial of adoptive cellular immunotherapy with APN401 in patients with solid tumors. Immun Cancer 3(Suppl 2):175
215. Alsina M et al (2012) Open-label extension study of the RNAi therapeutic ALN-VSP02 in cancer patients responding to therapy. J Clin Oncol 30(4):3062
216. Cervantes et al (2011) Phase I dose escalation study of ALN-VSP02, a novel RNAi therapeutic for solid tumors with liver involvement. J Clin Oncol 29:3025
217. Fitzgerald K et al (2014) Effect of an RNA interference drug on the synthesis of proprotein convertase subtilisin/kexin type 9 (PCSK9) and the concentration of serum LDL cholesterol in healthy volunteers: a randomised, single-blind, placebo-controlled, phase 1 trial. Lancet 383(9911):60–68
218. Leachman SA et al (2010) First-in-human mutation-targeted siRNA phase Ib trial of an inherited skin disorder. Mol Ther 18(2):442–446
219. Gillmore, et al (2016) Phase 2 open-label extension study of revusiran, an investigational RNAi thera-

sandra.alves@insa.min-saude.pt

peutic for the treatment of patients with transthyretin amyloidosis with cardiomyopathy: updated interim results. 2016: Abstract book, international symposium of amyloidosis, p PA84
220. Zimmermann TS et al (2017) Clinical proof of concept for a novel hepatocyte-targeting GalNAc-siRNA conjugate. Mol Ther 25(1):71–78
221. Xu CF et al (2015) Targeting glucose uptake of glioma cells by siRNA delivery with polymer nanoparticle. J Control Release 213:e23–e24
222. Zuckerman JE et al (2014) Correlating animal and human phase Ia/Ib clinical data with CALAA-01, a targeted, polymer-based nanoparticle containing siRNA. Proc Natl Acad Sci USA 111(31):11449–11454
223. Yuen et al (2017) Prolonged RNA interference therapy with ARC-520 Injection in treatment nai¨ve, HBeAg positive and negative patients with chronic HBV results in significant reductions of HBs antigen. J Hepatol 66:S27
224. Turner, et al. (2017) Hepatic targeted RNA interference provides deep and prolonged knockdown of alpha-1 antitrypsin levels in ZZ patients. J. Hepatol 66:S92
225. Drugs.com. Alnylam presents new clinical results from the APOLLO phase 3 study of patisiran at the 16th international symposium on amyloidosis. 2018 10 Aug 2018. Available from: https://www.drugs.com/clinical_trials/alnylam-presents-new-clinical-results-apollo-phase-3-study-patisiran-16th-international-symposium-17805.html
226. Drugs.com (2018) Available from: https://www.drugs.com/history/onpattro.html
227. Bobbin ML, Rossi JJ (2016) RNA interference (RNAi)-based therapeutics: delivering on the promise? Annu Rev Pharmacol Toxicol 56:103–122
228. Gilleron J et al (2013) Image-based analysis of lipid nanoparticle-mediated siRNA delivery, intracellular trafficking and endosomal escape. Nat Biotechnol 31(7):638–646
229. Wittrup A et al (2015) Visualizing lipid-formulated siRNA release from endosomes and target gene knockdown. Nat Biotechnol 33(8):870–876
230. Bartlett DW, Davis ME (2006) Insights into the kinetics of siRNA-mediated gene silencing from live-cell and live-animal bioluminescent imaging. Nucleic Acids Res 34(1):322–333
231. Tatiparti K et al (2017) siRNA delivery strategies: a comprehensive review of recent developments. Nanomaterials (Basel) 7(4):322–33
232. Han L, Tang C, Yin C (2014) Oral delivery of shRNA and siRNA via multifunctional polymeric nanoparticles for synergistic cancer therapy. Biomaterials 35(15):4589–4600
233. Akinc A et al (2008) A combinatorial library of lipid-like materials for delivery of RNAi therapeutics. Nat Biotechnol 26(5):561–569
234. Semple SC et al (2010) Rational design of cationic lipids for siRNA delivery. Nat Biotechnol 28(2):172–176
235. Shi B et al (2011) Biodistribution of small interfering RNA at the organ and cellular levels after lipid nanoparticle-mediated delivery. J Histochem Cytochem 59(8):727–740
236. Morrissey DV et al (2005) Activity of stabilized short interfering RNA in a mouse model of hepatitis B virus replication. Hepatology 41(6):1349–1356
237. Gooding M et al (2012) siRNA delivery: from lipids to cell-penetrating peptides and their mimics. Chem Biol Drug Des 80(6):787–809
238. Akinc A et al (2010) Targeted delivery of RNAi therapeutics with endogenous and exogenous ligand-based mechanisms. Mol Ther 18(7):1357–1364
239. Czech MP, Aouadi M, Tesz GJ (2011) RNAi-based therapeutic strategies for metabolic disease. Nat Rev Endocrinol 7(8):473–484
240. Robbins M, Judge A, MacLachlan I (2009) siRNA and innate immunity. Oligonucleotides 19(2):89–102
241. Chiu YL, Rana TM (2003) siRNA function in RNAi: a chemical modification analysis. RNA 9(9):1034–1048
242. Morrissey DV et al (2005) Potent and persistent in vivo anti-HBV activity of chemically modified siRNAs. Nat Biotechnol 23(8):1002–1007
243. Judge AD et al (2006) Design of noninflammatory synthetic siRNA mediating potent gene silencing in vivo. Mol Ther 13(3):494–505
244. Judge AD et al (2009) Confirming the RNAi-mediated mechanism of action of siRNA-based cancer therapeutics in mice. J Clin Invest 119(3):661–673
245. Jackson AL et al (2006) Position-specific chemical modification of siRNAs reduces "off-target" transcript silencing. RNA 12(7):1197–1205
246. Kenski DM et al (2012) siRNA-optimized modifications for enhanced in vivo activity. Mol Ther Nucleic Acids 1:e5
247. Tai W, Gao X (2017) Functional peptides for siRNA delivery. Adv Drug Deliv Rev 110-111:157–168
248. Ha D, Yang N, Nadithe V (2016) Exosomes as therapeutic drug carriers and delivery vehicles across biological membranes: current perspectives and future challenges. Acta Pharm Sin B 6(4):287–296
249. Boado RJ (2005) RNA interference and nonviral targeted gene therapy of experimental brain cancer. NeuroRx 2(1):139–150
250. Rossi JJ (2006) RNAi therapeutics: SNALPing siRNAs in vivo. Gene Ther 13(7):583–584
251. Li Z, Loh XJ (2016) Recent advances of using polyhydroxyalkanoate-based nanovehicles as therapeutic delivery carriers. Nanomed Nanobiotechnol 9(3):e1429
252. Coutinho MF et al (2016) Genetic substrate reduction therapy: a promising approach for lysosomal storage disorders. Diseases 4(4):1429
253. Buduru S et al (2018) RNA interference: new mechanistic and biochemical insights with application in oral cancer therapy. Int J Nanomedicine 13:3397–3409

sandra.alves@insa.min-saude.pt

254. Song E et al (2005) Antibody mediated in vivo delivery of small interfering RNAs via cell-surface receptors. Nat Biotechnol 23(6):709–717
255. Peer D et al (2007) Selective gene silencing in activated leukocytes by targeting siRNAs to the integrin lymphocyte function-associated antigen-1. Proc Natl Acad Sci USA 104(10):4095–4100
256. Peer D et al (2008) Systemic leukocyte-directed siRNA delivery revealing cyclin D1 as an anti-inflammatory target. Science 319(5863):627–630
257. McNamara JO 2nd et al (2006) Cell type-specific delivery of siRNAs with aptamer-siRNA chimeras. Nat Biotechnol 24(8):1005–1015
258. Berezhnoy A et al (2014) Aptamer-targeted inhibition of mTOR in T cells enhances antitumor immunity. J Clin Invest 124(1):188–197
259. Wheeler LA et al (2011) Inhibition of HIV transmission in human cervicovaginal explants and humanized mice using CD4 aptamer-siRNA chimeras. J Clin Invest 121(6):2401–2412
260. Soutschek J et al (2004) Therapeutic silencing of an endogenous gene by systemic administration of modified siRNAs. Nature 432(7014):173–178
261. Kortylewski M et al (2009) In vivo delivery of siRNA to immune cells by conjugation to a TLR9 agonist enhances antitumor immune responses. Nat Biotechnol 27(10):925–932
262. Davis ME et al (2010) Evidence of RNAi in humans from systemically administered siRNA via targeted nanoparticles. Nature 464(7291):1067–1070
263. Wong SC et al (2012) Co-injection of a targeted, reversibly masked endosomolytic polymer dramatically improves the efficacy of cholesterol-conjugated small interfering RNAs in vivo. Nucleic Acid Ther 22(6):380–390
264. Nair JK et al (2014) Multivalent N-acetylgalactosamine-conjugated siRNA localizes in hepatocytes and elicits robust RNAi-mediated gene silencing. J Am Chem Soc 136(49):16958–16961
265. Manoharan M(2014) GalNAc-siRNA with enhanced stabilization chemistry: ESC-GalNAc-siRNA. Available from: http://www.alnylam.com/web/assets/ALNY-ESC-GalNAc-siRNA-TIDES-May2014-Capella.pdf
266. Roberts TC et al (2016) Synthetic SiRNA delivery: progress and prospects. Methods Mol Biol 1364:291–310
267. Bruun J et al (2015) Investigation of enzyme-sensitive lipid nanoparticles for delivery of siRNA to blood-brain barrier and glioma cells. Int J Nanomedicine 10:5995–6008
268. Serramia MJ et al (2015) In vivo delivery of siRNA to the brain by carbosilane dendrimer. J Control Release 200:60–70
269. Bruck J et al (2015) Cholesterol modification of p40-specific small interfering RNA enables therapeutic targeting of dendritic cells. J Immunol 195(5):2216–2223
270. Haroon MM et al (2016) A designed recombinant fusion protein for targeted delivery of siRNA to the mouse brain. J Control Release 228:120–131
271. Gabathuler R (2012) New protein vectors for physiological transfer of therapeutic agents to the central nervous system. Biol Aujourdhui 206(3):191–203
272. Gabathuler R (2015) Using a peptide derived from transcend (mtf, p97) to deliver biologics to the cns using a physiologic pathway. Available from: http://www.brains4brain.eu/wp-content/uploads/2015/01/9th-B4B-Workshop-Scientific-Programme.pdf
273. Unniyampurath U, Pilankatta R, Krishnan MN (2016) RNA interference in the age of CRISPR: will CRISPR interfere with RNAi? Int J Mol Sci 17(3):291
274. Barrangou R et al (2007) CRISPR provides acquired resistance against viruses in prokaryotes. Science 315(5819):1709–1712
275. Sorek R, Kunin V, Hugenholtz P (2008) CRISPR–a widespread system that provides acquired resistance against phages in bacteria and archaea. Nat Rev Microbiol 6(3):181–186
276. Grissa I, Vergnaud G, Pourcel C (2007) The CRISPRdb database and tools to display CRISPRs and to generate dictionaries of spacers and repeats. BMC Bioinformatics 8:172
277. Mali P et al (2013) RNA-guided human genome engineering via Cas9. Science 339(6121):823–826
278. Cong L et al (2013) Multiplex genome engineering using CRISPR/Cas systems. Science 339(6121):819–823
279. Cornu TI, Mussolino C, Cathomen T (2017) Refining strategies to translate genome editing to the clinic. Nat Med 23(4):415–423
280. Yin H et al (2014) Genome editing with Cas9 in adult mice corrects a disease mutation and phenotype. Nat Biotechnol 32(6):551–553
281. Nelson CE et al (2016) In vivo genome editing improves muscle function in a mouse model of Duchenne muscular dystrophy. Science 351(6271):403–407
282. Tabebordbar M et al (2016) In vivo gene editing in dystrophic mouse muscle and muscle stem cells. Science 351(6271):407–411
283. Zetsche B et al (2015) Cpf1 is a single RNA-guided endonuclease of a class 2 CRISPR-Cas system. Cell 163(3):759–771
284. Sahin U, Kariko K, Tureci O (2014) mRNA-based therapeutics–developing a new class of drugs. Nat Rev Drug Discov 13(10):759–780
285. Stanton MG (2018) Current status of messenger RNA delivery systems. Nucleic Acid Ther 28(3):158–165
286. Pardi N et al (2018) mRNA vaccines – a new era in vaccinology. Nat Rev Drug Discov 17(4):261–279
287. Heiser A et al (2002) Autologous dendritic cells transfected with prostate-specific antigen RNA

sandra.alves@insa.min-saude.pt

stimulate CTL responses against metastatic prostate tumors. J Clin Invest 109(3):409–417
288. Morse MA et al (2002) The feasibility and safety of immunotherapy with dendritic cells loaded with CEA mRNA following neoadjuvant chemoradiotherapy and resection of pancreatic cancer. Int J Gastrointest Cancer 32(1):1–6
289. Morse MA et al (2003) Immunotherapy with autologous, human dendritic cells transfected with carcinoembryonic antigen mRNA. Cancer Investig 21(3):341–349
290. Weide B et al (2009) Direct injection of protamine-protected mRNA: results of a phase 1/2 vaccination trial in metastatic melanoma patients. J Immunother 32(5):498–507
291. Rittig SM et al (2011) Intradermal vaccinations with RNA coding for TAA generate CD8+ and CD4+ immune responses and induce clinical benefit in vaccinated patients. Mol Ther 19(5):990–999
292. Kübler, et al. (2011) Final analysis of a phase I/IIa study with CV9103, an intradermally administered prostate cancer immunotherapy based on self-adjuvanted mRNA. J Clin Oncol 29:4535
293. Sebastian M et al (2012) Messenger RNA vaccination and B cell responses in NSCLC patients. J Clin Oncol 30(15_suppl):2573–2573
294. Wilgenhof S et al (2013) A phase IB study on intravenous synthetic mRNA electroporated dendritic cell immunotherapy in pretreated advanced melanoma patients. Ann Oncol 24(10):2686–2693
295. Devoldere J et al (2016) Evading innate immunity in nonviral mRNA delivery: don't shoot the messenger. Drug Discov Today 21(1):11–25
296. Granot Y, Peer D (2017) Delivering the right message: challenges and opportunities in lipid nanoparticles-mediated modified mRNA therapeutics-An innate immune system standpoint. Semin Immunol 34:68–77
297. Zangi L et al (2013) Modified mRNA directs the fate of heart progenitor cells and induces vascular regeneration after myocardial infarction. Nat Biotechnol 31(10):898–907
298. Baba M et al (2015) Treatment of neurological disorders by introducing mRNA in vivo using polyplex nanomicelles. J Control Release 201:41–48
299. Matsui A et al (2015) Messenger RNA-based therapeutics for the treatment of apoptosis-associated diseases. Sci Rep 5:15810
300. DeRosa F et al (2016) Therapeutic efficacy in a hemophilia B model using a biosynthetic mRNA liver depot system. Gene Ther 23(10):699–707
301. Ramaswamy S et al (2017) Systemic delivery of factor IX messenger RNA for protein replacement therapy. Proc Natl Acad Sci USA 114(10):E1941–E1950
302. Kormann MS et al (2011) Expression of therapeutic proteins after delivery of chemically modified mRNA in mice. Nat Biotechnol 29(2):154–157
303. Wang Y et al (2013) Systemic delivery of modified mRNA encoding herpes simplex virus 1 thymidine kinase for targeted cancer gene therapy. Mol Ther 21(2):358–367
304. Schrom E et al (2017) Translation of angiotensin-converting enzyme 2 upon liver- and lung-targeted delivery of optimized chemically modified mRNA. Mol Ther Nucleic Acids 7:350–365
305. An D et al (2017) Systemic messenger RNA therapy as a treatment for methylmalonic acidemia. Cell Rep 21(12):3548–3558
306. Patel S et al (2017) Boosting intracellular delivery of lipid nanoparticle-encapsulated mRNA. Nano Lett 17(9):5711–5718
307. Ellington AD, Szostak JW (1990) In vitro selection of RNA molecules that bind specific ligands. Nature 346(6287):818–822
308. Tuerk C, Gold L (1990) Systematic evolution of ligands by exponential enrichment: RNA ligands to bacteriophage T4 DNA polymerase. Science 249(4968):505–510
309. Jayasena SD (1999) Aptamers: an emerging class of molecules that rival antibodies in diagnostics. Clin Chem 45(9):1628–1650
310. Yu Y et al (2016) Molecular selection, modification and development of therapeutic oligonucleotide aptamers. Int J Mol Sci 17(3):358
311. Cruz-Toledo J et al (2012) Aptamer Base: a collaborative knowledge base to describe aptamers and SELEX experiments. Database (Oxford) 2012:bas006

sandra.alves@insa.min-saude.pt